Model Documentation Report
East-Central Florida Transient Expanded (ECFTX) Model
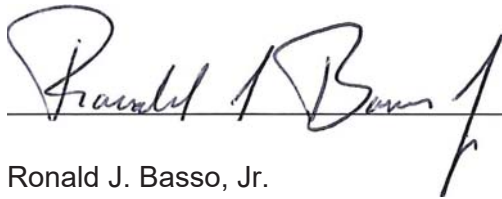

Prepared by Central Florida Water Initiative (CFWI)
Hydrologic Analysis Team (HAT)
February 2020

Model Documentation Report
East-Central Florida Transient Expanded (ECFTX) Model

February 2020

The geological evaluation and interpretation contained in the report entitled Model Documentation Report, East-Central Florida Transient Expanded Model has been prepared by or approved by a Certified Professional Geologist in the State of Florida, in accordance with Chapter 492, Florida Statutes.

Ronald J. Basso, Jr.
Professional Geologist
License No. PG 0001325

Table of Contents

FIGURES

TABLES

ACRONYMS AND ABBREVIATIONS

AFSIRS	Agricultural Field-Scale Irrigation Requirements Simulation
AG	Agricultural
AMC	antecedent moisture contents
APhpz	Avon Park high permeability zone
APPZ	Avon Park Permeable Zone
APT	aquifer performance test
BFI	Base-Flow Index
cfs	cubic feet per second
CFWI	Central Florida Water Initiative
CII	Commercial/Industrial/Institutional
CII_MD	Commercial/Industrial/Industrial and Mining/Dewatering
CN	curve Number
CUP	consumptive use permit
DCIA	directly connected impervious areas
DEM	digital elevation model
DMIT	Data, Monitoring and Investigations Team
DRN	Drain package
DRT	Drain Return package
DSS	Domestic Self-Supply
DV	deviation of volume
DWRM	District Wide Regulatory Model
dy^{-1}	ft per day per ft
ECF	East Central Florida
ECFM	East Coast Floridan Model
ECFT model	East-Central Florida Transient model
ECFTX	East-Central Florida Transient Expanded Model
EFH	equivalent freshwater head
ENV	Environmental
EMT	Environmental Measures Team
ET	evapotranspiration
ET_c	crop evapotranspiration
ETp	potential evapotranspiration
FAS	Floridan aquifer system
FASS	Florida Agricultural Statistics Service
FDACS	Florida Department of Agriculture and Consumer Services

FDEP	Florida Department of Environmental Protection
FLUCCS	Florida Land Use Cover Classification System
FP	fire protection
FSAID-4	Florida Statewide Agricultural Irrigation Demand-4
ft/d	feet per day
ft^2/d	Feet squared per day
FW	flowing wells
GAT	Groundwater Availability Team
GHB	General Head Boundary package
GLAUClpu	low permeability glauconitic marker unit
gpd	gallons per day
HAT	Hydrologic Analysis Team
HAT-ECFT	Hydrologic Analysis Team version of the ECFT model
HSGs	Hydrologic Soil Groups
HUC	Hydrologic Unit Classification coding system
HYSEP	Hydrograph Separation program
IAS	intermediate aquifer system
ICU	intermediate confining unit
ID	identification
IFAS	Institute of Food and Agricultural Sciences (University of Florida)
K	hydraulic conductivity
Kc	crop water use coefficient
KCOL	Kissimmee Chain of Lakes
Kh	horizontal hydraulic conductivity
KOE	Kissimmee-Okeechobee-Everglades system
Kv	vertical hydraulic conductivity
LFA	Lower Floridan aquifer
LFA-upper	First subdivision of the LFA – upper permeable zone
LF-basal	Lower Floridan aquifer – basal permeable zone
LRA	landscape/recreational/aesthetic
MAE	mean absolute error
MCU	middle confining unit
MCU_I	first component of the MCU
MCU_II	second component of the MCU
ME	mean error
mg/l	Milligrams per liter
MGD	million gallons per day
MOC	Management Oversight Committee

MODFLOW-2005	USGS Modular Groundwater Flow Model 2005
MORs	monthly operating reports
MSR	mean-square residual
NAVD88	North American Vertical Datum of 1988
NDM	Northern District Model
NFSEG	North Florida-Southeast Georgia
NGVD29	National Geodetic Vertical Datum of 1929
NHD	National Hydrography Data (USGS)
NIR	Net Irrigation Requirement
NLCD	National Land Cover Database
NOAA	National Oceanic and Atmospheric Administration
NRCS	Natural Resources Conservation Services
NS	Nash-Sutcliffe coefficient
NWS	National Weather Service
OCAPlpz	Ocala-Avon Park low-permeability zone
OMR	overall mean residual
Panel	independent scientific peer review panel
PET	potential evapotranspiration
PETc	total potential ET for a specific vegetation type
PS	public supply
PWS	Public Water Supply
PZ	Permeable Zone
R^2	coefficient of determination
RASA	Regional Aquifer System Study
RBOT	river bottom elevation
RIB	rapid infiltration basin
RMS	root mean square
RMSR	root-mean-square-residual
RWSP	Regional Water Supply Plan
RWSPT	Regional Water Supply Planning Team
SAS	Surficial Aquifer System
SCS	Soil Conservation Service
SFWMD	South Florida Water Management District
SJRWMD	St. Johns River Water Management District
Ss	Specific storage
Swamp	Green Swamp
SWFWMD	Southwest Florida Water Management District
Sy	Specific yield

SZ	saturated zone
TDS	total dissolved solids
TOC	Technical Oversight Committee
UFA	Upper Floridan aquifer
UFA-upper	Uppermost permeable zone of FAS
UPW	Upstream Weighting
USACE	United States Army Corp of Engineers
USF	University of South Florida
USGS	United States Geological Survey
USGS-ECFT model	USGS version of the ECFT model
UZF1	MODFLOW Unsaturated Zone Package
UZ	unsaturated zone
WAT	Water Resource Assessment Team
WMD	water management district
WUCA	Water Use Caution Area
WUP	water use permit

Model Documentation Report for the East-Central Florida Transient Expanded (ECFTX) Model

CHAPTER 1 – INTRODUCTION

Historically, central Florida has predominately utilized fresh groundwater to meet the increasing needs of public, agricultural, industrial, commercial, and other water users. To support these users, the Central Florida Water Initiative (CFWI) undertook a robust and cooperative effort to identify the extent of this groundwater system, support regional water supply planning, and understand groundwater resource limitations for sustainable water supplies while protecting natural systems. A primary tool for the groundwater assessment is the East-Central Florida Transient Expanded (ECFTX) groundwater flow model. This report describes the documentation for the development and calibration of the ECFTX Model.

1.1 Background

The CFWI Planning Area is in central Florida and consists of Orange, Osceola, Polk, and Seminole counties and southern Lake County (Figure 1), covering approximately 5,300 square miles. The CFWI Planning Area is based on the county boundaries for the four wholly included counties and the utility service areas for Lake County.

Due to the extent and complexities of the planning area, the CFWI required a collaborative effort by three water management districts (WMDs), other public agencies, and stakeholders. The participants in the CFWI include: South Florida Water Management District (SFWMD), St. Johns River Water Management District (SJRWMD), Southwest Florida Water Management District (SWFWMD), Florida Department of Agriculture and Consumer Services (FDACS), Florida Department of Environmental Protection (FDEP), public water supply utilities, and other interested parties and stakeholders.

Aspects of water supply planning for CFWI were divided among several project teams. The groundwater flow modeling was performed by the Hydrologic Analysis Team (HAT) of the CFWI. Other technical teams in the CFWI were the Minimum Flows and Levels/Reservations Team (MFLRT), Environmental Measures Team (EMT), Data, Monitoring and Investigations Team (DMIT), the Groundwater Availability Team (GAT), and the Regional Water Supply Planning Team (RWSPT). The Water Resource Assessment Team (WRAT) coordinates the technical efforts of the HAT, MFLRT, EMT, and GAT. The technical teams were provided guidance from the Steering Committee through the Management Oversight Committee (MOC). A detailed description of the activities and products of the CFWI is provided in the Regional Water Supply Plan (RWSP) (CFWI 2014a, CFWI 2015).

As the population of central Florida has grown, so has the pace of residential, agricultural, industrial, and commercial development. With that growth, the need for water has also increased. This trend is projected to continue, which will lead to the need for more water supply. However, hydrogeological, hydrological and ecological studies, water supply permitting, and public policy

have concluded the use of traditional groundwater[1] is nearing its sustainable limit. This means meeting future water needs may require the use of alternative, non-traditional water supplies.

The benchmarks used to assess the sustainable limit of groundwater supplies are:

- Unacceptably stressed ecological conditions of wetlands and lakes linked to groundwater withdrawals;

- Reduced groundwater levels that are insufficient to limit adverse salinity changes; and

- Reduced river and spring flows below regulatory thresholds directly attributable to predicted reduced aquifer water levels (drawdowns) from modeled historic or projected groundwater withdrawals in comparison to observed conditions.

The ECFTX model is an important tool for assessing changes in groundwater levels and spring flows by comparing the simulation results of various regional water supply scenarios to a baseline or reference condition. Assessments of the relationships between predicted drawdowns and changes to wetland and lake conditions and spring flows were performed.

1.2 Objectives of the CFWI Hydrologic Analysis Team

The objectives[2] of the HAT are to provide the necessary modeling tools and data analysis and work collaboratively with other CFWI teams to:

1. Estimate the potential availability of groundwater.

2. Produce model output that can be used by the other technical teams to evaluate the effects of groundwater withdrawals on natural systems.

3. Assess future water supply and management strategies.

4. Develop processes to assess the long-term effectiveness of management strategies.

5. Support collaborative water supply planning.

6. Support future regulatory actions.

1.3 Previous Studies

The East Central Florida (ECF) model was originally developed by the SJRWMD in 2002 and is a steady-state model (McGurk and Presley, 2002). In 2006, SFWMD converted that model into a transient model, and it was then referred to as the East Central Florida Transient (ECFT) model. The ECFT model underwent an independent peer review (2007) consisting of review of the model as well as documentation of suggested improvements (Andersen and others, 2007). The United States Geological Survey (USGS) was contracted to implement these and other improvements

---

[1] Traditional groundwater supplies refer to water from the surficial aquifer system (SAS), intermediate aquifer system (IAS), and Floridan aquifer system (FAS) that has been used to meet the needs of the area and requires minimal treatment to meet the water quality requirements for the expected use.
[2] Central Florida Water Initiative Guiding Document (http://cfwiwater.com/pdfs/2013/08-16/CFWI_Guiding_Document_updates.pdf)

as described by Sepúlveda, et al. (2012). The ECF, ECFT, and the USGS version of the ECFT Model (USGS-ECFT) models were developed prior to formal initiation of the CFWI effort and did not include the entire CFWI area.

The USGS delivered the USGS-ECFT groundwater flow model to the HAT in 2012. The HAT reviewed the model construction, distribution of input parameters, and model performance and determined that several items needed to be updated for its use in the CFWI process (HAT-ECFT). Through this process, the following model input data sets were identified for improvement:

1. The General Head Boundary water level values used for the Upper and Lower Floridan aquifer systems (Layers 3, 5, and 7).

2. Leakance (vertical hydraulic conductivity) values for Layer 6, which represents the Middle semi-confining unit between the Upper and Lower Floridan aquifers,

3. Specific storage.

4. Spring pool elevations (a factor used to calculate spring discharge),

5. Groundwater withdrawal amounts for various categories of water use.

6. Landscape irrigation using public water supply (PWS) and reclaimed water.

The HAT identified additional data were available to improve these inputs and thus improve the performance of the model. From a performance statistics perspective, the recalibrated HAT-ECFT model was similar to the USGS-ECFT calibration. Recalibration for the full model domain resulted in a slight improvement over the original calibration; however, depending on the model layer or the metric being evaluated, the recalibration results varied from a slight degradation to a slight improvement in the model calibration statistics. The main benefit of the recalibration effort was improvement in the transient response of many of the water levels and flows simulated by the model and the overall water balance. The domain or active area of the HAT-ECFT was the same as the USGS-ECFT model.

The HAT-ECFT model covers central Florida as shown in Figure 2 and encompasses nearly 10,300 square miles. The model domain included all of Seminole, Orange, and Osceola counties; most of Lake, Volusia, Brevard, and Polk counties; and small parts of Marion, St. Lucie, Okeechobee, Highlands, Hardee, and Sumter counties. The selected grid size was 1,250 feet by 1,250 feet, or approximately 36 acres, which resulted in 472 rows oriented east-west and 388 columns oriented north-south. A more complete description of the HAT-ECFT model is presented in Appendix C of the CFWI Regional Water Supply Plan (CFWI. 2014b). The model was fully three-dimensional and included seven layers to represent the hydrogeologic units from land surface to the base of the Floridan aquifer system (FAS). The thickness of the layers varies based on the position within the model grid and the hydrogeologic unit that a layer represents.

The HAT recognized the need for improvements to the HAT-ECFT Model as acknowledged in the CFWI Regional Water Supply Plan (CFWI. 2014b). In particular, the model domain needed to be expanded outward away from the CFWI area to minimize boundary condition effects on the simulation. The expanded version of the ECFT model is referred to as the ECFTX model. Figure 2 shows the domains of the ECFT and ECFTX models. The purpose of the expanded model is to

update the ECFT model to better represent current and future hydrologic conditions in the CFWI area and assist in planning decisions.

The major areas of model improvements or changes for the ECFTX model are summarized below:

Model Boundaries – The western and eastern boundaries coincide with offshore boundaries (i.e., Gulf of Mexico and Atlantic Ocean), while the southern boundary was extended southward to the Charlotte-DeSoto county line to incorporate groundwater withdrawals in the SFWMD's Lower Kissimmee Basin that might have an effect on MFL water-bodies on the Lake Wales Ridge. The northern boundary stayed the same as in the previous ECFT model.

Water Use -- Developed best estimates of water use recognizing each District has varying amounts of metered data above certain thresholds and use classes.

Hydrostratigraphic Framework -- Updated with new well information, resolved interpretation differences across District boundaries, and incorporated additional model layering within the FAS.

Runoff-Infiltration Partitioning – The ECFT model used the Green-Ampt method, suitable for surface water models with short (minutes/hours) time steps. In addition, the MODFLOW UZF package was used to account for the time lag incurred during surface infiltration through thick unsaturated zones. This approach was found to be computationally inefficient and data intensive for a regional groundwater model with 3-day time steps and monthly stress periods. Accordingly, the empirically based Natural Resources Conservation Service (NRCS) curve number method was used, which has been applied successfully in previous regional groundwater modeling efforts (Giddings, et al, 2015).

1.4 Peer Review

Given the scope of model improvements, the HAT determined it was best to convene an independent scientific peer review panel (Panel) during each major phase of the construction and calibration of the updated ECFTX Model. Three independent groundwater modeling experts with experience in Florida were assembled to conduct this review. They are:

- Peter F. Andersen, M.S. (Chair), Principal Engineer, Tetra Tech, Inc.

- Louis Motz, Ph.D., P.E., D. WRE

- Mark Stewart, Ph.D., P.G., Professor Emeritus (retired), University of South Florida

Traditionally, peer reviews have been implemented once the model is calibrated and the documentation developed. The HAT thought an improved approach was to convene the Panel earlier in the model development process. In this way, the Panel could provide early input to better minimize the chance that a major model revision would be needed at the conclusion of the project. Towards that end, the Panel was engaged at the conceptual model development phase and throughout calibration and model documentation. The Panel was formed, and the first meeting held in September 2016. Throughout the peer review process, periodic publicly noticed teleconference calls were conducted to update the Panel on the HAT's progress and solicit input. All communication with the Panel was conducted via a SWFWMD electronic web board, available to the public. Publicly noticed meeting dates were posted prior to the meetings, and all documents

and correspondence between staff and the Panel were conducted via the web board. Meeting summaries for each meeting were similarly posted on the web board.

Major topics discussed included the conceptual model of the system, resolving dry cells, baseflow estimation, boundary condition selection, rainfall-adjusted NEXRAD estimation, calibration approaches (e.g., automated vs. manual), calibration targets, statistical measures of calibration success, and modification of general head boundary fluxes.

1.5 Acknowledgements

CHAPTER 1 - FIGURES

Figure 1. Map of the Central Florida Water Initiative (CFWI) Planning Area and the ECFT Model Domain
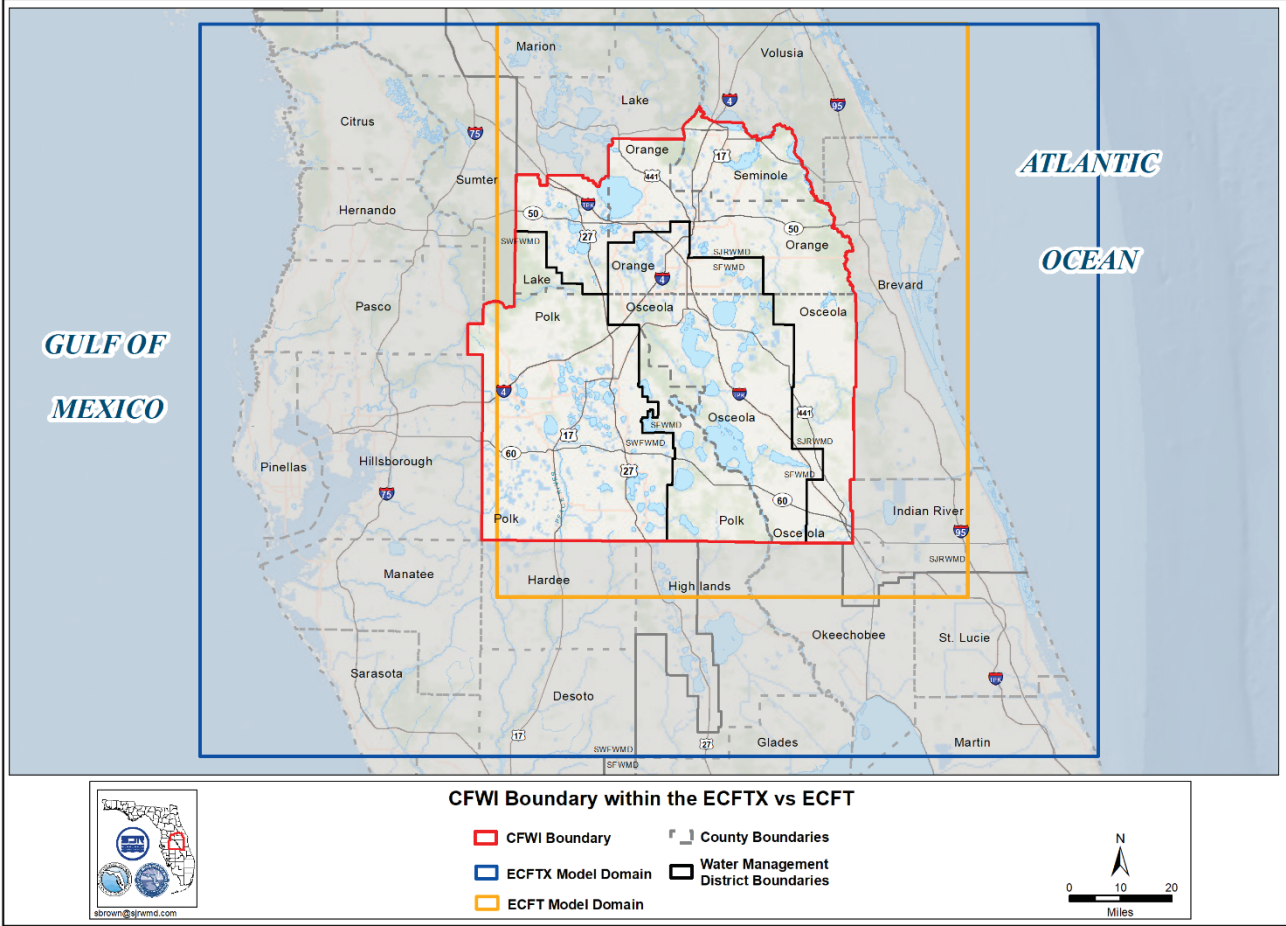
Figure 2. Model Boundaries for the existing (ECFT) and updated (ECFTX) models.

CHAPTER 2 - DESCRIPTION OF STUDY AREA

The ECFTX active model domain covers about a 23,800 square mile area of central Florida that stretches from the Atlantic Ocean to the Gulf of Mexico and from southern Marion - central Volusia counties in the north to Lake Okeechobee in the south. The study area spans approximately 143 miles on its eastern and western sides, approximately 175 miles on its northern and southern sides, and covers the entire CFWI area. It includes the major metropolitan areas of Tampa-St Petersburg, Orlando, Lakeland, Melbourne, Sarasota, and Vero Beach.

2.1 Topography and Physiography

Land-surface elevation ranges from sea level along the coasts of the Gulf of Mexico and Atlantic Ocean to more than 300 ft above National Geodetic Vertical Datum of 1929 (NGVD 29) in Polk and Lake counties along the Lake Wales Ridge (Figure 3). The Central Highlands Region of peninsular Florida consists of a series of near parallel north-south ridges that are remnants of beach and sand-dune systems associated with Miocene, Pliocene or Early Pleistocene shorelines (White, 1970). The region consists of xeric residual sand hills, beach ridges and dune fields which are interspersed with numerous sinkhole lakes and basins caused by erosion of the underlying limestone bedrock. The main axis of the Central Highlands is the Central Ridge, extending from southeastern Lake County in the north to southern Highlands County in the south (Wunderlin, 2010). This comprises the Lake Wales Ridge, Winter Haven Ridge, Lake Henry Ridge and Bombing Range Ridge. An outlying ridge system to the west in Polk County comprises the Lakeland Ridge. In general, thick sandy soils promote low runoff, rapid infiltration, and high recharge rates along these ridges. Exceptions are the Lakeland Ridge, and possibly the Lake Henry Ridge, where more poorly drained soils are prevalent and the clay below these soils are more competent and therefore inhibiting recharge.

In the southwestern and central parts of the domain west of the Central Highlands Region, there are large physiographic regions such as the Southern Gulf Coastal Lowlands, De Soto Plain, and Polk Upland that lie outside of the ridge areas (Figure 4). These are generally flat topographic regions with poorly drained soils, a shallow water table, extensive dendritic network of drainage, and thick competent clay beneath the surface soils. To the southeast of the Central Highlands Region, lie the Osceola and Okeechobee Plains that are very similar to the Gulf Coastal Lowlands and DeSoto Plain. Further east is the Eastern Valley and the Atlantic Coastal Ridge. With intermittent absences, the Atlantic Coastal Ridge parallels the Atlantic Ocean from near the St Mary's River close to the Georgia state line in the north to about 30 miles southwest of Miami in the south. It's comprised of relict beach dunes that occur as single or multiple ridge lines (White, 1970).

In the center part of the domain is the Green Swamp (Swamp). While not identified as a unique physiographic region, the Swamp is a largely undeveloped mosaic of cypress domes, hardwood forests, pine forests, prairies, and sand hills in central Florida (Figure 5). The Swamp occupies about 870 square miles in five Florida Counties - Polk, Sumter, Lake, Hernando, and Pasco (Basso, 2010). Land surface elevations vary between 75 and 200 feet NGVD 29. The Green Swamp is an extensive area of wetlands and open water that forms a broad, flat plateau. While the limestone is generally shallow (close to land surface), it is relatively dense and impermeable which allows rainfall that infiltrates into the soil to mound or stack up at the surface. This creates a rather large reservoir of standing water, marshes, and cypress wetlands which forms the headwaters of five rivers. The Swamp includes the headwaters of several important rivers

including the Ocklawaha, Withlacoochee, Little Withlacoochee, Hillsborough, and Peace. Water levels with the Upper Floridan aquifer (UFA) underlying the Swamp represent the highest potentiometric levels in peninsular Florida. Groundwater within the Floridan aquifer moves laterally away from the Swamp to supply downgradient parts of the aquifer in other parts of central Florida (Figure 6).

Transitioning to the northern half of the study area, the Brooksville Ridge extends from northern Citrus County into eastern Pasco County. The entire ridge overlies a clay unit up to 30 feet thick, with partial hydraulic connection to the underlying UFA by way of solution features and fractures (SWFWMD 1996). The Brooksville Ridge has the most irregular topography to be found in peninsular Florida (White 1970). There are few persistent valleys and little surface drainage. Some of the highest land surface elevations occur in this physiographic province within peninsular Florida, with some elevations as high as 300 feet NGVD 29. The Gulf Coastal Lowlands province lies to the west of the Brooksville Ridge, and includes an extensive lakes region in northwest Hillsborough County and south-central Pasco County. Soils are sandy, with little organic material (SWFWMD 1996). Elevations are generally between 20 and 100 feet NGVD 29. The Zephyrhills Gap lies to the south of the Brooksville Ridge and east of the Gulf Coastal Lowlands. The Zephyrhills Gap is an erosional watershed with sluggish surface drainage and many karst features (SWFWMD 1996). A thin layer of sand and clay overlies karst limestone, and springs and sinkholes are common. Elevations range from 10 to 140 feet NGVD 29, with poorly drained swamps and marshes in the lower elevations and pine flatwoods in the higher elevations.

Much of the area in the northwest quarter of the domain north of the Pasco-Hernando County line is where the UFA is unconfined and is a highly karst-dominated region. Dissolution of limestone is an active process via infiltration of rainwater because the limestone units of the UFA are close to land surface and the intermediate confining unit (ICU) is thin and discontinuous. The carbonate rocks of this region have been extensively and repeatedly subjected to chemical dissolution and deposition processes in response to sea-level fluctuations. Numerous sinkholes, internal drainage, and undulating topography that are typical of karst geology dominate the landscape. These active karst processes lead to enhanced permeabilities within the UFA. First-magnitude springs (> 100 cfs discharge) are found within this region. In addition, the highest recharge rates to the UFA occur here with values ranging between 10 and 30 inches per year (Sepulveda, 2002). Physiographic regions found within this area include the Tsala-Apopka Plain, Lake Upland, and Sumter Upland. The Tsala-Apopka Plain includes most of the Withlacoochee River drainage basin and contains numerous swamps and shallow water table areas. The Lake and Sumter Uplands are generally deep water-table areas of limited surface water drainage that contain relict and recent karst activity.

The northeast quarter of the domain is characterized by discontinuous highlands separated by broad valleys. Past sea level stands have created relict shorelines that consist of beach ridges that parallel the Atlantic Ocean. Areas in between these ridges are generally closed basins that contain numerous karst features, including sinkholes and springs. Sinkholes are common throughout much of the area and range from small depressions to large lakes. Many of these sinkholes can be areas of high recharge to the underlying aquifers. The springs in the northeastern part of the study area discharge water from the UFA into rivers and streams that eventually flow into the Atlantic Ocean. Prominent ridges include the Orlando Ridge, Mount Dora Ridge, Deland Ridge, and Geneva Hill. Interspersed between the ridges lie the Central Valley, Marion Uplands, Osceola Plain, and the Eastern Valley.

2.2 Land Use

Land use-cover areas were primarily used in the model to develop estimates of runoff, maximum evapotranspiration (ET), and recharge rates, agricultural pumping demands, and to estimate landscape and agricultural irrigation return flows. Land use-cover presents a distribution of pervious and impervious surfaces that are used in separating runoff and infiltration of the total rainfall and irrigation. The SCS Curve Number method is an empirical method that was used in an external preprocessing routine (ET-Recharge program) to separate runoff from the combination of rainfall and irrigation as a function of land use-cover and properties of the surface soil. Agricultural demands, however, were developed based on the Florida Statewide Agricultural Irrigation Demand-4 (FSAID-4) land use coverage, which provides more accurate estimates of irrigated acreage. A description of FSAID-4 land use coverage can be found in the Agricultural Demands section in Appendix A.

The distributions of land use-cover for 2004 (Figure 7), and for 2009 (Figure 8) were used for the model calibration. The use of time varying land use-cover data is essential in order to capture the change in hydrology of the system through time. For example, transitions from agricultural or forest land use to urban land use are particularly important because such changes could modify the runoff potential caused by changes in infiltration associated with impervious surfaces, soil compaction during development, or stormwater drainage systems. In the case of closed watersheds, it is also necessary to account for the effect of increased runoff that drains to isolated waterbodies where runoff becomes available as groundwater recharge.

Each water management district independently developed their own land use-cover for their jurisdictional boundaries and then combined them into a single coverage. In general, up to a level 4 Florida Land Use Cover Classification System (FLUCCS) code was assigned to each polygon depending upon available data. Since land use-cover data is not available for every year of the calibration period, interpolation of land use-cover for the years between each land use-cover update was conducted as follows. The 2004 land use-cover was used for stress periods of January 2003 through December 2006, and 2008/2009 land use-cover was used from January 2007 through December 2014.

In 2004, agriculture was the most extensive land use and covered 31 percent of the study area, followed by wetlands (22 percent), urban (20 percent), forest (12 percent), water (7 percent), upland non-forested (6 percent), transportation, communication and utilities (1.5 percent), and barren land (0.5 percent). In 2009 agricultural land use was reduced by 3 percent (28 percent), while urban area land use, forest area, and upland non-forested area increased by 1 percent (21 percent,13 percent, and 7 percent respectively) compared to 2004 land use-cover.

2.3 Hydrography

The model domain encompasses the headwaters of many major river basins in peninsular Florida (Figure 9). There are approximately 4,000 square miles of wetlands and approximately 1,200 square miles of open water bodies such as lakes in the ECFTX model (Figure 10). The CFWI Planning Area has hundreds of lakes, including the interconnected Alligator and Kissimmee Chains of Lakes. There are 16 springs in the region, five 2nd magnitude, seven 3rd magnitude, and four 4th magnitude or smaller (CFWI, 2014a). Well-drained soils and karst terrain occur in some areas and are internally drained with no outfall to a river or stream. This provides significant recharge to the UFA.

2.3.1 Rivers

Major rivers in the ECFTX model domain include the St. Johns, Kissimmee, Withlacoochee, Myakka, Alafia, Hillsborough, and Peace Rivers. In the eastern portion of the study area, the St. Johns River watershed covers approximately 6,400 square miles. The St Johns River is approximately 310 miles long and originates in marshy headwaters in Indian River and Brevard counties. The St. Johns River flows north and empties into the Atlantic Ocean near Jacksonville. Major tributaries, or smaller streams and rivers that flow into the St. Johns River, include the Wekiva River, the Econlockhatchee River and the Ocklawaha River. Further south, the Kissimmee Basin includes the Kissimmee River and floodplain. More than two dozen lakes form the Kissimmee Chain of Lakes (KCOL) within the watershed. The basin forms the headwaters of Lake Okeechobee and the Everglades; together they comprise the Kissimmee-Okeechobee-Everglades (KOE) system.

In the western part of the model area, the Withlacoochee River watershed covers approximately 2,100 square miles in parts of Citrus, Hernando, Lake, Levy, Marion, Pasco, Polk and Sumter counties. The Withlacoochee River is approximately 160 miles long and originates in the Green Swamp extending northward through eight counties before eventually discharging into the Gulf of Mexico near Yankeetown, Florida (Hood et al, 2010). Further south, the Myakka River flows southerly for 66 miles from Myakka Head in Manatee County to Charlotte Harbor. The river's watershed has a drainage area of approximately 602 square miles, which lies principally in Manatee and Sarasota Counties with small drainage areas extending into Hardee, Desoto, and Charlotte counties (Flannery et al, 2011). On the east side of Tampa Bay, the Alafia River is a tributary to the gulf coast of west-central Florida. The river's watershed is located predominantly in Hillsborough County, with headwater regions extending into Polk County. With a watershed area of 422 square miles, the Alafia represents the second largest river watershed contributing flow to Tampa Bay. It comprises approximately 19 percent of the total watershed area. (Flannery et al, 2008). The Hillsborough River originates in the Green Swamp, which is in Hernando, Lake, Pasco, Polk, and Sumter counties. The Hillsborough River is approximately 54 miles long. Flows in both the upper and lower reaches of the Hillsborough River are partially derived from spring discharges. The Hillsborough River drains an area that is approximately 675 square miles. The river ultimately discharges to Tampa Bay (Southwest Florida Water Management District, 2006).

Near the central part of the model area lies the Peace River, with a drainage basin of 2,350 square miles, it's approximately 105 miles long, beginning at the confluence of the Peace Creek Drainage Canal and Saddle Creek in Polk County to Charlotte Harbor. The watershed of the entire Peace River includes portions of Lakeland, Auburndale and Haines City in northern Polk County, and extends south to the city of Cape Coral in Lee County. Its western boundary includes portions of Hillsborough, Manatee and Sarasota counties and portions of Highlands and Glades counties on the east. The watershed includes major portions of Polk, Hardee, DeSoto and Charlotte counties (Southwest Florida Water Management District, 2010).

The rivers mentioned in the preceding discussion are major systems within the model domain. In the northwest quarter of the domain, most of the Hillsborough and Withlacoochee Rivers are hydraulically connected to the UFA over significant sections due to unconfined conditions in the UFA. Many springs and seepage from limestone within their riverbeds provide significant baseflow contribution to these systems. Most other rivers are located where the UFA is semi-confined or well-confined and are largely runoff-dominated systems. They receive baseflow contributions largely from the surficial aquifer.

2.3.2 Lakes

Many naturally formed lakes in the model domain are sinkhole lakes, which are the result of depressions that occur due to the collapse of cavities in the limestone of the underlying UFA. Resistance to downward vertical leakage due to the presence of the intermediate aquifer system/confining unit aids in the retention of water in the resulting depressions, thus helping to form lakes. Large numbers of sinkhole lakes are found in Central Florida and surrounding areas.

Sinkhole lakes can act as sources of relatively concentrated recharge to the underlying UFA in recharge areas. Leakage rates beneath them to the UFA are often enhanced by disturbances that occurred in the intermediate confining unit during the collapse(s) within the UFA that resulted in their formation. Rates of recharge, which are enhanced by downward leakage from numerous sinkhole lakes, are large enough to result in the formation of a potentiometric high along the Lake Wales Ridge in Polk County, a prominent, hydrologically important feature of the potentiometric surface of the Floridan aquifer system (FAS). This potentiometric high is centered near Polk City and extends south-southeast along the center of the state. Many relict sinkhole lakes are prevalent in the Winter Haven Ridge and Lake Wales Ridge areas. Other relict sinkhole lakes occur in areas in which the UFA is semi-confined in the Orlando area. Large lakes such as Tsala-Apopka in Citrus County are directly connected to the unconfined UFA with its stage close to the level of the potentiometric surface of the UFA.

2.3.3 Swamps/Wetlands

There are two main type of wetlands in the study area: isolated and those connected to riverine systems. Isolated systems consist of cypress wetlands or shallow wet prairie marshes. Riverine systems are located within the flood plains of rivers and creeks. They generally consist of wetland hardwood forests. The largest region of wetlands is, as the name implies, the Green Swamp. It's located in the central part of the study area and consists of a largely undeveloped system of cypress domes, hardwood forests, and wet prairies in central Florida. The Swamp occupies about 870 square miles in five Florida counties - Polk, Sumter, Lake, Hernando, and Pasco.

Wetlands within the model domain are related to the hydrogeology of the system in several ways. In recharge areas, confinement of the UFA in flat terrain areas can impede leakage into the system. The flatness of the terrain itself impedes runoff. Swamps can also occur in recharge areas in which the UFA is generally unconfined due to the absence or thinness of the intermediate confining unit. Due to lower horizontal and vertical hydraulic conductivity within the UFA, potential recharge runs off to the land surface and forms wetland areas. An additional type of wetland occurs in coastal discharge zones where the UFA is unconfined, and the potentiometric surface is above land surface. This creates artesian discharge to relatively flat land and results in the pooling of the discharged water onto the land surface (i.e., swamp formation).

2.4 Climate

The climate of the study area is classified as subtropical and is characterized by warm, normally wet summers and mild, dry winters. Maximum temperatures usually exceed 90 F during the summer but may fall below freezing for several days in the winter. The mean annual rainfall for the ECFTX model domain is 48.6 inches for 2003-2014. During the summer and early fall, tropical storms and hurricanes can produce substantial rainfall in the area. Winter rainfall is generally associated with large frontal systems that move from the northern latitudes southward.

The spatial and temporal distribution of rainfall between 2003 and 2014 was a key hydrologic parameter that influenced other variables in the model. It was based on Next Generation Weather Radar (NEXRAD) rainfall data. This period contains extreme wet (hurricanes of 2004 and 2005) and dry (drought of 2006 and 2012) conditions. As a result, the approach provides insight to the potential changes of hydrologic conditions to meet projected needs during extreme conditions. Daily rainfall data was used to develop recharge input to the ECFTX model.

Radar images from the U.S. National Weather Service (NWS) network cover much of the United States and provide a way of measuring the intensity of rain or snowfall. Radar can locate and follow clouds within a range of 200 to 400 kilometers. Weather radar emits microwave energy in short bursts or pulses, which are focused in a narrow conical beam that scans the atmosphere from a slowly rotating antenna. A beam passes through fog and clouds, but when it encounters rain, snow or ice particles (hail), some of the energy is scattered back to the radar's antenna as an echo. The amount of energy the antenna receives is proportional to the intensity of the precipitation; the heavier the rain or snow, the more energy is scattered back to the antenna.

There is a statistical tradeoff between rainfall measurement data collected by rain gauges and weather radar. Rain gauges can provide precise point values of rainfall depth and intensity but cannot economically provide the spatial distribution of rainfall. While rain gauges suffice for frontal-related rainfall events, the timing and orientation of the front is often not well represented and can miss convective rainfall events altogether. South and Central Florida receive most rainfall during the summer wet season, which is dominated by tropical and convective processes.

Next Generation Weather Radar (NEXRAD) data provides complete spatial coverage of rainfall amounts using a predetermined grid resolution (2 km by 2 km). The NEXRAD rainfall data is limited by relying on the measurement of raindrop reflectivity, which can be affected by factors such as raindrop size and signal reflection by other objects. Because the reflected signal measured by the radar is proportional to the sum of the sixth power of the diameter of the raindrops in a given volume of atmosphere, small changes in the size of raindrops can have a dramatic effect on the radar's estimate of the rainfall. For this reason, the radar is generally scaled to match volume measured at the rain gauges (Hoblit and Curtis, 2000). The best of both measurement techniques is realized by using rain gauge data to adjust NEXRAD values. The readers can obtain additional information on this subject from several references (Huebner et al., 2003 and Skinner, 2006).

Four NEXRAD sites operated by the NWS cover the ECFTX model domain: KBYX in Key West, KAMX in Miami, KMLB in Melbourne, and KBTW in Tampa. Although data is also available from several private radar installations, the Districts exclusively use NWS sites for its NEXRAD rainfall database due to longevity and reliability issues. NEXRAD technology offers the distinct advantage of providing water management officials with a spatial and temporal account of rainfall variability. Skinner (2006) provides additional details on the NEXRAD rainfall data and gauge-adjustment methodology used in derivation of the data.

OneRain, Inc. provides data to the Districts as near real-time, 15-minute rainfall amounts after acquiring radar rainfall accumulations from the NWS via WSI Corporation and reviews the results to identify and correct any anomalies or apparent errors. NEXRAD datasets that have been quality assurance/quality controlled (QA/QC) are acquired from OneRain and maintained by each District. The time-series data is maintained in each District's corporate database and represents

discrete points (or 2k by 2k cells/pixels) with rainfall amounts provided at 15-minute intervals. The NEXRAD points or pixels are evenly distributed across the three Districts. Use of a single vendor for processing NEXRAD data provides an opportunity to eliminate discontinuities at District boundaries.

SJRWMD and SWFWMD each provided overlapping data sets evenly distributed at the 2 square kilometer pixels which cover the ECFTX model domain. The daily rainfall amounts, aggregated from 15-minute data, provide a continuous dataset, spatially and temporally for the period of record of January 1, 2003 thru December 31, 2014. SFWMD provided daily rainfall from 2003 thru 2014. SFWMD maintains continuous NEXRAD data extending back to mid-1995. For those overlapping areas where pixel data was available from multiple Districts, the priority for the rainfall data was assigned to the pixel information from the District where it was located.

A distinct list of pixels (non-overlapping) were selected to represent the entire ECFTX model domain, and the daily data sets for each pixel were filtered and combined into single datasets by year. These sets of data represent 2 km by 2 km cells, so an additional ArcGIS geoprocessing step was necessary to assign a NEXRAD Pixel ID to each 1,250 ft by 1,250 ft model cell. This was accomplished using the ECFTX row and column number via spatial intersection. A new daily series of files were generated for each year and were organized into columns representing 365 to 366 days, as well as rows representing ECFTX model cells (a total of 603 rows by 704 columns).

2.4.2 Adjustment to NEXRAD Rainfall

A statistical analysis comparing the daily rain gauge timeseries values with nearby NEXRAD rainfall data revealed that there was a seasonal bias in the NEXRAD daily data. The relative bias between the monthly and yearly recorded rain gauge and estimated NEXRAD rainfall totals was calculated as follows:

$$Relative\ bias\ = \frac{\sum NRDi - \sum RGi}{\sum RGi} \times 100$$

Where NRD_i and RG_i represent the mean rainfall estimated by NEXRAD and recorded by the rain gauge, respectively. RD is the mean rainfall difference, which can be calculated as:

$$RD = \overline{NRDi} - \overline{RGi}$$

The bias was determined to represent over-estimation of small rainfall accumulations (<= .1 in/day) and an under-estimation of more extreme events. (> 20 in/day). A method was developed and used to adjust the NEXRAD data to reduce this bias. The bias was mainly observed in SFWMD and SWFWMD and therefore, the corrections were applied only to SFWMD and SWFWMD data sets. No corrections were applied to the SJRWMD data set.

The correction involves identifying some multiplier for each daily NEXRAD data value, applied in a manner that neither significantly increases nor decreases the overall volume of water for each year. Alternatively, it maintains the same general daily spatial distribution of rainfall patterns. The correction should not significantly increase or decrease the annual total NEXRAD data either, given its notable similarity to - and correlation with - rain gauge annual totals.

Other studies and alternative work have been done to adjust NEXRAD data for other models. Methods used to eliminate the bias have included use of a single, non-linear equation, as well as multiple equations to adjust for the wet and dry seasons separately. The spatial extents of these models, however, were significantly smaller than they are in this case. The efforts surrounding the ECFTX model have required the development of specific, suitable equations to account for the model's extent.

Linear regression of yearly, monthly, and daily rain gauge and NEXRAD rainfall totals was performed to evaluate the overall relationship between the variables. Furthermore, the Kolmogorov-Smirnov statistical test for normality showed a marked positive skew of the daily values, indicating a considerable number of small values near or equal to zero; this observation is not surprising since it does not rain every day. Therefore, the relationship between NEXRAD data and individual rain gauges was evaluated using the Kendall's Tau (τ) rank-based correlation method (Helsel and Hirsch, 1992). Monthly correlation for each rain gauge and NEXRAD pixel pair was calculated using daily values ($n \geq 14$), and correlation coefficients were used to discern which rain gauges displayed a good relationship ($\tau \geq 0.75$) with the NEXRAD pixels. Rain gauges showing a poor relationship with the NEXRAD pixels were excluded from further analysis. Yearly and monthly rain gauge and NEXRAD totals were calculated. The bias between the rain gauge and NEXRAD was determined by the ratio between the two (Steiner et al., 1999; Goudenhoofdt and Delobbe, 2009; Smith and Rodriguez, 2017). The resulting value was used as the NEXRAD adjustment factor, calculated as follows:

$$AdjF\ (bias) = \sum \frac{RGi}{n_1} \Big/ \sum \frac{NRDi}{n_1}$$

Where AdjF is the multiplicative factor used to adjust the daily NEXRAD value, RG_i and NRD_i are the monthly rainfall recorded by the rain gauge and estimated by NEXRAD, respectively, during an equally match-paired number of days ($n \geq 14$).

The statistical analysis performed did not consistently show a very good correlation when comparing daily rain gauge data with NEXRAD data at nearby pixels. There were, however, strong correlations for most rain gauges when comparing these same data for annual totals, as well as for monthly totals.

The method developed uses monthly adjustment factors at each rain gauge with a suitable correlation and number of observations within the selected month. The adjustment factor is calculated as the ratio of the monthly sum of rain gauge values divided by the sum of the nearest monthly NEXRAD rain pixel values. Rain gauge stations with adjustment factors were filtered prior to creating NEXRAD bias corrections. Stations included must have adjustment factors between 0 and 10, Kendall Tau correlation values greater than 0.6, and 15 or more non-missing daily values per month.

To prevent overcorrection of NEXRAD daily values (and to include the highest number of adjustment factors), the adjustment factor was arbitrarily capped at no less than 0.7, and no greater than 1.3. Adjustments less than 0.7 were assigned the minimum factor of 0.7, while those greater than 1.3 were defaulted to a value of 1.3. Rain gauges with monthly adjustment factors equal to 0 were set to 1, providing no adjustment. Visual examination of the resulting bias showed several rain gauges located less than 2 kilometers from each other. This can produce inconsistencies in the bias arising from high and low values in spatially close stations. Therefore, the resulting monthly bias value at each rain gauge station was normalized using a complete hierarchical cluster analysis (Müllner, 2013, Mächler, et al., 2018) in which bias points are the

result of the averaged bias of each rain gauge located within 2 kilometers of each other. The resulting monthly bias was used as the multiplicative adjustment factor to correct the daily NEXRAD pixel value using geostatistical processes.

Adjustment factors were interpolated across the entire NEXRAD grid using the automated autoKrige method described by Hiemstra et al. (2009). The autoKrige function tests different interpolation models (linear, spherical, exponential, Gaussian, and Matern [M. Stein's parameterization]) by estimating semi-variograms and selecting the best fit kriging model (Hiemstra et al., 2009). This process produced a monthly bias grid with adjustment factors at each NEXRAD pixel; these adjustment factors were applied to the uncorrected NEXRAD values to produce corrected NEXRAD values. Point values for the bias and the uncorrected and corrected NEXRAD were converted into a raster for visual evaluation. During this process, a few inconsistencies associated with the NEXRAD and rain gauge pairing were observed in the corrected NEXRAD raster. These inconsistencies resulted from mismatched NEXRAD and rain gauge daily values, these data were examined and removed from daily values. Subsequently, the entire process described above was repeated and a new set of raster plots created. The difference or change in rain was calculated by subtracting the corrected from the uncorrected NEXRAD, and the results were displayed in a separate raster. The model cell locations were used to extract values from the corrected NEXRAD raster and exported as data for each model mesh cell. All statistical and spatial data analyses were performed using R programming language (version 3.5.1; R Development Core Team, 2018).

The results obtained by applying adjustment factors for each temporal aggregation (for bias correction and recalculation of monthly and annual sums near observed locations) were reviewed to ensure that the correction neither created nor eliminated significant amounts of rain. Monthly totals provided significantly better correction than just wet season/dry season alone. Analysis further revealed that there was no substantial benefit to using bi-weekly or weekly data, given that the observed and NEXRAD values didn't show suitable correlation at those levels of discretization.

Figure 11 shows the locations of rainfall stations, measured rainfall data, unadjusted NEXRAD rainfall data and adjusted NEXRAD rainfall data for 2004. While Figure 11 only shows the comparison of the gauging stations within the CFWI planning area; corrections were also applied to all the gauging stations within SFWMD and SWFWMD areas. As a result of this correction, the differences were reduced between the annual gauged (measured) and NEXRAD data. Figure 12 and Figure 13 show the spatial distribution of adjusted NEXRAD data for 2004 (wet year) and 2012 (dry year) respectively.

2.5 Evapotranspiration

Evapotranspiration (ET) is accountable for the largest loss within the entire water budget in central Florida. ET is equal to about half to three quarters of the annual average rainfall, though it can well exceed rainfall in both dry periods, as well as for large open-water body systems in the central Florida region. ET is a physical process and is the sum of evaporation from water bodies plus transpiration losses from plant systems to the atmosphere.

Plants meet their ET requirements from the unsaturated zone (UZ) or the saturated zone (SZ). The total potential ET for a specific vegetation type (PETc), often referred to as the crop consumptive use in agricultural applications, can thus be expressed as:

$$PETc = PETc,uz + PETc,sz$$

The amount of water a plant extracts from the UZ is dependent on the amount of moisture available, which is a function of rainfall and climate conditions. For the SZ, the amount of water available to the plant depends on the water table depth and the plant's ability to extract water from deeper zones. If the plant is unable to extract enough water from either the UZ or SZ, then the plant will experience a moisture deficit. This occurs in areas with deep water tables (e.g., ridges), cultivated areas where drainage is necessary, and landscaped areas with shallow root zones (e.g., annual flowers, some grasses). To maintain plant vigor, irrigation can be applied to supplement the moisture deficit. The amount of water necessary to meet the vegetation's PETc is often expressed as the Net Irrigation Requirement (NIR).

Thus, incorporating the practice of irrigation, the equation for actual ET that occurs is as follows:

$$ETc = ETc,uz + ETc,sz + NIR$$

PETc for a crop or vegetation can be estimated by multiplying a time series for daily Reference ET (RET) by a crop coefficient (Kc). RET represents the amount of ET that can be expected to occur for a representative short (grass) or tall (alfalfa) crop. Kc factors are specific for a crops or vegetation types. Some Kc factors also vary by month for perennial vegetation to reflect preferential growing seasons (e.g., cool vs. warm weather grasses); for annuals the Kc factors vary according to the plant's growth stages.

The source of the RET data is the USGS Statewide Evapotranspiration Information and Data web page: http://fl.water.usgs.gov/et/. Data sets are available by county or statewide and by year. Daily values provided are organized in tabular format:

Column	Column Definition
date	Date data representation
latitude	Latitude of Pixel value
longitude	Longitude of Pixel value
pixel	Pixel ID number
PET	Potential ET(mm/day) (Priestly-Taylor method)
RET	Reference ET(mm/day) (ASCE-ET method)
solar	Solar Radiation - Daily Insolation (MegaJoules/sq meter/day)
RHmax	Maximum Relative Humidity for day (%)
RHmin	Minimum Relative Humidity for day (%)
Tmax	Maximum Temperature for day (C)
Tmin	Minimum Temperature for day (C)
Wind	Wind Speed (meters/second)

Annual statewide data sets were selected (versus counties) to reduce the number of steps required to download all necessary data. Reference ET was selected from the available columns presented in the USGS data and was reformatted into the file structure previously described for the NEXRAD data. The same Pixel ID numbers were used – as assigned to the ECFTX model rows and columns. Reference ET data files were generated for each year, organized in columns representing 365-366 days, and in rows representing reference ET values for each ECFTX model cell (603 rows by 704 columns).

Spatial distribution of reference evapotranspiration data for 2004 (wet year) and 2012 (dry year) for the model domain are shown in Figure 14 and Figure 15, respectively.

2.6 Soil Infiltration Groups

Infiltration rates of soils in the ECFTX model domain vary widely, from high infiltration capacity (low runoff potential), to low infiltration (high runoff) capacity. The runoff-rainfall potential is dependent upon hydrologic soil groups as classified by the NRCS. Soils are classified into four Hydrologic Soil Groups (HSGs) with specific letter designations. "A", "B", "C", and "D" designations indicate high, moderate, low, and poor infiltration capacities, respectively (TR-55). Dual designations, such as "A/D", "B/D", or "C/D" are assigned in areas where a high-water table may limit infiltration. In these cases, the first letter applies to the drained condition, while the second applies to the undrained condition. The ET-Recharge program that generates recharge to the ECFTX model utilizes the NRCS Curve Number (CN) approach to separate infiltration from rainfall and irrigation. It does this using the soil group (HSG) information previously discussed.

Soils in the ECFTX model domain have predominantly high infiltration rates that may be further limited by a shallow water table condition, with 49 percent of the areas are classified as "A/D" (Figure 16). This category of soil is mainly found in plain physiographic regions. The next most prevalent soil group is class "A" (25 percent); these are well drained, high infiltration soils commonly observed in the ridge and upland physiographic provinces. The third most common soil group is class "C/D" (13 percent), and consists of moderately drained, somewhat low infiltration capacity soils found primarily in the south east corner of the model domain (Martin, St. Lucie, and Indian River counties). The remaining 13 percent of the model domain consists of class "B/D" (10 percent), "D" (2 percent), and "B" (1 percent) soil classifications.

CHAPTER 2 - FIGURES

ECFTX Model Domain - Topographic Map

Elevation Contours (NAV88)

— 50 feet
— 100 feet
— 150 feet
— 200 feet
— 250 feet

ECFTX Model Domain
CFWI Boundary
County Boundaries
Water Management District Boundaries
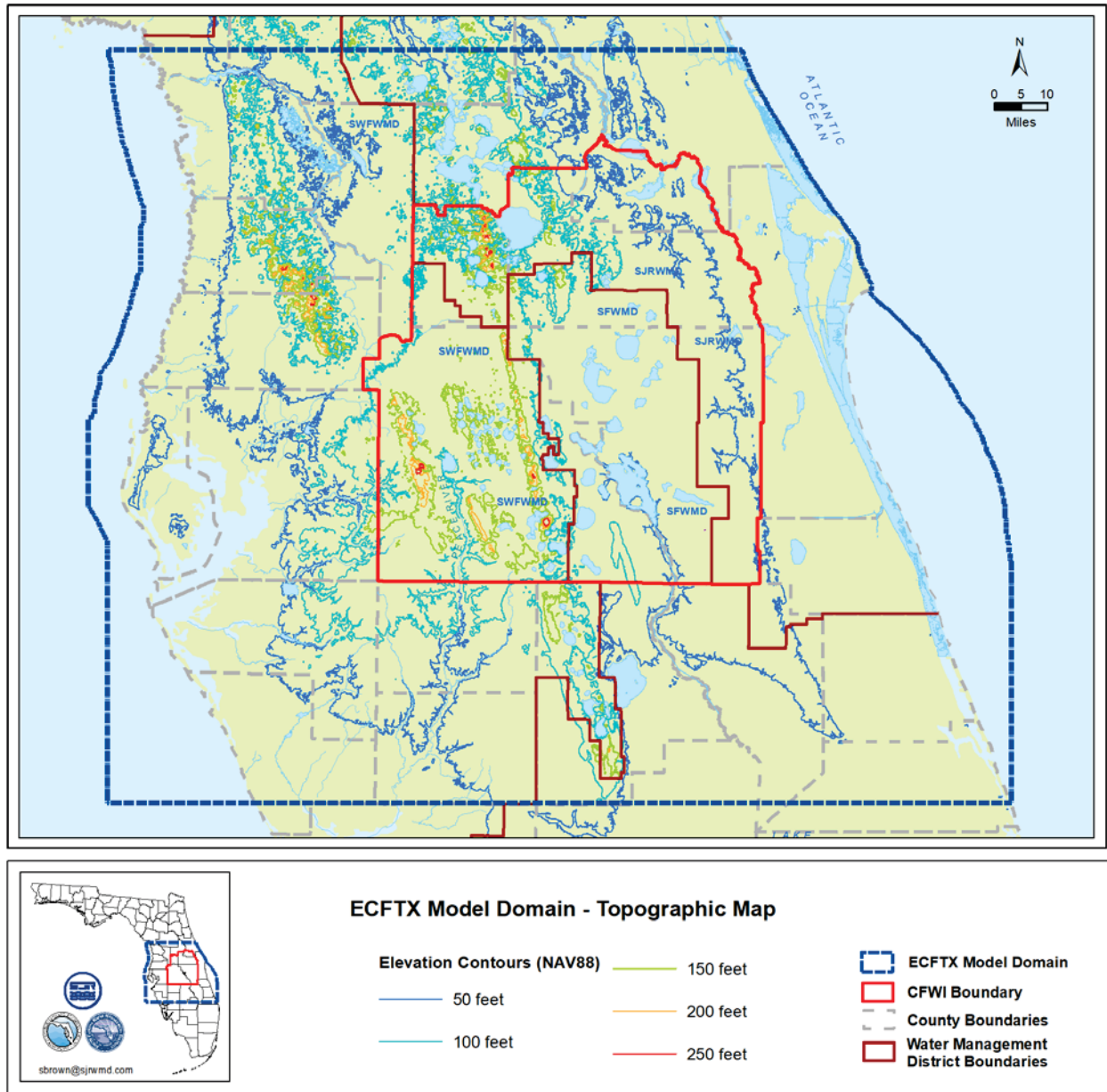
Figure 3. Land surface elevation across central Florida.
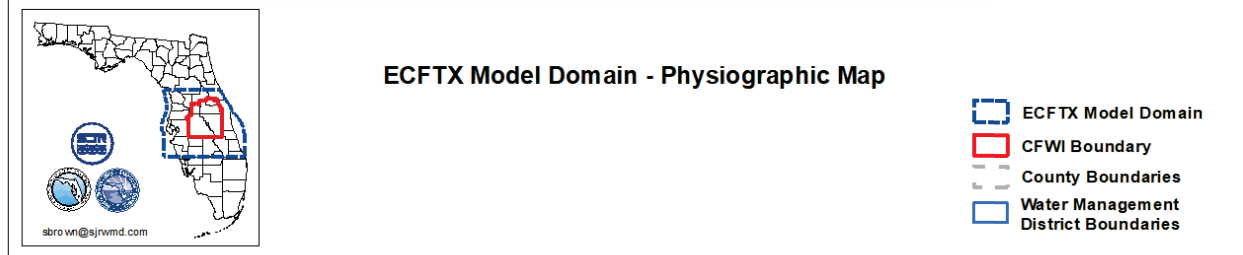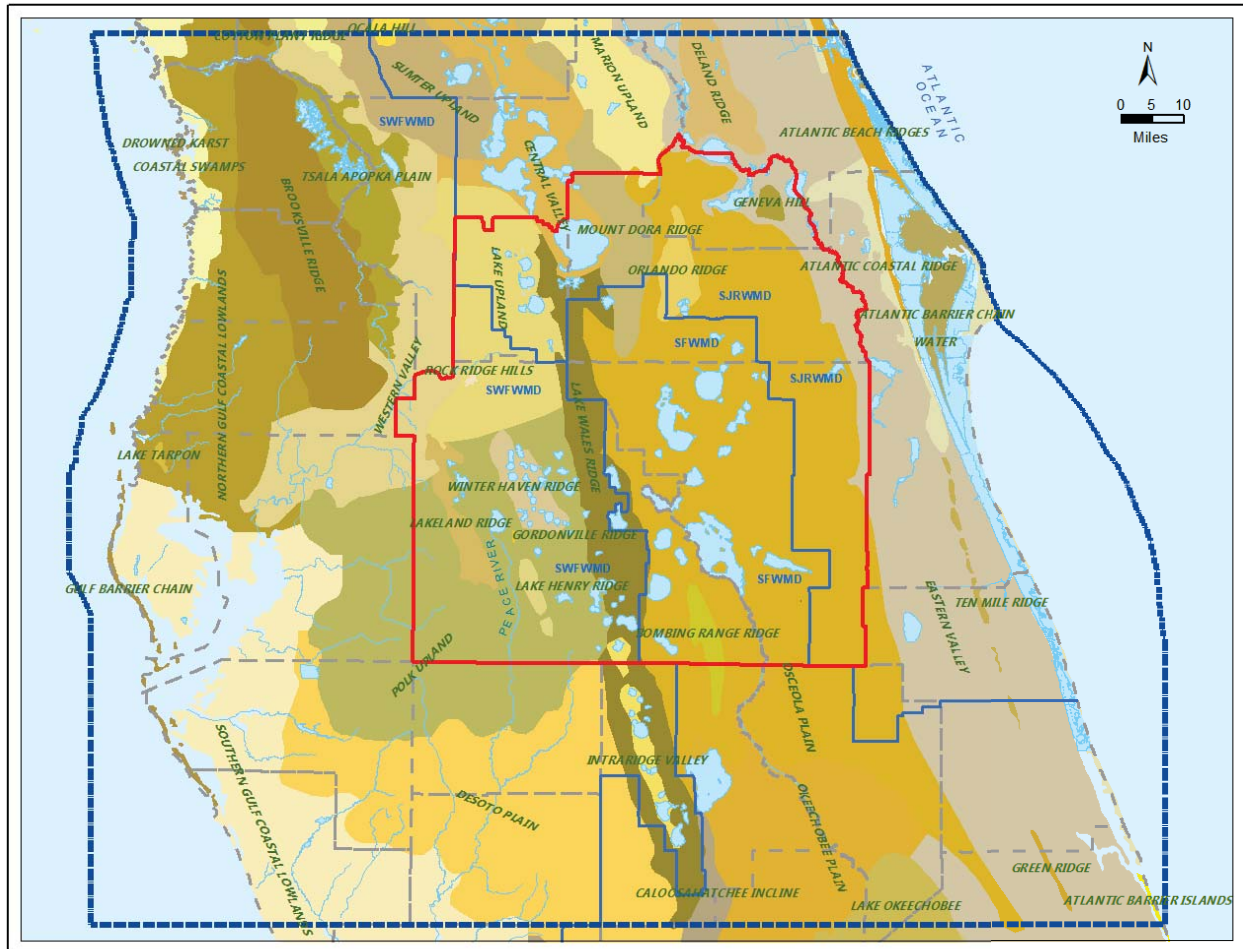
Figure 4. Physiographic regions located within central Florida (White, 1970).
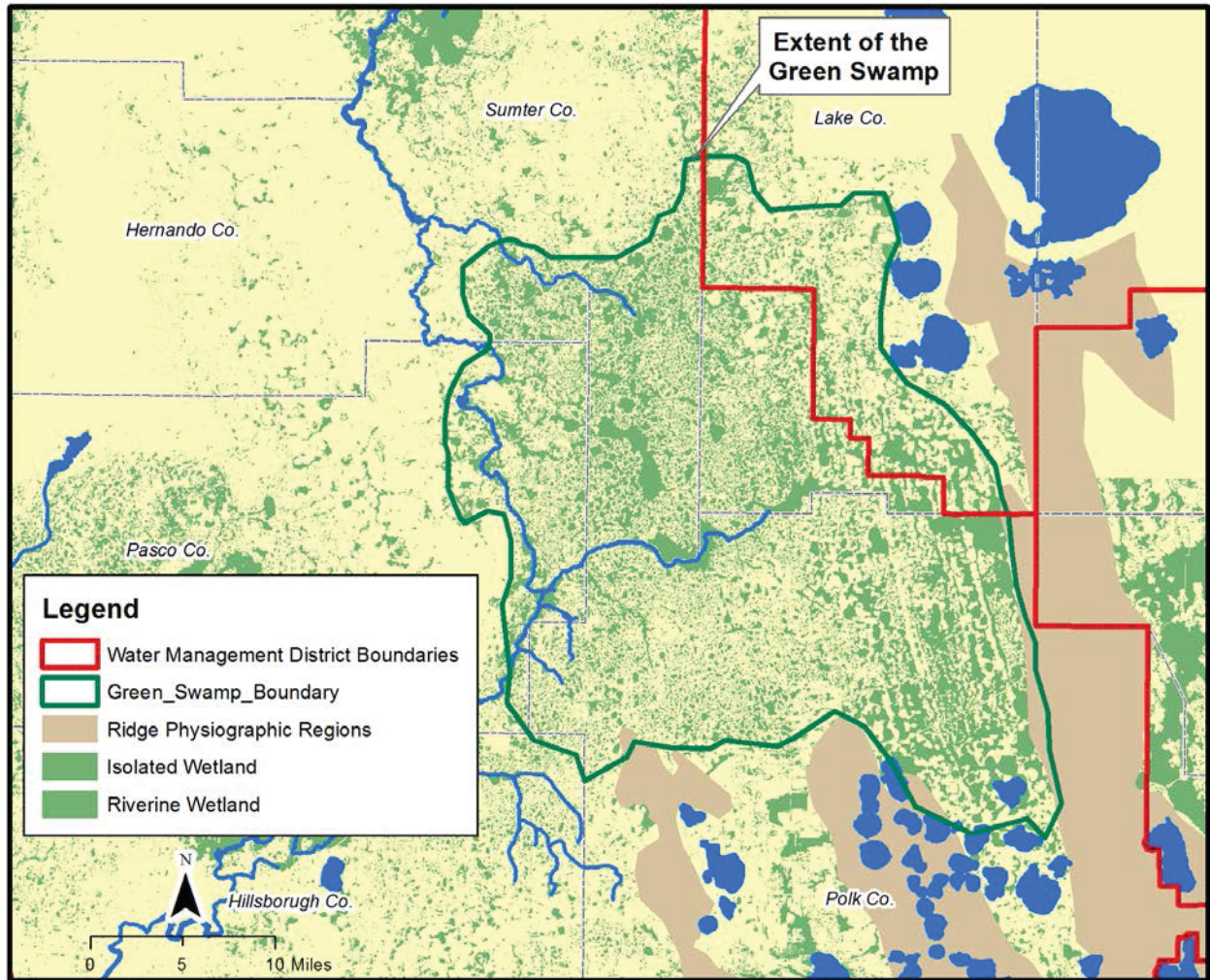
Figure 5. Location of the Green Swamp.
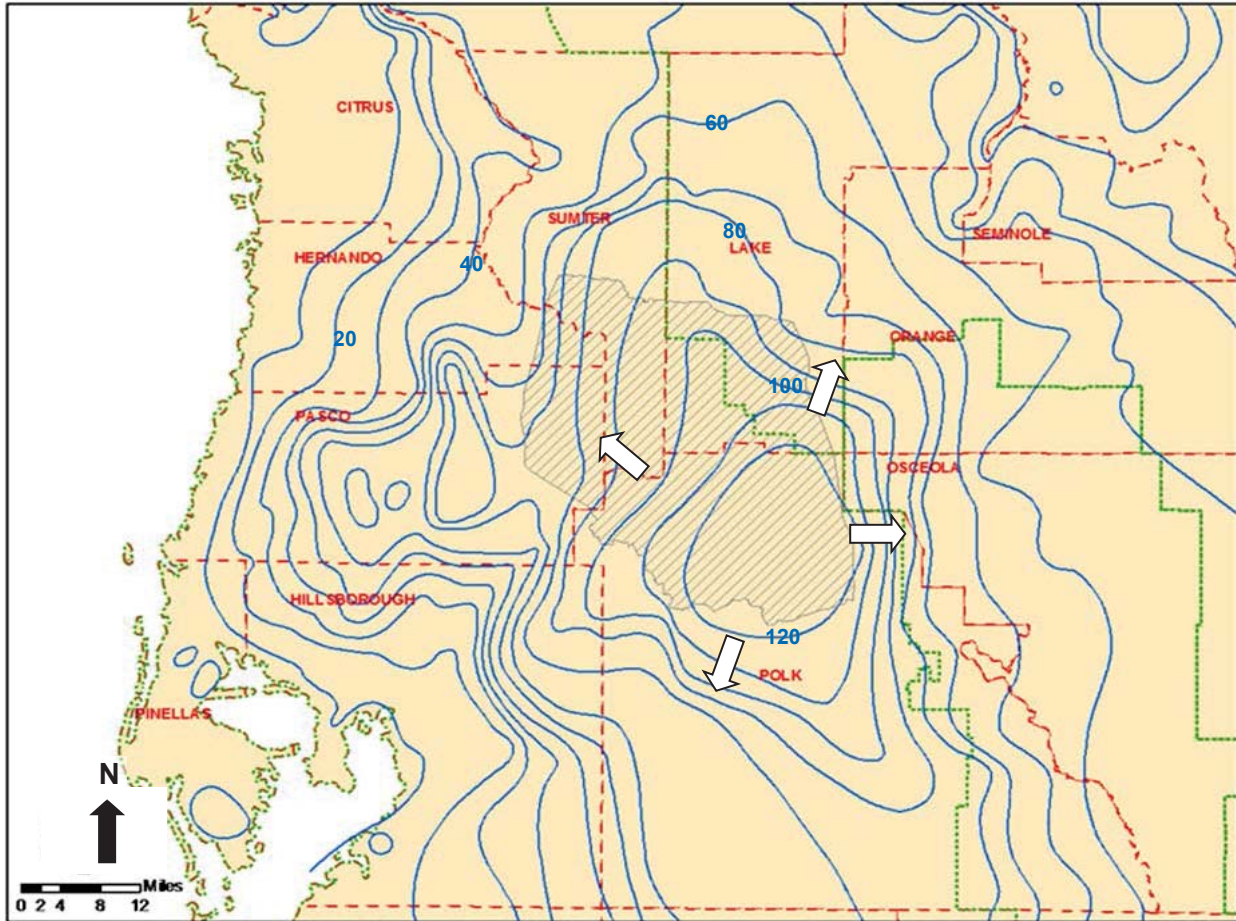
Figure 6. Groundwater flow direction and potentiometric surface of the Upper Floridan aquifer, September 2002. Hachured area the Green Swamp. Highest elevation (> 120 Ft NGVD) Is named the Polk City Potentiometric High.
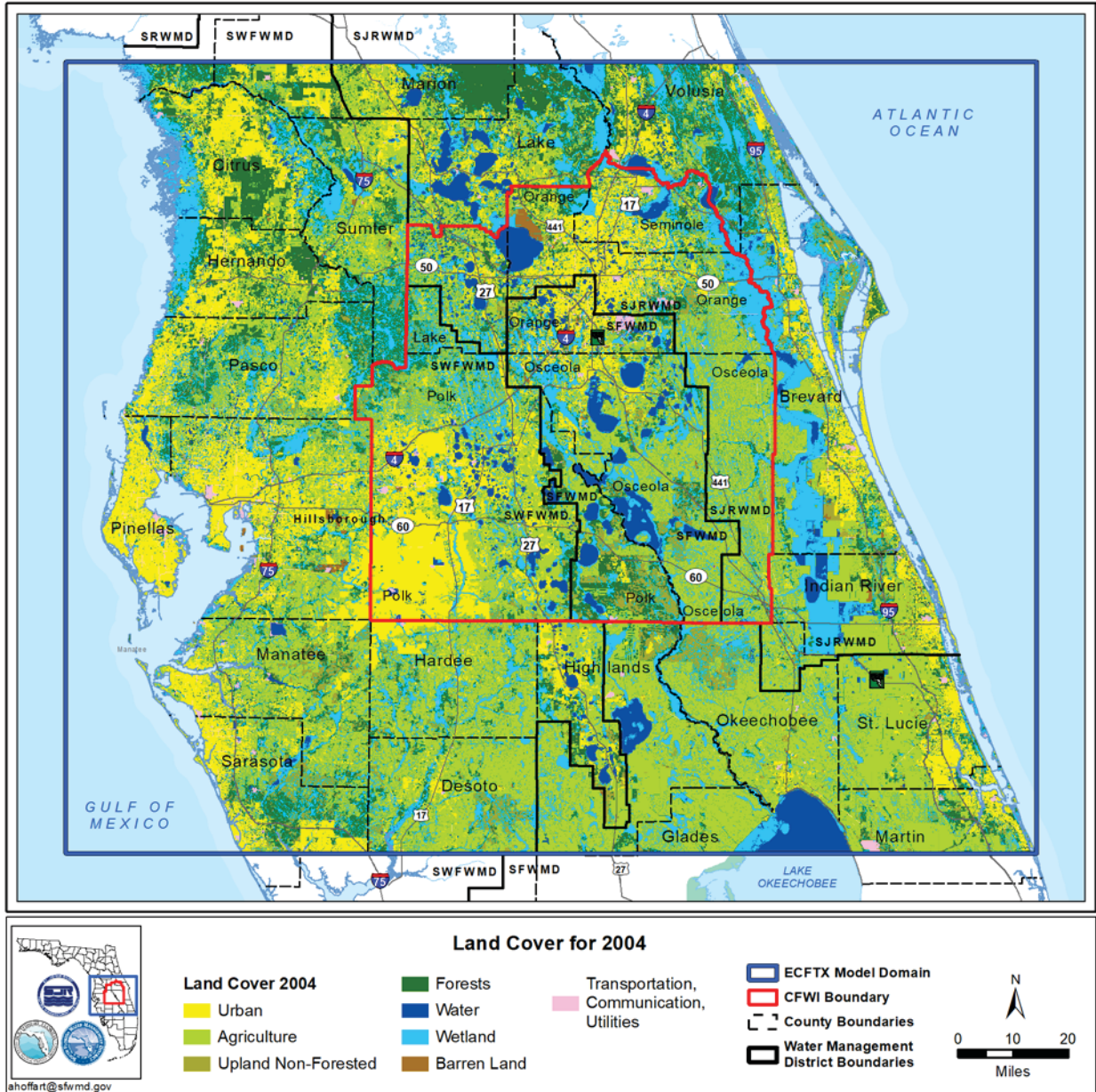
Figure 7. Generalized 2004 land use-cover (FLUCCS level 1) in the study area.
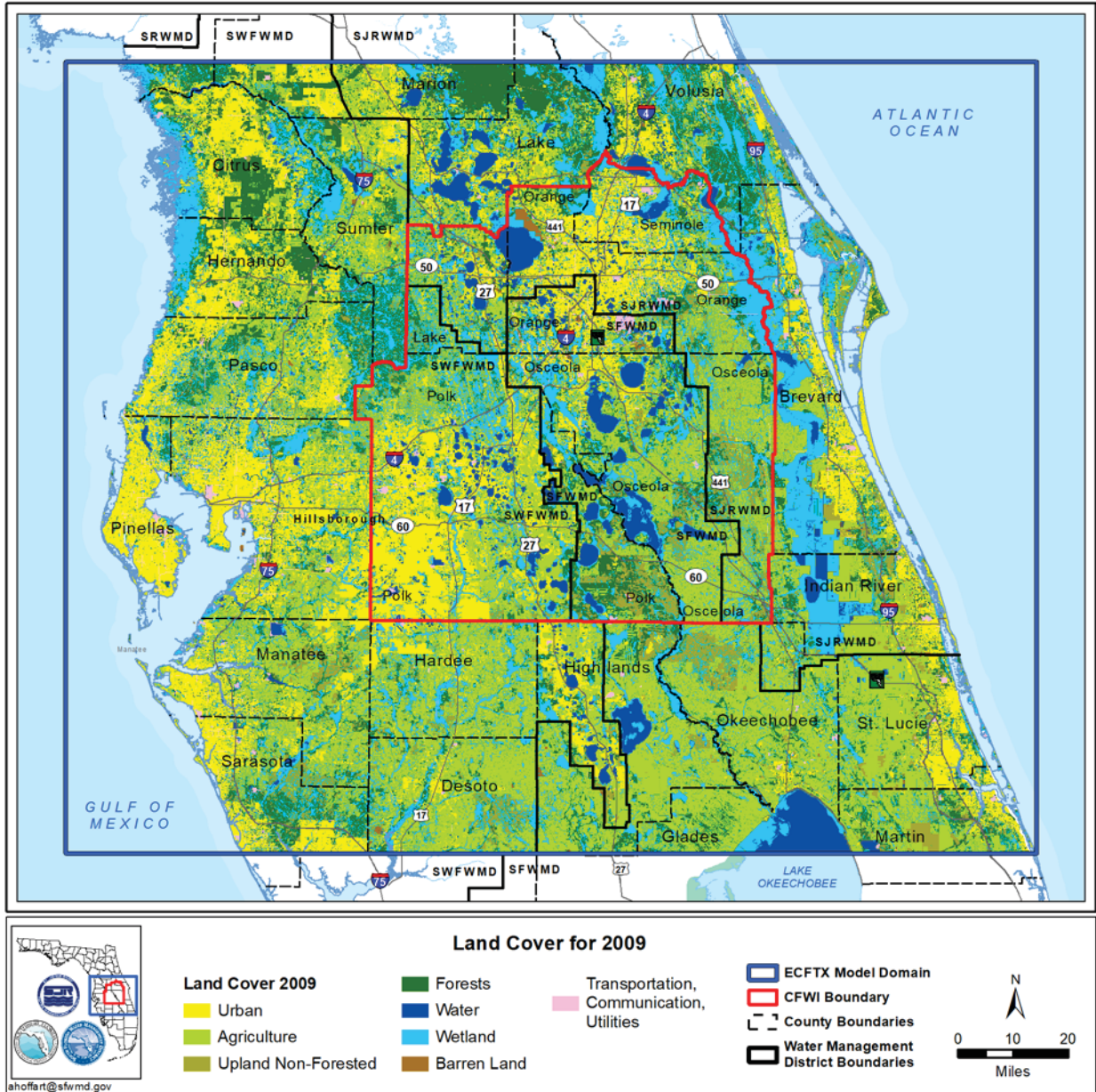
Figure 8. Generalized 2009 land use-cover (FLUCCS level 1) in the study area.
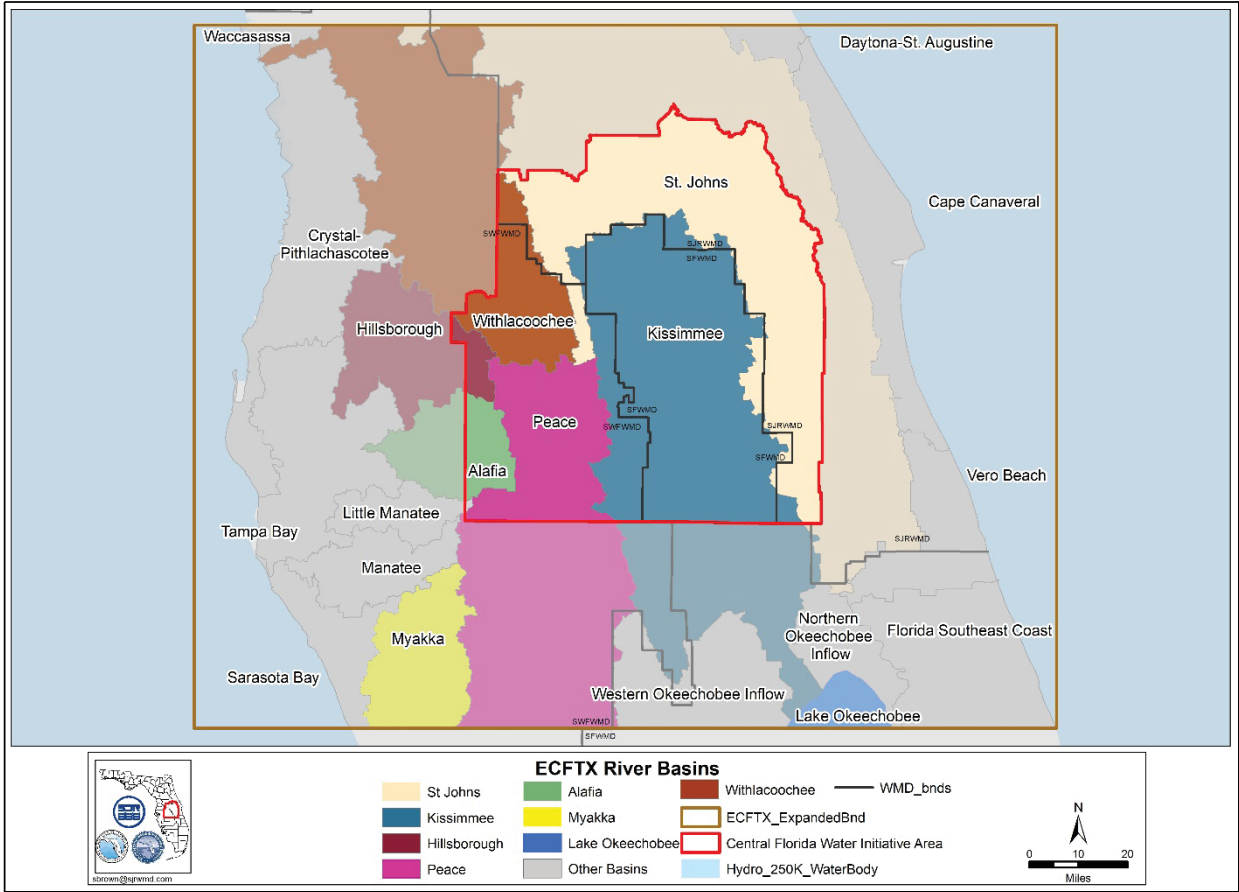
Figure 9. Major River Basins in the Central Florida Water Initiative (CFWI) Planning Area and the ECFTX Model Domain.
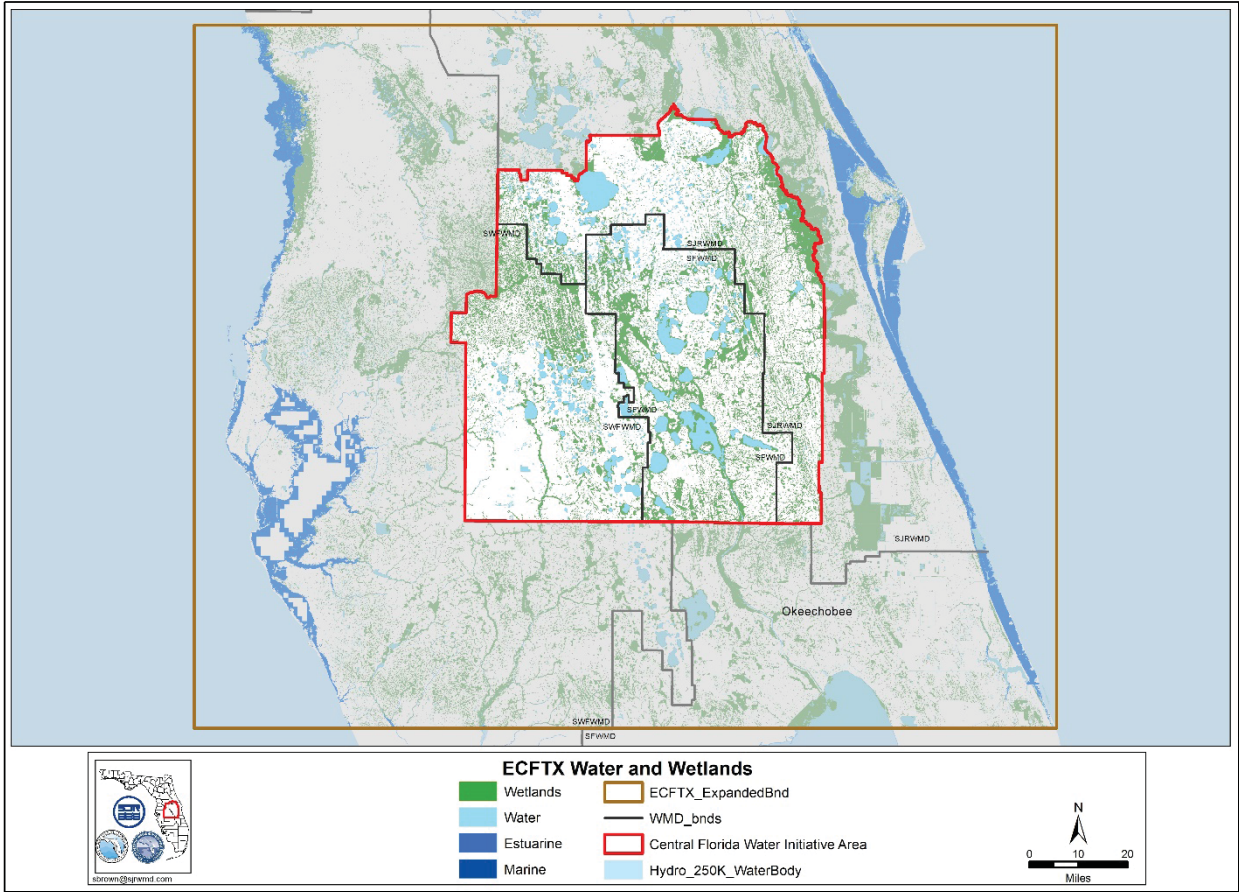
Figure 10. Wetlands and other bodies of water in the Central Florida Water Initiative (CFWI) Planning Area and the ECFTX Model Domain.
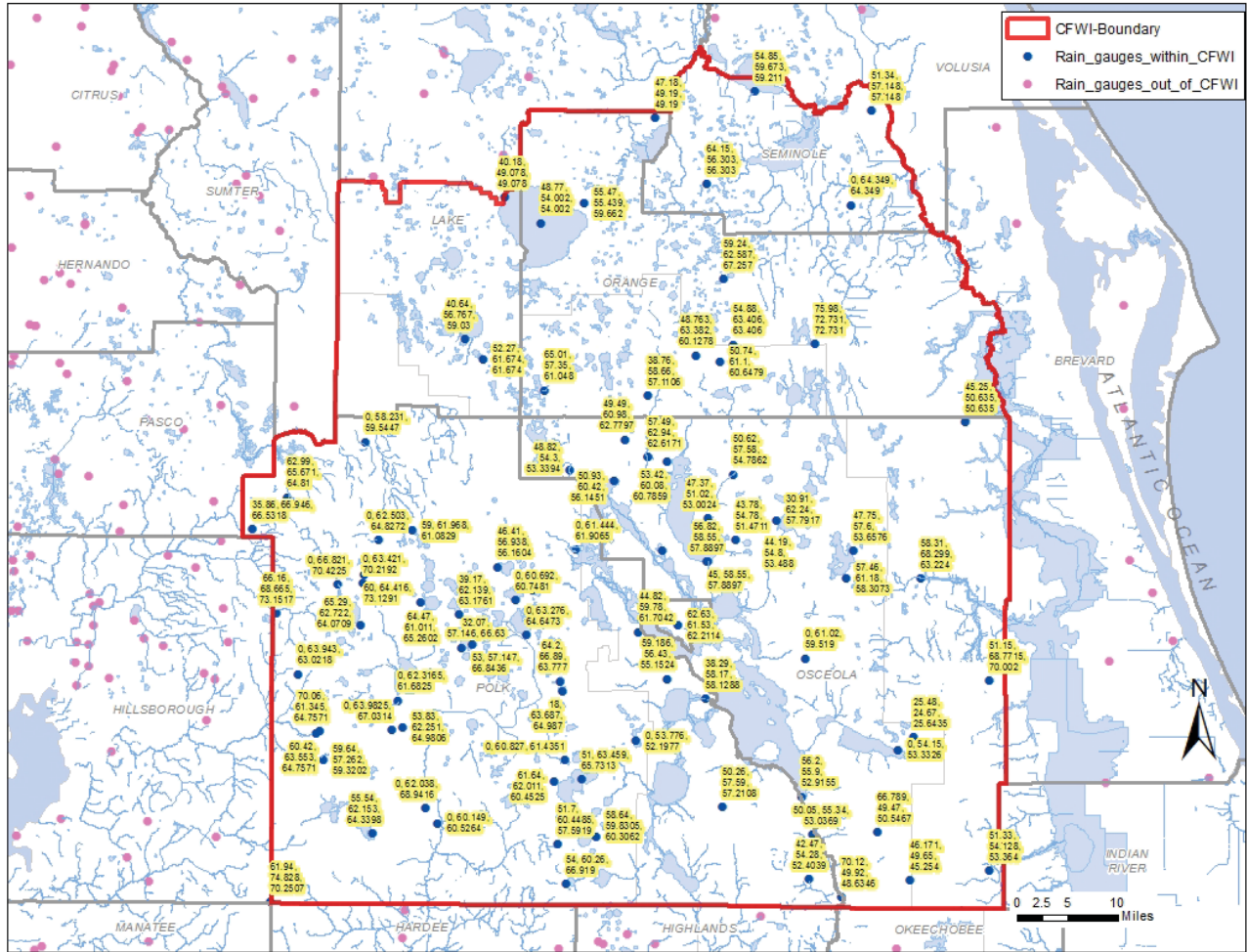
Figure 11. Locations of rainfall stations, measured 2004 rainfall at the stations, and unadjusted and adjusted rainfall from Next Generation Weather Radar (NEXRAD) within the CFWI planning area, top: gauged data, middle: uncorrected NEXRAD data, bottom: corrected N. All units in inches per year.
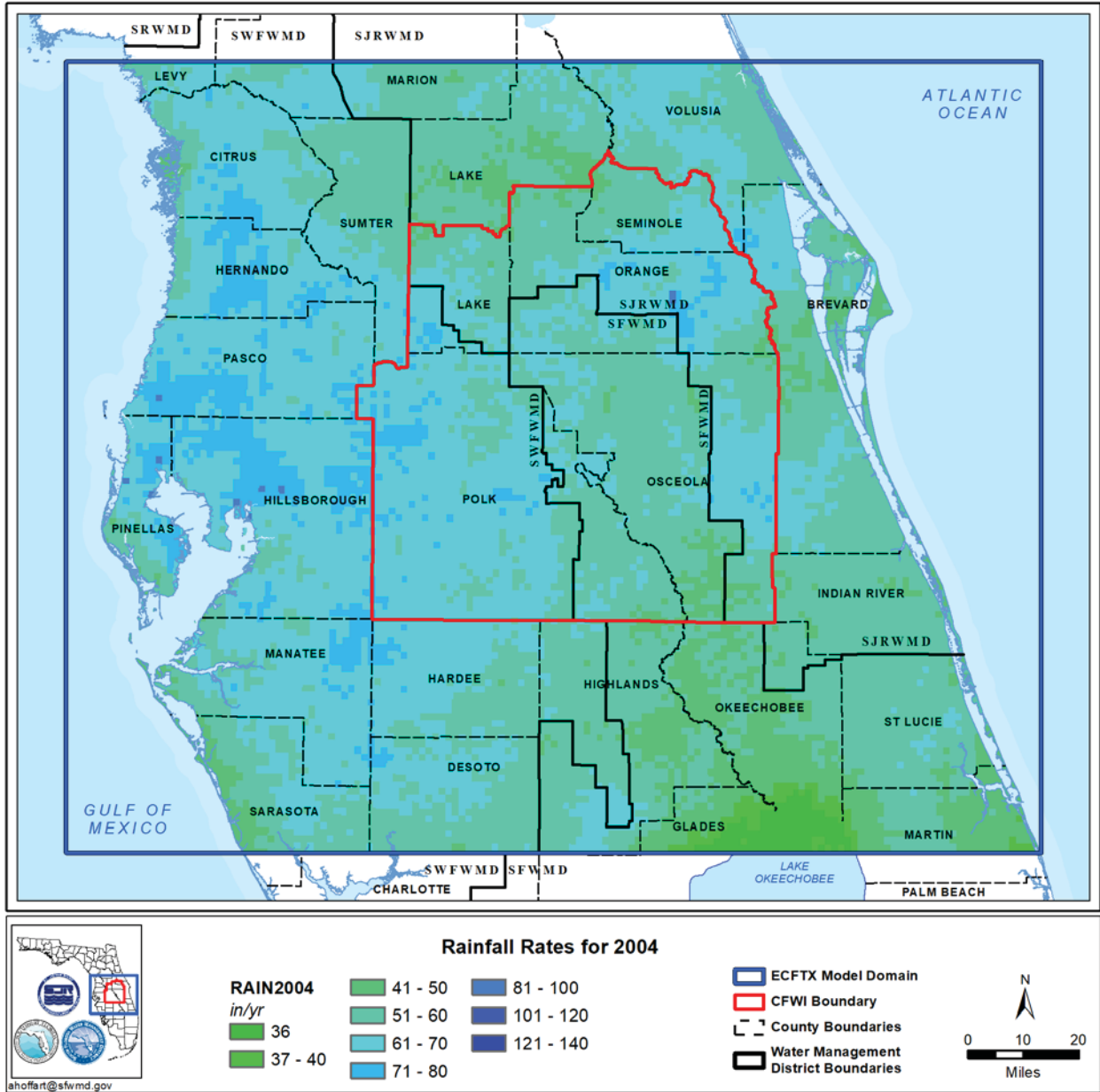
Figure 12. Spatial distribution of adjusted Next Generation Weather Radar rainfall data for 2004 (wet year).
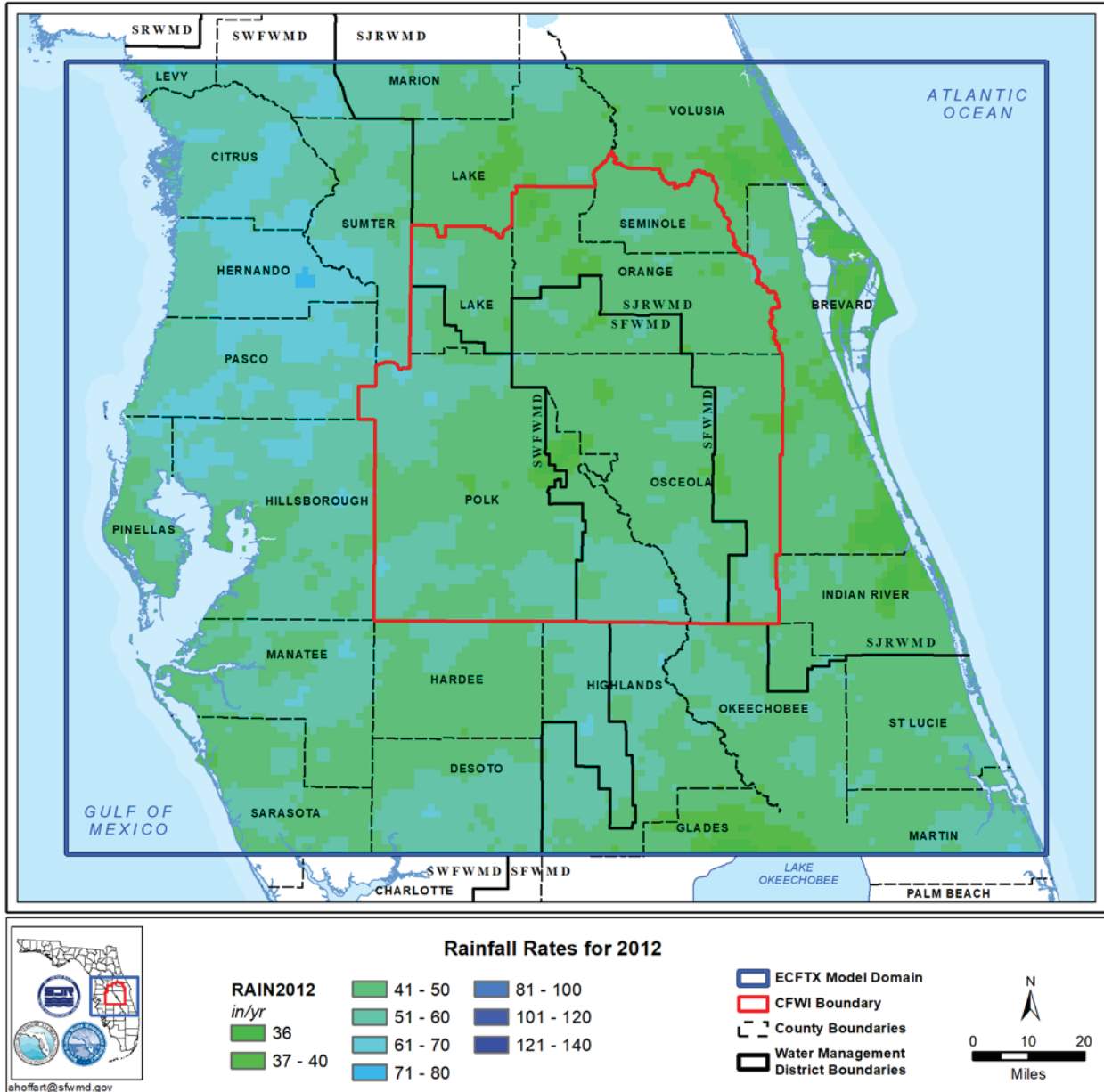
Figure 13. Spatial distribution of adjusted Next Generation Weather Radar rainfall data for 2012 (dry year).
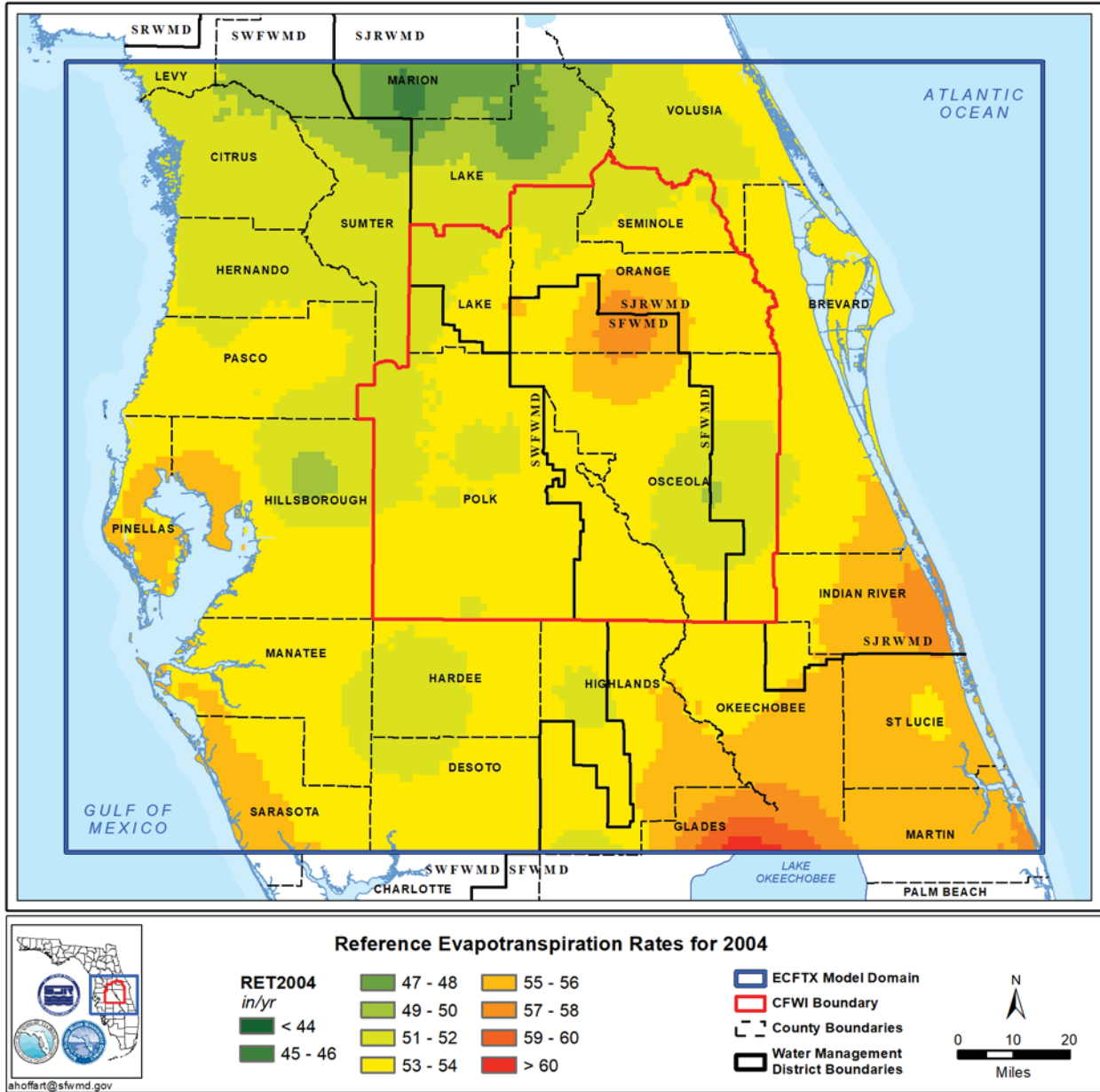
Figure 14. Spatial distribution of reference evapotranspiration from United States Geological Survey for 2004 (wet year).
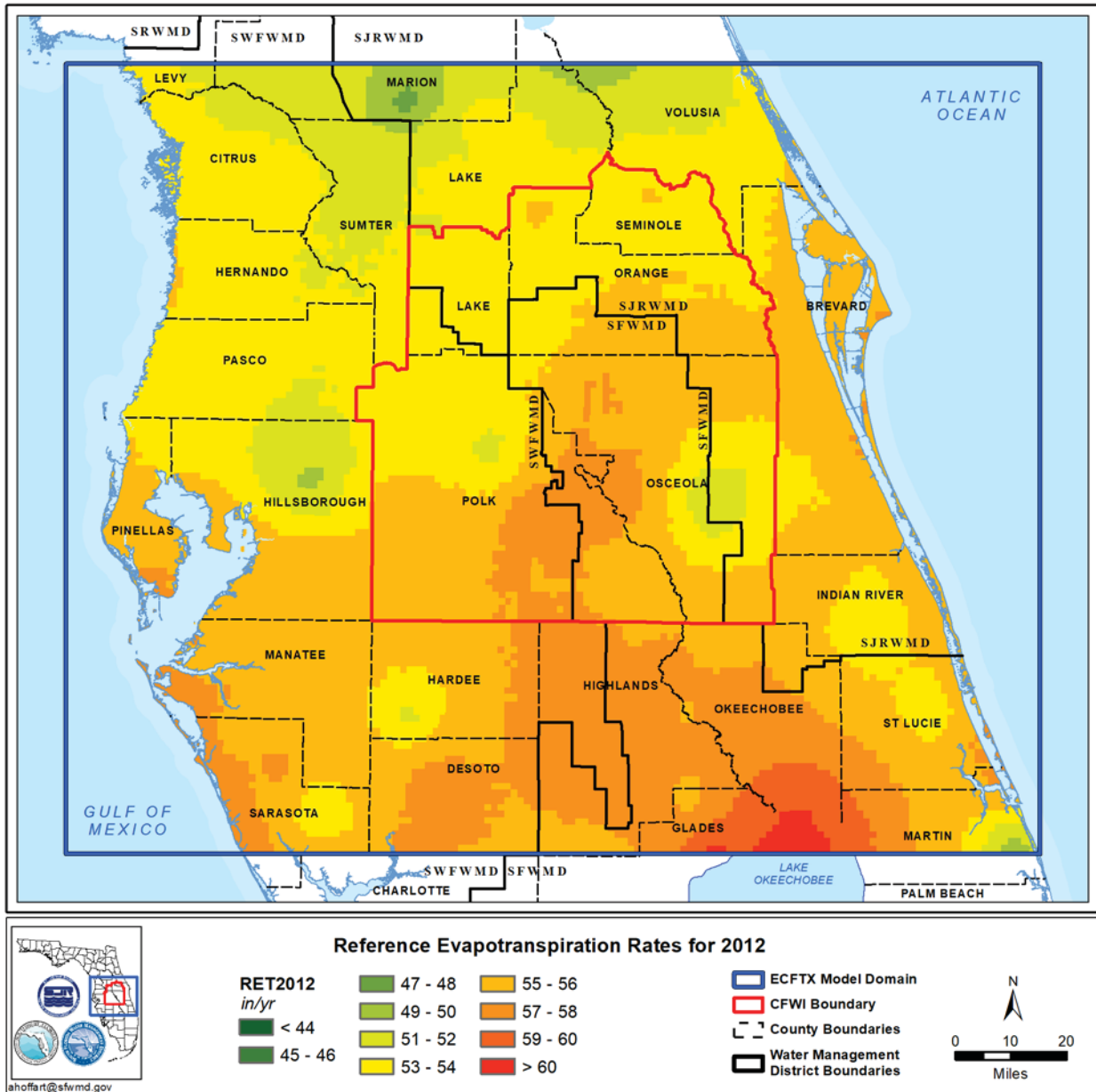
Figure 15. Spatial distribution of reference evapotranspiration from United States Geological Survey for 2012 (dry year).
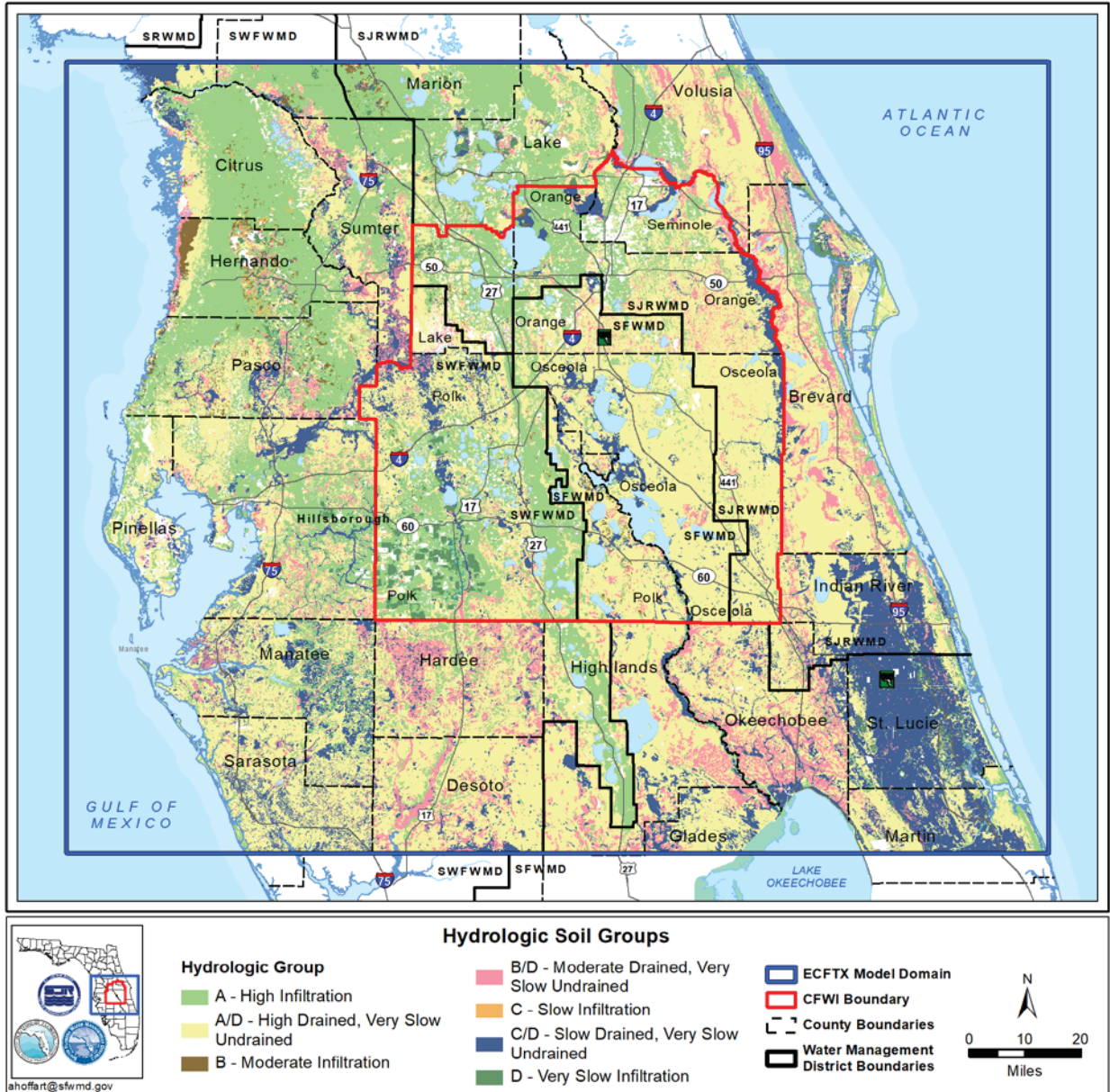
Figure 16. Spatial distribution of hydrologic soil groups as classified by the Natural Resource Conservation Service (NRCS).

CHAPTER 3 – PHYSICAL SETTING

3.1 Geologic Framework

The geological framework of central and south Florida has been described by several investigators including: Miller (1990), Meyer (1989), Reese and Richardson (2008), and Williams and Kuniansky (2016). Most of the following is summarized directly from Reese and Richardson (2008).

Florida is underlain by a thick sequence of carbonate and clastic sedimentary rocks ranging in age from Paleocene to recent. The geologic units that compose the FAS generally include the Cedar Keys Formation of Paleocene age, the Oldsmar Formation of early Eocene age, the Avon Park Formation of middle Eocene age, the Ocala Limestone of late Eocene age, the Suwannee Limestone of Oligocene age (when present), and the base of the Hawthorn Group, which ranges in age from late Oligocene to Miocene. A generalized geologic/hydrogeologic framework of central Florida is shown in Figure 17.

The Cedar Keys Formation consists of dolomite, dolomitic limestone, and anhydrite. The anhydrite exists as massive beds in the lower part of the formation and forms the base of the FAS. The Oldsmar Formation, which includes the Boulder Zone, consists primarily of interbedded micritic limestone and dolomite. The Avon Park Formation consists of micritic and fossiliferous limestone, dolomitic limestone, and dolostone or dense dolomite. The Ocala Limestone consists of micritic or chalky limestone, calcarenitic limestone, and coquinoid limestone. Miller (1986) maps the Ocala Formation as absent in the extreme southeastern area of Florida. The Hawthorn Group, which includes the Arcadia and Peace River formations, consists of varying lithologies including clay, limestone, mudstone, dolomite, dolosilt, shell, and quartz sand, existing as both an interbedded sequence and mixtures of all these materials. Geologic materials that overlie the Hawthorn Group include undifferentiated clastic sediments of the Pliocene, Pleistocene, and Holocene Epochs.

3.2 Hydrostratigraphic Framework

Four main hydrostratigraphic units describe the regional hydrogeologic framework of Florida. From the uppermost to the lowermost units, there are: (1) the surficial aquifer (SA), composed mainly of sand; (2) intermediate confining unit (ICU), composed mainly of fine-grained clastic sediments, or if this rock sequence has water supply potential, intermediate aquifer system (IAS) composed mainly of carbonate rocks that are layers within the ICU; (3) Floridan aquifer system (FAS), composed mainly of limestone and dolostone with some carbonate rock intervals containing evaporites; and (4) sub-Floridan confining unit (SFCU), composed mainly of Paleocene Series evaporite beds (Hickey and Wilson, 1982). The concept of a "hydrogeologic system" was used by SEGS (1986) as a means of recognizing that each of the essential units could be further subdivided depending upon the purpose of an investigation. Miller (1986) subdivided the Floridan aquifer system (FAS) into: an Upper Floridan aquifer (UFA), a series of middle confining units (MCUs) – each varying in lateral extent (and one containing evaporites), and a Lower Floridan aquifer (LFA).

3.3 Surficial Aquifer

The surficial aquifer (SA) consists of unconsolidated sediments, predominantly quartz sand with varying amounts of silt, clay, and shell deposits. It is unconfined and mostly produces small quantities of fair-to-good quality water with total dissolved solids (TDS) content typically less than 500 milligrams per liter (mg/l). In the northwest part of the study area, where clay of the intermediate confining unit is thin, discontinuous, and breeched by numerous karst features, the SA is largely absent, and the surface sands are either unsaturated or in direct hydraulic connection with the underlying limestone. In all other areas of the domain, a relatively competent basal clay unit of varying thickness exists and forms a perennial shallow-sand surficial aquifer distinct from the underlying UFA.

Thickness of the surficial sands is generally less than 50 feet over much of the study area, except along ridge areas. In the Central Highlands Region, thickness along the Lake Wales Ridge can range from 200 to 300 feet, resulting in a thick permeable SA. In this region, withdrawals from the aquifer from large diameter wells can often exceed 500 gallons per minute. In 2006, existing water use permitted (WUP) withdrawals from the SA consisted of approximately 12.3 million gallons per day (mgd) in the Lake Wales region of the SWFWMD. Nearly 83 percent of this total occurred in Highlands County. Another 13 percent of the total withdrawals occurred in Polk County. Elsewhere, the thickness of surficial sand is much less and wells utilizing this aquifer are mostly limited to small diameter household irrigation wells.

Except for the northwest part of the domain and along ridges, the depth-to-the-water table is mostly shallow. Typical water table depth ranges from near land surface to as much as ten feet (Figure 18). Along the ridge areas, however, the depth to the water table is deep - generally ranging from greater than 10 feet to more than 50 feet. Shallow water table conditions are generally concomitant with thick clay confinement underlying the surface sands. In the Green Swamp, however, the clays are thin and carbonate rocks underlying the sands are relatively low in permeability. Shallow water table areas are prevalent in most of the Tampa Bay region, southern half of the domain (excluding ridge areas), areas adjacent to lakes, wetlands, and rivers, and along coastal environments. Deep water table conditions exist where the UFA is largely unconfined in the northwest portion of the domain, along the Central Highlands ridges, and those ridges in the northeast part of the domain near Orlando.

3.4 Intermediate Aquifer System/Intermediate Confining Unit

The intermediate aquifer system/intermediate confining unit (IAS/ICU) mostly consists of Hawthorn Group clay. In the southwest part of Florida, there are thin permeable zones within the Hawthorn Group clays that form local aquifers (Figure 19). These thin permeable zones are named the intermediate aquifer system (IAS) and they lie between the SA and UFA. Unlike the FAS, the IAS is comprised of thin, often discontinuous layers of limestone, gravel, shell, and sand that make up individual permeable units that are separated by thick clays. In descending order, these units are Permeable Zone (PZ) 1, PZ 2 and PZ 3 (Basso and Hood, 2005). While these aquifers within the Hawthorn Group have been developed for local household use and small water users in the southwestern portion of Florida, the Hawthorn Group clays generally act as a regionally extensive confining unit over the underlying UFA. In 2006, total groundwater withdrawn from the IAS was 26.2 mgd from DeSoto, Hardee, Highlands, Hillsborough, Manatee, Polk, and Sarasota counties within the domain. Over 75 percent of that total occurred in just four counties: DeSoto, Hardee, Manatee, and Sarasota.

This confining zone, hereafter referred to as the intermediate confining unit (ICU), varies in thickness from essentially absent (or a few feet thick) in the northwestern portion of the study area, to over 700 feet in the southeastern portions of the study area. The thickness of the ICU generally increases from north to south across the central Florida region (Figure 20). The USGS, in their most recent Regional Aquifer System Study (RASA) of the FAS (now termed Floridan Aquifer System Groundwater Availability Study; https://fl.water.usgs.gov/floridan/), identified regions of the UFA distinguished as unconfined, thinly confined, or well-confined (Figure 21). Where the ICU is thin and discontinuous in the northwest quarter of the domain, the UFA is largely unconfined. Where the ICU is more competent but still thin and mostly leaky, is (1) in the area around Tampa Bay, (2) in the Green Swamp, and (3) within the northeast corner of the domain in the Orlando region. In the south half of the domain, from about Interstate 4 southward, the ICU thickens considerably, and the UFA is generally well-confined. The exception is along the Lake Wales Ridge area of the Central Highlands Region, where relict and active karst activity locally increases the hydraulic connection between the SA and UFA. This results in a semi-confined UFA in this area of the domain.

Vertical hydraulic head difference from nested monitor well pairs in the SA and UFA is often used as a qualitative guide of relative confinement of the UFA by the ICU (Figure 22). In areas of less than a foot of difference, the UFA is mostly unconfined. Where vertical head difference is more than one but less than 20 ft, the UFA is semi-confined. Where the vertical head difference is greater than 20 ft, the UFA is typically well-confined (Basso, 2011). These qualitative criteria generally hold true except in transition areas between downward and upward head potentials in the extreme southern part of the domain, Kissimmee River basin, and coastal regions of the UFA where there is an upward vertical head gradient from the UFA. These areas are all well-confined based on the thickness of the ICU, which is several hundred feet thick. Other qualitative factors used in determining the relative degree of confinement of the ICU include sinkhole density and the degree of natural surface water drainage pattern (Figure 23 and 24). Highly dendritic networks of surface water drainage imply a tight ICU, as well as areas with little to no sinkhole development. High densities of reported sinkholes and a lack of surface water drainage imply little to no confinement with respect to the hydraulic properties of the ICU. Most of the reported sinkhole locations are where the UFA is either unconfined or semi-confined. The highest density of natural surface water drainage exists where the UFA is well-confined, generally within the southern half of the study area outside of ridges.

3.5 Floridan Aquifer System

The FAS is comprised of three major divisions: the Upper Floridan aquifer (UFA), various Middle confining units (MCUs), and the Lower Floridan aquifer (LFA) (Miller 1986). Reese and Richardson (2008) refined the description of these units to provide a more consistent hydrogeologic framework for groundwater model development. The results of that work were generally adhered to in the original ECFT model (2006). The 2012 update to the model (Sepulveda et al, 2012) updated the hydrostratigraphic surfaces, and adopted a revised hydrostratigraphic nomenclature for the FAS. In the ECFTX model, the LFA has been further subdivided to accommodate the needs of CFWI plan development. Additionally, all the hydrostratigraphic surfaces have been supplemented with more recently published data compiled and contributed by each of the three WMDs. Figure 25 reflects the hydrogeologic conceptualization used for ECFTX model development. It should be noted the hydrostratigraphic nomenclature of the FAS has been a subject of significant debate and controversy in recent years. There is no formally accepted state-wide terminology for sub-divisions of the UFA and LFA, and preferred terminology may vary between WMDs. The nomenclature used in this report reflects

the most common usage in the CFWI region (e.g., OCAPlpz), or simply the physical position of the unit (e.g. UFA-upper, LFA-upper etc.). The nomenclature of the FAS is currently under review by the Florida Geological Survey.

3.5.1 Upper Floridan Aquifer

The UFA generally occurs at the base of the Hawthorn Group, though it may include permeable units within the lower Hawthorn Group. It includes the Suwanee limestone (where present), the Ocala Limestone, and portions of the Avon Park Formation. It generally consists of several thin, highly permeable water bearing zones interbedded with thicker zones of lower permeability. Three regionally mappable units were used to represent the vertical heterogeneity of the UFA, the UFA-upper, OCAPlpz and APhpz.

The UFA-upper is the uppermost permeable zone of the FAS. It is predominantly limestone characterized by intergranular, vuggy or moldic porosity, and well-developed secondary porosity (Davis & Boniol, 2011). It is highly productive in the karst-dominated unconfined portion of the UFA in the northwestern portion of the study area, but that productivity declines to the south. Reported transmissivity of the UFA-upper ranges from less than 10,000 to over 1,000,000 feet^2/day within the study area. The elevation of the top of the UFA-upper in the study area varies from more than 100 feet above sea level within the Green Swamp to more than 800 feet below it in the extreme southeastern part of the study area. The thickness of the UFA-upper varies from less than 100 feet in central Florida to more than 700 feet in some areas of southern Florida. The bottom of the UFA-upper tends to be gradational in nature and its elevation is difficult to define precisely. The UFA-Upper is largely unconfined in the northwest portion of the study area. In the Tampa Bay, Green Swamp, Central Ridge and Orlando regions, it is semi-confined. Throughout the remainder of the domain, the UFA-Upper is observably more well-confined.

The Ocala-Avon Park low-permeability zone (OCAPlpz) is distinguished from the UFA-Upper by a reduction in the secondary permeability that provides most of the unit's productive capacity. There is exception to this in the northwest quarter of the study area, where it represents the uppermost unit of the UFA, and is karst-dominated. This unit is equivalent to the MCU 1 unit of Reese and Richardson (2008), but the OCAPlpz terminology is preferred in the study area, as it prevents confusion with the MCU I unit of Miller (1986). It also recognizes that, though it is generally semi-confining, minor permeable zones can be found within this unit. In SWFWMD it is of persistently lower permeability than the rest of the UFA, but not considered confining. It is significantly thicker and more confining to the south and east where it may contain portions of Miller's MCU I rock. As stated above, the boundary between the UF-upper and OCAPlpz is gradational and difficult to define precisely; therefore, the altitude of the top of the OCAPlpz shows a significant degree of variability. The thickness of the OCAPlpz varies from less than 50 feet in the northwest, to greater than 800 feet in the south and southwest portions of the model area.

The Avon Park high permeability zone (APhpz) is composed primarily of massive dolostone with inter-bedded limestone and dolomitic limestone. It is a primary source of supply to many public and agricultural wells in the CFWI region. Productivity in this unit is primarily associated with fracturing, but karstic, intergranular and inter-crystalline permeability may exist as well (Reese and Richardson, 2008). It is present throughout the entire CFWI region, but thins, and may become absent along the southeast coast of Florida in the expanded model area. It is absent in the northwest portion of the model domain as well. The fractured nature of the APhpz produces considerable variability in both the thickness (0 feet in the north to more than 600 feet in the south) and elevation of the top (less than 200 to more than 1,700 feet below NAVD88) of the unit.

In SFWMD and SJRWMD, south of Orange County, the APhpz begins to drop deeper in the stratigraphic section. In those southern regions, the APhpz often consists of multiple discrete fracture zones separated by much less permeable rock. There are large portions of the ECFTX model area where supporting discrete head and water-quality are not available to assess the hydraulic continuity of these discrete zones. Consequently, some hydrogeologists tend to lump the fracture zones into a single unit, while others split it and view the deeper fractured zone as part of the LFA. Such deviations may account for some of the variability in the mapped thickness of this unit.

There is further debate over whether the contiguous fracture zone (prevalent in the north and west) is hydraulically connected to the thinner, bifurcated fracture zones that are more predominant in the south-central and southeast portions of the expanded model area. There are often large distances between control points in this region, making continuity difficult to establish. This is an area of uncertainty in the hydrogeology of the region that can only be addressed with additional drilling and testing. Transmissivity is variable, ranging from less than 100,000 to 1,600,000 feet^2/day, in central Florida. The highest permeability regions, particularly in the southern part of the model area, are associated with more mineralized groundwater. Relatively lower permeabilities observed along the central ridge provinces are typically attributed to sand in-filling of the fractured dolostone.

3.5.2 Middle Confining Units

The Middle confining unit divides the upper and lower Floridan aquifers. Miller (1986) defined the MCU and subdivided it into eight regional units designated by roman numerals I - VIII. Two of these units (MCU_I and MCU_II) comprise the MCU for the ECFTX model region. MCU_I (the shallower unit) is absent from the western half of the study area, and MCU_II is absent in the eastern half (Figure 26). Along the western reaches of the Kissimmee River valley and Lake Wales Ridge, these two units overlap each other, greatly increasing the thickness of the MCU in that region. Though not discretely mapped for the development of the ECFTX model, permeable zones are known to be present between MCU_I and MCU_II in parts of the overlap area. MCU_I, which ranges in lithology from dolostone to micritic limestone, is the leakier of the two units. The lithologic composition of the MCU_II unit is more distinct. It is composed of hard crystalline dolostone to dolomitic limestone and characterized by the occurrence of evaporites as beds or pore in-filling. These attributes are what greatly reduce the permeability of MCU_II. The elevation of the top of the MCU ranges from less than 200 to more than 1,700 feet below NAVD88, with a sharp drop in this elevation occurring where MCU_I pinches out. Mean hydraulic head difference between nested monitor wells from the UFA and LFA is shown in Figure 27. Hydraulic head difference is generally much smaller across MCU I versus MCU II which is reflective of its leakier nature.

3.5.3 Lower Floridan Aquifer

The Lower Floridan aquifer (LFA) consists of a sequence of permeable zones separated by lower permeability units. One or two of these permeable zones, such as the Boulder zone of south and east-central Florida, are regionally mapped units. In most cases, however, the availability and distribution of deep well data is not enough to establish the continuity of permeable zones between wells. The top of the LFA is located near the base of the Avon Park Formation. It occurs at variable reported elevations ranging from less than 500 to greater than 2,300 feet below sea level within the ECFTX model region. Its upper reaches are lithologically like MCU_I, but identifiable by the presence of secondary permeability; fractures or solution zones, which are lacking in MCU_I

(O'Reilly et al, 2002). The base of the LFA is the base of the FAS (i.e. top of the sub-Floridan confining unit). Miller (1986) generally associated this with the uppermost occurrence of persistent evaporite minerals near the top of the Paleocene Cedar Keys formation, occurring at elevations form 1800 to more than 4000 feet below sea-level in the ECFTX model domain. In the greater Orlando region, where the LFA has been extensively utilized for water supply, O'Reilly et al (2002) reported a loss of productivity was frequently observed considerably higher than the evaporite beds of the Cedar Keys Formation. The practical thickness of this unit, therefore, is considerably reduced. Williams and Kuniansky (2016) mapped the total thickness of the LFA, including intra-aquifer confining units, as ranging from 1000 to greater than 1900 feet within the study area. Discretizing this thickness into less hydraulically diverse subdivisions is one of the objectives of the model update.

The ECFTX model hydrostratigraphic team compiled a unified hydrostratigraphic database as the first task of its assignment to provide boundary surfaces for the expanded model area. The original datasets that each WMD contributed contained hydrostratigraphic picks (elevation of the unit) in the local preferred nomenclature. The majority of wells contained only picks for the top of the LFA. SJRWMD picks were restricted mainly to the uppermost permeable zone but did incorporate some lower unit picks based on limited hydrogeologic data. SFWMD picks referenced multiple observed flow zones within the LFA but did not provide a means of correlating these zones between wells. SWFWMD picks subdivided the LFA based on whether it was overlain by MCU_I or MCU_II but did not further subdivide the LFA below MCU_II. A method was needed to consolidate these disparate approaches and provide a practical sub-division of the LFA that would illustrate its heterogeneity more realistically than the single-layer approach.

For the ECFTX model, the LFA has been subdivided into upper (LFA-upper) and basal (LFA-basal) permeable zones. These divisions are roughly equivalent to the lower Avon Park permeable zone and Oldsmar permeable zone described by the USGS in their recently published update on the hydrogeologic framework of the FAS (Williams and Kuniansky, 2016). Although the surfaces from that report are not utilized here, in both cases the regionally mappable low permeability glauconitic marker unit (GLAUClpu) is used as the dividing line between the upper and lower permeable zones. The general approach: 1) Map elevation of the glauconitic gamma marker (GLA) within the expanded ECFT model region, 2) Identify this elevation at all of the wells in our hydrostratigraphic database, 3) Based on the GLA elevation, parse identified permeable zones within the LFA as either upper (above the GLA) or basal (Below the GLA).

The mapped thickness of LFA-upper ranged from zero to greater than 800 feet based on data from 73 wells. The distribution of wells fully penetrating this unit is densest in the north central region of the model area, particularly Orange County, where it contains both fresh water and is a source of public supply. The availability of data outside that region is much more limited, but some general trends can be observed. The productivity of LFA-upper decreases significantly to the south and west of the freshwater region. Reported transmissivities range from more than 500,000 ft^2/d in metropolitan Orlando, to less than 500 ft^2/d in southwestern Polk County. This is potentially attributable to evaporitic infilling of pore spaces. Salinity in LFA-upper increases rapidly toward the east coast where the unit is largely below the 10,000 milligram per liter mg/L total dissolved solids (TDS) interface. Quantitative hydraulic data in that area are generally limited to small-scale packer-testing and laboratory core data from coastal deep injection wells. These tend to be focused on identification of confinement rather than producing zones.

The GLAUClpu forms the base of the upper LFA. The top of the GLAUClpu is found near the top of the Oldsmar formation, at elevations ranging from less than 1,200 to more than 2,400 feet below sea-level in the ECFTX model region. Its thickness ranges from zero to more than 500 feet. Duncan et al. (1994) first noted a distinctive gamma log signature from an inter-bedded series of wackestone and dolostone near the top of the Oldsmar formation. They associated the gamma signature with the presence of glauconite, clay and collophane accessory minerals within that rock assemblage, and made use of it to correlate the wells across their Brevard and Indian River study area. Duncan referred to the gamma signature as the 'glauconitic zone marker', and this name has remained, despite the marker being identifiable in numerous wells where no glauconite was observed. It was noted by SFWMD that test wells drilled in the Kissimmee River Basin also showed a generally excellent confining unit at the position of the log marker, as reported by Duncan et al. (1994) in the Brevard and Indian River regions. Williams and Kuniansky (2016) mapped the unit across most of peninsular Florida. They considered it semi-confining, but noted that, locally, it might contain zones of high permeability. Given the importance of the assumption of low permeability, further investigation has been undertaken to evaluate its validity within the ECFTX model area (Janzen et al, in progress).

To date, ancillary information (associated report or test data) to indicate relative permeability of the GLAUClpu has been found and reviewed for sixty-one wells for which the marker was identified. Preliminary results indicate 93% of these were found to be in a confining or low-permeability unit and 7% were productive zones (Figure 28). It's interesting to note that - of the low permeability wells - the majority were comprised of limestone, while all the productive wells were fractured dolostone. It may be inferred, then, that post-depositional history could be the decisive factor in determining the permeability of this unit. Looking at the distribution of the exceptional 7%, all but one are located in the saline portion of the LFA near the southern border of the model. The final exception is SWFWMDs' ROMP 119.5 well, at the far northern border of the model area in Marion County. The GLAUClpu unit thins to the northwest of the Orlando area, and is absent altogether by ROMP 119.5. No exceptions to the general rule have been observed within the CFWI area, however, so it is believed this approach to LFA discretization is a reasonable one. It is important to be aware, however, of these exceptional locations, and the potential that there could be others in the more data-poor regions of the ECFTX model domain.

The basal LFA, Williams and Kuniansky's Oldsmar permeable zone, is a massive dolostone unit, characterized by fracture permeability. The top of LFA-upper ranges from less than 1,400 to more than 3,000 feet below sea-level in the ECFTX model domain. In south Florida and along the central east coast, its top is coincident with the top of the previously mapped Boulder-zone; a cavernous and highly transmissive unit with salinities commensurate with seawater. Reported transmissivities in the Boulder zone often exceed 1,000,000 ft^2/d. In the north central portion of the ECFTX model region, the basal LFA also includes freshwater producing zones. These have been reported as far south as northeast Polk County, and extending northwest into Marion County, where the basal LFA is not overlain by a confining unit. Polk County Utilities reported transmissivity in excess of 190,000 ft^2/d and TDS of 450 mg/l from the LFA well in the Northeast Regional Utility Service Area. The fractured dolostone and associated permeability both disappear toward the southwest from this point. Polk County's northwest facility (~22 miles distant) reported massive limestone and transmissivity of less than 2,000 ft^2/d from the basal LFA. Well control for the basal LFA is most limited in the far western portion of the model domain. The availability of high salinity productive zones in the Avon Park Permeable Zone (APPZ) reduced the need for deep well drilling on the south-central coast. In Pinellas County, where some deeper exploratory wells were drilled, they were characterized by low permeability gypsiferous limestone and dolostone (Hickey, 1979).

3.6 Upper Floridan Aquifer – Groundwater Flow System

Groundwater flow in the UFA, within Florida, generally radiates outward from four prominent high-water level areas observed on the potentiometric surface map for the state shown in Figure 29 (Miller 1990). Two of these exist in the Panhandle (northwest Florida) near the Georgia border, one northeast of Gainesville, and the other around Polk City in central Florida. The Polk City high generally dictates the direction of flow within the aquifer for central and southern Florida. The high is oblong in shape and trends north/south from northern Polk County, southward into Highlands County. It generally follows the Lake Wales Ridge. Although not as pronounced, this potentiometric surface high progresses southward and continues to provide freshwater recharge to the FAS in Polk and Highlands counties, and to a lesser extent, Osceola County. These potentiometric highs form the focal points of regional groundwater basin boundaries as originally described by Bush and Johnston (1988) in the first RASA study of the FAS.

The topographically high area at the center of the state forms a persistent groundwater divide resulting in recharge entering the UFA on its eastern side to move laterally toward the east coast. Conversely, it causes recharge entering west of the divide to move toward the west coast. Fisk (1983) and others further subdivided the UFA flow field into five smaller regional GW basins across the study area (Figure 30). Over the west half of the peninsula within the SWFWMD they are named the Northern West-Central Florida Groundwater Basin, the Central West-Central Florida Groundwater Basin, and the Southern West-Central Florida Groundwater Basin. Over the east half of the Peninsula, they are called the Volusia Groundwater Basin and the East-Central Florida Groundwater Basin. Groundwater basins represent semi-permanent lateral flow boundaries that are largely controlled by the underlying geology and hydraulics of the system. The basin boundaries may shift slightly from year to year based on recharge and pumping variations. However, in their most recent RASA (Groundwater Availability Study) of the FAS, the USGS indicated little change between major groundwater basin boundaries in the FAS between predevelopment and 2010 conditions (Bellino and others, 2018).

The SA is an important component of the overall water budget for the FAS because it provides storage of freshwater that can eventually reach the UFA. The Winter Haven, Lake Wales, Deland and Avon Park Ridges, among others, are characterized by thick permeable deposits of sand and shell with deep water tables. This area, compared to most others in the state (where the water table is much closer to the surface), allows for greater downward percolation of rainfall that would otherwise be lost to ET. Surface water drainage networks are also poorly developed along the ridges, restricting runoff and allowing the potential for additional recharge. In addition, several areas along the ridges are closed basins where no runoff occurs. Recharge to the UFA beneath these ridges takes place where the ICU is thin or where it has been partially or totally breached by sinkhole development (Spechler, 2010).

Topographically, these ridges are areas of higher elevation than the surrounding regions. In the high elevation portions of the Lake Wales Ridge, the water table is generally deep and a very subtle reflection of land surface. The water table elevation beneath the associated ridges is also higher than the adjacent flatlands. These higher SA water level elevations provide the driving mechanism for recharge into the UFA. The rate of recharge then becomes a function of the head difference between the SA and the UFA, as well as the vertical hydraulic conductivity and thickness of the ICU. Recharge is also higher along the Lake Wales Ridge because of sinkholes and a thin confining unit in the more northern portions of the Ridge. In the southeastern and southwestern portions of the model area, the ICU is much thicker and restricts interaction between the SA and the UFA. There are also areas within these regions where the head of the UFA is

higher than the SA, further reducing the possibility of downward leakance from rainfall into the UFA.

Rainfall provides direct recharge in the northwest quarter of the model area within the Northern West-Central Florida Groundwater Basin area because the ICU is thin and discontinuous. The UFA in this area is regionally unconfined and is located within a highly karst-dominated region. Dissolution of limestone is an active process via infiltration of rainwater because the limestone units of the UFA are close to land surface and poorly confined. Numerous sinkholes, internal drainage, and undulating topography that is typical of karst geology dominates the landscape. These active karst processes lead to enhanced permeability within the UFA. The mean transmissivity value of the UFA based on seven aquifer performance tests in northern Citrus, Levy, and western Marion Counties are 1,070,000 ft^2/day (SWFWMD 1999). There are five first-magnitude springs (flow greater than 100 cfs discharge) found here: Rainbow Springs, Crystal River group, Homosassa group, Chassahowitzka group, and Weeki Wachee Springs. In addition, some of the highest recharge rates to the UFA in the state occur in this region, with values ranging between 10 and 30 inches per year (Sepulveda 2002).

In the remainder of the area outside the unconfined UFA region and the sand ridges, recharge to the UFA is low to moderate. In the well-confined regions in the southern half of the study area, thick ICU clays limit the amount of leakage from the overlying SA to the UFA. In the Tampa Bay region and the area near Orlando, some moderate recharge reaches the UFA via karst connections through the ICU or thinner clay units. Average recharge rates to the UFA vary from zero to five inches per year in the well-confined areas, and from five to 15 inches per year in the semi-confined or more leaky regions (Bellino and others, 2018). Discharge from the UFA in the study area occurs via six primary mechanisms: offshore discharge, spring flow, groundwater withdrawals, ET in the unconfined region, baseflow in northern rivers, and upward seepage into the SA and surface water bodies. Each of these components can be large within specific geographical regions across the model domain.

In summary, the conceptual groundwater flow model has water entering the FAS either as horizontal inflow into the study area from the Polk City high, or from downward percolation of rainfall along the ridge systems or semi-confined/unconfined karst regions. Flow generally moves east/southeastward toward the ocean and west/southwest toward the gulf from the center of the state. Discharges from the FAS occur as groundwater withdrawals, ET in unconfined areas, flow into the ocean along the eastern outcrops, discharges to the gulf, spring flow, upward leakage into the overlying SA or IAS, and as baseflow into the some northern river systems that are hydraulically connected to the UFA (such as the Hillsborough and Withlacoochee Rivers). Flow within the FAS generally has an upward component near the coasts and the extreme southern part of the domain because of density, pressure, and temperature differentials between the aquifers.

3.7 Water Use

SJRWMD, SFWMD, and SWFWMD each have separate water use databases that are independently maintained based on information (source, location, depth, water use, etc.) provided by permittees as a condition of their consumptive/water use permits (CUP/WUP). For this 2020 Central Florida Water Initiative (CFWI) Regional Water Supply Plan (RWSP) effort, the water use data for 2003 – 2014 (simulation period) for each District were compiled into a single database. The overall goal was to use best available information for each District. Water use for the ECFTX model is categorized as agricultural (AG), commercial/industrial/industrial and mining/dewatering

(CII_MD), domestic self-supply (DSS), landscape/recreational/aesthetic (LRA), and public supply (PS). The ECFTX model database also includes water use for environmental (ENV), fire protection (FP), flowing wells (FW), other (OTH), and unknown (UNK). The water use database also includes return flows associated with rapid infiltration basins (RIBs).

Surface water and groundwater withdrawals were included in the ECFTX model's water use database. However, the ECFTX model is not an integrated surface water/groundwater model and is not suitable for simulating the details of surface water flow systems. Therefore, surface water withdrawals were only used to estimate return flow. Water use associated with RIBs is simulated as injection wells in Layer 1. This information forms the basis to develop the input files necessary to develop and calibrate the ECFTX model. Table 1 shows the average groundwater withdrawals by water use category and year within the ECFTX model domain. Table 2 shows the average groundwater withdrawals by water use category and year within the CFWI Planning Area. It should be noted the nomenclature and definition of water use categories for the 2020 CFWI RWSP do vary from what has been used in the ECFTX model; however, the water use compiled for both the ECFTX model and 2020 CFWI RWSP are consistent (Appendix A, 2020 CFWI RWSP). For water use category definitions not defined here, refer to Appendix A, 2020 CFWI RWSP.

Table 1. Average groundwater withdrawals (including rapid infiltration basins) in million gallons per day by water use category and year (ECFTX model domain).

Use	2003	2004	2005	2006	2007	2008	2009	2010	2011	2012	2013	2014	Avg
AG	629.0	657.5	486.2	837.5	767.7	637.5	778.5	750.5	662.2	742.3	636.8	539.4	677.1
CII_MD	141.2	126.1	120.7	120.0	118.5	121.2	110.9	104.0	98.4	107.5	110.6	102.0	115.1
DSS	113.1	115.7	110.9	119.5	116.8	116.2	113.2	118.5	111.3	104.7	89.3	89.5	109.9
LRA	94.9	110.2	95.9	143.0	142.4	127.6	127.0	108.3	119.9	123.7	108.7	96.2	116.5
PS	747.5	791.1	813.7	937.3	886.2	815.1	806.1	776.0	778.5	760.8	760.8	742.4	801.3
ENV	0.5	0.5	0.5	0.2	0.2	0.1	0.0	0.1	0.3	1.4	1.8	1.8	0.6
FP	0.0	0.0	0.0	0.0	0.0	0.0	0.0	0.1	0.1	0.1	0.2	0.5	0.1
FW	0.0	0.0	0.0	0.0	0.0	0.0	0.0	0.0	0.0	0.0	0.0	0.0	0.0
OTH	0.6	0.7	0.2	0.9	0.8	0.7	2.6	0.9	0.6	1.4	1.0	0.9	0.9
RIBS	-69.5	-68.2	-77.1	-67.6	-60.6	-70.7	-67.2	-71.8	-69.9	-72.6	-74.5	-80.1	-70.8
UNK	0.0	0.0	0.0	0.0	0.0	0.0	0.0	0.0	0.0	0.0	0.0	0.0	0.0
Total w/o RIBS	1,726.8	1,801.6	1,628.2	2,158.4	2,032.6	1,818.3	1,938.4	1,858.4	1,771.2	1,841.9	1,709.3	1,572.6	1,821.5
Total with RIBS	1,657.3	1,733.5	1,551.1	2,090.7	1,972.1	1,747.6	1,871.1	1,786.6	1,701.4	1,769.3	1,634.8	1,492.5	1,750.7

Table 2. Average groundwater withdrawals (including rapid infiltration basins) in million gallons per day by water use category and year (CFWI Planning Area).

Use	2003	2004	2005	2006	2007	2008	2009	2010	2011	2012	2013	2014	Avg
AG	126.6	133.1	89.5	168.5	155.9	131.8	160.5	157.4	130.1	165.2	139.6	119.7	139.8
CII_MD	78.0	61.3	55.9	58.8	53.8	65.0	60.9	53.6	48.1	52.3	56.1	51.0	57.9
DSS	35.2	35.6	29.3	31.1	30.6	31.9	33.8	40.5	33.4	29.8	18.1	16.6	30.5
LRA	26.3	32.2	25.2	42.3	38.8	33.2	34.3	31.8	35.6	35.9	31.2	28.1	32.9
PS	365.8	386.6	392.7	448.3	434.4	403.4	392.9	383.1	387.4	384.0	377.9	373.5	394.2
ENV	0.2	0.2	0.2	0.1	0.1	0.1	0.0	0.1	0.3	0.3	0.7	0.7	0.2
FP	0.0	0.0	0.0	0.0	0.0	0.0	0.0	0.0	0.0	0.0	0.0	0.0	0.0
FW	0.0	0.0	0.0	0.0	0.0	0.0	0.0	0.0	0.0	0.0	0.0	0.0	0.0
OTH	0.2	0.2	0.0	0.2	0.2	0.2	0.2	0.2	0.0	0.6	0.2	0.6	0.2
RIBS	-47.6	-46.7	-55.3	-46.7	-41.5	-51.4	-46.0	-48.7	-49.8	-52.1	-54.7	-59.8	-50.0
UNK	0.0	0.0	0.0	0.0	0.0	0.0	0.0	0.0	0.0	0.0	0.0	0.0	0.0
Total w/o RIBS	632.3	649.3	592.8	749.3	713.8	665.7	682.7	666.6	635.0	668.1	623.8	590.0	655.8
Total with RIBS	584.8	602.6	537.6	702.7	672.4	614.3	636.7	617.9	585.1	616.0	569.1	530.3	605.8

3.7.1 Agricultural Water Use

Apart from SWFWMD, historical metered withdrawals for AG are mostly unavailable and confined to the last several years of the calibration period. SWFWMD, through its WUP program, collects monthly metered withdrawal data at the well level. For permits and withdrawals without metered data, estimates were made based on reported pumping amounts for similar uses and quantities withdrawn. In a few instances, SJRWMD did use submitted historic withdrawal data, but mostly relied on the method described below.

Due to the uncertainty and lack of AG metered data for SJRWMD and SFWMD, a secondary method was implemented to estimate any missing or anomalous AG withdrawals for the simulation period. AG water use was estimated using the Agricultural Field Scale Irrigation Requirements Simulation (AFSIRS) model. AFSIRS, described below, provides a reasonable estimate of daily irrigation requirements based upon observed rainfall and ET rates, crop types, and land use.

The AFSIRS model was developed for Florida's water management districts by the University of Florida Institute of Food and Agricultural Sciences to provide a method to determine agricultural water use allocations for CUP/WUP programs. AFSIRS estimates irrigation requirements for crops, soils, irrigation systems, and climate conditions. The irrigation requirement for crop production is the amount of water, exclusive of precipitation, that should be applied to meet a crop's supplemental demand requirements without a significant reduction in yield.

The AFSIRS model is based on a water budget of the crop root zone and the concept that crop ET can be estimated from potential ET and crop water use coefficients. The water budget includes inputs to the crop root zone from rain and irrigation, and losses from the root zone by drainage and ET. The water storage capacity in the crop root zone is defined as the product of the water-holding capacity of the soil and the depth of the effective root zone for the crop being grown. Daily ET for each crop is calculated as the product of potential ET and the crop water use coefficient for that day. Irrigation is scheduled based on an allowable level of soil water depletion from the

crop root zone. This level of simulation model development produces a functional model that could address the wide variety of crops, soils, and irrigation systems typical of Florida and include variations in daily rainfall and ET rates needed for a transient model simulation.

SJRWMD's and SFWMD's CUP/WUP databases were used to determine the crop type, acreage, irrigation efficiency, source used, and the dates of operation for each permitted user. This data was also compared to the information published by the Florida Department of Agriculture and Consumer Services (FDACS) in their Florida Statewide Agricultural Irrigation Demand (FSAID) report (FDACS, 2017). The FSAID report contains estimated and projected agricultural acreage and water use/demand in the State of Florida. In addition, the FSAID deliverable includes a spatial component of irrigated agricultural areas that includes crop type, acreage, irrigation efficiency, and use by each area. Using FSAID, the database was expanded to include areas of known agricultural irrigation that were not required to have CUP/WUPs.

The crop type, acreage, and irrigation efficiency were then fed into AFSIRS for each area, producing monthly water use estimates for the calibration period. If available, the date the wells were constructed during the calibration period were used to avoid wells being simulated that may have not been in operation. Changes in source and reuse were also taken into consideration to avoid wells being simulated that may not have been in use. For those permits where well specific pumpage was not available, the estimated volumes were distributed equally among all the active wells.

Water uses associated with non-irrigated agriculture (e.g., aquaculture, livestock, dairy, etc.) were also included in the database. These users account for a minor fraction of the overall water use and when metered data was not available, were assigned their respective permitted allocation throughout the calibration period.

Model layer assignments for individual wells were made by correlating model layers with permitted casing and total well depths and assigning the well to the deepest model layer penetrated. When casing and well depth information was not available, a nearest neighbor approach was used to assign the model layer. In this case, the model layer assigned to the use correlated with the model layer of a permitted user that was close by.

3.7.2 Commercial/Industrial and Mining Water Use

The CII_MD category for the ECFTX model effort includes the uses associated with power generation, whereas in the 2020 CFWI RWSP, power generation is classified as its own water use category. Historical withdrawals for CII_MD are generally available throughout the ECFTX model domain and the calibration period through metered data submitted to the water management districts if required via the CUP/WUP programs. For permits and withdrawals without metered data (in all three water management districts), estimates were made based on reported pumping amounts for similar uses and quantities withdrawn. In addition, there are some CII_MD facilities that are required to submit monthly operating reports (MORs) to FDEP. In instances where there were no metered data, but there was MOR data, the MOR data was utilized. For those permits where well specific pumpage was not available, the estimated water use was distributed equally among all the active wells. Model layer assignments for individual wells were made by correlating model layers with permitted casing and total well depths and assigning the well to the deepest model layer penetrated.

3.7.3 Landscape/Recreational/Aesthetic Water Use

Historical withdrawals for LRA are generally available throughout the ECFTX model domain and the calibration period through metered data submitted to SJRWMD and SWFWMD if required via the CUP/WUP programs. For permits and withdrawals without metered data, estimates were made based on reported pumping amounts for similar uses and quantities withdrawn.

For SFWMD golf courses, an effort was undertaken to identify the timeframes of when a specific golf course began irrigating with reuse water. For golf courses that employed reuse during the calibration period, groundwater irrigation withdrawals were reduced or stopped once reuse application began. Golf course permits identified as having a groundwater source as back-up only were not included in the model dataset. For golf courses not using reclaimed water, the water use was estimated using AFSIRS and the irrigated acreages for the respective golf course. For non-golf course LRA uses, water use reflects those reported plus an estimated volume based on the ratio (percentage) of reported pumpage to allocation for permittees who did report multiplied by the allocation of the permits that did not report.

For those permits where well specific pumpage was not available, the estimated volumes were distributed equally among all the active wells. Model layer assignments for individual wells were made by correlating model layers with permitted casing and total well depths and assigning the well to the deepest model layer penetrated.

3.7.4 Domestic Self-Supply Water Use

DSS water use is calculated by the Districts yearly report at the county level using a county-wide residential per capita rate and estimate of domestic self-supply population for that respective county. For specific details and methodology on the development of DSS water use, the District's respective annual water use reports are available on their respective web sites (SFWMD, 2016; SJRWMD, 2015; SWFWMD, 2015).

Once DSS water use for the calibration period was obtained, the water use was distributed at the well level. For SJRWMD and SFWMD, the respective well databases were used to identify the location of DSS wells. The county-wide DSS water use was then distributed equally among all the wells. For SWFWMD, DSS wells were aggregated into each grid and a single point represented the aggregation of the wells (i.e., one point in the grid centroid could represent 100 DSS wells). The county-wide water use was then proportionally distributed to each centroid based on the representation of wells for the centroid. Model layer assignments for individual wells were made by correlating model layers with permitted casing and total well depths and assigning the well to the deepest model layer penetrated. When casing and well depth information was not available, a nearest neighbor approach was used to assign the model layer.

3.7.5 Public Supply Water Use

Historical withdrawals for PS are generally available throughout the ECFTX model domain and the calibration period through MORs submitted to FDEP and/or metered data submitted to the Districts if required via the CUP/WUP programs. MORs generally include the raw water that is pumped into a water treatment plant, but do not include withdrawals from individual wells. Usually, more than one well provides water to a treatment plant. For purposes of this CFWI effort, the MOR volumes reported by the utility were distributed equally among all wells for each specific PS permit. When available, individual well pumpage records were used instead of the MOR data. If

available, the date that wells were constructed during the calibration period was used to avoid wells being simulated that may have not been in operation.

Production wells with open-hole sections that penetrate multiple model layers were examined. The affected wells were divided into two categories:

1. Wells where the straddling of layers was thought to be real.

2. Wells where the straddling of layers was thought to be an artifact of the layer definition interpolation methods used to convert layer definitions at points with lithologic logs into cell-by-cell definitions across the model domain.

For wells in the first category, the withdrawal at the affected well location were split between the contributing layers in proportion to the transmissivities of the contributing layers. For wells in the second category, the apparent straddling of layers were overridden, and the wells' withdrawals were assigned completely to the model layer within which the open-hole section of the well was thought to be contained.

3.7.6 All Other Water Use

Water use for ENV, FP, FW, OTH, and UNK were only included in the dataset when metered data submitted to SJRWMD and SWFWMD via the CUP/WUP programs was available. Model layer assignments for individual wells were made by correlating model layers with permitted casing and total well depths and assigning the well to the deepest model layer penetrated.

RIBs are included in the calibration data set to represent volumes and areas of aquifer recharge. Complete data records were used if available and provided by wastewater utilities. In instances where no data was provided, the FDEP Reuse Inventory was utilized. The FDEP publishes an annual Reuse Inventory report of wastewater treatment plants with a capacity to treat greater than 0.1 million gallons per day. Flows for all recharge facilities were assigned to a centroid in each cell that occupied a recharge facility. A weighted approach was taken when assigning flows to centroids.

The aquifer recharge facilities are mostly RIB facilities, except for those at Orange County's Northwest Water Reclamation Facility, which includes a substantial wetland treatment system that discharges several million gallons per day of treated reclaimed water to Lake Marden. Because Lake Marden is an isolated depressional lake, water discharged into it infiltrates from there to the underlying UFA. All these facilities were represented by "injection" of appropriate quantities of water into Layer 1 of the model (the surficial aquifer system). Treatment wetlands that discharge to free-flowing streams and rivers were not represented in the model because the discharge of reclaimed water at these locations had negligible effects on recharge to the groundwater system.

3.8 Previous Water Budget Studies

Water budget information is useful to describe the major components of the hydrologic system. Over the central Florida area, water budgets were constructed over two different hydrogeologic regimes: (1) an unconfined UFA, deep water table, internally-drained pasture area at Ferris Farms in Citrus County, and (2) a shallow water table, semi-confined UFA, with surface water runoff in the Anclote River Basin at the Starkey Preserve in southwest Pasco County. Information was

mostly obtained from Sumner and others (2017). The purpose of examining local-scale water budgets was to estimate recharge where sufficient data was collected that could then be used as a comparison to similar hydrologic settings in the model domain.

The equation for a water budget is below:

Recharge = Rainfall – Evapotranspiration (ET) – Runoff– Storage

This equation can be further simplified for internally drained areas like the Citrus County Ferris Farms site by eliminating runoff as follows:

Recharge = Rainfall – Evapotranspiration (ET) – Storage

If water budgets are examined over a long-term period, the change in storage is negligible and can be eliminated from the preceding equations. Data was analyzed at each site above from 2004-2015. Rainfall for the Ferris Farms site was obtained from the SWFWMD website for Citrus County annual totals (https://www.swfwmd.state.fl.us/resources/data-maps/rainfall-summary-data-region). Rainfall data from the Starkey site was directly measured on location. Water table depths are greater than 16 ft at the Ferris Farms site and generally less than 3 feet deep at the Starkey site. Both land use types were Bahia pastureland.

Table 3 and 4 show the water budget terms each year from 2004 through 2015. Average values indicate that while rainfall for the period at both sites was very similar, 53 in/yr (inches per year) at the Starkey site and 52.8 in/yr at Ferris Farms, average recharge varied from about 9 in/yr at the Starkey site to approximately 28 in/yr at Ferris Farms. These recharge values are consistent with previous estimates by the USGS for semi-confined regions of central Florida of 5-15 in/yr (Bellino and others, 2018). The values for unconfined deep-water table areas in the northwest part of the model area are also consistent at 10-30 in/yr from Sepulveda (2002). Similar recharge values could be expected in semi-confined regions with surface water runoff and internally drained, deep water table areas of the sand ridge regions within the model area. Along the Lake Wales Ridge in another deep-water table setting, Sumner (1996) indicated recharge values ranging from 22 to 28 in/yr under average rainfall conditions of 52 in/yr during a 1993-1994 period.

Table 3. Annual rainfall, ET, runoff, and recharge values for the Starkey preserve site in southwest Pasco County, Florida (Sumner and others, 2017).

Year	Rainfall (in)	ET (in)	Runoff[1] (in)	Recharge (in)
2004	70.08	35.04	25.26	9.78
2005	51.18	31.10	4.19	15.89
2006	42.52	30.31	1.58	10.62
2007	33.66	28.35	0.48	5.03
2008	49.21	33.46	6.19	9.56
2009	51.18	32.28	6.75	12.15
2010	52.36	35.43	16.09	0.84
2011	53.15	29.92	10.23	13.00
2012	63.78	31.69	23.36	8.72
2013	50.00	32.28	12.70	5.02
2014	55.31	32.28	15.31	7.72
2015	61.42	30.31	24.14	6.96
Avg:	**52.8**	**31.9**	**12.2**	**8.8**

[1] Surface water runoff based on the Anclote River nr Elfers gauge (adjusted for baseflow contribution by estimating 85% of flow is runoff (Geurink and others (2000)).

Table 4. Annual rainfall, ET, and recharge values for the Ferris Farms site in southeast Citrus County, Florida (Sumner and others, 2017).

Year	Rainfall[1] (in)	ET (in)	Recharge (in)
2004	61.50	27.69	33.81
2005	62.40	24.58	37.82
2006	40.42	23.96	16.46
2007	44.93	22.40	22.53
2008	52.34	26.45	25.89
2009	50.10	25.51	24.59
2010	52.97	28.00	24.97
2011	49.31	23.65	25.66
2012	56.11	25.05	31.06
2013	50.25	25.51	24.74
2014	62.54	25.51	37.03
2015	53.38	23.96	29.62
Avg:	**53.0**	**25.2**	**27.8**

[1] Rainfall data for Citrus County from (https://www.swfwmd.state.fl.us/resources/data-maps/rainfall-summary-data-region)

CHAPTER 3 - FIGURES

Series	Geologic Unit		Lithology		Hydrogeologic Unit		
Holocene and Pleistocene	Anastasia Formation	Consolidated to unconsolidated shell beds, molluskan limestone, quartz sand		Sand	Surficial aquifer system		
	Nashua Formation	Variably calcareous, shelly sand and sandy shell coquina		Silt,			
Pliocene	Cypresshead Formation	Variably argillaceous quartz sand, silt and gravel occurring on higher elevations		Clay & shell			
	Hawthorn Group	Highly variable, clay, silt quartz sand, shell beds, limestone, dolostone, chert (especially in lower section), phosphate. Intervals with abundant clay mineral or clay size material can be very impermeable. Sand and shell beds may be locally very permeable			Intermediate confining unit		
Oligocene	Suwanee Limestone	Dolomitic, micro-fossiliferous limestone with silt-sized phosphate. Present eastern Indian River and southeastern Brevard Counties, and in localized areas of central Florida			Upper Floridan aquifer system	Upper permeable zone	
Late Eocene	Ocala Limestone	Thickly bedded, foraminiferal limestone with abundant echinoids, mollusks, corals, and bryozoans. Productive where secondary permeability well developed, but low permeability where recrystallized or lime mudstone dominant.				Ocala-Avon Park low permeability zone	
Middle Eocene	Avon Park Formation	Upper lithozone consists of recrystallized dolostone interbedded with white to tan recrystallized foraminiferal limestone. Beds of tan to brown to gray dolomitic limestone and dolostone are common and may be very impermeable unless fractured. May contain peat beds or other organic material. A lower dolostone lithozone may contain pyrite and glauconite grains			Floridan aquifer		Avon Park high permeability zone
							Middle confining unit I
							Overlap unit of LFA
							Middle confining unit II
Early Eocene	Oldsmar Formation	Upper: white to grey, dolomitic limestone & brown recrystallized dolostone. Lower: very hard and massive dolostone, traces of glauconite, pyrite, peat and phosphate. Extremely permeable where fractured.				lower Floridan aquifer	Upper permeable zone
							Glauconite marker unit
							Basal permeable zone
Paleocene	Cedar Keys Formation	Dolostone, dolomitic limestone, and evaporites. The lower two-thirds consisting of finely crystalline dolostone with interbedded anhydrite forms the sub-Floridan confining unit			Sub-Floridan confining unit		

Figure 17. Relation between stratigraphic and hydrogeologic units and ECFT model layers (identified in the hydrogeologic unit column) for the CFWI Planning Area (modified from Sepúlveda, et al., 2012).
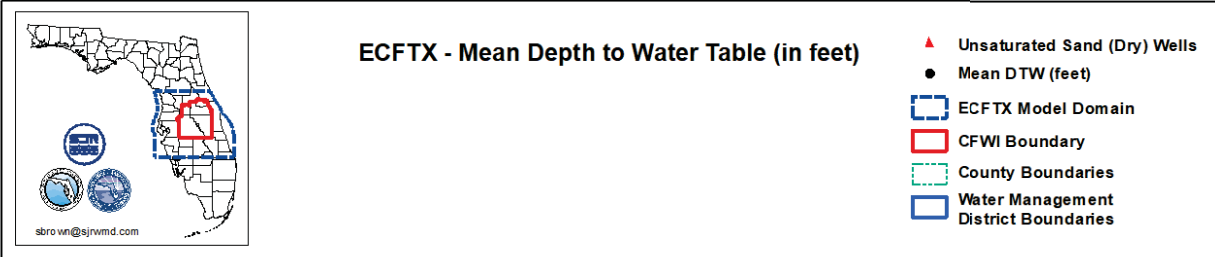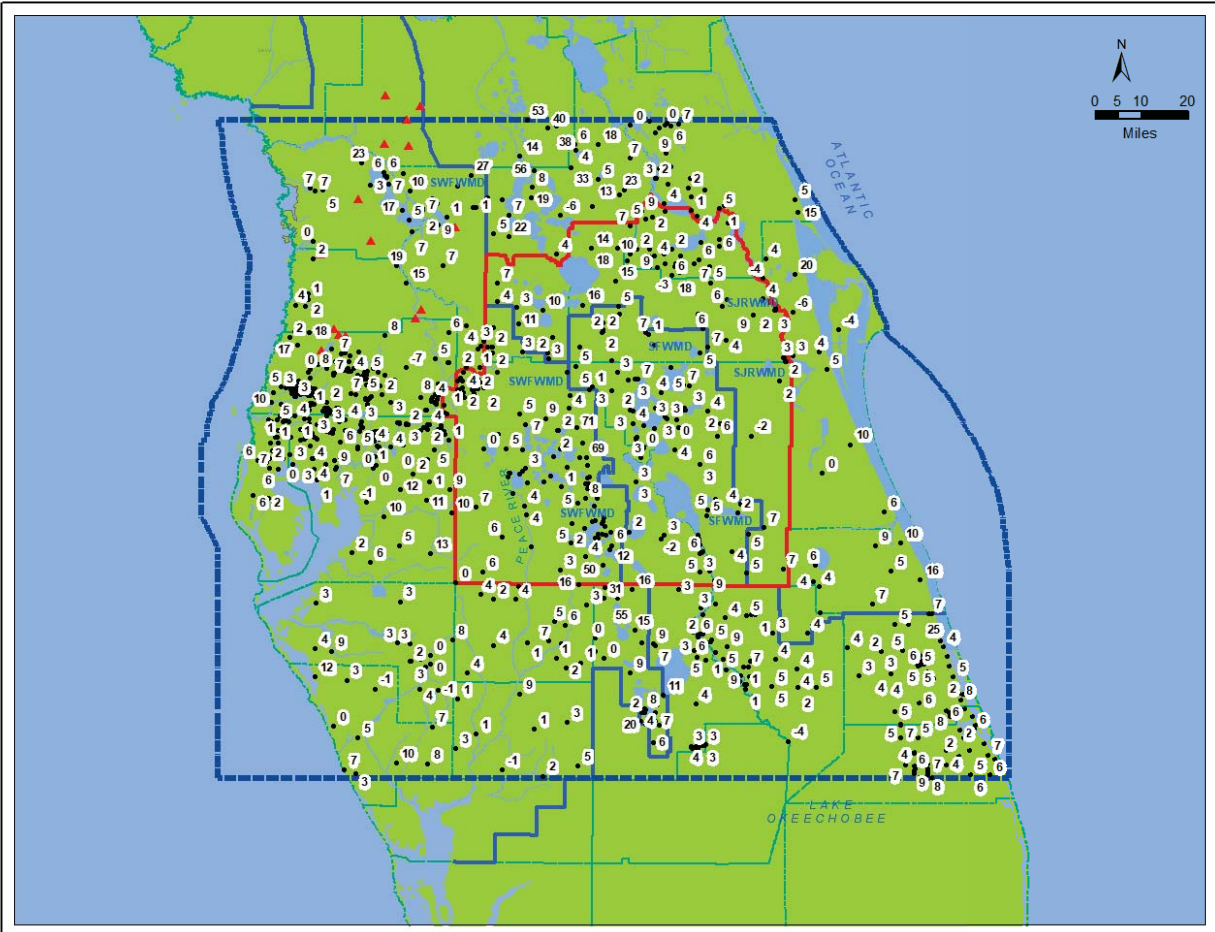
Figure 18. Long-term average depth to the water table from monitor wells in central Florida (Minimum 5-year average period-of-record. Note: negative above land surface).
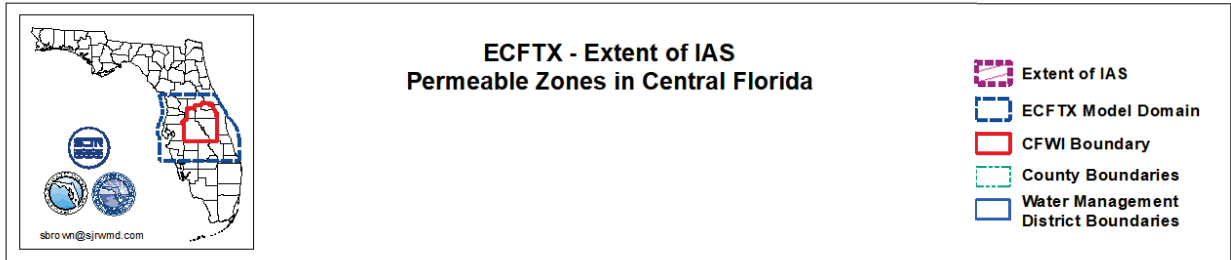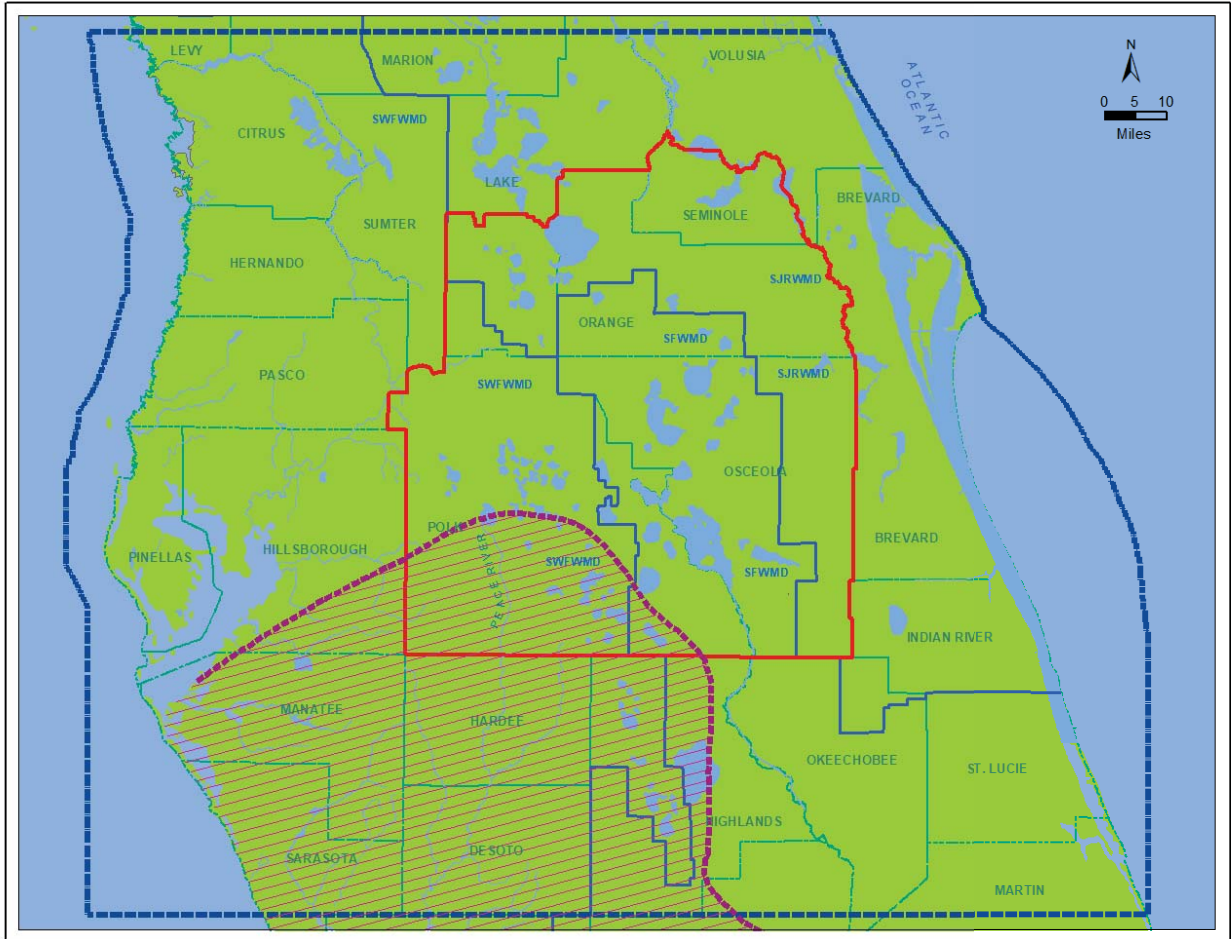
Figure 19. Extent of Intermediate Aquifer System (IAS) permeable zones in central Florida.
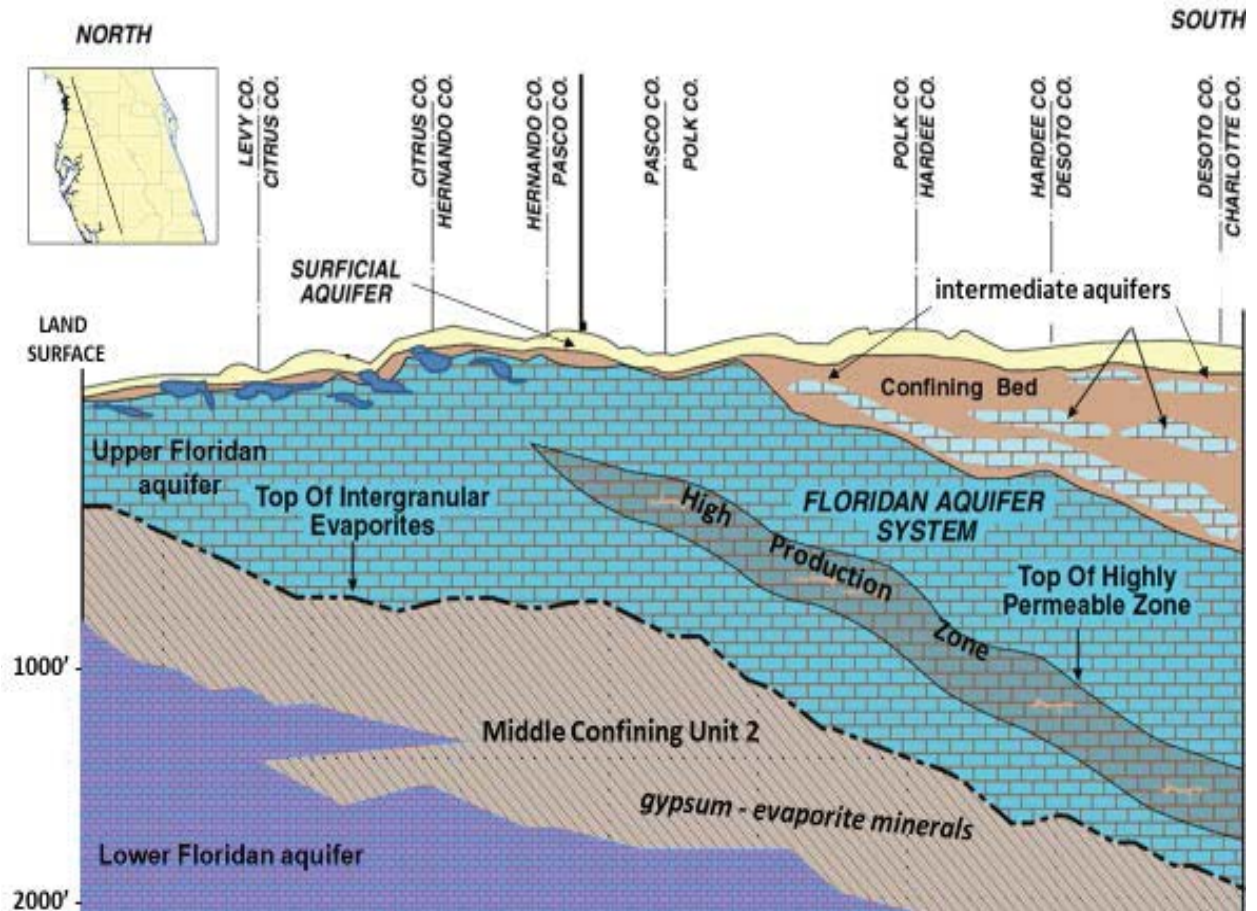
Figure 20. Hydrogeologic cross-section from north to south across the western half of the ECFTX model domain.
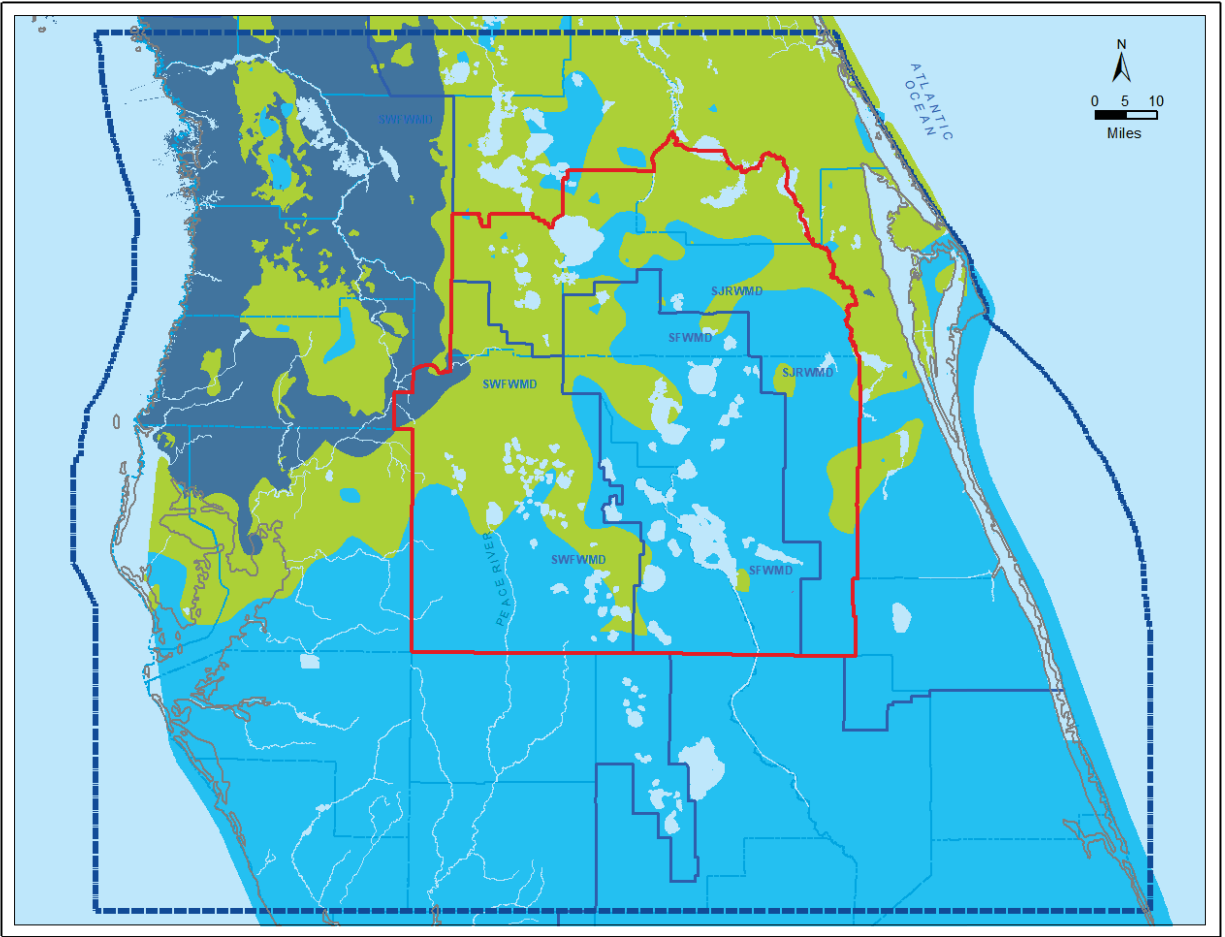
Figure 21. Generalized degree of confinement of the Upper Floridan aquifer (Williams and Kuniansky, 2016).
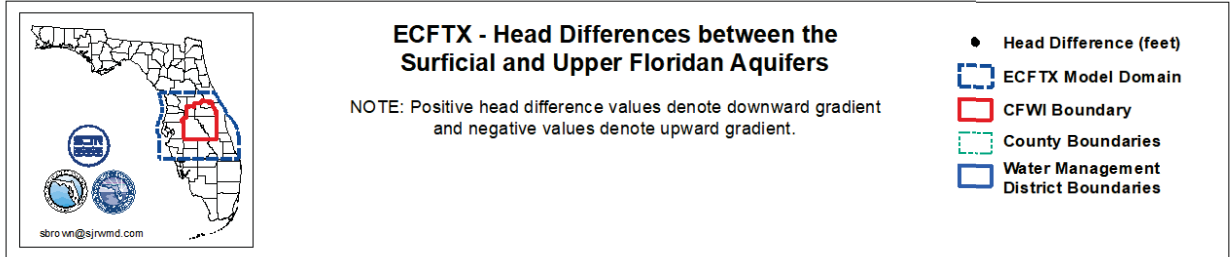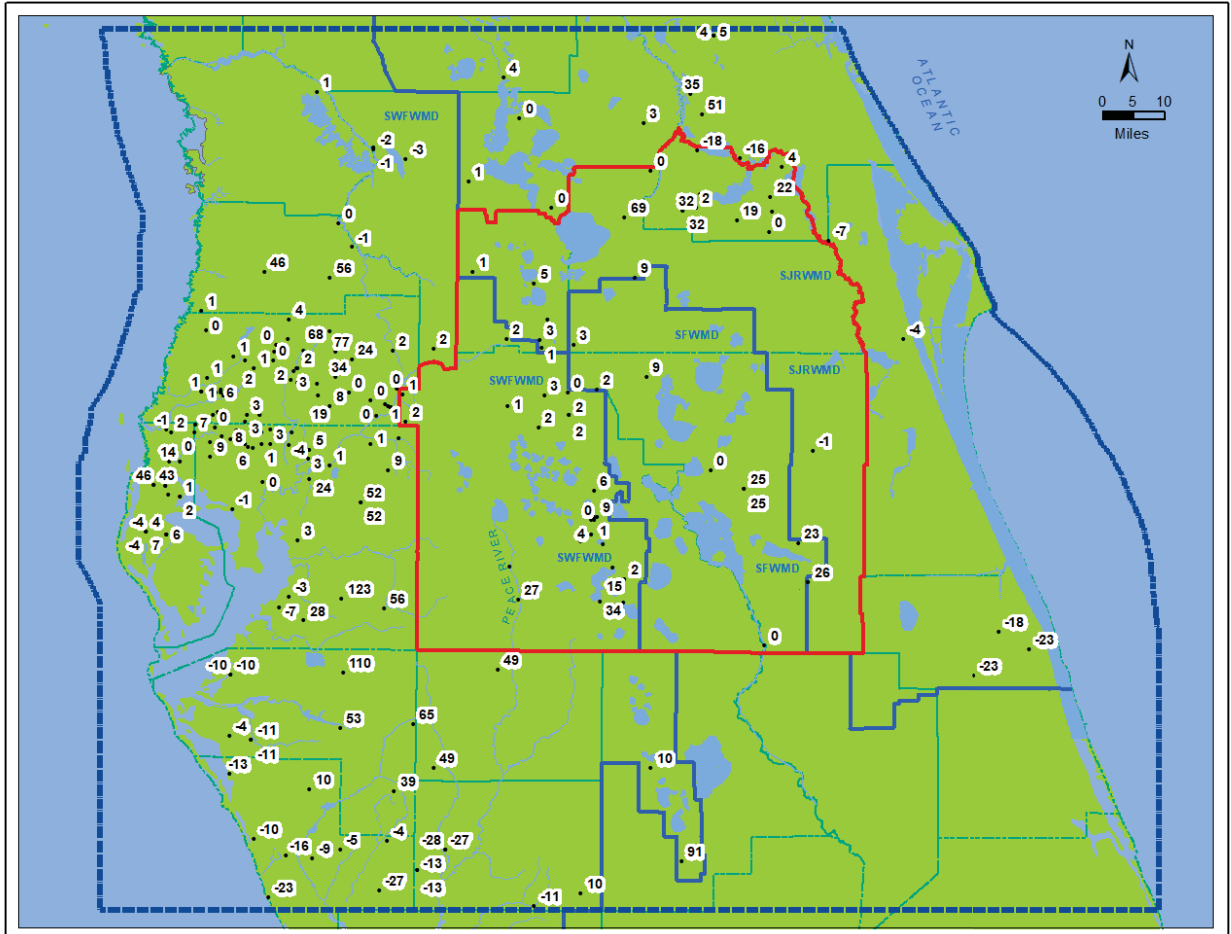
Figure 22. Long-term average hydraulic head difference between nested surficial and Upper Floridan aquifer monitor wells in central Florida (Minimum 5-year average period-of-record).

ECFTX Model Domain - Sinkhole Coverage

* Subsidence data / sinkhole locations acquired from Florida Department of Environmental Protection -
https://floridadep.gov/fgs/sinkholes/content/subsidence-incident-reports

▲ Sinkhole Location

▯ ECFTX Model Domain

▯ CFWI Boundary

County Boundaries

Water Management District Boundaries
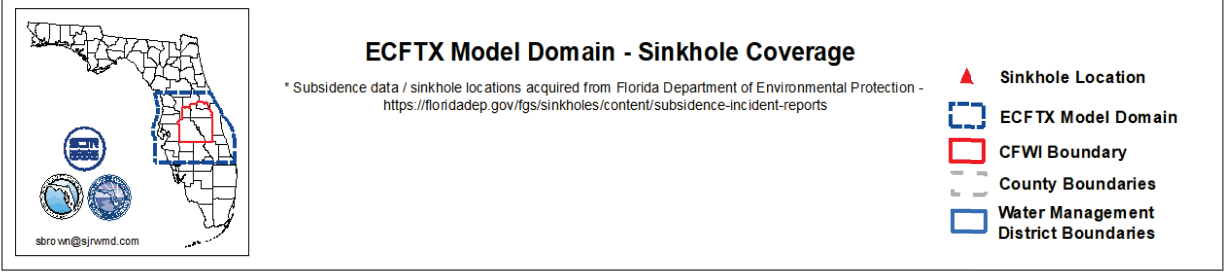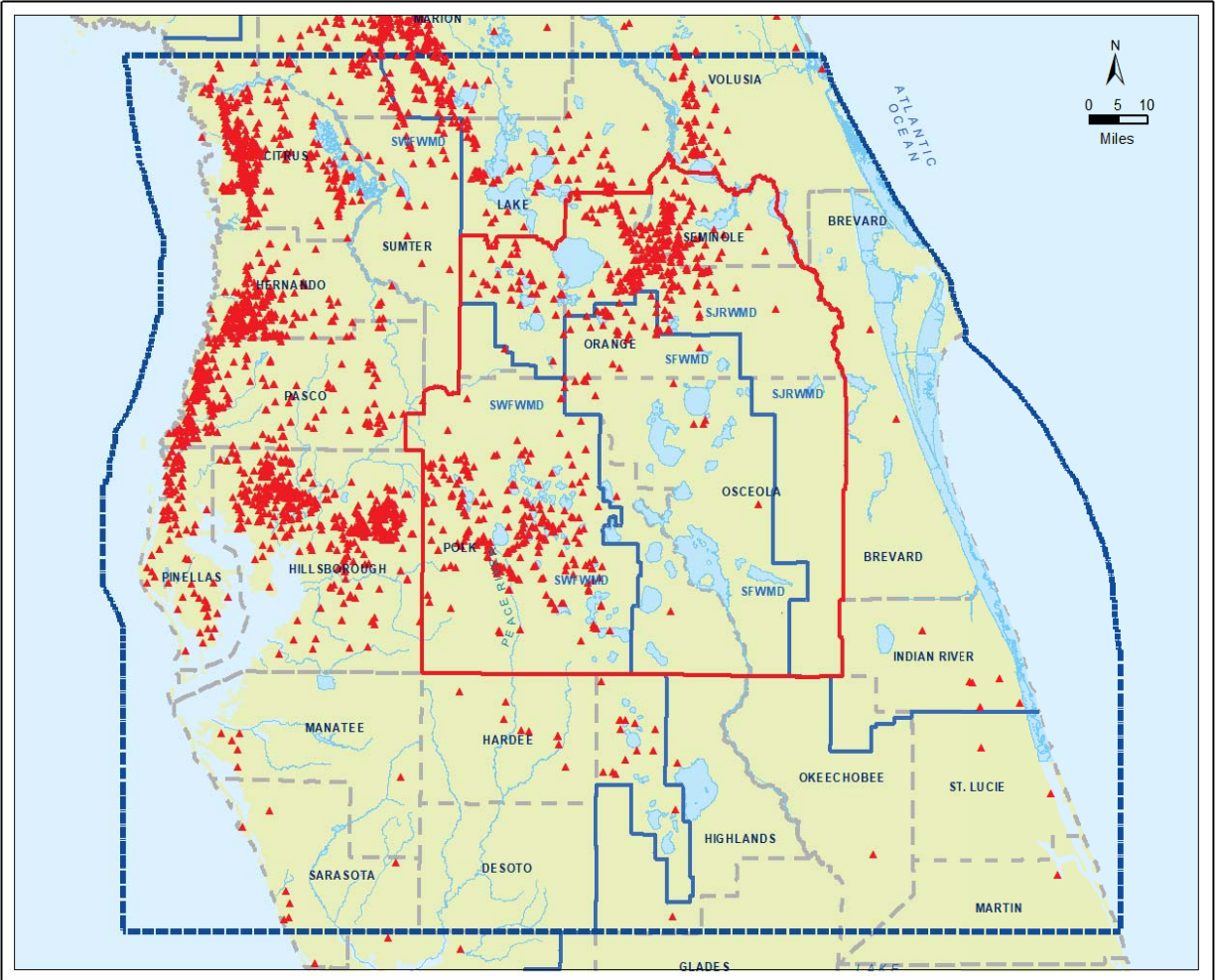
Figure 23. Reported sinkholes within the central Florida area.
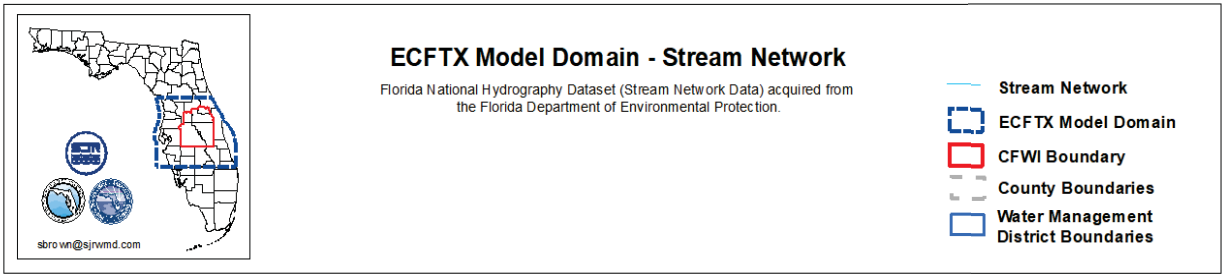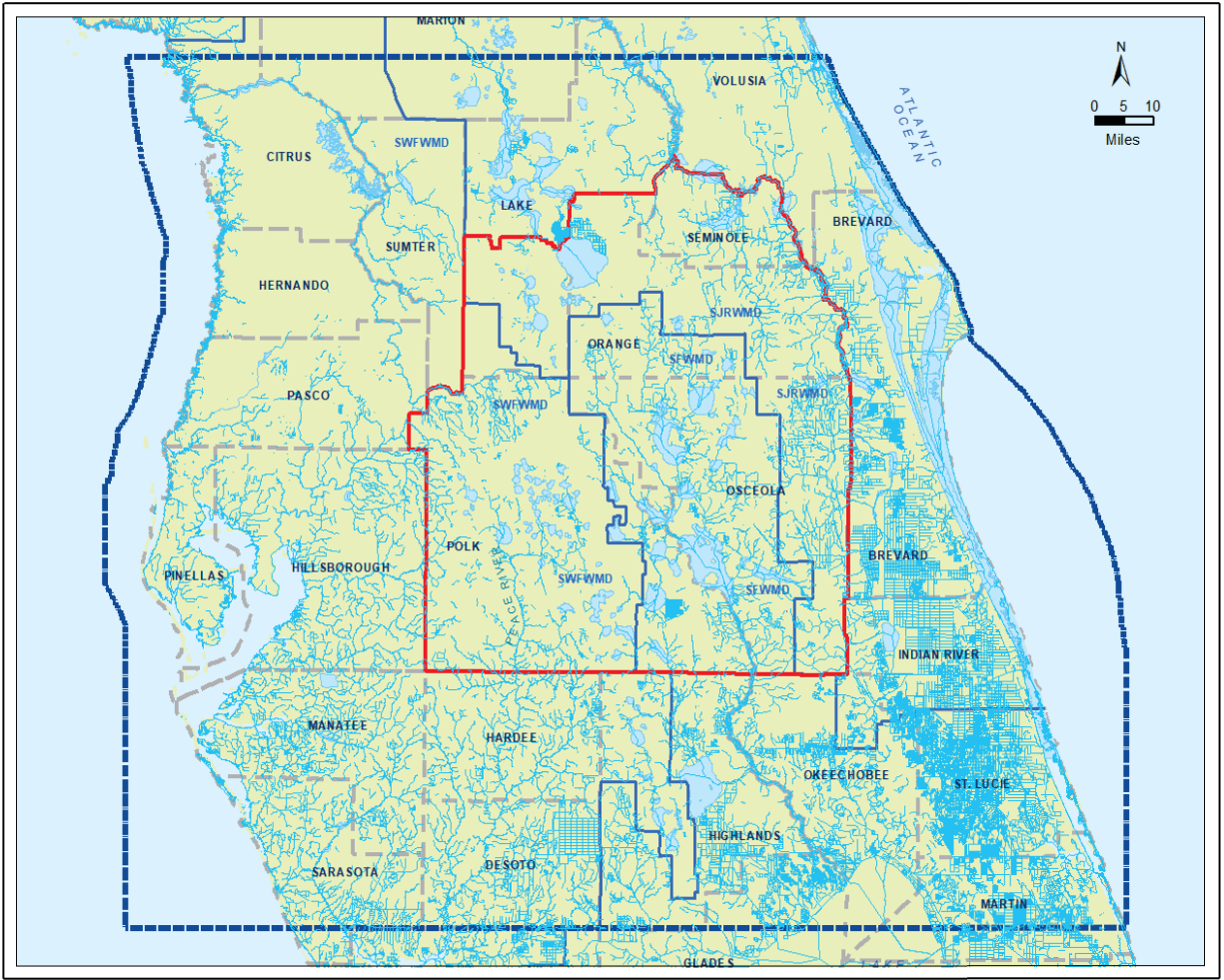
Figure 24. Hydrography within the central Florida area.

Hydrostratigraphic Conceptualization

West Half	East Half

Surficial Aquifer | **Surficial Aquifer**

Intermediate Confining Unit | **Intermediate Confining Unit**

Upper Floridan Aquifer - Upper

Ocala Low-Permeability Zone (OCAPlpz)

Avon Park High-Permeability Zone (APhpz) | **Upper Floridan Aquifer (UFA)**

Middle Confining Unit I

Overlap Unit of the LFA | **LFA** | **Middle Confining Units**

Middle Confining Unit II

Lower Floridan Aquifer – Upper

Glauconite Marker Low-Permeability Unit (GLAUC-lpu)

Lower Floridan Aquifer – Basal | **Lower Floridan Aquifer (LFA)**

Figure 25. Hydrogeology within the central Florida area.
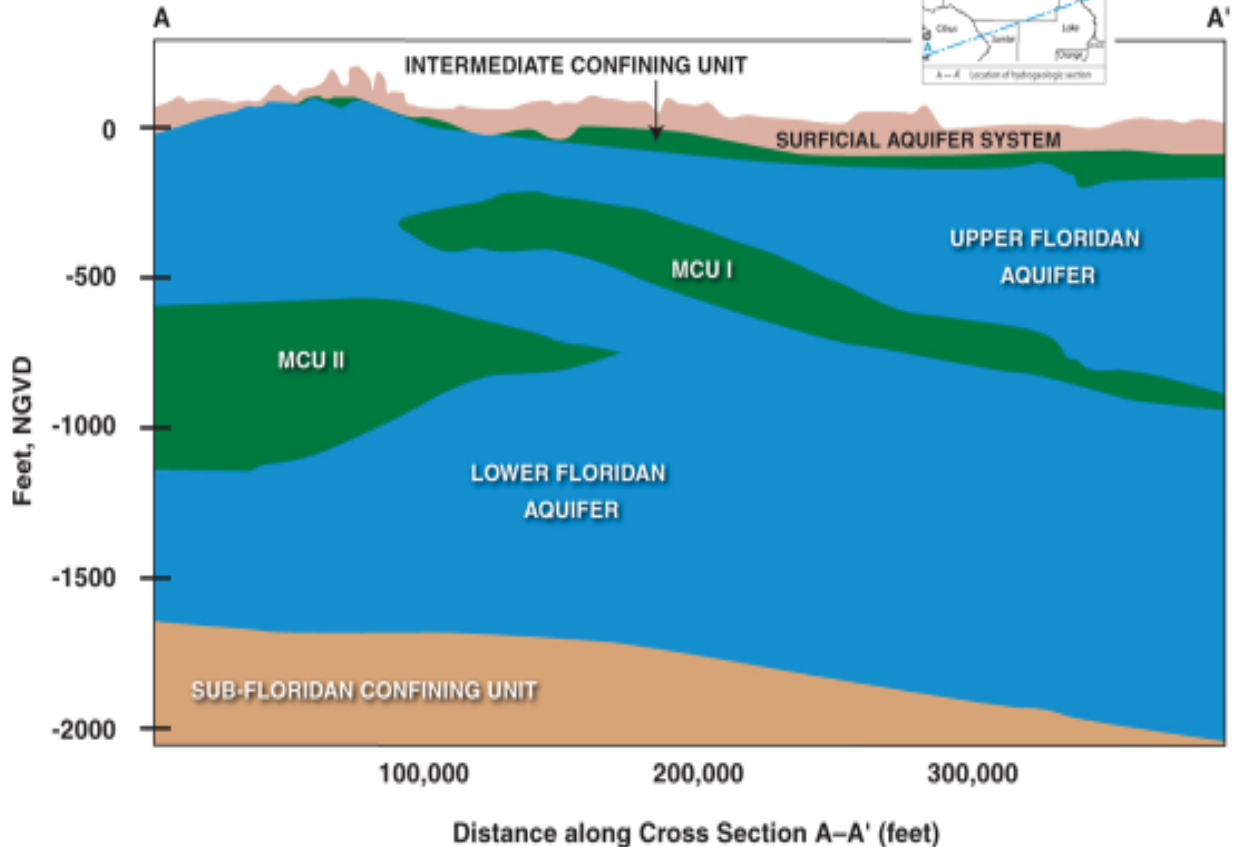
Figure 26. Hydrogeologic cross-section showing the relation between MCU 1 and MCU 2 units within the FAS in the northern portion of the ECFTX model domain.
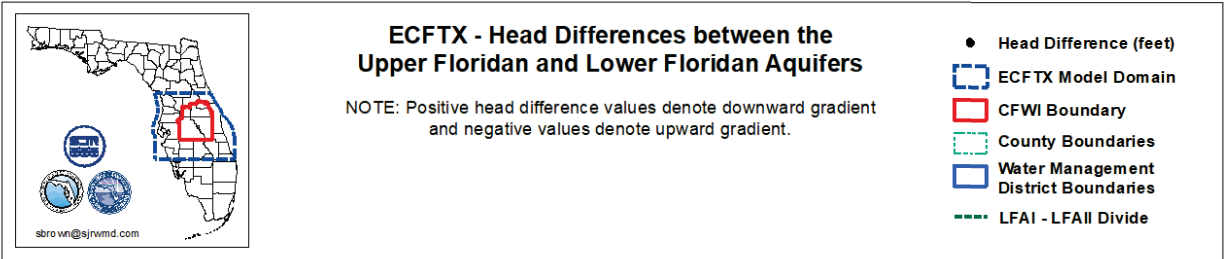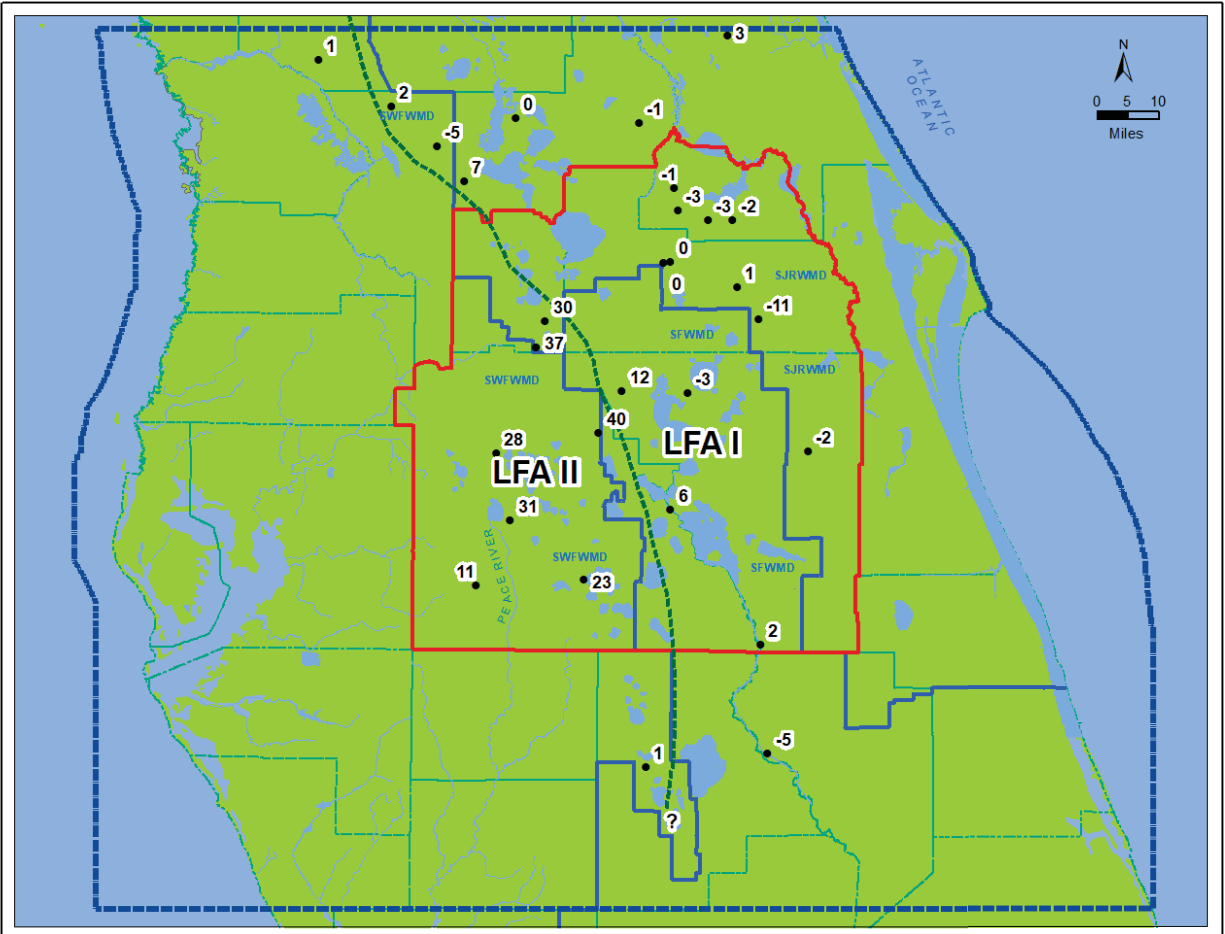
Figure 27. Long-term average hydraulic head difference between nested Upper Floridan and Lower Floridan aquifer monitor wells in central Florida (Minimum 1-year average period-of-record).
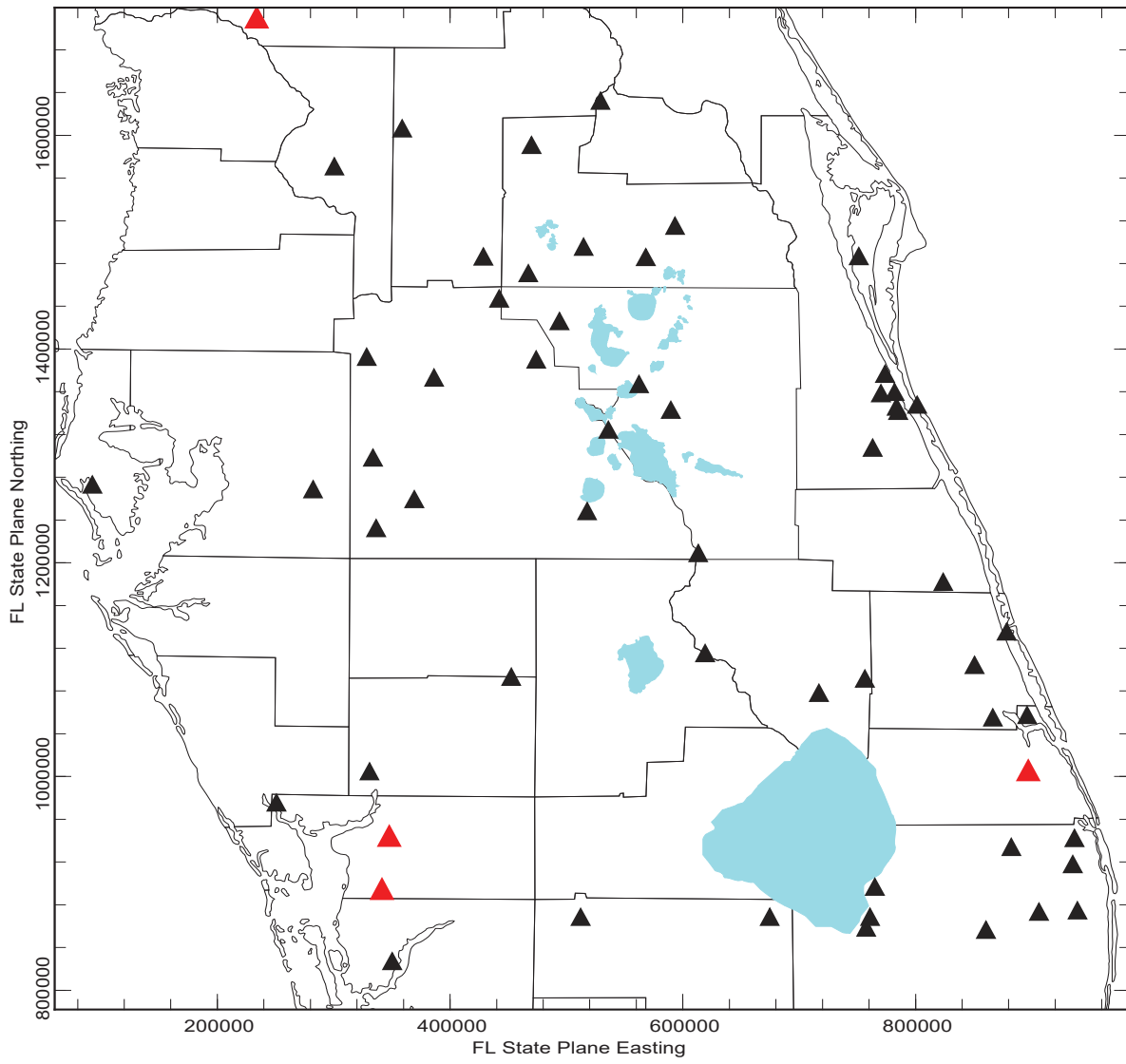
▲ GLA Marker: within overall Low Permeability unit
▲ GLA Marker: within overall Productive unit

Figure 28. Results of spot-checks on relative permeability of the GLAUClpu.
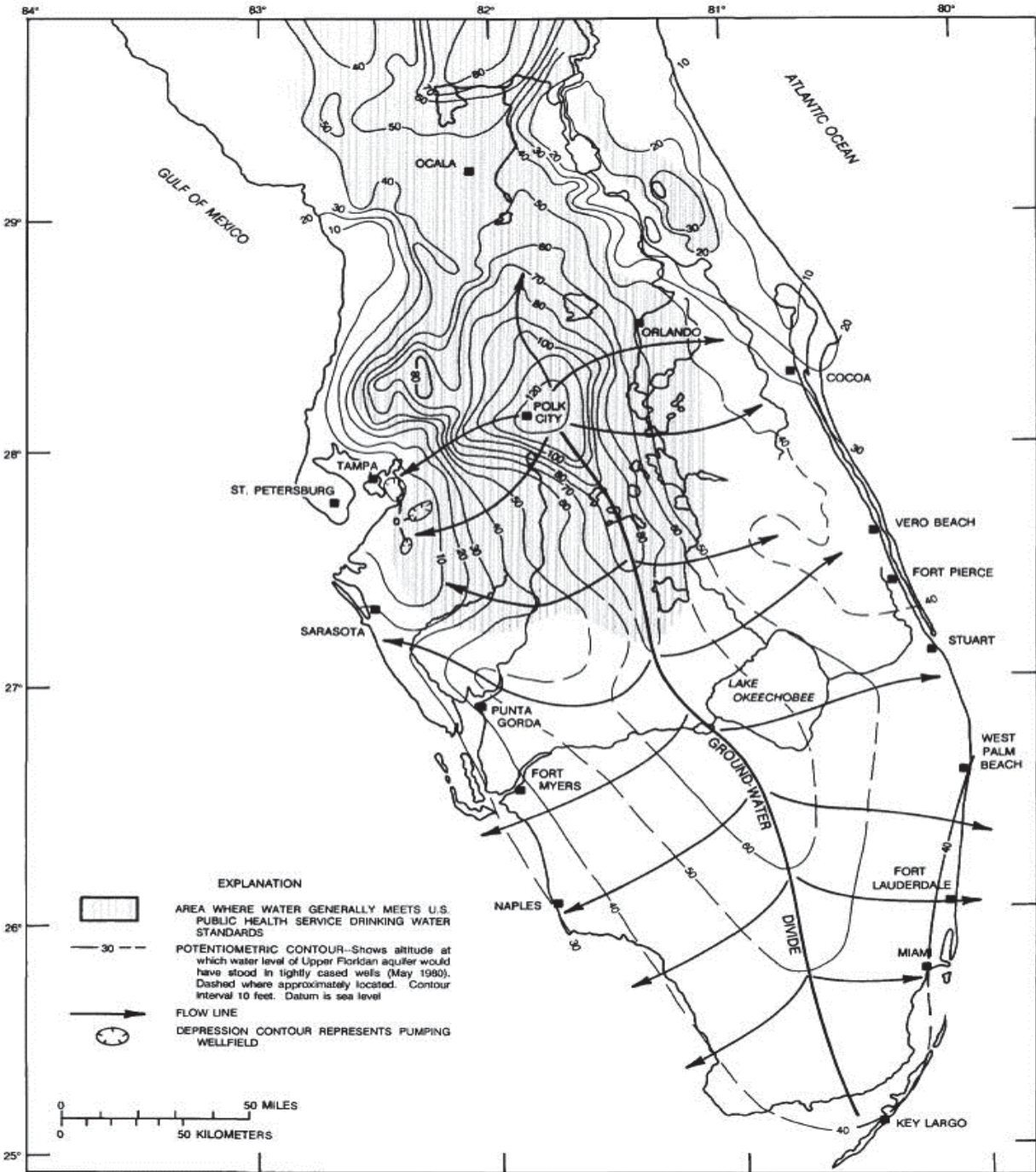
Figure 29. Flow Patterns in the Upper Floridan Aquifer (Meyer, 1989).
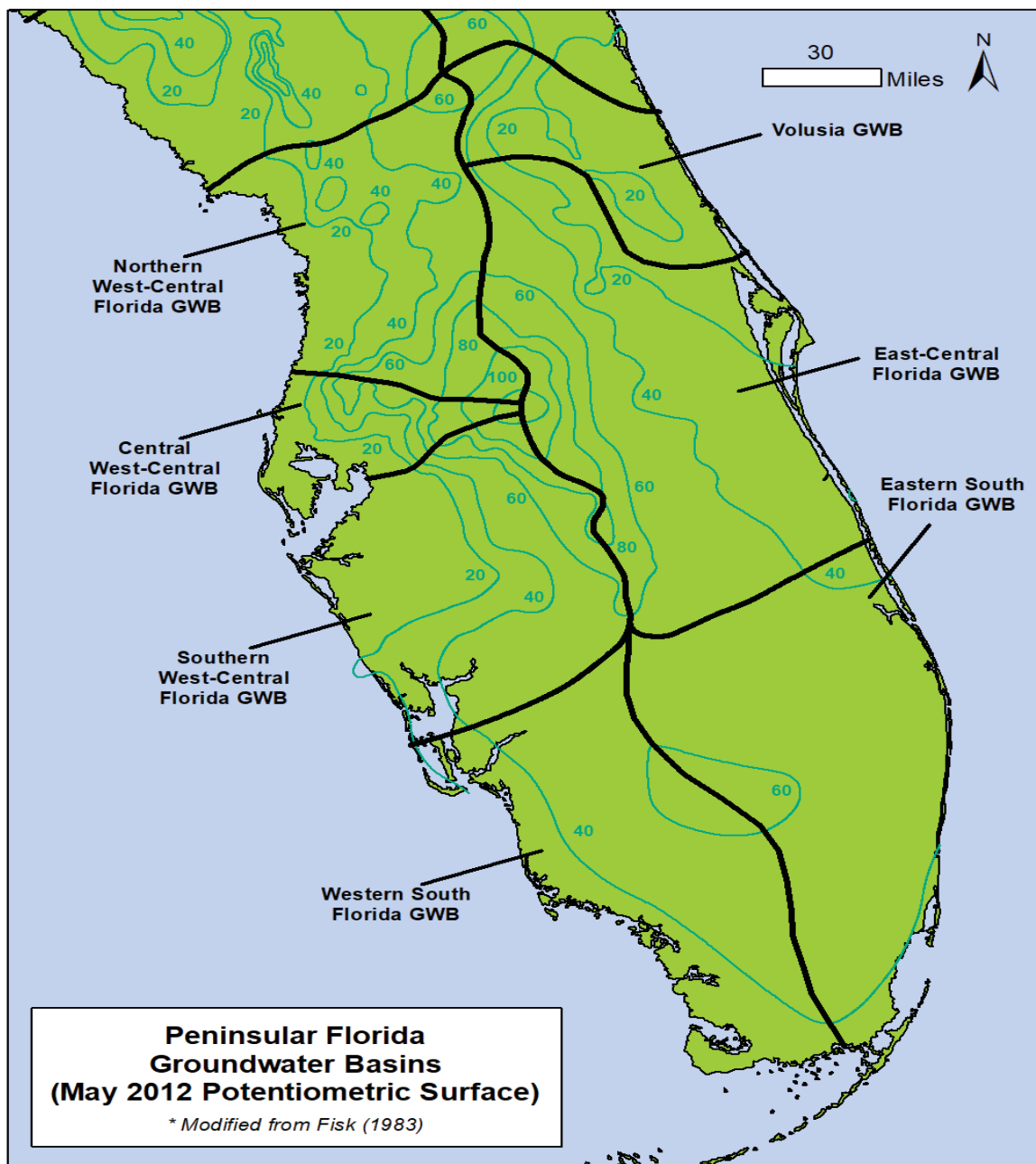
Figure 30. Regional groundwater basins of the Upper Floridan aquifer over the Florida peninsula (Fisk, 1983; Bellino and others, 2018).

CHAPTER 4 – SIMULATION OF GROUNDWATER FLOW

4.1 Model Development

The ECFTX model is a fully three-dimensional (3D) groundwater flow model and uses MODFLOW NWT (Niswonger, et al., 2011) as the simulation code. All elevation data for the model are assigned a vertical datum of NAVD 88. Active and inactive areas of the model layers are delineated. In general, for those areas of the model where total dissolved solids concentrations exceed 10,000 mg/l (or chloride concentrations approximately equal to or greater than 5,000 mg/l), the layers are populated with appropriate aquifer parameters but are inactivated and general head boundaries are set along the edge of the active areas. The Upstream Weighting (UPW) package – associated with MODFLOW NWT – was developed to incorporate aquifer layering and parameters. Within the ECFTX model domain, topography was used as the top of model layer 1 over the entire model area, based on information received by each district.

Numerous types of hydraulic data are required to develop a numerical model. For this section of the model development discussion, the data are divided into the following five categories:

- Hydraulic conductivities and storage coefficients

- Groundwater withdrawal rates

- Recharge rates

- Boundary conditions

- Initial conditions

4.2 Model Grid and Layers

The model domain covers an area ranging from Daytona Beach (to the north), to the Charlotte-Desoto county line (to the south). It spans from the Atlantic Ocean on the east coast, to the Gulf of Mexico on the west (Figure 31). The model grid is aligned in a north-to-south direction. The model has 603 rows and 704 columns with a uniform grid spacing of 1,250 feet. It consists of approximately 23,800 total square miles – more than twice the area of the ECFT model. The selection of the grid size was based on the planned use of the model, data availability, and computational considerations. The model coordinates, based on state plane coordinates of NAD83 Florida East, located at the northeast corner of the model are:

X-direction: 24352

Y-direction: 1737103

Vertically, the model includes eleven hydrostratigraphic layers. In descending order, they are: (1) the Surficial Aquifer (SA); (2) the Intermediate Aquifer System/Confining Unit (IAS/ICU); (3) the Upper Floridan aquifer – upper permeable zone (UFA-upper); (4) the Ocala-Avon Park low permeability zone (OCAPlpz); (5) the Avon Park high-permeability zone (APhpz); (6) MCU_I, the first component of the Middle Confining Unit; (7) the overlap unit of the Lower Floridan aquifer (second component, where MCU_I and MCU_II overlap without touching); (8) MCU_II, the third

component of the MCU; (9) the upper permeable zone (the first subdivision of the LFA called the LFA-upper); (10) the low permeability glauconitic marker unit (second subdivision of the LFA called GLAUClpu); and (11) the Lower Floridan aquifer – basal permeable zone (LF-basal). Each of these hydrostratigraphic units is treated as a separate layer in the model (as shown in Figure 32).

The collection of data and the assembly of input data sets is one of the most important and time-consuming parts of model development, particularly for a model with a large geographic extent and complex hydrostratigraphy, such as the ECFTX model.

The conceptual model was initially divided into similar hydrostratigraphic units following the primary water producing units and confining units identified in Reese and Richardson (2008). Data from that work and the respective WMD databases provides most of the information used to construct the conceptual model. The groundwater flow model was then constructed based upon hydrostratigraphic units and may not necessarily follow geological formation contacts. Additional data points from wells constructed post 2008 were also obtained. These newly obtained sites were checked against the existing database and corrected as necessary to meet the conceptual model specifications.

Once data were gathered and checked for quality assurances, they were combined into a single dataset for development of the model layers. The hydrostratigraphic layers were then created by a thickness-kriging method using a moving geostatistical technique developed by Geovariances and SJRWMD (2011). Additional modifications were also incorporated based on newly mapped UFA, MCU, and LFA units. The surfaces of each of the major hydrostratigraphic units are created with a 150-meter cell size for units above and including the UFA top, and a 500-meter cell size for units below the UFA top.

Most layers show a southerly dip from the Polk County portion of the model to the south. The degree and extent of this dip varies between hydrologic units. The UFA shows a relatively consistent increase in depth of the top of the unit in a southerly direction. The higher areas in Hendry County can be attributed to the basal portion of the ICU showing productivity and are therefore included in the UFA. North of Lake Okeechobee, the APPZ exhibits a southerly trend, but develops a more southwestwardly trend south of Lake Okeechobee. Because of the density and distribution of the existing data (both spatially and vertically), the upper units of the FAS are relatively better defined than the deeper units.

After the 500- and 150-m surfaces were resampled to the model grid, analysis of these results showed locations where units were extremely thin or absent (e.g., ICU, MCU_1, MCU_II). To ensure numerical stability during model execution, a minimum thickness of 10 feet was assigned. When this minimum thickness rule was applied, the aquifer hydraulic properties were assigned based on the properties of the over or underlying units.

4.3 Drain Return (DRT)

The Drain (DRN) Package simulates groundwater flow out of the drain cells and removes the total amount of simulated drain flow out of the model (McDonald and Harbaugh, 1988). The Drain Return (DRT) Package simulates groundwater flow out of the drain cells but returns a fraction of that simulated drain flow simultaneously to any cell in the model (Banta, 2000). That fraction is referred to as the return-flow proportion. The user can specify the return-flow proportion, which is a value valid in the range of 0.0 to 1.0. When the return-flow proportion is chosen as 0.0, the DRT

package is identical to the DRN package. When the return-flow proportion is chosen as 1.0, the total drain flow is fully returned to the model.

As in the DRN Package, the DRT Package evaluates the drain flow $QD_{i,j,k}$ from the drain cell (i, j, k) as

$$QD_{i,j,k} = \begin{cases} CD_{i,j,k}(h_{i,j,k} - d_{i,j,k}), & h_{i,j,k} > d_{i,j,k} \\ 0, & h_{i,j,k} \leq d_{i,j,k} \end{cases}$$

where $QD_{i,j,k}$ is the volumetric flow rate (L³/T) computed from cell (i, j, k) for the drain-return feature, $CD_{i,j,k}$ is the drain conductance (L²/T) for the drain-return feature in cell (i, j, k), $h_{i,j,k}$ is the hydraulic head (L) computed for cell (i, j, k), $d_{i,j,k}$ is the drain elevation (L) for the drain-return feature in cell (i, j, k) (Banta, 2000). Groundwater only flows out of the drain cell when the simulated head at the cell is higher than the drain elevation.

The DRT package also evaluates the return flow that is received at an associated recipient cell (ir, jr, kr) in the model as

$$QRF_{ir,jr,kr} = RFPROP_{i,j,k} \times QD_{i,j,k}$$

where $QRF_{ir,jr,kr}$ is the volumetric flow rate (L³/T) into the recipient cell, and $RFPROP_{i,j,k}$ is the return-flow proportion (dimensionless) specified for the drain-return feature in cell (i, j, k) (Banta, 2000).

In the ECFTX model, for each DRT cell either a value of 0.0 or a value of 1.0 is specified for the cell's return-flow proportion. When the return-flow proportion is set to 0.0, the DRT cell returns no drain flow to the model; such 0.0-RFPROP DRT cells are used to represent irrigation ditches, stream headwater reaches, and shallow surface-water bodies not represented by RIV cells. When the return-flow proportion is set to 1.0, the DRT cell returns drain flow fully to the model; such 1.0-RFPROP DRT cells are used to represent drainage-well lakes and numerous drainage wells in the Orlando area (some of which are the outfall for stormwater ponds) whose drain flow is returned to recipient cells immediately beneath the DRT cells in layer 3 (the upper part of the UFA).

The drain cells associated with the surface water hydrography elements such as irrigation ditches, headwater drainage features, and shallow surface water bodies are represented by traditional drainage type cells allowing discharge only if the simulated aquifer water level is above the drain cell elevation (Figure 33). There is zero discharge once the simulated aquifer water level falls to or below the elevation of the drainage cell stage. In contrast, the DRT cells used in the Orlando area to represent drainage wells within lakes that are used to control flooding or surface water runoff drainage wells route water to the uppermost layer of the UFA (Figure 34). The water routed to the UFA is controlled by the simulated Surficial aquifer head and surface water stage elevation prescribed for each DRT cell and can vary month-to-month in the transient simulation. Average drainage well discharge to the UFA in the Orlando area from 2003-2014 was 59.8 mgd (Figure 35).

4.4 Boundary Conditions (Lateral)

Model boundaries for the ECFTX model were selected at a distance from the CFWI region that would not have an appreciable effect on the groundwater system within the CFWI region. Boundaries are required in numerical models to constrain the area of interest and are ideally situated corresponding to presence of hydrologic boundaries. The northern model boundary occurs along an east-west line in central Volusia County just south of Daytona Beach. Previously evaluated influence coefficients resulting from the steady-state ECFT-HAT model concluded the northern boundary location does not influence the performance of the model within the CFWI region. The eastern boundary corresponds to the hydrologic boundary of the Atlantic Ocean and the western boundary corresponds to the hydrologic boundary of the Gulf of Mexico. The southern model boundary occurs along an east-west line corresponding to the Charlotte-DeSoto county line extending to both coasts. The southern boundary is located approximately 42 miles south of the CFWI boundary and is not anticipated to influence model performance within the CFWI region. Model boundaries were simulated using either a specified-head boundary condition, no-flow boundary condition, or a general head boundary condition (GHB).

Specified-Head Boundary

In a specified-head boundary condition, the water level is fixed at a given elevation and does not change during the simulation unless a CHD package is used that allows it to vary by stress period. In the ECFTX model, the specified-head boundary condition was fixed and did not change by stress period. This type of boundary condition is typically used for lateral inflow/outflow from the model or to represent large surface water features (Rumbaugh, 2019). Specified heads were set at sea level for the SA (Layer 1) along the east and west boundaries where model cells extended into the Atlantic Ocean and Gulf of Mexico.

No-Flow Boundary

No-flow boundary conditions were used at the lateral boundaries or edges for layers that reflected confining units between aquifers. These boundary conditions were specifically assigned to the eastern portion of layer 6 (MCU I), the western portion of layer 8 (MCU II), and all of layer 10 (GMU). No-flow boundary conditions do not allow transfer of water across the boundary. This boundary condition approach is reasonable for confining units with low permeability.

General-Head Boundary

General-head boundaries (GHBs) are lateral boundary conditions for this application of MODFLOW. The function of the GHB Package is to simulate flow into or out of a cell from an external source in proportion to the difference between the head in the cell and the head assigned to the external source (Harbaugh, 2005). GHBs are used to effectively extend the hydrologic influence of the model and to buffer the effects of simulating stresses within the model domain without extending the active model domain. The lateral location of the assigned heads for the GHBs are 1,250 feet away from cell-centers of the outer ring of active cells for each layer. The hydrologic parameter, described as the conductance term, is calculated as the product of hydraulic conductivity of the aquifer and the cross sectional area of flow at each boundary cell divided by the distance from the location of the boundary head (center of the boundary cell) to the location of the source head. The values for these parameters are those of the boundary cells at each cell around the perimeter of the model.

Numerical and GIS methods were used to estimate a monthly water level surface that was then used as an input to the GHB. The estimation of water levels with a monthly time step for the 11 years of the simulation created 133 monthly UFA surfaces that were then used to develop water levels for the aquifer and adjacent aquifers based on head differences for observed wells in each of the lower layers.

For the northern and southern boundaries, heads in the UFA (Layer 3) were developed from UFA potentiometric surface maps and supplemented with simulated water levels from existing groundwater models in areas of sparse observed data. Heads in the permeable layers associated with layers 4, 5, 7, 9, and 11 were estimated based on observed differences between heads in the UFA and the respective layers in paired wells. Water levels for the confining layers in the model were based on linear interpolation of boundary heads between the adjacent upper and lower aquifers. For the western (Gulf of Mexico) and eastern (Atlantic Ocean) boundaries, head-dependent flux boundaries were simulated using GHBs for layers 2, 3, 4, 5, western portion of 6, and eastern portion of 8, 9, and 11 based on equivalent freshwater heads. Figure 36 through 46 show each type of boundary condition for each layer within the model.

Estimation of Heads for Layer 3

The process to estimate monthly heads for the GHB Package involved constructing potentiometric surface maps for the UFA (Layer 3) for each monthly stress period of the simulation. Each well was assigned a model layer based on its casing and total depths in relation to the thickness of each layer defined in the model. If a well was open to multiple aquifers, the well was assigned to the model layer corresponding with the total well depth. Monitoring wells within the model domain were considered to establish a reasonable coverage over the area. Additional wells outside the active model domain were identified and used to ensure trends in the potentiometric surface beyond the model area were captured and adequately characterized. A minimum data availability of May and September for each year was established, though in some areas, where well coverage is poor, wells missing these values were infilled. In areas with highly sparse information, especially the southern boundary, simulated water levels from existing models that cover the same calibration period were utilized to fill in these areas.

To construct a potentiometric surface map for each month, the selected wells needed a minimum of one water level value per month during the simulation period. Two types of data infilling techniques were performed for wells with missing data: 1) linear infilling when data gaps of less than four months occurred, and 2) estimating missing water levels based on observed water level fluctuations from a nearby well or wells when more than four consecutive months of data are missing. Data for the well with available data were standardized to the standard deviation as follows:

$$X_{1,SV,m} = \frac{\left(X_{1,m} - \bar{X}_1\right)}{SD_{X1}}$$

where:
$X_{1,SV,m}$ = standardized value of X_1 (well with available data), for month m
$X_{1,m}$ = monthly value of X_1
$\bar{X}_1$ = mean value of X_1
SD_{X1} = standard deviation of X_1

The assumption is that the well with missing data will respond the same or similarly to the well with data, so the monthly standardized values would be the same. The monthly values for the infilled well data was estimated as follows:

$$X_{2,m} = \left(X_{1,SV,m} * SD_{X2}\right) + \bar{X}_2$$

where:
$X_{2,m}$ = estimated monthly value of X_2 (well with missing data) for month m
$\bar{X}_2$ = mean value of X_2
SD_{X2} = standard deviation of X_2

Monthly potentiometric surfaces were created using a Python script developed in the Spatial Analyst Tools extension in ArcGIS using the splining interpolation method. The interpolation extended beyond the active model boundary to capture trends beyond the active model domain. The monthly value used for the northern and southern GHB boundaries were selected as the value of the potentiometric surface located 1,250 feet from the center of the boundary cell in the direction outside the model grid perpendicular to the boundary (Figure 38).

Estimation of Heads for Layer 5

Existing wells completed in both the UFA (Layer 3) and APhpz (Layer 5) were used to estimate the head differences between the two model layers. A consideration was the proximity of the layer 5 well to the layer 3 well. To compare head differences between layers, only layer 5 wells in proximity (within a few hundred feet) to a layer 3 well were used as a paired well. Paired wells outside the model domain were identified and used to ensure trends beyond the active model area were captured and adequately characterized. The minimum data availability for inclusion was at least one observed value for every month during any given year for the paired wells.

The layer 3-layer 5 differences were obtained by subtracting the observed water levels in layer 5 from the observed water levels in layer 3 for the same month and year. The average difference for each well pair for each month of the simulation was calculated and contoured using ArcGIS to estimate the variability over the area. Though the differences typically vary along the model boundary, the differences did not significantly change over time and were therefore held constant throughout the simulation period. These head differences were applied to the layer 3 GHB heads to estimate layer 5 GHB heads.

Estimation of Heads for Layer 7

The process for selecting wells and obtaining differences between layers 3 and 7 is the same as for determining differences between layers 3 and 5. Only wells monitoring water levels in the UFA (Layer 3) and the LFA (Layer 7) were considered. To compare head differences between layers, only layer 7 wells near a layer 3 well were considered as a paired well. Paired wells outside the model domain were identified and used to ensure trends beyond the active model area are captured and adequately characterized. The minimum data availability for inclusion was at least one observed value for every month during any given year for the paired wells. Infilling was not performed for missing data. The layer 3 to layer 7 differences were created by subtracting the observed water levels in layer 7 from the observed water levels in layer 3. Though the differences may vary along the model boundaries, the differences between layers 3 and 7 should not significantly change over time and were held constant throughout the simulation period.

Estimation of Heads for Layer 9

Layer 9 head estimations were obtained by subtracting the observed water levels in layer 3 from the observed water levels in layer 9. Only wells monitoring water levels in the UFA (Layer 3) and the LFA (Layer 9) were considered. To compare head differences between layers, only layer 9 wells near a layer 3 well were considered as a paired well. Paired wells outside the model domain were identified and used to ensure trends beyond the active model area were captured and adequately characterized. The minimum data availability for inclusion was at least one observed value for every month during any given year for the paired wells. Infilling was not performed for missing data. The layers 3 to 9 differences were created by subtracting the observed water levels in layer 9 from the observed water levels in layer 3. Though the differences may vary along the model boundaries, the differences between layers 3 and 9 should not significantly change over time and were held constant throughout the simulation period.

Estimation of Heads for Layer 11

Water level information for aquifers below the upper most zone of the LFA (LFA I) is extremely limited and generally restricted to data collected during exploratory well construction. Continuous water level monitoring is generally unavailable and therefore a relationship was developed between existing LFA I and LFA II, similar to those described for the UFA and APPZ/LFA I. Several deep drilling sites suggest a noticeable head change occurs between LFA I and LFA II. The head drop variability across the model domain was established spatially using available borehole and geophysical logging information.

Estimation of Heads for Layer 2, Layer 4, Layer 6, and Layer 8

For the three confining layers in the model (Layers 2, 6, and 8) and the OCAPlpz (Layer 4), the boundary heads were linearly interpolated between the estimated heads for the two high producing layers vertically adjacent to layer 4 and for the confining layers. Therefore, boundary heads for layer 2 were linearly interpolated between heads in layers 1 and 3; boundary heads for layer 4 were linearly interpolated between heads in layers 3 and 5; for layer 6, the boundary heads were linearly interpolated between layers 5 and 7; and for layer 8 the boundary heads were linearly interpolated between layers 7 and 9.

Equivalent Freshwater Heads

The model simulates the freshwater flow system, and cells representing areas where each layer contained water with total dissolved solids (TDS) exceeding 10,000 milligrams per liter (mg/l) were made inactive. MODFLOW calculates head at the center of the grid cell reflects the equivalent freshwater head (EFH) corresponding to the elevation at the location. If the water quality is fresh, there is effectively no difference in head between the well casing depth and cell center. If there is a concentration gradient, there will be differences based on elevation and concentration. EFHs were assigned to the GHBs using the following formula:

$$h_f = \left(\frac{\rho_0}{\rho_f}\right) h_i - \frac{(\rho_0 - \rho_f)}{\rho_f} Z$$

Where:
ρ_f =Freshwater density at approximately 60 degrees F
ρ_0 =Density of groundwater at the given TDS concentration

h_i =Average measured (environmental) head in the well
h_f = Equivalent freshwater head
Z = Mid-point of the open interval if known, midpoint of layer if not

Estimated TDS values at each well with water quality data was based on X-Y location of the well and a "best estimate" calculated using measured values and previous GIS gridding work conducted by the SFWMD. These two approaches were combined in a single point shapefile and interpolated together using the natural neighbor algorithm in ArcMap. The rasters were generated for layers 3, 5, and 9. Layer 4 values were approximated using an average value between layers 3 and 5. Layers 6, 7, and 8 were set to the layer 5 values, and layers 10 and 11 were set to the layer 9 value.

Reasonable maximum and minimum TDS concentrations were calculated at each well based only on the interpolated values in the x-y plane to account for interpolation and measurement uncertainty. For most targets in all layers, the maximum TDS added was 500 mg/L and the minimum subtracted was 500 mg/L. Exceptions included three wells along the southeastern Atlantic coast in layer 5. The interpolated values at these locations seemed low compared to inland values, so the maximum value added 2,000 mg/L. In Desoto County, two high measurements believed to be possible isolated "upconing" interpolated out to cover more distance than may have been accurate. To handle the greater uncertainty at those targets, a range of +/- 2,000 mg/L was used.

MODFLOW calculates head at the cells center making estimates of conditions at the center of the cell important for the proper calibration of the model. The maximum and minimum TDS values were re-calculated using the mid-point elevation of the layer the target is in as the depth of the well. At some target locations, the bottom of the casing (where the EFH is typically computed) is over 100 to 200 feet above the cell center, below the cell center, or in a confining unit above the aquifer where it target is placed. In these instances, the casing elevations were adjusted so the bottom of the casing could not have an elevation above the layer in which the target is monitoring. If the casing elevation was above the top of the layer, the casing elevation was above the top of the layer, thereby assuming the TDS concentrations measured in the well were representative of the top of the aquifer the target is placed in. The TDS from the top/bottom of the modified target casing to the cell center was computed using the following assumption:

   i.   For measured/estimated TDS < 1,000 mg/L assume concentration gradient is 1,000 mg/L per 100 feet
   ii. For measured/estimated TDS > 1,000 mg/L assume concentration gradient is 5,000 mg/L per 200 feet

Although completed with a different methodology and approach, the freshwater extent of the aquifers based on the 10,000 mg/L TDS concentration in the ECFTX model very closely aligns with the delineation of freshwater zones in the UFA and LFA as defined in Figure 45, 49, and 50 by Williams and Kuniansky (2016) in their study of the Floridan aquifer system.

4.5 Aquifer and Confining Unit Properties

Hydraulic properties within the ECFTX model include hydraulic conductivity (both vertical and horizontal) and specific storage properties. The ECFTX model is fully 3-D in that top and bottom elevations (thicknesses) are assigned to each of the 11 layers. Initial estimates of hydraulic properties were assigned using field measurements, past modeling efforts, and prior knowledge

and are discussed below. During the calibration process, the initial estimates were adjusted within reasonable limits in order to improve the agreement between simulated and observed conditions while maintaining parameterization consistent with the conceptual model of the system described previously in Chapters 2 and 3. Results of the calibration are described in detail in Chapter 5.

Many aquifer performance test (APT) results were available for incorporation into the model. Most of the data are available for the UFA, which is the principal aquifer used throughout much of the state. The database was compiled from multiple sources including the SFWMD, SWFWMD, SJRWMD, USGS, USACE, various county governments, and numerous consultant reports. The APT points were analyzed and distributed throughout the model grid via kriging. Past modeling efforts within the ECFTX model domain were used to interpolate between APTs and in areas with sparse data. Models used were the ECFT model, Northern District Model (NDM), East Coast Floridan Model (ECFM), and District Wide Regulatory Model (DWRM). The ECFT model was used as highest priority, NDM and ECFM were second, and the DWRM was third.

HYDRAULIC CONDUCTIVITY

Hydraulic conductivity (K) is typically one of the most important input parameters used to develop and calibrate a groundwater model, as is the case with the ECFTX model. It represents the aquifer's ability to transmit water under a hydraulic gradient. K values are given in the horizontal and vertical flow direction. The horizontal K (Kh) value establishes how water flows between each cell within a given aquifer and the vertical K (Kv) establishes the relationship between different aquifers and confining units.

In the SA (Layer 1), K values typically range from 1 to 50 feet per day (ft/d) with most values between 10 and 20 ft/d. K values in the northwest portion of the model were 10 ft/d. The higher values of K were 50 ft/d in the ridge areas and along the east coast. Some lakes within the model domain were simulated as "high K" lakes. For these lakes, a K value of 1×10^6 ft/d was used.

The initial K values were based on APT data, past modeling efforts, and physiographic region locations. Hydraulic conductivity fields for Layers 1, 3, 5, 9, and 11 are shown in Figure 47 through 51. The hydraulic conductivity fields for all other layers are found in Appendix A.

TRANSMISSIVITY

Transmissivity is defined as the rate at which water is transmitted through a unit width of aquifer under a unit hydraulic gradient. Transmissivity is the product of the aquifer K and the saturated thickness and is expressed as feet squared per day (ft^2/d). Transmissivity is driven by Kh and represents a cell-to-cell transfer of water within an aquifer. MODFLOW requires the Kh and thickness as model input. Transmissivity can readily be calculated directly from these values.

As stated, the UFA is the primary water source within the CFWI region. An extensive amount of APTs have been conducted and were used as initial values for the model. Cumulative transmissivity values for the UFA (layers 3, 4, and 5) within the ECFTX model range between 2.5×10^3 ft^2/d to over 1×10^7 ft^2/d. Transmissivity values in the model domain were mostly between 2.5×10^3 ft^2/d and 2.5×10^4 ft^2/d. High transmissivity values are in the northwest, unconfined karst regions and southeast portions of the model domain. Additional areas of high transmissivity are from known localized karst features in Orange, Volusia, Hillsborough, and Desoto counties.

Middle confining unit I (layer 6) is simulated as below the APhpz within the UFA west of the Lake Wales Ridge. The Kh and Kv values within the western portion of the model domain for layer 6 were set uniformly at 10 ft/d. The transmissivity values range from 30 ft^2/d to 56,000 ft^2/d, with an average transmissivity of approximately 2,000 ft^2/d. As a product of thickness and horizontal hydraulic conductivity, the variations in transmissivity for this layer are a result of changes in aquifer thickness.

Layer 7 is simulated as the aquifer where MCU I and MCU II overlap within the central portion of the model (mostly in Polk, Lake, and Sumter Counties). Transmissivity values in the overlap area range from 20 ft^2/d to 2,800 ft^2/d. Transmissivity values to the west are uniformly set at 200 ft^2/d to represent the UFA below the APhpz. To the east of the overlap area, transmissivity values range from 10 ft^2/d to 100 ft^2/d and were derived during the calibration process. The small range of transmissivity values within layer 7 of the model is due to a uniform thickness of 20 feet, with variability in thickness only within the overlap area.

Middle confining unit II (layer 8) is simulated as part of the LFA east of the Lake Wales Ridge. The transmissivity ranges from 8 ft^2/d to 5,700 ft^2/d. Final transmissivity values were derived during calibration.

Several counties in the CFWI are currently using the LFA as a water source. However, for most of the state, APT data within the LFA is sparse. Data collected from areas where APTs have been performed were used to establish a starting value for hydraulic conductivity fields in the model within the LFA. Cumulative transmissivity values for the LFA (layers 9 and 11) ranged from 700 ft^2/d to greater than 1×10^6 ft^2/d. Transmissivity values in the LFA are generally low (700 – 5×10^3 ft^2/d) in the western portion of the model below MCU II and increase moving west-to-east towards Osceola and Orange counties where transmissivity is greater than 1×10^6 ft^2/d. Transmissivity of the UFA (layers 3-5) and LFA (layers 9-11) are shown in Figure 52 and 53.

LEAKANCE

Leakance coefficient is the volume of water that flows through a unit area of a semi-confining layer separating two aquifers per unit of head difference per unit of time. Leakance coefficient units are expressed in ft per day per ft (d^{-1}). Leakance is determined by the analysis of constant-rate aquifer test data from observation wells. Like the relationship between Kh and transmissivity, leakance is controlled by Kv and confining unit thickness and represents the vertical transfer of water between layers. The equation for the leakance coefficient is Kv/thickness. Leakance values are of importance for confining layers 2, 6, 8, and 10 as they represent the ICU, MCUs between the UFA and LFA, and semi-confining unit within the LFA. Initial values were implemented using APT data and past modeling efforts.

The intermediate confining unit (Layer 2) separates the unconfined SA and UFA. Most leakance values range from 1×10^{-3} d^{-1} to 1×10^{-6} d^{-1} except the northwest portion of the model. The UFA in this area is considered unconfined and layer 2 values were part of the UFA with values as high as 1×10^6 d^{-1}. The smallest Layer 2 leakance values occur within the tightly confined southern half of the ECFTX model domain. The average leakance value for layer 2 was approximately 1×10^{-4} d^{-1}.

Middle confining unit I (layer 6) is simulated as a confining unit in the eastern portion of the model separating the UFA from the LFA east of the Lake Wales Ridge. Typical leakance values east of the ridge vary between 1×10^{-3} d^{-1} to 1×10^{-6} d^{-1}. Final leakance values within the confining portion

of layer 6 were derived during calibration. West of the Lake Wales Ridge, layer 6 is simulated as below the APhpz.

Middle confining unit II (Layer 8) is simulated as a confining unit on the western portion of the model separating the UFA from the LFA west of the Lake Wales Ridge. Typical leakance values west of the ridge varied between $1x10^{-4}$ d^{-1} to $1x10^{-6}$ d^{-1}. Final leakance values within the confining portion of layer 8 were derived during calibration. East of the Lake Wales Ridge, layer 8 is simulated as the upper part of the LFA.

Layer 10 separates the LFA I from LFA II (layer 9 and 11). It has been described as a low permeability glauconitic layer. Limited data has been collected from this stratigraphic unit. However, data that has been collected from geophysical logging indicates a reduced hydraulic connection between the LFA I and LFA II. Leakance values for the model were based on the above-mentioned geophysical logs and ranged from $1x10^{-3}$ d^{-1} in the northwest and central portion of the model to $1x10^{-6}$ d^{-1} along the eastern and southern portion of the model.

Leakance coefficient values for layer 2 (ICU), layer 6 (MCU I), layer 8 (MCU II), and layer 10 (LFA semi-confining unit) are shown in Figure 54 through 57. Vertical K values assigned to these same layers are contained in Appendix B.

STORAGE

Specific yield (Sy) is defined as the volume of water an aquifer releases from storage per unit surface area of the aquifer per unit decrease in the water table elevation. Sy is dimensionless and is expressed as a decimal fraction The SA (Layer 1) is an unconfined aquifer with an initial Sy between 0.1 and 0.25. Most of the model domain had a Sy of 0.15 to 0.25. Sy values of 0.1 to 0.15 are within the southern portion of the Lake Wales Ridge and a small section in the northwest portion of the model running longitudinal just east of the Lake Wales Ridge that are the result of adjustments during calibration.

Storage coefficient is also a dimensionless term and is expressed as a decimal fraction. It is defined as the total volume of water an aquifer releases from or takes into storage per unit horizontal surface area of the aquifer per unit change in the component of head normal to that surface. Specific storage (Ss) is the volume of water a unit volume of saturated aquifer releases from storage for a unit decline in hydraulic head by expansion of water or compression of rock/soil matrix. Storage coefficients can be readily obtained from the APTs. Like the relationship between hydraulic conductivity and transmissivity, the model code requires a Ss value, which is calculated by dividing the storage coefficient by the aquifer thickness. The Ss values for layers 6 through 11 are assumed to be low and a constant value of 1x10-6/ft was assigned uniformly for all confining units. Storage coefficients for layers 2 through 5 were initially assigned based APT data and previous modeling efforts. The Ss value for layers 2 through 5 were adjusted during calibration. Final Ss values within the model ranged from $1x10^{-3}$/ft to $8x10^{-8}$/ft.

Sy values for layer 1 are shown in Figure 58. Storage coefficient values (specific storage x thickness) for the UFA (layers 3-5) and LFA (layers 7, 9, and 11) are displayed in Figure 59 and 60. Ss values assigned to all layers in the model are contained in Appendix C.

ANISOTROPY

Anisotropy is characterized as the ratio of horizontal to vertical hydraulic conductivity (Kh/Kv). The ratio of the horizontal hydraulic conductivity to the vertical hydraulic conductivity within a cell is defined as the anisotropy ratio. Anisotropy ratios used in the ECFTX model were determined based on layer conceptualization. For layers simulated as aquifers throughout the model domain (layers 1, 3, 4, 5, 7, 9, and 11), an anisotropy ratio (Kh/Kv) of 1:1 was used, allowing principal flow to exist in both the vertical and horizontal direction. For confining layers 2 and 10, an anisotropy ratio of 10:1 was applied allowing principal flow to exist in the horizontal direction. For layers 6 and 8, an anisotropy ratio of 10:1 was assigned within the confining portion of the layer, 5:1 within the transition zone between the confining unit and the aquifer, and 1:1 within the aquifer. Due to the uncertainty of anisotropy within each hydrostratigraphic unit, the anisotropy ratios were not modified during the calibration process.

4.6 Recharge and Evapotranspiration

Within Florida, recharge is derived primarily from rainfall in the area, the amounts of which can vary dramatically throughout the year. Mean rainfall and temperatures are similar in much of south Florida. In Fort Pierce (St. Lucie County), the mean average temperature is 62°F in January and 82°F in July and August. The mean annual rainfall is 53.96 inches, with most occurring in the month of September. Mean annual temperature for Lake Placid in Highlands County is 61°F in January and 81°F in July and August. The mean average rainfall there is 52.25 inches, with August being the wettest month.

Although the average annual rainfall and temperatures are relatively similar across the ECFTX model domain, large variations in the spatial and temporal distributions occur daily. These differences are obtained daily from rain gauges, NEXRAD radar, and climatic stations. This site-specific information is used when calculating the supplemental irrigation demands at the property level.

The amount of rainfall available for recharge to the SA is reduced by runoff and evapotranspiration (ET). ET generally accounts for approximately 70 percent of rainfall and the remaining 30 percent either runs off the land into drainage networks/streams/rivers or percolates into the ground as recharge. Recharge to the FAS within the study area occurs primarily from downward leakage from the SA through the Intermediate Confining Unit (ICU) into the Upper Floridan Aquifer (UFA). Stewart (1980) identified areas in Florida where recharge occurs to the FAS.

The amount of water available from the SA as recharge to the UFA depends on several variables. Areas where the soil is well drained are potentially good areas of moderate to high recharge capacity, while in areas with poorly drained soil, the recharge potential could be near zero because more runoff usually occurs in these areas. A second variable is the thickness and characteristics of the ICU. Areas where the ICU is not well developed and thin, or where local aquifers in the ICU make up a dominant percentage of the overall unit thickness, are prime areas for recharge because flow through this unit is less restrictive. The third primary variable is the downward hydraulic gradient between the SA and UFA. In other words, recharge requires the water levels in the SA to be higher than water levels in the underlying UFA and is proportional to the magnitude of the differences in water levels.

In the model domain, the area where all three of these variables exist is along the well-drained hills of the Lake Wales Ridge and Brooksville Ridge. A similar, but smaller ridge that acts as a

significant source of recharge to the model lies adjacent to the Kissimmee River, and is referred to as the Bombing Range Ridge. A third area of low-to-moderate recharge potential, termed the Osceola Plain, is along the east and west sides of the Kissimmee River. The Kissimmee River itself does not provide recharge, but rather, receives some discharge from the UFA depending on the degree of Middle Confining Unit (MCU) confinement.

Rainfall infiltration into the model domain was compared with studies conducted along the Lake Wales Ridge area that attempted to estimate recharge from the SA into the UFA as a result of rainfall and local stresses. Spechler and Kroening (2007) estimated the annual recharge to the FAS in Polk County at 2.1 inches/year over a 10-year period. Stokes (2005) calculated the average recharge to the FAS east of the Kissimmee River in Osceola and northern Okeechobee counties were generally between 0 and 4 inches/year in 1998 and 2004. This was determined from the hydraulic pressure differences between the FAS and SA aquifers, and aquifer/confining unit properties. Similar values for the same area were determined by Boniol et al. (1993). Sepulveda et al. (2012) calculated an average rainfall recharge rate to the ICU of 3.7 inches/year for central Florida. Stewart (1980), Tibbals (1990), and Yobbi (1996) calculated similar values -- generally less than 5-10 inches/year.

Simulated recharge rates will vary monthly based upon historical rainfall and vary spatially within the recharge zones. Total and spatial distribution of recharge was further adjusted during the calibration process as discussed in the calibration section.

4.6.1 Recharge and Evapotranspiration applied to the ECFTX model

The methodology used to develop Evapotranspiration (ET) and recharge to the SAS uses AFSIRS (Agricultural Field Scale Irrigation Requirement Simulations, Smajstrla 1990) together with the USDA National Resources Conservation Service (NRCS) Curve Number (CN) method for partitioning rainfall and runoff. (Restrepo and Giddings 1994, Bandara 2018). A program has been written to call AFSIRS for different land use polygons to calculate daily ET and recharge requirements, which are translated into model cell values. The model uses time-dependent data such as rainfall, irrigation return flows, potential evapotranspiration (PET), land use, crop types and time-independent data such as drainage basins, soil types, irrigated fractions of the model cell, and irrigation efficiencies.

First, drainage basins that contribute to the river flows were delineated and a GIS coverage was developed. Once the basins were delineated, gauged drainage basins were identified as candidates for the calibration process. Each model cell was assigned a predominant land use and soil type using the land use and soil type GIS coverages. The effective rainfall that goes into the AFSIRS program was calculated by subtracting runoff estimated using the NRCS CN method from rainfall (i.e., rainfall plus irrigation return flows) for each model cell. The effective rainfall was calibrated using the observed surface water flow data, which represents the surface runoff and baseflow components. By calibrating the effective rainfall, the correct ET and recharge values were passed to MODFLOW.

Within a given basin several land use types could exist. Therefore, the initial CN for a given basin was estimated as the area-weighted CN using all the land use types and associated curve numbers. Since CNs are dependent upon the antecedent moisture content of the soil, the CNs were adjusted based on the rainfall events during the calibration period (described in detail later in this section). Two different land use maps were used during the calibration periods 2004, and 2008/2009. Basin CNs were also adjusted to reflect the change in land use over the calibration

period. Figure 61 is a schematic showing the various input data and output data that the ET-recharge program uses and produces and how the different model components fit together.

Input Requirements:

GIS Coverage Input: Spatially referenced data are read from the program after overlaying the model grid with land use, soil-type, topography, and climatic (i.e., rainfall and ET) GIS coverages. The main inputs to the program are developed from the overlay process, which produce area-weighted values for each model cell.

Model Grid Arrays: The main inputs to the program related to model-grid-referenced data include: basin identification (ID) for water budget calibration purposes, basin ID for runoff curve number, and cell ID for active/inactive designation (Note: Curve numbers are empirical parameters and are used to estimate runoff from rainfall based on land use, etc.).

Reference Land Use Table: Look-up related land use tables to the following: crop type, curve numbers (CN), growing season, percent vegetation, impervious area; switch indicating if a polygon is irrigated or not; and water use type classification. Irrigated types include citrus, sugar cane, vegetable, pasture, sod, among others. Non-irrigated land use types include rangeland, upland forest, among others.

Evapotranspiration Input: The USGS Florida evapotranspiration (ET) database was used to assign reference ET across the model domain. The potential ET was computed from the reference ET and crop coefficients.

Rainfall Input: NEXRAD and/or National Weather Service data were used to assign rainfall data across the model domain as described under RAINFALL section.

Return Flow Input: Irrigation flows and other applications that introduce water into the unsaturated zone were included and added directly into the rainfall arrays.

Evapotranspiration: Evapotranspiration (ET) is the sum of vaporization by the combined process of evaporation and transpiration (Jensen et al. 1990). ET is the largest loss in the water budget in Florida. The ET rate from a crop depends on the type of crop, stage of growth, soil moisture content, and the amount of energy available. The reference crop ET (ET_R) was used to represent a baseline rate of ET for actively growing grass, which has an unlimited supply of soil water. Potential ET for other crops ($ET_{C,P}$) was calculated as the multiplication of ET_R and the crop coefficient (K_c).

$$ET_{PC} = K_c * ET_R$$

The source of the ET_R data was the USGS Statewide Evapotranspiration Information and Data web page: http://fl.water.usgs.gov/et/, where ET_R was developed based on ASCE Penman-Monteith method. (Jensen et al. 1990). The value of the crop coefficient depends on several factors including growth stage, the development of the crop canopy, and the amount of rainfall. It varies from 0.4-1.2 for most agricultural crops and varies from month to month during a year. The low values occur early in the crop growing seasons when vegetation canopies are incomplete, while the high values occur during peak growth stages. The crop coefficients increase following rain or irrigation due to increased evaporation from wet soil. AFSIRS provides tables of monthly crop coefficients for both perennial and annual crops. Daily crop coefficients were calculated within the AFSIRS program using linear interpolation and adjusted based on the daily rainfall.

Since the AFSIRS program is designed to estimate agricultural irrigation demands, it does not provide crop coefficients for non-irrigated crop types, such as upland forests. In such cases, K_c values were determined by comparing the crop type in the land use GIS coverages with the AFSIRS data base crop description. During the calibration process, these assumed K_c values were adjusted if necessary, to better reflect the reality.

Total crop evapotranspiration (ET_c) was calculated as the sum of unsaturated zone ET (ET_{UZ}) and groundwater ET (ET_{GW}) as,

$$ET_c = ET_{UZ} + ET_{GW}$$

Unsaturated zone ET (ET_{UZ}) was calculated within the AFSIRS program. The AFSIRS program does not directly output ET_{UZ}, thus source code was modified to properly account and output ET_{UZ}. Once ET_{UZ} is calculated, maximum ET_{GW} is calculated using the above equation. The maximum ET_{GW} was provided as an input to MODFLOW, which uses the simulated depth to the water table and the crop root zone depth to calculate the actual ET_{GW}. Actual groundwater ET varies linearly with water table depth, with maximum ET rate at the ground level and zero at the root zone depth (Extd).

Groundwater ET for a model cell, $V_{cell,ET}$ is calculated as:

$$V_{cell,ET} = \sum_{i=1}^{nLU} (ET_{C,P,i} - ET_{UZ,i}) * A_{perv,i}$$

where $A_{perv,i}$ is the pervious area of the land use class i. Pervious areas are calculated using the National Land Cover Database (NLCD) data set. In well irrigated areas, crop ET requirement is assumed to be met by irrigation. Therefore, in well-irrigated areas, groundwater ET approaches zero. In open water conditions where surface water and groundwater are connected, it was assumed the ET requirement was completely met by groundwater and therefore groundwater ET approaches potential ET (PET).

The CN method developed by NRCS, formerly known as the Soil Conservation Service (SCS),) (1986), was used to compute runoff (SCS, 1986). The net rain (infiltration and retention) was computed as the rainfall, plus return flows, minus runoff; however, additional criteria was used to consider antecedent conditions and high rainfall conditions.

Curve numbers were selected according to the antecedent moisture contents (AMC) as per the SCS classification (Soil Conservation Service, 1972, Table 42. P. 4.12.). According to this classification, a dry condition was defined as the condition when the total 5-day antecedent rainfall (in) is less than 0.5 during the dormant season or less than 1.4 during the growing season. Wet condition is defined as the condition when the total 5-day antecedent rainfall (in) is over 1.1 during the dormant season or over 2.1 during the growing season. The condition in between these two are defined as normal conditions. Curve numbers are selected from AMC I, AMC II, or AMC III categories for the dry, normal, and wet conditions, respectively.

If dry conditions existed, an additional retention factor was added to the NRCS initial abstraction. The retention factor is a user input and was adjusted during calibration. This procedure considers antecedent conditions to limit runoff when there is potential for additional soil storage.

The majority of Florida soils are sandy with very high infiltration capacity; therefore, runoff generation occurs mainly due to a saturation excess mechanism. Runoff was calculated for each model cell and accumulated by watershed. Runoff volume for each model cell ($V_{cell,roff}$) was calculated as:

$$V_{cell,roff} = \sum_{i=1}^{nLU} D_{roff,i} * A_{roff,i}$$

where subscript i indicates the land use class i within the model cell, $D_{roff,i}$ is the runoff depth, $A_{roff,i}$ is the area of runoff, nLU is the number of land uses within the cell. In the present work nLU is limited to 3 predominant land use categories. The area of runoff is the area that is directly connected to drainage features that contribute to the basin outflows. The directly connected impervious areas ($DCIA$) are calculated using Sutherland's equations (Sutherland, 2000; Table 5).

In open water conditions, runoff was assumed to be negligible during the dry season and assumed to be high during the wet season. Thus, the model calculates runoff only during the wet season using a higher CN. In closed basins, where runoff does not leave the basin and ridge physiographic province areas, where runoff potential is very small, runoff was assumed to be zero.

Effective rainfall ($Rain_{eff}$) is the portion of rainfall that is available for plant evapotranspiration and is calculated as:

$$Rain_{eff} = Rain - Runoff - IA$$

where *IA* is the initial abstraction

For closed basins and in ridge areas, runoff was assumed to stay within the watershed. Thus, the total rainfall was effective after accounting for initial losses in closed basins and ridge areas.

The ET-Recharge program was used to transform the direct runoff (from NRCS) to a routed flood hydrograph using the Muskingum hydrologic routing procedure (Cunge 1969). The direct runoff computed with the NRCS equation for all areas was accumulated by basin in preparation for the Muskingum hydrologic routing procedure.

The Muskingum method is a hydrologic river routing technique based on the continuity equation and the linear reservoir relationship. This method is adaptable to a simple mathematical solution with variables such as a weighting factors for inflow and outflow rates, a storage time constant, and travel time constant. The inflow hydrograph was made up of the direct runoff from each basin. The result of the Muskingum transformation was a routed hydrograph curve with an equivalent volume to the inflow hydrograph curve. The Muskingum parameters were calibrated by correlating routed runoff with the actual observed flow values.

Table 5. Sutherland Equations to Determine DCIA (%).

Watershed Selection Criteria	Assumed Land Use	Land Use FLUCCS Code	Equation (where ImpA(%)>= 1)
Average: Mostly storm sewered with curb & gutter, no dry wells or infiltration, residential rooftops not directly connected	Commercial, Industrial, Institutional, Open land, and Medium density residential	1200, 1400, 1500	$DCIA=0.1(ImpA)^{1.5}$
Highly connected: Same as above but residential rooftops are connected	High density residential	1300	$DCIA=0.4(ImpA)^{1.2}$
Totally connected: 100% storm sewered with all IA connected	-	3000-7000	$DCIA=ImpA$
Somewhat connected: 50% not storm sewered, but open section roads, grassy swales, residential rooftops not connected, some infiltration	Low density residential	1100	$DCIA=0.04(ImpA)^{1.4}$
Mostly disconnected: small percentage of urban area is storm sewered, or 70% or more infiltrate/disconnected	Agricultural Forested	2000	$DCIA=0.01(ImpA)^{2}$

Note: ImpA = Impervious area.

AFSIRS simulates a daily water balance in the unsaturated zone (UZ). Originally developed for determining irrigation demands, it was adapted to simulate the UZ water balance in non-irrigated areas as well. Databases for AFSIRS include a crop database, an irrigation data base, and a soils data base. The crop database includes the crop type, monthly crop coefficients, the total and irrigated crop root depths and allowable soil water depletion by month. The irrigation database contains the irrigation system type, the application efficiency of the irrigation system, the percent irrigated soil surface areas and the ET fraction assumed to be extracted from the irrigated portion of the crop root zone. The soils database includes available soil type, vertical conductivity and porosity.

The AFSIRS model is based on a water budget of the crop root zone and the concept of crop ET can be estimated from PET. The water budget includes inputs to the crop root zone from rain and irrigation, and losses from initial abstraction, runoff, deep percolation and potential crop ET (ET_{PC}). The water balance equation within the crop root zone of a polygon can be written as:

$$\Delta STO = Rain + IRR - RCH - Runoff - IA - ET_{PC}$$

where ΔSTO is the change in soil storage (inches), $RAIN$ is the rainfall (inches), IRR is the irrigation (inches), RCH is the deep percolation or groundwater recharge (inches), $Runoff$ is the runoff (inches), and IA is the initial abstraction (inches). In non-irrigated areas IRR term becomes zero.

In AFSIRS, the control volume is the available water content of the plant's root zone. If incoming rainfall (or irrigation) exceeds this control volume, the excess volume ("drainage") is simply discarded as the combined process of runoff and recharge to the SZ. In the current approach, runoff (from the CN calculations) is removed from the daily rainfall, aka 'effective rainfall', and then used as input to AFSIRS. This essentially makes the AFSIRS "drainage" output equal to the recharge to the SZ, which is passed to the MODFLOW model.

Recharge volume for a model cell ($V_{cell,RCH}$) is calculated as:

$$V_{cell,RCH} = \sum_{i=1}^{nLU} DRN_i * A_{perv,i} + Rain_{eff} * (A_{imperv,i} - DCIA_i)$$

where $A_{imperv,i}$ is the impervious area of the land use polygon i. The second term in the equation represents the groundwater recharge that can occur within impervious areas such as urban developments where runoff is routed to on-site lakes or ponds.

For non-irrigated areas, the vegetation utilized the available water in the unsaturated zone and, if the plant's water extraction depth is deep enough, supplemented the additional demands from the water table. AFSIRS was used to calculate both the overall PET for the crop (from PETc=RET*Kc) as well as the amount of water extracted from the unsaturated zone (ETc,uz). ETc, uz is based on the daily water balance of rainfall, PETc and available soil water storage. The potential saturated zone ET (PETc,sz) is equal to PETc minus ETc,uz. PETc,sz was passed to MODFLOW, which calculated actual saturated zone ET (ETc,sz) based on the distance from the ET surface to the water table, and on the extinction depth for a specific crop type.

In well-irrigated areas, the calculations were the same except irrigation was applied when the soil moisture storage was depleted to a specified level (the maximum allowable depletion). Thus, the potential saturated zone ET (PETc,sz) approached zero for irrigated areas. Nonetheless, PETc,sz for irrigated areas was also passed to MODFLOW. Both ET and recharge are assumed to be negligible in the impervious areas due to runoff. Figure 62 is a flow chart that describes the ET-Recharge program.

4.6.2 Recharge and Evapotranspiration model validation

The ET-Recharge program was successfully verified against field-measured data within the ECFTX model domain. The field data represents different geographic regions with the study area and includes the Lake Wales Ridge area in Orange County, Blue Cypress marsh site in Indian River County, Starkey pasture site in Pasco county, and University of Central Florida (UCF) site in Orange County (Bandara, 2018).

Figure 63 and 64 show the spatial distribution of simulated runoff for 2004 (wet year) and 2012, (dry year) respectively. Generally, the simulated runoff is lowest in highly drained soil conditions or in deep water table conditions such as in Lake Wales Ridge, Brooksville Ridge, Bombing Range Ridge, Deland Ridge and in closed basins. Simulated runoff is highest in areas where the soil is poorly drained or areas where shallow water table conditions exist, such as the southwest portion

of the model domain (Manatee, Hillsborough, Hardee, Pasco, Pinellas Counties) and river flood plains (Peace river, Kissimmee river, St. Johns river). Figure 65 and 66 show the spatial distribution of unsaturated evapotranspiration (UZET) developed using the ET-Recharge program for 2004 (wet year) and 2012 (dry year), respectively. UZET is highest when the thickness of the unsaturated zone is greater or in deep water table conditions such as Lake Wales Ridge, Brooksville Ridge, Bombing Range Ridge and Deland Ridge. UZET is lowest when the thickness of the unsaturated zone is small to non-existent or in shallow water table conditions such as river flood plains.

Figure 67 and 68 show the spatial distribution of maximum evapotranspiration developed using the ET-Recharge program for 2004 (wet year) and 2012 (dry year), respectively. Maximum ET is an input to MOFLOW and is highest in open water bodies and shallow water table conditions, while it is lowest in deep water table conditions. Figure 69 and 70 show the spatial distribution of gross recharge developed using the ET-Recharge program for 2004 (wet year) and 2012 (dry year), respectively. Gross recharge is an input to MODFLOW and is highest in highly drained soil conditions, deep water table conditions, closed basins, or in open water bodies, while it is lowest in poorly drained soil conditions or shallow water table conditions.

Figure 71 and 72 show the spatial distribution of MODFLOW simulated groundwater evapotranspiration (ET) for 2004 (wet year) and 2012 (dry year), respectively. MODFLOW simulated ET depends on the maximum ET provided (Figure 67 and 68), simulated depth to the water table, and extinction depth of the plants. Figure 73 shows the spatial distribution extinction depths used for 2004 (Shat et al. 2007). Generally, the simulated groundwater ET is highest underneath open water or shallow water table conditions, such as rivers, lakes, wetlands and river flood plains. The simulated groundwater ET is lowest in deep water table conditions or in urban areas due to lack of tree cover. Figure 74 and 75 show the spatial distribution of simulated net recharge for 2004 (wet year) and 2012 (dry year), respectively. Net recharge here is defined as the difference between the gross recharge and the MODFLOW simulated groundwater ET. Generally, the net recharge is highest in highly drained soil conditions and in deep water table conditions such as in Lake Wales Ridge, Brooksville Ridge, Bombing Range Ridge and Deland Ridge areas. Net recharge is lowest or negative (aquifer is discharging) in poorly drained soil conditions and shallow water table conditions such as in river flood plains of the Kissimmee River, St. Johns River and Peace River.

4.7 Baseflow

The consulting firm Jones Edmunds and Associates, Inc., in agreement with the water management districts, estimated the groundwater baseflow using a separation technique developed by Perry (1995). The method uses a low-pass filter that works with a window of a characteristic time length using USGS gages with flow data. A time length of 121 days was used, which includes a time span of 60 days before and 60 days after the specified date. The 121-day period was selected due to Florida generally having low slope, large surface storage attenuation, and a four-month summer rainy season. A minimum daily flow is calculated for each 121-day period as the window is advanced each day through the record. The resulting calculated minimum daily flow values are a smoothed series of minimum flows that represent the estimated daily baseflow. With the model calibration period of 1/1/2003 to 12/31/2014, flow measurements from 11/2/2002 to 2/28/2015 were used. Baseflow estimates are only representative of the available data. If a gap in flow data greater than the 121-day window occurred, the baseflow separation was not performed and no data was recorded for the period. Baseflow was also not estimated at gages with managed structures.

Baseflow estimates using the "Perry" method or also referred to as the USF method were compared to other baseflow estimation methodologies. The USGS Groundwater Toolbox (version 1.3.1) includes six hydrograph-separation methods and two digital filtering methods to calculate baseflow (Barlow et al., 2017). The six hydrograph-separation methods include two Base-Flow Index (BFI) methods adopted from the BFI program developed by Wahl and Wahl (1995) with slight modifications, three Hydrograph Separation Program (HYSEP) methods adopted from the HYSEP program developed by Sloto and Crouse (1996), and PART method adopted from the PART program developed by Rutledge (1998) with a small change. The two BFI methods are Standard BFI and Modified BFI, and the three HYSEP methods are Fixed Interval HYSEP, Sliding Interval HYSEP, and Local Minimum HYSEP. The two digital filtering methods include the SWAT BFLOW method and the Eckhardt method. The SWAT BFLOW method is a one-parameter digital filtering method using the Lyne and Hollick (1979) low-pass filter based on the assumption that baseflow is the low frequency component of streamflow. The Eckhard method uses a two-parameter filter based on the assumption that aquifer outflow is linearly proportional to storage (Eckhard, 2005).

Comparison of baseflow estimation methods for the North Florida-Southeast Georgia (NFSEG) model for the St. Mary's River gage using the USF and USGS toolbox methods yielded values ranging between 50 and 280 cfs in 2009. The USF method (Perry, 1995), initially used to estimate baseflow for the ECFTX model, was the lowest of nine different methodologies to estimate baseflow. This analysis suggests total estimated baseflow may be up to 10 times greater than the USF methodology. Therefore, a range of estimated baseflow was defined at each of the 18 non-structured gages using the various methodologies described above (Table 6). The location of the unstructured gages is shown in Figure 76.

4.8 Rivers

The MODFLOW River Package was used to simulate effects of flow between rivers, streams, and canals on the groundwater system. This is accomplished by adding terms representing seepage to or from the surface water features to the groundwater flow equation for each river cell affected by seepage (USGS, 2005). The river boundary condition is head-dependent in which the model computes the difference in head between the boundary stage (river cell) and the head in the corresponding active model cell (aquifer). This head difference is multiplied by the conductance term to calculate the flux of water flowing in or out of the aquifer. MODFLOW performs an additional check prior to computing flow rates for cells with modeled head below the river bottom elevation (RBOT); the difference in head is computed as stage minus RBOT. Therefore, flow rates reach a maximum value when an unsaturated zone exists beneath the river (GWV6, 2011).

Table 6. Ranges of 2003-2014 average baseflow estimates using the USF method and eight USGS Groundwater Toolbox methods.

Gauge	Station	Min (cfs)	Max (cfs)	Max/Min Ratio
02232400	ST JOHNS RIVER NR COCOA FL	222	932	4.20
02232500	ST JOHNS RIVER NR CHRISTMAS FL	314	1125	3.59
02234000	ST JOHNS RIVER ABOVE LAKE HARNEY NR GENEVA FL	496	1549	3.12
02236000	ST JOHNS RIVER NR DELAND FL	491	3233	6.59
02238000	HAYNES CREEK AT LISBON	17	86	5.06
02294650	PEACE RIVER AT BARTOW	23	140	6.04
02294898	PEACE RIVER AT FORT MEADE	22	163	7.26
02295637	PEACE RIVER AT ZOLFO SPRINGS	86	385	4.48
02296750	PEACE RIVER AT ARCADIA	130	684	5.27
02298830	MYAKKA RIVER NR SARASOTA	18	181	9.90
02300500	LITTLE MANATEE RIVER NR WIMAUMA	25	96	3.80
02301500	ALAFIA RIVER AT LITHIA	58	203	3.51
02303000	HILLSBOROUGH RIVER NR ZEPHYRHILLS	69	159	2.29
02310000	ANCLOTE RIVER NR ELFERS	5	46	9.20
02312000	WITHLACOOCHEE RIVER AT TRILBY	38	209	5.54
02312500	WITHLACOOCHEE RIVER AT CROOM	74	277	3.71
02312762	WITHLACOOCHEE RIVER NR INVERNESS	194	471	2.43
02313000	WITHLACOOCHEE RIVER NR HOLDER	288	616	2.14

The MODFLOW input files for rivers and streams in the ECFTX model were initially prepared by Jones Edmunds & Associates, Inc. While developing the River package, bi-monthly meetings were held between Jones Edmunds & Associates, Inc. and water management districts to make decisions discussed below. Additional information on the River package development can be found in Appendix D.

Identification for rivers and streams to simulate using river cells in the ECFTX model included: rivers/streams previously simulated in the ECFT model, perennial rivers/streams identified in the Florida Department of Environmental Protection (FDEP) National Hydrologic Dataset (NHD) with a Strahler Order greater than or equal to 3, and rivers/streams with a Strahler Order of less than 3 if the river/stream had sufficient data (defined as more than 6 months of continuous data). Some cells that did not meet the above-stated criteria were added to create continuous reaches along the NHD flowlines that connected to higher order flowlines. River cells that met the above-stated criteria and overlapped drain cells were removed as long as they did not belong to rivers/streams from the ECFT model, were not part of a gauged river/stream segment and did not create a gap in a continuous river segment.

River stage and bottom elevations were assigned using a Digital Elevation Model (DEM) provided by the districts and the NHD. River elevations were determined using 357 gauging stations within the model domain and infilled between each gauge using the Inverse Distance Weighting interpolation method in GIS. All river bottom elevations were set at a minimum of 2 feet below the minimum stage elevation. A bed thickness of 1 foot was assigned to all river segments.

Vertical hydraulic conductivities were initially assigned from previous modeling efforts. If a river/stream cell overlapped a simulated river/stream in the ECFT model, the vertical hydraulic conductivity from the ECFT model was used. Other models used were SWFWMD's Northern District Model (NDM) and the District Wide Regulatory Model (DWRM). In some instances, an overlap from previous modeling efforts did not exist. In these cases, the vertical hydraulic conductivity was assigned based on Strahler Order with higher conductivity (connection) associated with a lower Strahler number.

Drainage basin boundaries used for the River package were supplied by the districts. The United States Geological Survey (USGS) Hydrologic Unit Classification (HUC) coding system was used, interpreted and digitized from the USGS 1:24,0000 quadrangles.

During model construction and calibration, modifications were made to the final RIV Package deliverable from Jones Edmunds & Associates, Inc. A total of 224 river cells were deleted due to overlapping drain cells for a total of 15,620 rivers/streams simulated using the River package (Figure 77). Conductance values were modified during calibration process to better represent baseflow.

4.9 Lakes

Like rivers, all lakes that met the criteria to be represented as a boundary condition were initially simulated using the River package. The MODFLOW input files for the lakes in the ECFTX model were prepared by Interflow Engineering, LLC. While developing the River package for the lakes, bi-monthly meetings were held between Interflow Engineering, LLC and the water management districts to make the conceptual decisions discussed below. Additional information on the River package development for the lakes can be found in Appendix E.

Lakes simulated as river cells in the ECFTX model included lake areas greater than or equal to half a grid cell and lakes monitored during the simulation period with observed stage data. Lakes also simulated as river cells included areas less than one grid cell but greater than half a grid cell at least one mile away from other lakes or hydraulically connected to another lake. The number of lakes simulated using the River package (RIV) was 483. This number included closed basin and open basin lakes.

Lake stage data was provided by the districts to Interflow Engineering, LLC. In the case of missing data, the dataset was infilled using one of four different infilling methods selected on a case-by-case basis. Bathymetry data for lake bottoms were provided for most of the lakes within the model domain. An offset of 5 feet below the lowest recorded lake stage was used as the lake bottom for lakes with no bathymetry.

Lakebed conductance values were compared with those used in previous modeling efforts, including 350 lakes modeled in the ECFT model within the CFWI region. Lakebed conductance values that did not overlap previous modeling efforts were based on assumed lakebed thicknesses of 5 feet, and 10-20 feet in the case of sandy bottom lakes. Typical initial conductance values ranged from 0.1 ft^2/d for sandy bottom lakes to 0.001 ft^2/d for silty/clayey bottom lakes.

During model construction and calibration, modifications were made to the River package for simulating lakes. Based on peer review comments, lakes were subdivided into two categories: closed basin and open basin lakes. Closed basin lakes were simulated as high conductivity features with a specific yield of 1. Some closed basin lakes within the SJRWMD were known to have drainage wells on the lakes and were simulated using the DRT package. Open basin lakes continued to be simulated using the River package. A total of 94 lakes were simulated as high conductivity features, 23 lakes were simulated using the DRT package, and 366 lakes were simulated using the River package for a total of 17,001 river cells (Figure 78).

Lakebed conductance values were modified during the calibration process. A targeted flux of 10 to 20 in/yr from a river cell to the underlying aquifer was considered reasonable based on previous Minimum Lake Level modeling within the SWFWMD and the SJRWMD. Lakebed conductance values were modified accordingly until this range of flux was achieved.

4.10 Wetlands

Individual wetlands are not directly simulated in the ECFTX model due to localized water level variations and their small size. The CFWI Environmental Measures Team (EMT) have defined three wetland classes based on long-term water level data, wetland edge elevation, and known hydrologic stress conditions (CFWI EMT, 2019). Class 1 wetlands meet all the aforementioned conditions and are the only wetland class with long-term water level data. There are 53 Class 1 wetlands within the model domain and 42 within the CFWI region. Of the 42 CFWI wetlands, 4 Class 1 wetlands are simulated as high conductivity features, 16 are simulated as River package lakes or are adjacent to River package lakes, and 22 did not meet the criteria or were not adjacent to a water body that met the criteria to be simulated as a high conductivity feature or as part of the River package. Of the 42 CFWI Class 1 wetlands, 20 are significantly influenced by open-water boundary conditions.

4.11 Springs

Springs are represented in the ECFTX model using MODFLOW's drain (DRN) package (McDonald and Harbaugh, 1988). The drain package is used to simulate the head-dependent transfer of water from groundwater to surface water; however, drains do not allow water to be transferred from surface water to groundwater. Once simulated head in the model cell falls below the threshold elevation, the flux to the spring drain cell drops to zero.

The locations of all 158 springs simulated in ECFTX model are shown in Figure 79 and spring information is given in Table 7. Data for the springs, including discharge rates, elevations, and conductance, were provided by the SWFWMD and the SJRWMD (2013). The springs shown in Figure 79 and Table 7 include magnitude 1 and 2 springs with relatively continuous discharge measurements. Of the 158 springs, 17 in total have continuous observed discharge data. The remaining 141 springs are mostly smaller magnitude 3 or 4 flow rates, with either no continuous discharge, or very few estimated values. Many of these small springs have no measured flow values and were assigned flow rates of 5 cfs or less based on previous model estimates or published literature. Observed discharge was estimated from published literature or previous models. The total annual mean spring flow within the model domain is approximately 2,159 cfs for the 2003-2014 simulation period.

Based on hydrogeologic and water quality evidence, each spring drain cell is assigned to one model layer. All spring drain cells are assigned to layer 3 (UFA) except for two springs: Warm Mineral Spring and Little Salt Spring. These two are assigned to layer 5 (APPZ) based on their more mineralized water quality characteristics and published information (Metz, 2016). Values of hydraulic conductance of spring drain cells are initially estimated from hydrogeologic evidence and previous models. Values of pool stage elevation for spring drain cells were based on measured or estimated elevations from previous models or reports.

The Rainbow spring group is located along the northern boundary of the model. Only 12 percent of the springshed is represented in the active ECFTX model domain. Therefore, flows were adjusted downward to approximately 12 percent of measured values for the calibration process. This was done to minimize potentially large, lateral boundary fluxes along the northern part of the model domain if the entire observed flow was simulated.

Wekiva Falls was an artesian well with no method of flow control prior to 2014. It was simulated using the DRN package during the calibration period just like the other springs. This method was chosen because the flow from Wekiva Falls was dependent on groundwater levels in the UFA during the calibration period. After the calibration and verification period of 2003-2014, the well was equipped with a method to control the flow from the well. Therefore, Wekiva Falls was simulated differently in the future projection simulations. This location was changed to a well designation and was set to zero conductance in the DRN package (zero flow). It was added as a constant withdrawal rate in the well package for the scenario runs that simulate projected future groundwater withdrawals.

Table 7. Estimated and measured flow from springs in the ECFTX model domain from 2003-2014.

Spring ID	SPRING_NAM	COUNTY	Mean Annual Flux (CFS)	Model Layer
1	WARM MINERAL SPRING	Sarasota	9	5
2	LITTLE SALT SPRING	Sarasota	2	5
3	LITHIA SPRING MAJOR	Hillsborough	35	3
4	BUCKHORN MAIN SPRING	Hillsborough	12	3
5	ULELE SPRING	Hillsborough	1	3
6	EUREKA SPRING	Hillsborough	1	3
7	LOWERY PARK SPRING	Hillsborough	2	3
8	LETTUCE LAKE SPRING	Hillsborough	8	3
9	SULPHUR SPRING (HILLSBOROUGH)	Hillsborough	35	3
10	PURITY SPRING	Hillsborough	0.1	3
11	CRYSTAL BEACH SPRING (PINELLAS)	Pinellas	3	3
12	HEALTH SPRING	Pinellas	1	3
13	TARPON SPRINGS (PINELLAS)	Pinellas	2.5	3
14	CRYSTAL MAIN SPRING (PASCO)	Pasco	45	3
15	SEVEN SPRINGS (PASCO)	Pasco	5	3
16	SALT SPRINGS (PASCO) #1	Pasco	8	3
17	HUDSON SPRINGS	Pasco	5	3
18	HORSESHOE SPRING	Pasco	10	3
19	ISABELLA SPRING	Pasco	5	3
20	MAGNOLIA SPRING	Hernando	1	3
21	GATOR SPRING (HERNANDO)	Hernando	0.5	3
22	BOBHILL SPRING	Hernando	2	3
23	ARIPEKA SPRING #2	Hernando	5	3
24	BOAT SPRINGS	Hernando	0.4	3
25	WEEKI WACHEE SPRING	Hernando	160	3
26	JENKINS CREEK SPRING	Hernando	15	3
27	HOSPITAL SPRING	Hernando	1	3
28	SALT SPRING (HERNANDO)	Hernando	22	3
29	MUD SPRING (HERNANDO)	Hernando	17	3
30	WILDERNESS SPRING	Hernando	1	3
31	BLIND SPRING	Hernando	43	3
32	BLUE RUN SPRING (HERNANDO)	Hernando	5	3
33	RYLES SPRING	Hernando	8	3
34	RITA MARIE SPRINGS #2	Hernando	1	3
35	BETEEJAY SPRING	Hernando	7	3
36	BAIRD SPRING #1	Citrus	3	3
37	CHASSAHOWITZKA SPRING MAIN	Citrus	60	3
38	CRAB CREEK SPRING	Citrus	47	3

Spring ID	SPRING_NAM	COUNTY	Mean Annual Flux (CFS)	Model Layer
39	LETTUCE CREEK SPRING	Citrus	1	3
40	SALT CREEK HEAD SPRING (CITRUS)	Citrus	0.4	3
41	POTTER CREEK SPRING (CITRUS)	Citrus	17	3
42	SHADY BROOK HEAD SPRING #4	Sumter	1	3
43	BELTONS MILLPOND MAIN SPRING	Sumter	1	3
44	BELTONS MILLPOND HEAD SPRING 1	Sumter	1	3
45	BELTONS MILLPOND HEAD SPRING 2	Sumter	1	3
46	BELTONS MILLPOND HEAD SPRING 2A	Sumter	1	3
47	BELTONS MILLPOND HEAD SPRING 2B	Sumter	1	3
48	BELTONS MILLPOND HEAD SPRING 3	Sumter	1	3
49	BELTONS MILLPOND HEAD SPRING 4	Sumter	1	3
50	BIG HOLE SPRING (SUMTER)	Sumter	3	3
51	CANAL 485 SPRING 5	Sumter	3	3
52	CANAL 485A SPRING 1B	Sumter	3	3
53	CANAL 485A SPRING 2	Sumter	3	3
54	HIDDEN RIVER HEAD SPRING	Citrus	13	3
55	OTTER CREEK SPRING	Citrus	1	3
56	SHADY BROOK HEAD SPRING #3	Sumter	1	3
57	SUMTER BLUE SPRING	Sumter	5	3
58	BLUEBIRD SPRINGS	Citrus	1	3
59	FENNEY SPRING	Sumter	15	3
60	HOMOSASSA SE FORK HEADSPRING	Citrus	40	3
61	MCCLAIN SPRING	Citrus	6	3
62	TROTTER SPRING #1	Citrus	6	3
63	TROTTER MAIN SPRING	Citrus	6	3
64	PUMPHOUSE SPRINGS	Citrus	6	3
65	BELCHER SPRING	Citrus	7	3
66	ABDONEY SPRING	Citrus	6	3
67	HOMOSASSA SPRING #1	Citrus	83	3
68	ALLIGATOR SPRING (CITRUS)	Citrus	1	3
69	HALLS RIVER SPRING #1	Citrus	6	3
70	HALLS RIVER HEAD SPRING	Citrus	123	3
71	A. WAYNE LEE SPRING	Sumter	5	3
72	HENRY GREEN SPRING	Sumter	5	3
73	SIDS SPRING	Citrus	1	3
74	BLACK SPRINGS (CITRUS)	Citrus	1	3
75	GOLFVIEW BOATHOUSE SPRING	Citrus	1	3
76	DAVES QUEST SPRINGS #1	Citrus	1	3

Spring ID	SPRING_NAM	COUNTY	Mean Annual Flux (CFS)	Model Layer
77	TARPON HOLE SPRINGS #2 COMPLEX	Citrus	3	3
78	FWS SPRING COMPLEX	Citrus	1	3
79	ART SPRING	Citrus	1	3
80	PARKER ISLAND SPRING (CRYSTAL SPRING GROUP)	Citrus	350	3
81	IDIOTS DELIGHT SPRING #2	Citrus	3	3
82	THREE SISTERS SPRING #1	Citrus	3	3
83	MANATEE SANCTUARY SPRING COMPLEX	Citrus	100	3
84	HUNTER SPRING	Citrus	1	3
85	HOUSE SPRING	Citrus	5	3
86	CATFISH SPRING (CITRUS)	Citrus	1	3
87	POOL SPRINGS	Citrus	1	3
88	MILLERS CREEK SPRING COMPLEX	Citrus	1	3
89	GUM SPRING MAIN	Sumter	64	3
90	ALLIGATOR SPRING (SUMTER)	Sumter	5	3
91	CITRUS BLUE SPRING	Citrus	3	3
92	WILSON HEAD SPRING (MARION)	Marion	2	3
93	RAINBOW SPRING #8	Marion	2	3
94	RAINBOW CAVE SPRING	Marion	2	3
95	RAINBOW SPRING #7	Marion	2	3
96	RAINBOW SPRING #6	Marion	2	3
97	INDIAN CREEK SPRING (MARION) #3	Marion	1	3
98	INDIAN CREEK SPRING (MARION) #4	Marion	1	3
99	INDIAN CREEK SPRING (MARION) #1	Marion	1	3
100	INDIAN CREEK SPRING (MARION) #2	Marion	1	3
101	RAINBOW SPRING #5	Marion	2	3
102	BUBBLING SPRING	Marion	2	3
103	WATERFALL SPRINGS	Marion	5	3
104	RAINBOW SPRING #4	Marion	2	3
105	RAINBOW BRIDGE SEEP SOUTH	Marion	2	3
106	RAINBOW BRIDGE SEEP NORTH	Marion	2	3
107	RAINBOW SPRING #3	Marion	2	3
108	RAINBOW SPRING #2	Marion	2	3
109	RAINBOW SPRING #1	Marion	72	3
110	RAINBOW SPRING NORTH	Marion	2	3
111	APOPKA SPRING	Lake	25	3
112	DOUBLE RUN SPRING (LAKE)	Lake	1.9	3
113	SANLANDO SPRINGS	Seminole	19	3
114	PALM SPRINGS (SEMINOLE)	Seminole	5.5	3

Spring ID	SPRING_NAM	COUNTY	Mean Annual Flux (CFS)	Model Layer
115	GINGER ALE SPRING	Seminole	0.1	3
116	PEGASUS SPRING	Seminole	2.8	3
117	STARBUCK SPRING	Seminole	12	3
118	CLIFTON SPRINGS	Seminole	1.5	3
119	LAKE JESSUP SPRING	Seminole	0.01	3
120	MIAMI SPRING	Seminole	5.3	3
121	WEKIWA SPRING (ORANGE)	Orange	61	3
122	WITHERINGTON SPRING	Orange	2.4	3
123	HOLIDAY SPRING	Lake	2.7	3
124	LAKE BLUE SPRING	Lake	2.7	3
125	MOORING COVE SPRINGS	Lake	0.7	3
126	BUGG SPRING (LAKE)	Lake	11	3
127	ROCK SPRINGS (ORANGE)	Orange	55	3
128	SULFUR SPRING (ORANGE)	Orange	0.5	3
129	NOVA SPRING	Seminole	8.1	3
130	ISLAND SPRING	Seminole	8.6	3
131	SNAIL SPRINGS COMPLEX	Lake	0.3	3
132	DROTY SPRING	Lake	0.6	3
133	PALM SPRINGS (LAKE)	Lake	0.9	3
134	SEMINOLE SPRING (LAKE)	Lake	30	3
135	MOCCASIN SPRINGS	Lake	0.01	3
136	MESSANT SPRING	Lake	15	3
137	ENTERPRISE SPRINGS	Volusia	0.4	3
138	GREEN SPRING	Volusia	1.2	3
139	GEMINI SPRINGS #2	Volusia	3.0	3
140	GEMINI SPRINGS #1	Volusia	6.9	3
141	MARKEE SPRING	Lake	0.2	3
142	MARKEE MINOR SPRING #1	Lake	0.2	3
143	TRICKLE SPRING	Lake	0.01	3
144	BOULDER SPRINGS	Lake	0.2	3
145	SHARKS TOOTH SPRING	Lake	0.2	3
146	HELENE SPRING	Lake	1.2	3
147	BLUE ALGAE BOIL SPRING	Lake	0.1	3
148	GREEN ALGAE BOIL SPRING	Lake	0.1	3
149	BLACKWATER SPRINGS	Lake	0.01	3
150	BLACKWATER MINOR #4	Lake	0.01	3
151	BLACKWATER MINOR #1	Lake	0.01	3
152	BLACKWATER MINOR #3	Lake	0.01	3
153	BLACKWATER MINOR #2	Lake	0.01	3

Spring ID	SPRING_NAM	COUNTY	Mean Annual Flux (CFS)	Model Layer
154	VOLUSIA BLUE SPRING	Volusia	144	3
155	CAMP LE NO CHE SPRING	Lake	0.8	3
156	MOSQUITO SPRINGS	Lake	1.2	3
157	ALEXANDER SPRING	Lake	100	3
158	WEKIVA FALLS RESORT	Seminole	12	3

4.12 Pumping Wells and Return Water

Groundwater withdrawals in the form of well pumping are represented in the ECFTX model using the Well package in MODFLOW NWT. Within the model domain, a database of monthly historical groundwater use data over the calibration period was prepared by the three Districts and integrated for use in the model. Surface water withdrawals, which are also part of the water use database, are not included in the Well package.

Additions to the aquifer system are also part of the Well package and include inflows from Rapid Infiltration Basins (RIBs) represented as recharge to the SA (Layer 1). These are simulated as injection wells in layer 1. Like RIBs, lake drainage wells in the Orlando area also add recharge - but to the UFA; however, these are included as part of the Drain Return package (DRT) outlined in Section 4.3.

The Upstream Weighting (UPW) Package is used to specify properties controlling flow between cells in MODFLOW-NWT (Niswonger, et al., 2011). To create the Well package, the historical water use data is run through a program that calls on the calibrated model upstream weighting (UPW) package in MODFLOW-NWT to extract hydraulic conductivity and top and bottom layer elevations to assign a layer to each water use station. Groundwater withdrawals in the Well package can further be subdivided into single-layer or multi-layer withdrawals. Single-layer well withdrawals are those in which the open interval of the well only spans one simulated aquifer layer. A layer is assigned based on provided casing and depth information and model layer elevations. Multi-layer wells have open intervals in more than one simulated aquifer layer. In most occurrences, the multi-layer wells are open to one or more discrete aquifer layers in the FAS (i.e., the UFA and LFA). The approach to apportion the groundwater withdrawals between hydrogeologic units within the FAS is described below.

First, for each layer, the transmissivity of the layer (T_W) interval open to the well is calculated by multiplying the well's open interval (QLEN) within the layer by the simulated horizontal hydraulic conductivity (Kh) of the entire layer (T_W= QLEN * Kh). Next, the "well fraction" was calculated by dividing transmissivity of the layer (T_W) interval open to the well by the transmissivity of the entire layer. The well fraction is used as a multiplier for the flow rate (Q). Finally, flow out of each layer is calculated by multiplying the well fraction by the historical pumping rate for each stress period. Groundwater withdrawals occur in nearly every layer of the model except for the lower portion of the LFA (Layer 11) and the lower confining unit in the LFA (LCU, Layer 10). Average annual withdrawals from all three layers comprising the UFA total 1,524 mgd and represent 87% of total groundwater withdrawals in the model domain (Table 8). Average annual withdrawals from the LFA (Layer 9) represent 8% of total groundwater withdrawals. Figure 80 and 81 illustrate the groundwater withdrawals by year and by aquifer in the ECFTX model domain. Figure 82 through 86 show the spatial distribution of withdrawals by aquifer over the model domain.

Table 8. Average annual withdrawals (mgd) in each layer of the model. Withdrawals from the SA (Layer 1) include additions from RIBs.

Layer		2003	2004	2005	2006	2007	2008	2009	2010	2011	2012	2013	2014	Avg
1	SAS	66.5	78.9	52.4	114.5	96.8	70.8	80.2	68.6	63.3	64.0	49.0	30.1	69.6
2	ICU/IAS	21.0	23.7	21.8	24.3	23.9	21.8	22.9	21.9	20.3	23.5	22.7	22.0	22.5
3	UFA	624.3	655.7	562.3	758.6	720.4	651.4	702.3	662.0	631.5	647.5	590.2	542.5	645.7
4	UFA	300.9	301.4	270.3	354.7	335.2	298.7	325.4	309.6	284.6	310.1	284.2	258.7	302.8
5	UFA	516.6	538.9	506.1	683.8	652.1	569.6	612.6	596.5	572.8	590.4	557.8	509.4	575.5
6	MCU	0.2	0.2	0.1	0.6	0.2	0.1	0.2	0.1	0.1	0.2	0.1	0.1	0.2
7	MCU	0.0	0.3	0.3	0.1	0.1	0.0	0.0	0.1	0.1	0.1	0.1	0.1	0.1
8	MCU	0.4	0.5	0.5	0.6	0.6	0.5	0.5	0.5	0.5	0.5	0.5	0.5	0.5
9	LFA	127.4	133.9	137.3	153.5	142.8	134.7	126.9	127.5	128.2	133.0	130.2	129.1	133.7
10	LCU	0.0	0.0	0.0	0.0	0.0	0.0	0.0	0.0	0.0	0.0	0.0	0.0	0.0
11	LFA	0.0	0.0	0.0	0.0	0.0	0.0	0.0	0.0	0.0	0.0	0.0	0.0	0.0
Total		1,657.3	1,733.5	1,551.1	2,090.7	1,972.1	1,747.6	1,871.1	1,786.6	1,701.4	1,769.3	1,634.8	1,492.5	1,750.7

4.12.1 Return Flow

Irrigation return flow was applied using the same methodology for all model simulations. Return flow is irrigated water that gets returned to the SA (model Layer 1) from inefficient irrigation practices. This occurred in agricultural areas and public water supply (PWS) service areas, where landscape irrigation utilized either potable or reclaimed water. There are three principal uses of irrigation that were applied in the model: agricultural, landscape/LRA and domestic self-supplied (DSS). Agricultural irrigation was based on observed or calculated water need in excess of rainfall, considering soil type and crop type (Table 9). Landscape/LRA irrigation return flow was estimated as a portion of PWS and reclaimed water use and applied to irrigated areas within the PWS utility and reclaimed water service boundaries (Table 10). DSS water demands were generated based upon the per capita usage rate for each county and the irrigation rates were assumed to be 50% of the total demand for each pumping well (Table 11). DSS irrigation was applied directly at the pumping locations. Total groundwater and surface water use by LSI groups is given in Table 12. An LSI group can be a county or combination of multiple counties depending on the spatial distribution of PWS and reclaimed water utility service areas. Potable and reclaimed water return flow as a percentage of total water use within LSI groups are given in Table 13. A more detailed discussion of the methodology used for agricultural return flow and landscape irrigation return flow is presented in Appendix F. A county-level break down of agricultural, landscape and DSS irrigation used for the calibration period is shown in the tables below.

Table 9. Agricultural irrigation return flows applied in the calibrated model.

COUNTY	2003	2004	2005	2006	2007	2008	2009	2010	2011	2012	2013	2014	Avg
BREVARD	28.28	29.89	10.36	24.41	33.1	30.76	39.26	40.08	35.17	30.93	28.88	18.87	29.2
CITRUS	1.9	2.34	1.48	2.73	2.46	1.71	2.32	2.01	1.38	2.14	1.93	1.49	2.0
DE SOTO	53.3	51.82	37.36	70.29	68.91	50.23	72.11	68.57	61.07	70.11	56.9	46.94	59.0
GLADES	22.33	25.37	21.66	33.74	26.55	23.43	31.97	27.93	26.98	25.94	21.79	15.75	25.3
HARDEE	39.64	43.42	26.29	50.1	49.19	37.51	50.85	47.85	36.34	50.49	42.59	36.75	42.6
HERNANDO	3.4	3.23	2.13	3.24	4.68	3.58	4.16	4.8	3.58	5.11	4.32	4.2	3.9
HIGHLANDS	122.18	120.72	100.97	169.92	148.05	125.23	148.49	133.34	134.97	135.06	121.32	104.92	130.4
HILLSBOROUGH	60.43	60.75	47.58	67.08	63.9	52.88	63.65	61.7	50.7	63.15	52.15	46.28	57.5
INDIAN RIVER	19.69	25.91	10.92	26.49	23.07	22.51	28.69	40.53	37.35	34.82	32.62	35.95	28.2
LAKE	22.69	22.49	18.41	25.08	21.54	21.82	23.69	32.07	24.43	29.11	27.96	21.51	24.2
LEVY	0.06	0.26	0.16	0.3	0.3	0.23	0.3	0.09	0.07	0.07	0.06	0.06	0.2
MANATEE	61.02	63.79	69.36	82.18	76.04	60.2	67.2	71.31	61.42	67.96	57.74	51.05	65.8
MARION	3.58	3.21	2.25	4.82	4.94	5.4	5.32	6.46	6.14	6.68	6.79	6.33	5.2
MARTIN	13.67	16.14	11.92	27.59	21.79	16.29	18.23	17.32	18.77	18.06	15.4	9.9	17.1
OKEECHOBEE	28.27	29.17	24.73	40.59	34.23	31.47	35.8	33.99	33.9	33.01	29.45	24.78	31.6
ORANGE	9.03	9.05	7.18	13.85	10.31	9.1	10.6	13.84	11.9	13.07	12.97	11.97	11.1
OSCEOLA	18.7	20.3	14.52	31.95	28.36	24.72	29.16	23.32	27.18	26.54	27.28	19.7	24.3
PASCO	14.73	16.11	9.98	17.23	18.02	10.34	15	13.37	9.78	12.26	8.54	7.45	12.7
PINELLAS	0.32	0.34	0.26	0.33	0.32	0.27	0.34	0.14	0.1	0.2	0.05	0.04	0.2
POLK	90.13	96.49	61.01	115.23	109.43	89.2	113.15	111.05	88.39	122.46	96	86.75	98.3
SARASOTA	3.61	3.45	3.47	9.84	5.86	4.8	4.59	3.66	4.07	4.73	3.36	3.44	4.6
SEMINOLE	2.5	2.42	1.87	3.09	2.98	2.55	3.05	4.2	2.86	2.77	2.87	2.98	2.8
ST. LUCIE	47.95	54.14	35.81	86.9	68.61	59.12	68.78	67.29	59.4	58.4	51.82	42.51	58.4
SUMTER	9.86	9.59	6.14	10.36	10.64	8.63	9.77	9.1	7.79	8.55	7.51	7.02	8.7
VOLUSIA	4.2	4.32	2.87	5.1	4.85	4	4.75	8.08	4.99	4.93	4.44	4.69	4.8
TOTAL	681.47	714.72	528.69	922.44	838.13	695.98	851.23	842.1	748.73	826.55	714.74	611.33	748.0

Note: All units in mgd.

Table 10. Landscape and LRA irrigation return flows applied in the calibrated model.

COUNTY	2003	2004	2005	2006	2007	2008	2009	2010	2011	2012	2013	2014	Avg
BREVARD	32.9	36.77	26.55	40.72	39.91	35.83	28.84	40.78	38.48	35.21	38.56	31.3	35.5
CITRUS	11.88	12.57	14.56	17.24	14.27	15.41	14.2	13.46	15.76	14.03	13.94	12.97	14.2
DE SOTO	2.36	2.75	2.89	7.13	5.05	2.73	4.28	1.03	0.56	0.49	0.52	0.51	2.5
GLADES	0.01	0.01	0.01	0.02	0.01	0.01	0.02	0.01	0.01	0.01	0.01	0.01	0.0
HARDEE	1.69	2.04	0.7	1.65	2.1	1.75	1.86	0.26	1.62	2.17	1.75	1.1	1.6
HERNANDO	18.28	21.47	21.55	25.78	25.13	23.06	21.05	19.64	20.39	18.3	16.13	15.9	20.6
HIGHLANDS	9.36	9.1	8.96	10.68	9.37	8.38	8.1	8.51	8.59	8.51	8.04	7.55	8.8
HILLSBOROUGH	33.98	46.37	51.31	53.04	63.4	53.17	64.4	40.21	45.73	43.83	40.57	55.1	49.3
INDIAN RIVER	17.28	16.95	13.98	17.6	15.85	14.08	15.11	26.99	28.59	24.62	25.86	27.03	20.3
LAKE	32.11	38.95	34.45	49.22	49.95	43.3	38.24	44.64	47.13	46.89	45.42	46.51	43.1
LEVY	0	0	0.01	0.01	0.01	0.01	0.01	0.01	0.01	0.01	0.01	0	0.0
MANATEE	25.32	32.01	32.39	41.08	45.51	46.53	46.37	32.51	32.72	34.06	30.56	30.71	35.8
MARION	11.3	13.81	13.41	19.34	17.14	16.34	15.71	16.38	16.29	13.61	13.74	13.26	15.0
MARTIN	27.11	34.8	30.91	47.59	39.59	33.8	35.85	32.35	33.68	33.87	29.46	24.98	33.7
OKEECHOBEE	1.77	2.1	2.88	4.29	3.32	3.62	4.04	3.51	3.91	3.39	3.05	2.86	3.2
ORANGE	98.22	112.8	106.78	149.5	148.13	124.64	119.93	117.98	133.35	119.75	105.12	101.23	119.8
OSCEOLA	22.6	28.49	26.13	39.2	40.49	32.92	32.5	31.13	32.98	29.8	30.95	29.55	31.4
PASCO	11.89	16.78	18.56	19.2	22.95	20.85	25.23	15.76	17.93	17.18	16.22	22	18.7
PINELLAS	36	47.1	52.17	53.89	64.44	51.03	61.84	38.58	43.88	42.07	37.98	51.62	48.4
POLK	42.08	45.73	50.78	67.04	61.86	56.3	58.18	48.87	50.43	55.11	52.79	46.97	53.0
SARASOTA	15.61	20.57	18.33	20.89	25.3	25.98	28.2	19.61	20.2	21.7	21.3	20.41	21.5
SEMINOLE	26.06	33.1	31.33	43.86	43.46	36.91	35.51	34.95	39.49	35.45	31.44	30.26	35.2
ST. LUCIE	30.81	34.82	32.79	54.66	36.96	39.74	44.09	39.61	40.9	41.02	37.08	34.18	38.9
SUMTER	9.51	10.81	9.71	11.59	13.79	16.73	16.82	16.06	17.54	16.72	16.92	14.31	14.2
VOLUSIA	21.12	24.59	21.66	30.24	30.45	26.78	24.55	26.63	28.93	25.89	25.71	24.07	25.9
TOTAL	539.25	644.49	622.8	825.46	818.44	729.9	744.93	669.47	719.1	683.69	643.13	644.39	690.4

Note: All units in mgd.

Table 11. Landscape irrigation return flows from Domestic Self Supplied (DSS) wells applied in the calibrated model.

COUNTY	2003	2004	2005	2006	2007	2008	2009	2010	2011	2012	2013	2014	Avg
BREVARD	0.76	0.79	0.54	0.55	0.94	0.93	1	0.98	0.96	0.94	0.75	1.25	0.9
CITRUS	3.8	3.33	4.71	5.75	4.5	3.91	3.51	3.89	3.11	3.08	2.94	2.4	3.7
DE SOTO	1.03	1.08	1.07	1.12	1.05	1.02	0.93	0.98	0.9	0.74	0.76	0.68	0.9
GLADES	0	0	0	0	0	0	0	0	0	0	0	0	0
HARDEE	0.39	0.9	0.8	0.63	0.65	0.56	0.45	0.39	0.4	0.36	0.39	0.29	0.5
HERNANDO	2.67	2.85	2.88	3.01	2.72	2.65	2.58	2.52	2.54	2.39	2.29	2.78	2.7
HIGHLANDS	2.09	2.04	2.05	2.11	2.09	2.1	2.17	2.26	2.17	2.15	2.14	2.02	2.1
HILLSBOROUGH	3.29	3.43	3.35	3.37	3.19	2.98	2.82	2.52	2.62	2.58	2.43	4.54	3.1
INDIAN RIVER	0.84	0.88	0.83	0.87	0.67	0.65	0.62	0.42	0.44	0.42	0.11	0.08	0.6
LAKE	3	3.15	3.24	3.65	4.87	4.62	4.06	3.88	4.33	4.09	3.03	3.7	3.8
LEVY	0.19	0.21	0.21	0.21	0.19	0.19	0.13	0.09	0.12	0.09	0.08	0.08	0.1
MANATEE	0.87	0.91	0.93	0.95	0.97	0.98	0.98	1.03	1.03	1.07	1.1	1.17	1.0
MARION	2.32	2.87	3.16	4.31	3.73	3.39	3.23	2.94	3.24	2.87	2.98	2.69	3.1
MARTIN	1.54	1.38	1.23	1.19	1.15	1.11	1.07	1.04	0.86	0.72	0.6	0.5	1.0
OKEECHOBEE	0.74	0.74	0.72	0.71	0.71	0.7	0.69	0.69	0.7	0.72	0.76	0.78	0.7
ORANGE	8.31	8.63	6.36	6.45	6.42	6.56	6.57	8.26	7.41	7.34	3.4	4.16	6.7
OSCEOLA	2.45	2.48	2.46	2.46	2.37	2.36	2.34	2.33	1.46	0.93	0.56	0.35	1.9
PASCO	5.35	5.63	5.77	6.35	5.62	5.62	5.41	5.6	5.48	5.86	5.36	4.43	5.5
PINELLAS	1.78	1.91	1.99	2.08	2.17	2.25	2.31	2.37	2.46	2.54	2.58	2.47	2.2
POLK	4.48	4.3	4.02	4.61	4.73	5.42	6.46	8.03	6.19	5.09	4.29	2.62	5.0
SARASOTA	2.97	3.07	3.11	3.12	3.07	3.17	3.05	3.01	3.09	3.13	3.11	3.3	3.1
SEMINOLE	1.92	1.97	1.37	1.4	0.99	0.88	0.83	0.89	0.86	0.82	0.4	0.62	1.1
ST. LUCIE	2.66	2.41	2.17	2.14	2.11	2.08	2.05	2.02	1.73	1.49	1.28	1.1	1.9
SUMTER	1.96	1.89	1.55	1.87	2.32	2.98	2.25	2.01	2.29	1.85	1.7	1.05	2.0
VOLUSIA	1.1	1.13	0.88	0.89	1.19	1.09	1.1	1.18	1.24	1.19	1.64	1.69	1.2
TOTAL	56.51	57.98	55.4	59.8	58.42	58.2	56.61	59.33	55.63	52.46	44.68	44.75	55.0

Note: All units in mgd.

Table 12. Total utility groundwater and surface water use by LSI group.

COUNTY	2003	2004	2005	2006	2007	2008	2009	2010	2011	2012	2013	2014
BREVARD	33.17	35.18	33.94	36.11	29.90	32.90	22.16	29.28	28.79	28.56	28.10	27.61
CITRUS	13.06	13.48	15.85	18.48	13.66	14.61	14.40	13.42	15.35	13.99	13.87	13.55
DESOTO	20.63	18.30	21.72	19.34	16.51	11.91	23.86	20.30	22.86	20.44	22.01	28.72
GLADES	0.00	0.00	0.00	0.00	0.00	0.00	0.00	0.00	0.00	0.00	0.00	0.00
HARDEE	1.28	1.60	1.50	1.68	2.00	1.91	1.59	1.44	1.18	1.34	1.32	1.34
HERNANDO	19.78	22.70	23.33	27.26	23.72	20.50	19.89	19.80	20.79	19.28	18.23	17.99
HIGHLANDS	8.11	7.61	7.96	9.26	8.85	7.87	7.26	7.70	7.86	7.93	7.88	7.89
HILLSBOROUGH[a]	258.75	246.71	272.60	293.58	273.57	244.26	286.74	251.67	237.92	236.40	258.69	288.76
INDIAN RIVER	17.43	18.47	17.42	18.63	17.08	16.42	16.25	16.80	14.94	15.39	15.96	16.13
LAKE	39.47	43.77	44.40	57.28	56.10	51.32	45.99	46.50	46.44	45.33	45.53	49.05
LEVY	0.18	0.15	0.21	0.21	0.22	0.24	0.18	0.15	0.16	0.14	0.15	0.14
MANATEE	47.68	49.66	51.67	55.65	52.41	52.48	46.10	44.26	45.01	45.43	43.77	44.66
MARION	11.75	14.29	14.75	20.73	18.33	17.08	16.45	15.86	15.99	13.01	12.50	12.37
MARTIN	14.94	20.06	18.81	22.14	19.94	19.37	19.72	17.57	17.70	18.20	18.11	17.41
OKEECHOBEE	1.01	1.35	2.60	2.80	2.35	2.78	2.81	2.65	2.75	2.68	2.67	2.71
ORANGE[b]	259.27	277.19	272.63	306.72	300.69	281.99	265.17	265.30	265.60	263.75	257.48	254.96
OSCEOLA	25.88	29.27	29.69	35.64	37.56	34.31	33.75	33.40	34.53	33.04	34.77	38.04
POLK	69.90	66.26	77.79	87.77	81.78	75.69	75.40	71.25	72.38	73.02	73.25	68.38
SARASOTA	21.80	21.26	22.30	22.48	19.56	22.93	21.72	14.93	15.32	15.22	14.66	15.42
ST. LUCIE	21.08	23.71	26.29	29.83	28.03	28.04	28.37	28.08	27.27	28.03	28.61	29.49
SUMTER	11.86	12.59	11.05	13.07	15.67	18.64	19.00	18.04	19.86	19.60	19.33	15.67
VOLUSIA	31.09	38.97	32.02	38.79	36.55	34.31	32.07	29.91	30.10	27.66	28.60	27.76

Note: All units in mgd.

[a]: Multiple counties are considered as a single LSI group because utilities providing service outside of the service areas/county via agreement between utilities (includes Hillsborough, Pasco, and Pinellas counties as a total).

[b]. (Includes Orange and Seminole counties as a total).

Table 13. Potable and reclaimed water return flow as a percentage of total water use within the LSI groups (%)

COUNTY	2003	2004	2005	2006	2007	2008	2009	2010	2011	2012	2013	2014
BREVARD	95.38	104.03	73.69	106.07	123.69	102.74	122.02	120.46	112.30	100.42	116.55	92.32
CITRUS	64.55	65.95	68.14	72.35	68.81	69.27	68.13	65.95	69.12	70.48	71.52	71.37
DESOTO	28.47	13.89	32.87	31.98	29.79	14.63	39.23	16.35	25.24	11.84	18.72	33.60
GLADES	0.00	0.00	0.00	0.00	0.00	0.00	0.00	0.00	0.00	0.00	0.00	0.00
HARDEE	51.56	61.25	7.33	15.48	38.00	32.46	16.98	9.72	5.93	5.22	3.03	8.96
HERNANDO	75.38	76.96	75.38	78.17	75.51	74.80	74.36	72.47	74.07	70.28	69.72	69.98
HIGHLANDS	70.65	69.51	71.11	69.33	68.70	65.82	66.80	66.75	67.43	67.09	65.23	61.34
HILLSBOROUGH[a]	24.20	34.78	36.51	34.79	44.52	39.00	43.83	31.75	38.96	36.77	31.28	40.10
INDIAN RIVER	79.63	76.32	73.08	78.82	78.23	72.31	74.28	77.98	85.81	63.94	73.62	72.72
LAKE	68.35	73.31	68.99	76.24	78.99	75.32	74.41	74.80	80.12	80.06	80.45	79.82
LEVY	0.00	0.00	5.24	6.67	6.82	5.00	5.56	6.67	6.25	7.14	6.67	0.00
MANATEE	37.93	46.09	44.35	53.08	59.69	58.08	65.03	50.77	47.52	46.29	42.33	43.84
MARION	74.10	76.40	74.56	77.37	75.73	76.04	76.23	73.33	74.61	71.64	71.04	72.19
MARTIN	76.26	80.58	83.04	81.17	77.92	73.33	78.80	74.39	73.79	70.77	66.15	65.59
OKEECHOBEE	5.94	26.67	51.54	57.14	52.34	56.47	60.50	58.11	60.00	53.73	53.18	53.14
ORANGE[b]	41.21	44.68	45.08	52.55	55.66	51.20	49.02	49.25	55.17	48.83	43.86	44.19
OSCEOLA	55.11	64.32	61.49	65.27	73.02	65.39	64.50	63.14	63.94	56.36	62.76	59.83
POLK	48.05	49.85	52.85	59.56	58.26	56.43	57.72	53.73	54.48	58.60	58.87	57.31
SARASOTA	68.92	103.87	75.07	79.33	91.90	108.35	112.06	135.43	144.84	155.06	145.84	128.08
ST. LUCIE	63.22	61.91	61.76	72.41	34.75	64.02	76.88	67.02	66.70	63.43	63.12	67.75
SUMTER	67.25	68.05	73.55	69.10	77.52	79.84	79.16	78.05	78.70	79.34	79.00	79.71
VOLUSIA	65.77	71.99	66.15	74.86	80.65	75.23	74.03	77.73	83.29	77.87	74.48	68.30

Note: All units in mgd.

[a]: Multiple counties are considered as a single LSI group because utilities providing service outside of the service areas/county via agreement between utilities (includes Hillsborough, Pasco, and Pinellas counties as a total).

[b]. (Includes Orange and Seminole counties as a total)

Figure 87 through 90 show the spatial distribution of return flow in the domain for a wet (2004) and dry year (2012), respectively.

Return flows from septic tanks were assumed to be 50% of the total DSS withdrawals. Septic tank returns flows were directly added to the recharge array. A county- level use of septic tank return flows is shown in Table 14.

Table 14. Septic tank return flows from DSS wells applied in the calibrated model.

COUNTY	2003	2004	2005	2006	2007	2008	2009	2010	2011	2012	2013	2014	Avg
BREVARD	0.76	0.79	0.54	0.55	0.94	0.93	1	0.98	0.96	0.94	0.75	1.25	0.9
CITRUS	3.8	3.33	4.71	5.75	4.5	3.91	3.51	3.89	3.11	3.08	2.94	2.4	3.7
DE SOTO	1.03	1.08	1.07	1.12	1.05	1.02	0.93	0.98	0.9	0.74	0.76	0.68	0.9
GLADES	0	0	0	0	0	0	0	0	0	0	0	0	0
HARDEE	0.39	0.9	0.8	0.63	0.65	0.56	0.45	0.39	0.4	0.36	0.39	0.29	0.5
HERNANDO	2.67	2.85	2.88	3.01	2.72	2.65	2.58	2.52	2.54	2.39	2.29	2.78	2.7
HIGHLANDS	2.09	2.04	2.05	2.11	2.09	2.1	2.17	2.26	2.17	2.15	2.14	2.02	2.1
HILLSBOROUGH	3.29	3.43	3.35	3.37	3.19	2.98	2.82	2.52	2.62	2.58	2.43	4.54	3.1
INDIAN RIVER	0.84	0.88	0.83	0.87	0.67	0.65	0.62	0.42	0.44	0.42	0.11	0.08	0.6
LAKE	3	3.15	3.24	3.65	4.87	4.62	4.06	3.88	4.33	4.09	3.03	3.7	3.8
LEVY	0.19	0.21	0.21	0.21	0.19	0.19	0.13	0.09	0.12	0.09	0.08	0.08	0.1
MANATEE	0.87	0.91	0.93	0.95	0.97	0.98	0.98	1.03	1.03	1.07	1.1	1.17	1.0
MARION	2.32	2.87	3.16	4.31	3.73	3.39	3.23	2.94	3.24	2.87	2.98	2.69	3.1
MARTIN	1.54	1.38	1.23	1.19	1.15	1.11	1.07	1.04	0.86	0.72	0.6	0.5	1.0
OKEECHOBEE	0.74	0.74	0.72	0.71	0.71	0.7	0.69	0.69	0.7	0.72	0.76	0.78	0.7
ORANGE	8.31	8.63	6.36	6.45	6.42	6.56	6.57	8.26	7.41	7.34	3.4	4.16	6.7
OSCEOLA	2.45	2.48	2.46	2.46	2.37	2.36	2.34	2.33	1.46	0.93	0.56	0.35	1.9
PASCO	5.35	5.63	5.77	6.35	5.62	5.62	5.41	5.6	5.48	5.86	5.36	4.43	5.5
PINELLAS	1.78	1.91	1.99	2.08	2.17	2.25	2.31	2.37	2.46	2.54	2.58	2.47	2.2
POLK	4.48	4.3	4.02	4.61	4.73	5.42	6.46	8.03	6.19	5.09	4.29	2.62	5.0
SARASOTA	2.97	3.07	3.11	3.12	3.07	3.17	3.05	3.01	3.09	3.13	3.11	3.3	3.1
SEMINOLE	1.92	1.97	1.37	1.4	0.99	0.88	0.83	0.89	0.86	0.82	0.4	0.62	1.1
ST. LUCIE	2.66	2.41	2.17	2.14	2.11	2.08	2.05	2.02	1.73	1.49	1.28	1.1	1.9
SUMTER	1.96	1.89	1.55	1.87	2.32	2.98	2.25	2.01	2.29	1.85	1.7	1.05	2.0
VOLUSIA	1.1	1.13	0.88	0.89	1.19	1.09	1.1	1.18	1.24	1.19	1.64	1.69	1.2
TOTAL	56.51	57.98	55.4	59.8	58.42	58.2	56.61	59.33	55.63	52.46	44.68	44.75	55.0

Note: All units in mgd.

4.13 Quality Control/Quality Assurance (QA/QC)

The model underwent a very extensive process of quality assurance and quality control (QA/QC) during its development. This section highlights the major QA/QC activities conducted. The three principal types of QA/QC conducted were (1) general coordination amongst team members, (2) data compilation, synthesis, and review of work products and (3) peer review procedures.

The overall modeling approach, in general, was for staff members from each District be responsible for data compilation, model development, and model calibration for their District's portion of the model domain. This approach achieved workload balancing as well as leveraging each District's expertise in their portion of the model domain. This expertise included a better understanding of the sub regional hydrogeology as well as knowledge of calibration parameters from previous models that overlapped with the ECFTX Model domain. The team initially met weekly and then bi-weekly to coordinate efforts and data was shared via web meetings and displayed with team members. This allowed staff to review interim work products and data errors or omissions were more easily identified prior to proceeding with a subsequent modeling task.

District databases were queried to develop historical water use. These data were compiled for each District, and duplicates, false zeros, etc. were removed. Aquifer test data were also compiled from each District database and reviewed. Kriging techniques were used to smooth the transitions of these parameters along District boundaries. This also ensured that values in each model layer were generally consistent, recognizing that there could be variations across the model domain. Recognizing the several methods of estimating baseflow and the inherent limitations of these methods, multiple techniques were evaluated and conducted to develop the selected estimated baseflow quantities. Structure flow calibration was conducted, and water budgets were developed in gauged watersheds. This calibration was useful in cross checking the baseflow estimates against the measured surface water flows as one component of the overall watershed water budget. The desire to maintain reasonable water budgets sometimes resulted in a slightly reduced statistical calibration for water levels, which staff agreed was the most appropriate stopping point for model calibration.

Rainfall estimates from NEXRAD data sets were found to be lacking in the earlier periods of their development. Rainfall gauges were used to tension these NEXRAD values to develop a more reliable rainfall data set upon which recharge estimates were ultimately developed. Evapotranspiration (ET) estimates were developed from the ET-Recharge program and used as input to MODFLOW, again evaluated as part of the overall basin water budget. The NRCS curve number method was used to estimate runoff, with values calculated and used as part of the water budget.

Dry cells and flooded cells were minimized through the calibration process, recognizing that these occurrences should be limited to known areas and extreme events. Lakebed conductance values were calibrated using estimated lakebed fluxes to preserve mass balance within watersheds. GHB fluxes were calculated and reviewed on a per-layer and per-segment basis to ensure that brackish/saltwater fluxes into the model were not major contributors to the freshwater flow system. Adjustments along these boundaries were also made to ensure conformance with the conceptual model (i.e., fluxes were higher in aquifer layers compared to confining and semi-confining units). Drainage well flows estimated using the MODFLOW Drain package were compared to published estimated drainage well flows to ensure that the magnitudes of flow were appropriate. Metered agricultural demands in SWFWMD were compared to AFSIRS-estimated demands in SJRWMD and SFWMD for similar crop types to ensure a reasonable comparison, recognizing that climatic

differences between the Districts would result in some differences that were appropriate. Measured and estimated springflows were used as a calibration metric given that one of the model's objectives was to evaluate the effect of groundwater withdrawals upon natural systems including springs. Published potentiometric surface maps for May and September each year were compared to simulated potentiometric maps for those months. These simulated water levels were compared to these maps to ensure that the model was reasonably simulated potentiometric highs, lows, and hydraulic gradients.

The peer review process itself was a form of QA/QC. Periodically and at major milestones, the Peer Review Panel was convened to discuss the proposed modeling methodology, interim data compilation or calibration results at milestones, and solicit feedback from the Panel to adjust the approach as needed to ensure quality work products that meet groundwater modeling standards. This required that staff compile information, develop PowerPoint presentations that could be shared via web meeting and posted on a web board, and discussed with the Peer review panel. The displayed information was first shared amongst District staff and this frequently resulted in QA/QC checks before the Peer Review meetings, with data adjustments made accordingly. During and following the meetings, feedback from the Panel was useful in making real-time adjustments, especially during model calibration. These PowerPoint presentations and meeting summaries were developed, shared during the meetings, and later posted on the web board to document the modeling process. Finally, development of the model documentation report and subsequent review by the Peer Review Panel resulted in recommendations to improve the report, as well as be a reference so that future upgrades to the model can be more easily implemented by staff.

CHAPTER 4 - FIGURES
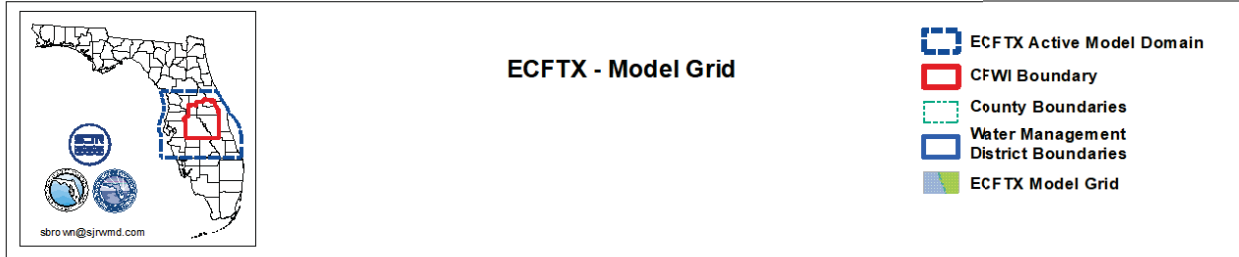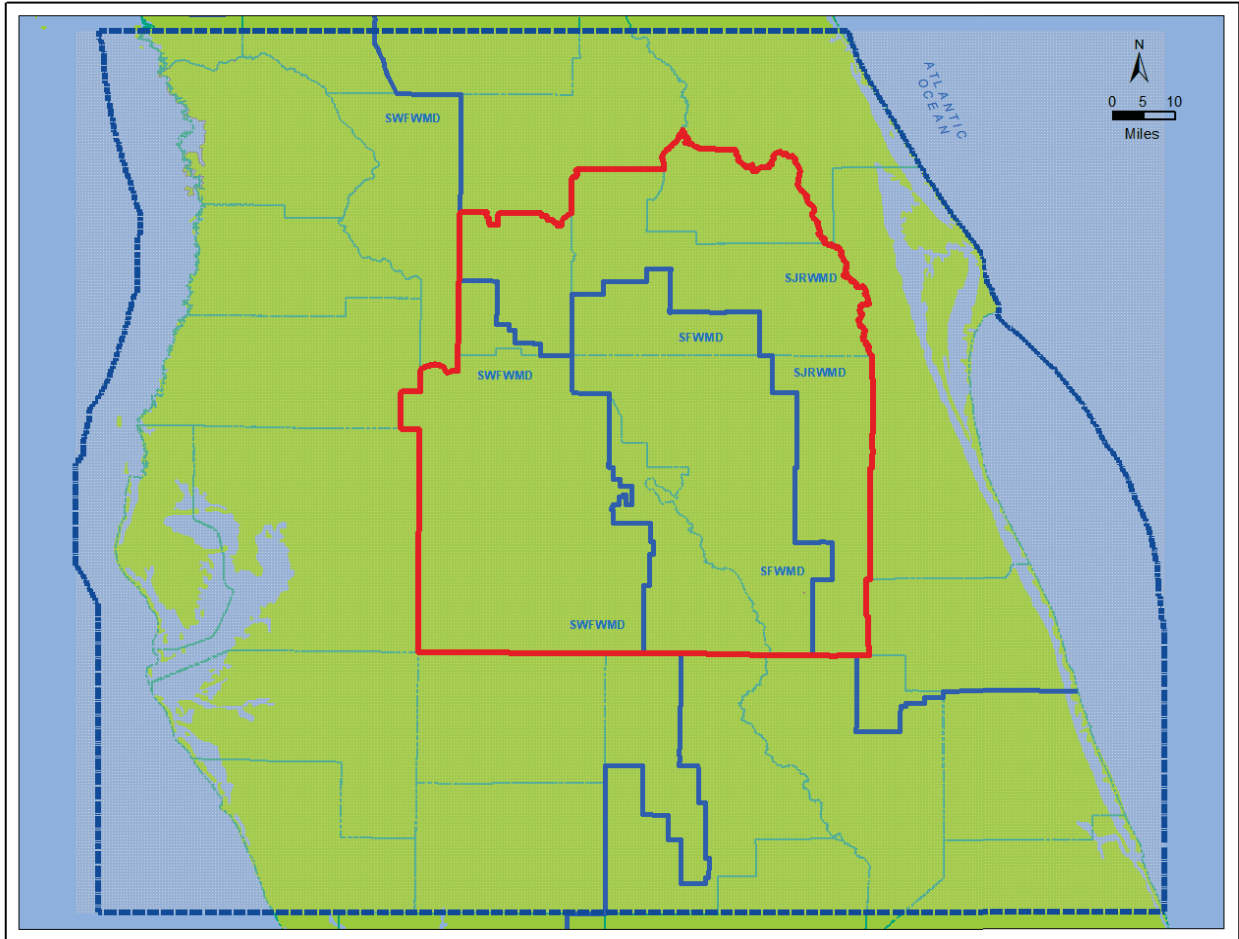
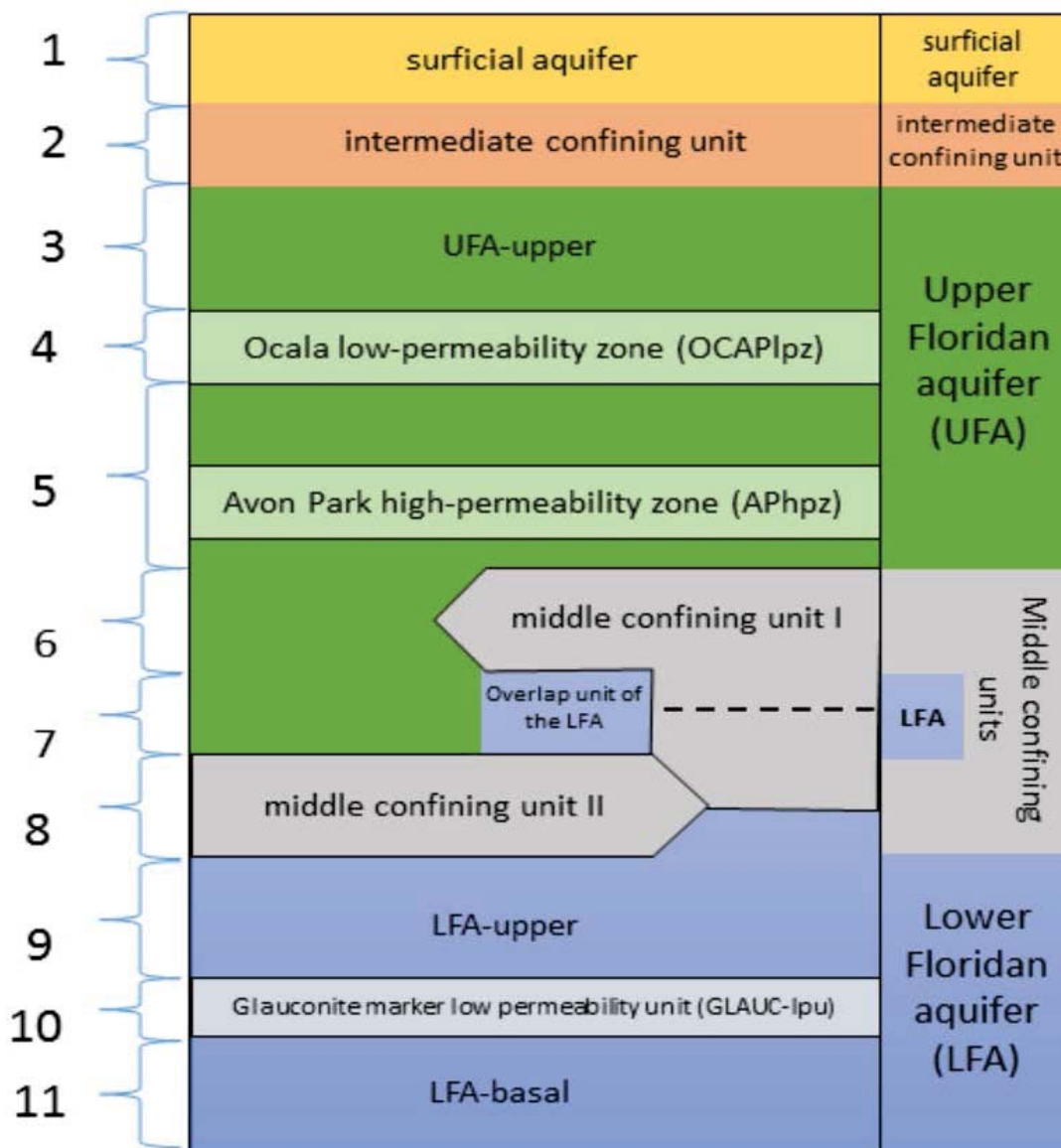Figure 31. Model grid for the ECFTX Model Domain.
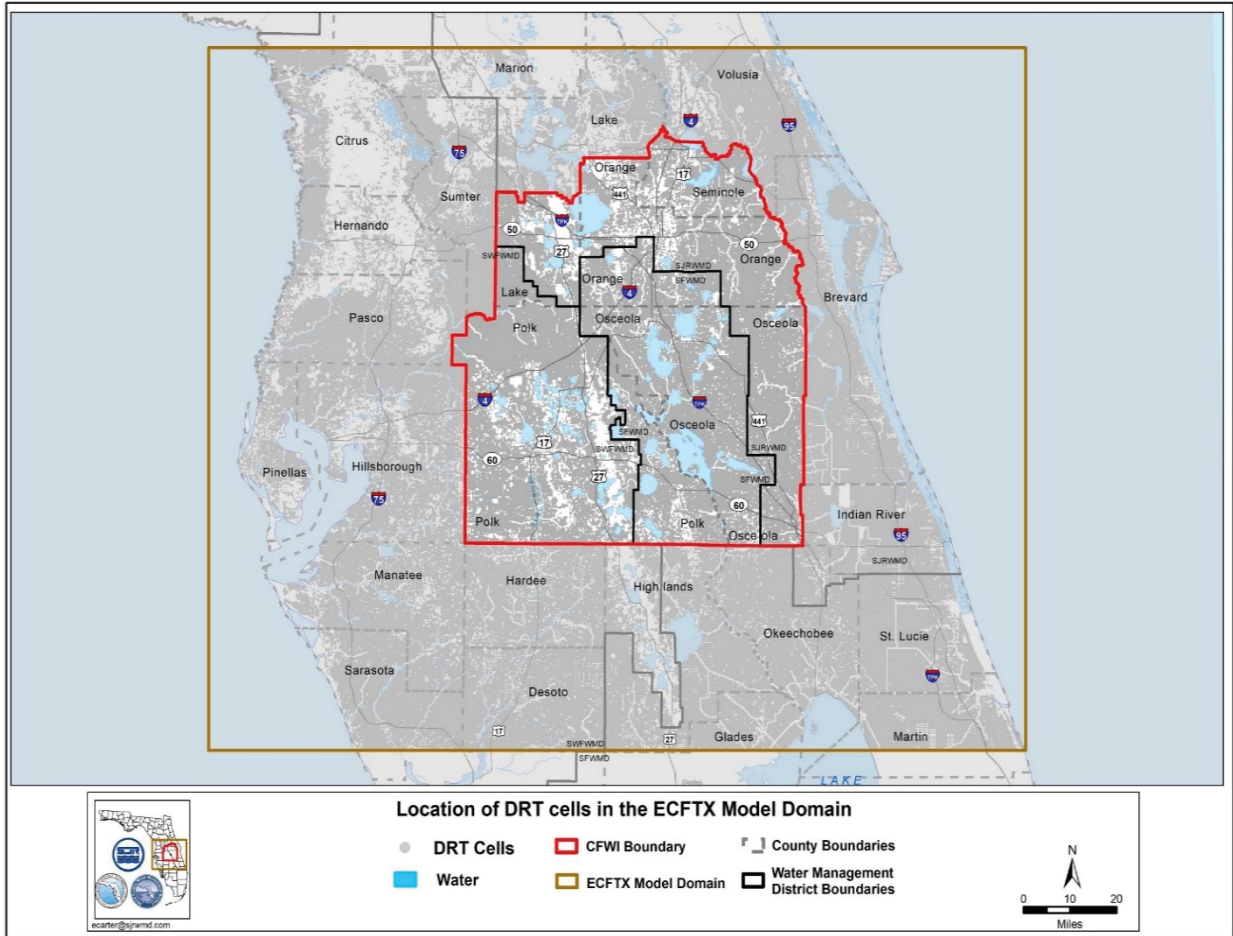
Figure 32. Vertical discretization of the ECFTX Model.

Figure 33. DRT cells in the ECFTX model that represent surface water hydrography elements (drainage well lakes and non-river package smaller waterbodies). Most cells are standard drainage cells without return water (see section 4.3).
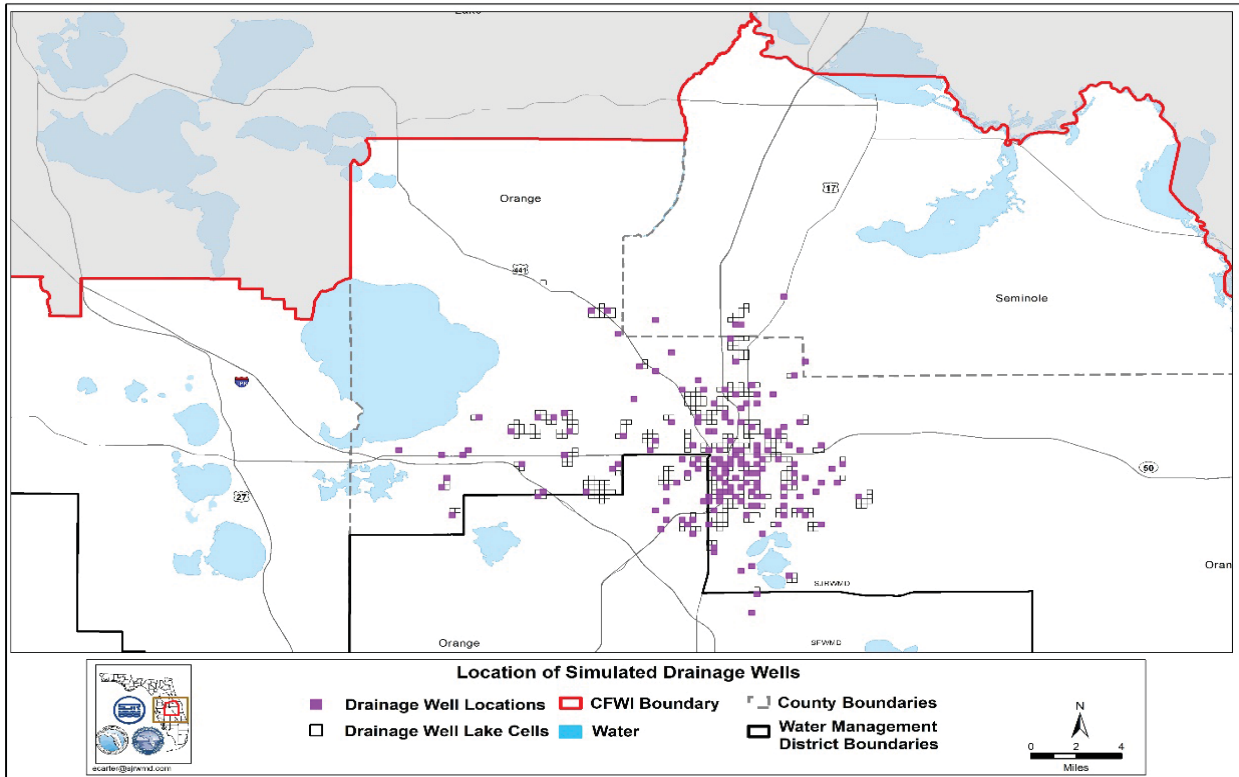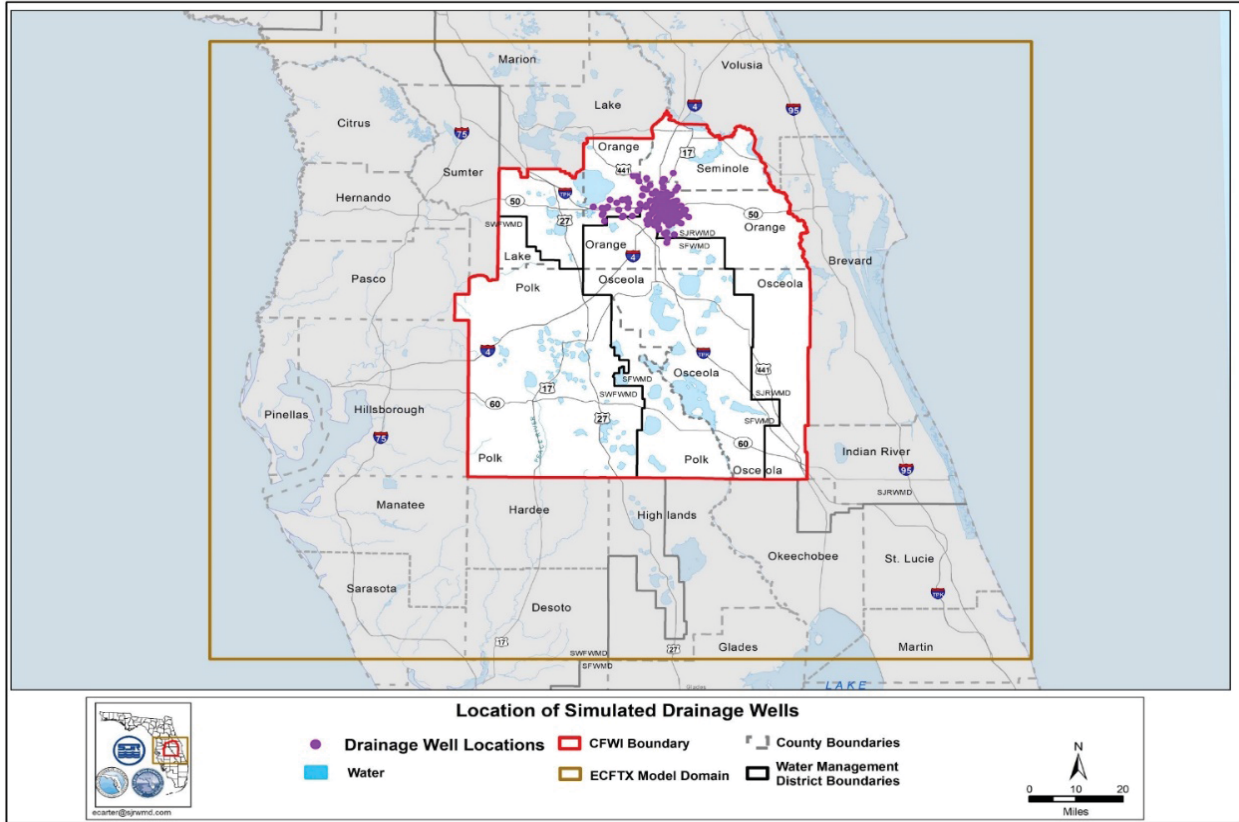
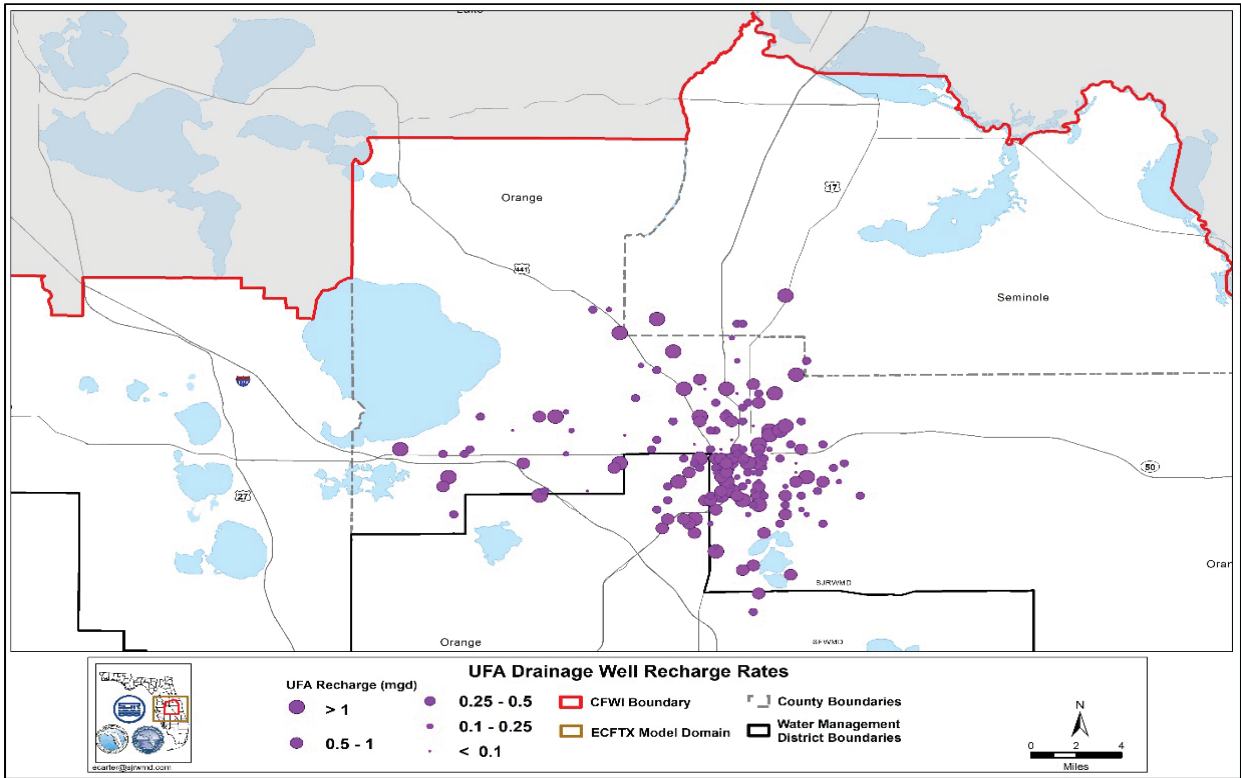Figure 34. DRT cells in the ECFTX model that represent drainage wells.

Figure 35. Drainage well recharge (average 2003-2014) to the UFA in the ECFTX model.
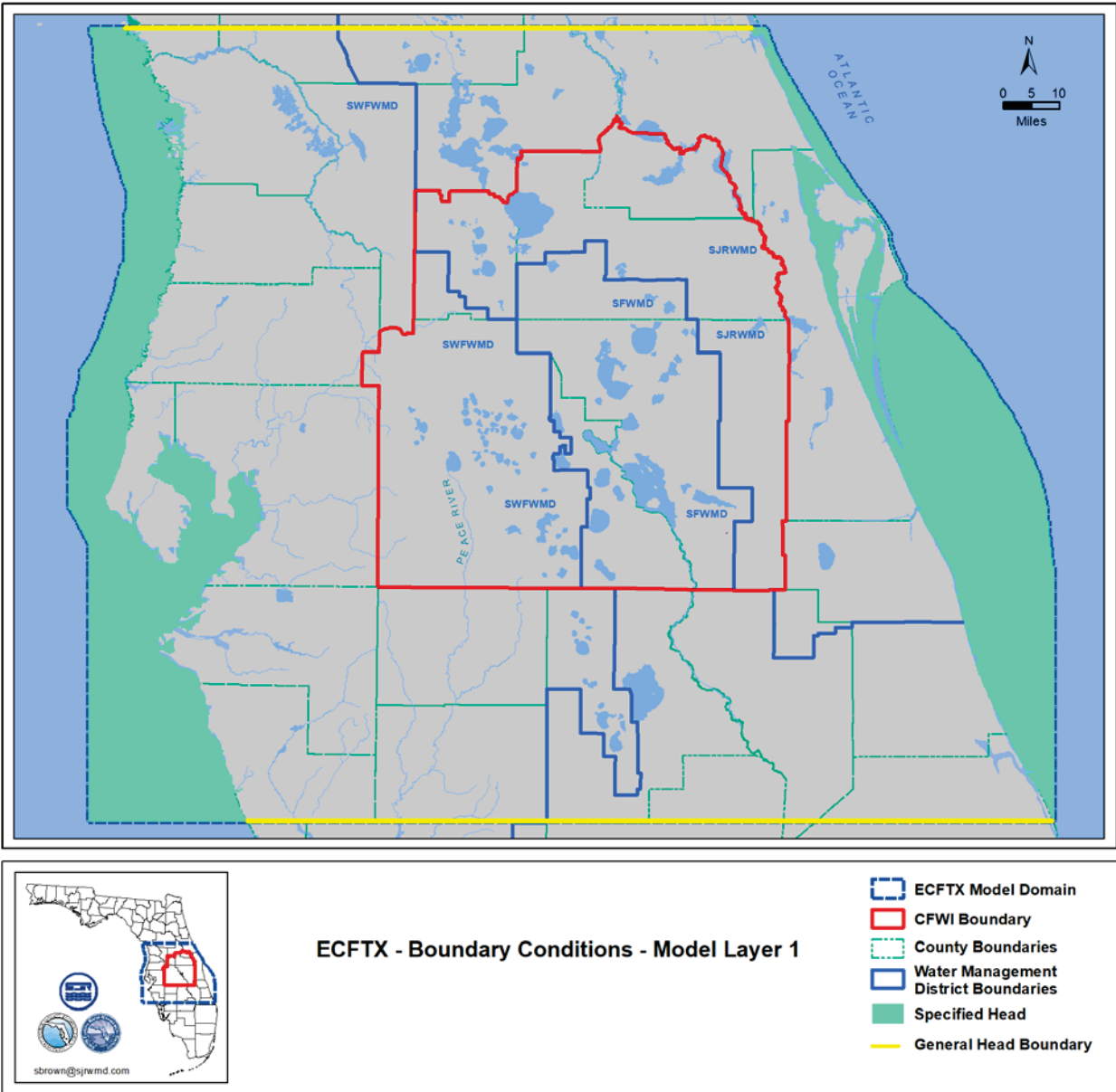
Figure 36. Boundary conditions for layer 1 in the ECFTX model.
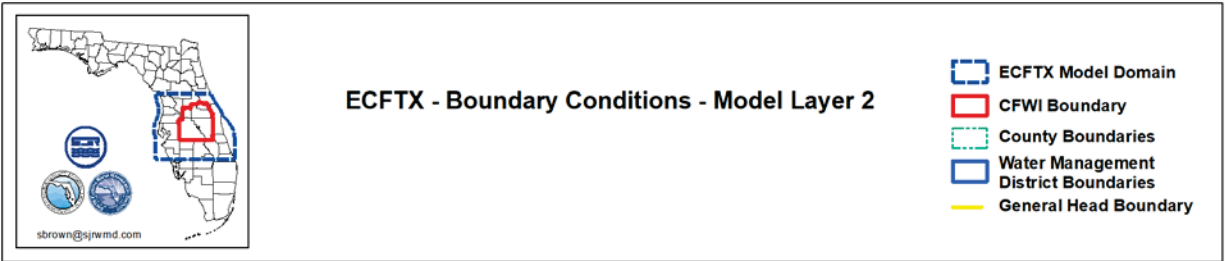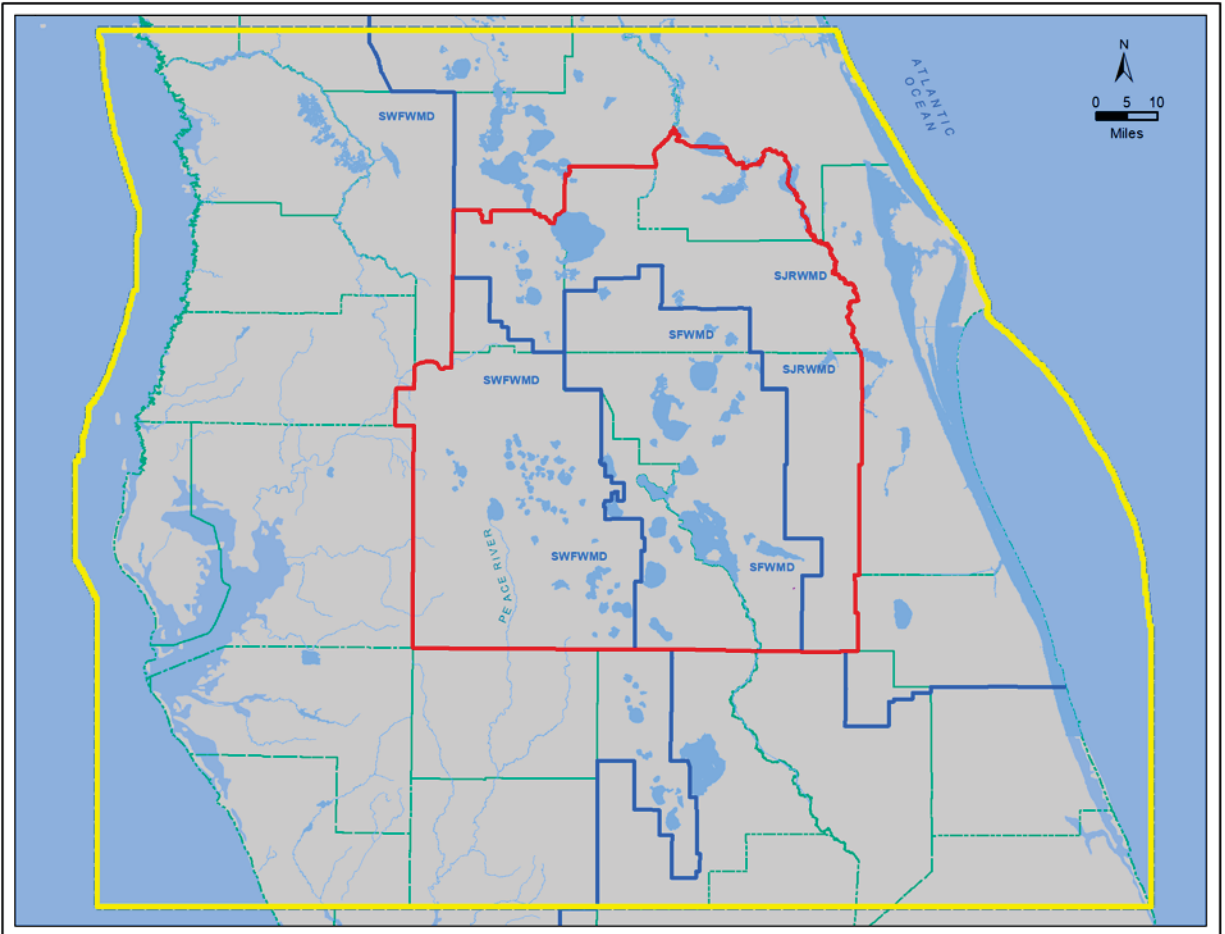
Figure 37. Boundary conditions for layer 2 in the ECFTX model.
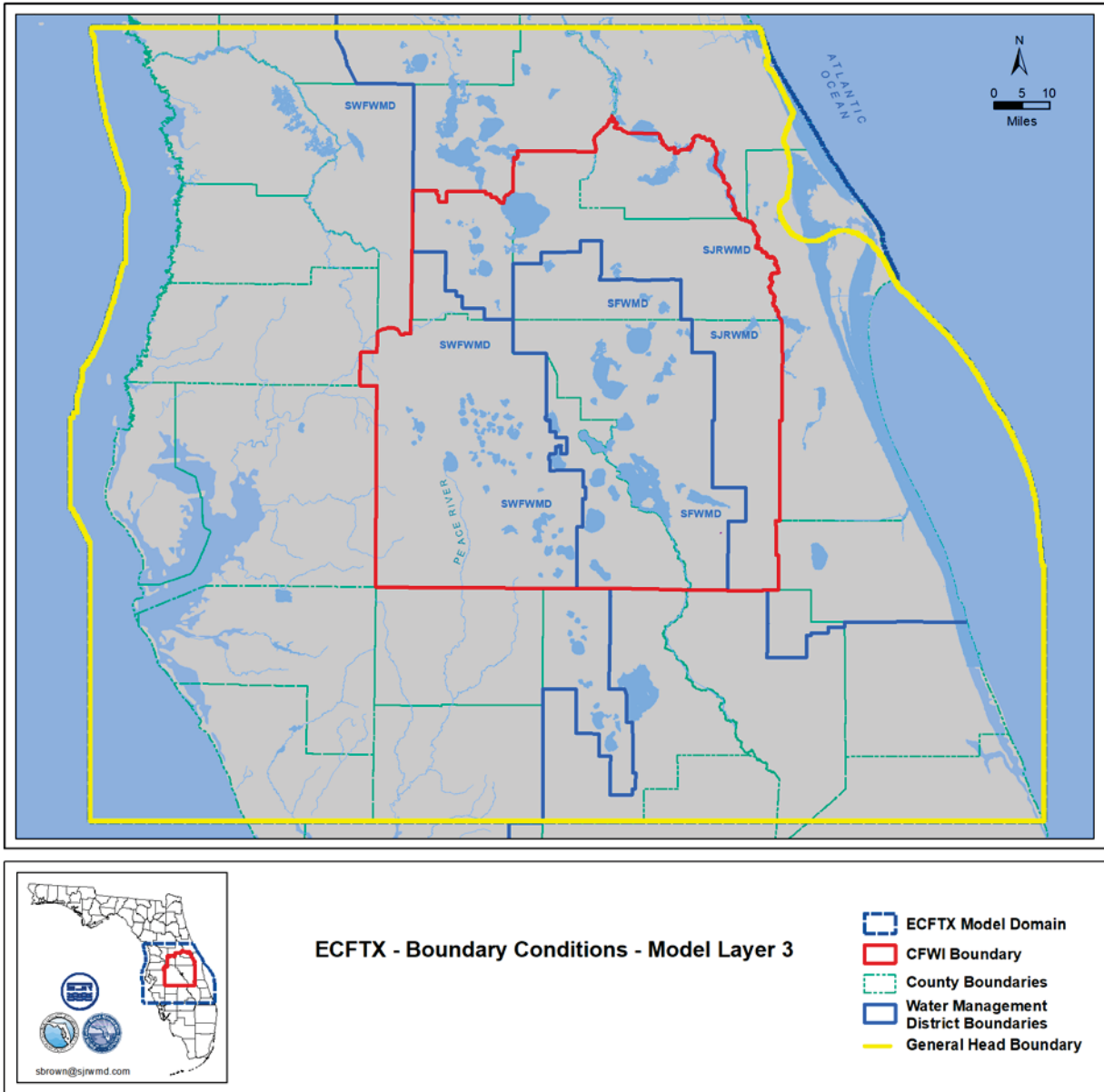
Figure 38. Boundary conditions for layer 3 in the ECFTX model.
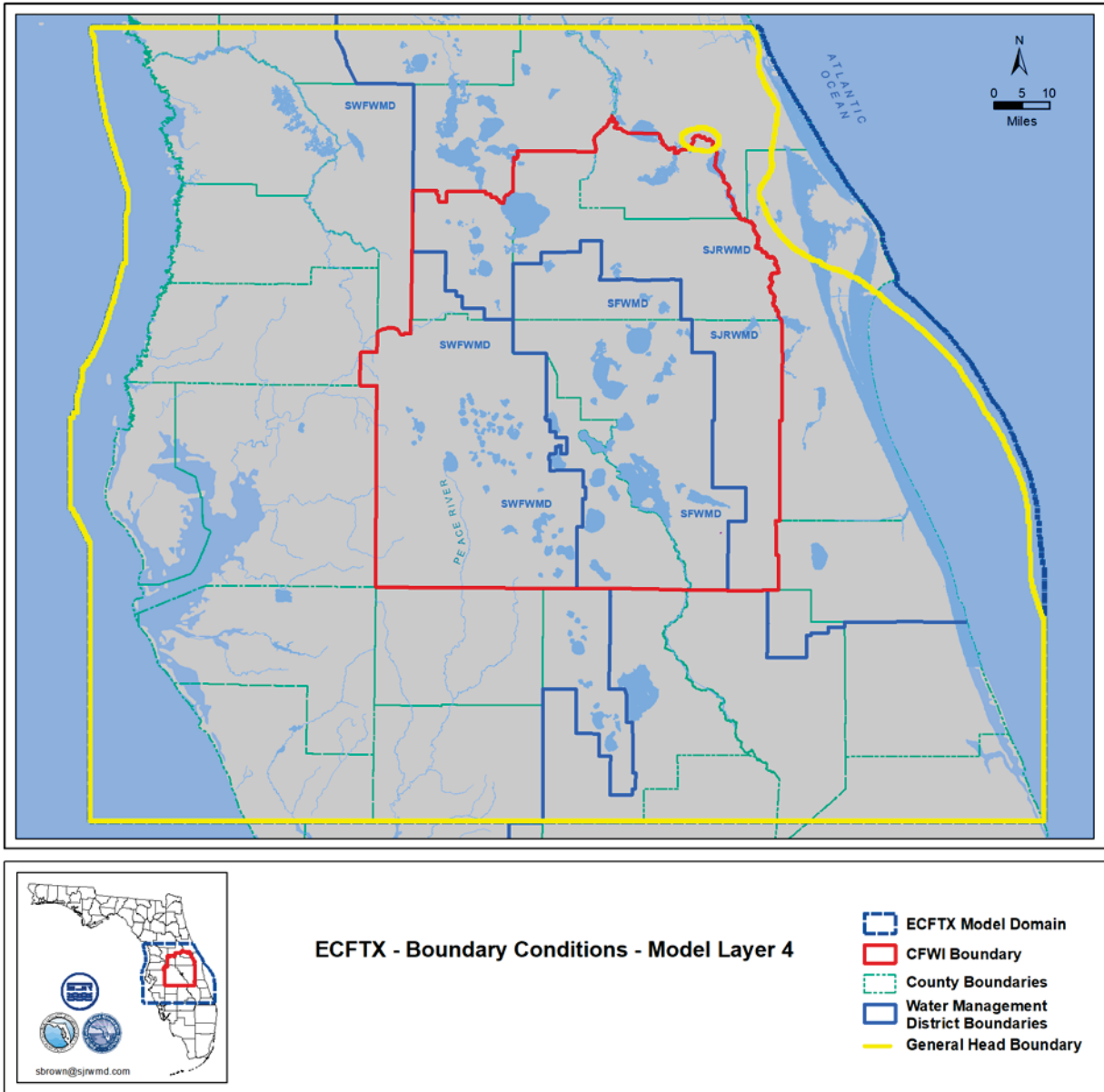
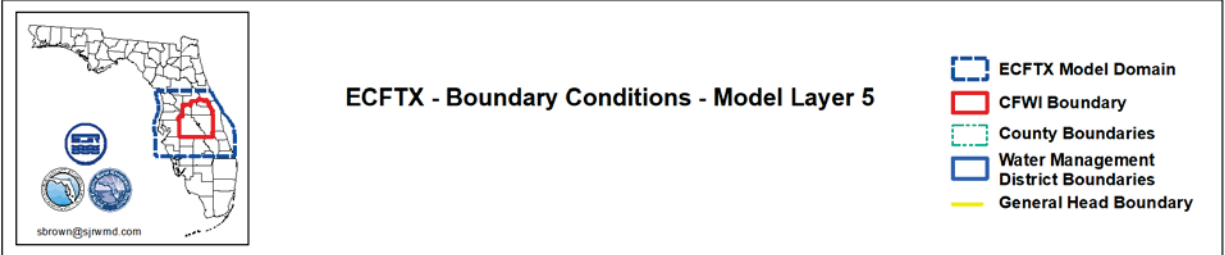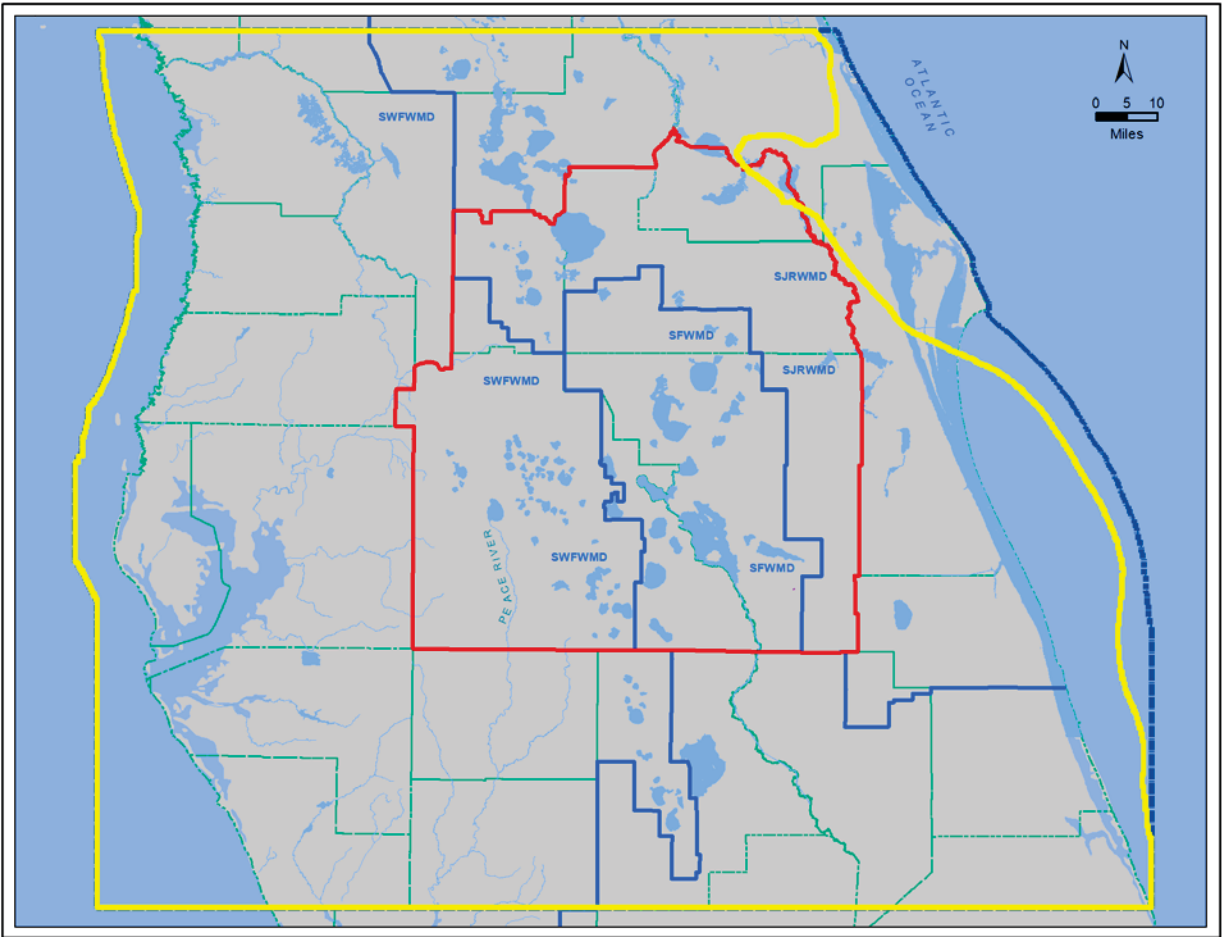Figure 39. Boundary conditions for layer 4 in the ECFTX model.

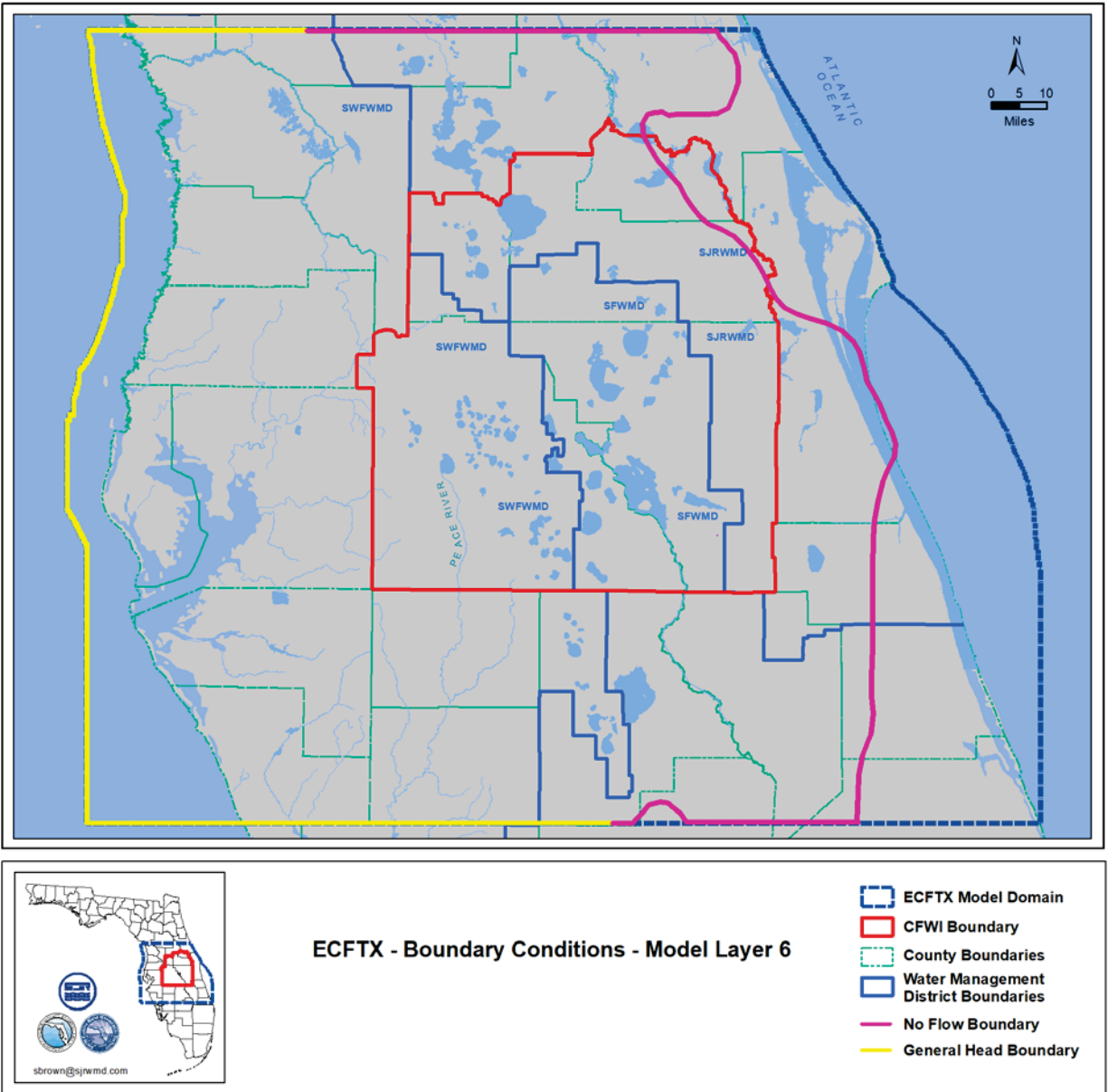Figure 40. Boundary conditions for layer 5 in the ECFTX model.

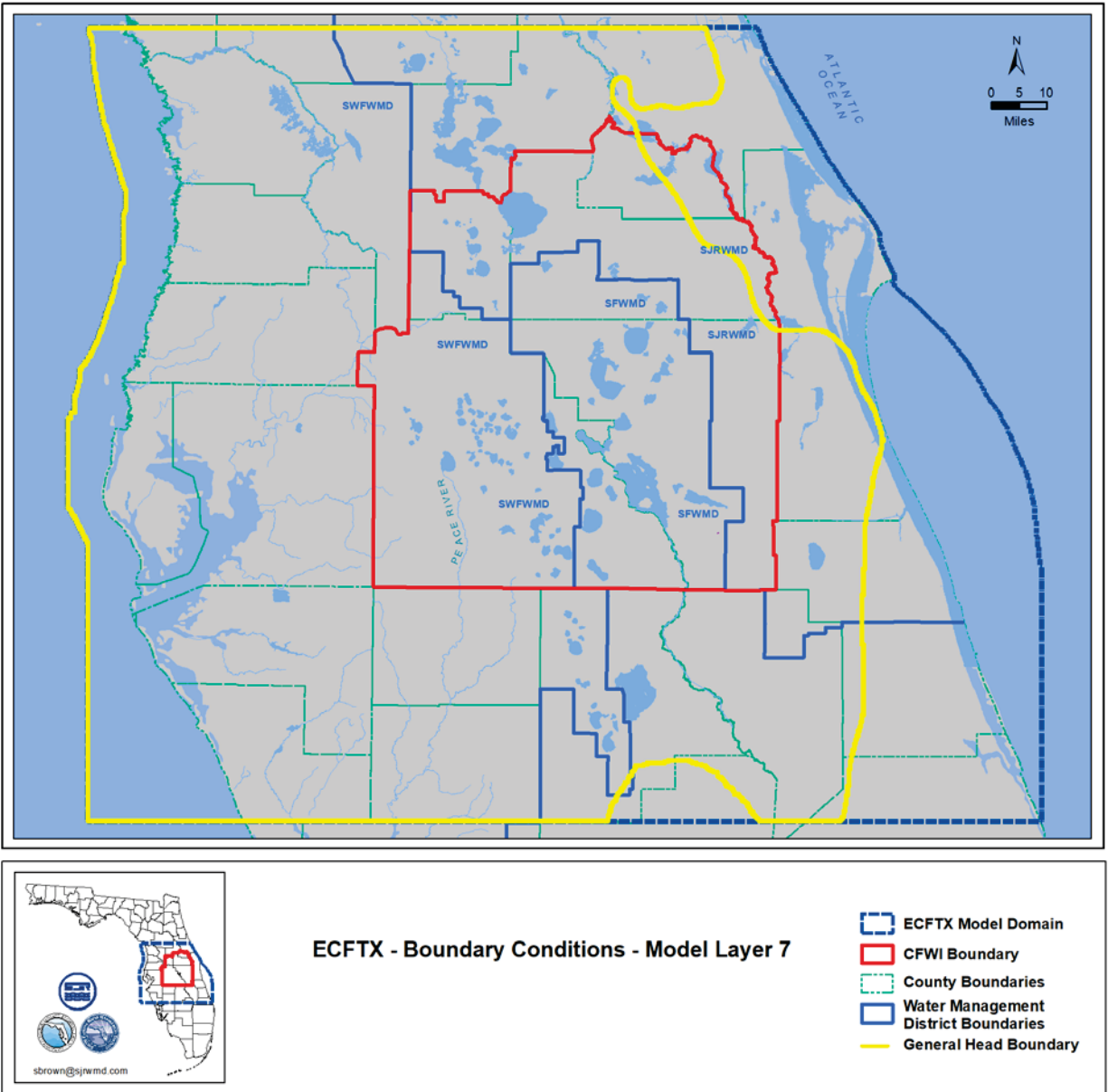Figure 41. Boundary conditions for layer 6 in the ECFTX model.

Figure 42. Boundary conditions for layer 7 in the ECFTX model.
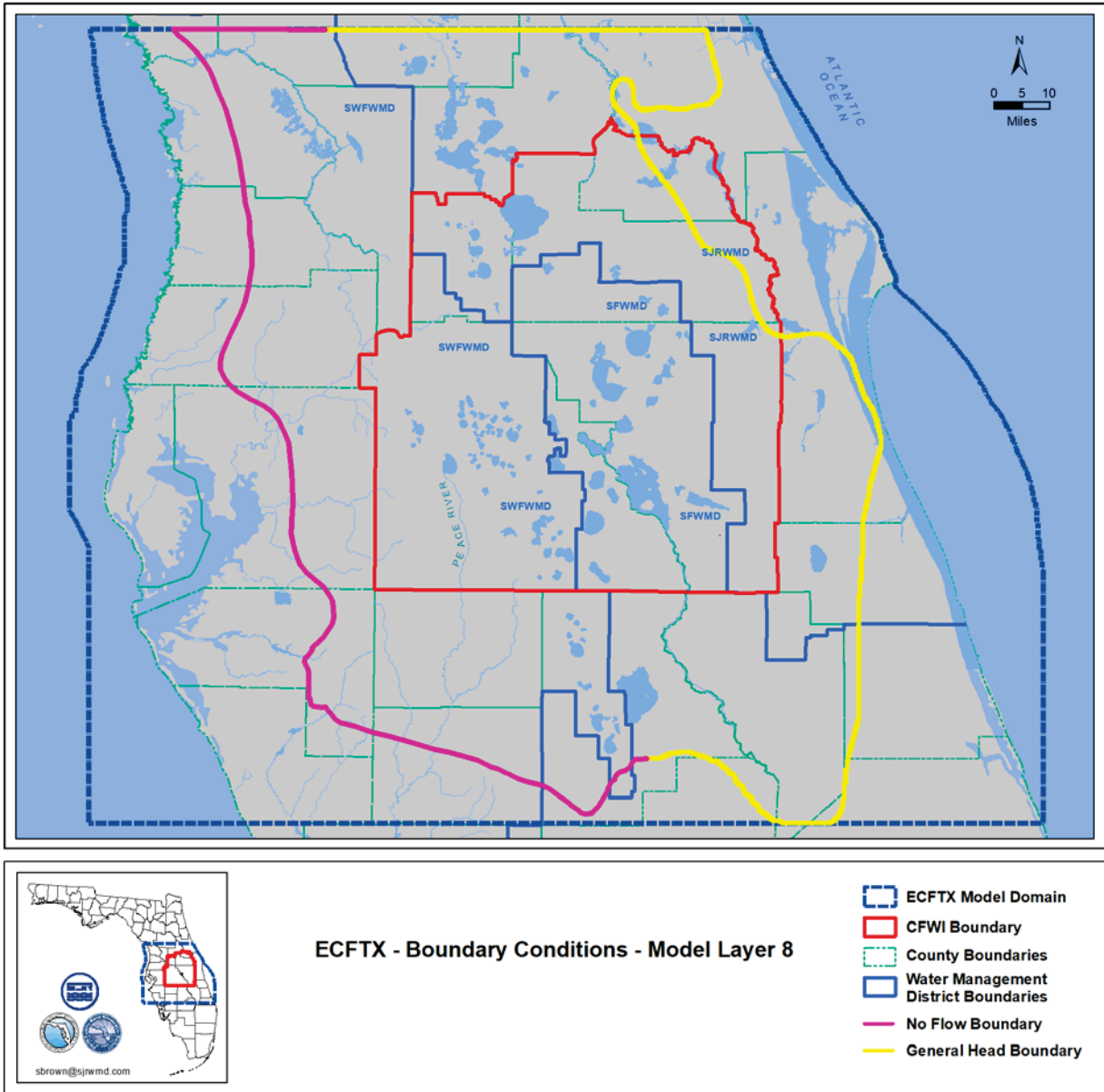
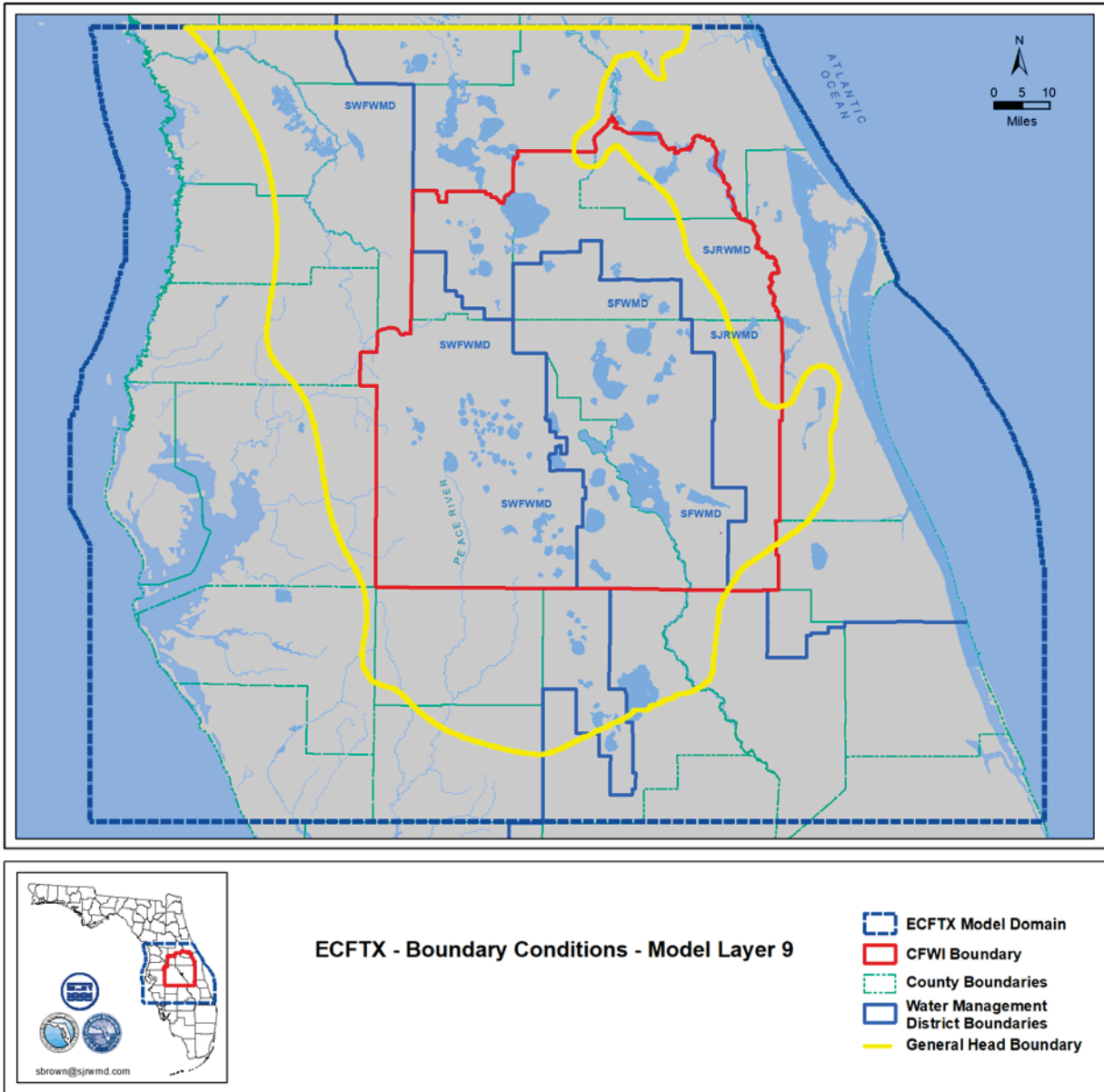Figure 43. Boundary conditions for layer 8 in the ECFTX model.

Figure 44. Boundary conditions for layer 9 in the ECFTX model.

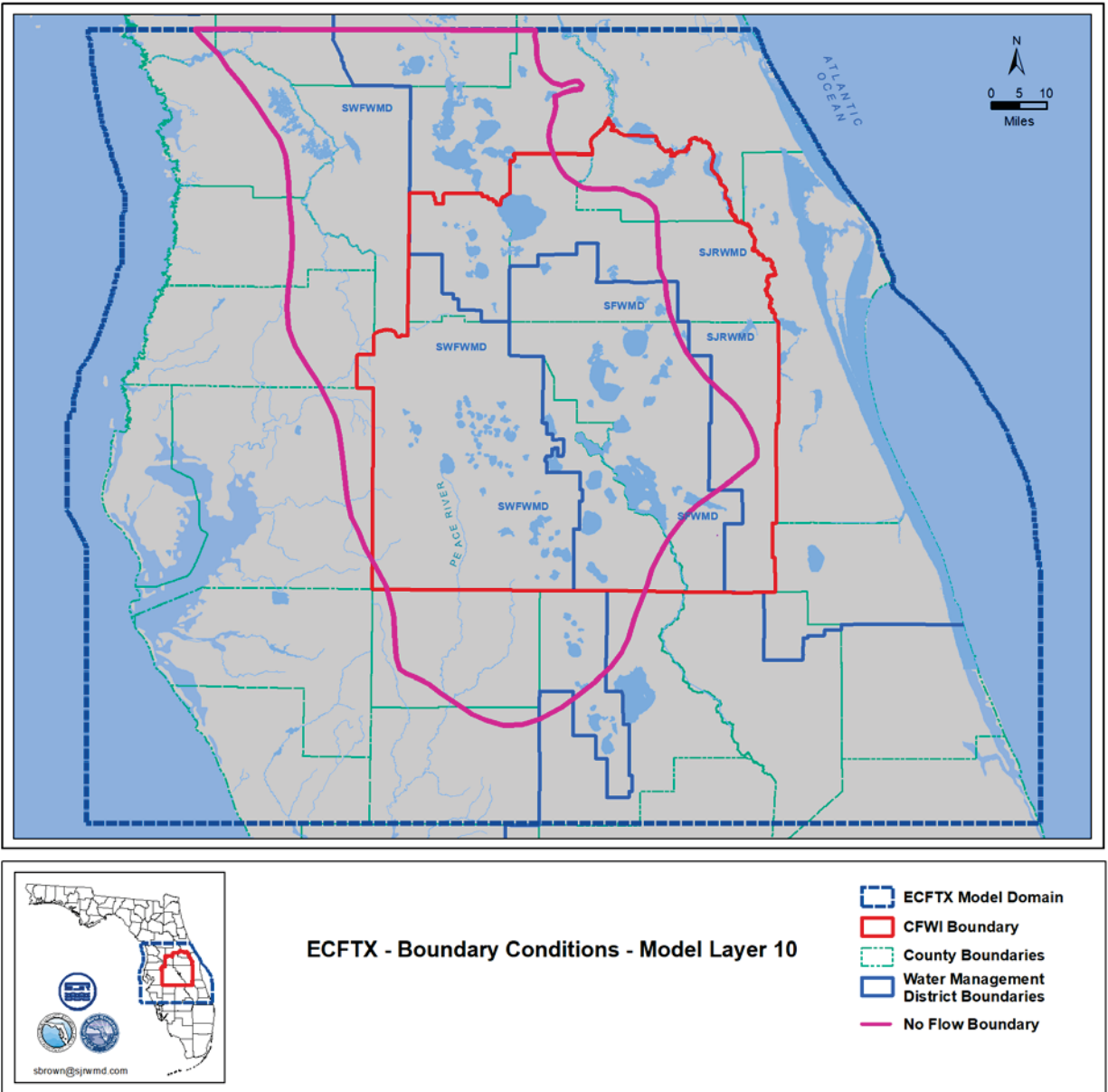Figure 45. Boundary conditions for layer 10 in the ECFTX model.
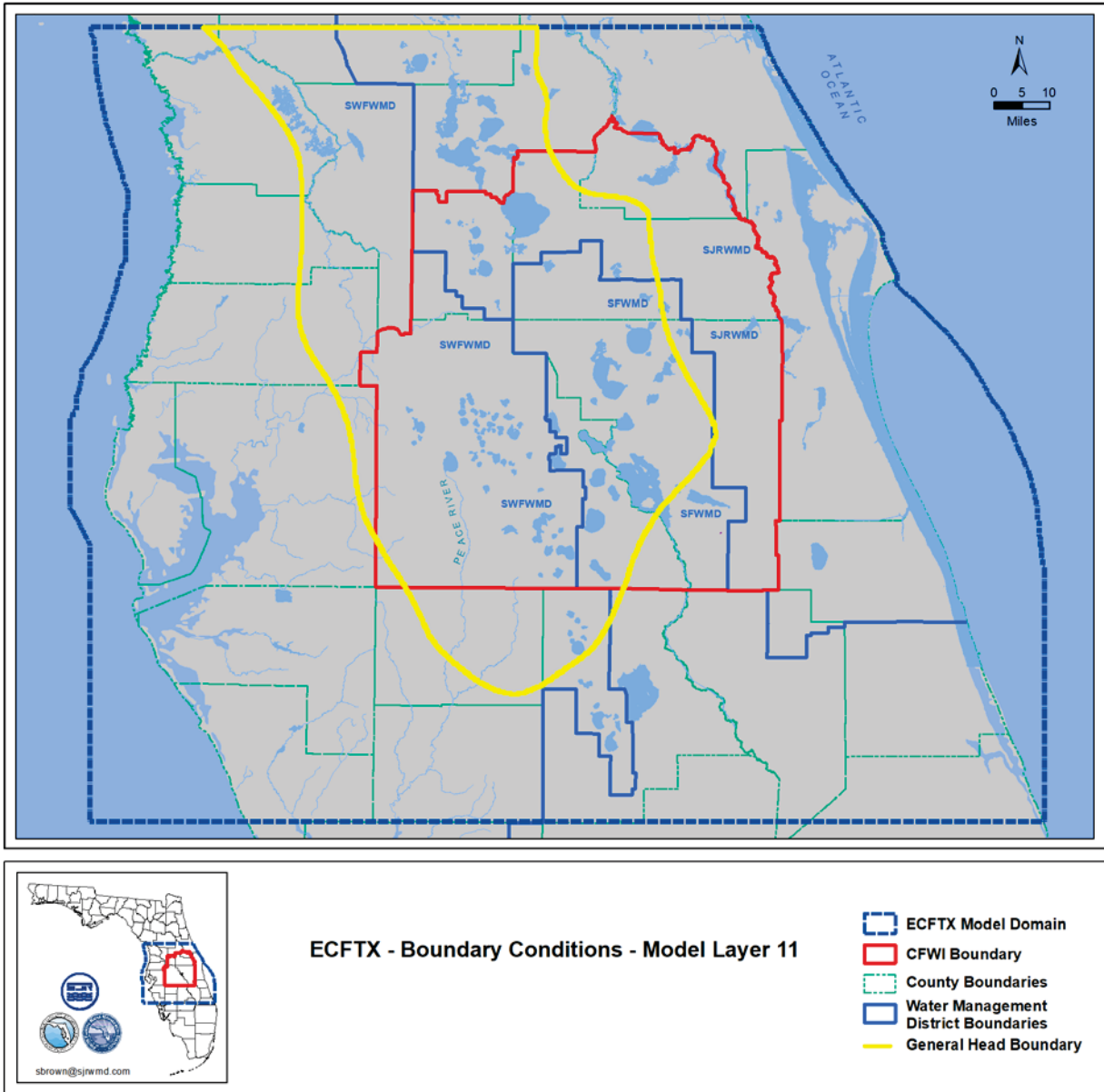
Figure 46. Boundary conditions for layer 11 in the ECFTX model.
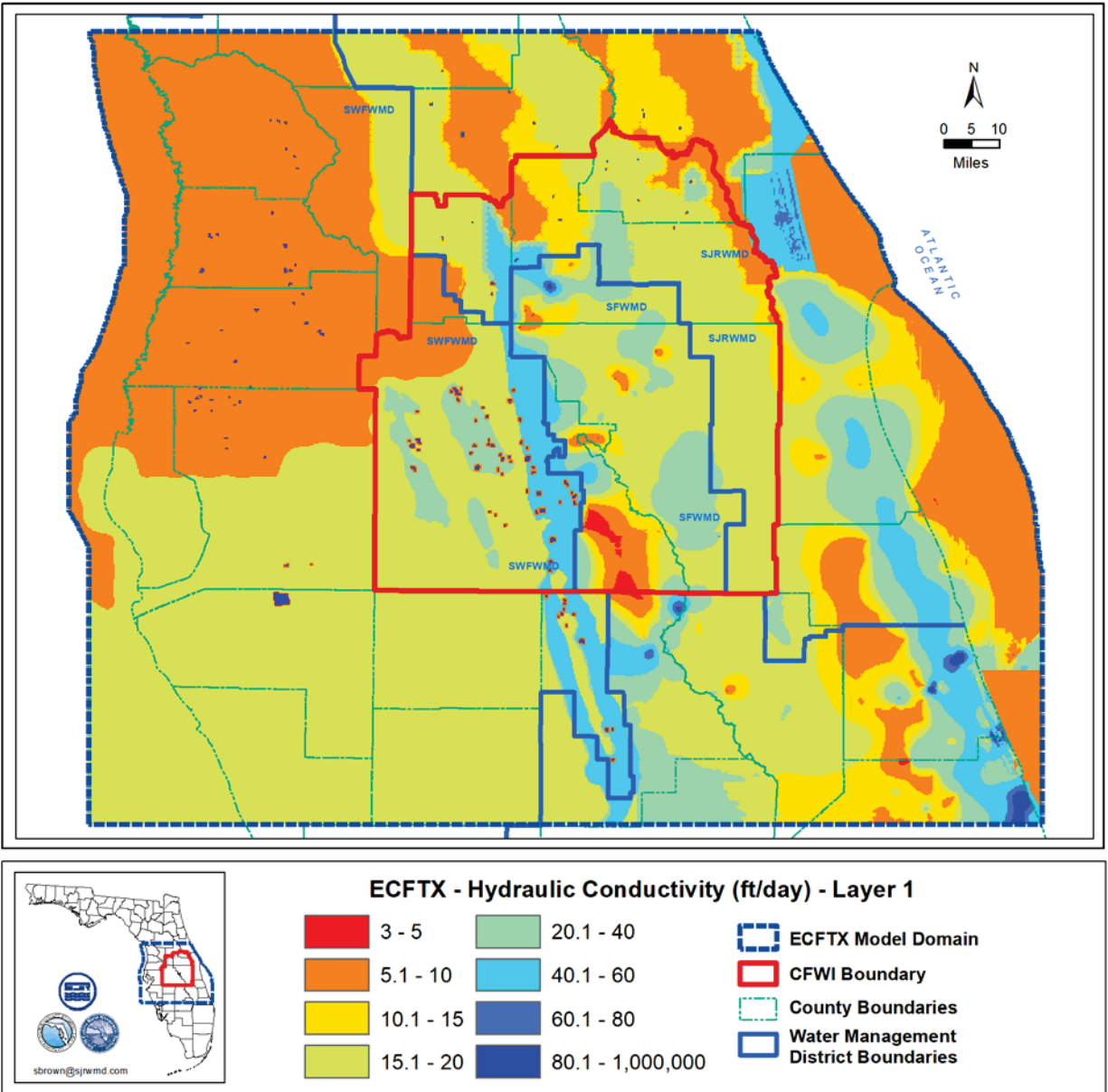
Figure 47. Hydraulic conductivity values in layer 1 in the ECFTX model.
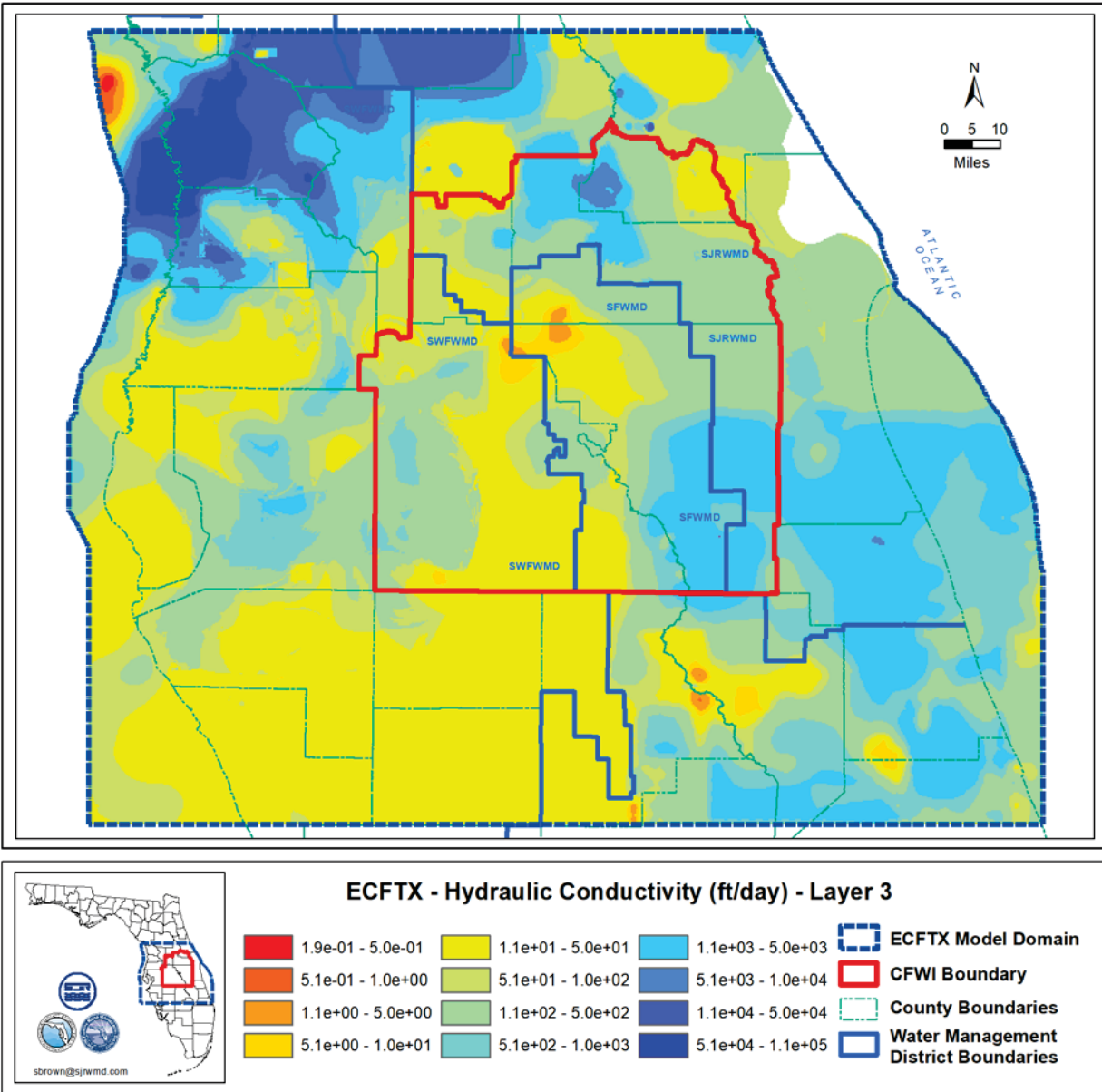
Figure 48. Hydraulic conductivity values in layer 3 in the ECFTX model.
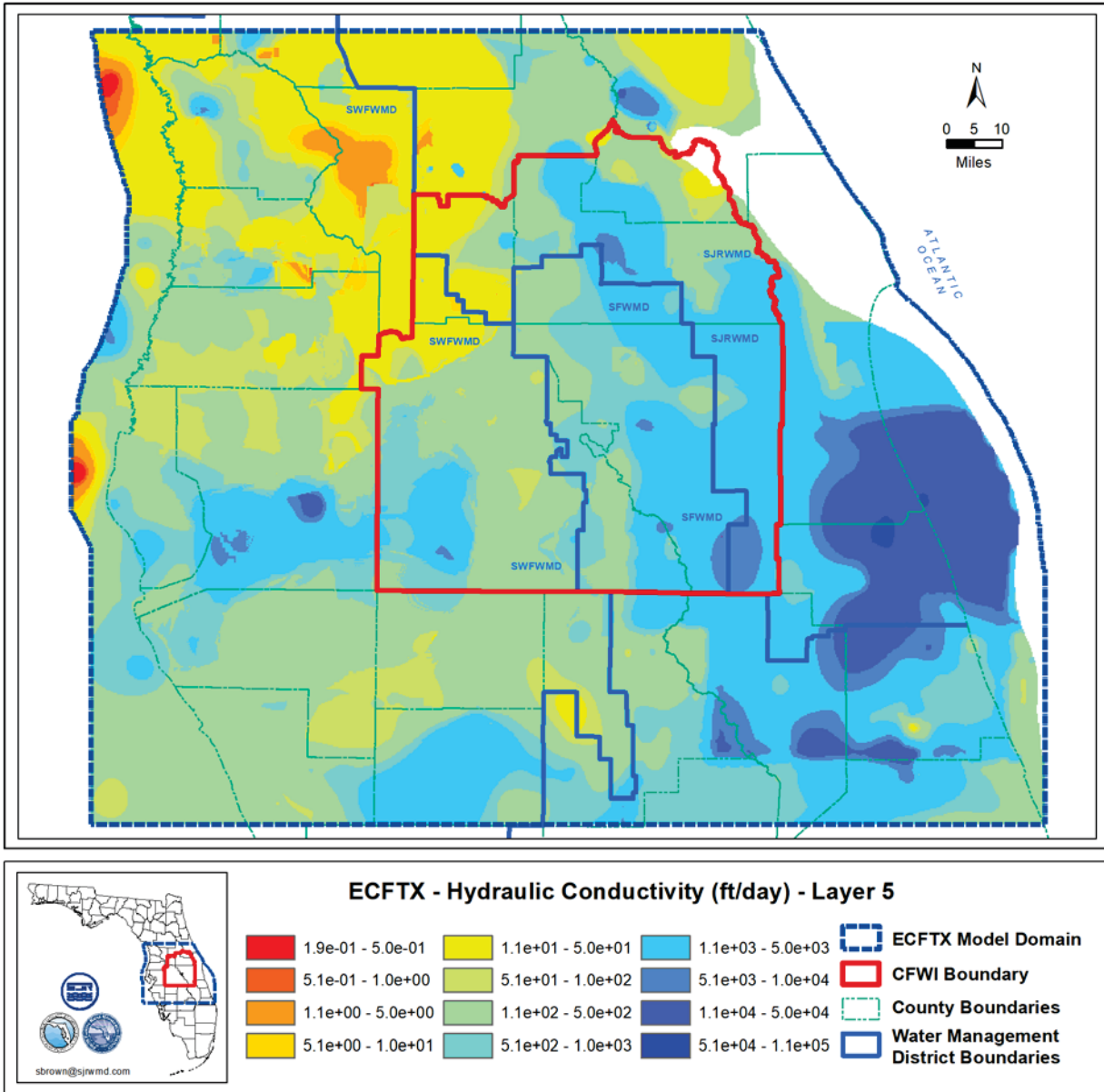
Figure 49. Hydraulic conductivity values in layer 5 in the ECFTX model.
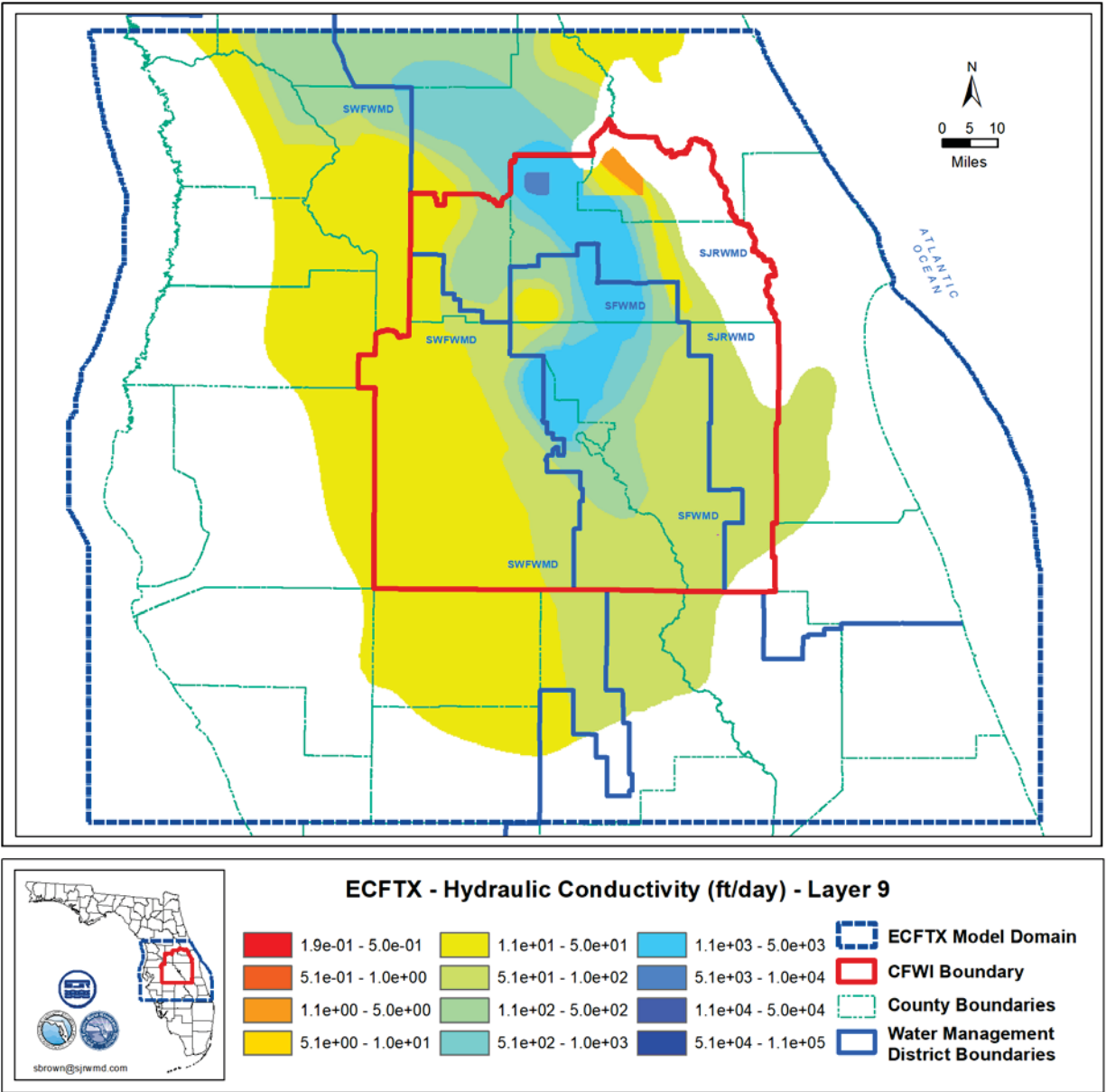
Figure 50. Hydraulic conductivity values in layer 9 in the ECFTX model.
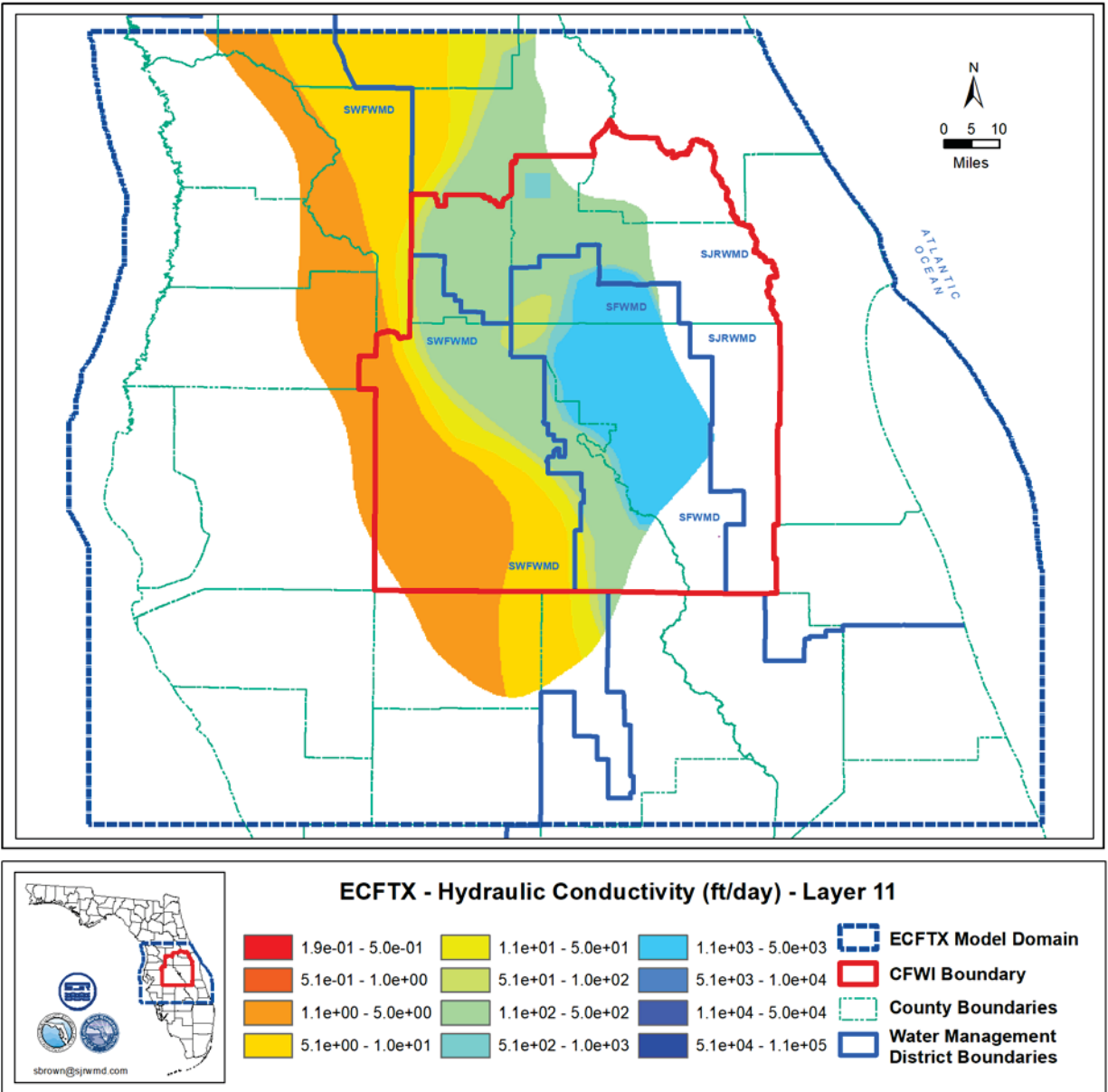
Figure 51. Hydraulic conductivity values in layer 11 in the ECFTX model.
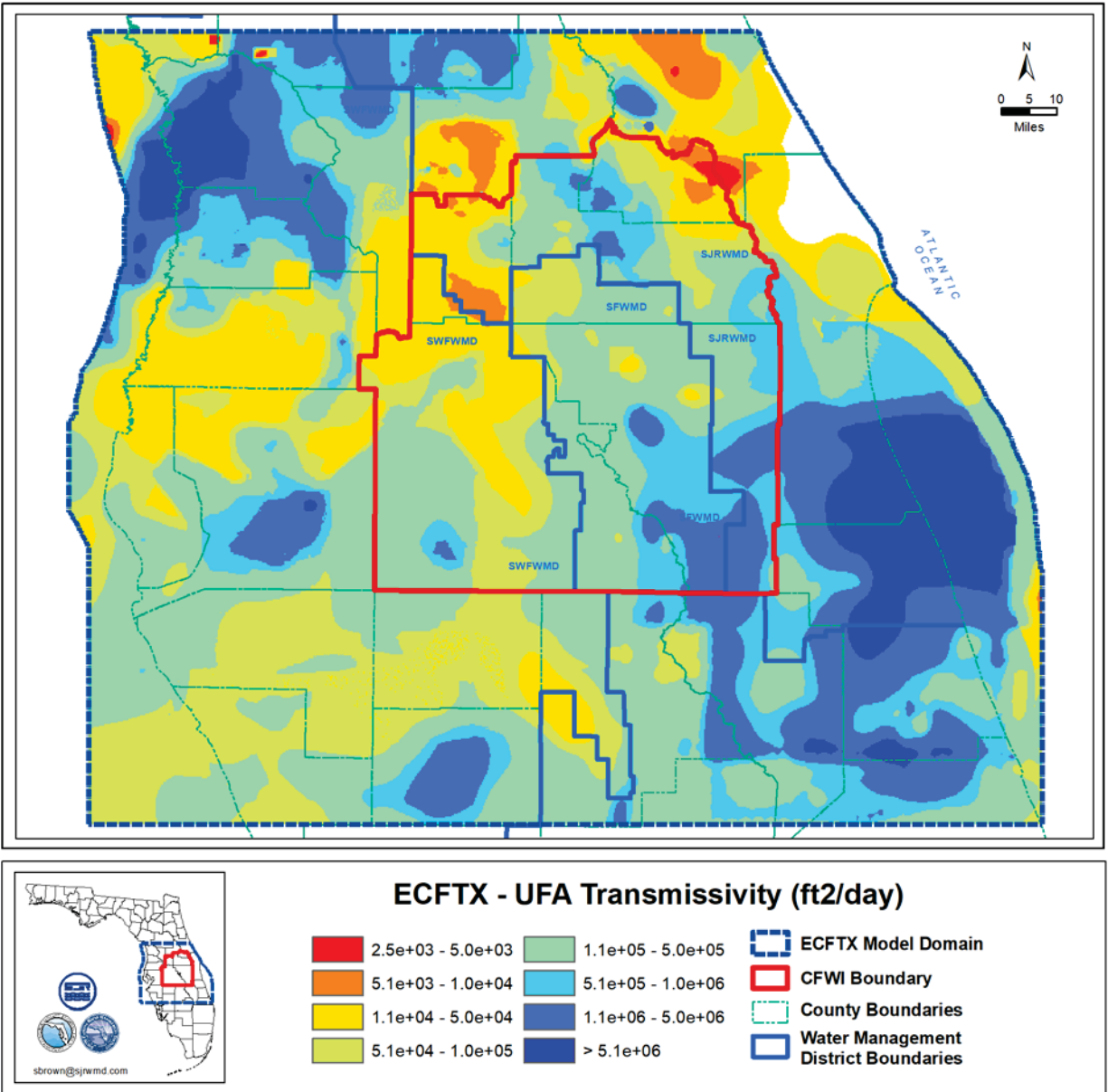
Figure 52. Transmissivity values for the UFA (layers 3-5) in the ECFTX model.
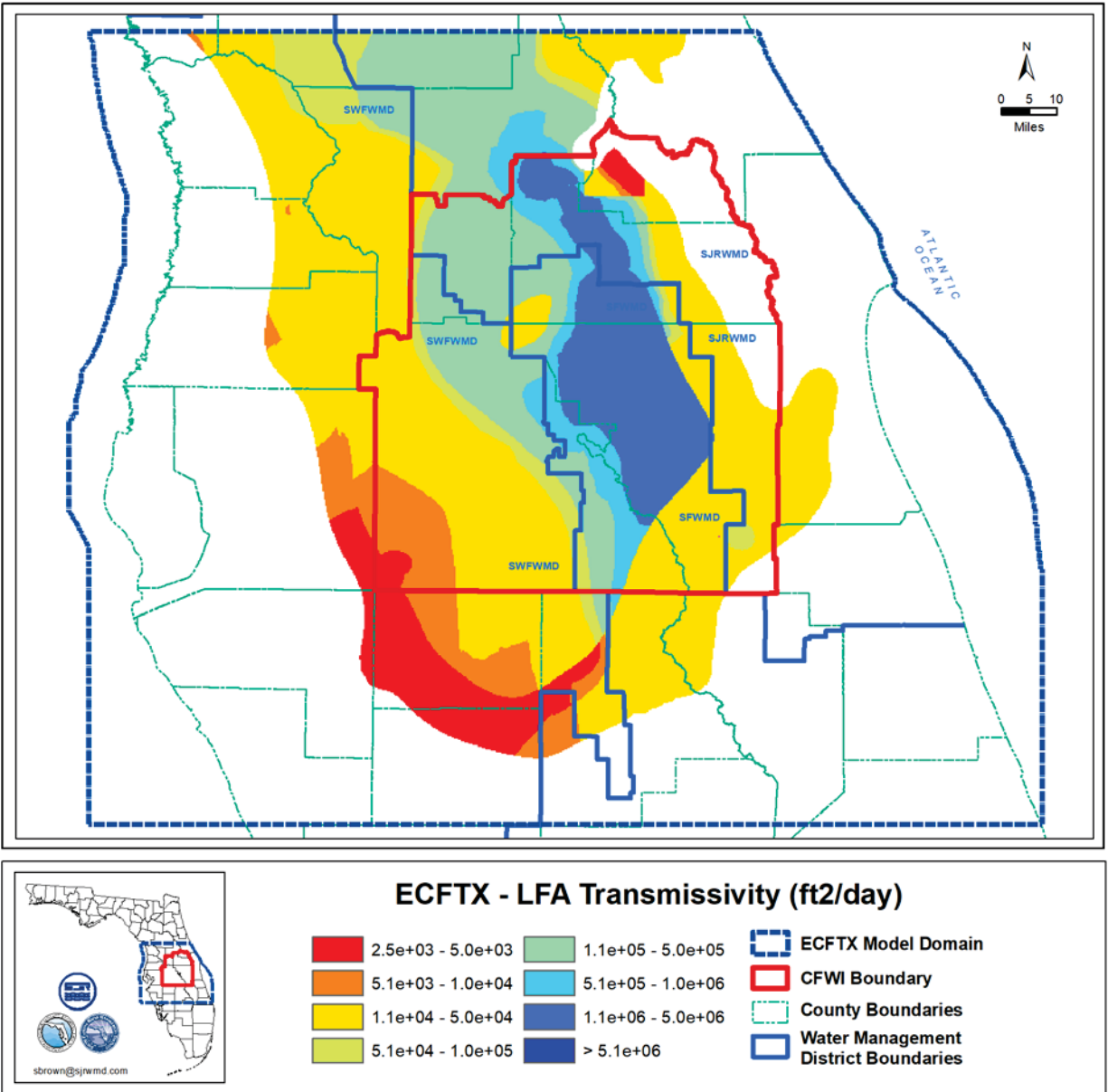
Figure 53. Transmissivity values for the LFA (layers 9-11) in the ECFTX model.
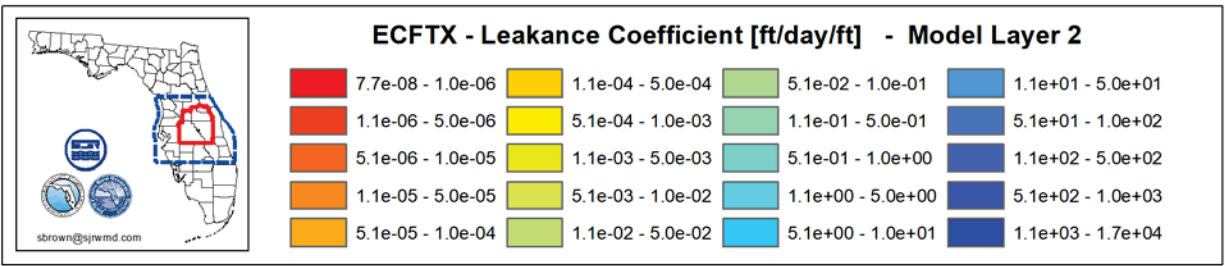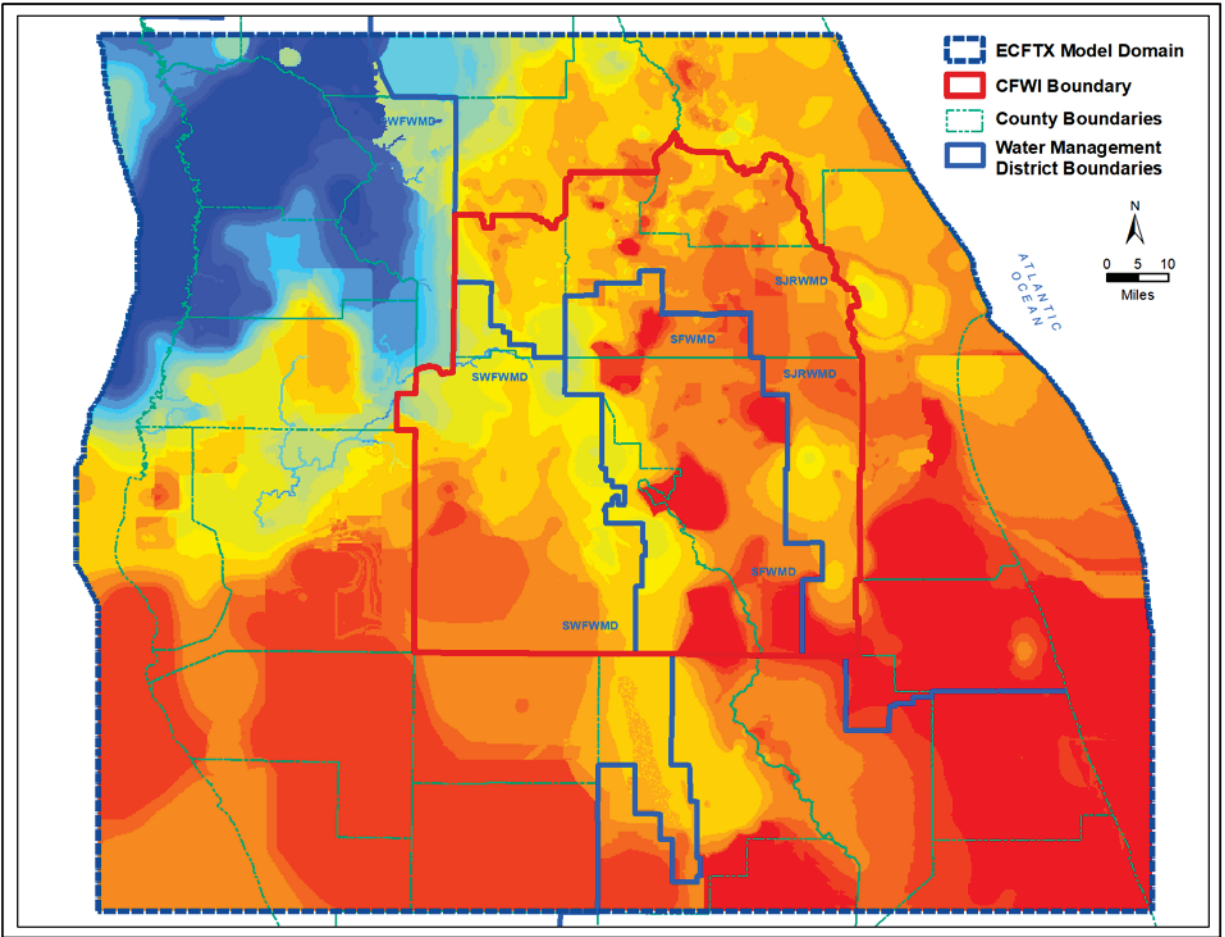
Figure 54. Leakance coefficient values for layer 2 in the ECFTX model.
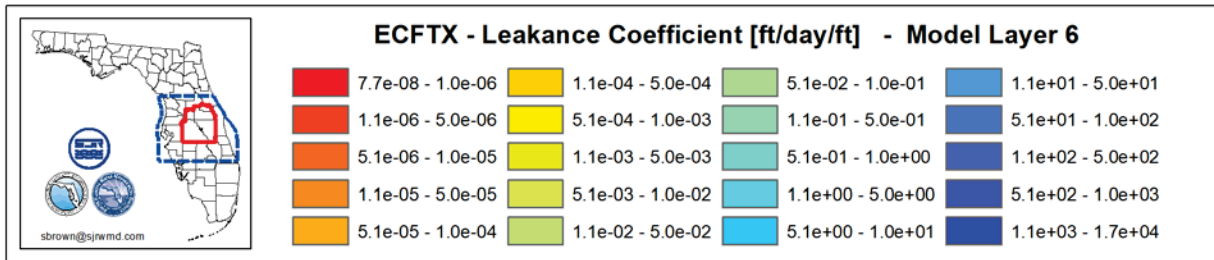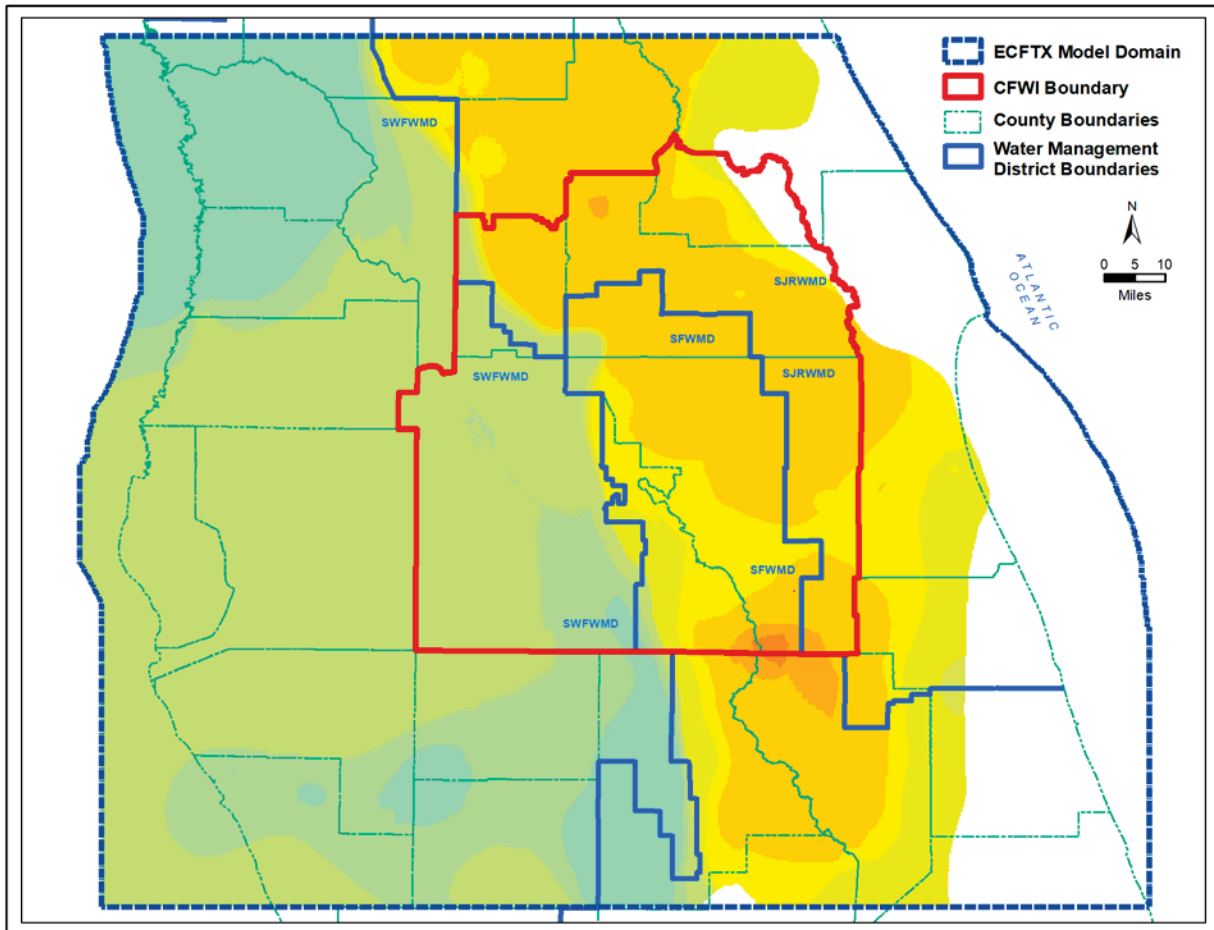
Figure 55. Leakance coefficient values for layer 6 in the ECFTX model.
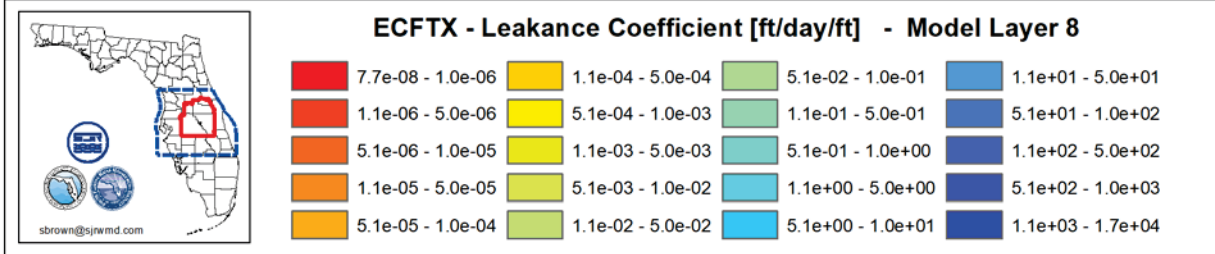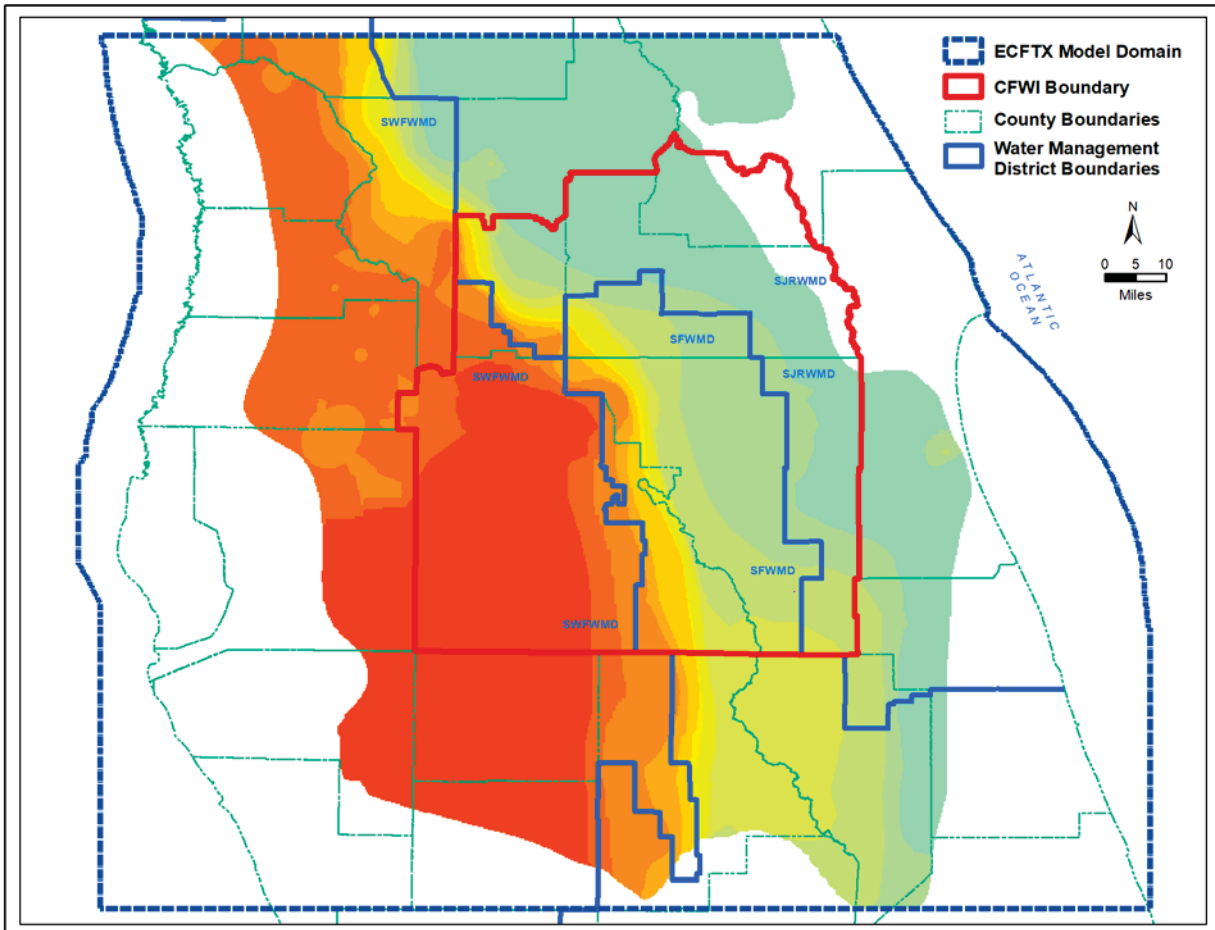
Figure 56. Leakance coefficient values for layer 8 in the ECFTX model.
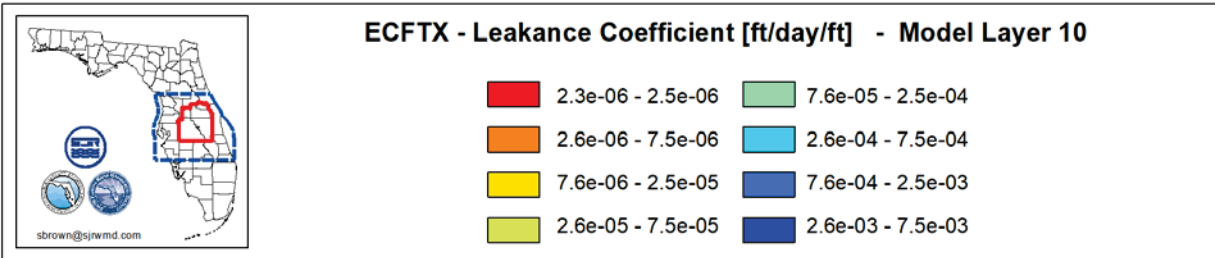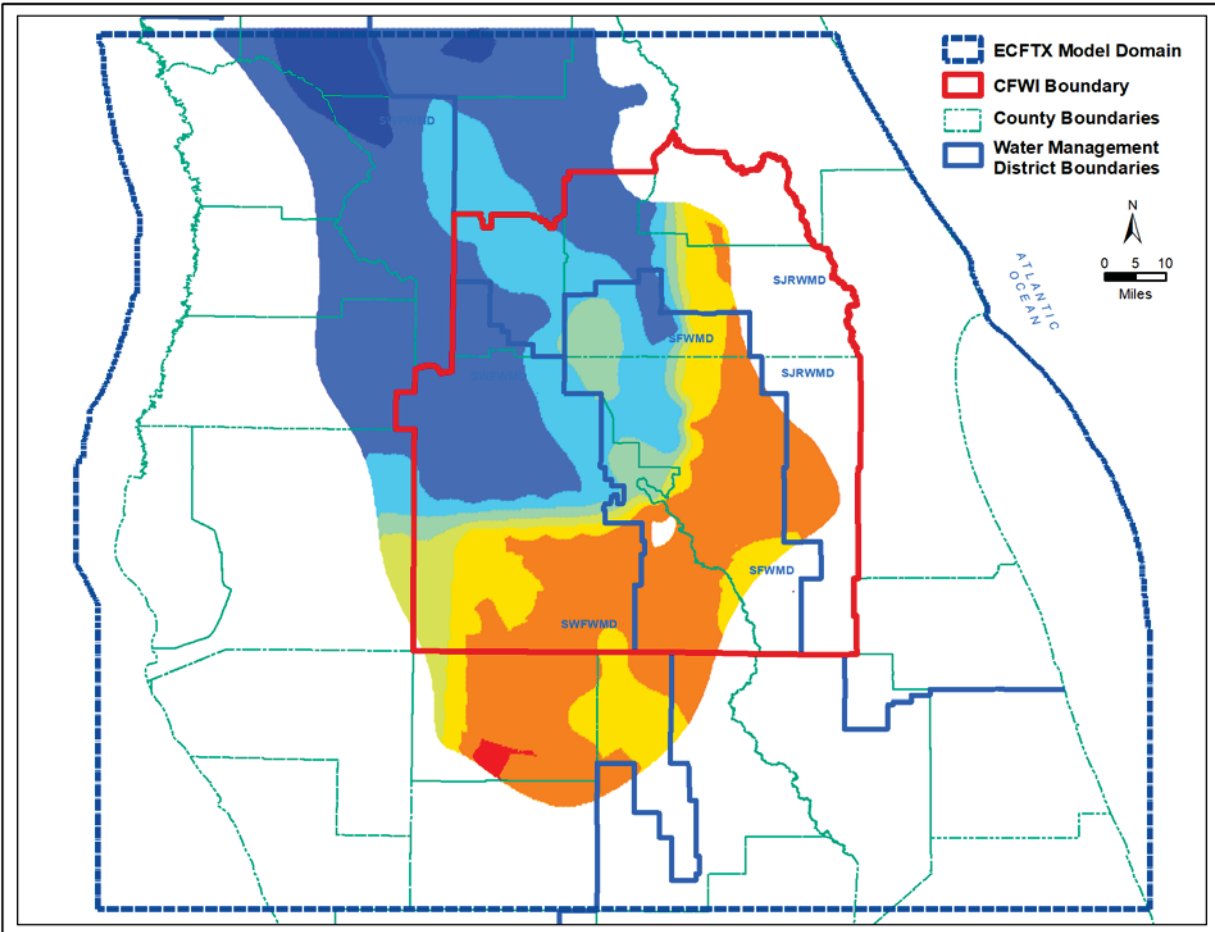
Figure 57. Leakance coefficient values for layer 10 in the ECFTX model.
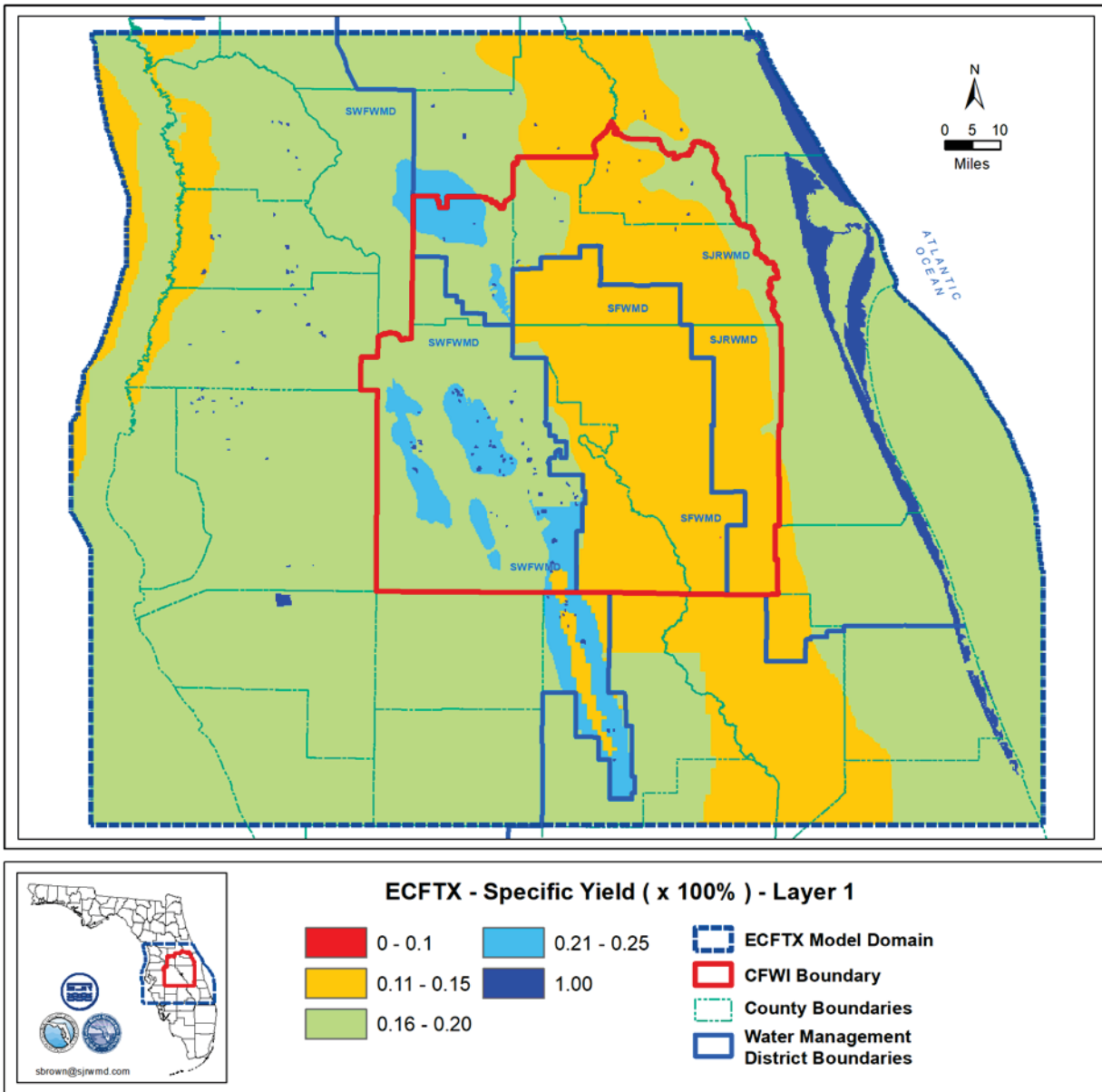
Figure 58. Specific yield values for layer 1 in the ECFTX model.
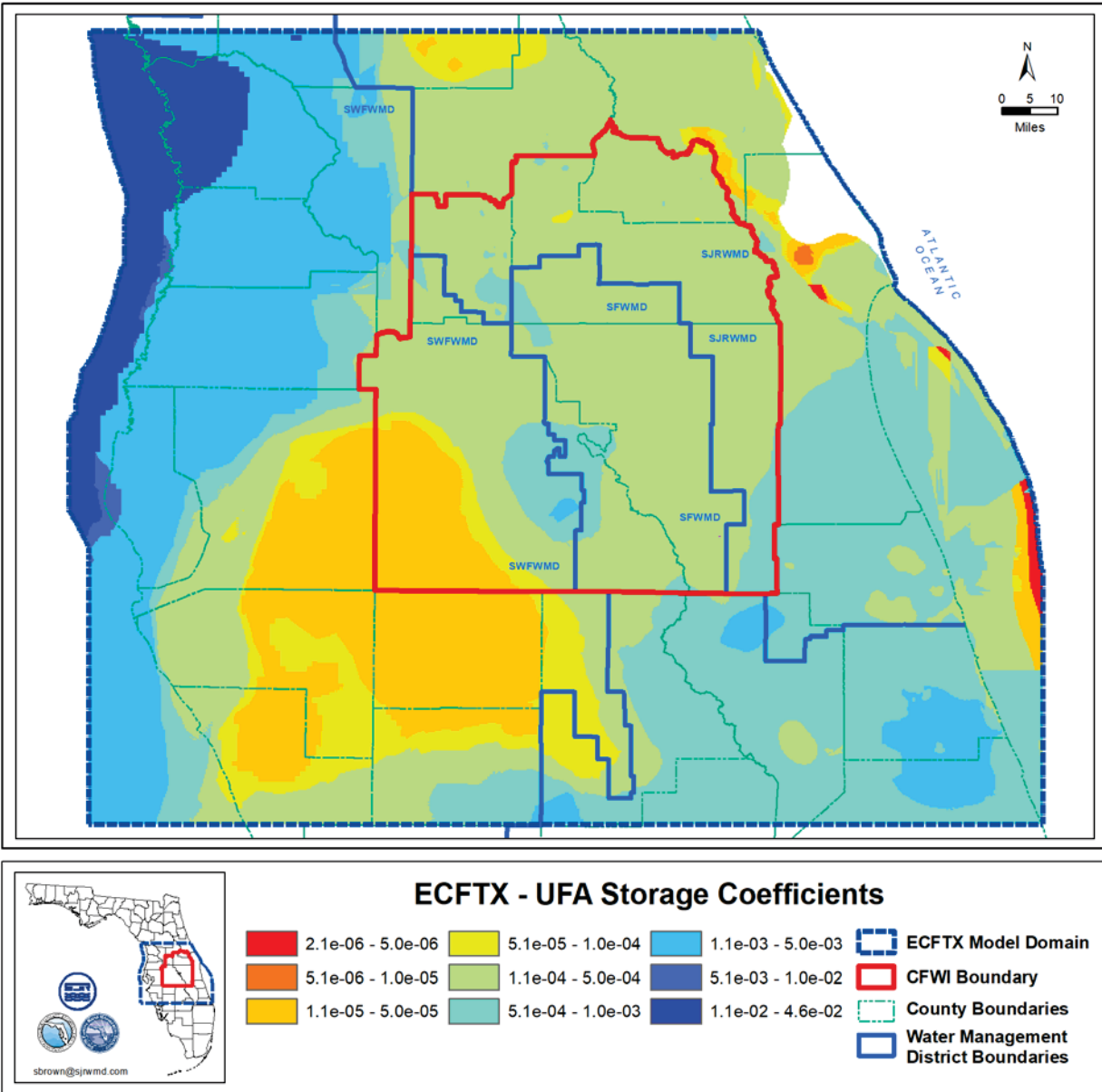
Figure 59. Storage coefficient values for the UFA (layers 3-5) in the ECFTX model.
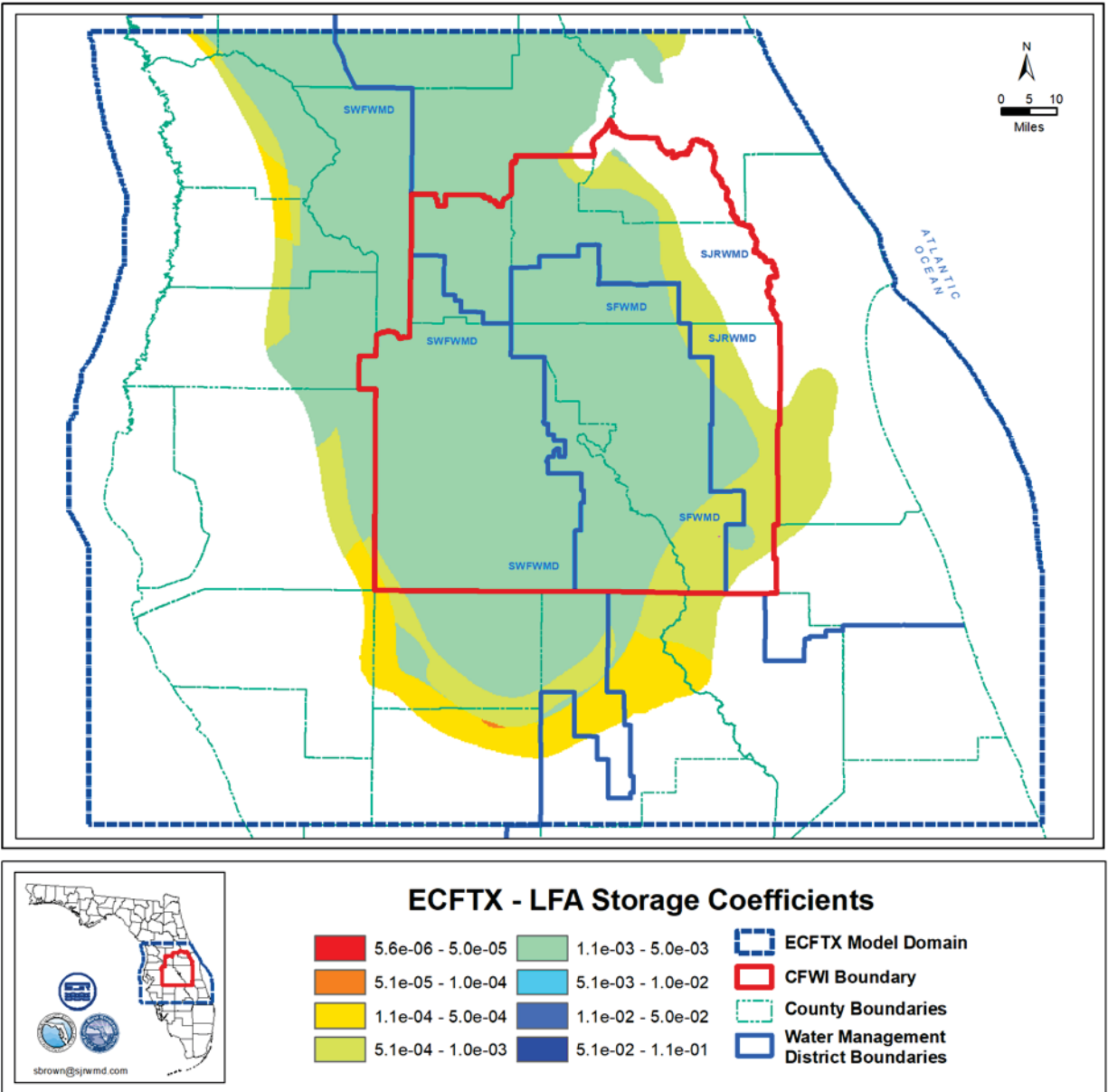
Figure 60. Storage coefficient values for the LFA (layers 9-11) in the ECFTX model.
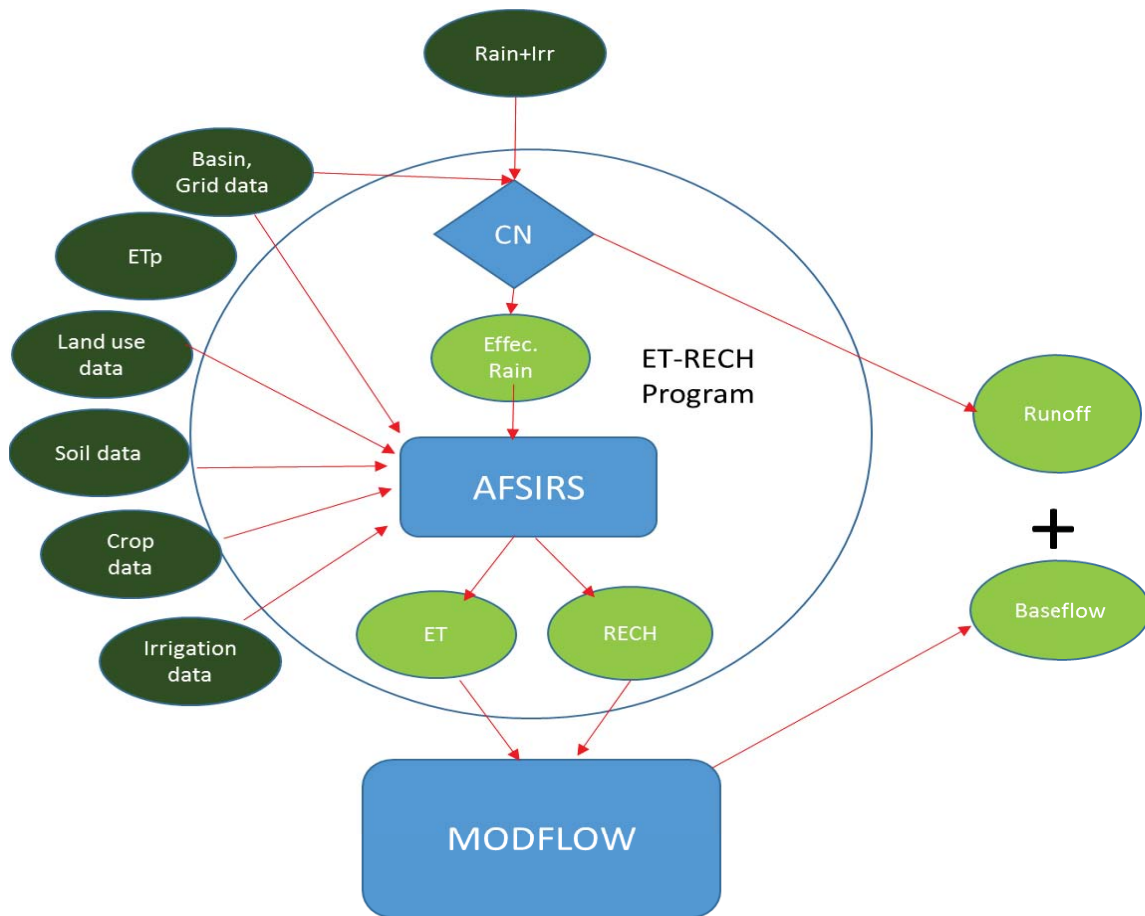
Figure 61. Data Inputs and Outputs for the ET/Recharge Methodology.
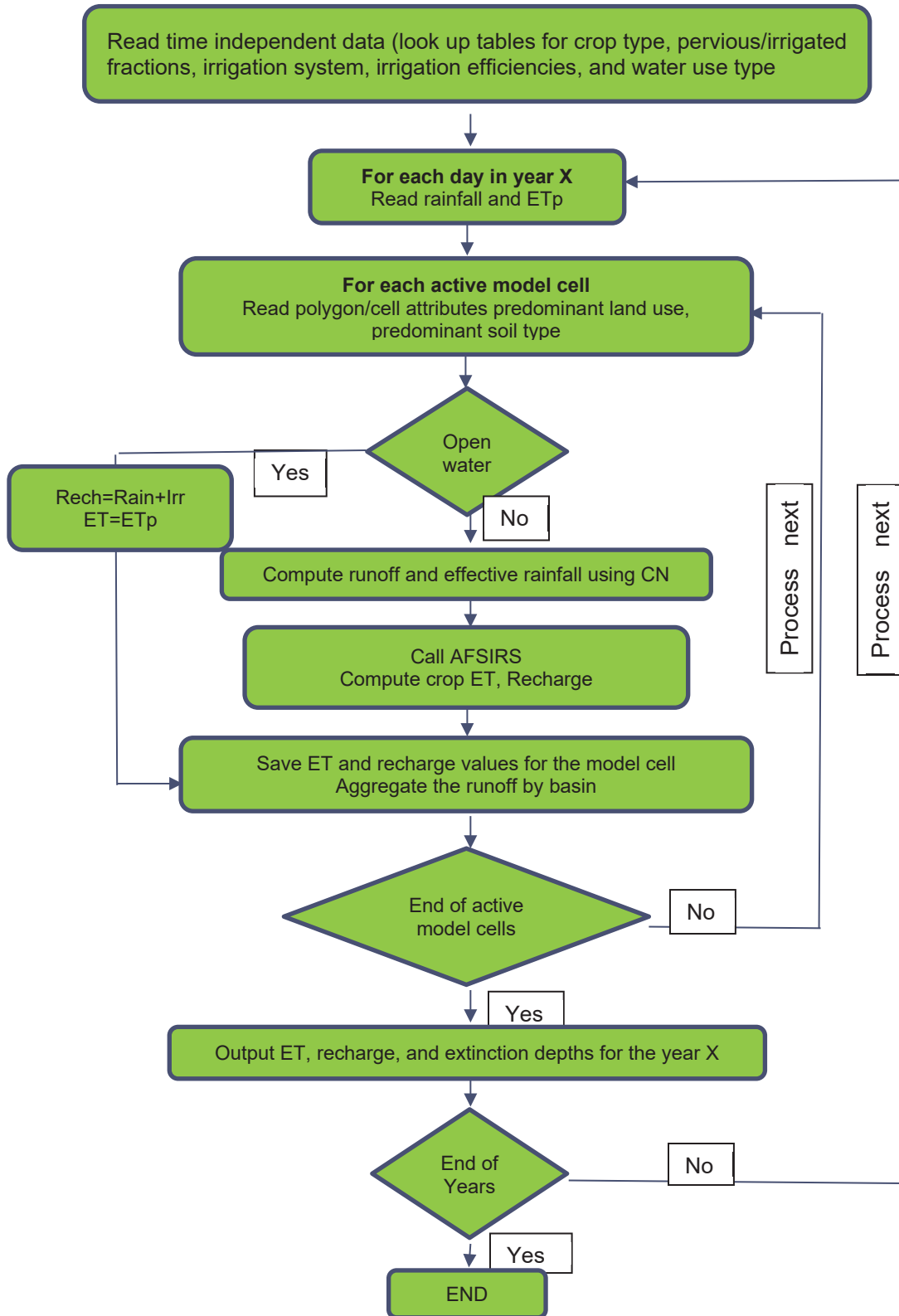
Figure 62. Flow Chart Showing the ET/Recharge Methodology.
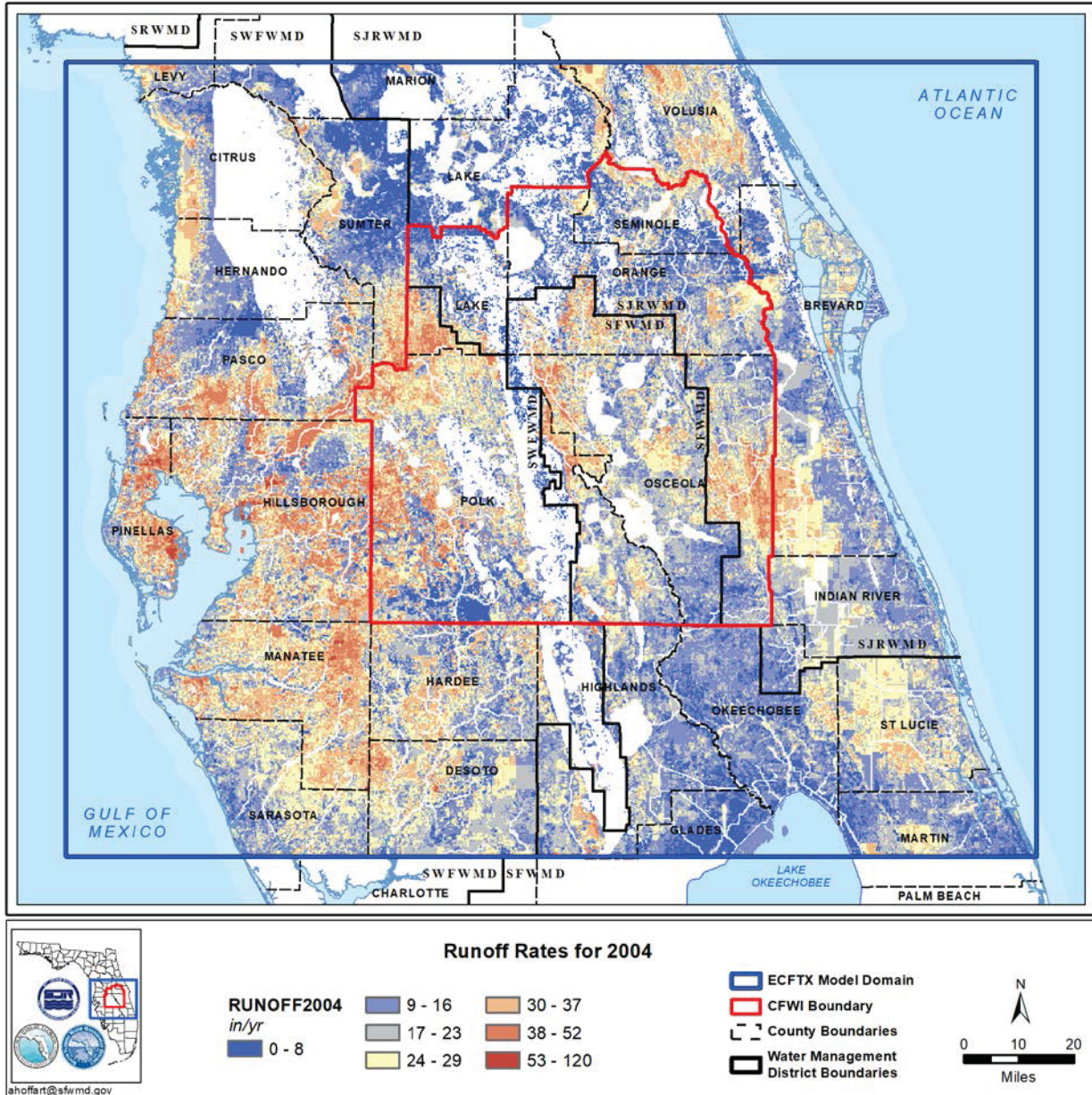
Figure 63. Spatial distribution of simulated runoff for 2004 (wet year).
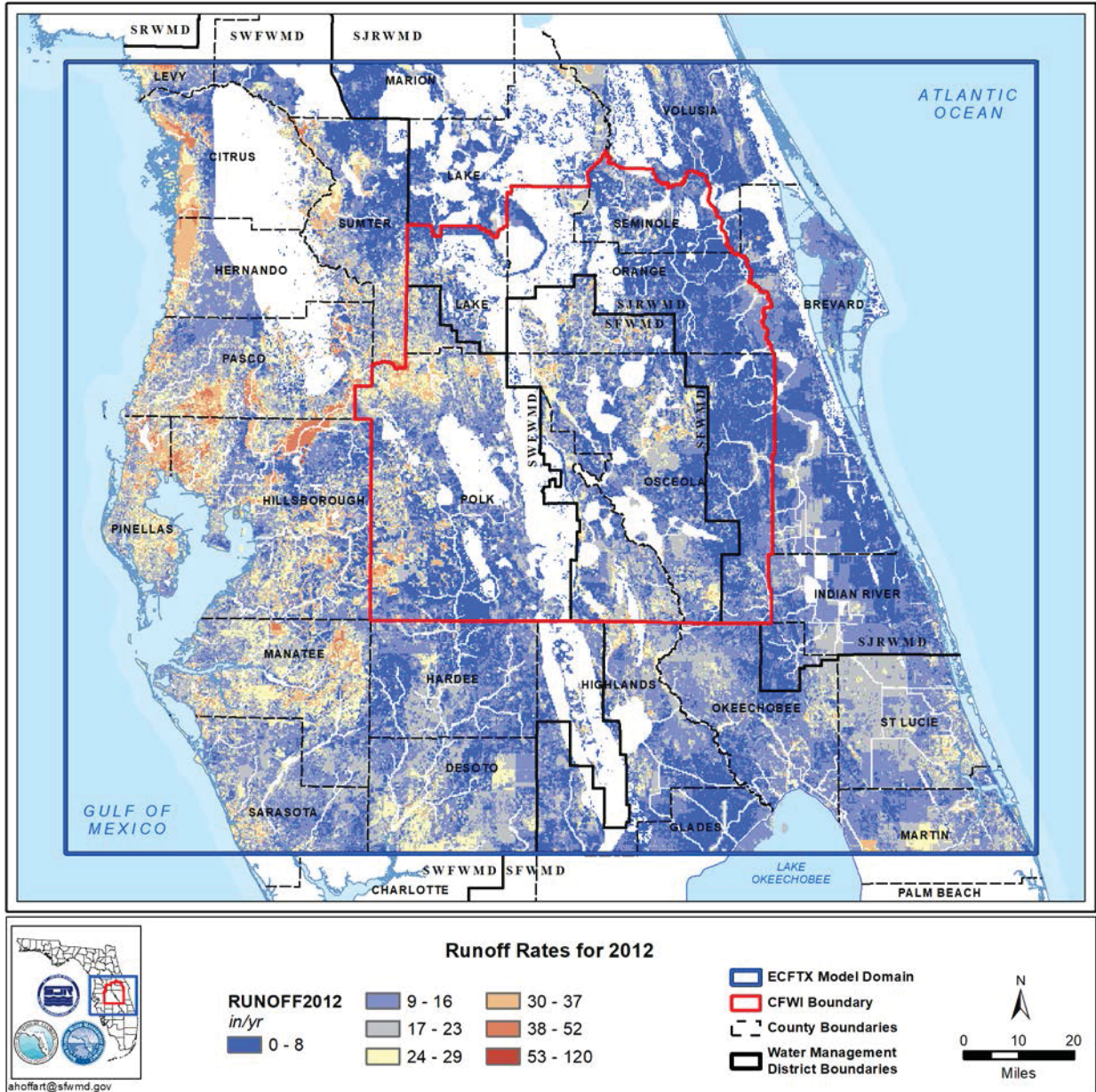
Figure 64. Spatial distribution of simulated runoff 2012 (dry year).
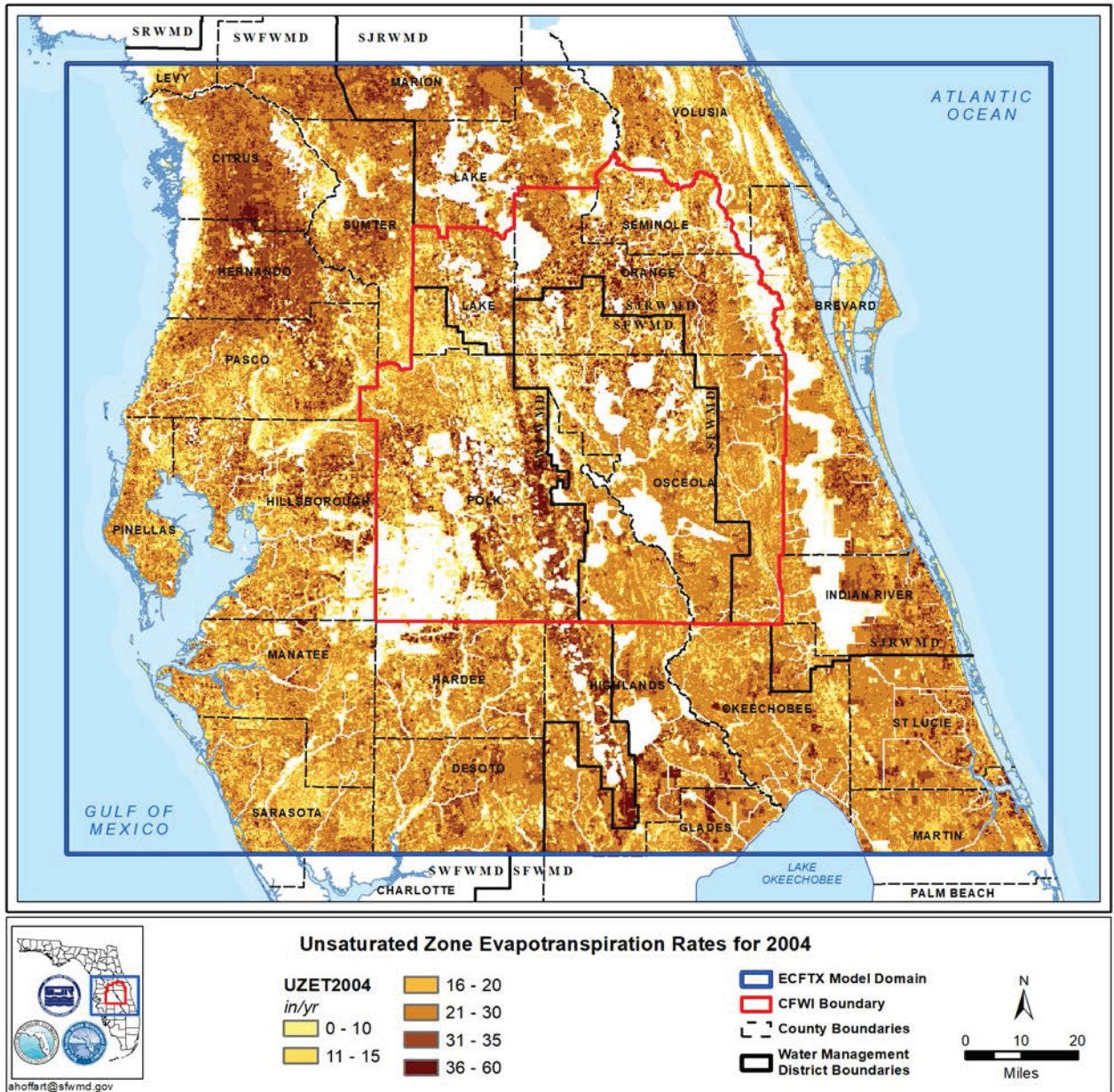
Figure 65. Spatial distribution of unsaturated zone evapotranspiration for 2004 (wet year).
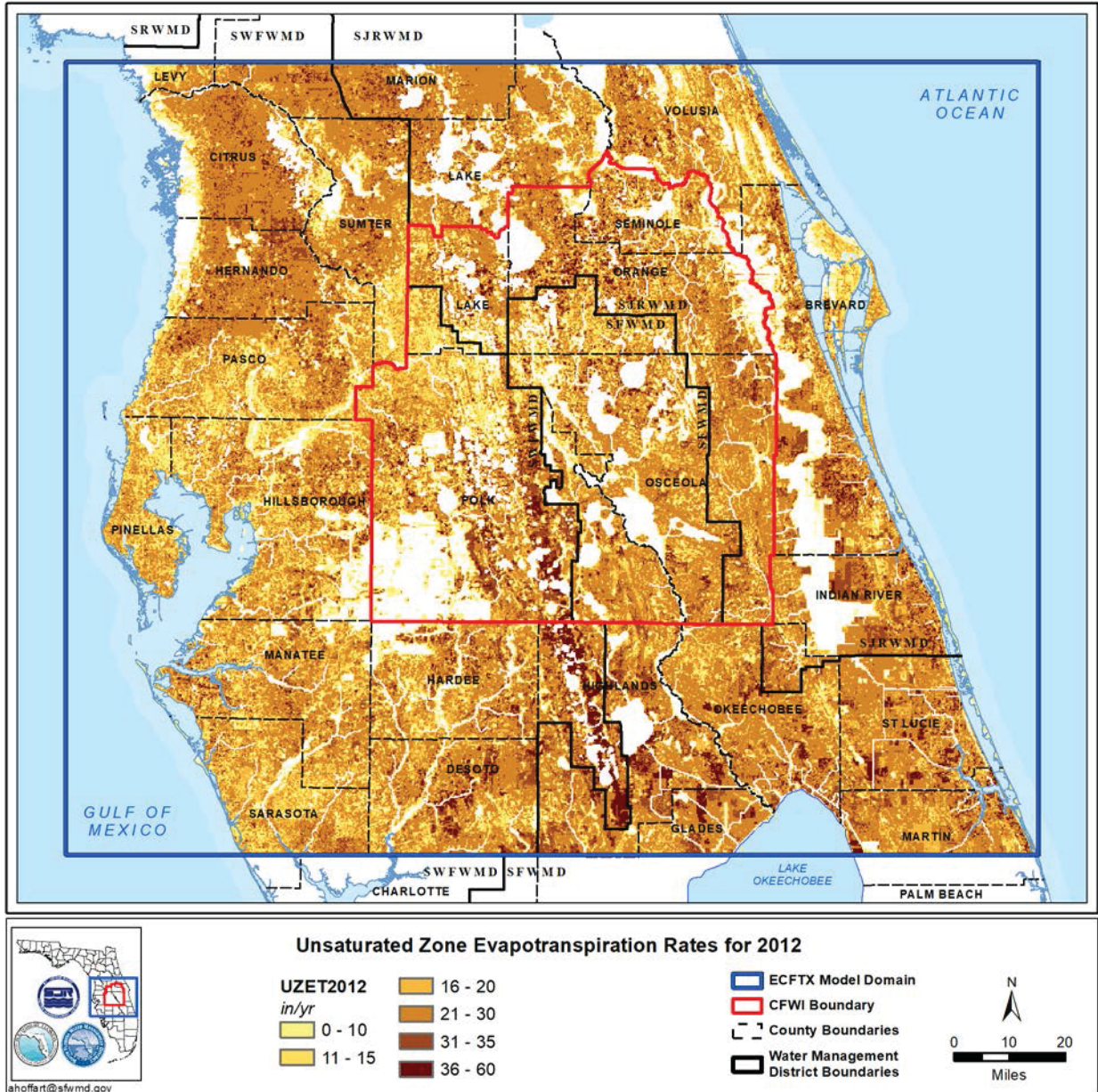
Figure 66. Spatial distribution of unsaturated zone evapotranspiration for 2012 (dry year).
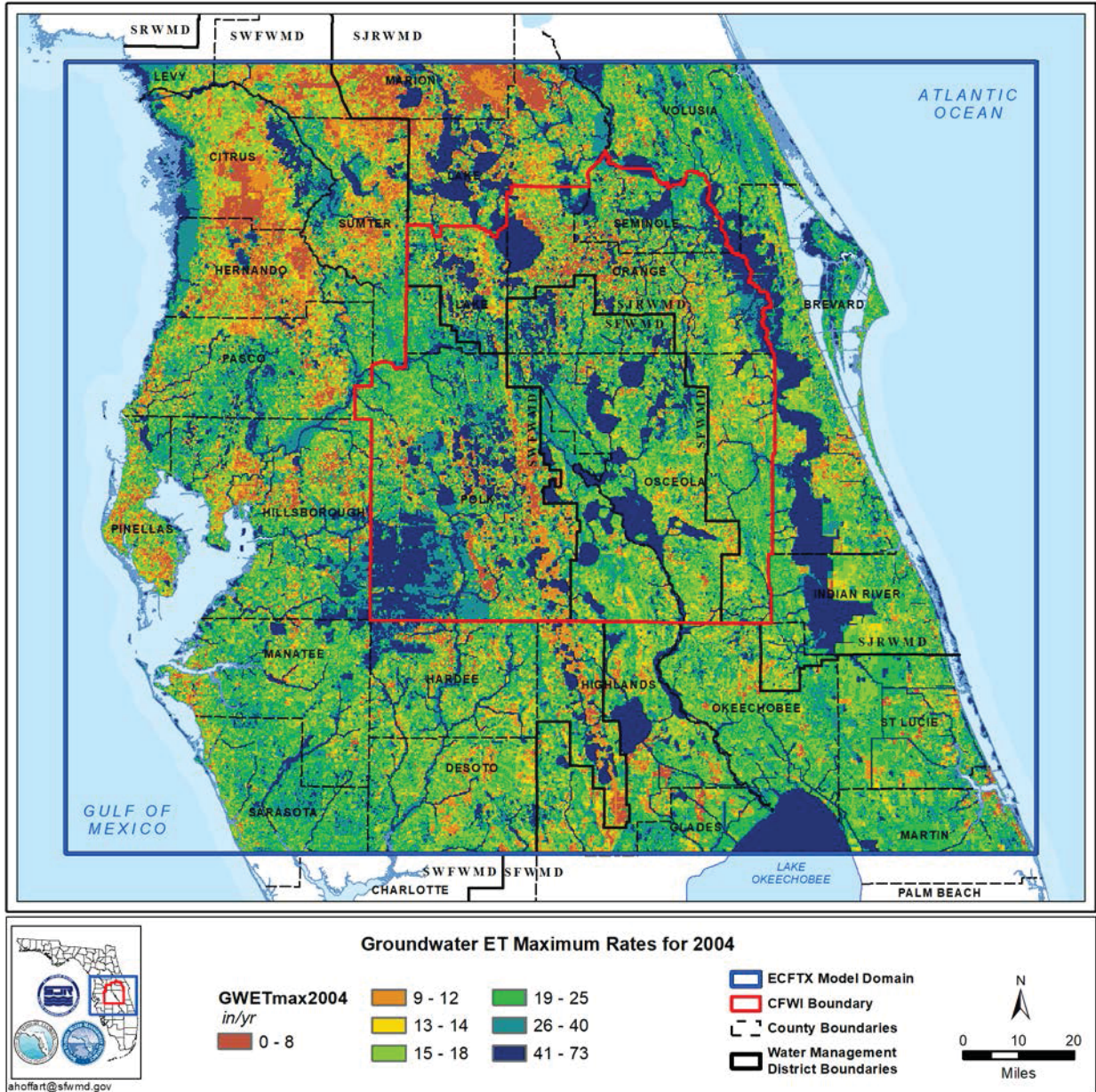
Figure 67. Spatial distribution of applied maximum evapotranspiration for 2004 (wet year).
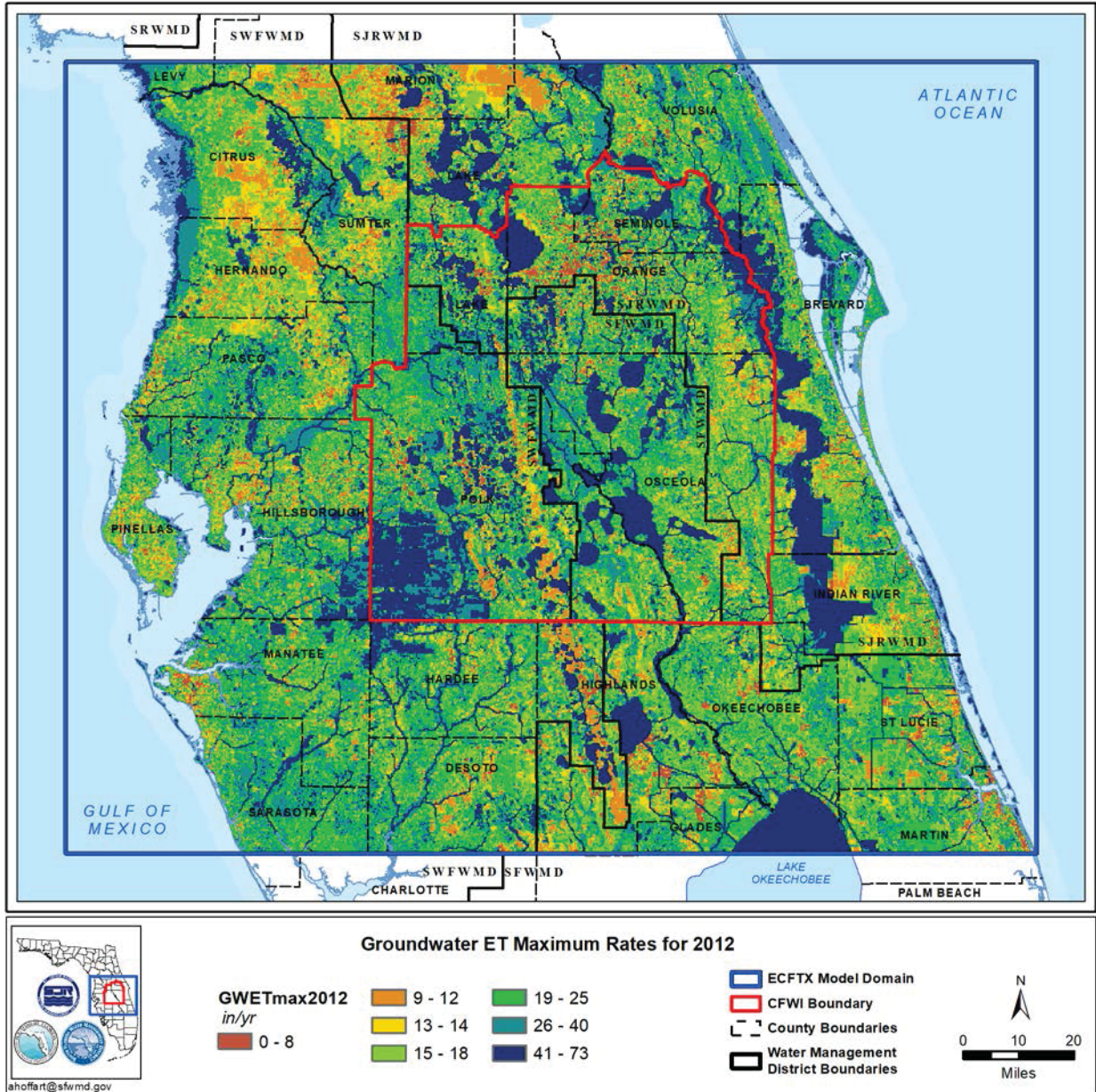
Figure 68. Spatial distribution of applied maximum evapotranspiration for 2012 (dry year).
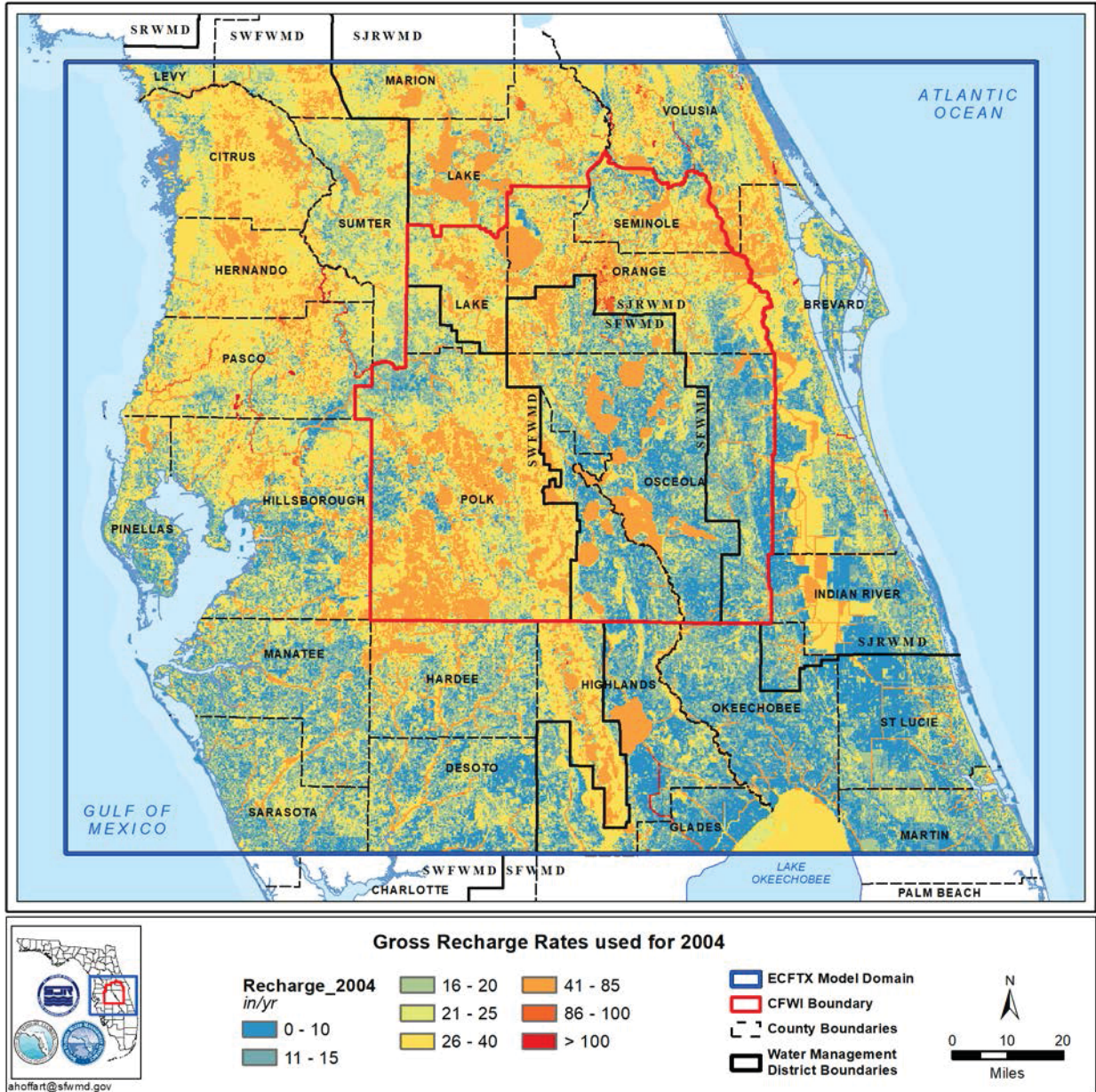
Figure 69. Spatial distribution of applied gross recharge 2004 (wet year).
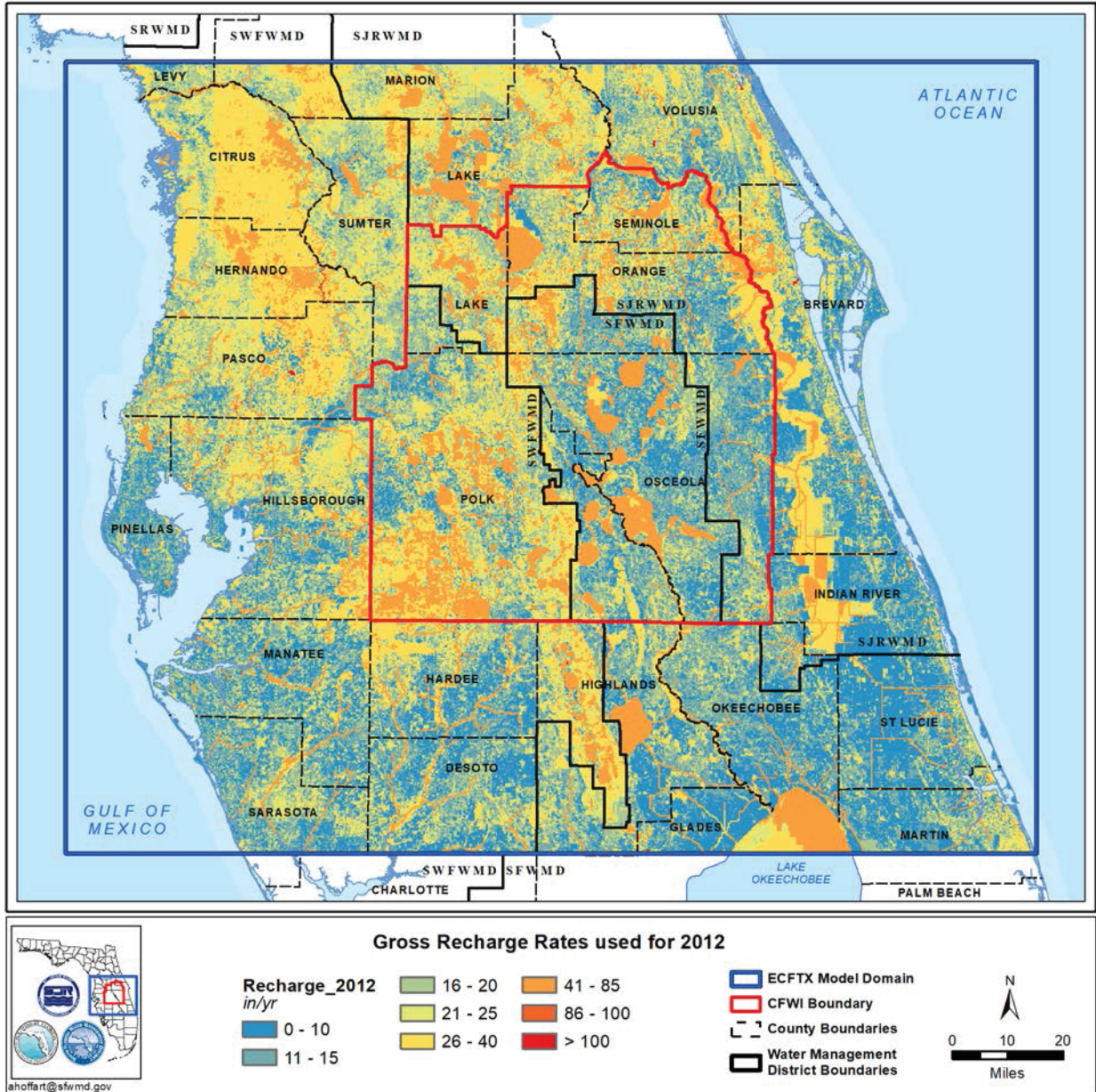
Figure 70. Spatial distribution of applied gross recharge 2012 (dry year).

MODFLOW Simulated Evapotranspiration Rates for 2004

ET_2004
in/yr
- 0 - 2
- 3 - 5
- 6 - 10
- 11 - 17
- 18 - 28
- 29 - 46
- 47 - 73

- ECFTX Model Domain
- CFWI Boundary
- County Boundaries
- Water Management District Boundaries

0   10   20
Miles
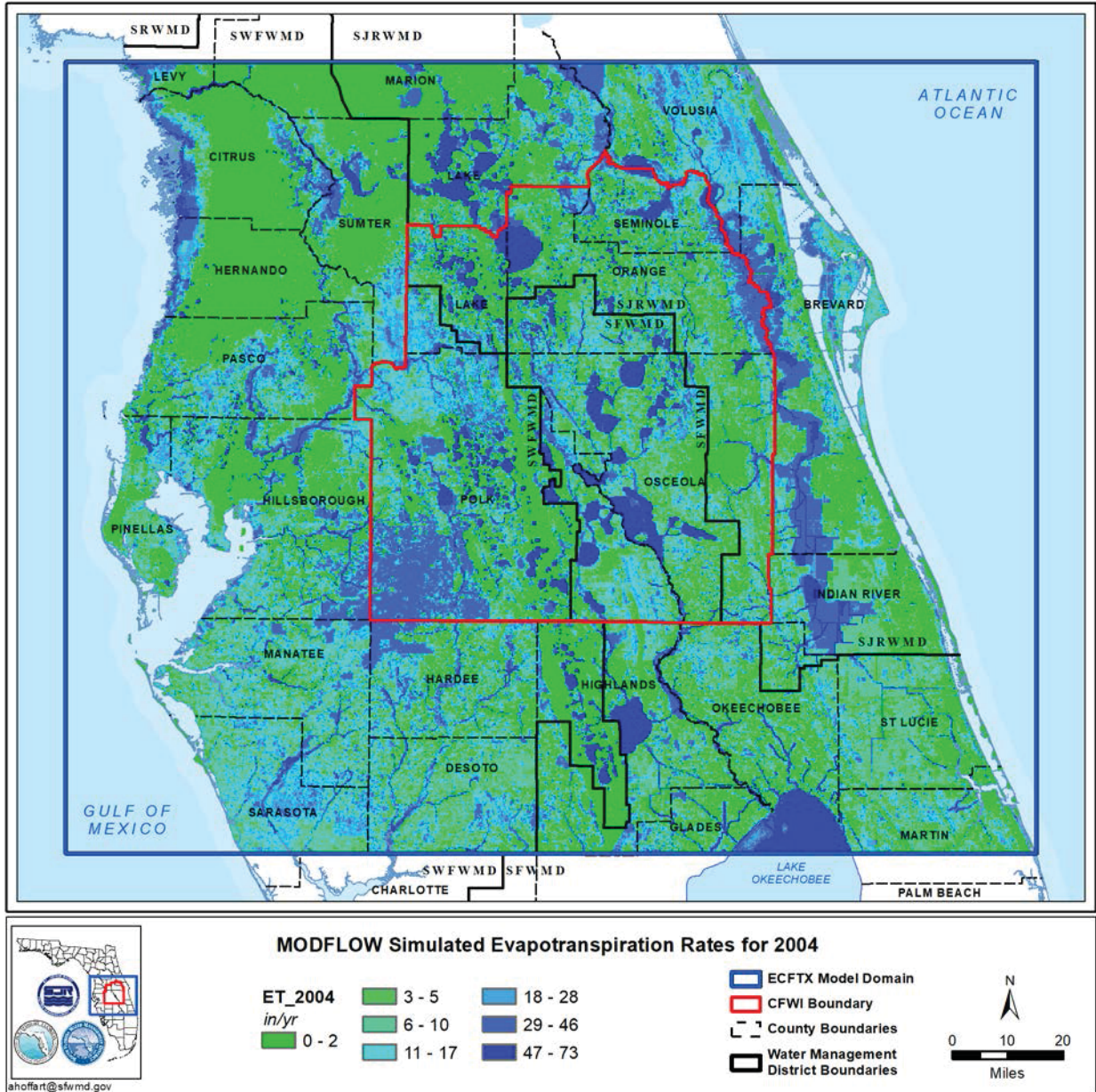
Figure 71. Spatial distribution of MODFLOW simulated groundwater ET 2004 (wet year).
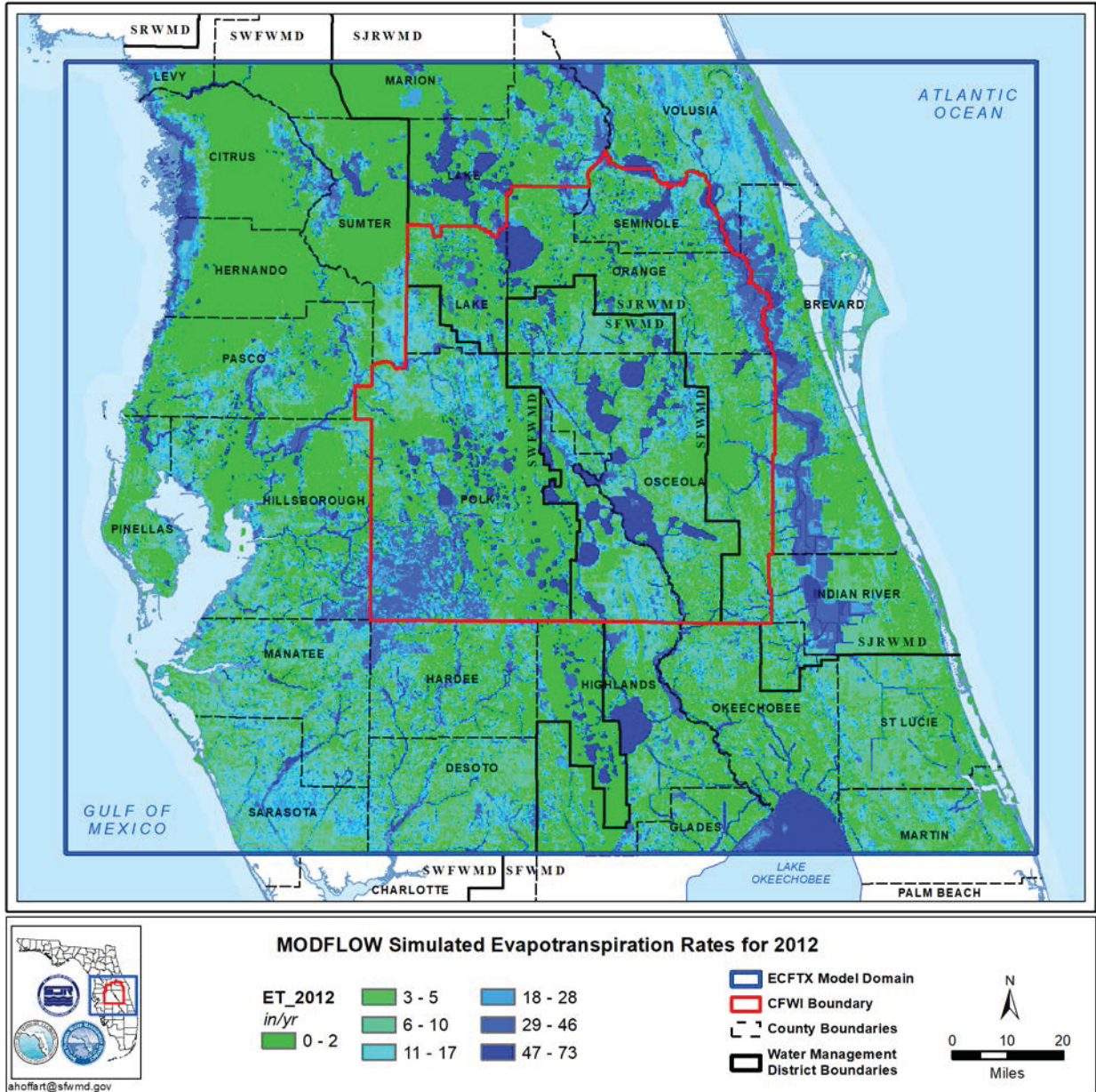
Figure 72. Spatial distribution of MODFLOW simulated groundwater ET for 2012 (dry year).
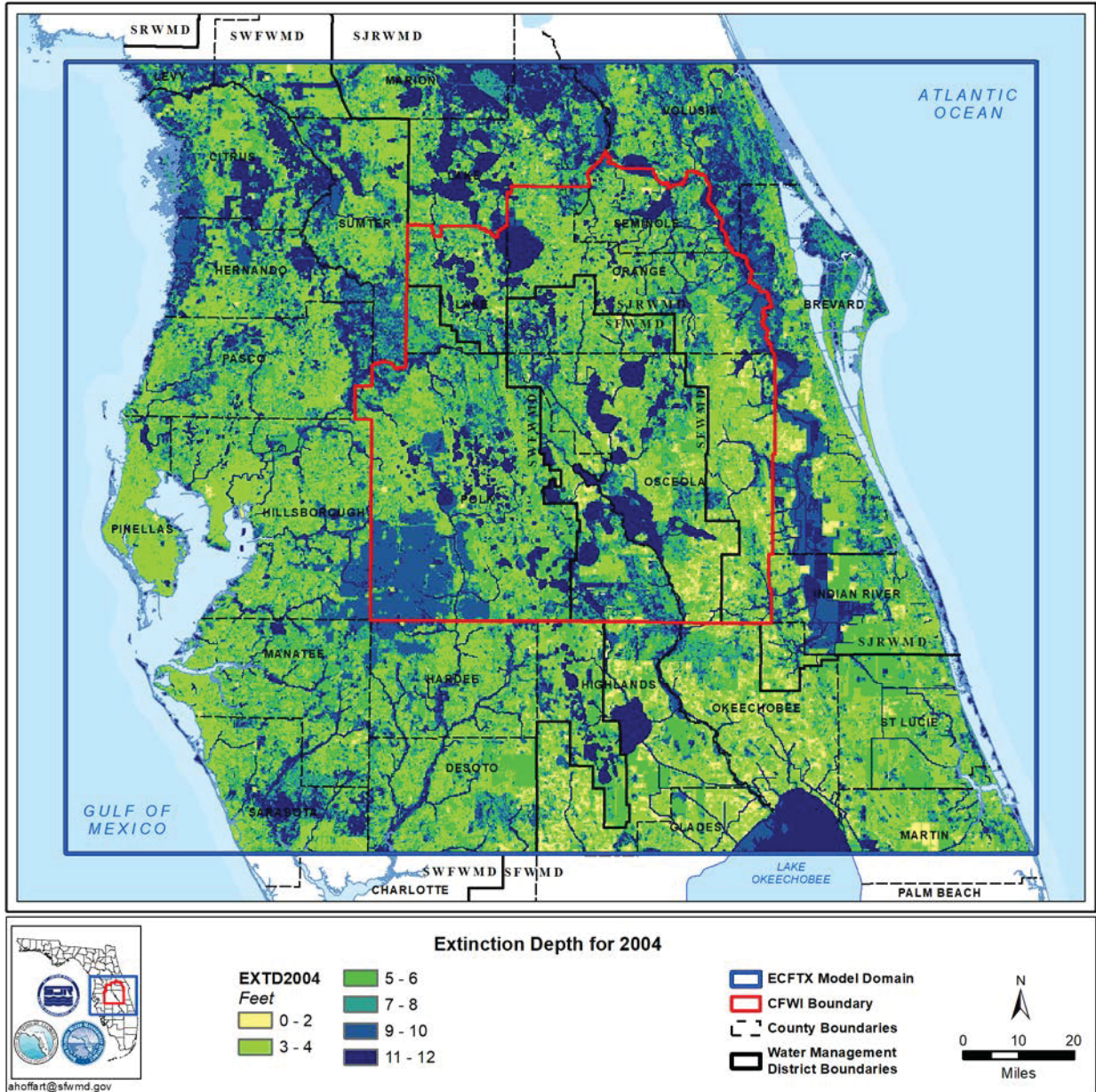
Figure 73. Extinction depth of simulated groundwater ET for 2004 (wet year).
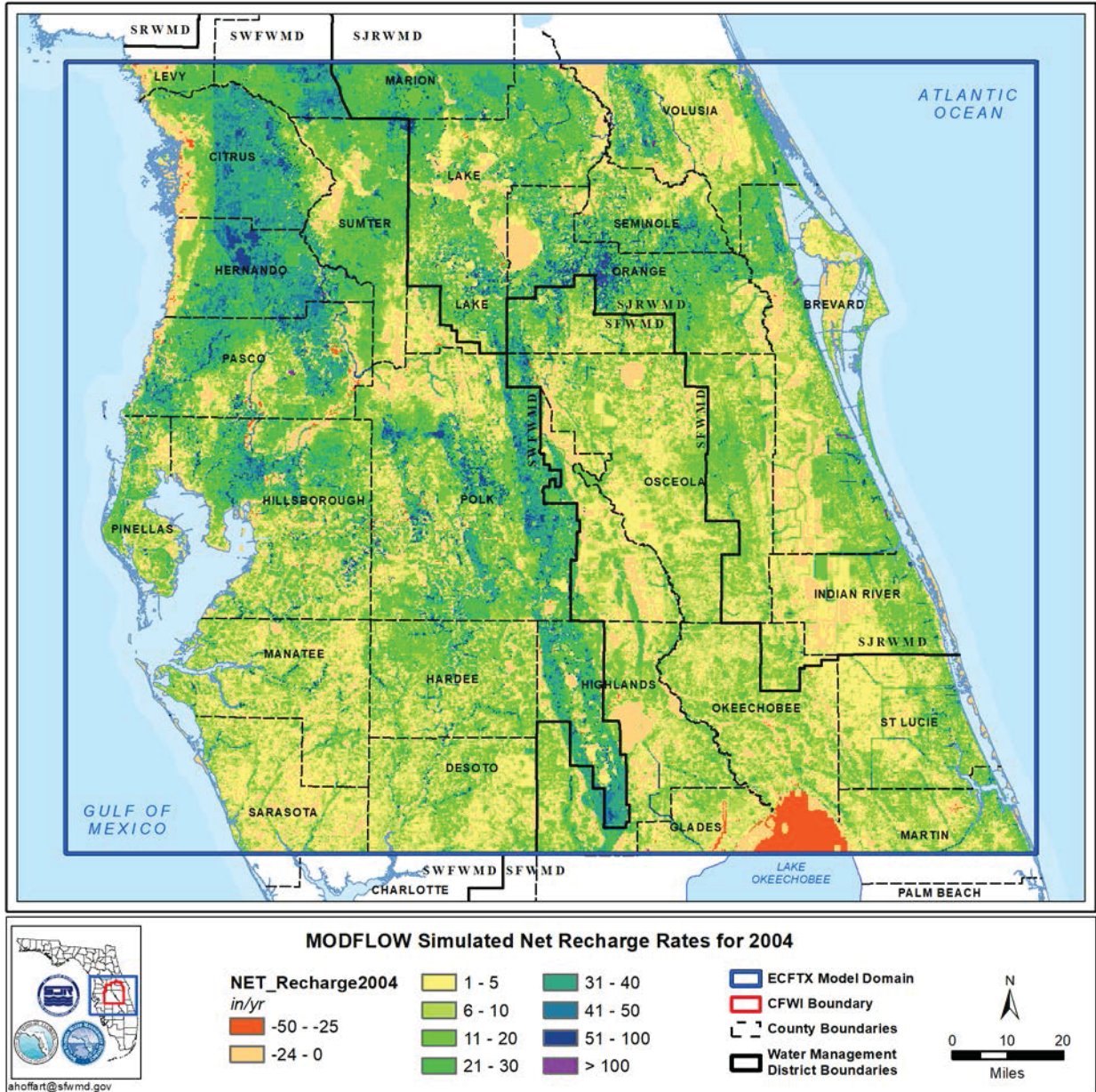
Figure 74. Spatial distribution of MODFLOW simulated net recharge for 2004 (wet year).
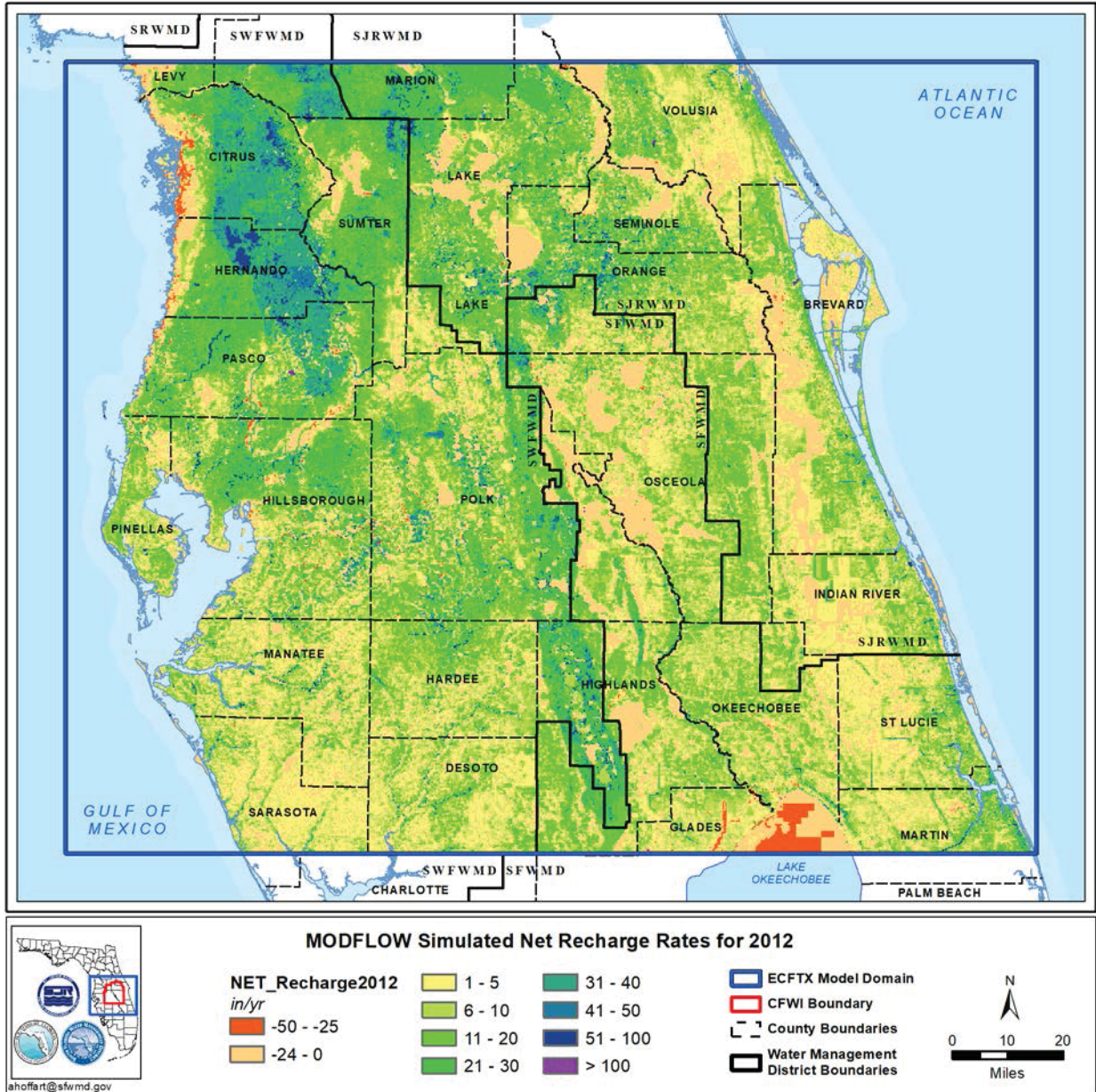
Figure 75. Spatial distribution of MODFLOW simulated net recharge for 2012 (dry year).
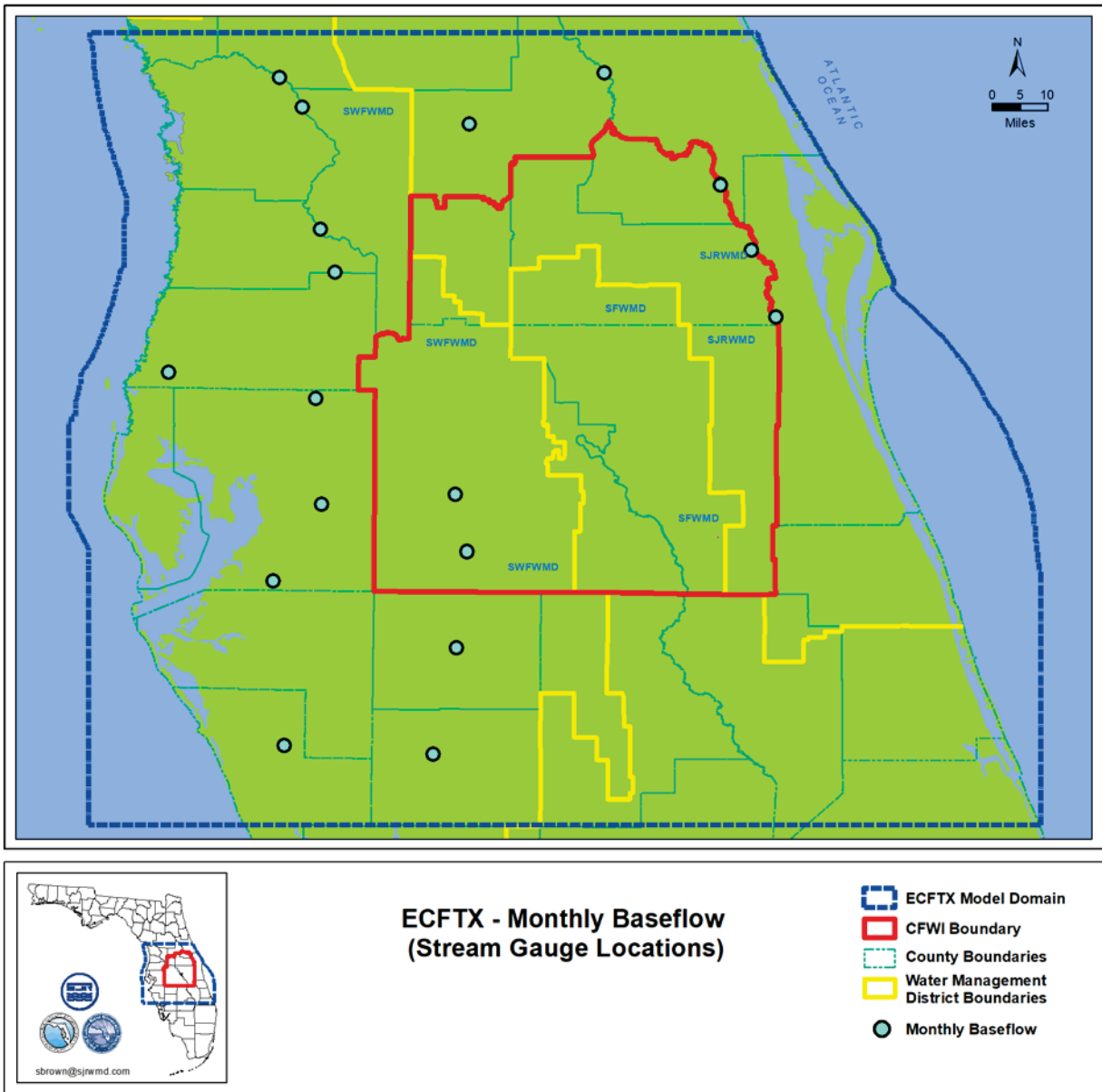
Figure 76. Location USGS streamflow gauging stations used to estimate baseflow in the ECFTX model domain.
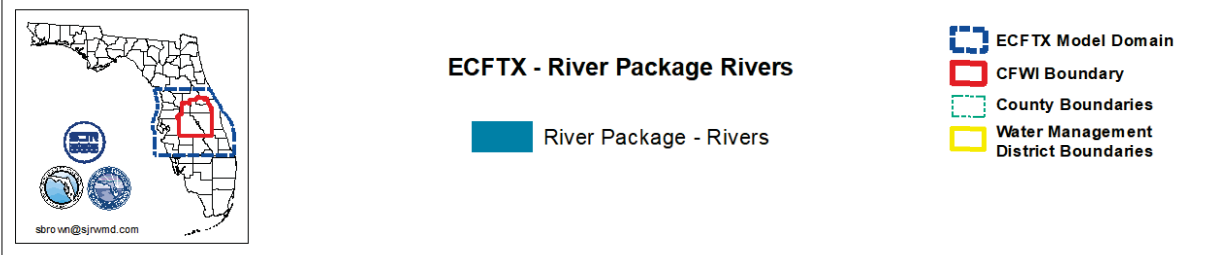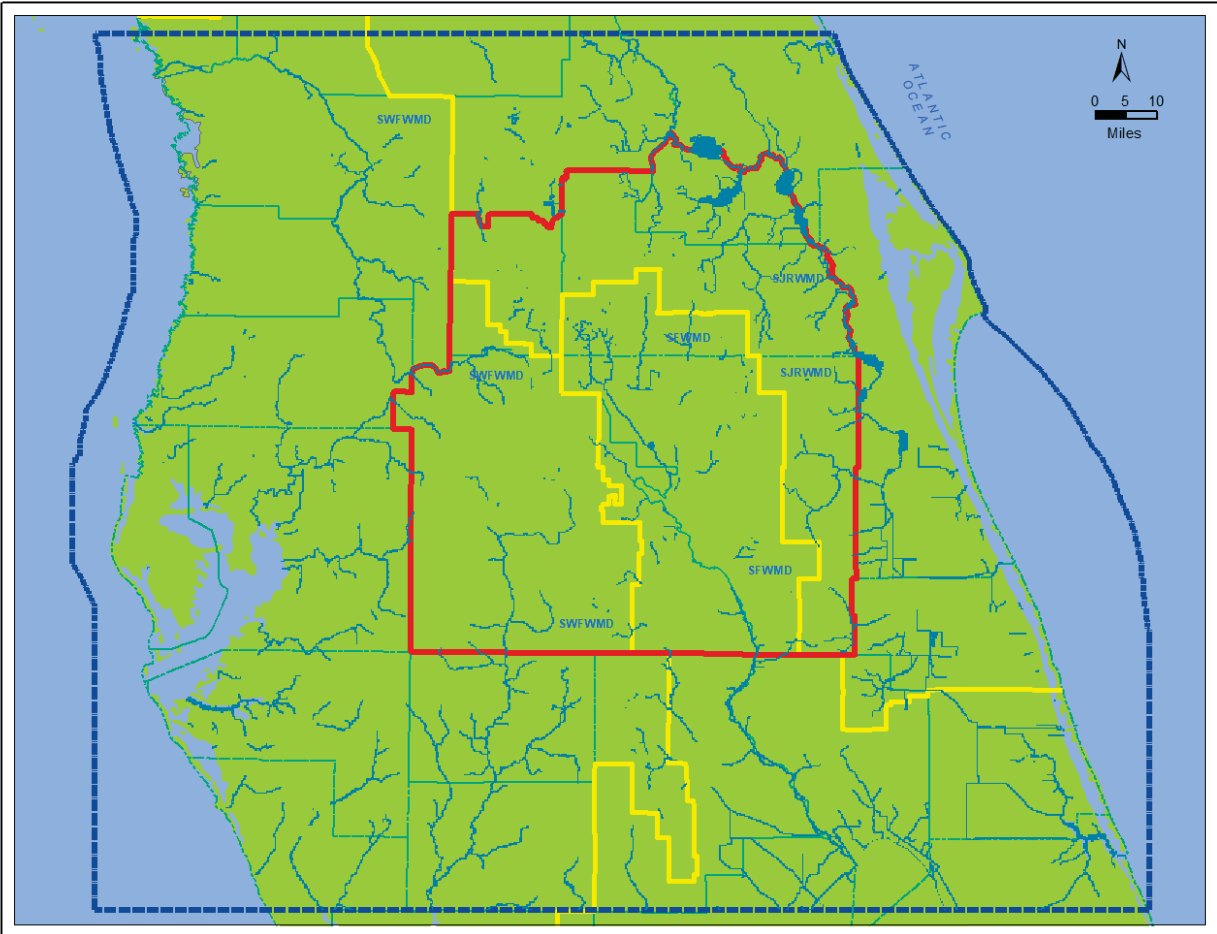
Figure 77. Location of streams represented by the MODFLOW River package in the ECFTX model domain.
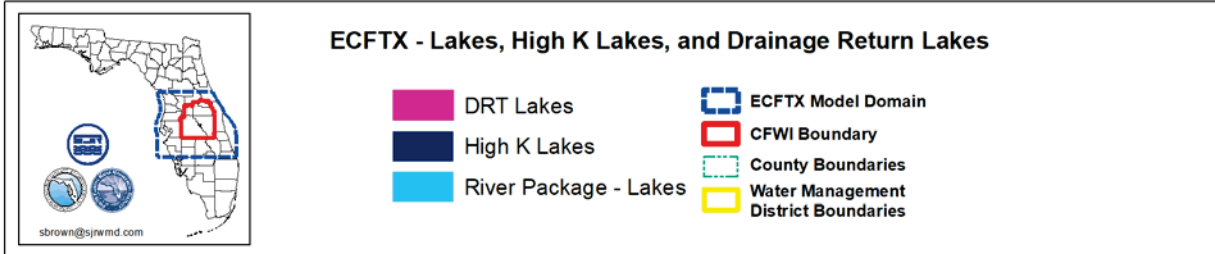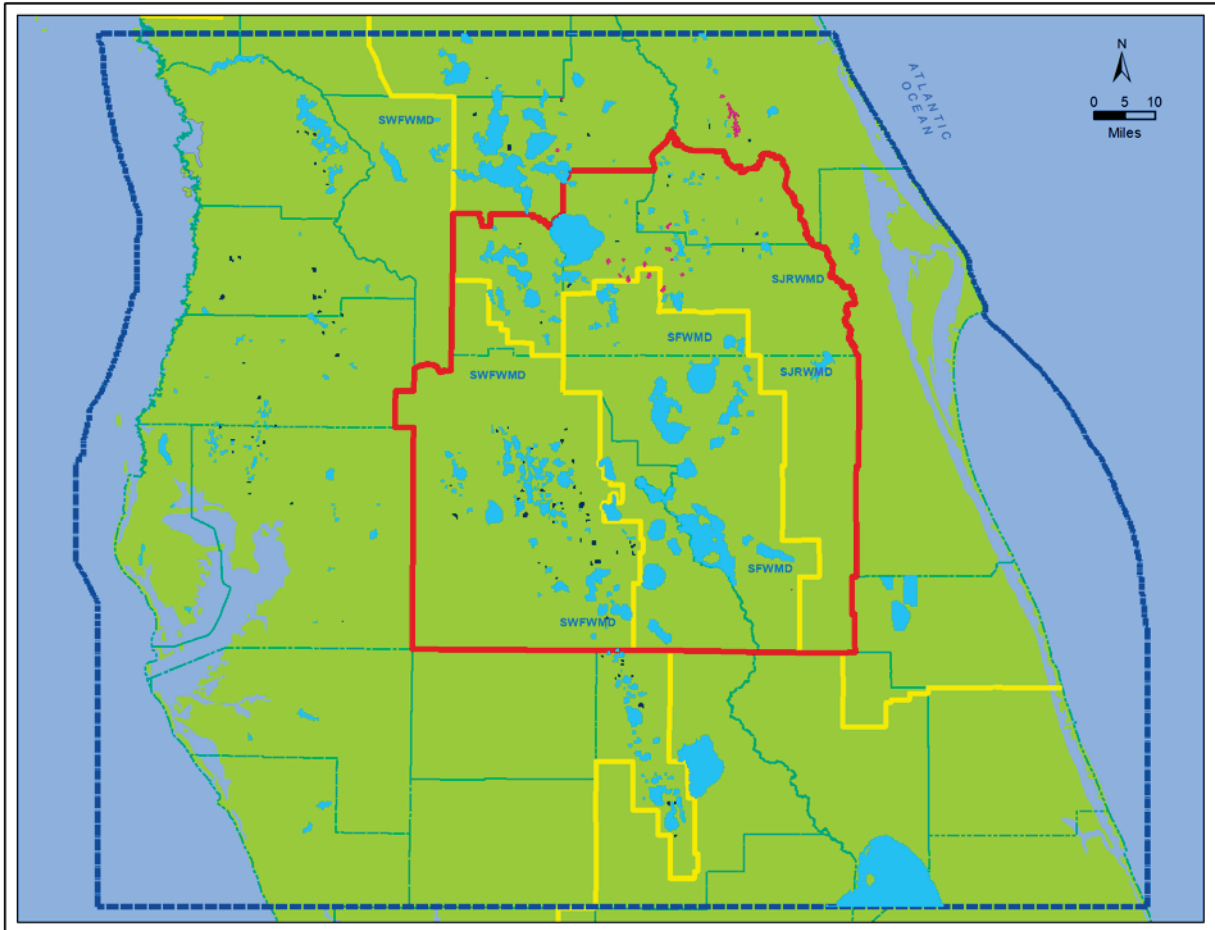
Figure 78. Location of lakes, high K lakes, and drainage return lakes in the ECFTX model domain.
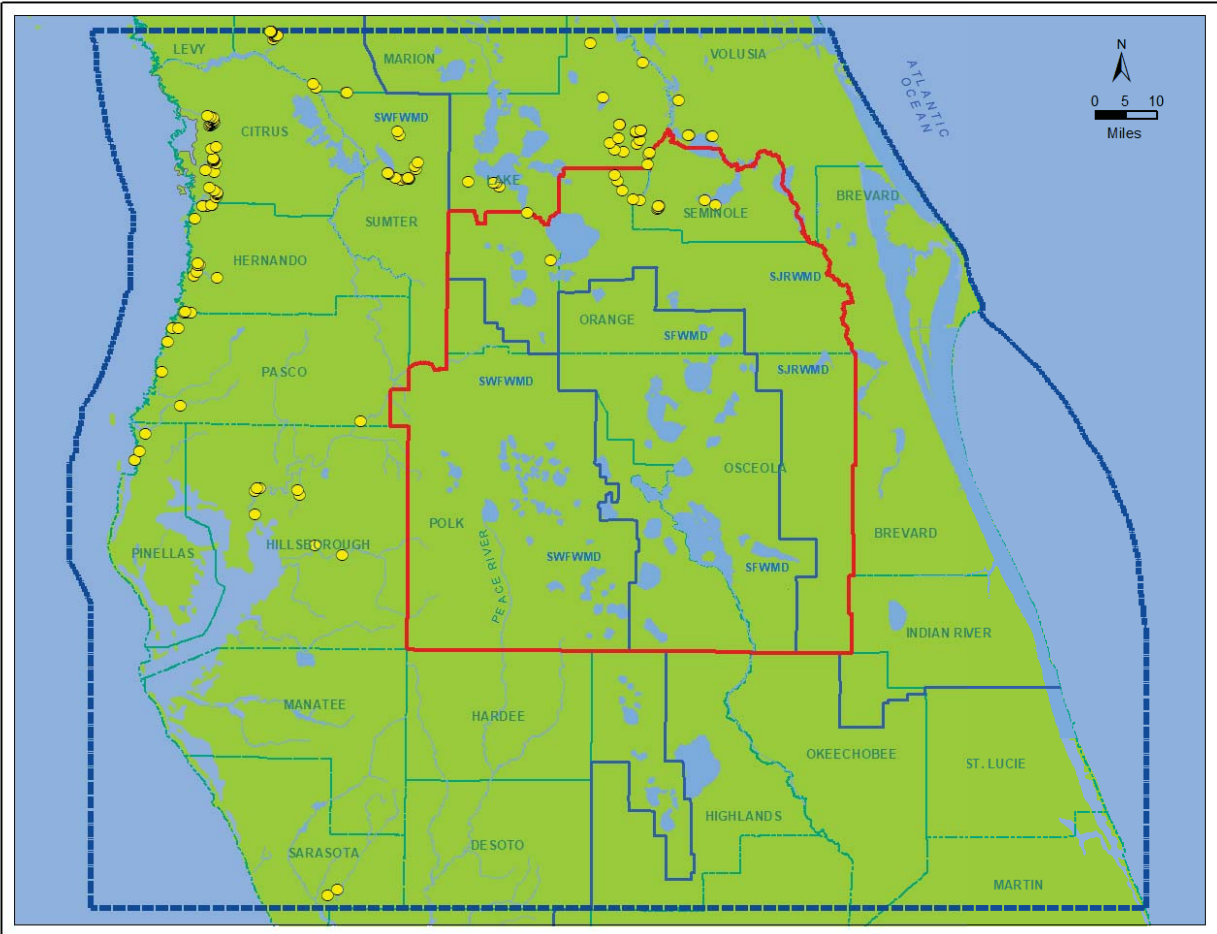
Figure 79. Location of simulated springs in the ECFTX model domain.
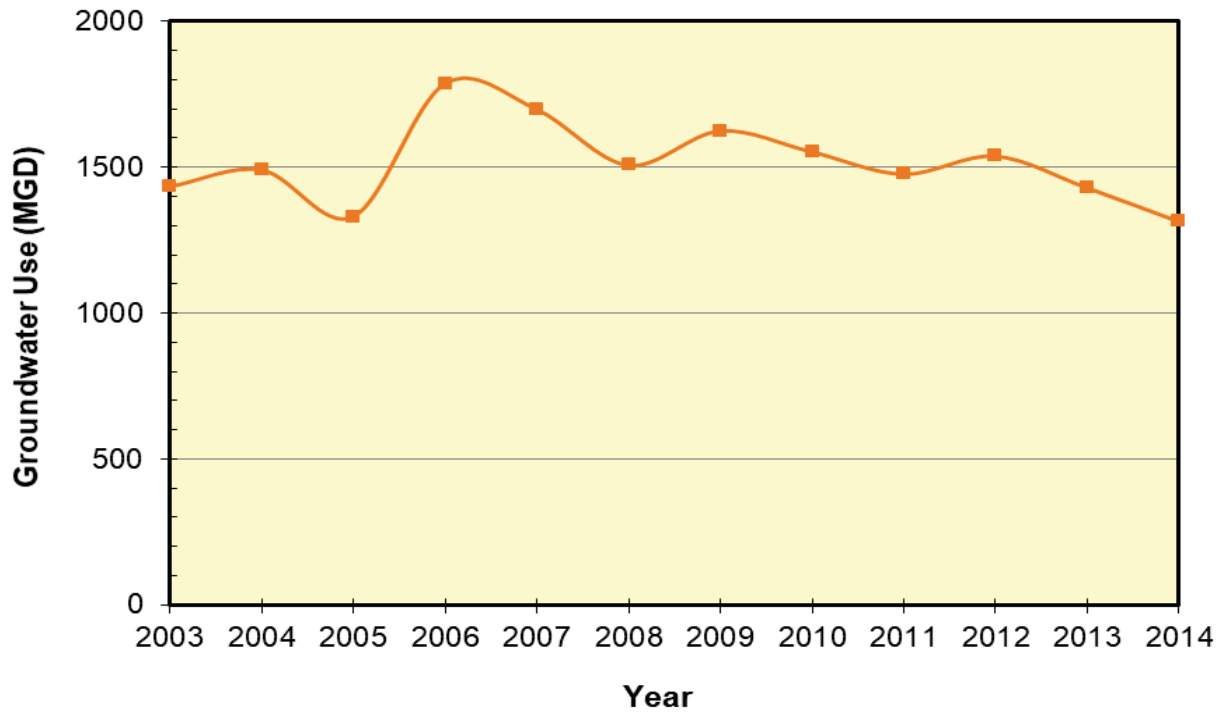
Figure 80. Upper Floridan aquifer withdrawals by year in the ECFTX model domain.
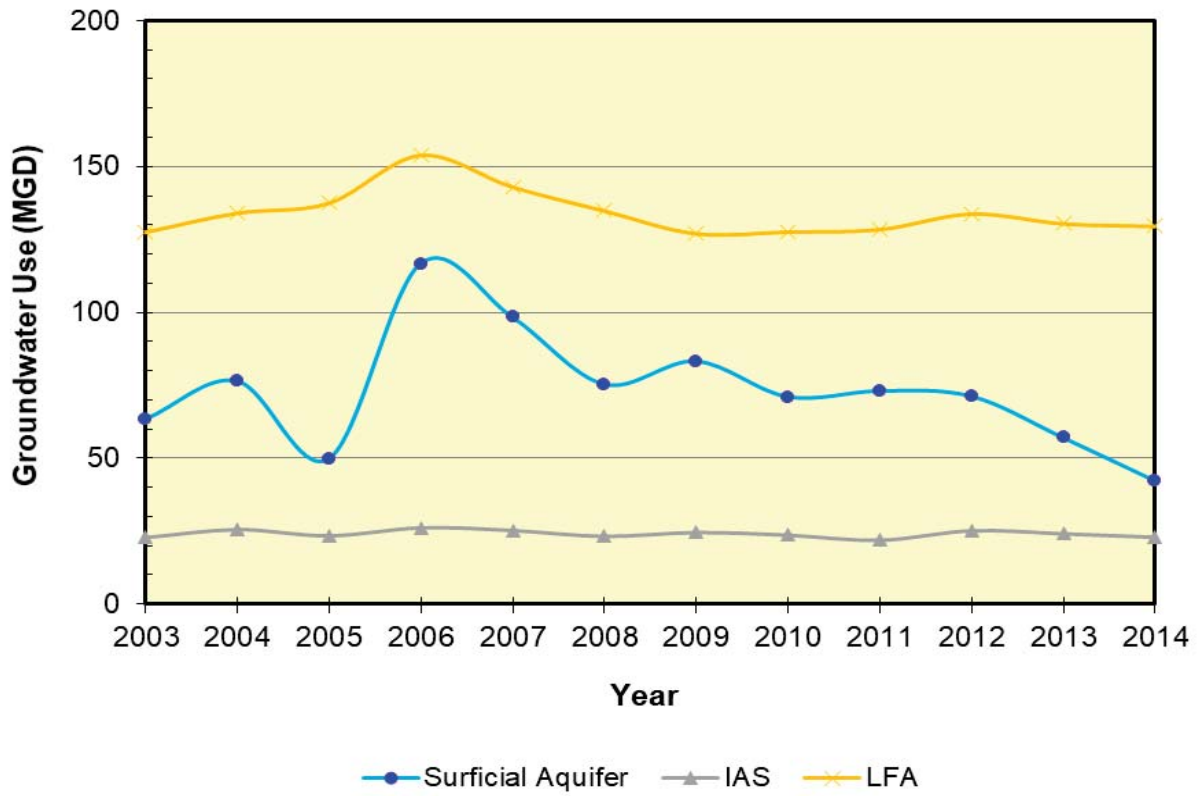
Figure 81. Surficial Aquifer, Intermediate aquifer system (IAS), and Lower Floridan aquifer (LFA) withdrawals by year in the ECFTX model domain.
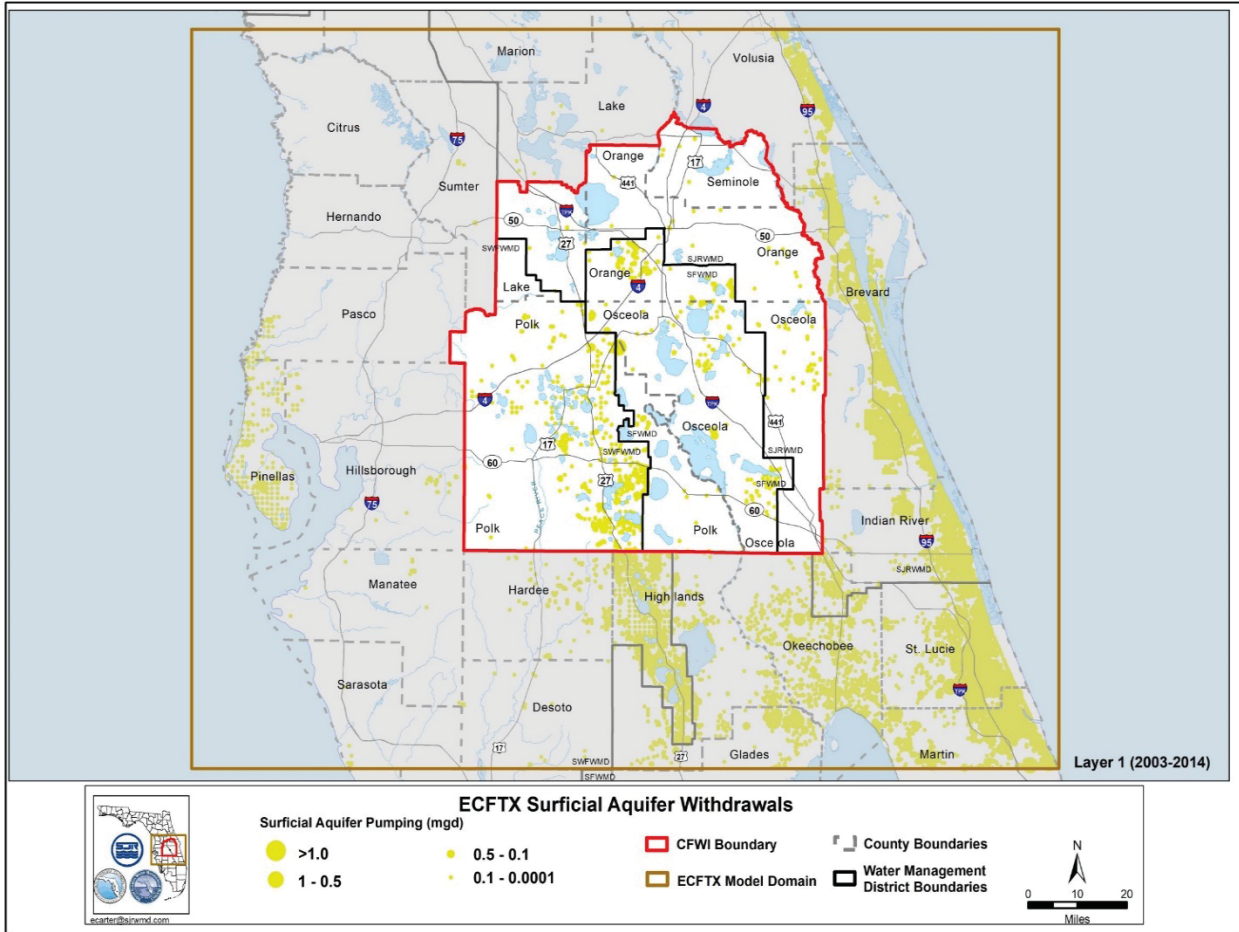
Figure 82. SA withdrawals (average 2003-2014) in the ECFTX model.
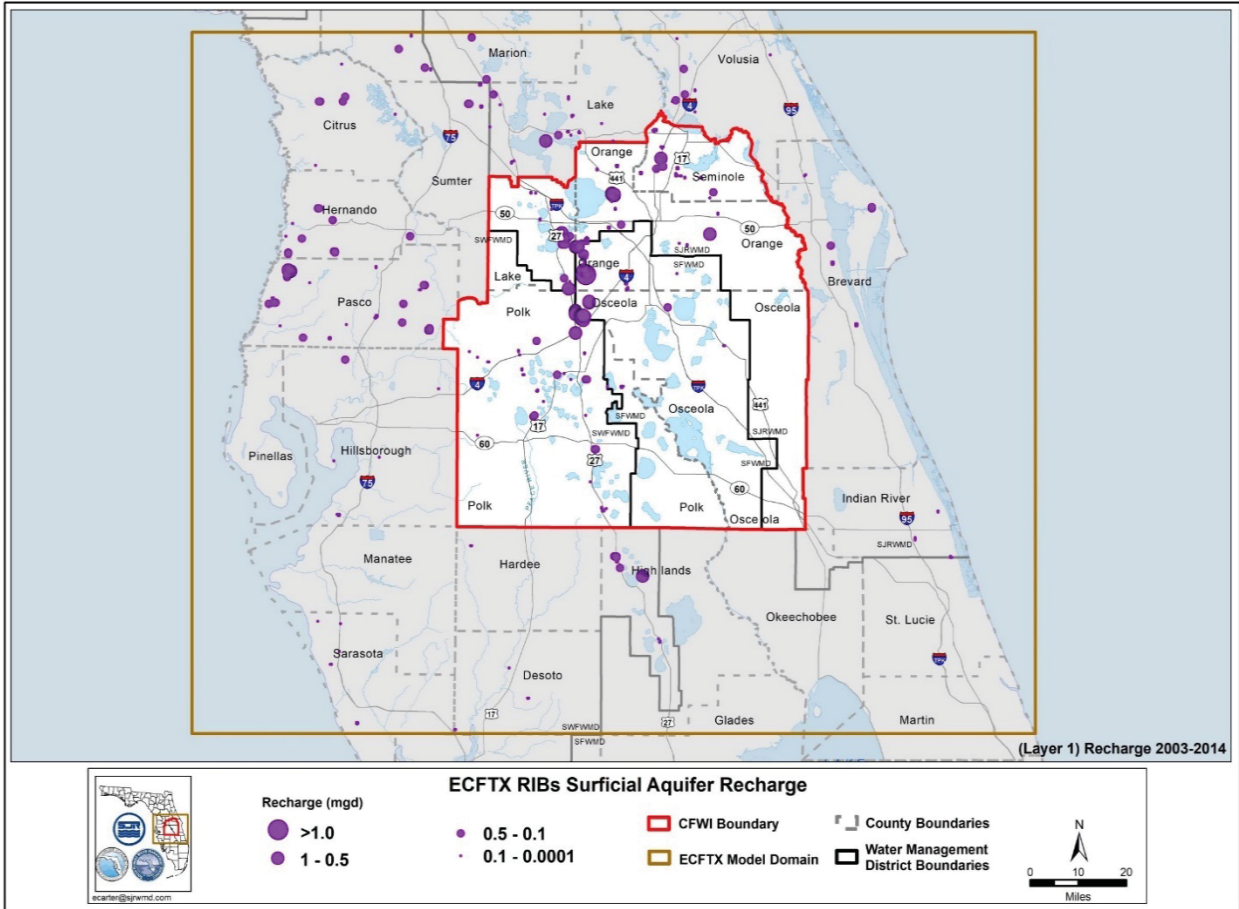
Figure 83. Rapid Infiltration Basin (RIB) recharge represented as Layer 1 injection (average 2003-2014) in the ECFTX model.
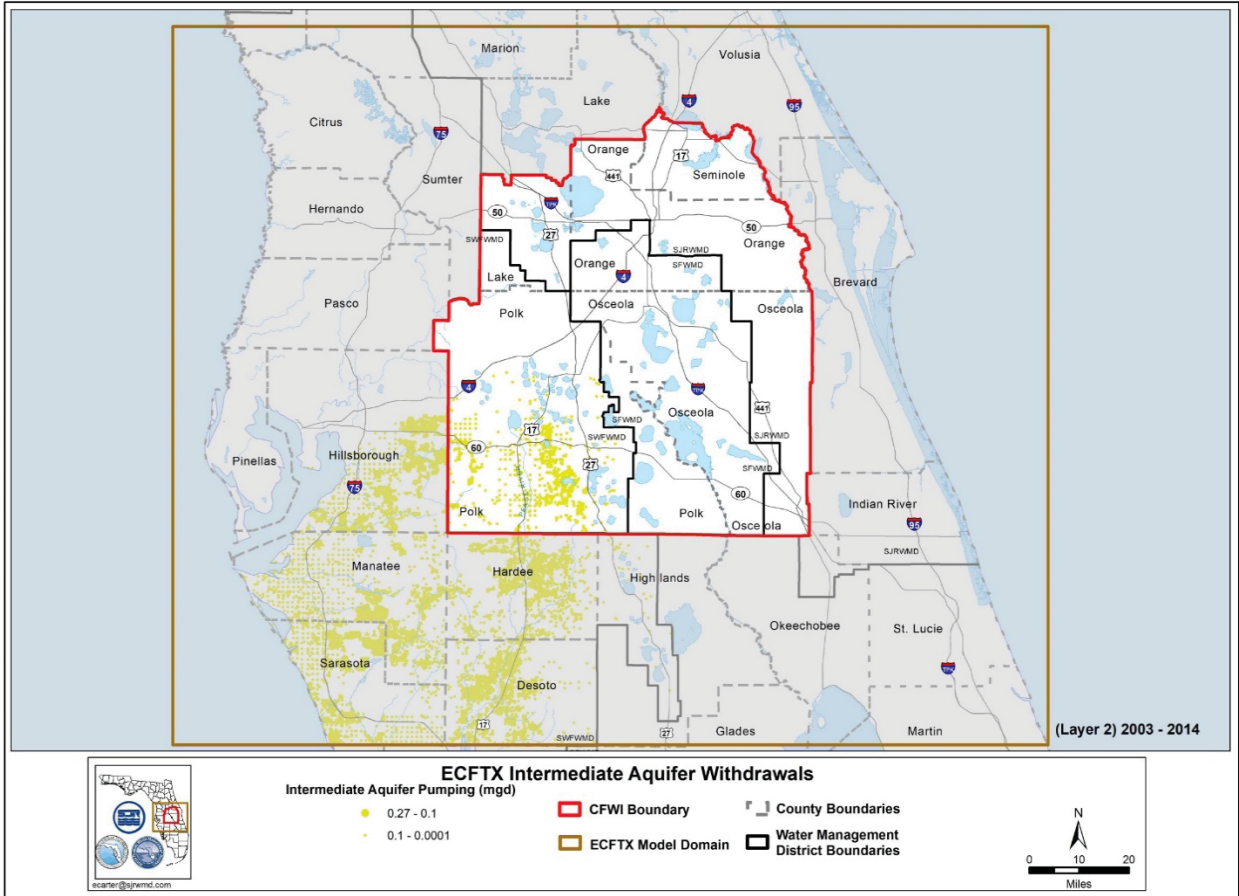
Figure 84. IAS withdrawals (average 2003-2014) in the ECFTX model.
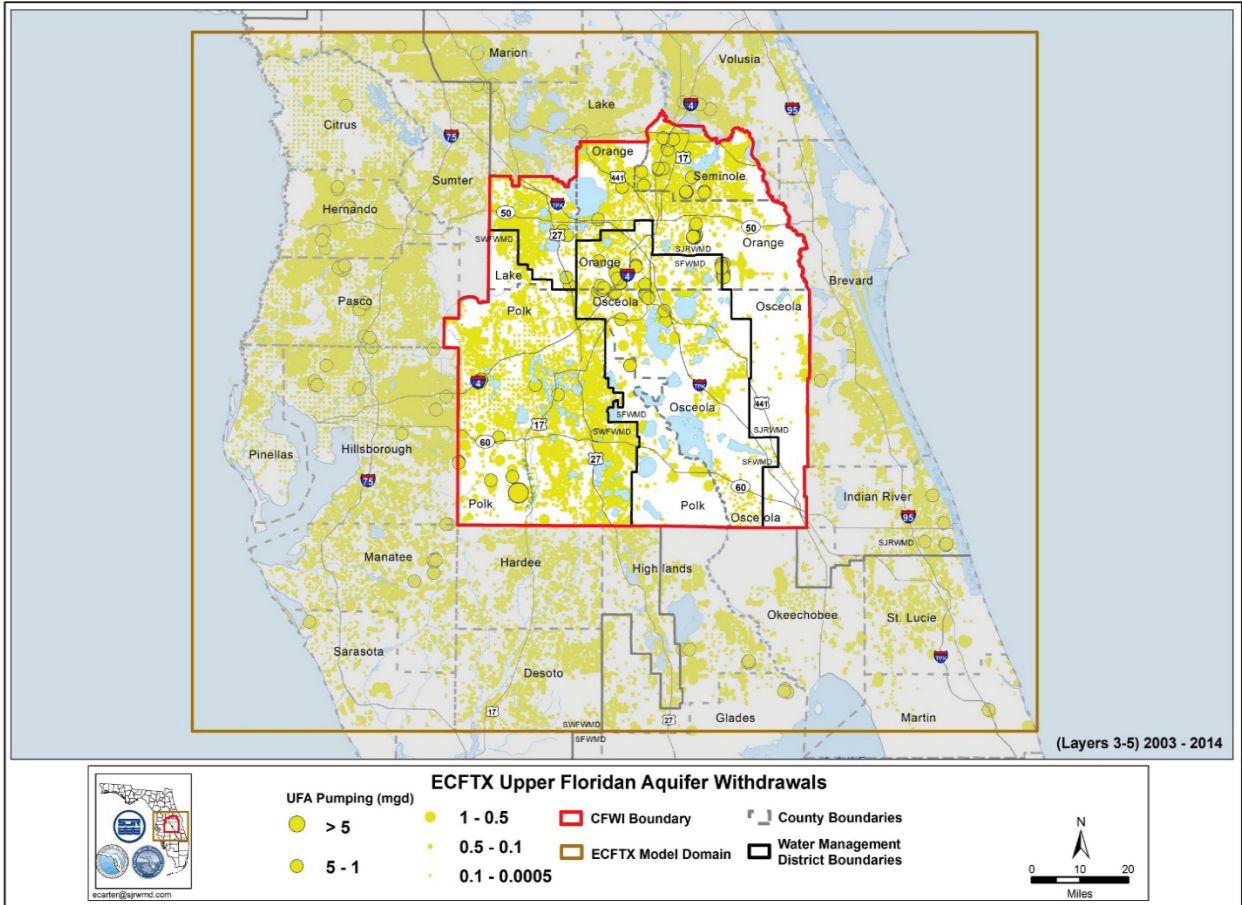
Figure 85. UFA withdrawals (average 2003-2014) in the ECFTX model.
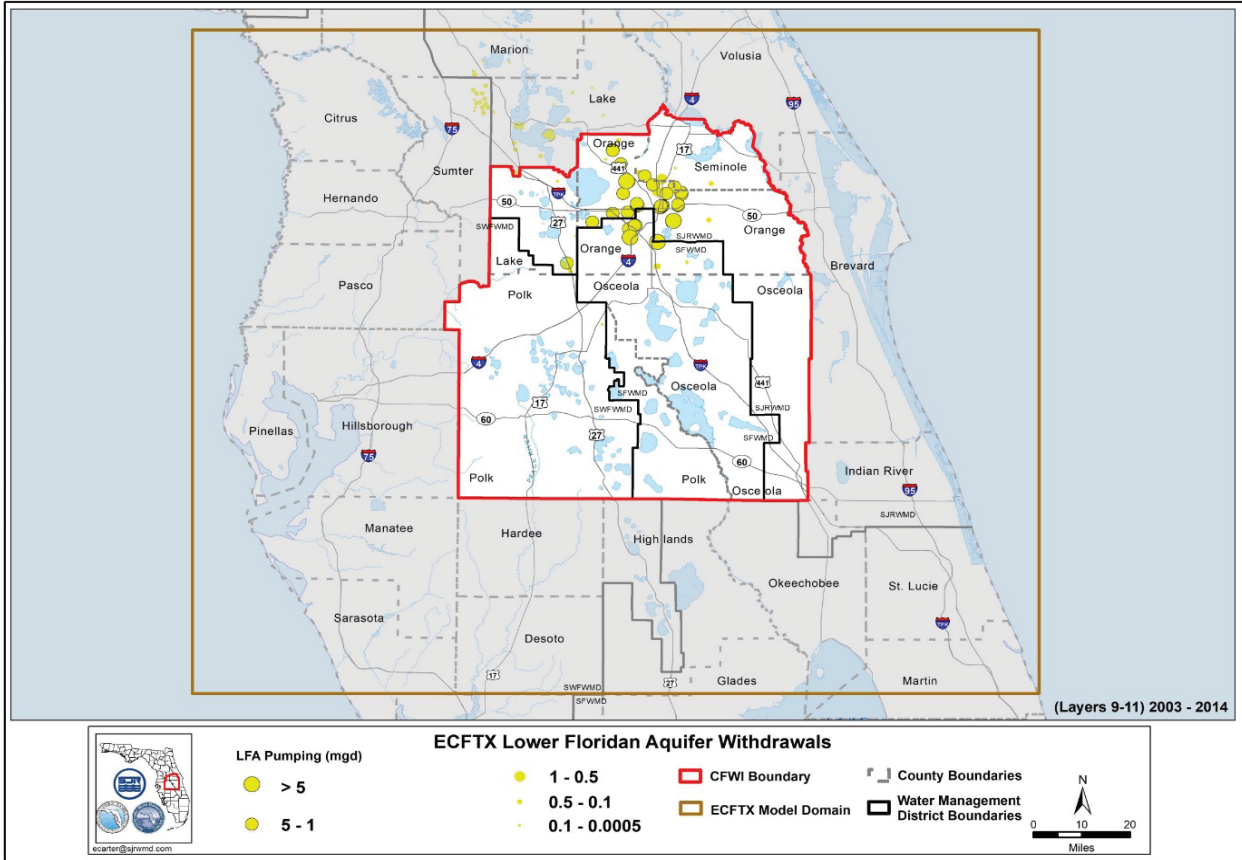
Figure 86. LFA withdrawals (average 2003-2014) in the ECFTX model.
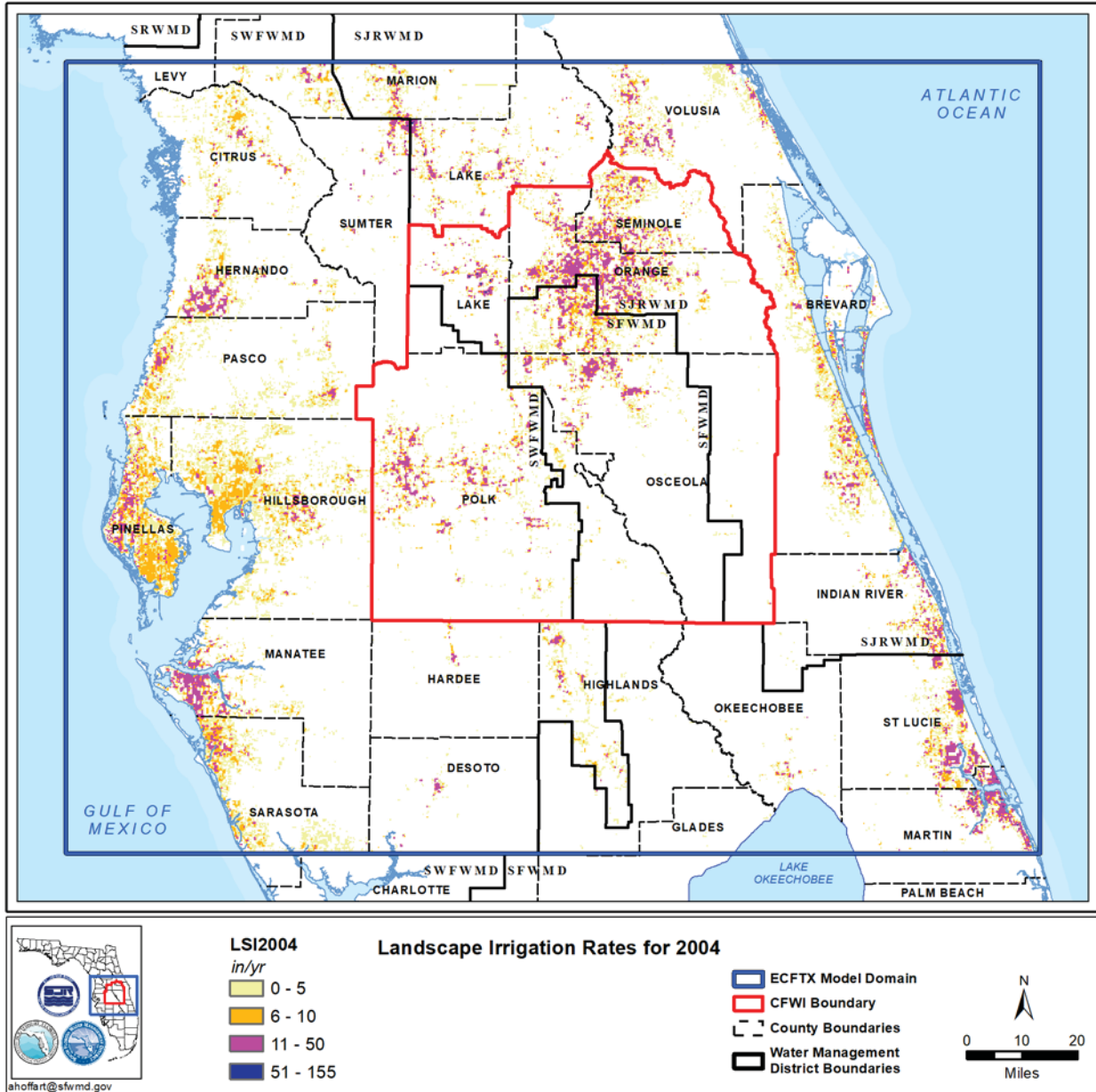
Figure 87. Spatial distribution of public water supply and reclaimed water and LRA landscape irrigation rates for 2004 (wet year).
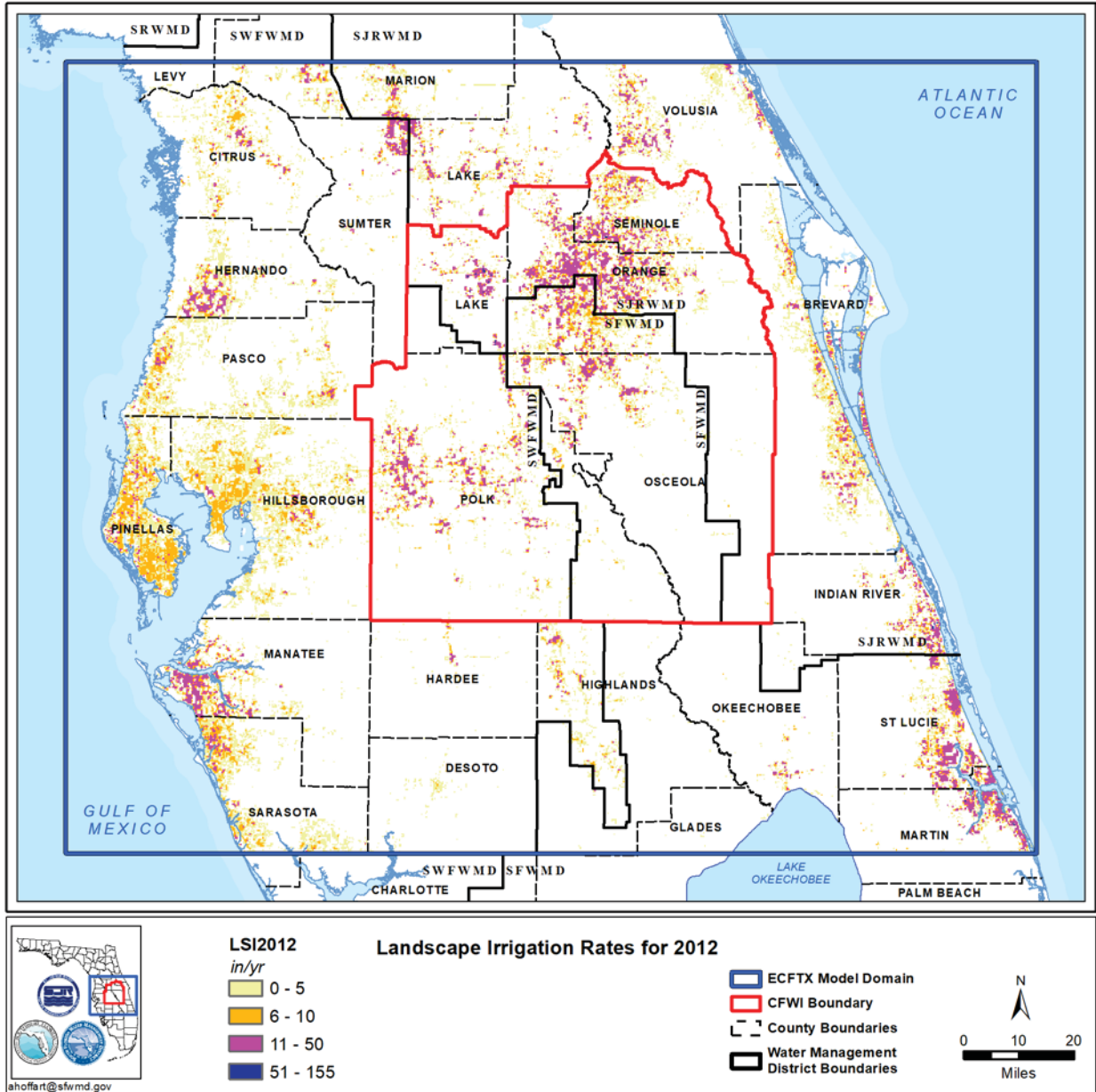
Figure 88. Spatial distribution of public water supply and reclaimed water landscape irrigation rates for 2012 (dry year).
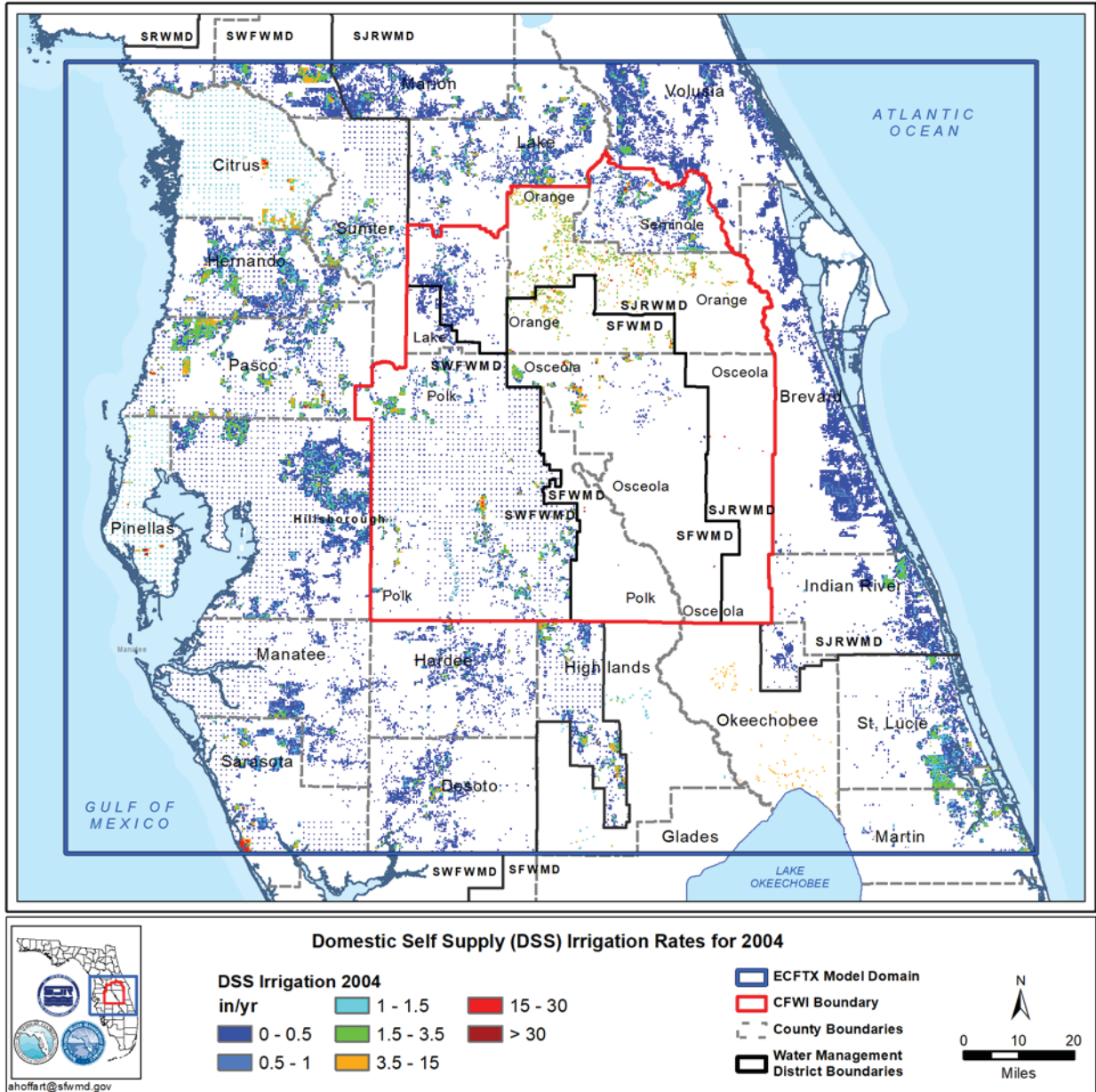
Figure 89. Spatial distribution of domestic self-supplied landscape irrigation rates for 2004 (wet year).
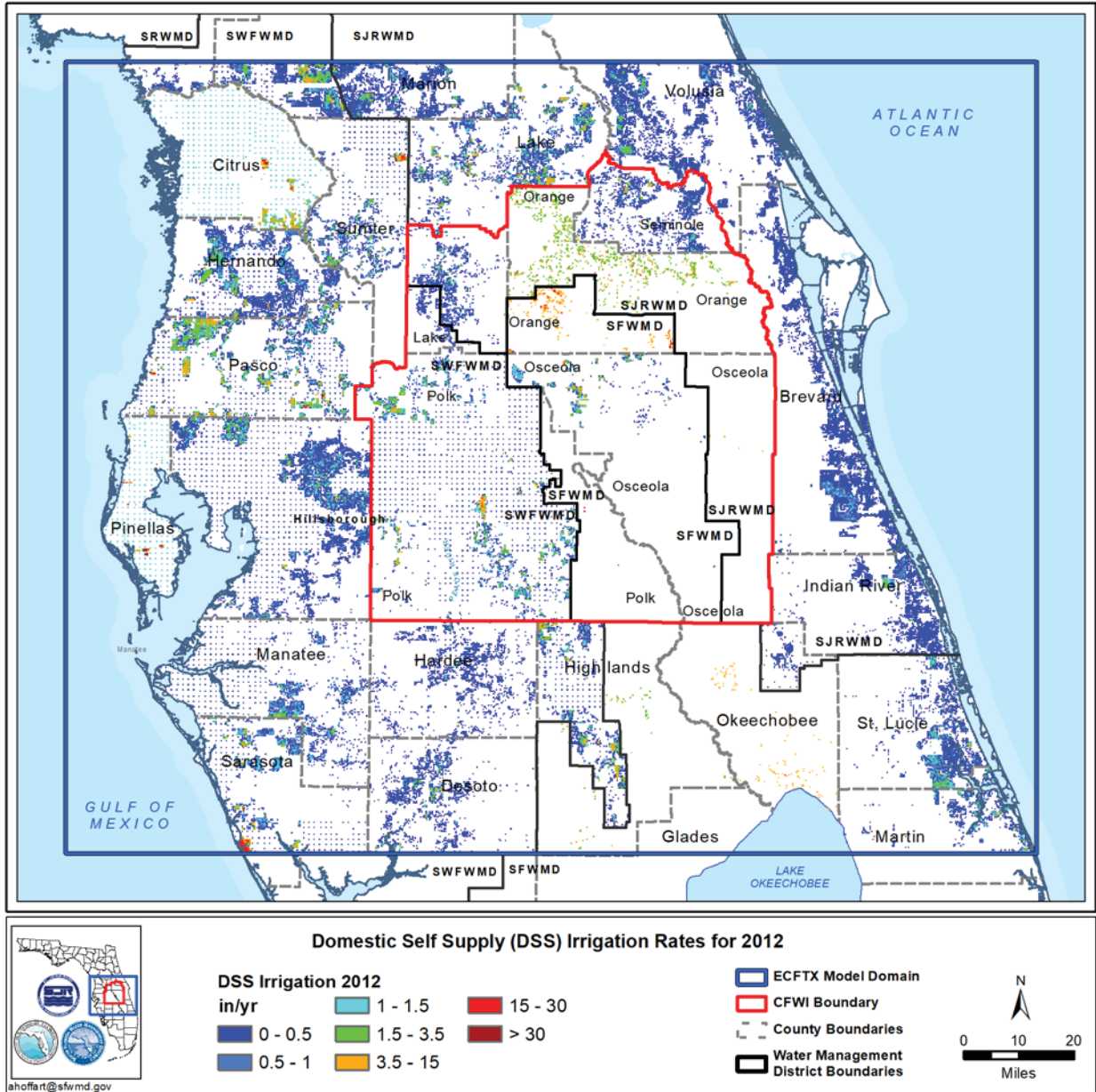
Figure 90. Spatial distribution of domestic self-supplied landscape irrigation rates for 2012 (dry year).

CHAPTER 5 – MODEL CALIBRATION

5.1 Steady-State Calibration

The ECFTX model is a long-term transient simulation of the central Florida hydrologic system. The first step in calibrating the model was to introduce parameterization from previous modeling efforts/prior knowledge of the system and run an average 2003 steady-state condition. The steady-state simulation served as the initial conditions for a long-term monthly transient simulation from 2004 through 2014. The period 2004-2012 being the calibration period with the final two years assigned as the verification period. The 2003 calendar year period was the first stress period for the subsequent 132 monthly stress period run of the transient model. Average annual aquifer water levels, springflow, and baseflow estimates were calculated during the calendar year 2003 period to calibrate the model to a steady-state condition. Average heads from observation wells for the SA (layer 1), UFA (layers 3-5), and the LFA (layers 9-11) were assigned as calibration targets that served as benchmarks for the steady-state calibration.

The 2003 steady-state head residuals comparing simulated versus observed water levels is shown in Table 15. Mean error (simulated minus observed) for all wells in the ECFTX domain within the SA, UFA, and LFA was -0.47 feet, -0.31 feet, and +1.67 ft, respectively. Mean absolute error for all wells in the ECFTX domain within the SA, UFA, and LFA was 2.48 feet, 3.32 feet, and 2.09 ft, respectively. For the CFWI area, 50% of the mean absolute simulated head residuals for all wells in the SA, UFA, and LFA were within 2.5 feet of observed and 80% of the mean absolute simulated head residuals for all wells in the SA, UFA, and LFA were within 5 feet of observed values for the steady-state period. Additional qualitative information included a review of the average potentiometric surface for 2003 with simulated UFA head to see how well the model matched the regional flow configuration. The UFA flow field is matched well with significant features such as the Polk City High and its extension along the Lake Wales Ridge, the East Pasco High, and steep gradient areas in northeastern Hillsborough County represented accurately. A defined set of calibration criteria was assigned for the transient model calibration (Figure 91).

5.1.1 Calibration Procedure

Calibration consisted of manually adjusting hydraulic conductivity fields to improve matches between simulated and observed heads. Starting parameterization was imported from other regional models of the area from SWFWMD's NDM, INTB, DWRM and SFWMD's ECFM outside the original ECFT model footprint. Starting conditions within the original ECFT model domain were from that model. An important approach in the calibration process was honoring the conceptualization of the system described previously in chapters 2 and 3. Parameters were constrained within reasonable ranges based on previous modeling efforts and prior knowledge of the hydrogeologic system. As noted earlier, no definitive calibration criteria were defined for the steady-state calibration (stress period 1). The approach was to use the steady-state period as the starting condition for the subsequent transient calibration from 2004-2012. Stress period 1 was incorporated into the transient calibration as the starting period (stress period 1 - 365 days, with subsequent stress periods each month starting in January 2004 through December 2012). While no definitive calibration criteria were assigned for stress period 1, head statistics are provided to note model performance as a starting condition.

Table 15. Steady state (year 2003) calibration statistics of the target monitor wells in the ECFTX and CFWI domain.

	ECFTX Model Domain			CFWI Area		
	SA	UFA	LFA	SA	UFA	LFA
Residual Mean	-0.47	-0.31	1.67	-0.38	-0.32	2.1
Error Standard Dev	3.81	4.47	2.14	3.3	3.68	2.03
5% of Observation Range	8.05	6.41	2.24	7.71	5.92	2.09
Absolute Residual Mean	2.48	3.32	2.09	2.28	2.81	2.32
Error Sum of Squares	10351	15616	128	2162	2178	124
RMS Error	3.84	4.48	2.67	3.31	3.68	2.87
Minimum Residual	-26.89	-23.03	-2.06	-15.46	-13.51	-1.37
Maximum Residual	13.92	14.21	6.4	10.02	9.38	6.4
Number of Observations	703	779	18	197	161	15
Percentage with MAE < 2.5 ft	66%	50%	61%	70%	56%	53%
Percentage with MAE < 5.0 ft	90%	79%	94%	88%	87%	93%

Note: All values in feet except as noted. Mean error expressed as simulated minus observed.

A parameter estimation (PEST) method was conducted initially during steady-state calibration. While some improvement in heads and fluxes occurred as a result of the PEST calibration, there were some results that were troublesome including a persistent dry-cell issue and some areas with relatively poor calibration results. After confirming that our conceptualization was correct -- and after adjustments were made to assist in solving the dry-cell issue -- the persistence of the dry-cell issue resulted in decision to pivot from that approach to manual calibration. This decision was made recognizing (1) staff experience with other regional models that overlapped the ECFTX Model domain, (2) staff understanding of the hydrogeologic system and (3) staff knowledge of aquifer parameterization. The manual calibration process was generally conducted to leverage the expertise of each District with regional models that overlapped the ECFTX Model domain. To avoid boundary inconsistency issues, staff periodically met to share information to ensure model input data sets including aquifer parameters were smoothed along District boundaries. Some model calibration processes including development of ET-Recharge-Runoff values, structure flow calibration, and return flow were conducted over the entire model domain. Combined, this resulted in a relatively seamless model calibration process and result.

5.1.2 Observed and Estimated Data

Within the CFWI area, there were 197, 161, and 15 monitor wells within the SA, UFA, and LFA, respectively to match or compare simulated water levels with observed water levels. These served as targets during the steady-state calibration. In addition, there were 8 springs with measurements during 2003 within the CFWI area that served as springflow targets. There were also five USGS streamflow gages within the CFWI area where simulated baseflow was compared to the range of estimated baseflow from multiple methods (see Chapter 4). In the greater ECFTX model domain, there were 703, 779, and 18 monitor wells within the SA, UFA, and LFA, respectively to match or compare simulated water levels with observed water levels in 2003. In addition, there were 17 springs with measurements during 2003 within the entire model area that

served as springflow targets during the steady-state calibration. There were also 18 USGS streamflow gages within the entire model domain where simulated baseflow was compared to the range of estimated baseflow.

In addition to the targets mentioned previously, qualitative criteria such as long-term depth to water table measurements from 807 SA observation wells, vertical head difference from 214 SA and UFA nested wells, and vertical head difference between 29 UFA and LFA nested wells were reviewed during the calibration process to guide adjustments for leakance (vertical hydraulic conductivity/thickness) using the water table depth and head difference data.

5.1.3 Model Fit/Statistics

The steady-state calibration served as a starting point for the ECFTX model transient calibration. The main focus of the ECFTX model effort was the creation of a successfully calibrated transient model. Head residuals during the steady-state period, however, were similar to the transient calibration period (Table 15). The steady-state simulated UFA head compared well with the observed regional configuration of the UFA water levels under average 2003 conditions with the Polk City potentiometric high, East Pasco potentiometric high, and steep hydraulic gradient areas represented well (Figure 92). Additional information regarding the steady-state calibration included minimizing areas of the water table above land surface and the number of dry cells during the simulation.

5.2 Transient Calibration

Monthly average aquifer water levels, springflow, and baseflow estimates were obtained from recorded observations or estimated during the 2004 through 2012 period to calibrate the transient model. Average monthly heads from observation wells for the SA (layer 1), UFA (layers 3-5), and the LFA (layers 9-11) were assigned as calibration target criteria that served as measuring sticks for a successful transient calibration. More qualitative criteria such as extent of flooded cells, dry cells, vertical hydraulic head comparisons, depth-to-water table information, and comparison with the regional potentiometric surface at specific time intervals within the transient period were also reviewed and used to guide the transient calibration process. Finally, review of simulated versus observed water levels at key monitor wells and simulated versus observed springflows were also examined to note the degree of transient response across the simulation period. Appendix G includes graphs of simulated versus observed water levels for each target well grouped by major aquifer. Appendix H contains graphs of simulated versus observed springflow where it was continuously measured.

Specific calibration target criteria for the entire ECFTX domain included: 1) a mean error for SA, UFA, and LFA aquifer heads from all wells of less than one foot, 2) a root mean squared error of less than 5 feet from all wells within each aquifer, and a mean absolute error within 5% of the total head elevation range for each aquifer. Total modeled springflow had to be within 10% of the estimated/measured and simulated mean springflow for each magnitude 1 and 2 spring with continuous observations had to be within 10% of mean average observed flow over the calibration period (Figure 91). Specific only to the CFWI area, 50% of the mean absolute simulated head residuals for all wells in the SA, UFA, and LFA had to be within 2.5 feet of observed and 80% of the mean absolute simulated head residuals for all wells in the SA, UFA, and LFA were required to be within 5 feet of observed values.

5.2.1 Calibration Procedure

Calibration primarily consisted of manually adjusting hydraulic conductivity, specific storage, and drain/river cell conductance's to improve matches between simulated and observed heads and fluxes. For springs, calibration involved modifying conductance values within reasonable limits to meet their calibration targets. Starting conditions and initial parameters were from the steady-state calibrated model for 2003. A continuing emphasis during the calibration process was honoring the conceptualization of the system described previously in Chapters 2 and 3. Parameters were constrained within reasonable ranges based on previous modeling efforts and prior knowledge of the hydrogeologic system.

5.2.2 Observed and Estimated Data

Within the CFWI area, there were 277, 194, and 24 monitor wells within the SA, UFA, and LFA, respectively to match or compare simulated water levels with observed water levels. These served as targets during the transient calibration. In addition, there were 8 springs with measurements from 2004-2012 within the CFWI area that served as springflow targets. There were also five USGS streamflow gages within the CFWI area where simulated baseflow was compared to the range of estimated baseflow from multiple methods. In the greater ECFTX domain, there were 997, 928, and 30 monitor wells within the SA, UFA, and LFA, respectively to match or compare simulated water levels with observed water levels from 2004-2012. In addition, there were 17 springs with measurements during the transient period within the entire model area that served as springflow targets during the calibration. There were also 18 USGS streamflow gages within the entire domain where simulated baseflow was compared to the range of estimated baseflow.

In addition to the targets mentioned previously, qualitative criteria such as long-term depth to water table from 807 SA observation wells, vertical head difference from 214 SA and UFA nested wells, and vertical head difference between 29 UFA and LFA nested wells were reviewed during the calibration process. May and September potentiometric surface maps from the USGS and other agencies were compared to simulated May and September UFA water levels across the domain each year during the calibration period as another qualitative guide to model calibration. Other qualitative criteria included minimizing water above land surface (flooded cells) and dry cells for each monthly stress period of the simulation. Additionally, r-squared values greater than 0.4 were generated by regressing all simulated versus observed water levels for all target wells by aquifer in the model to note percent reached during transient periods within the ECFTX domain and CFWI area. This methodology provided a measure of how well the model performed matching shorter-term transient response (see section 5.2.3. for a more detailed assessment of model performance during extreme events (wet and dry periods) and by year within the transient period).

5.2.3 Model Fit/Statistics

Head calibration targets were achieved for the CFWI area and the ECFTX model domain. While not specified as a calibration target for the CFWI area, the mean error slightly exceeded one foot for the LFA within the CFWI area for the transient calibration period (Table 16). For the entire domain, however, the mean error criteria for the LFA was achieved. Monitor well targets were limited in the LFA; however, with only 24 wells available in the CFWI area and 30 wells total for the entire model domain - compared to over 900 observation wells for the SA and UFA within the entire model domain.

The spatial distribution of error for the target wells for the SA, UFA, and LFA is shown in Figure 93 through 95. Spatial distribution of error for all aquifers within the CFWI area is smaller than the domain outside the CFWI area. Elevation of SA simulated water levels are underpredicted in the southern half of the Lake Wales Ridge in Highlands County and within some deep-water table areas near Orlando. Simulated water levels in eastern portions of Citrus, Hernando, Pasco, and Hillsborough are generally simulated higher than observed in the UFA. Much of the error during the transient calibration is associated with initial starting conditions of the steady-state period that is carried forward during the transient calibration period. In addition, localized, hydraulically steep gradient areas along ridges in the SA are sometimes difficult to match given large grid cell sizes in regional models. Other than these areas, there appears to be little to no spatial bias in mean error of simulated water levels in the model.

Simulated versus observed potentiometric surfaces for May 2010 and September 2012 are shown in Figure 96 and 97 to view matches during wet and dry periods during the transient calibration. Like the steady-state calibrated flow field, the Polk City potentiometric high, the East Pasco potentiometric high, the high along the Lake Wales Ridge, and the configuration of the UFA flow field are well-represented by the transient model. Appendix I contains a full suite of May and September comparisons with the simulated UFA surface from 2004 through 2014.

Histograms and regression plots of simulated versus observed water levels for each aquifer are shown in Figure 98 through 109 for the CFWI area and ECFTX model domain. Figures 110 through 115 show individual simulated versus observed water level response at selected wells across the CFWI area within the SA, UFA, and LFA (Figure 116). A full suite of model hydrographs are also contained within Appendix G.

Review of the simulated versus observed head residual histograms for the SA and UFA for both the ECFTX domain and CFWI area show a normal distribution pattern centered around zero. The LFA histograms illustrate more scatter in residuals although the highest number is still centered near zero. This situation is likely due to the relatively small number of targets from the LFA (24 CFWI, 30 ECFTX domain) and overall limited amount of hydraulic data in this aquifer compared to the overlying SA and UFA.

Review of regression plots of simulated versus observed water levels for the SA, UFA, and LFA show a very close alignment between the solid line (theoretical 1:1 match, $r^2 = 1$) and dashed line (model simulated versus observed). The coefficient of determination (r^2) from the simulated versus observed heads for the SA and UFA ranges from 0.98 to 0.99 for the CFWI area and 0.97 to 0.98 for the ECFTX domain. R-squared values associated with the LFA target well set range from 0.97 for the CFWI area and 0.95 for the ECFTX domain. Review of the scatter plots indicates little observable bias toward over or under prediction of water levels in the SA and UFA with points generally scattered equidistant above and below the line. In the LFA, there is a slight bias toward higher simulated water levels than observed at lower head elevations and this is reflected in simulated minus observed mean error slightly larger than one foot in the model.

Springflow calibration targets were achieved for the CFWI area and the ECFTX domain. For the calibration period from 2004-2012, mean simulated springflow in the model from all 158 springs was 2,082 cfs, while observed (estimated and measured) was 2,158 cfs, resulting in a mean error of -3.5%.

Table 16. Transient model calibration statistics of the target monitoring wells in the ECFTX Model domain and CFWI area.

	ECFTX Model Domain			CFWI Area		
	SA	UFA	LFA	SA	UFA	LFA
Residual Mean	-0.46	0.46	0.46	-0.64	0.34	1.23
Error Standard Dev	4.24	4.7	3.33	3.47	3.75	2.68
5% of Observation Range	8.97	7.59	2.79	8.6	6.2	2.62
Absolute Residual Mean	2.83	3.78	2.65	2.61	3.24	2.48
Error Sum of Squares	18156	20666	329	3442	2729	202
RMS Error	4.27	4.72	3.31	3.53	3.75	2.9
Minimum Residual	-31.65	-22.1	-10.19	-16.51	-11.93	-5.46
Maximum Residual	21.15	19.14	5.73	13.29	10.11	5.73
Number of Observations	997	928	30	277	194	24
Percentage with MAE < 2.5 ft	68%	48%	60%	71%	52%	58%
Percentage with MAE < 5.0 ft	88%	76%	87%	87%	85%	88%
Percentage with R2> 0.4	78%	93%	93%	78%	96%	92%

All values in feet except as noted. Calibration period is 2004-2012. Mean error expressed as simulated minus observed.

Calibration target statistics were also achieved for each of the 17 magnitude 1 and 2 springs that had continuous measurements during the calibration period (Table 17). Each magnitude 1 and 2 spring with measurements had to have a mean error less than 10 percent to meet calibration criteria. Spatial distribution of error for the 17 simulated springs is shown in Figure 117. There are generally small errors in simulated mean springflow with 12 of 17 springs individually having mean error less than five percent. A regression plot of simulated versus observed mean spring flow is shown in Figure 118. The regression plot shows a very tight fit with an r-squared value of 0.99. Simulated versus observed monthly flow hydrographs for Wekiwa and Gum Springs are shown in Figure 119. Simulated versus observed springflow hydrographs for all 17 springs with continuous measurements are shown in Appendix H.

The baseflow calibration targets were achieved for the ECFTX domain. For the calibration period from 2004-2012, mean simulated baseflow in the model from all 18 USGS gages was 5,170 cfs, while observed (estimated) varied between 2,226 and 9,160 cfs. Calibration criteria for estimated baseflow was to have the model simulate it within an order of magnitude due to the variability of estimation methods for this more uncertain flow statistic. A total of 15 out of 18 USGS gages where baseflow was estimated were within the range of flows estimated by the methods described in Chapter 4 (Table 18; Figure 120).

In addition to the model fit statistics, water above land surface (flooded cells) and the number of dry cells per month were minimized during the calibration process. Figure 121 and 122 show the worst months (i.e. most flooded cells and dry cells) within the transient calibration period of the model. For flooded cells, it was the high rainfall month of September 2004 when three hurricanes crossed the model domain. For dry cells, it was an unusually dry May in 2012. Most months in the transient calibration contained few flooded cells or any dry cells at all. Appendix J includes

maps of the flooded cells per month in the transient model. Appendix K shows the number of dry cells in layer 1 per month from 2004-2014.

Model simulated mean depth-to-water table, SA-UFA hydraulic head difference, and UFA-LFA head difference were also compared to observed well data (Figure 123 through 125). With some local differences, the model simulation compares favorably to the observed data indicating deep water table areas along the Lake Wales Ridge and ridges in the Orlando area. Shallow water table areas are also well represented where the system is well-confined in the southern half of the domain. SA-UFA head difference is greatest in the model where the UFA is tightly confined and smallest in the unconfined or leaky areas of Tampa Bay, Green Swamp, northern Lake Wales Ridge, and portions of the Orlando area. UFA-LFA simulated head difference shows the largest values where the gypsum-dominated MCU 2 separates the UFA and LFA with smaller values where the leakier MCU 1 largely-carbonate unit exists.

5.3 Model Verification

Once a model is deemed calibrated, a verification period outside of the calibration period is selected to note the model's performance and determine if the simulation continues to meet the calibration metrics previously assigned. In this case, the two-year monthly transient period from 2013-2014 was selected as the model verification period.

Table 17. Transient model calibration statistics of the target springs simulated in the ECFTX model.

Spring Name	Observed Flux (cfs)	Simulation	
		Flux (cfs)	Error
Lithia Spring Major	34.7	33.2	-4.4%
Buckhorn Main Spring	12.2	12.1	-0.9%
Sulphur Spring (Hillsborough)	34.7	35.4	2.0%
Crystal Main Spring (Pasco)	45.5	46.4	2.0%
Weeki Wachee Spring	160.4	167.3	4.4%
Chassahowitzka Spring Main	59.6	59.3	-0.6%
Homosassa Spring #1	83.5	84.5	1.1%
Gum Spring Main	63.8	64.8	1.5%
Rainbow Spring #1	71.8	73.3	2.0%
Apopka Spring	24.9	24.8	-0.1%
Sanlando Springs	18.8	19.9	5.4%
Starbuck Spring	12.1	12.6	3.9%
Wekiwa Spring (Orange)	61.0	64.6	5.8%
Bugg Spring (Lake)	10.6	9.7	-8.2%
Rock Springs (Orange)	54.9	51.6	-6.1%
Volusia Blue Spring	143.6	132.4	-7.9%
Alexander Spring	100.1	98.9	-1.2%

Calibration period is 2004-2012. Mean error expressed as simulated minus observed.

Within the CFWI domain, there were 220, 161, and 25 monitor wells within the SA, UFA, and LFA, respectively to compare simulated water levels with observed water levels. In addition, there were 8 springs with measurements from 2013-2014 within the CFWI area that served as targets to evaluate model performance. There were also 15 USGS streamflow gages within the CFWI area where simulated baseflow was compared to the range of estimated baseflow from multiple methods. In the greater ECFTX model domain, there were 796, 709, and 31 monitor wells within the SA, UFA, and LFA, respectively to compare simulated water levels with observed water levels from 2013-2014. In addition, there were 17 springs with measurements during the verification period within the entire model area. There were also 18 USGS streamflow gages within the entire model domain where simulated baseflow was compared to the range of estimated baseflow.

Table 18. Simulated mean baseflow from 2004-2012 compared to estimated ranges using the USF method and USGS Groundwater Toolbox methods at 18 stations.

Gauge	Station	Min (cfs)	Max (cfs)	Simulated Mean Baseflow (cfs)
02232400	ST JOHNS RIVER NR COCOA FL	221	928	293
02232500	ST JOHNS RIVER NR CHRISTMAS FL	282	1085	384
02234000	ST JOHNS RIVER ABOVE LAKE HARNEY NR GENEVA FL	441	1473	856
02236000	ST JOHNS RIVER NR DELAND FL	389	3186	1768
02238000	HAYNES CREEK AT LISBON	19	86	73
02294650	PEACE RIVER AT BARTOW	21	125	77
02294898	PEACE RIVER AT FORT MEADE	19	144	129
02295637	PEACE RIVER AT ZOLFO SPRINGS	80	350	331
02296750	PEACE RIVER AT ARCADIA	118	596	533
02298830	MYAKKA RIVER NR SARASOTA	14	150	50
02300500	LITTLE MANATEE RIVER NR WIMAUMA	23	88	70
02301500	ALAFIA RIVER AT LITHIA	53	189	110
02303000	HILLSBOROUGH RIVER NR ZEPHYRHILLS	65	145	102
02310000	ANCLOTE RIVER NR ELFERS	4	38	11
02312000	WITHLACOOCHEE RIVER AT TRILBY	28	153	165
02312500	WITHLACOOCHEE RIVER AT CROOM	56	211	190
02312762	WITHLACOOCHEE RIVER NR INVERNESS	156	378	36
02313000	WITHLACOOCHEE RIVER NR HOLDER	237	505	-8

5.3.1 Model Fit/Statistics (Heads, Springflow, and Baseflow)

Head calibration targets were achieved for the CFWI area during the verification period and were comparable to the calibrated model. For the ECFTX model domain, all head targets were within the defined calibration criteria except the mean error for the SA was -1.01 ft, which very slightly exceeded the less than one-foot criteria assigned to the domain as a whole for each aquifer (Table 19).

Table 19. Verification period statistics (2013-2014) of the target monitoring wells in the ECFTX model domain and CFWI area.

	ECFTX Model Domain			CFWI Area		
	SA	UFA	LFA	SA	UFA	LFA
Residual Mean	-1.01	-0.11	0.65	-0.71	-0.09	1.55
Error Standard Dev	4.39	4.56	3.26	3.57	3.68	2.2
5% of Observation Range	8.66	6.95	2.52	8.56	6.02	2.38
Absolute Residual Mean	2.87	3.53	2.52	2.62	3.06	2.25
Error Sum of Squares	16133	14720	331	2895	2171	177
RMS Error	4.5	4.56	3.27	3.63	3.67	2.66
Minimum Residual	-31.95	-21.99	-10.83	-16.38	-12.08	-4.68
Maximum Residual	21.2	18.77	5.55	11.67	10.17	5.55
Number of Observations	796	709	31	220	161	25
Percentage with MAE < 2.5 ft	66%	49%	65%	67%	54%	68%
Percentage with MAE < 5.0 ft	87%	78%	90%	85%	84%	96%
Percentage with R2> 0.4	80%	87%	94%	77%	92%	100%

All values in feet except as noted. Verification period is 2013-2014. Mean error expressed as simulated minus observed.

The spatial distribution of error for the verification period wells for the SA, UFA, and LFA is shown in Figure 126 through 128. Spatial distribution of error for all aquifers within the CFWI area is smaller than the domain outside the CFWI region. Like the transient calibration period, elevation of SA simulated water levels is underpredicted in the southern half of the Lake Wales Ridge in Highlands County. Some improvement in underprediction was seen within some deep-water table areas near Orlando. Simulated water levels in eastern portions of Citrus, Hernando, and Pasco continued to be generally simulated higher than observed in the UFA. Simulated versus observed potentiometric surfaces for May and September 2014 are shown in Figure 129 and 130. Like the calibration period flow field, the Polk City potentiometric high, the East Pasco potentiometric high, the high along the Lake Wales Ridge, and the configuration of the UFA flow field are well-represented by the transient model.

For the verification period from 2013-2014, mean simulated springflow in the model from all 158 springs was 2,121 cfs, while observed (estimated and measured) was 2,165 cfs, resulting in a mean error of +2%. Simulated springflow comparison with estimated/observed for the verification period was similar for the CFWI area during the calibration period but not for two springs within the larger ECFTX model domain. Verification period statistics were comparable to the calibration

period for the 17 springs with measurements except for the Rainbow No. 1 and Lithia Major spring which slightly exceeded the calibration period metric at 11% and 14%, respectively (Table 20).

Table 20. Verification period statistics (2013-2014) of the target springs simulated in the ECFTX model.

Spring Name	Observed Flux (cfs)	Simulation	
		Flux (cfs)	Error
Lithia Spring Major	41.1	35.4	-14%
Buckhorn Main Spring	11.6	12.7	10%
Sulphur Spring (Hillsborough)	41.1	38.1	-7%
Crystal Main Spring (Pasco)	49.6	46.5	-6%
Weeki Wachee Spring	175.1	176.9	1%
Chassahowitzka Spring Main	61.9	65.1	5%
Homosassa Spring #1	84.2	77.4	-8%
Gum Spring Main	64.2	65.6	2%
Rainbow Spring #1	74.9	83.1	11%
Apopka Spring	22.1	24.4	10%
Sanlando Springs	18.3	19.3	5%
Starbuck Spring	11.5	12.5	9%
Wekiwa Spring (Orange)	58.7	63.6	8%
Bugg Spring (Lake)	10.0	9.1	-8%
Rock Springs (Orange)	53.2	51.0	-4%
Volusia Blue Spring	125.1	127.0	2%
Alexander Spring	90.3	95.0	5%

Verification period is 2013-2014. Mean error expressed as simulated minus observed.

The baseflow match for the verification period was similar to the calibration period for the ECFTX domain. For the verification period from 2013-2014, mean simulated baseflow in the model from all 18 USGS gages was 4,774 cfs, while observed (estimated) varied between 3,352 and 9,814 cfs. A total of 10 out of 18 USGS gages where baseflow was estimated were within the range of flows estimated by the methods described in Chapter 4 for the verification period (Table 21).

5.4 Model Fit during High and Low Periods

The Nash-Sutcliffe efficiency coefficient (NS) is often used to assess the predictive power of hydrologic models. The coefficient can range from -infinity to 1. An efficiency of 1 corresponds to a perfect fit between simulated and observed data. An efficiency of 0 means that the model predictions are as accurate as the mean of the observed data while less than zero means the observed data is a better predictor than the model. Like the coefficient of determination (r^2), the closer the value is to 1 the more accurate the model matches the behavior of the observed data. NS coefficients were generated for each target well of simulated versus observed water levels along with mean error, mean absolute error, and r-squared in Appendix G. Both the unadjusted

NS and adjusted NS are listed on each graphic. The adjusted NS coefficient is normalized by removing the starting condition error for each hydrograph.

Table 21. Simulated mean baseflow from 2013-2014 compared to estimated ranges using the USF method and USGS Groundwater Toolbox methods at 18 stations.

Gauge	Station	Min (cfs)	Max (cfs)	Simulated Mean Baseflow (cfs)
02232400	ST JOHNS RIVER NR COCOA FL	245	934	225
02232500	ST JOHNS RIVER NR CHRISTMAS FL	458	1210	297
02234000	ST JOHNS RIVER ABOVE LAKE HARNEY NR GENEVA FL	753	1737	711
02236000	ST JOHNS RIVER NR DELAND FL	813	3368	1568
02238000	HAYNES CREEK AT LISBON	0	2	136
02294650	PEACE RIVER AT BARTOW	14	97	93
02294898	PEACE RIVER AT FORT MEADE	17	119	144
02295637	PEACE RIVER AT ZOLFO SPRINGS	71	321	347
02296750	PEACE RIVER AT ARCADIA	128	675	579
02298830	MYAKKA RIVER NR SARASOTA	31	200	59
02300500	LITTLE MANATEE RIVER NR WIMAUMA	26	87	74
02301500	ALAFIA RIVER AT LITHIA	54	174	117
02303000	HILLSBOROUGH RIVER NR ZEPHYRHILLS	73	154	110
02310000	ANCLOTE RIVER NR ELFERS	7	56	14
02312000	WITHLACOOCHEE RIVER AT TRILBY	45	192	174
02312500	WITHLACOOCHEE RIVER AT CROOM	78	234	196
02312762	WITHLACOOCHEE RIVER NR INVERNESS	210	385	-6
02313000	WITHLACOOCHEE RIVER NR HOLDER	329	525	-65

Histograms of normalized NS statistics for the SA, UFA, and LFA target wells were generated for the CFWI area and ECFTX model domain (Figure 131 through 136). For the CFWI area, Nash-Sutcliffe statistics were good with the largest number of targets within the 0.4-0.8 range for the SA and UFA, and within the 0.8-1.0 range for the LFA. Likewise, NS statistics were consistent with the CFWI targets within the larger ECFTX model domain.

Another statistic frequently used to assess model performance over the full range of hydrologic conditions from extreme high to extreme low period is stage duration (in this case head duration). A stage duration curve is a plot of stage elevation versus percent of time that a stage was equaled or exceeded. Figure 137 through 142 show simulated versus observed head duration at selected

wells across the CFWI area within the SA, UFA, and LFA (well location shown in Figure 116). These are the same wells shown previously for the times series plots of simulated versus observed heads in Section 5.2.3. While some target wells show almost identical head duration curves between observed and simulation water levels such as UFA well OR-47 and LFA well S-1329, others show a distinct separation such as LFA well OSF-52. Wells that show an elevation separation do tend to maintain that distance consistently throughout the range of elevations in the record – suggesting a starting condition offset carried throughout the transient simulation. In addition, the maximum-minimum difference in water levels or range between observed and simulated water levels for the period is approximated closely – even if the duration curves are separated. This all suggests model simulated water levels are replicating high and low periods within the record. Plots of simulated versus observed head duration for all target wells over the 2003 through 2014 period are contained in Appendix L.

To assess model statistics through time, the mean error (simulated minus observed) for all target wells for each year from 2003 through 2014 for the CFWI and ECFTX areas is presented by aquifer (Figure 143 and 144). Annual rainfall in the ECFTX domain is superimposed on the plot to note any variation due to unusually wet or dry periods. There is no apparent trend in mean error with time except for the LFA where error becomes gradually smaller from the beginning to the end of the simulation period. This is due to the limited dataset where additional target well water levels are being added through the period that reach their maximum extent during the more recent time frame. There is also no significant difference in mean error head statistics between wet and dry periods from 2004 through 2014.

Calibration statistics were also examined for a dry year (2006) and a wet year (2014) within the CFWI and ECFTX areas. Table 22 and 23 show the statistics for 2006 and 2014, respectively. Interestingly, mean absolute error and root mean squared error calibration statistics were either equal to or slightly better than for the calibration period from 2004-2012. This suggests the model is well calibrated even during dry or wet periods within the simulation.

5.5 Water Budget

Simulated water budgets illustrating boundary condition inflow and outflows from the ECFTX model by layer were prepared for both the calibration and verification periods (Table 24-27; Figure 145-146). The total flux (IN-OUT) balances to within less than 0.05 inches/year. Net fluxes for each major component of the water budget during the calibration period included recharge of 8.7 in/yr, GHB lateral flux of 0.7 in/yr into the model with constant head, well, river, springs, and drains having net outflow components of 2.3, 2.0, 0.9, 1.3, and 3.4 inches per year, respectively. A total net storage change of +0.4 in/yr occurred over the 2004-2012 period based on the model results.

About 60% of the net GHB inflow (a total of 0.7 in/yr in the calibration period) occurs along the northern boundary along its western half primarily in the unconfined karst region of the UFA – and about 30% along the southern GHB boundary. These fluxes are consistent with a net flow into the model from the active part of the aquifer system based on the configuration of the potentiometric surface and where transmissivity of the UFA is very high. They represent less than 10% of the net recharge and are far removed from the CFWI area of interest. The remaining 10% of net GHB influx (< 0.1 in/yr) occurs along the western boundary. There is approximately zero net GHB flux along the eastern boundary of the model.

Table 22. Water level statistics of the target monitoring wells for dry (2006) and wet (2014) years in the ECFTX model domain.

ECFTX	Dry Year (2006)			Wet Year (2014)		
	SA	UFA	LFA	SA	UFA	LFA
Residual Mean	-0.29	0.39	1.00	-0.94	-0.21	0.12
Error Standard Dev	3.87	4.41	2.18	4.38	4.66	3.33
5% of Observation Range	8.71	7.20	2.63	8.54	6.47	2.52
Absolute Residual Mean	2.59	3.45	2.05	2.84	3.54	2.46
Error Sum of Squares	11813	12020	133	15815	13840	289
RMS Error	3.9	4.4	2.4	4.5	4.7	3.3
Minimum Residual	-29.4	-20.9	-2.7	-31.4	-20.5	-10.9
Maximum Residual	18.3	15.9	4.8	22.6	19.0	4.4
Number of Observations	787	615	24	789	636	27
Percentage with MAE < 2.5 ft	66%	49%	67%	65%	50%	67%
Percentage with MAE < 5.0 ft	89%	79%	100%	88%	77%	93%
Percentage with R2 > 0.4	75%	85%	100%	60%	64%	89%

All values in feet except as noted. Mean error expressed as simulated minus observed.

Table 23. Water level statistics of the target monitoring wells for dry (2006) and wet (2014) years in the CFWI area.

CFWI	Dry Year (2006)			Wet Year (2014)		
	SA	UFA	LFA	SA	UFA	LFA
Residual Mean	-0.91	-0.21	1.37	-0.78	-0.63	1.16
Error Standard Dev	3.54	3.71	2.00	3.57	3.54	2.10
5% of Observation Range	8.45	6.02	2.54	8.45	5.80	2.33
Absolute Residual Mean	2.52	3.03	2.05	2.61	2.94	2.04
Error Sum of Squares	2805	1936	113	2891	1619	117
RMS Error	3.6	3.7	2.4	3.6	3.6	2.4
Minimum Residual	-17.6	-11.6	-2.4	-17.3	-12.2	-4.6
Maximum Residual	9.9	9.0	4.8	11.3	7.6	4.4
Number of Observations	211	141	20	218	126	21
Percentage with MAE < 2.5 ft	67%	50%	70%	67%	56%	71%
Percentage with MAE < 5.0 ft	86%	84%	100%	85%	86%	100%
Percentage with R2 > 0.4	77%	94%	100%	67%	74%	95%

All values in feet except as noted. Mean error expressed as simulated minus observed.

Net fluxes for each major component of the water budget during the verification period included recharge of 10.4 in/yr, GHB lateral flux of 0.5 in/yr into the model with constant head, well, river, springs, and drains having net outflow components of 2.5, 1.7, 1.0, 1.3, and 3.6 inches per year, respectively. A total net storage change of -0.8 in/yr occurred over the 2013-2014 period.

Vertical leakage downward (into) or upward (out) of the UFA during the calibration period is shown in Figure 147. Largest values of 10 to 30 in/yr occur within the unconfined karst region in the northwest part of the domain, along the Lake Wales Ridge, and deep water-table areas near Orlando. Smallest vertical leakage values varying from one to five in/yr, are found within the well-confined parts of the UFA in the southern half of the domain except for the central ridge area. Upward flux occurs in the coastal regions, Kissimmee River valley, and the southeast part of the domain. A more detailed water budget showing vertical flow components between each layer is contained in Appendix M.

Table 24. Annual average boundary condition influx in the ECFTX transient model during the calibration period (2004-2012).

Layer	Constant Head in/yr	GHB in/yr	Well in/yr	River in/yr	Rech in/yr	ET in/yr	Spring in/yr	Drain Return in/yr	Drain in/yr	Storage in/yr
1	0.22	0.04	0.08	3.60	21.89	-	-	-	-	0.38
2	-	0.26	-	-	-	-	-	-	-	0.01
3	-	0.48	-	-	-	-	-	0.06	-	0
4	-	0.23	-	-	-	-	-	-	-	0
5	-	0.57	-	-	-	-	-	-	-	0
6	-	0.10	-	-	-	-	-	-	-	0
7	-	0.08	-	-	-	-	-	-	-	0
8	-	0.06	-	-	-	-	-	-	-	0
9	-	0.22	-	-	-	-	-	-	-	0
10	-	-	-	-	-	-	-	-	-	0
11	-	0.11	-	-	-	-	-	-	-	0.01
Total	0.22	2.15	0.08	3.60	21.89	-	-	0.06	-	0.40

Note: Units = inches per year.

Table 25. Annual average boundary condition outflux in the ECFTX transient model during calibration period (2004-2012).

Layer	Constant Head in/yr	GHB in/yr	Well in/yr	River in/yr	Rech in/yr	ET in/yr	Spring in/yr	Drain Return in/yr	Drain in/yr	Storage in/yr
1	-2.56	-0.02	-0.17	-3.92	-	-13.17	-	-	-3.50	0
2	-	-0.03	-0.02	-	-	-	-	-	-	0
3	-	-0.46	-0.64	-	-	-	-1.28	-	-	0
4	-	-0.11	-0.30	-	-	-	-	-	-	0
5	-	-0.06	-0.59	-	-	-	-0.01	-	-	0
6	-	-	-	-	-	-	-	-	-	0
7	-	-	-	-	-	-	-	-	-	0
8	-	-	-	-	-	-	-	-	-	0
9	-	-0.18	-0.30	-	-	-	-	-	-	0
10	-	-	-	-	-	-	-	-	-	0
11	-	-0.57	-	-	-	-	-	-	-	0
Total	-2.56	-1.43	-2.03	-3.92	-	-13.17	-1.29	-	-3.50	0

Note: Units = inches per year.

Table 26. Annual average boundary condition influx in the ECFTX transient model during the verification period (2013-2014).

Layer	Constant Head in/yr	GHB in/yr	Well in/yr	River in/yr	Rech in/yr	ET in/yr	Spring in/yr	Drain Return in/yr	Drain in/yr	Storage in/yr
1	0.19	0.04	0.09	2.84	23.08	-	-	-	-	0
2	-	0.24	-	-	-	-	-	-	-	0
3	-	0.39	-	-	-	-	-	0.05	-	0
4	-	0.22	-	-	-	-	-	-	-	0
5	-	0.54	-	-	-	-	-	-	-	0
6	-	0.09	-	-	-	-	-	-	-	0
7	-	0.08	-	-	-	-	-	-	-	0
8	-	0.06	-	-	-	-	-	-	-	0
9	-	0.20	-	-	-	-	-	-	-	0
10	-	-	-	-	-	-	-	-	-	0
11	-	0.10	-	-	-	-	-	-	-	0
Total	0.19	1.96	0.09	2.84	23.08	-	-	0.05	-	0

Note: Units = inches per year.

Table 27. Annual average boundary condition outflux in the ECFTX transient model during the verification period (2013-2014).

Layer	Constant Head in/yr	GHB in/yr	Well in/yr	River in/yr	Rech in/yr	ET in/yr	Spring in/yr	Drain Return in/yr	Drain in/yr	Storage in/yr
1	-2.72	-0.02	-0.14	-3.88	-	-12.63	-	-	-3.67	0.76
2	-	-0.03	-0.02	-	-	-	-	-	-	0.01
3	-	-0.49	-0.54	-	-	-	-1.31	-	-	0
4	-	-0.10	-0.26	-	-	-	-	-	-	0
5	-	-0.07	-0.53	-	-	-	-0.01	-	-	0
6	-	-	-	-	-	-	-	-	-	0.01
7	-	-	-	-	-	-	-	-	-	0
8	-	-	-	-	-	-	-	-	-	0
9	-	-0.18	-0.29	-	-	-	-	-	-	0
10	-	-	-	-	-	-	-	-	-	0
11	-	-0.58	-	-	-	-	-	-	-	0.01
Total	-2.72	-1.48	-1.79	-3.88	-	-12.63	-1.32	-	-3.67	0.79

Note: Units = inches per year.

5.6 Structure Flow Calibration

The ET-Recharge (AFSIRS) program is not coupled to MODFLOW; therefore, an iterative process was used to calibrate structure flows using ET and recharge parameters and canal/drain bed conductance. The interaction between the surface water system and groundwater system was facilitated by a simple canal water budget module, along with the ET-Recharge (AFSIRS) program.

The simple canal water budget module neglects storage in the canals and is represented by the following equation:

Runoff +Baseflow= structure canal outflows – structure canal inflows

where: runoff is the routed runoff computed with the NRCS/Muskingum method, structure canal inflows and outflows are obtained from measured flow at gauges, and baseflow (Q) is calculated using the by MODFLOW equation:

Q (baseflow) = (K*L*W/M) * (h_river - h)

where: h_river is the river stage, h is the aquifer hydraulic head, K is the hydraulic conductivity of riverbed material, L is the length of reach, W is the width of the river, and M is the thickness of riverbed sediments.

Gauged basins were used for the calibration. For ungauged basins, parameters from calibrated basins with similar characteristics (land use, soil type, etc.) were used. The first step was to generate initial ET and recharge MODFLOW files using the ET-RCH program. For the initial ET and recharge estimates, an average 2003 depth to water table values were used. Then MODFLOW was run with these estimated ET and recharge files (first iteration). MODFLOW was then run with these estimated ET and recharge files. Baseflows for each basin were extracted from RIV, DRN (spring flows) and DRT (drains) flow budgets using another Fortran program (MULTIBUD). The extracted baseflows were combined with the routed basin runoff from ET-Recharge to develop the simulated total stream flow hydrograph. This hydrograph was then compared with the observed stream flow hydrograph. Both runoff and baseflow components were adjusted to achieve a reasonable match with the observed stream flow hydrograph and the cumulative flow.

In cases where the drainage basin area is significantly larger, the outflow hydrograph peak can be less pronounced and takes more time to occur than the inflow hydrograph. Runoff was routed using the Muskingum method to correct the time lag and attenuate the peak of the output flood hydrograph. When runoff was adjusted, the effective rainfall that passed to the ET-recharge program was changed as described in the ET/Recharge methodology. Baseflows were adjusted based on the estimated values (described in RIVERS section) by adjusting the river and drain bed conductance. The ET-recharge program was re-run using the adjusted CNs effective rainfall values and MODFLOW simulated depth to water table values. Then MODFLOW was re-run (second iteration) with the updated parameters and extracted the baseflows from RIV, DRN and DRT budget files, added to basin runoff and then compared with the observed stream flow hydrograph. This procedure was repeated until a reasonable match between the observed stream flow hydrograph and the simulated hydrograph was achieved.

The calibration criteria for structure flows were selected based upon the criteria used in previous regional models in the area and are described as follows:

- Deviation of Volume (DV) < 15%

- Nash-Sutcliffe (NS)   > 0.5

- R squared (R2)   > 0.5

5.6.1 Structure Flow Calibration Results

Within the ECFTX model domain, 39 gaged basins were selected for structure flow calibration based on the availability of continuous measured inflow/outflow stream data. Gaged basins were delineated by combining multiple HUC12 watersheds to ensure the availability of inlet and outlet stream gaging stations of the basins. Heavily managed basins within the SFWMD, such as the Kissimmee basin, were not included in the calibration process due to the difficulty in simulating changing river geometry through time. Figure 148 shows the basins and stream gages selected for the calibration. Table 28 shows a summary of average runoffs, baseflows, and total flows and calibration statistics of total structure flows. The basins are assigned a unique identification number (Basin ID) in column 1 in Table 28 and their location are shown in Figure 148.

Figure 149 shows an example of simulated vs observed runoff, baseflow, and total structure flow hydrographs for the Shingle Creek watershed (basin ID 28). Simulated runoff is obtained by subtracting the estimated baseflow from the total stream flow. Simulated runoff compared well with the estimated runoff, except during September 2004 ($NS=0.46, R^2=0.55$) as shown in Figure 149 (a). Comparison of estimated vs. simulated baseflows (b). Simulated baseflows are derived from river and drain leakage terms within the basin from MODFLOW output. Total simulated structure flows, which is the sum of the simulated runoffs and the simulated baseflows, are compared with total measured stream flows (c). Except during September 2004, a very good agreement between the simulated and observed total structure flows (**$NS=0.45, R^2=0.59$**) is shown (c). The study area received heavy rainfall during September 2004 due to three major hurricane events, which is an extraordinary condition. Uncertainty in both NEXRAD and measured rainfall data is quite high in this type of extreme situation. As such, the simulated structure flow underestimates the peak flow (~ 1300 cfs measured vs. 700 cfs simulated) that occurred in September 2004, which caused a deviation in the simulated cumulative flows from the observed (d). In general, the majority of the basins meet the NS (>0.5) and R^2 (0>0.5) criteria, however, the DV (<15%) criteria is not met in many occasions, mainly due to not capturing September 2004 extreme rainfall condition correctly (Table 28). Recharge developed using the ET-Recharge program for the basins that meet the calibration criteria has a high level of confidence. Conversely, recharge developed for the areas where no surface water calibration took place may have a lower level of confidence.

Table 28. Summary of runoff, baseflow, total structure flow and total structure flow calibration statistics; (a) basin ID (b) basin name, (c) 12-year average simulated runoff, (d) 12-year average simulated base flow (e) 12-year average total flow ((b)+(c)), (f) total flow statistics for 12 years.

(a) Basin ID	(b) Basin Name	(c) Runoff-12 yr Avg (cfs)		(d) Baseflow-12 yr Avg (cfs)		(e) Total Flow-12 yr Avg (cfs)		(f) Total Flow Statistics		
		Est	Sim	Est	Sim	Obs	Sim	%DV	NS	Rsq.
5	Reedy Creek	56.9	76.3	6.3	14.2	63.2	90.6	-42.3	0.44	0.59
28	Shingle Creek	157.9	120.0	52.7	24.4	210.5	144.4	31.7	0.45	0.59
29	Lake Toho*	211.3	92.1	-52.7	2.9	158.6	95.0	41.2	0.22	0.22
31	Alligator Lake-Lake Gentry-Lonesome Camp Swamp	104.6	119.3	11.6	3.9	116.2	123.3	-6.2	0.57	0.61
33	Lake Arbuckle	167.9	173.3	62.0	133.3	229.9	306.6	-29.5	0.36	0.67
48	Upper Bay Swamp-Upper Harney Pond Canal	208.4	89.1	0.0	122.9	208.4	212.0	0.3	0.53	0.51
50	Lower Canal C-41A	39.9	27.9	0.0	32.3	39.9	60.2	-43.8	0.76	0.83
55	Cypress Creek-C23	138.7	106.3	1.0	69.5	139.7	175.9	-12.6	0.82	0.79
62	Boggy Creek	74.4	69.0	11.4	34.2	85.8	103.2	-21.5	0.74	0.79
80	C-24	174.9	166.0	0.0	29.2	174.9	195.1	-11.5	0.79	0.78
81	C-25	193.9	181.6	0.0	20.8	193.9	202.3	-4.3	0.80	0.78
3	Triplet Lake	13.4	d	2.0	17.2	15.4	26.9	-76.1	-0.41	0.63
7	Wekiva River	99.6	66.0	168.4	376.9	268.0	442.9	-66.4	-6.73	0.49
9	North Branch of Crab Grass Creek	25.0	23.4	0.0	10.4	25.0	33.8	-37.0	0.40	0.60
10	Wolf Creek	28.7	24.6	0.7	17.4	29.4	42.0	-44.6	0.62	0.73
11	Bird Lake + Halfway Lake etc. SJ River	131.9	147.8	59.8	62.5	191.7	210.3	-10.9	0.31	0.33
12	South Fork of Taylor Creek + Taylor Creek-SJ River	42.7	37.9	1.4	21.2	44.1	59.1	-36.8	0.66	0.74
13	South Branch of St. Sebastian River	48.8	35.6	0.0	47.5	48.8	83.0	-70.6	0.07	0.75
20	Six-mile Creek	25.4	20.9	0.7	4.8	26.0	25.7	0.6	0.54	0.50
21	Econ River	392.9	244.0	157.9	447.4	550.8	691.5	-27.7	0.30	0.63
24	Lake Dorr + Lake Norris	40.7	12.3	15.6	98.1	56.2	110.3	-98.4	-2.04	0.59
25	Soldier Creek	10.6	10.8	1.6	12.9	12.2	23.8	-95.5	-0.19	0.77
27	Bear Gully Lake + Howell Creek	47.7	30.2	16.2	52.8	63.9	83.0	-30.9	0.74	0.82
58	Turbull Creek	21.2	4.4	0.4	18.3	21.6	22.6	-2.1	0.58	0.51
6	Lake Ariana + Lake Hancock + Lake Parker	26.4	1.3	20.5	31.4	46.9	32.7	28.1	0.54	0.64
17	Payne Creek	94.6	85.1	17.0	51.5	111.6	136.7	-23.5	0.70	0.71
34	Hawthorn Creek + Lower Joshua Creek etc	104.9	83.2	13.9	65.5	118.8	148.7	-23.9	0.83	0.85

(a) Basin ID	(b) Basin Name	(c) Runoff-12 yr Avg (cfs)		(d) Baseflow- 12 yr Avg (cfs)		(e) Total Flow- 12 yr Avg (cfs)		(f) Total Flow Statistics		
		Est	Sim	Est	Sim	Obs	Sim	%DV	NS	Rsq.
35	Maple Creek + Owen Creek + Wingate Creek + Oglegy Creek	115.9	116.2	6.9	30.6	122.8	146.8	-19.1	0.76	0.78
36	Alderman Creek	26.3	38.1	2.1	9.9	28.4	47.9	-68.6	0.35	0.73
38	Horse Creek	140.5	129.8	9.8	89.8	150.3	219.6	-45.2	0.78	0.80
40	Blackwater Creek + Branch Borough Channel + Hillsborough River Drain	112.0	186.7	65.0	105.6	177.0	292.3	-66.8	0.42	0.64
46	Brooker Creek	20.4	26.3	0.3	8.7	20.6	35.0	-67.3	0.19	0.74
47	Sweetwater Creek	18.2	21.0	1.7	-3.5	19.8	17.5	14.8	0.38	0.68
49	Charlie Creek	193.2	229.0	11.6	137.5	204.8	366.5	-76.7	0.65	0.74
53	Lake Okahumpka	16.6	18.9	15.5	11.0	32.1	29.9	6.6	-0.20	0.26
66	South Branch of Alafia River	68.4	44.6	14.5	22.6	82.9	67.1	19.4	0.68	0.74
70	03100205+Cypress Creek	41.7	9.0	1.7	56.5	43.3	65.4	-42.4	0.65	0.67
71	Rocky Creek	39.6	26.0	3.5	14.0	43.1	40.0	8.6	0.70	0.77
75	3100206+Brooker sub watershed	14.7	9.7	0.0	0.2	14.6	9.9	33.5	0.56	0.61

* Lake Toho (ID No 29) baseflow is negative because it's a managed system.

CHAPTER 5 - FIGURES

Calibration Criteria

- Structure Flow Criteria:
  - Deviation of Volume (DV) < 15%
  - Nash-Sutcliffe Efficiency (NS) > 0.5
  - Coefficient of Determination (R^2) > 0.5

- Springflow Criteria:
  - ME within +/- 10% for each Mag 1 and Mag 2 spring with continuous measurements
  - ME of within +/- 10% for total springflow

- Baseflow Criteria:
  - ME within an order of magnitude for the sum of all simulated baseflow

- Water Level Criteria:
  - Within CFWI, by Aquifer (SAS, UFA, and LFA):
    - 50% of the wells with MAE < 2.5 ft and 80% of the wells with MAE < 5 ft
  - Model Wide, by Aquifer (SAS, UFA, and LFA):
    - Average RMSE < 5 ft
    - Average Overall ME < 1 ft
    - Average MAE < 5% of the range of all observed heads within that aquifer

1

Figure 91 Calibration targets applied to the ECFTX transient model (2004-2012 period)
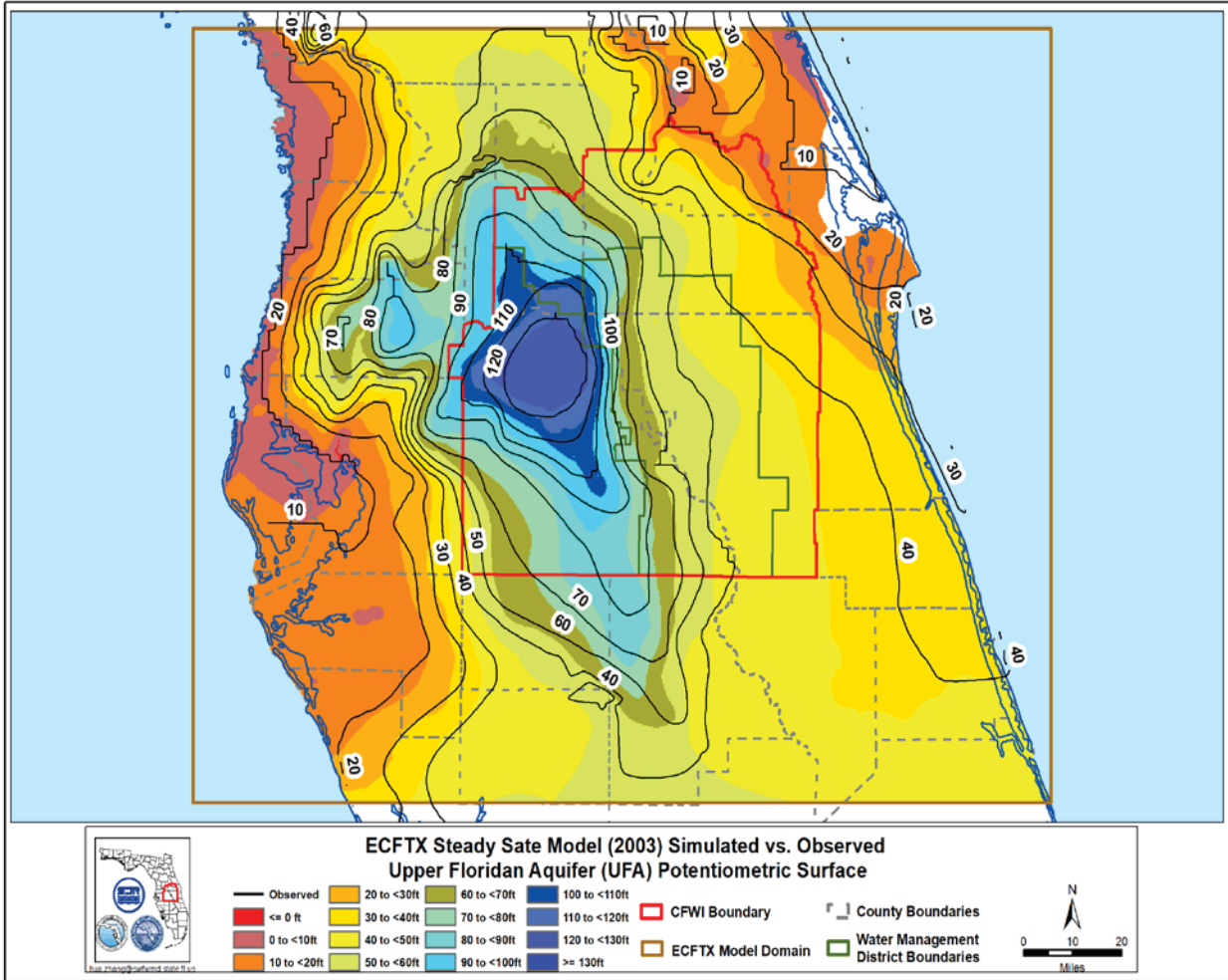
Figure 92. Comparison of average 2003 potentiometric surface with the simulated UFA potentiometric surface from the steady-state model.
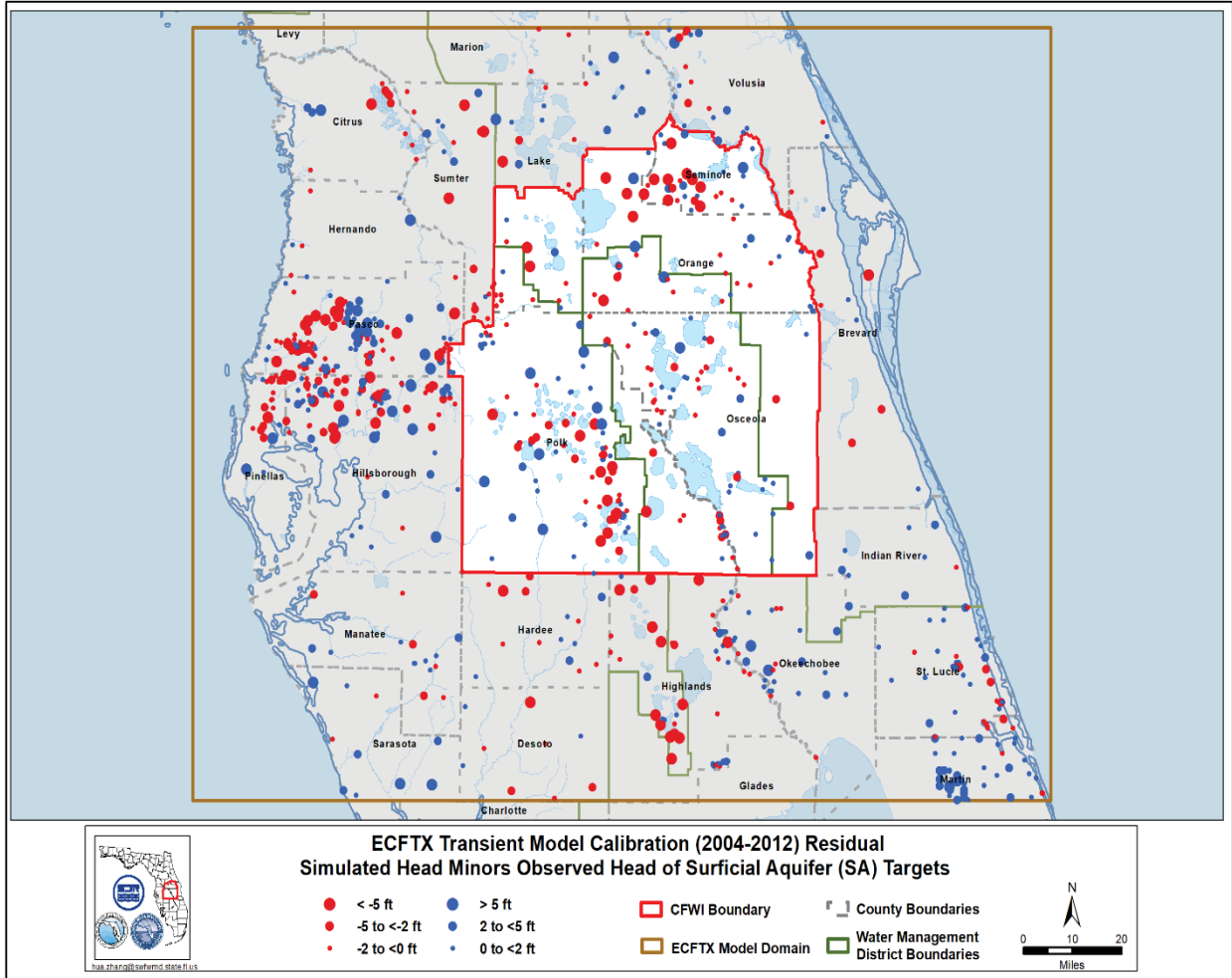
Figure 93. Spatial distribution of mean error for the SA in the ECFTX transient model calibration.
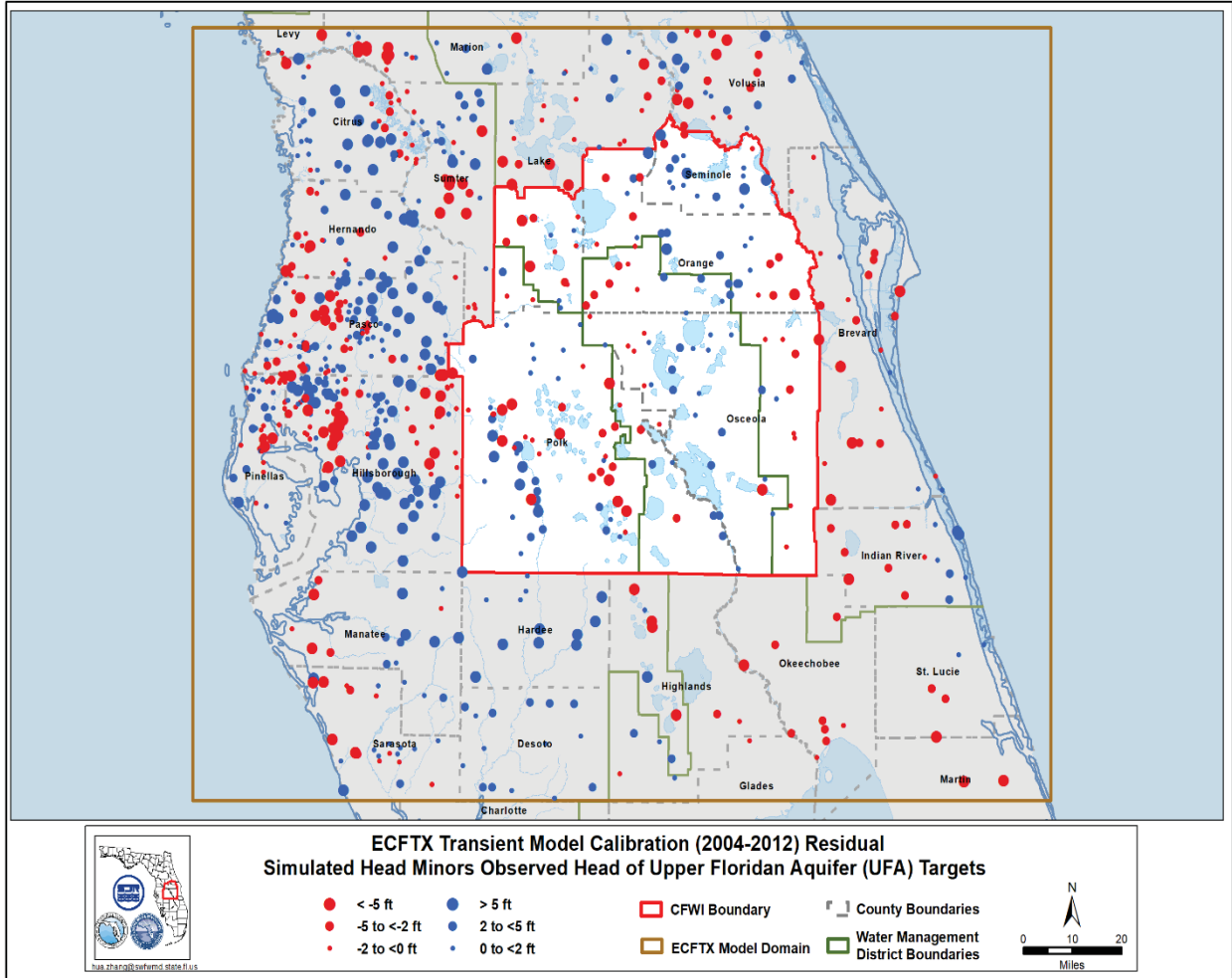
Figure 94. Spatial distribution of mean error for the UFA in the ECFTX transient model calibration.
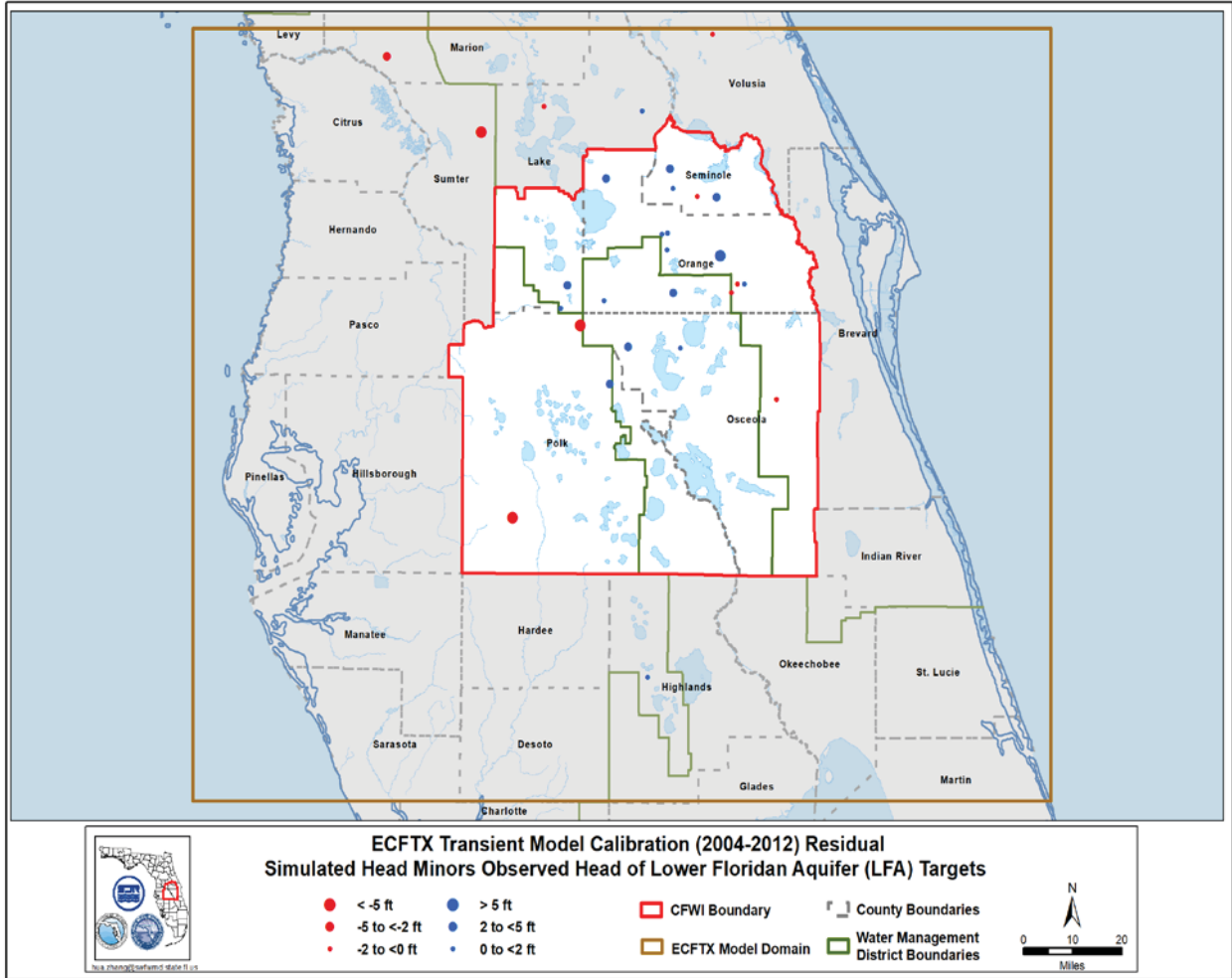
Figure 95. Spatial distribution of mean error for the LFA in the ECFTX transient model calibration.
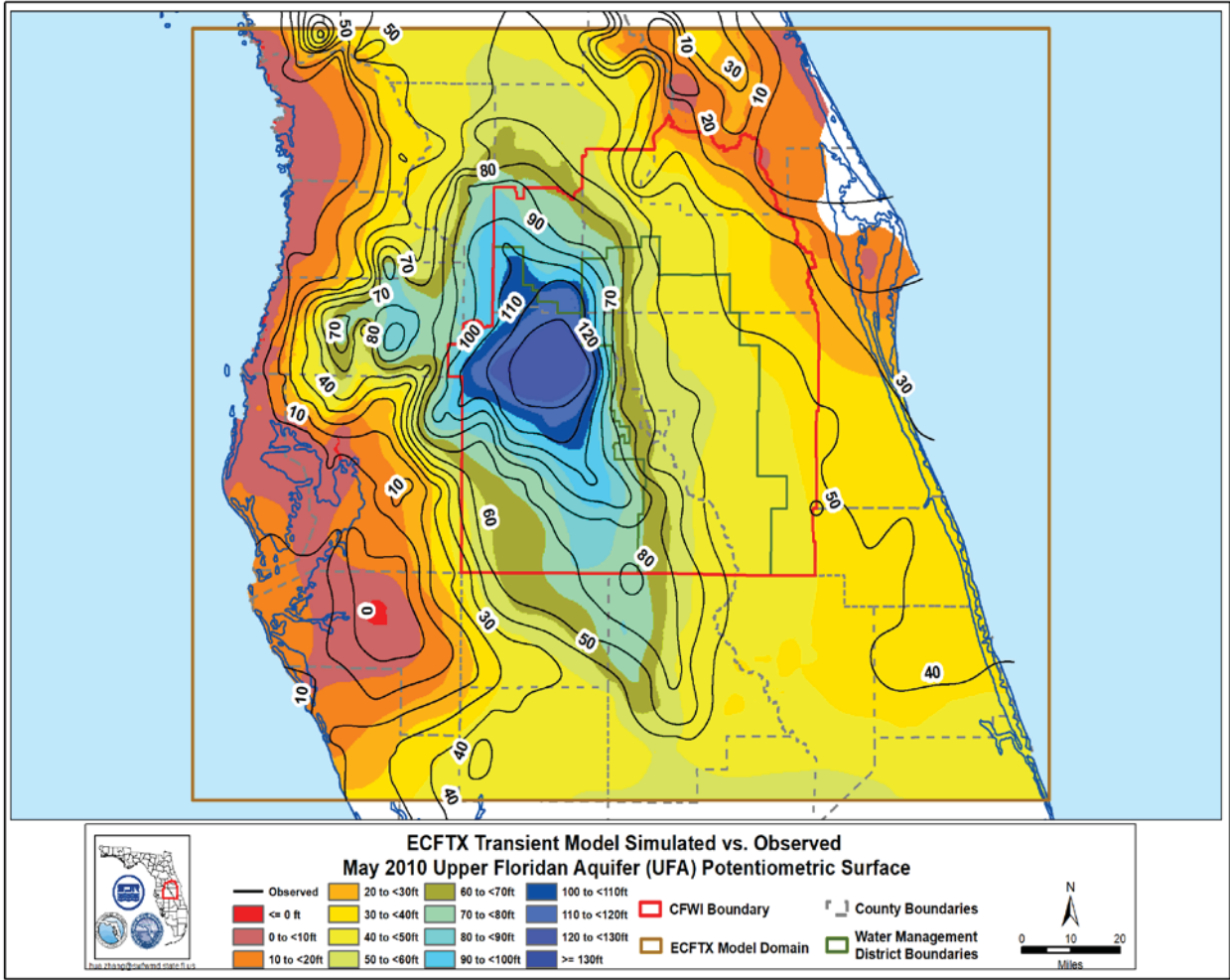
Figure 96. Comparison of May 2010 potentiometric surface with the simulated UFA potentiometric surface from the ECFTX transient model.
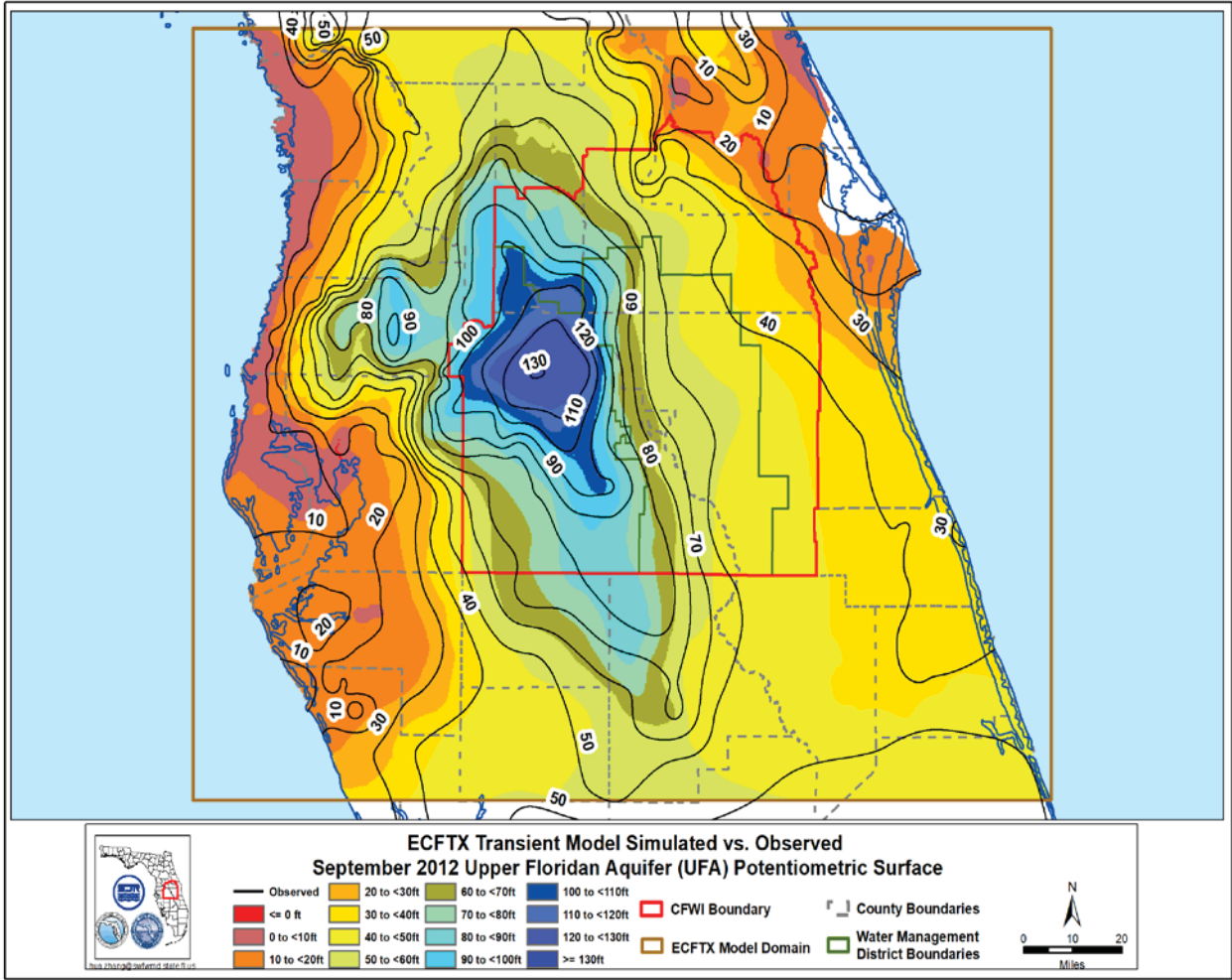
Figure 97. Comparison of September 2012 potentiometric surface with the simulated UFA potentiometric surface from the ECFTX transient model.
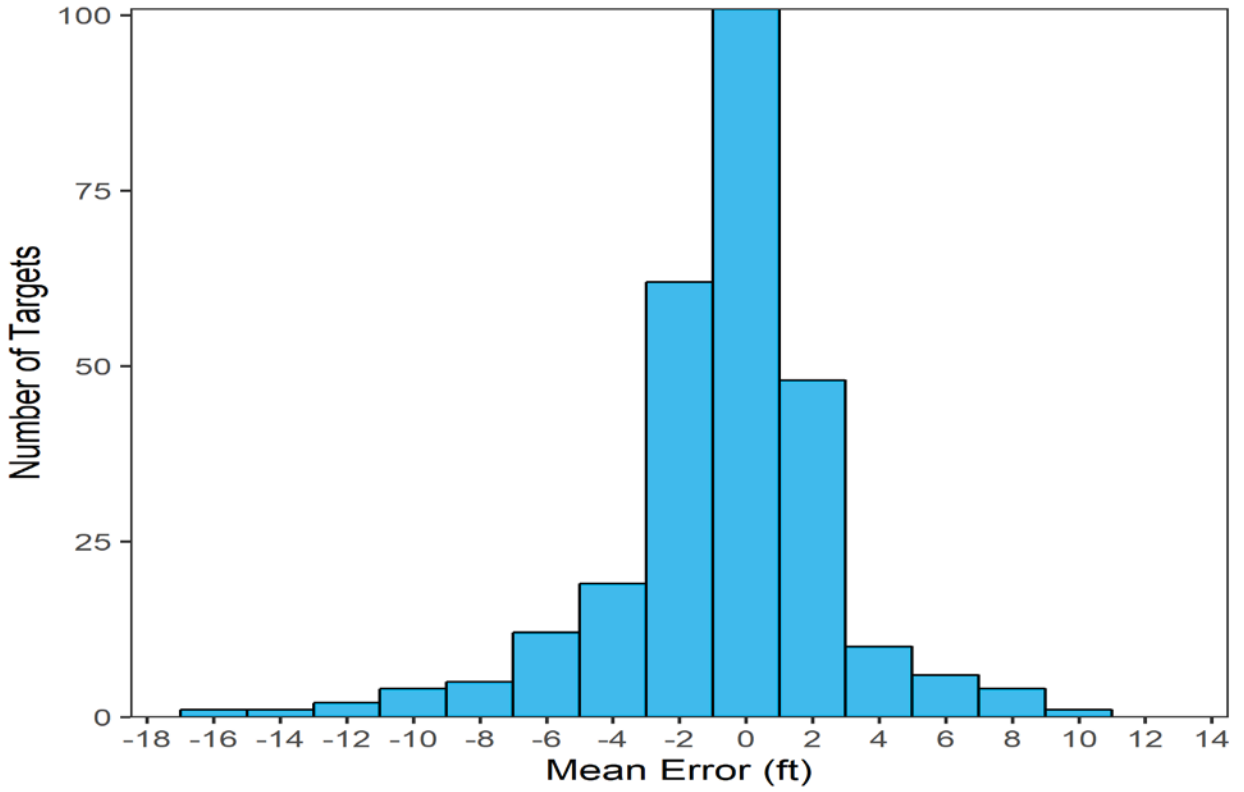
Figure 98. Histogram of simulated versus observed water level differences for the SA within the CFWI area in the ECFTX transient model.
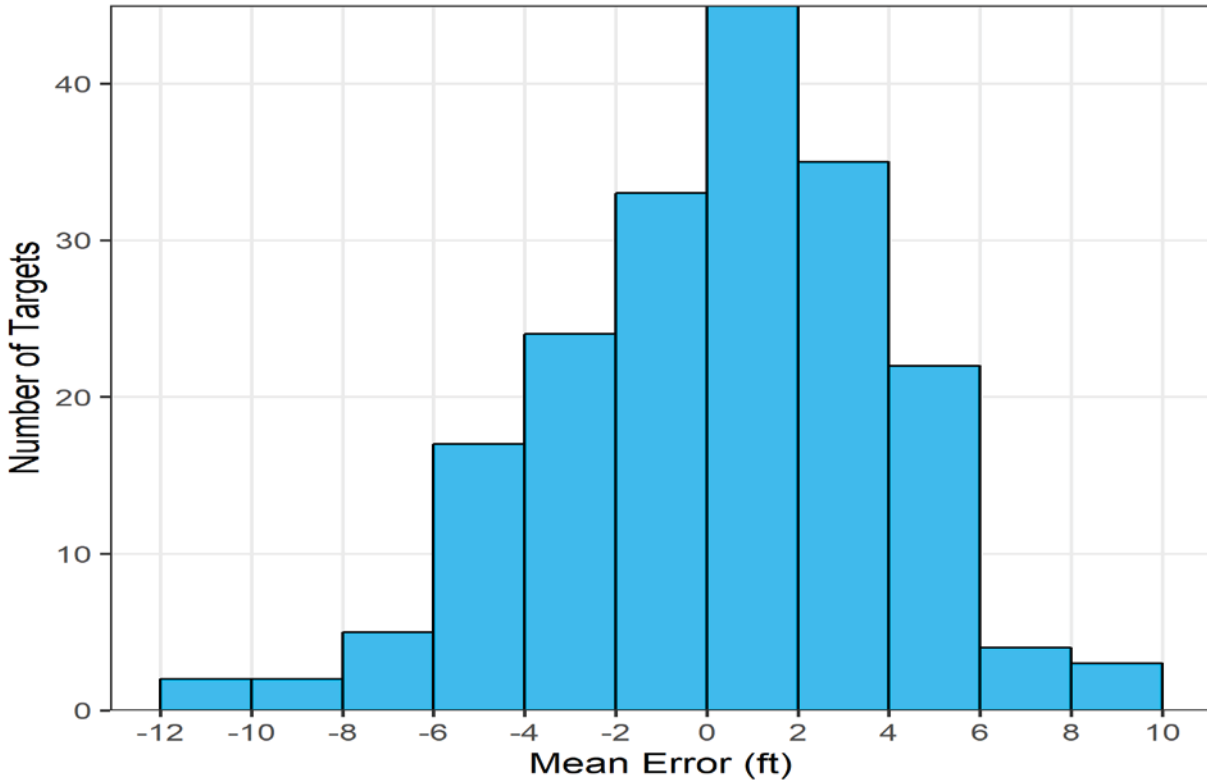
Figure 99. Histogram of simulated versus observed water level differences for the UFA within the CFWI area in the ECFTX transient model.
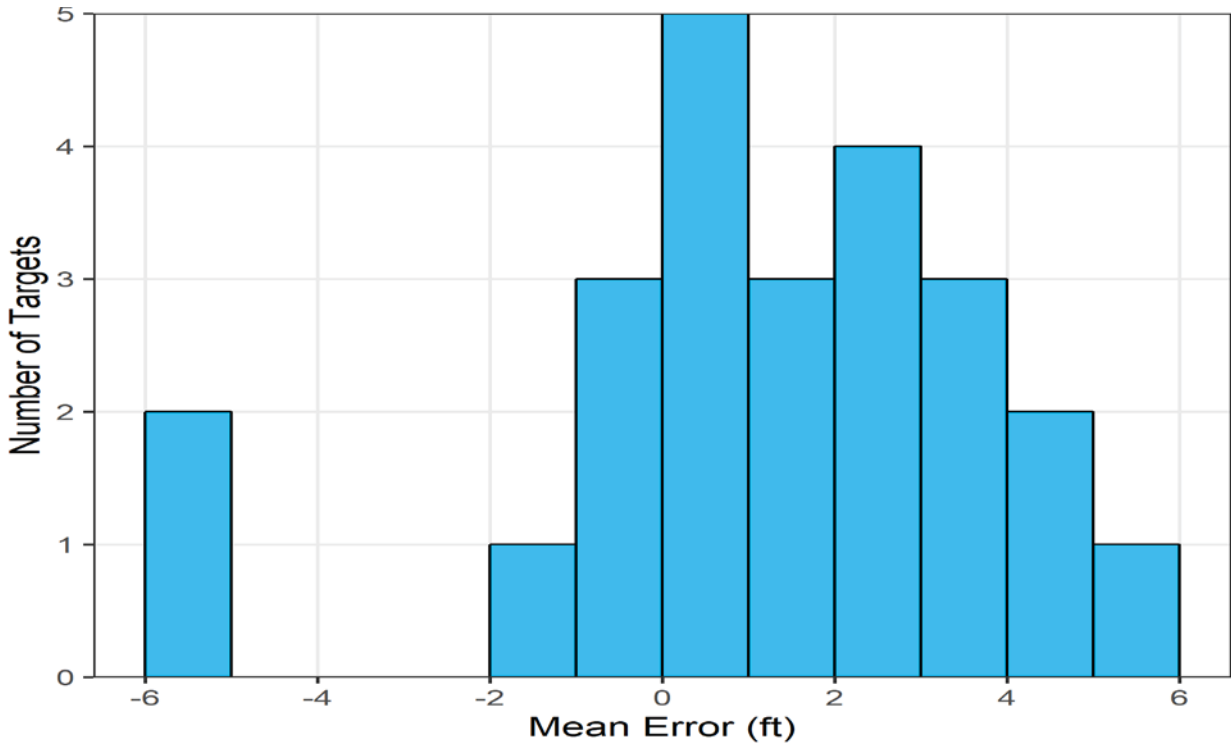
Figure 100. Histogram of simulated versus observed water level differences for the LFA within the CFWI area in the ECFTX transient model.
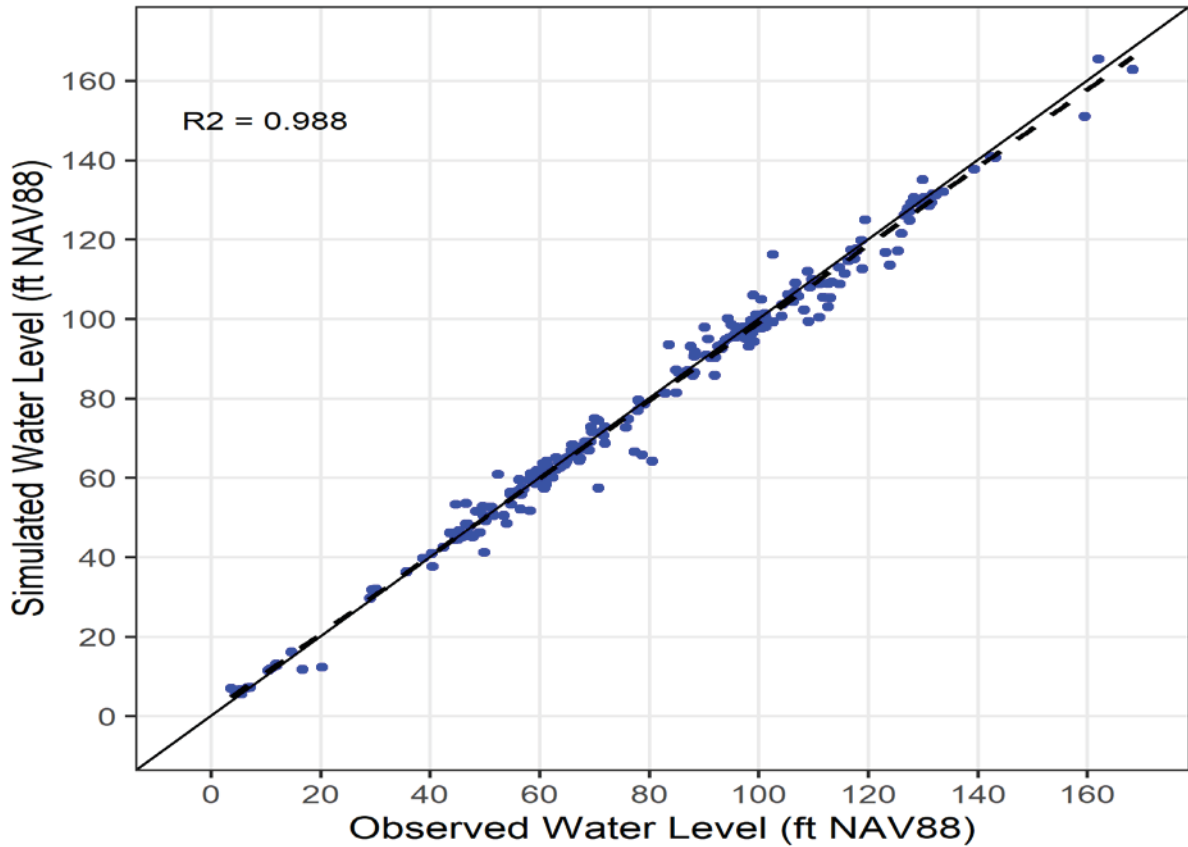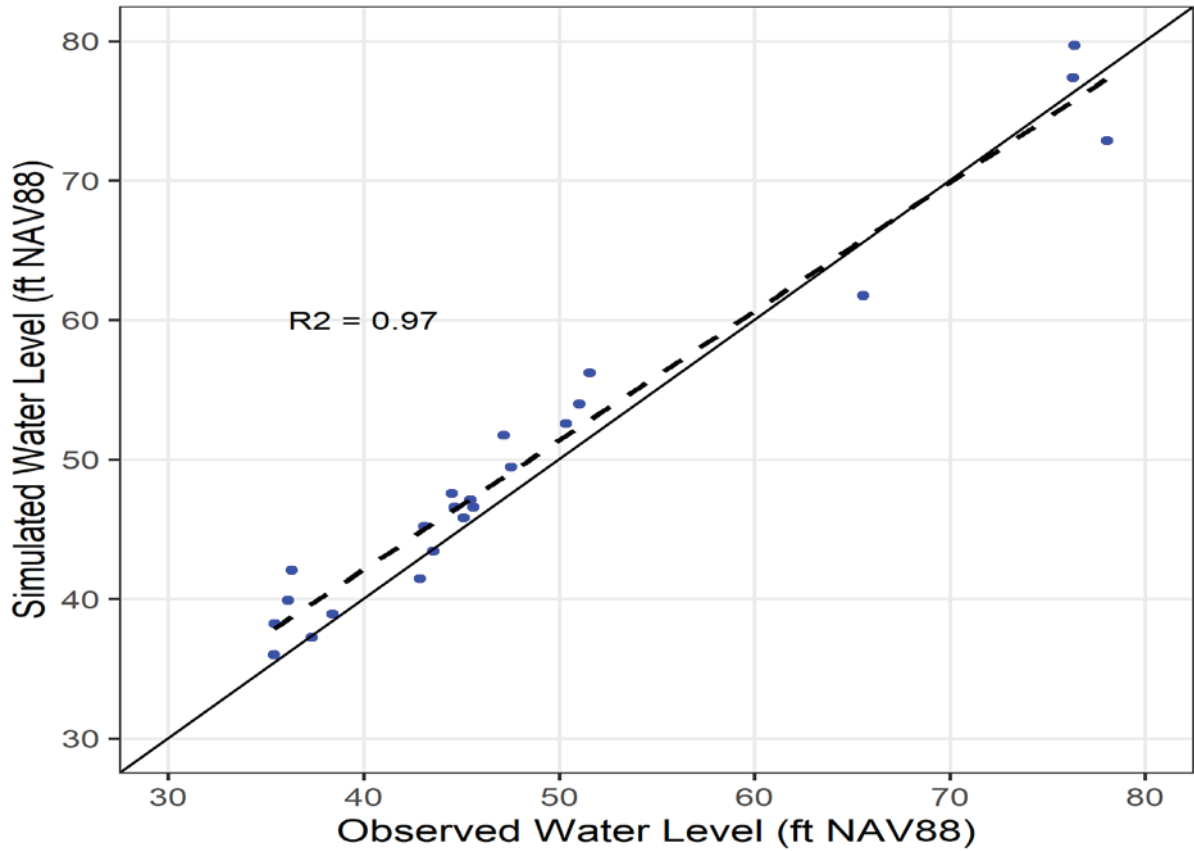
Figure 101. Mean simulated versus observed water levels for the SA within the CFWI area in the ECFTX transient model. (Note: Solid line is 1:1 relation between simulated and observed water levels; dashed line is linear regression of simulated versus observed water levels from target wells).
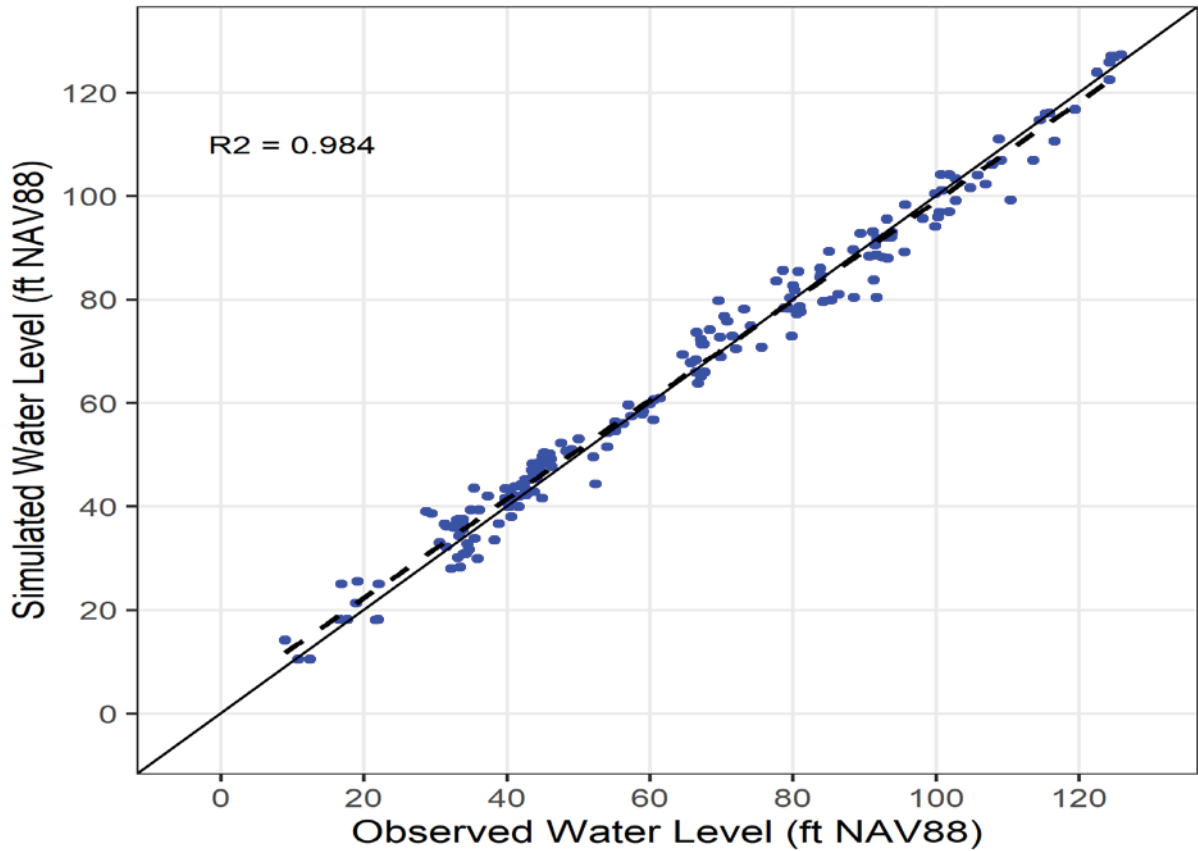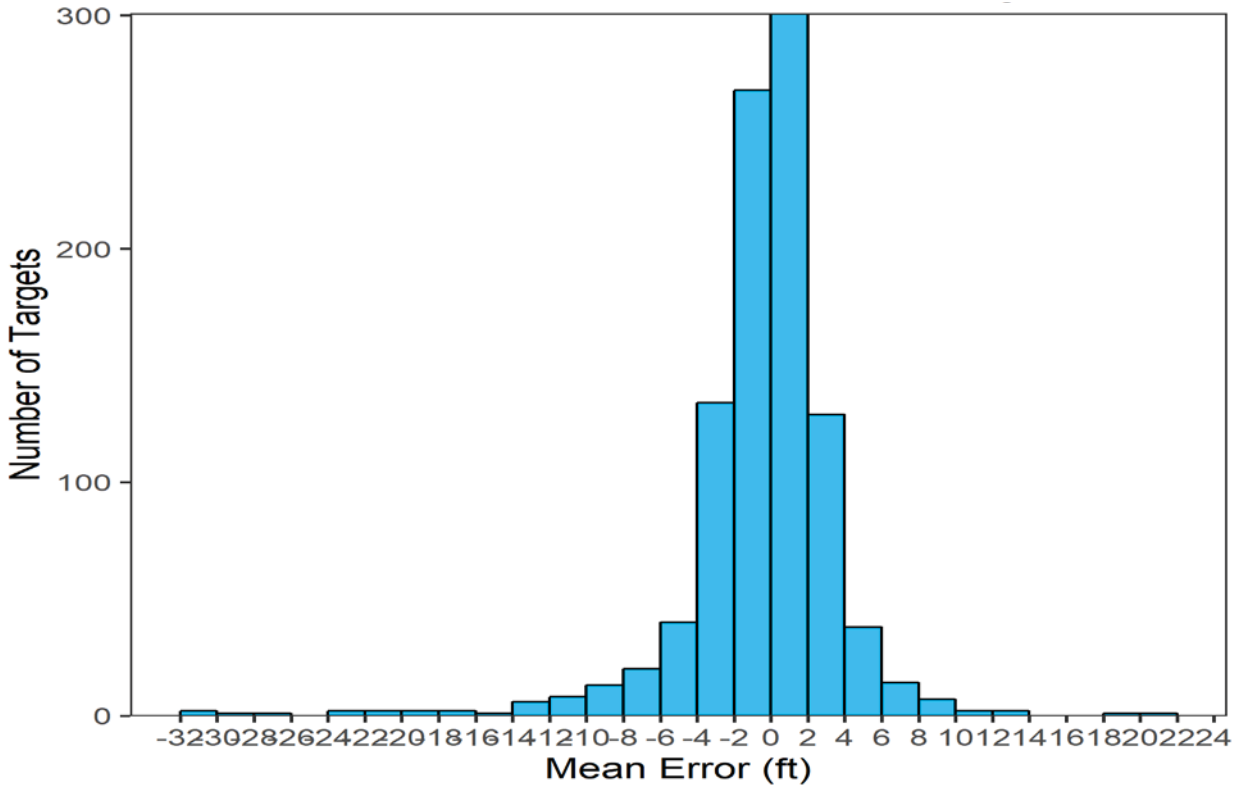
Figure 102. Mean simulated versus observed water levels for the UFA within the CFWI area in the ECFTX transient model. (Note: Solid line is 1:1 relation between simulated and observed water levels; dashed line is linear regression of simulated versus observed water levels from target wells).

Figure 103. Mean simulated versus observed water levels for the LFA within the CFWI area in the ECFTX transient model. (Note: Solid line is 1:1 relation between simulated and observed water levels; dashed line is linear regression of simulated versus observed water levels from target wells).

Figure 104. Histogram of simulated versus observed water level differences for the SA from target wells within the entire ECFTX transient model domain.
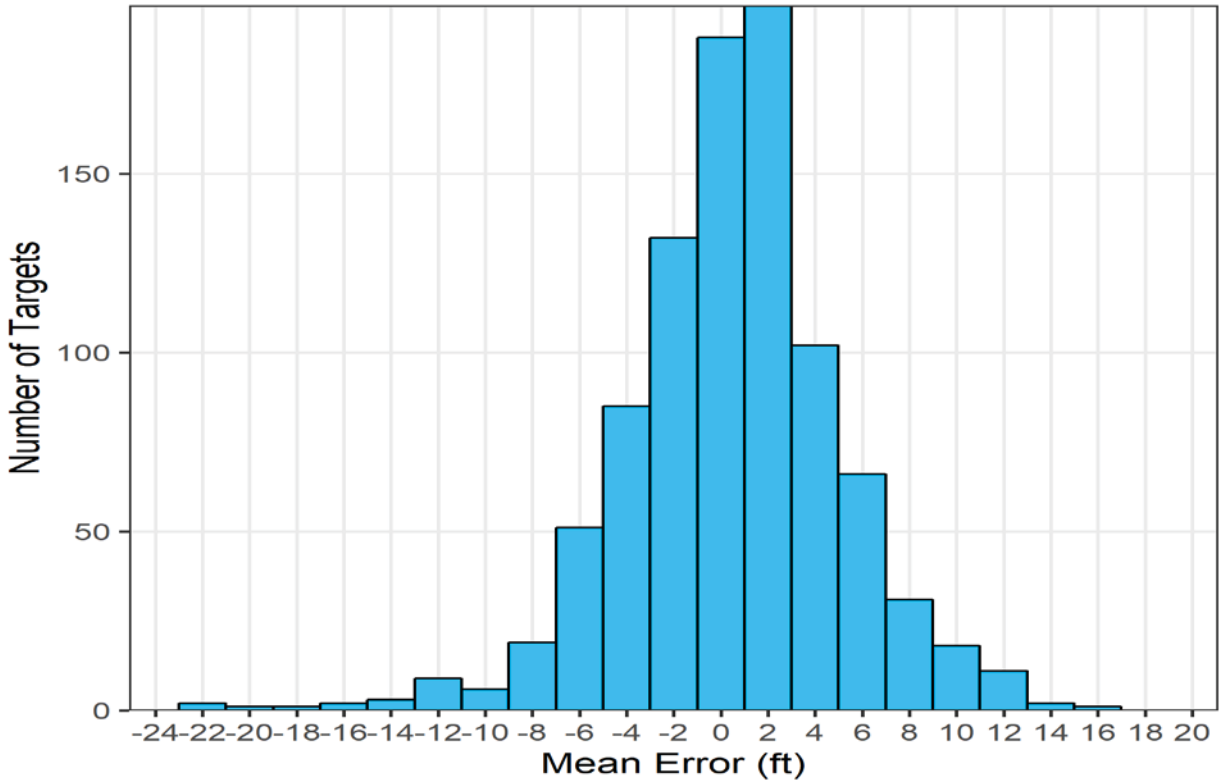
Figure 105. Histogram of simulated versus observed water level differences for the UFA from target wells within the entire ECFTX transient model domain.
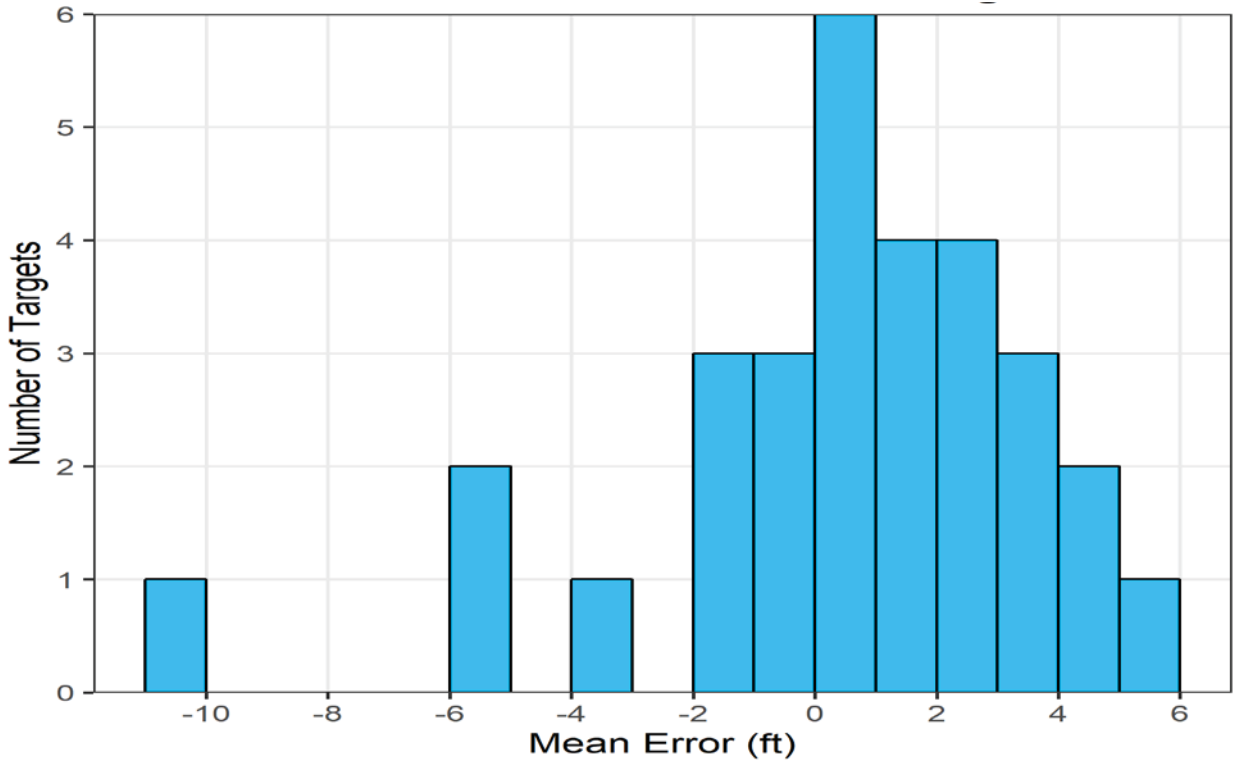
Figure 106. Histogram of simulated versus observed water level differences for the LFA from target wells within the entire ECFTX transient model domain.
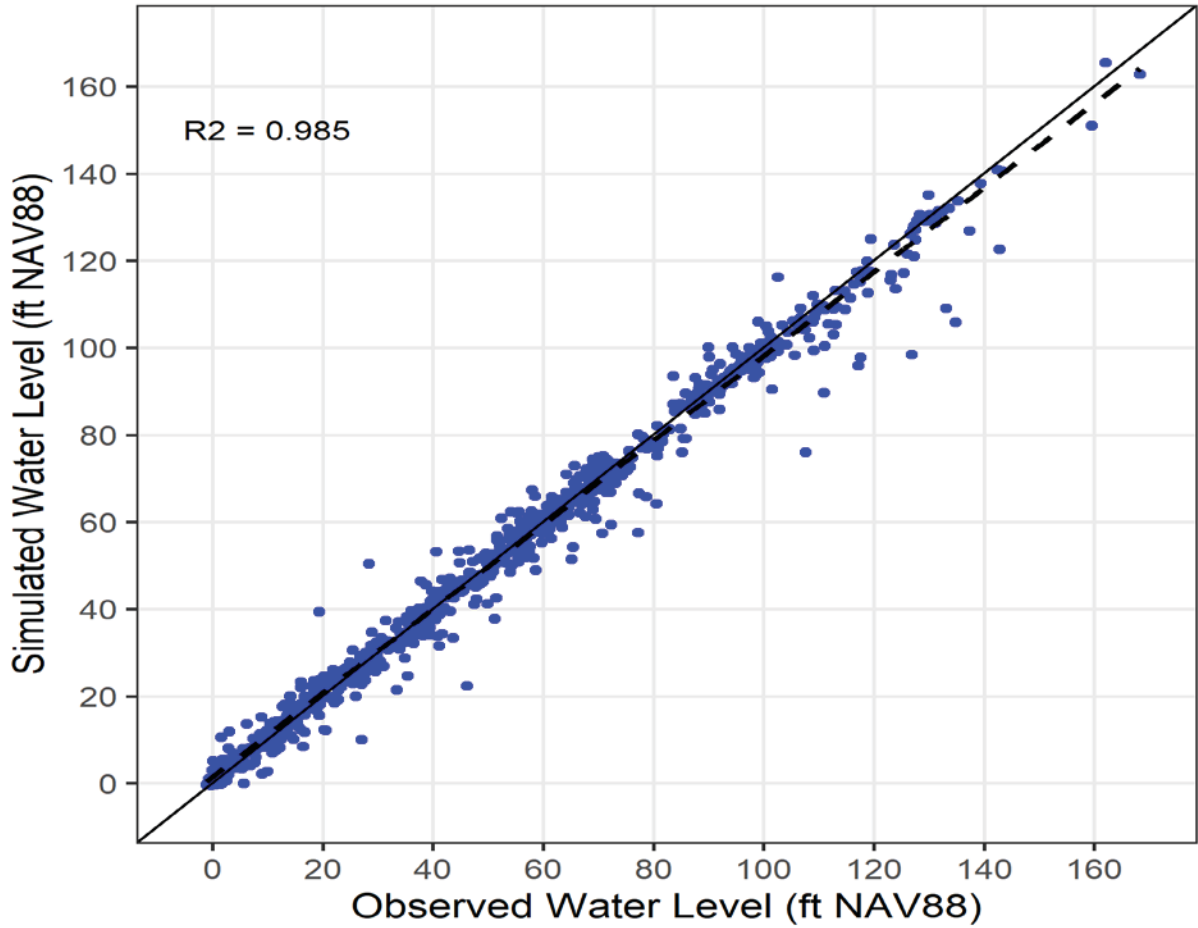
Figure 107. Mean simulated versus observed water levels for the SA within the ECFTX transient model domain. (Note: Solid line is 1:1 relation between simulated and observed water levels; dashed line is linear regression of simulated versus observed water levels from target wells).
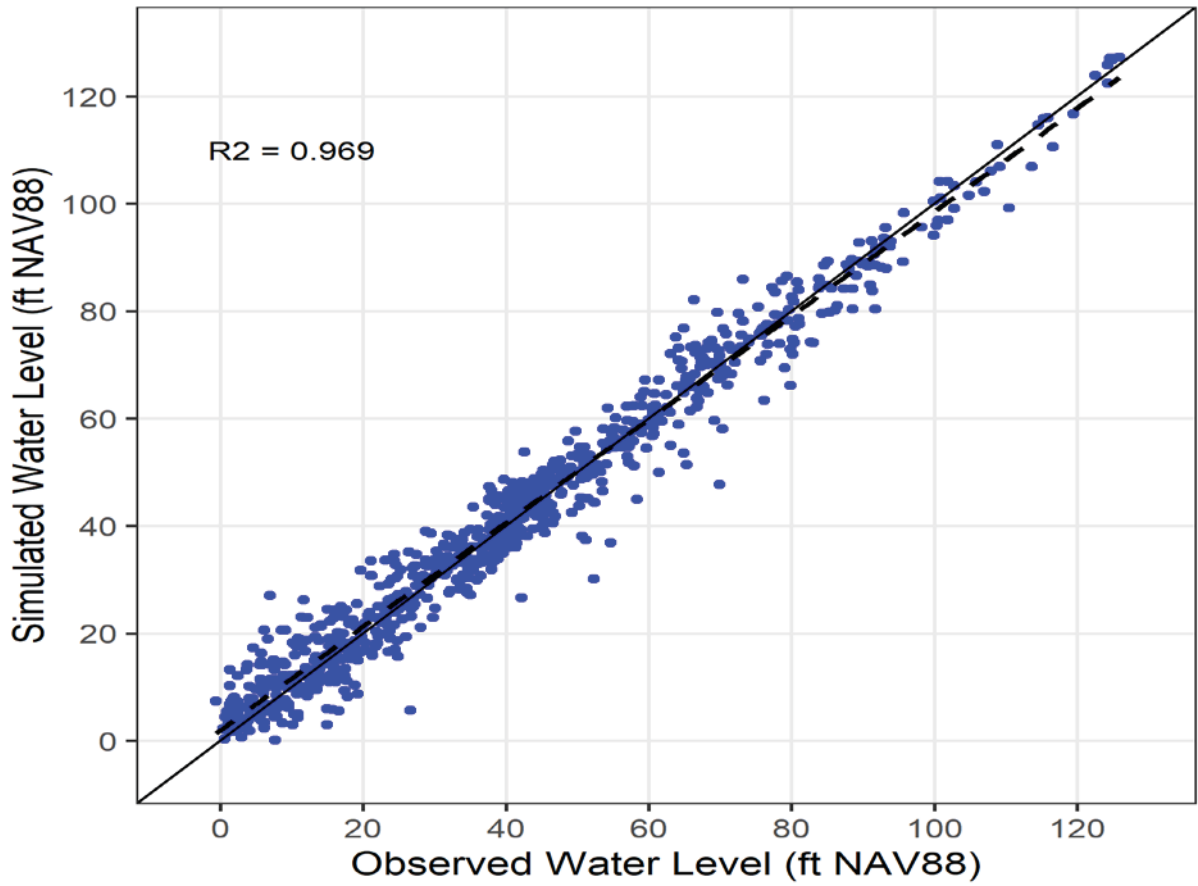
Figure 108. Mean simulated versus observed water levels for the UFA within the ECFTX transient model domain. (Note: solid line is 1:1 relation between simulated and observed water levels; dashed line is linear regression of simulated versus observed water levels from target wells).
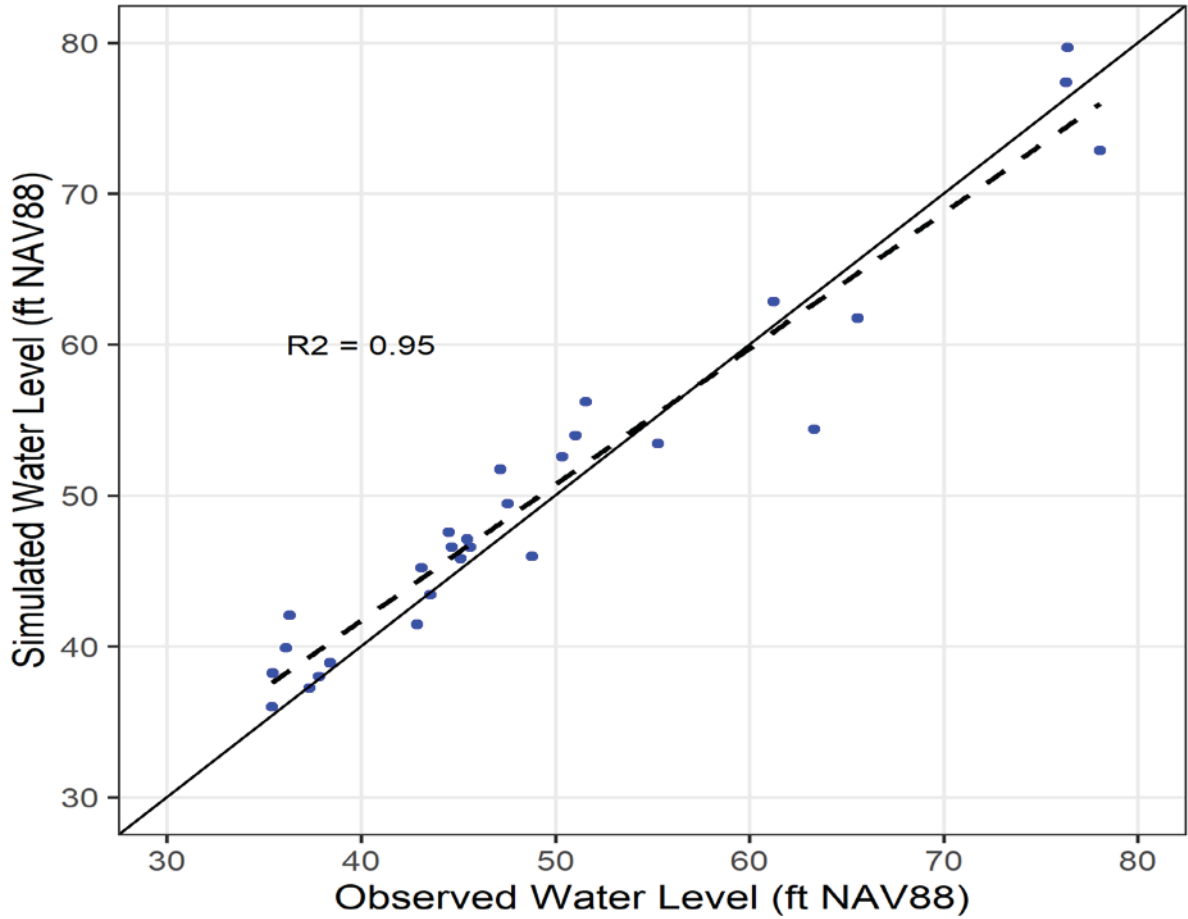
Figure 109. Mean simulated versus observed water levels for the LFA within the ECFTX transient model domain. (Note: solid line is 1:1 relation between simulated and observed water levels; dashed line is linear regression of simulated versus observed water levels from target wells).
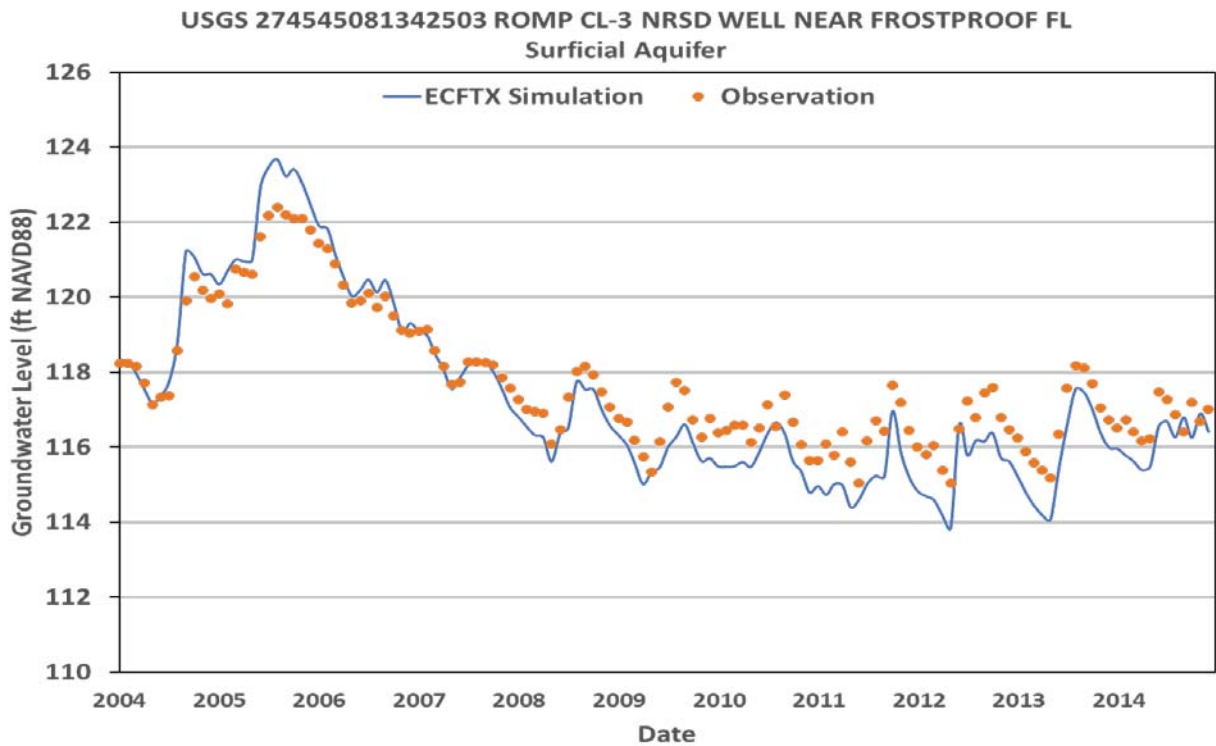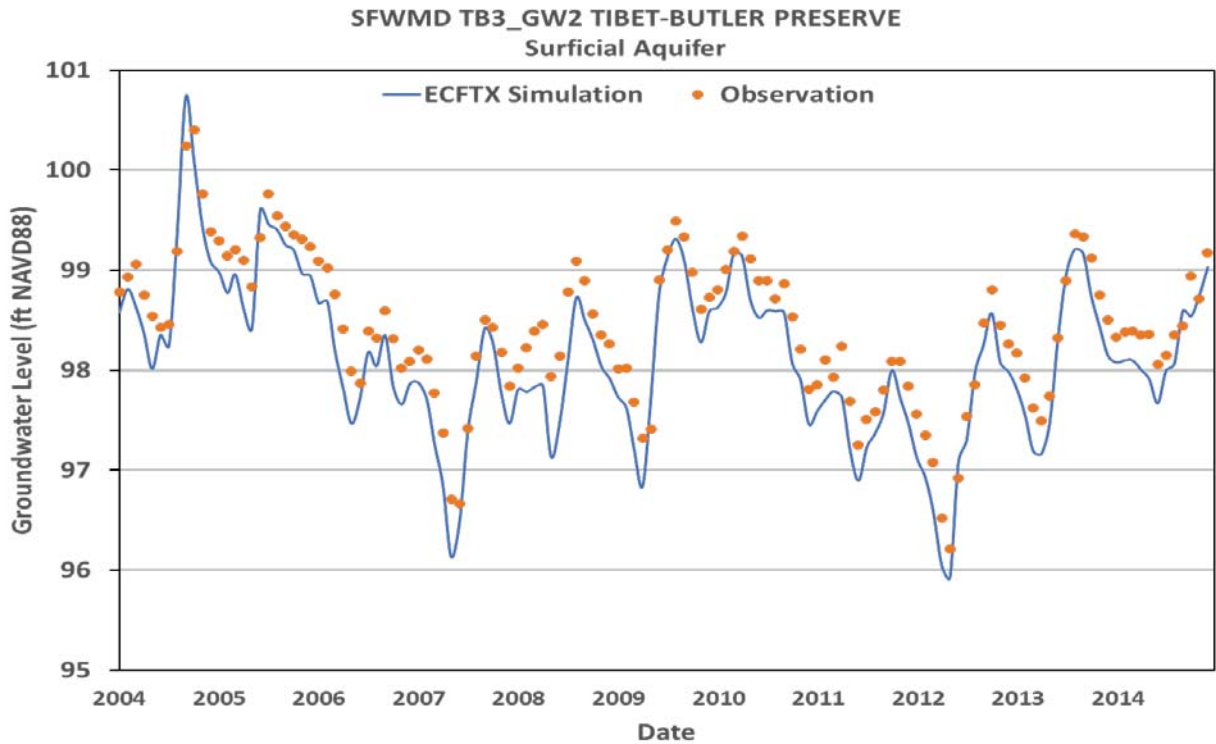
Figure 110. Simulated versus observed water levels for the SA at monitor wells TB3_GW2 Tibet-Butler Preserve and Romp CL-3 within the CFWI area of the ECFTX model.
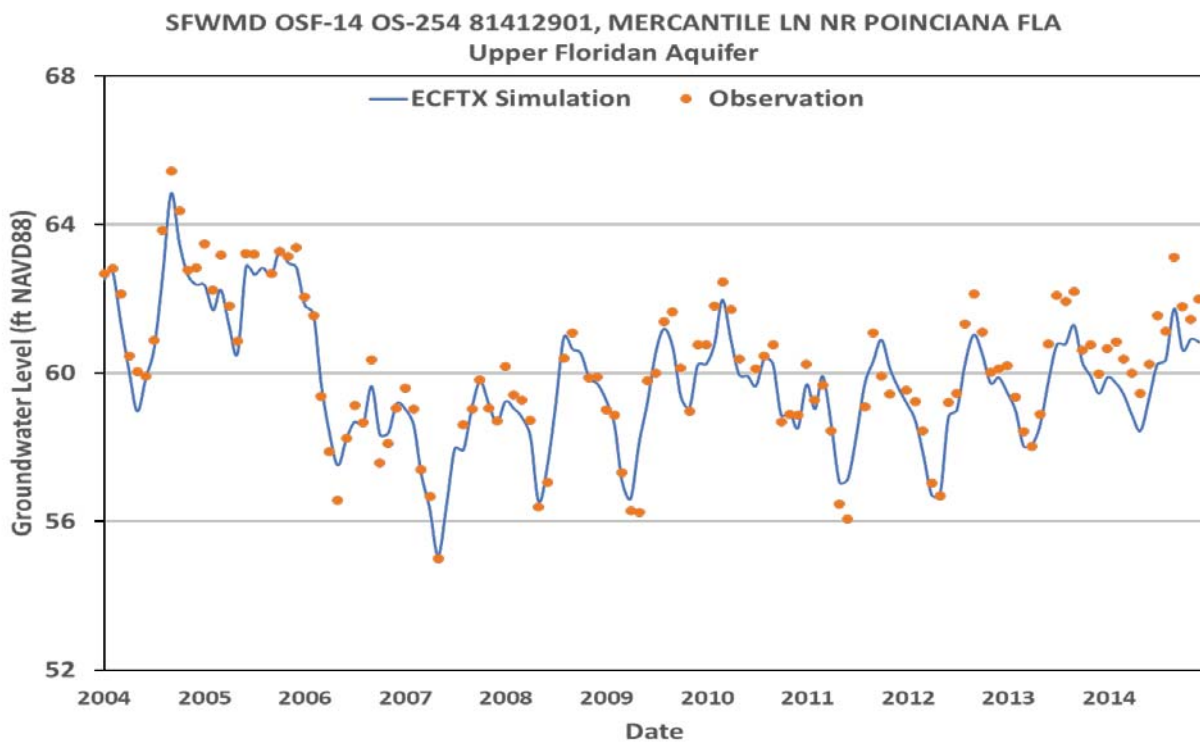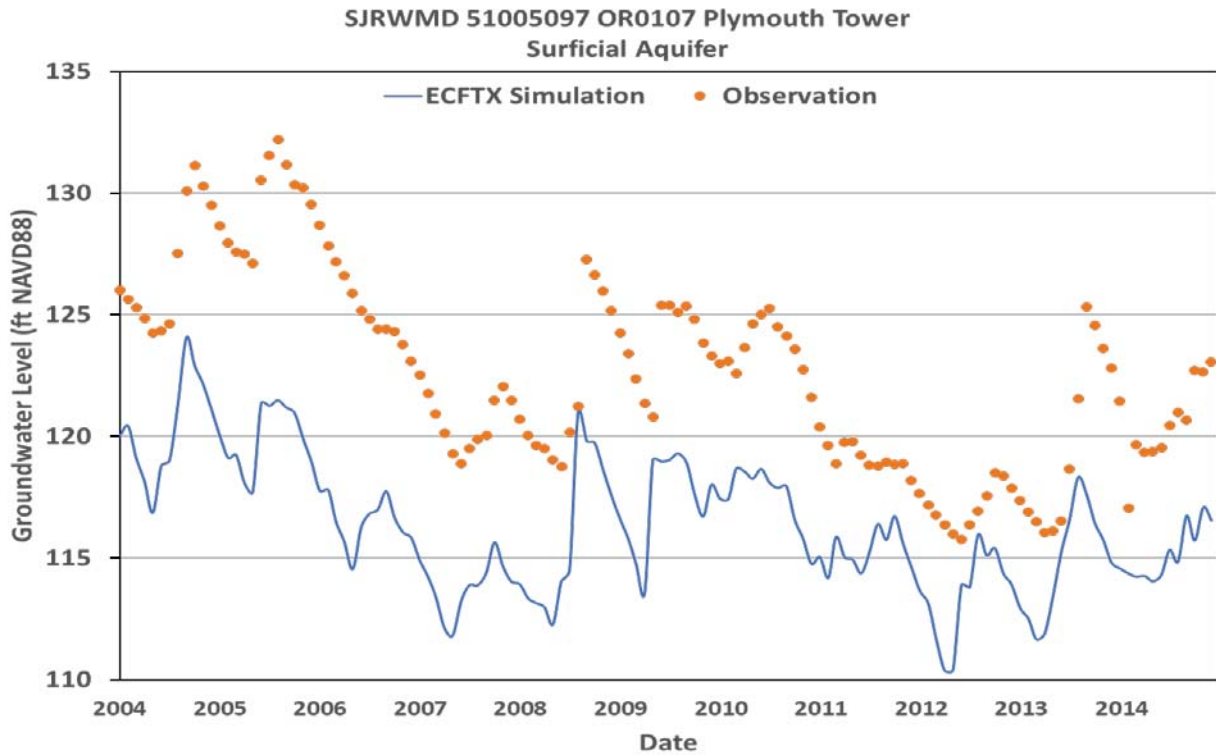
Figure 111. Simulated versus observed water levels for the SA at monitor well Plymouth Tower and the UFA monitor well OSF-14 within the CFWI area of the ECFTX model.

Figure 112. Simulated versus observed water levels for the UFA at monitor wells Romp 88 and L-0877 Hilochee within the CFWI area of the ECFTX model.
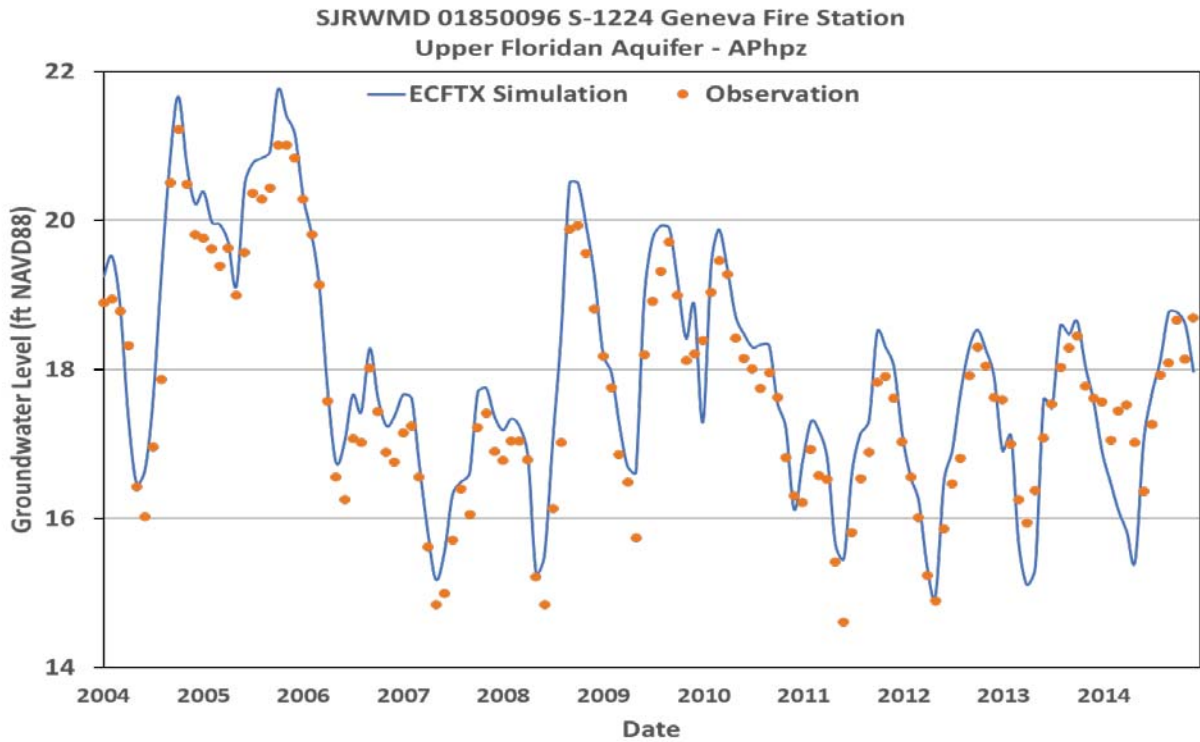
Figure 113. Simulated versus observed water levels for the UFA at monitor well S-1224 Geneva Fire Station and OR-47 within the CFWI area of the ECFTX model.
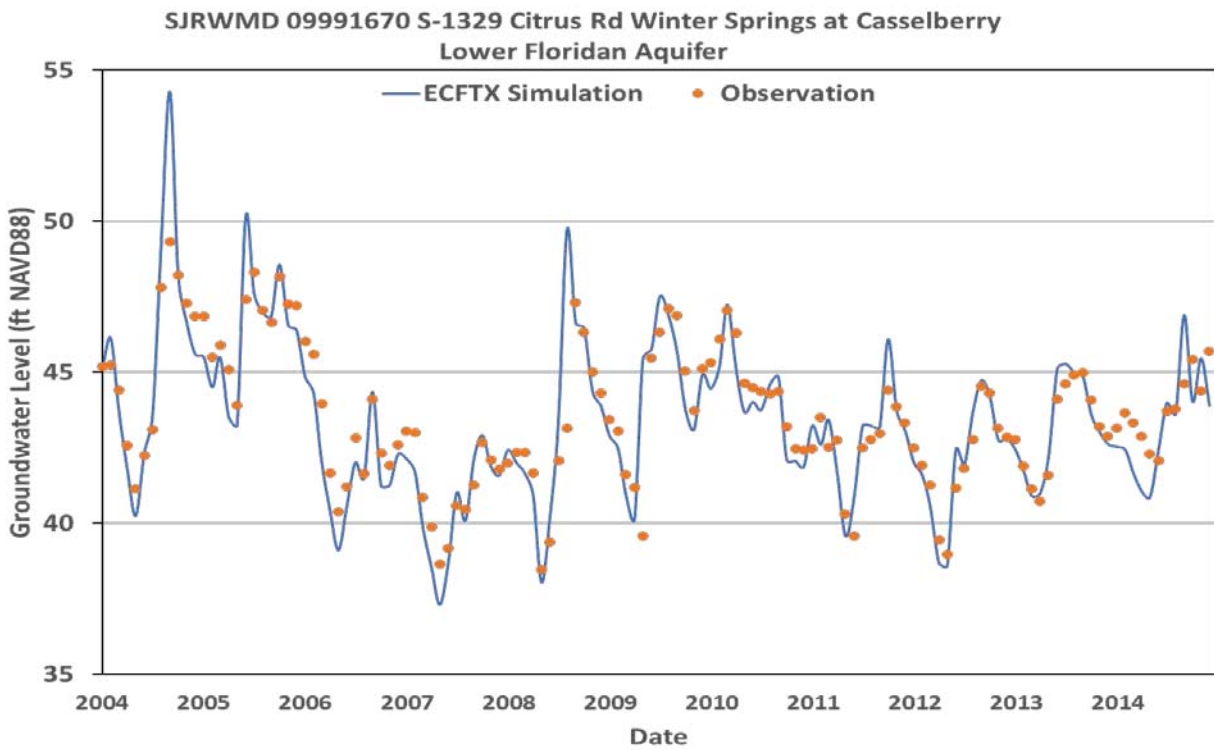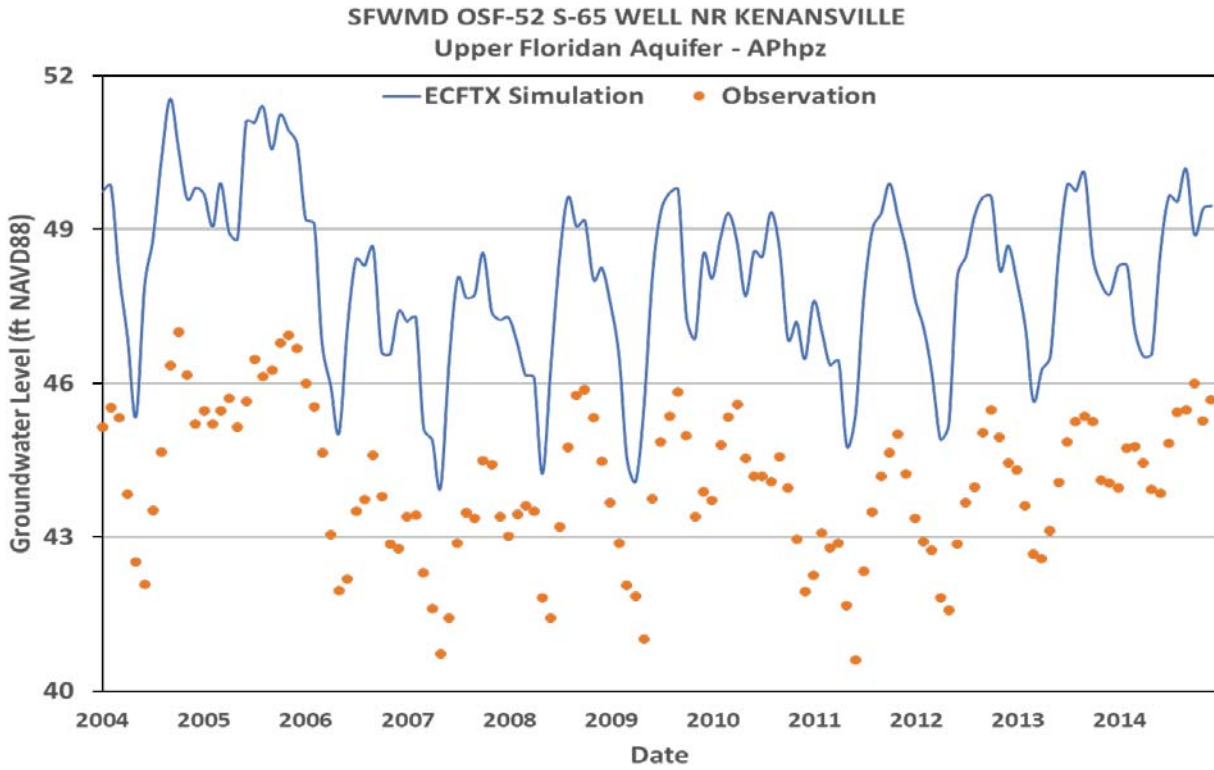
Figure 114. Simulated versus observed water levels for the UFA at monitor well OSF-52 and LFA monitor well S-1329 within the CFWI area of the ECFTX model.
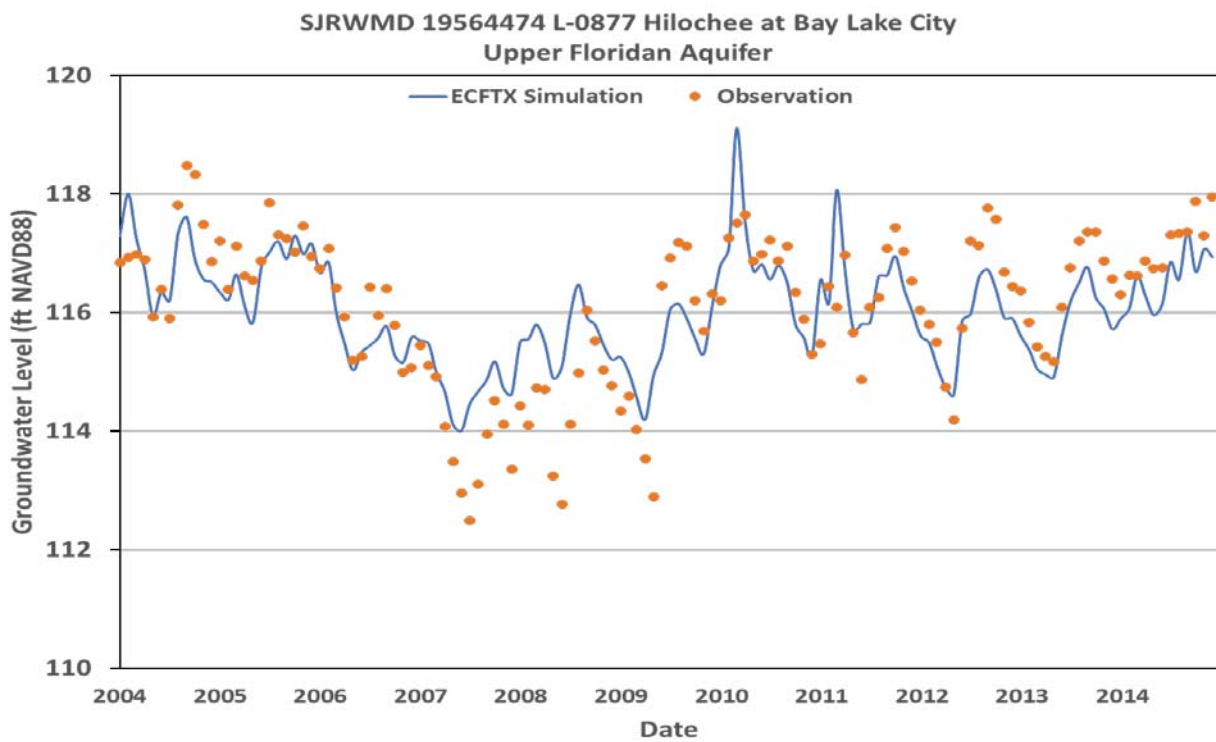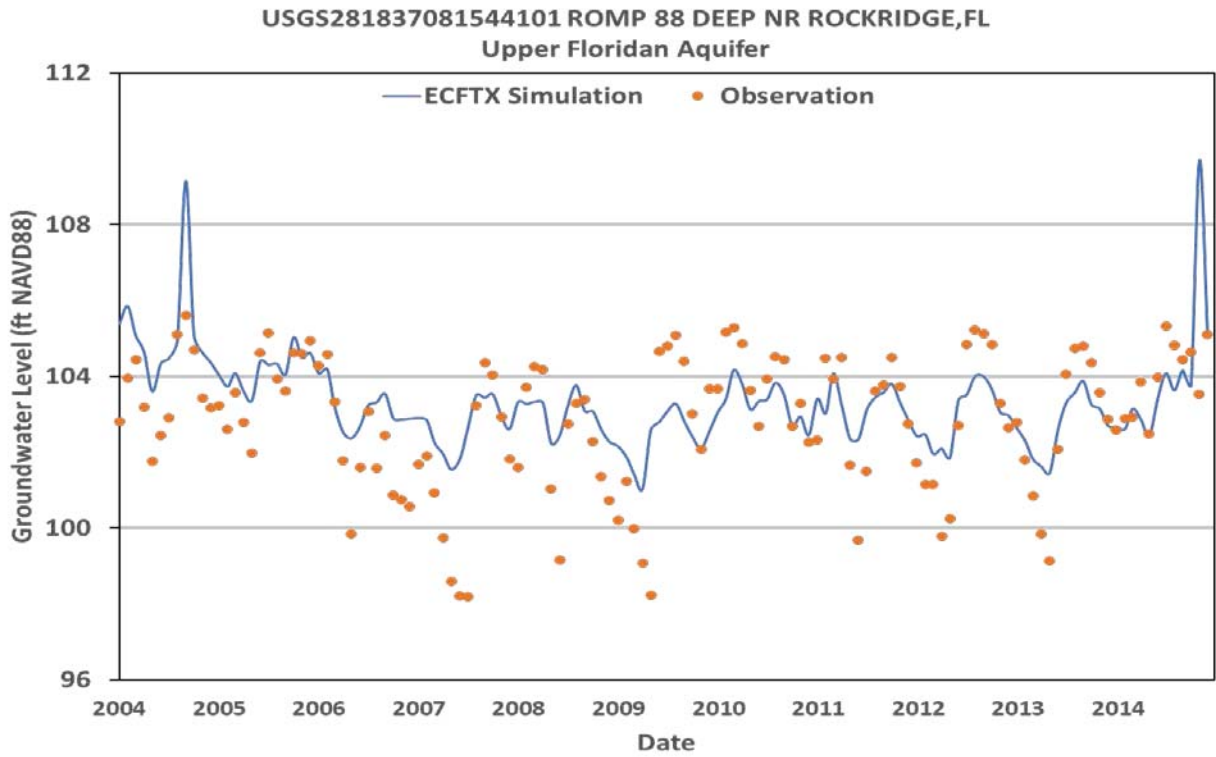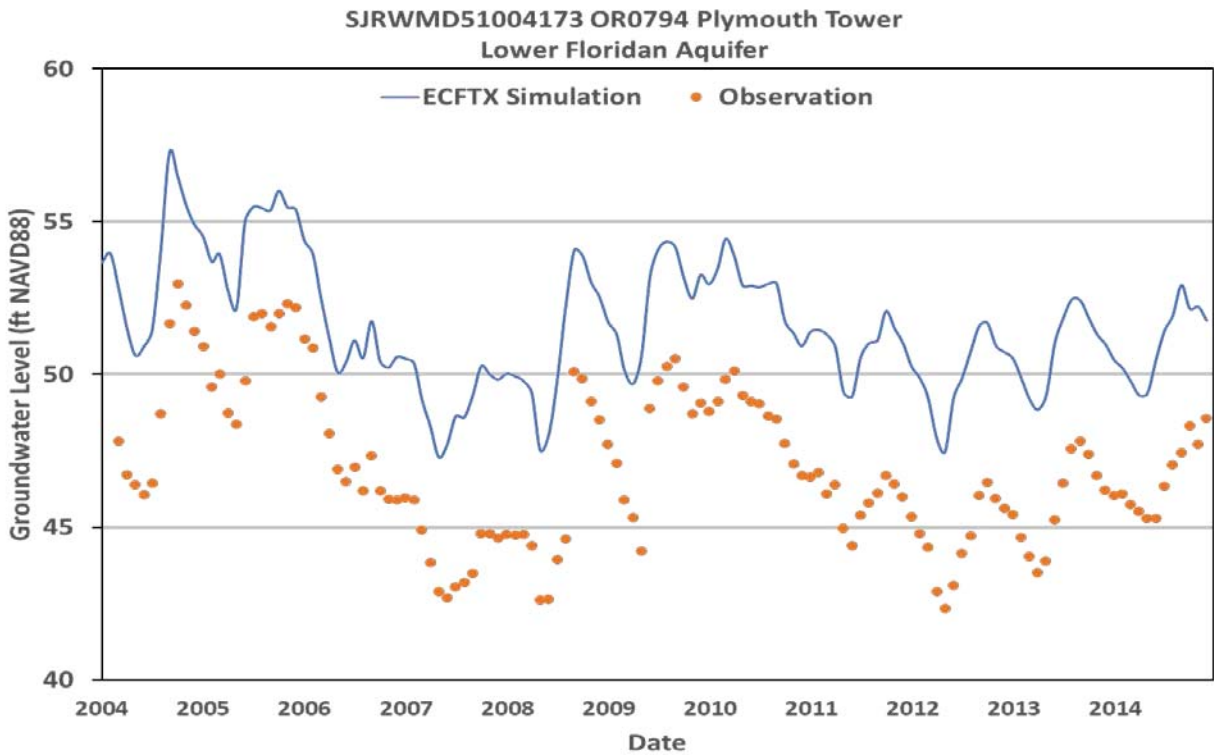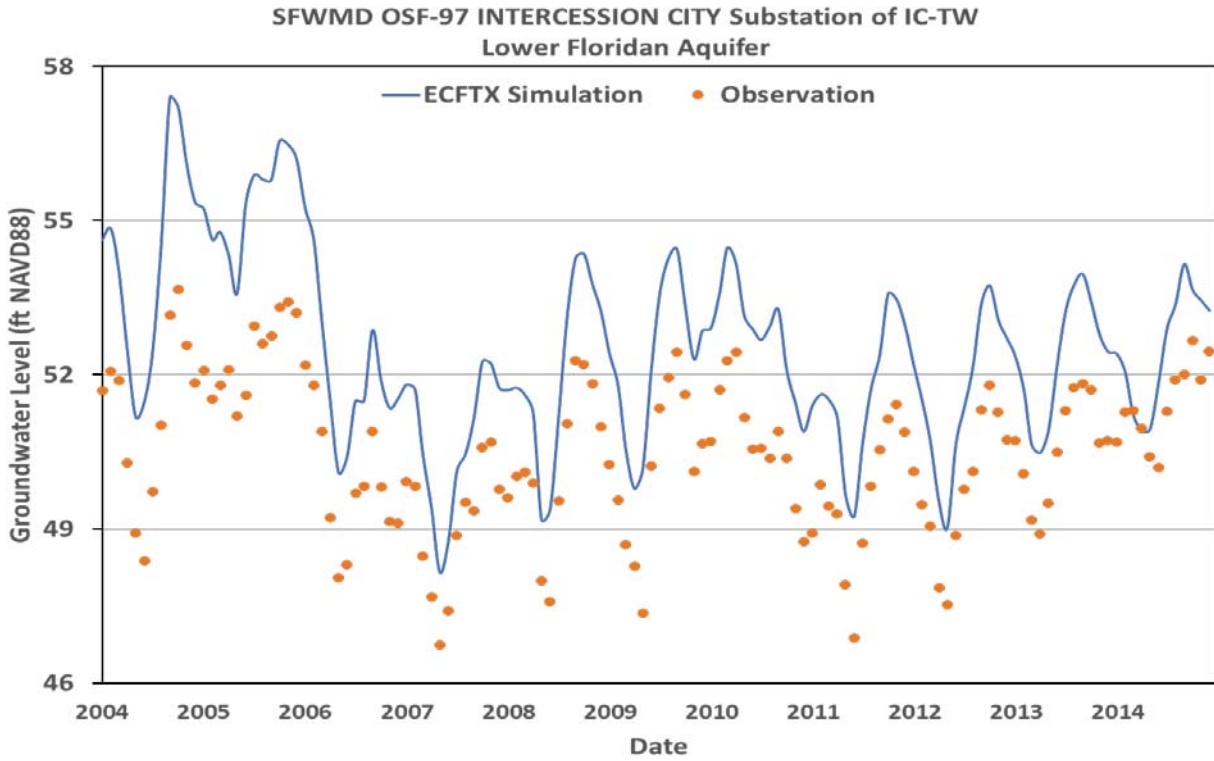
Figure 115. Simulated versus observed water levels for the LFA at monitor wells OSF-97 and ORD794 Plymouth Tower within the CFWI area of the ECFTX model.
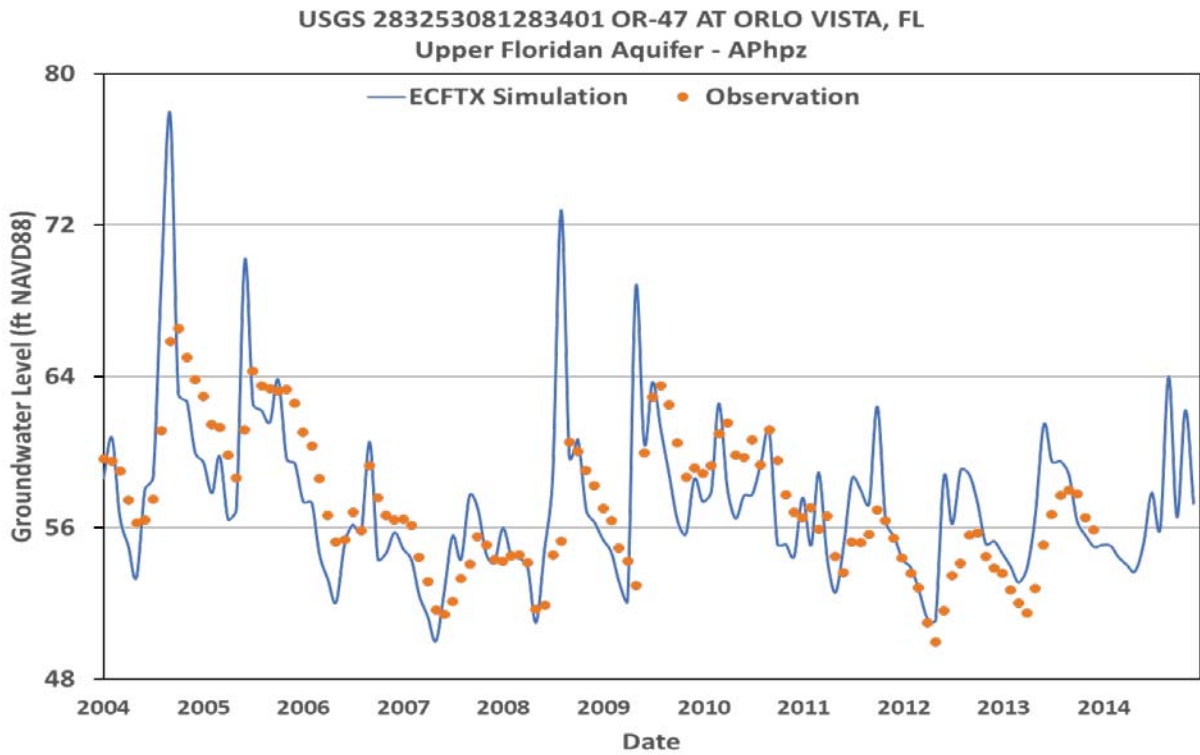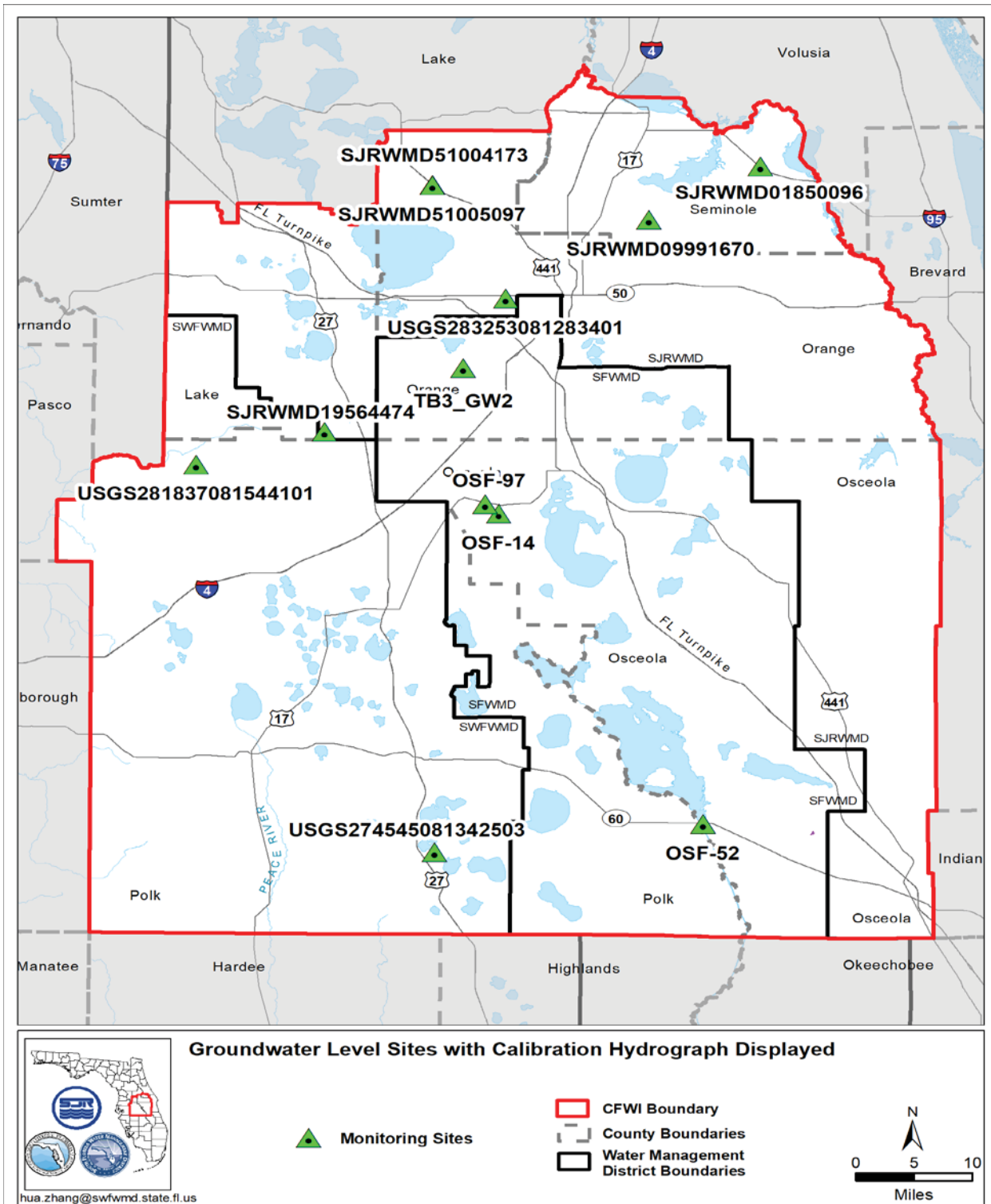
Figure 116. Location of hydrographs of selected simulated versus observed water levels for the SA, UFA, and LFA within the CFWI area of the ECFTX model.
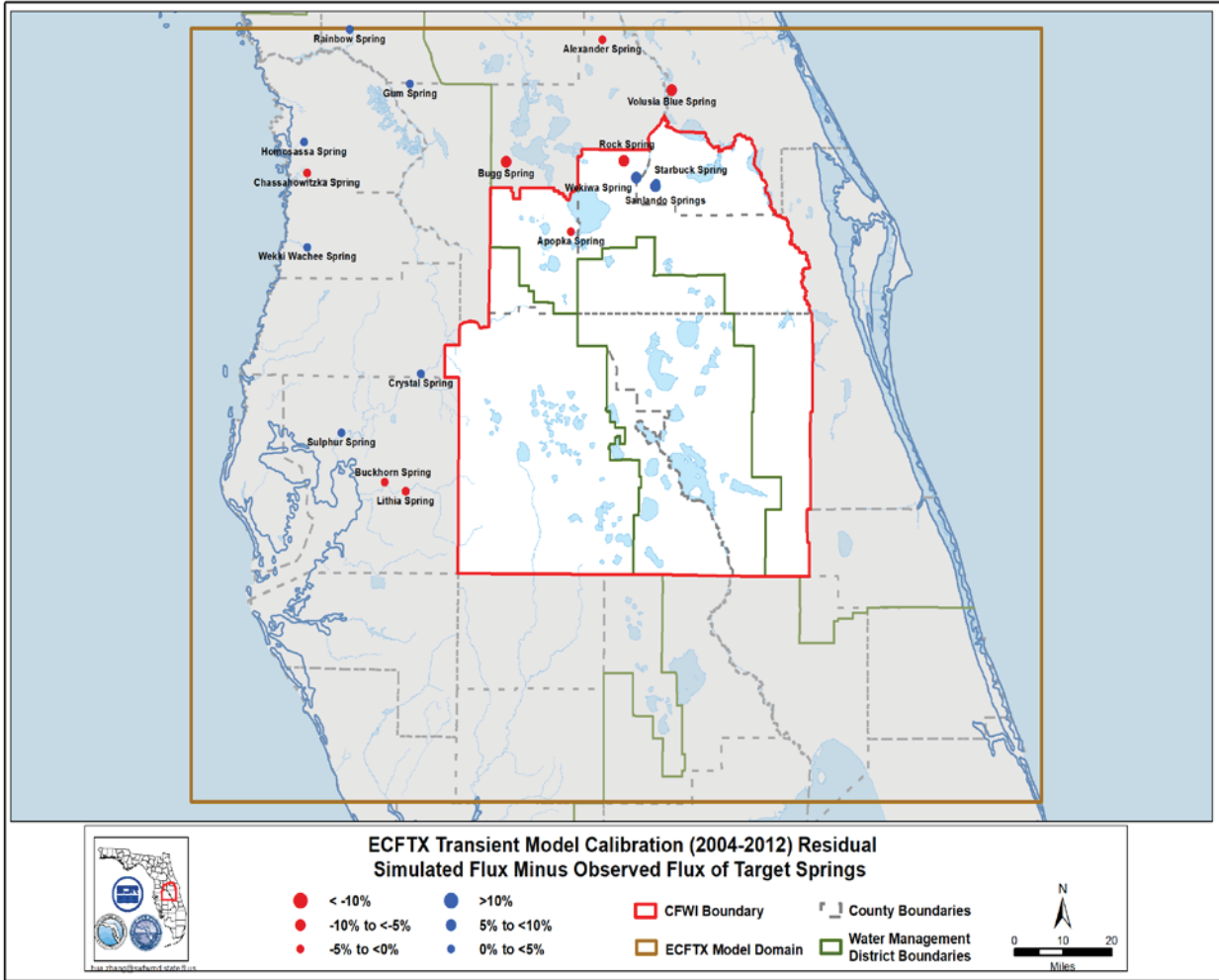
Figure 117. Spatial distribution of mean error for 17 magnitude 1 and 2 springs within the ECFTX model during calibration period. Mean simulated versus observed springflow from 2004-2012; blue indicates simulated flows higher than observed, red indicates simulated flows lower than observed.
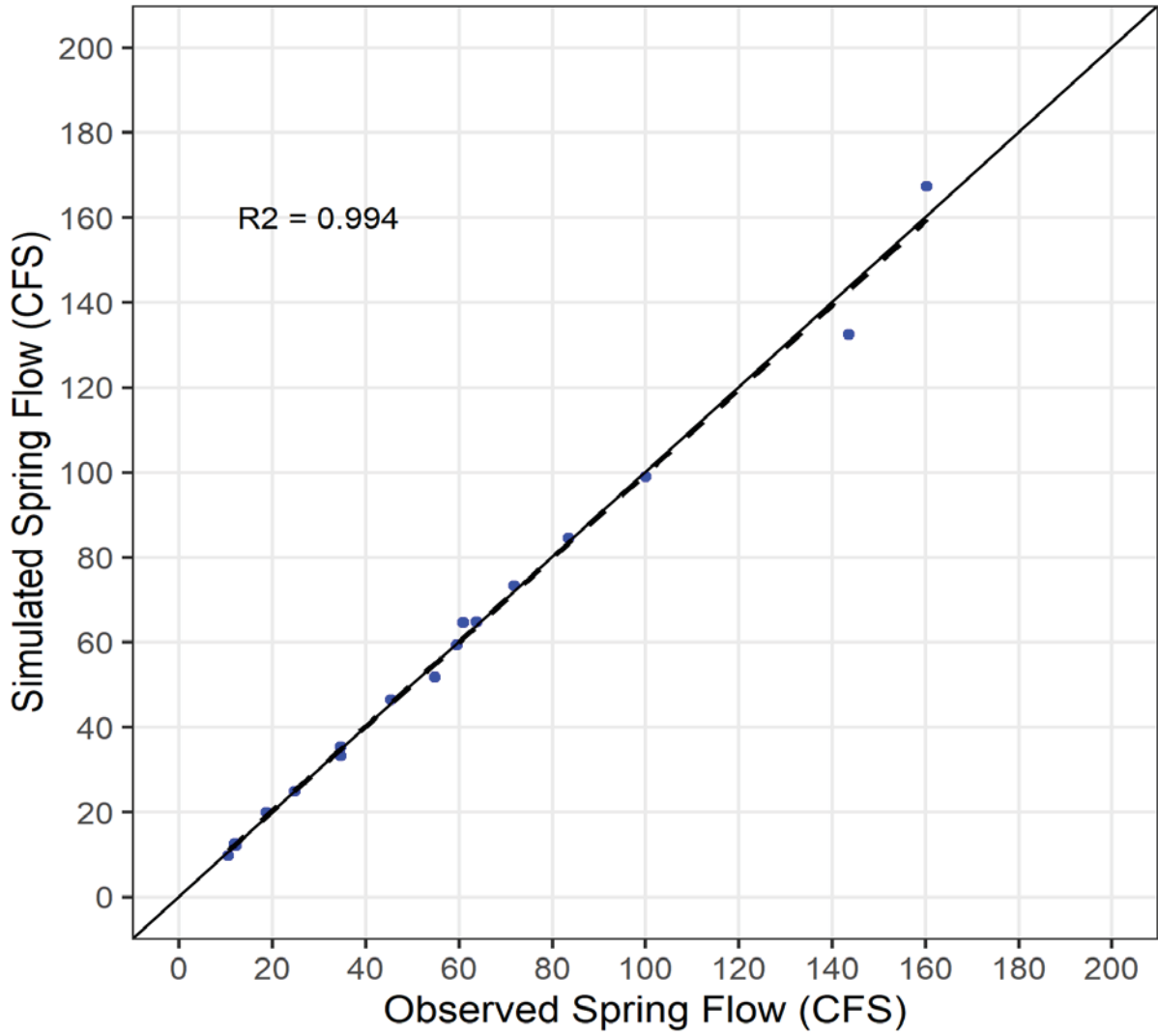
Figure 118. Mean simulated versus observed flow for all measured magnitude 1 and 2 springs within the ECFTX transient model domain. (Note: solid line is 1:1 relation between simulated and observed flow; dashed line is linear regression of simulated versus observed flow from 17 springs with measured flow).
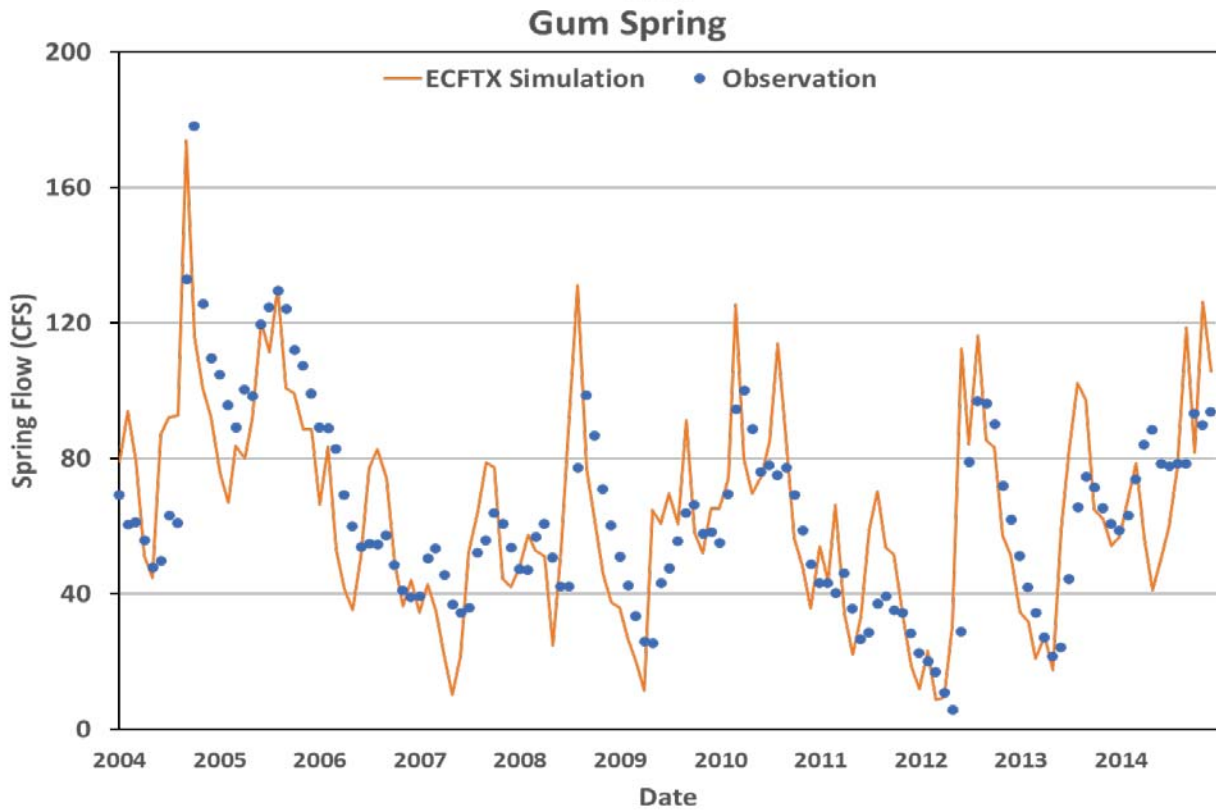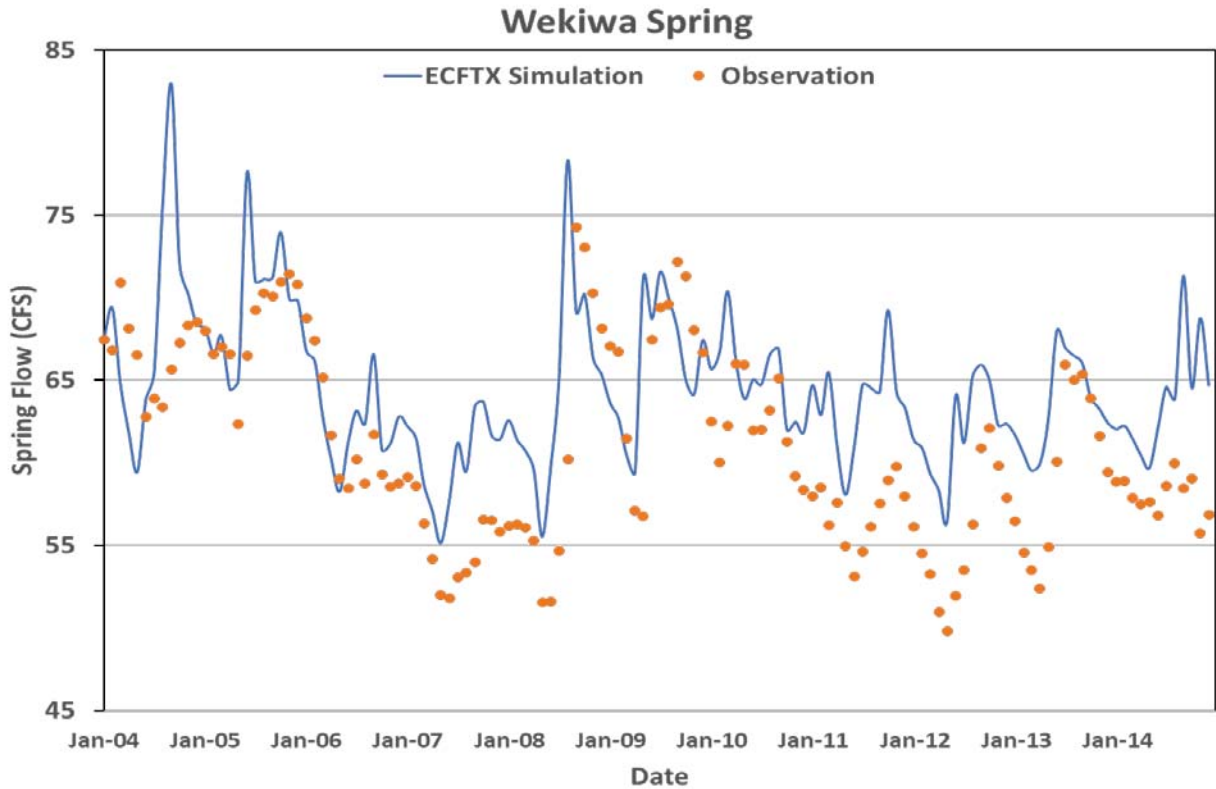
Figure 119. Simulated versus observed flows at Wekiwa and Gum Springs within the ECFTX model.
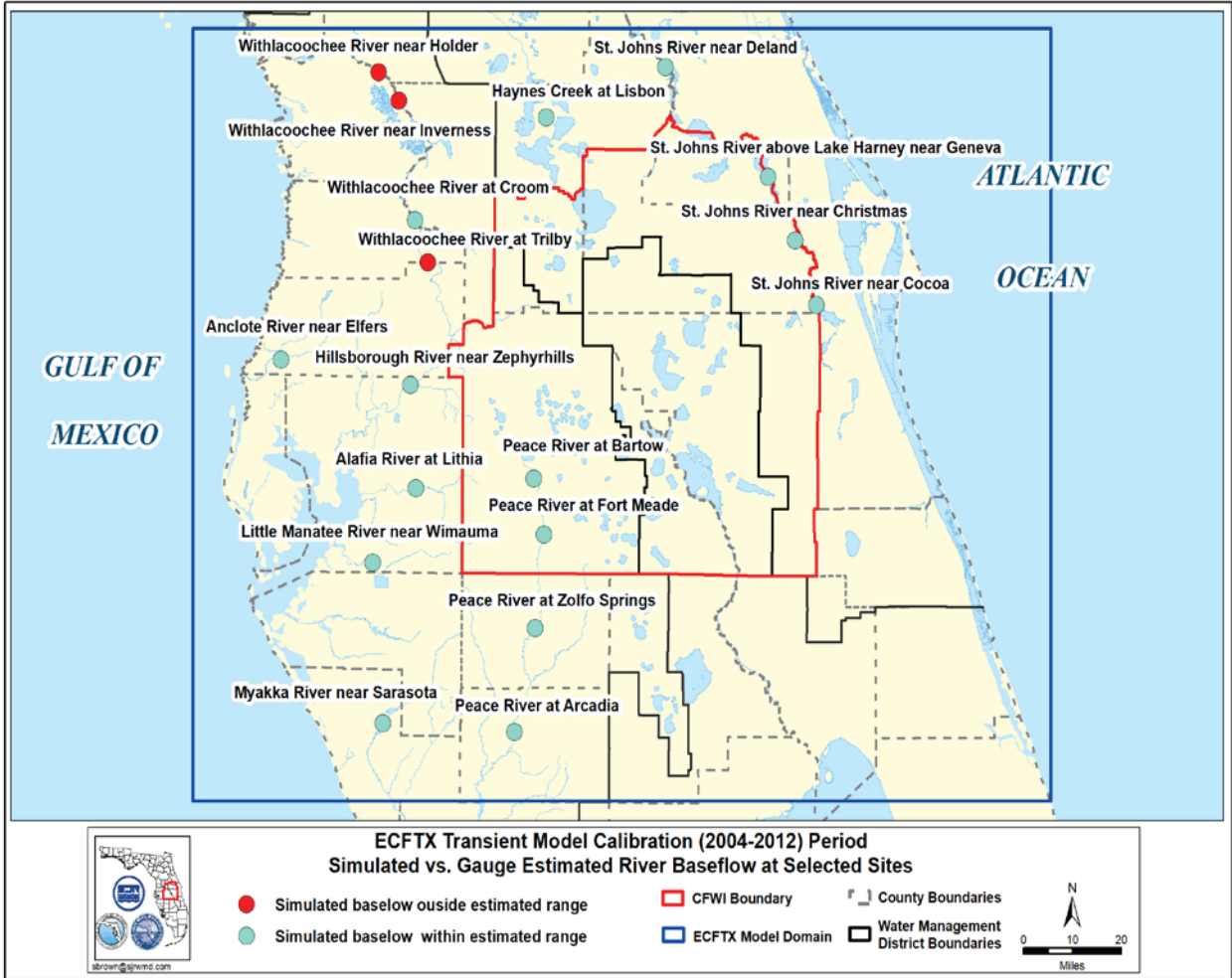
Figure 120. Spatial distribution of the USGS streamflow gages that were within or outside the baseflow estimation ranges within the ECFTX domain for the calibration period.
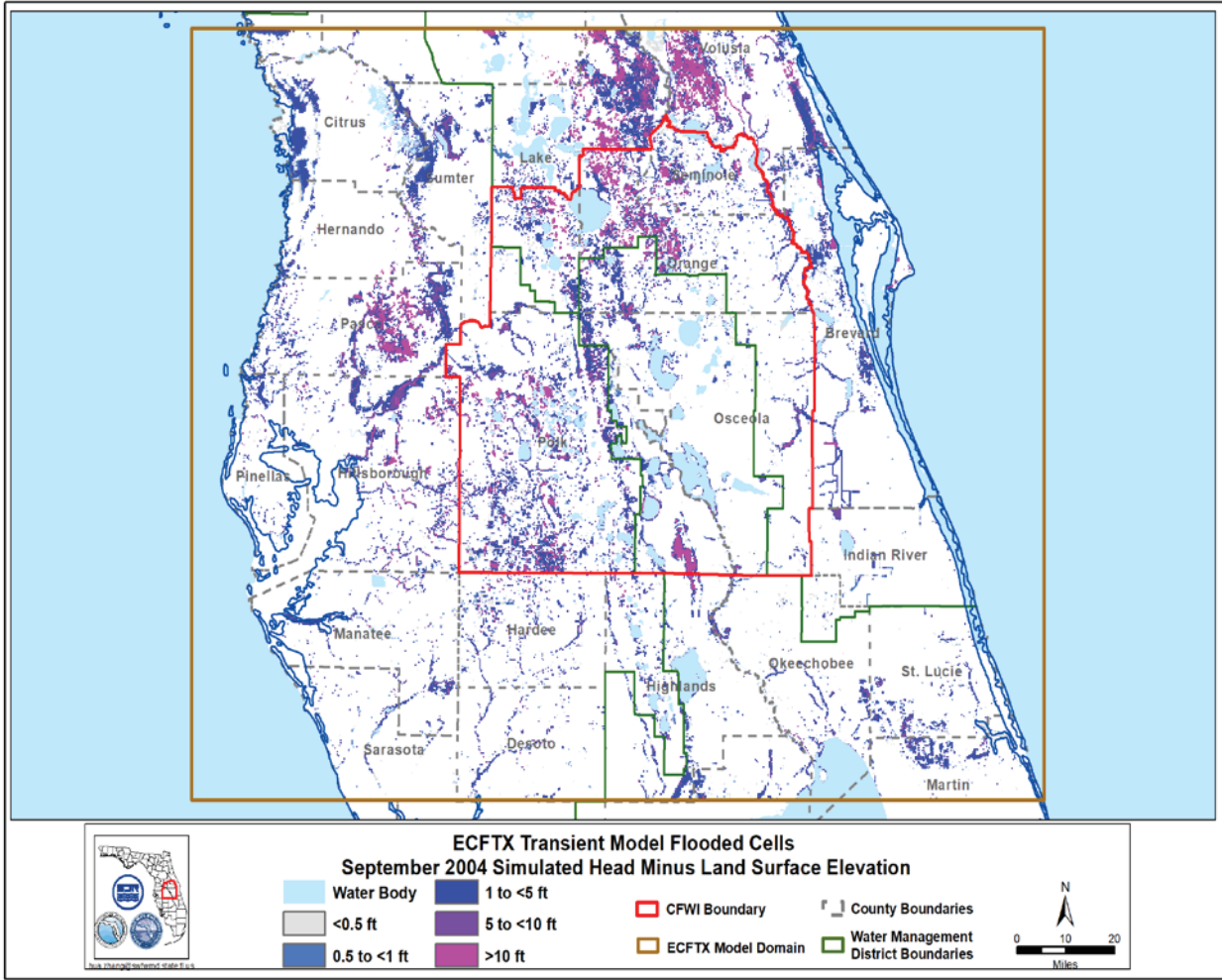
Figure 121. Spatial distribution of the flooded cells in September 2004 within the ECFTX domain.
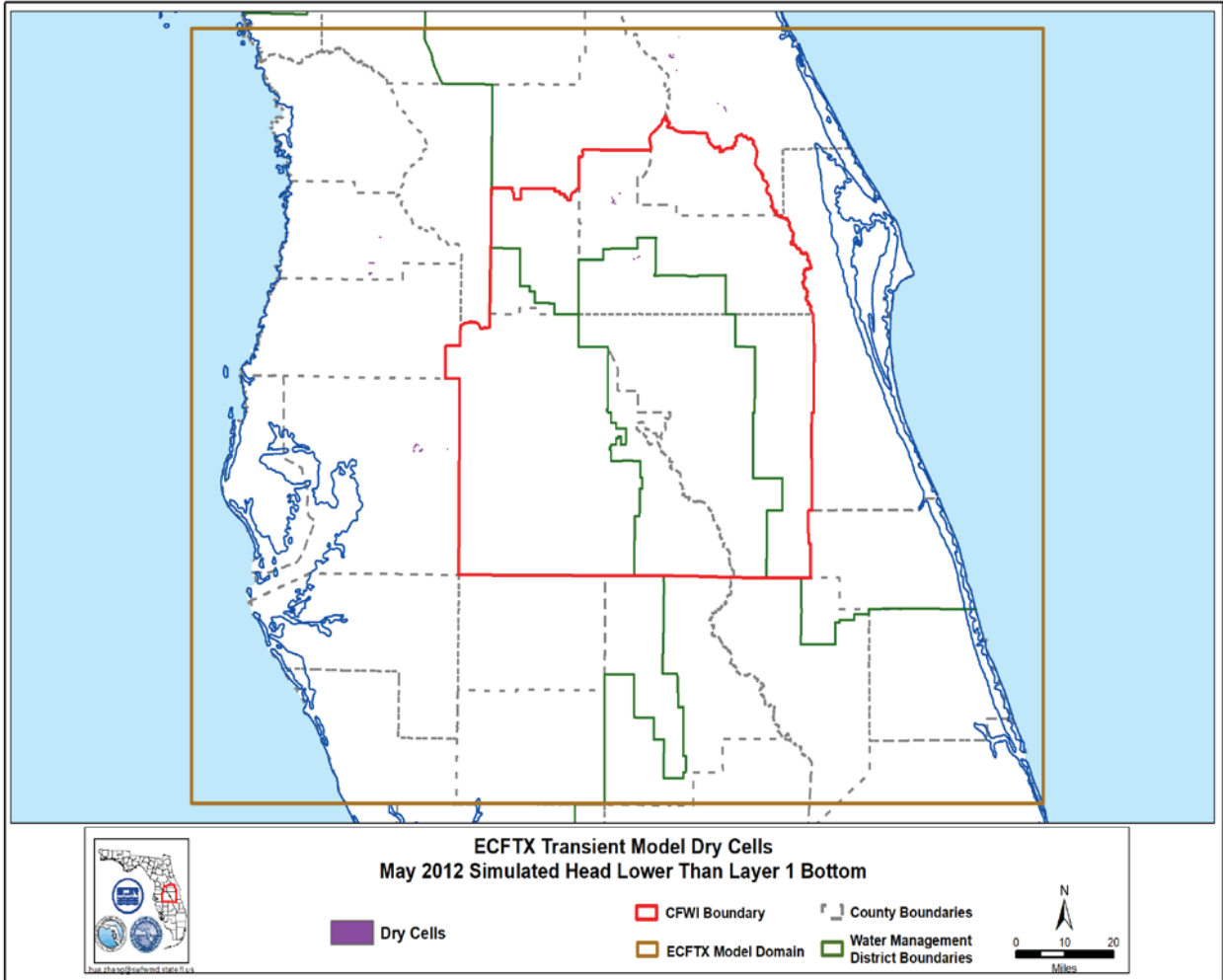
Figure 122. Spatial distribution of the dry cells in May 2012 within the ECFTX domain.
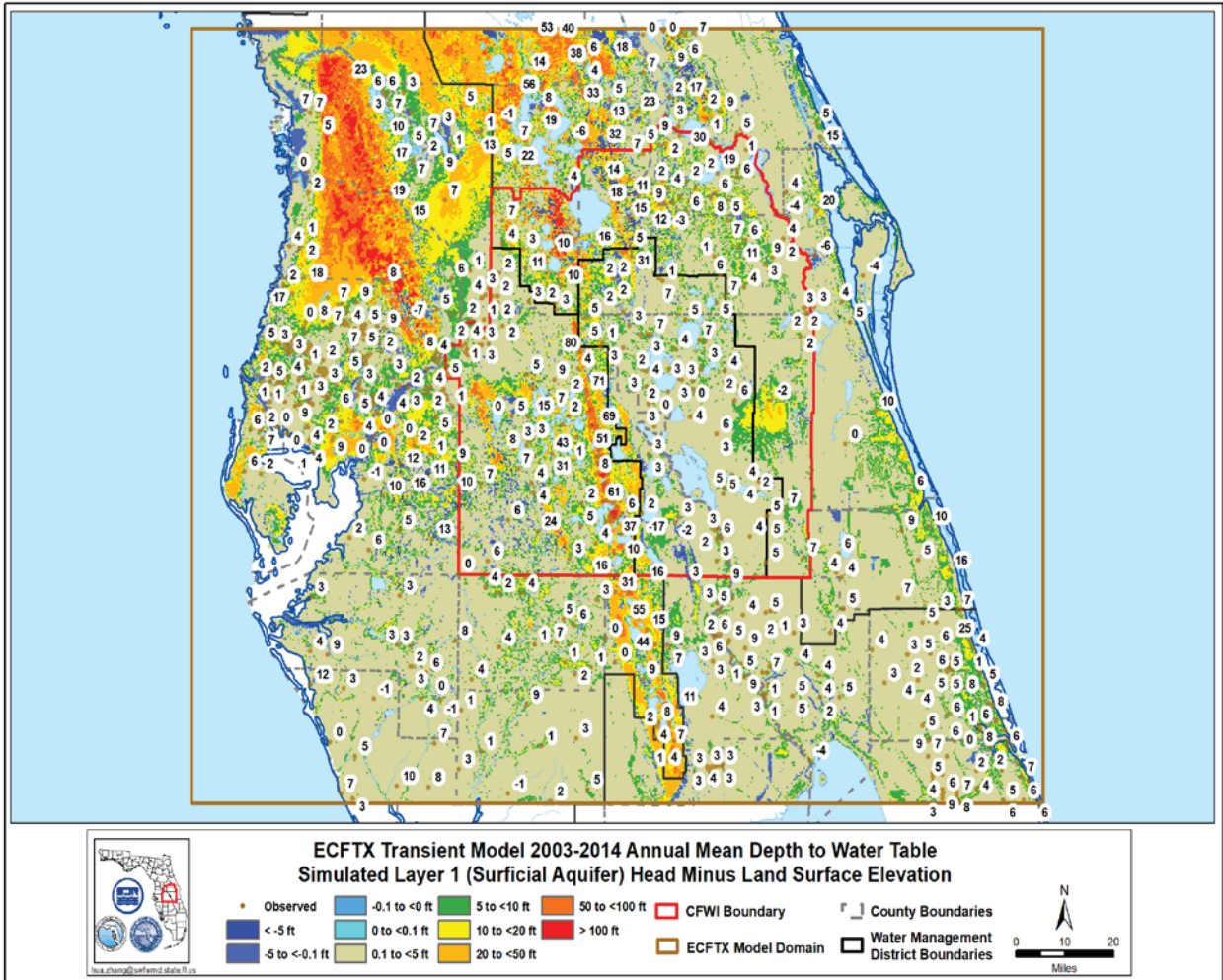
Figure 123. Simulated depth of the water table versus observed water table depth within the ECFTX domain (2003-2014 average).
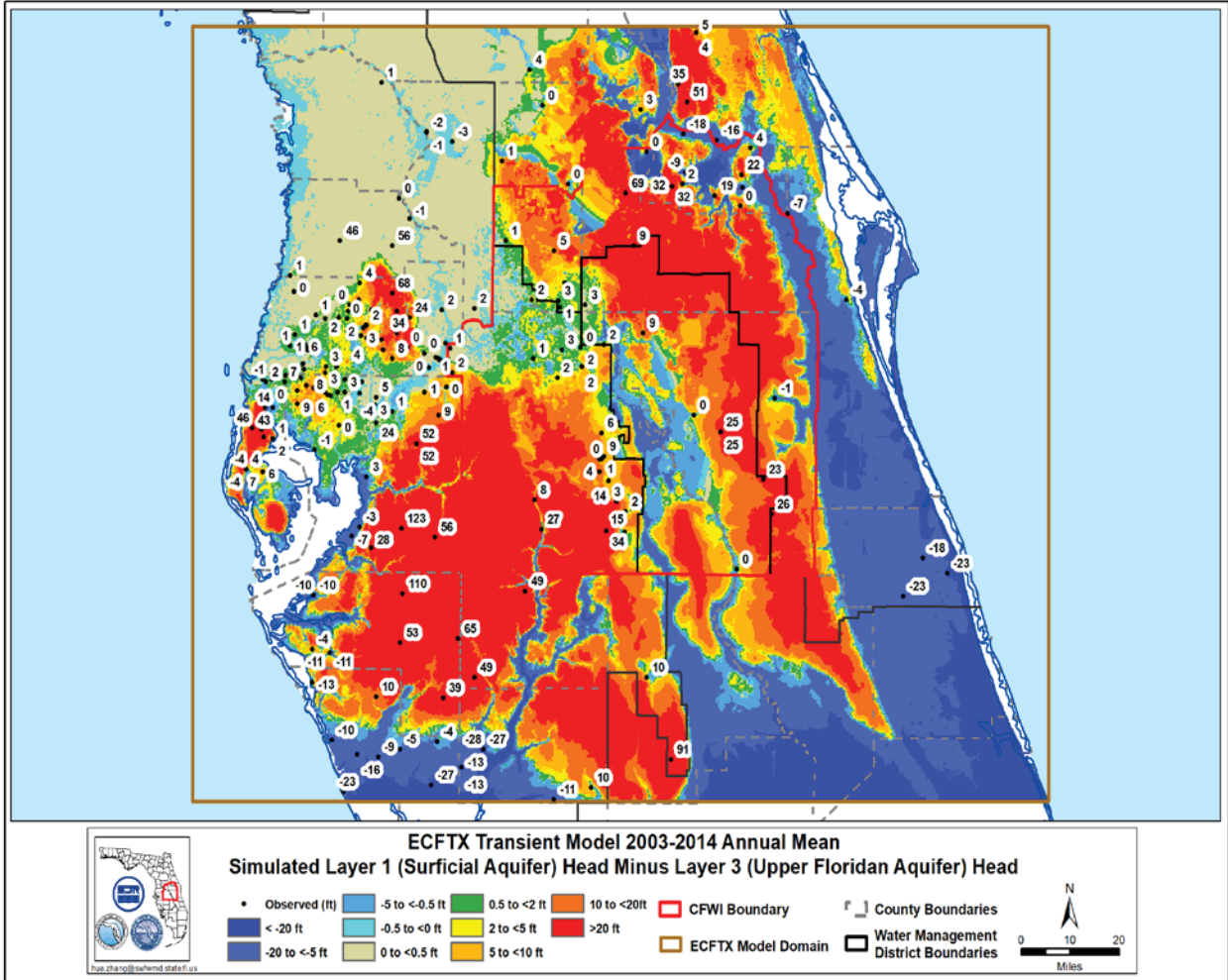
Figure 124. Simulated SA-UFA head difference versus observed long-term SA-UFA head difference within the ECFTX domain (2003-2014 average).
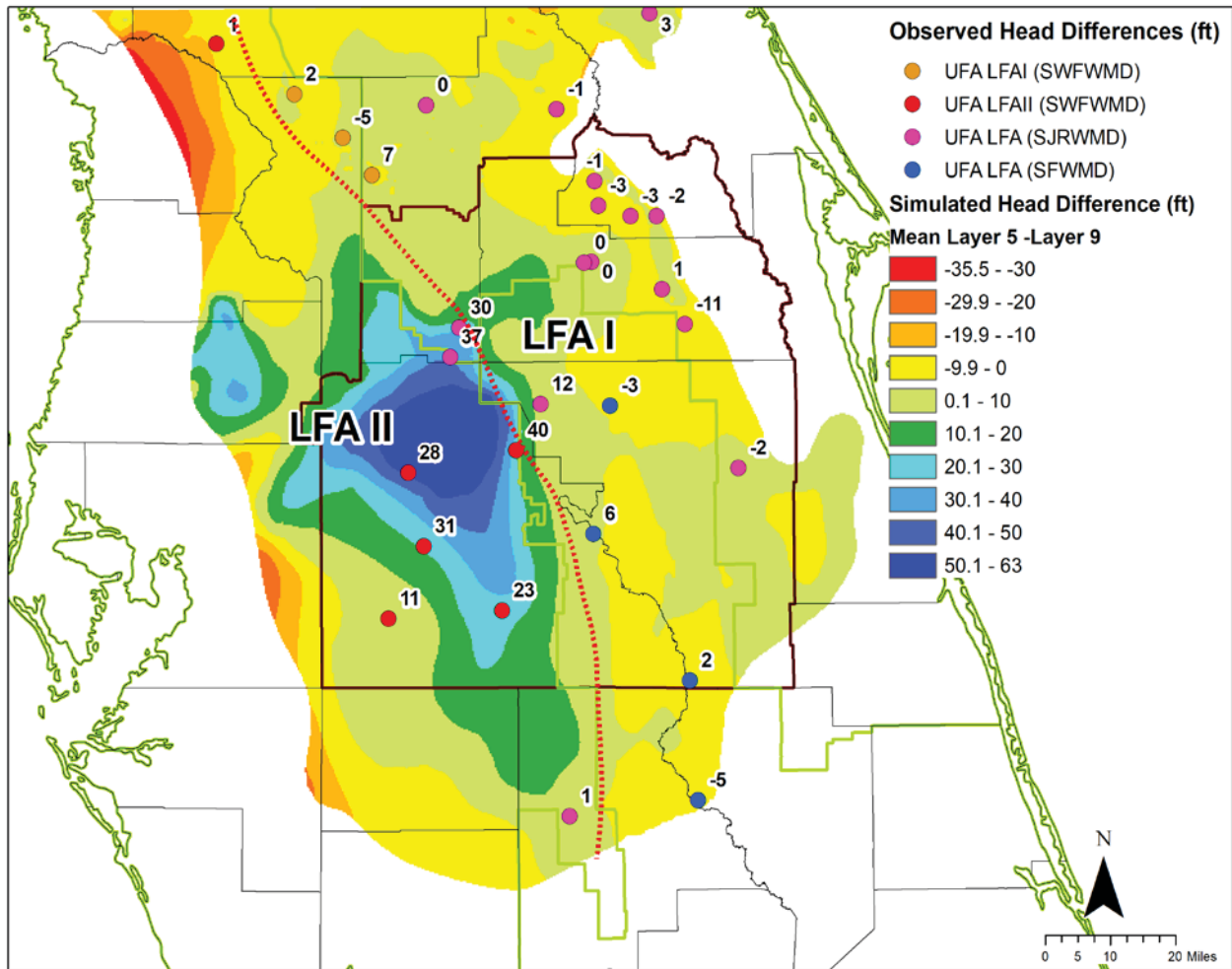
Figure 125. Simulated UFA-LFA head difference versus observed long-term UFA-LFA head difference within the ECFTX domain (2003-2014 average).
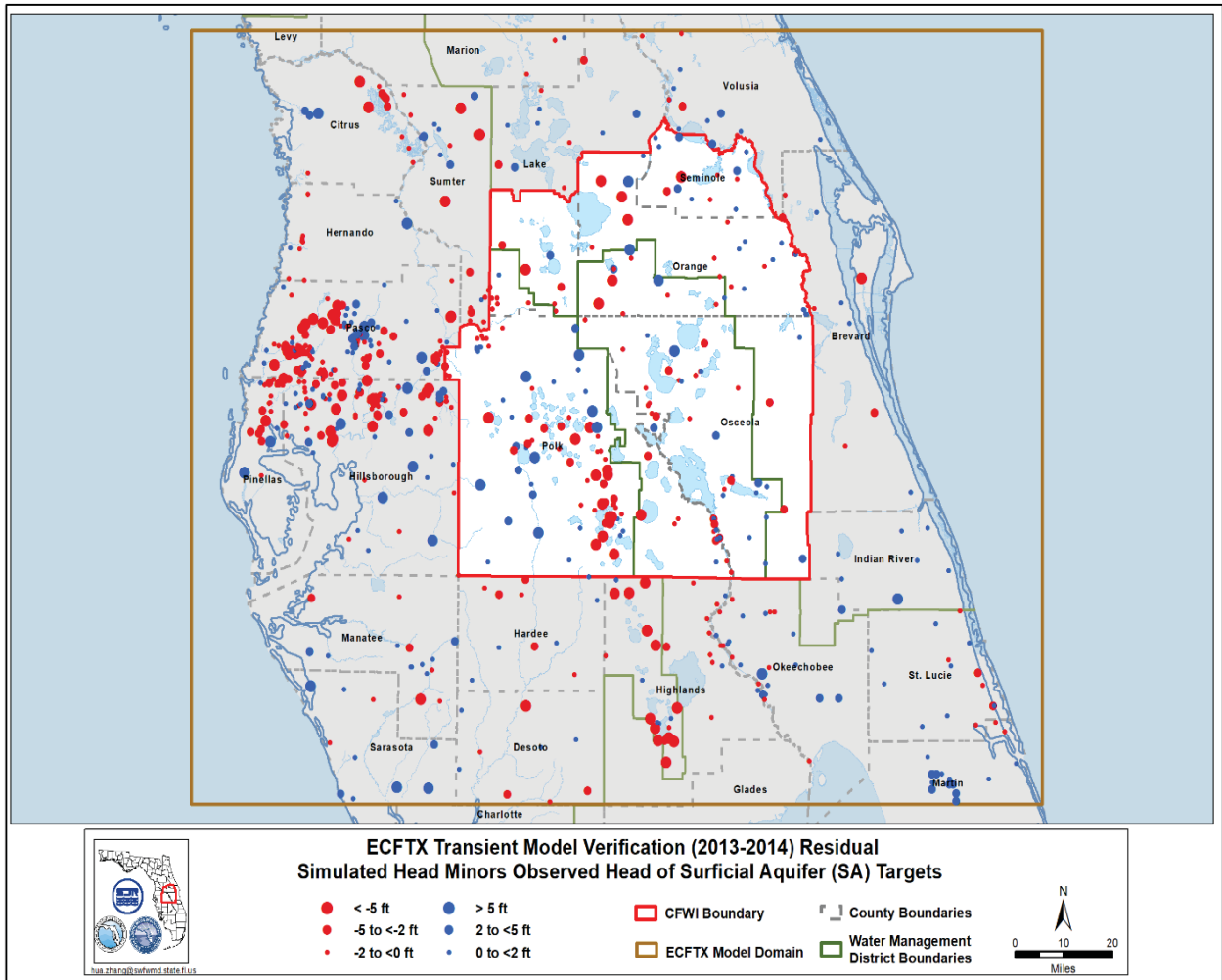
Figure 126. Spatial distribution of mean error during the verification period for the SA in the ECFTX transient model calibration.
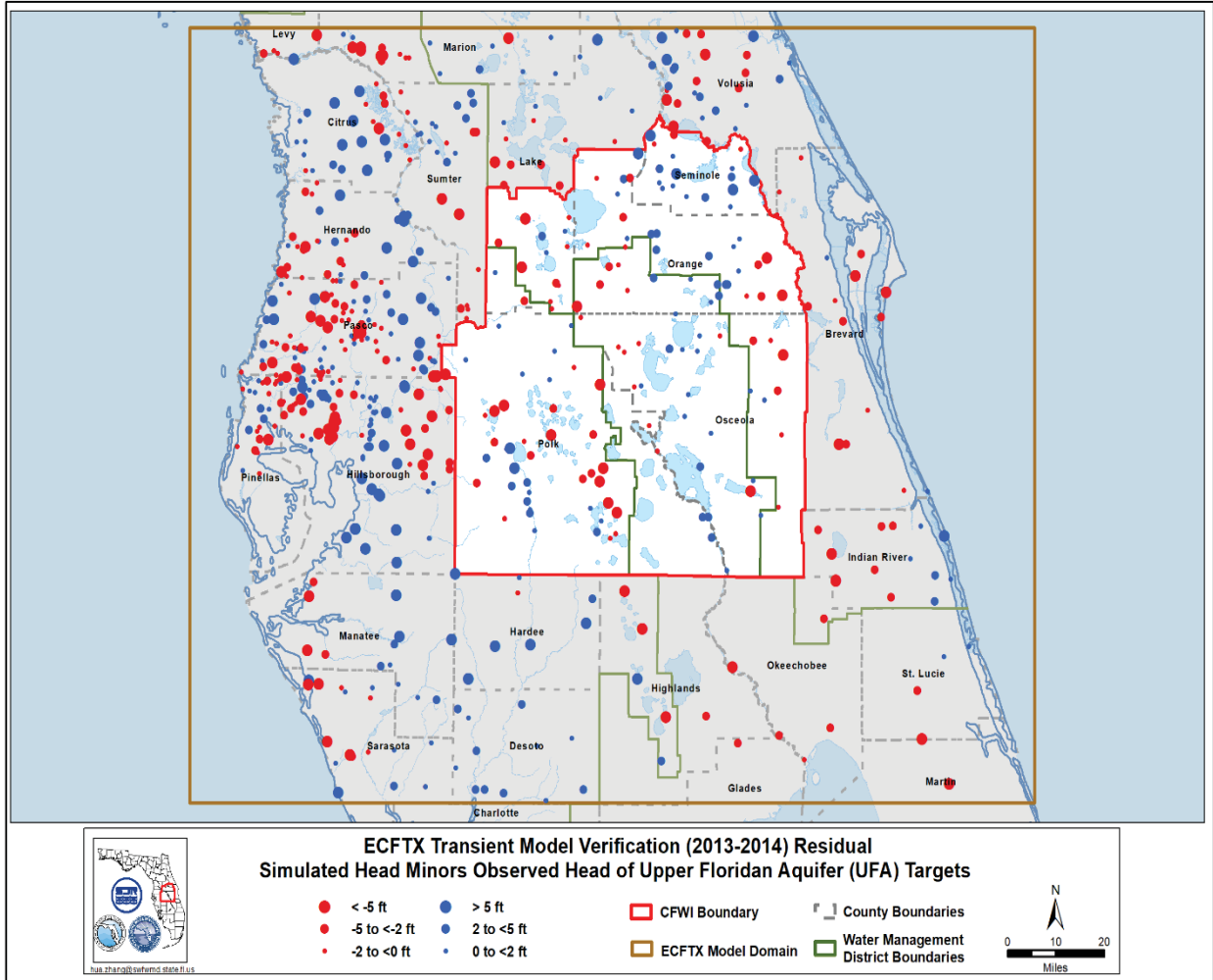
Figure 127. Spatial distribution of mean error during the verification period for the UFA in the ECFTX transient model calibration.
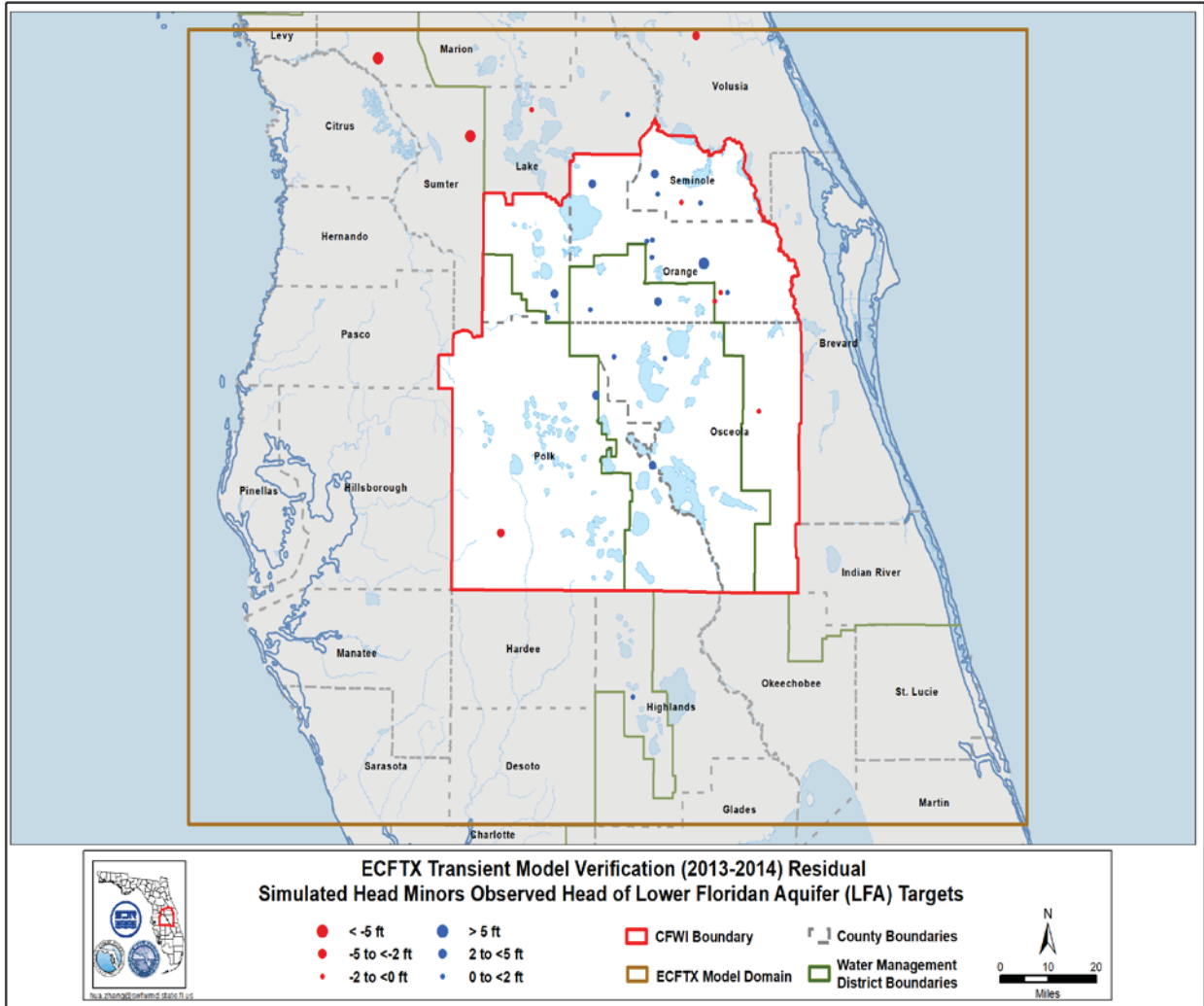
Figure 128. Spatial distribution of mean error during the verification period for the LFA in the ECFTX transient model calibration.
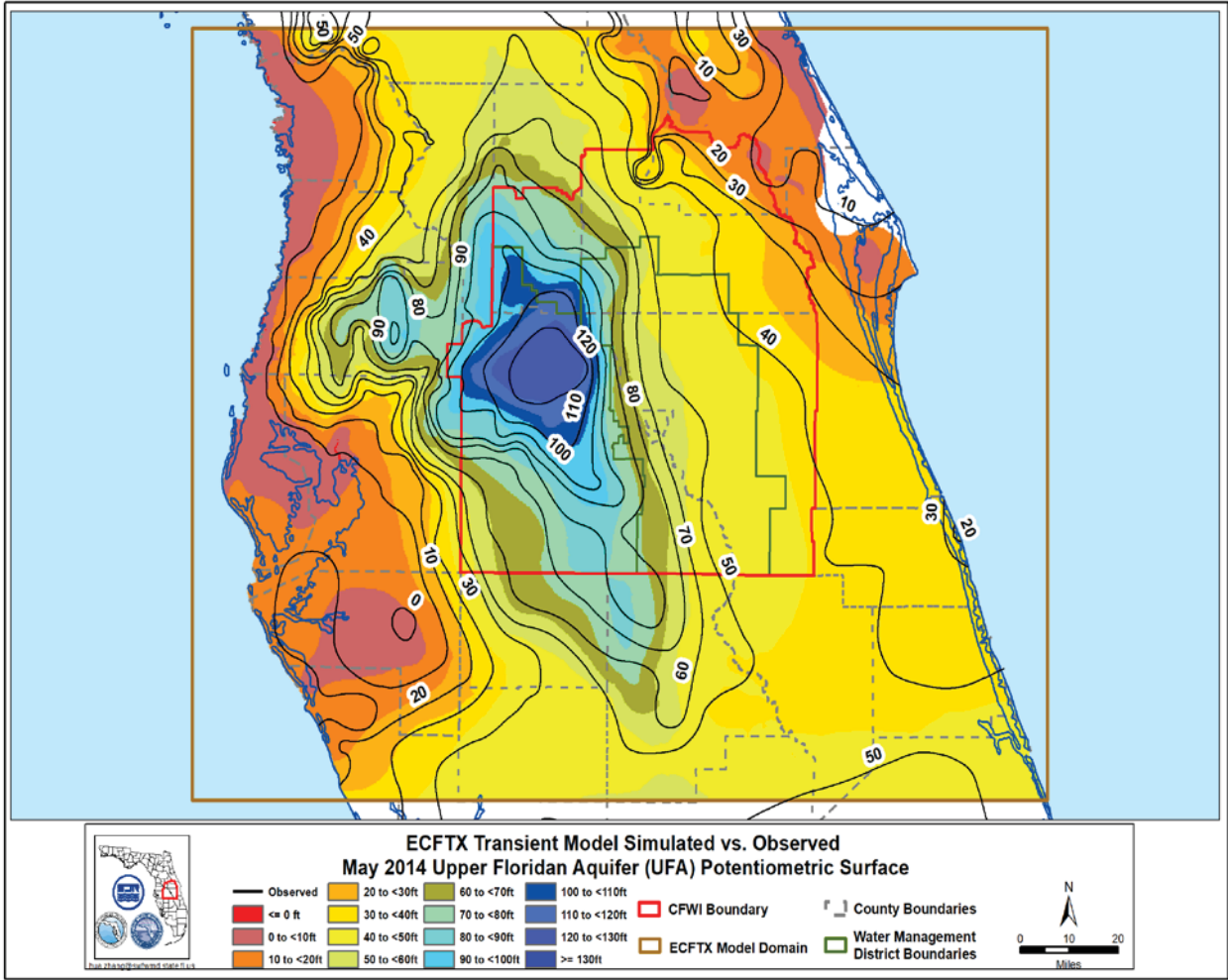
Figure 129. Comparison of May 2014 potentiometric surface with the simulated UFA potentiometric surface from the ECFTX transient model.
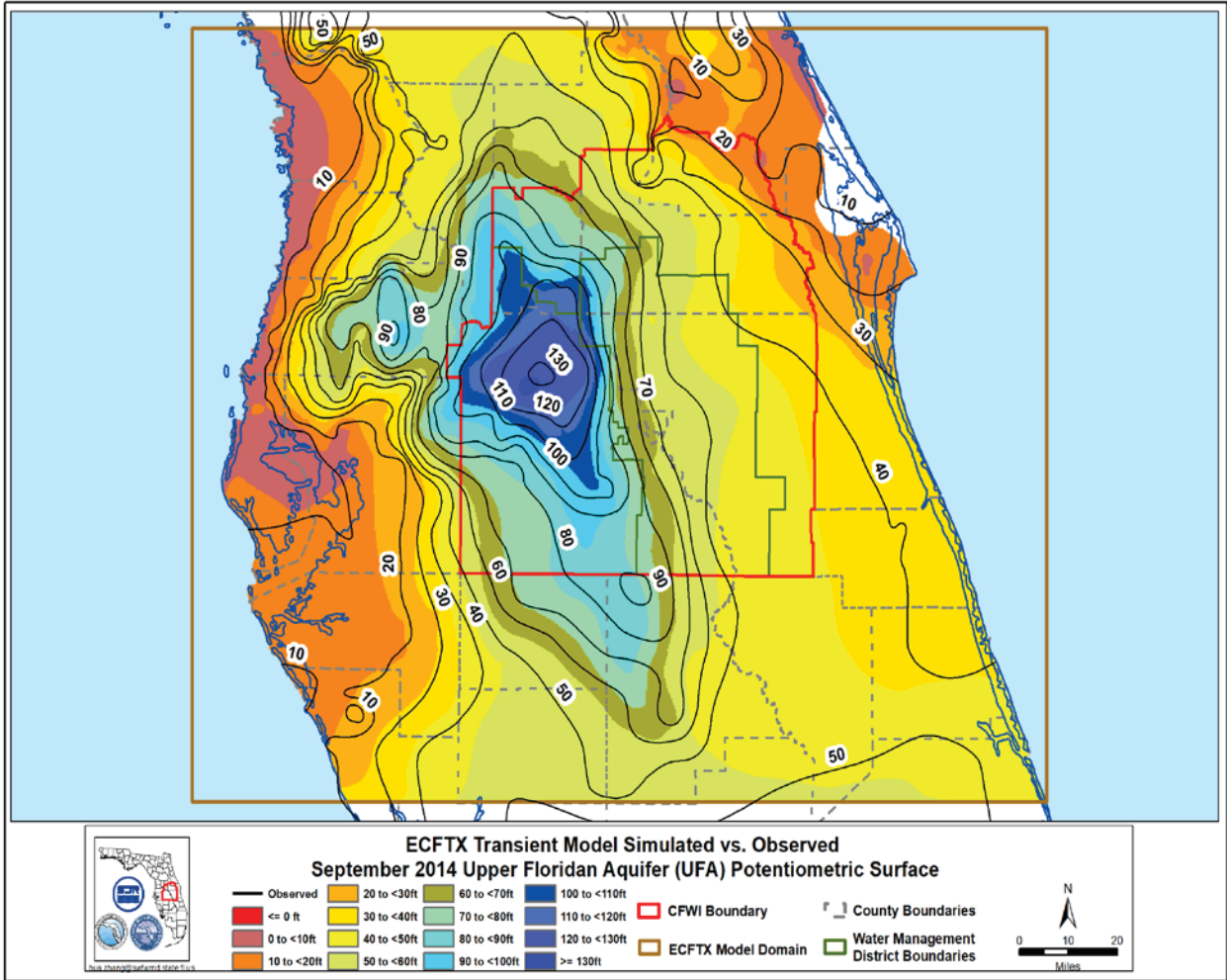
Figure 130. Comparison of September 2014 potentiometric surface with the simulated UFA potentiometric surface from the ECFTX transient model.
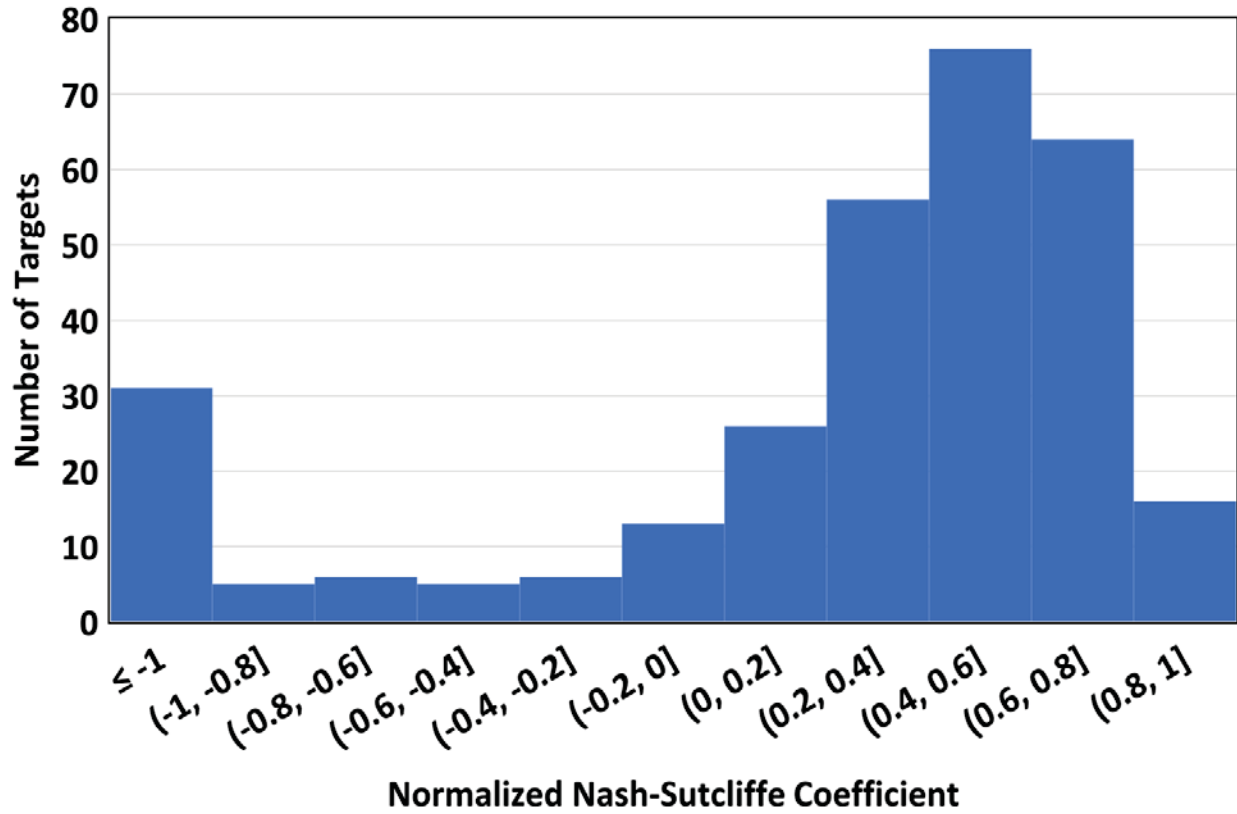
Figure 131. Histogram of Nash-Sutcliffe normalized coefficients for the SA within the CFWI area in the ECFTX transient model.
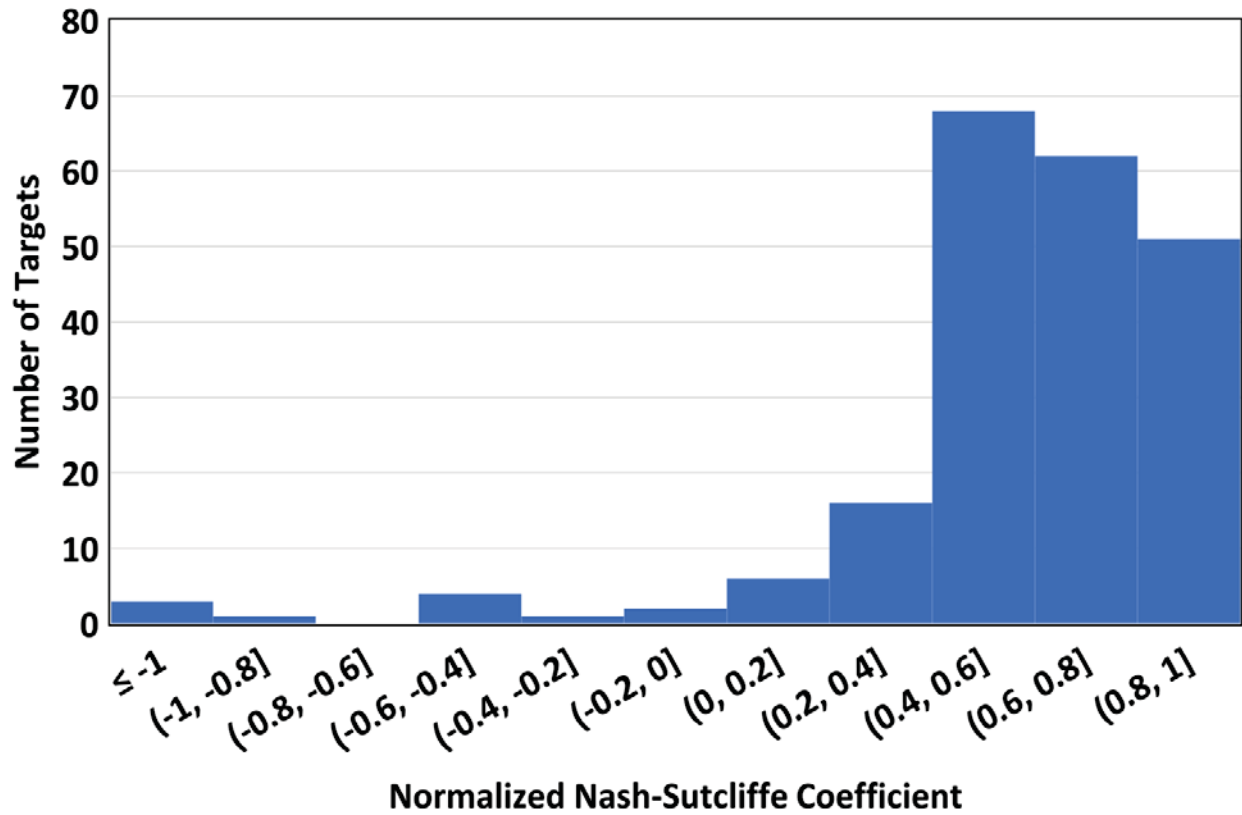
Figure 132 Histogram of Nash-Sutcliffe normalized coefficients for the UFA within the CFWI area in the ECFTX transient model.
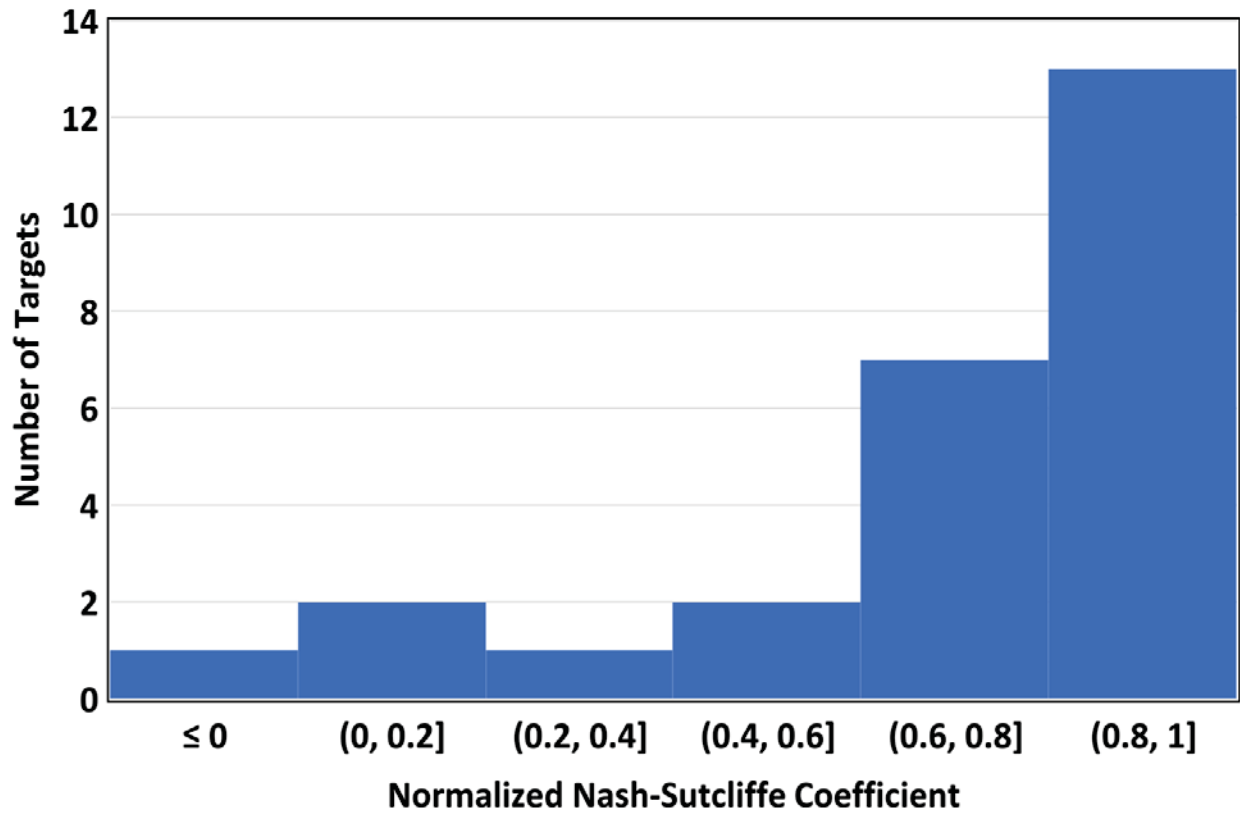
Figure 133 Histogram of Nash-Sutcliffe normalized coefficients for the LFA within the CFWI area in the ECFTX transient model.
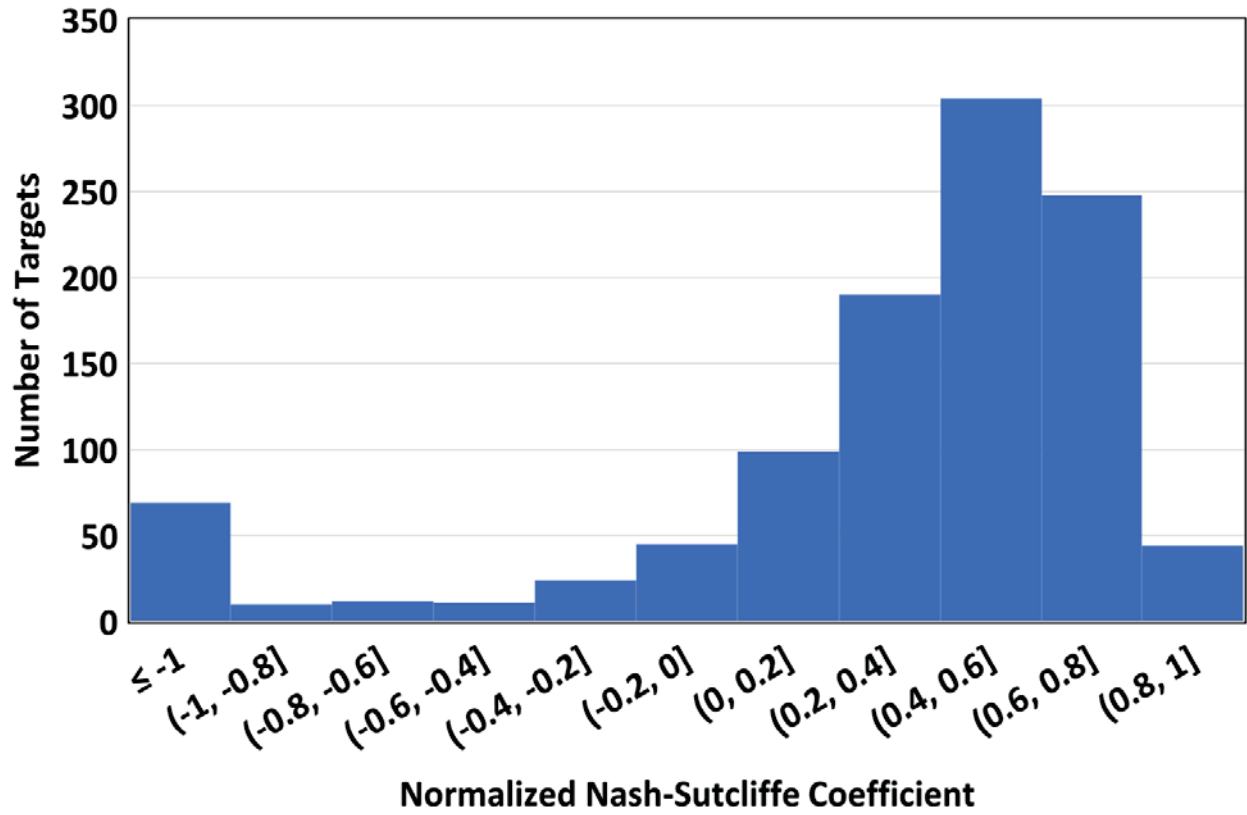
Figure 134. Histogram of Nash-Sutcliffe normalized coefficients for the SA within the ECFTX domain.
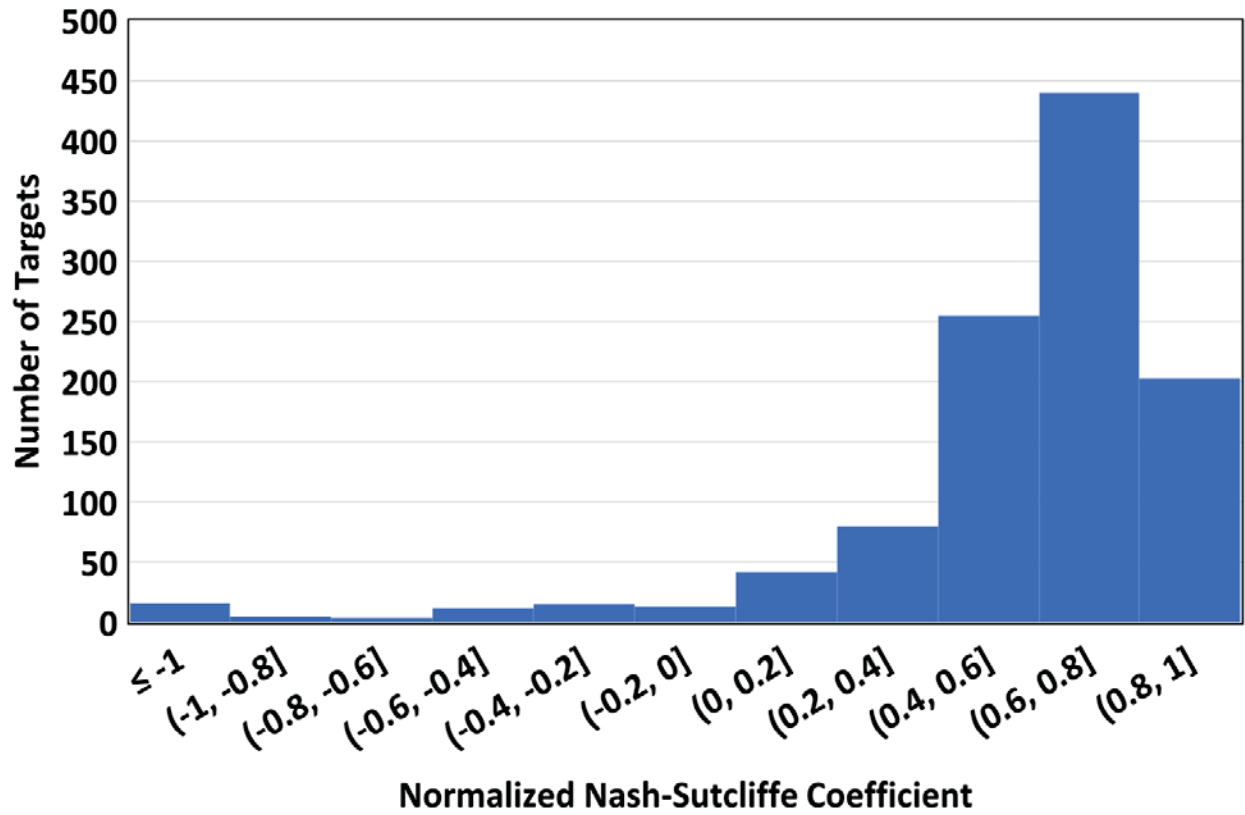
Figure 135. Histogram of Nash-Sutcliffe normalized coefficients for the UFA within the ECFTX domain.
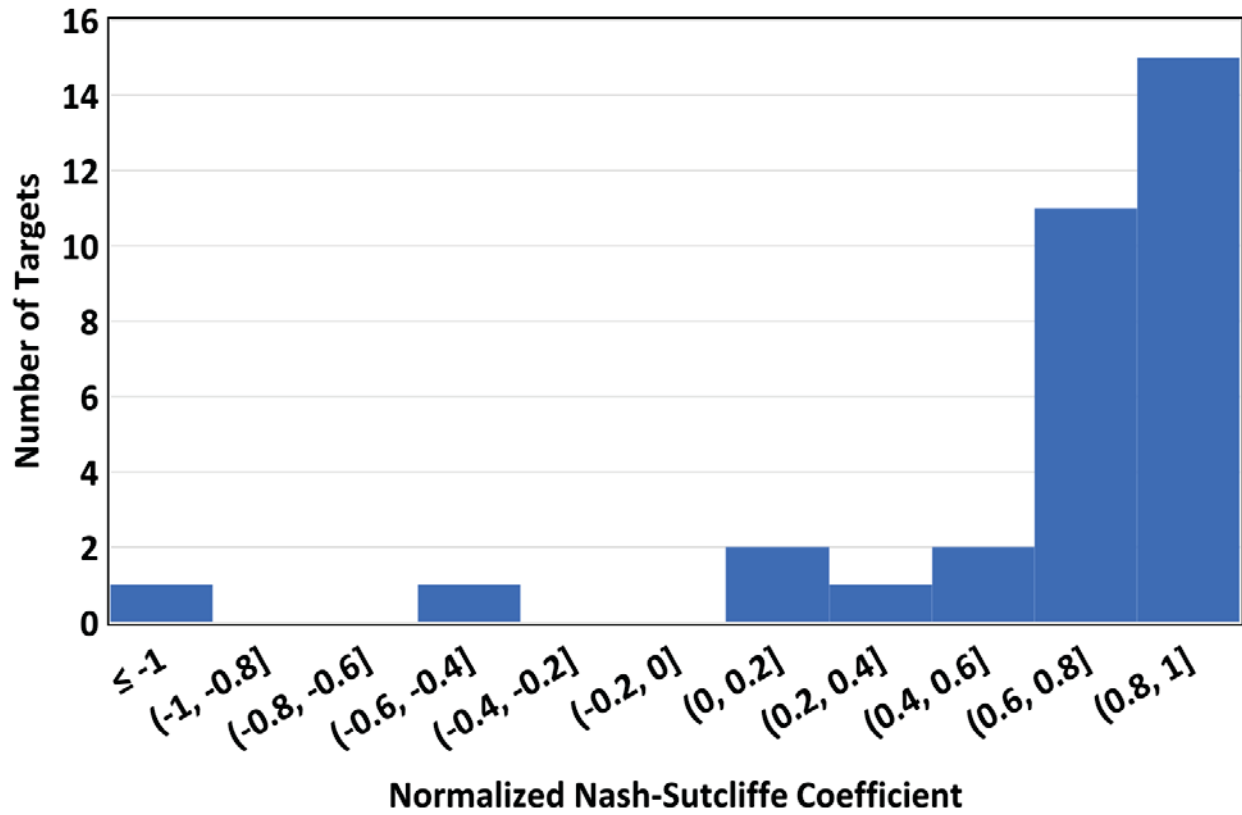
Figure 136. Histogram of Nash-Sutcliffe normalized coefficient for the LFA within the ECFTX domain.
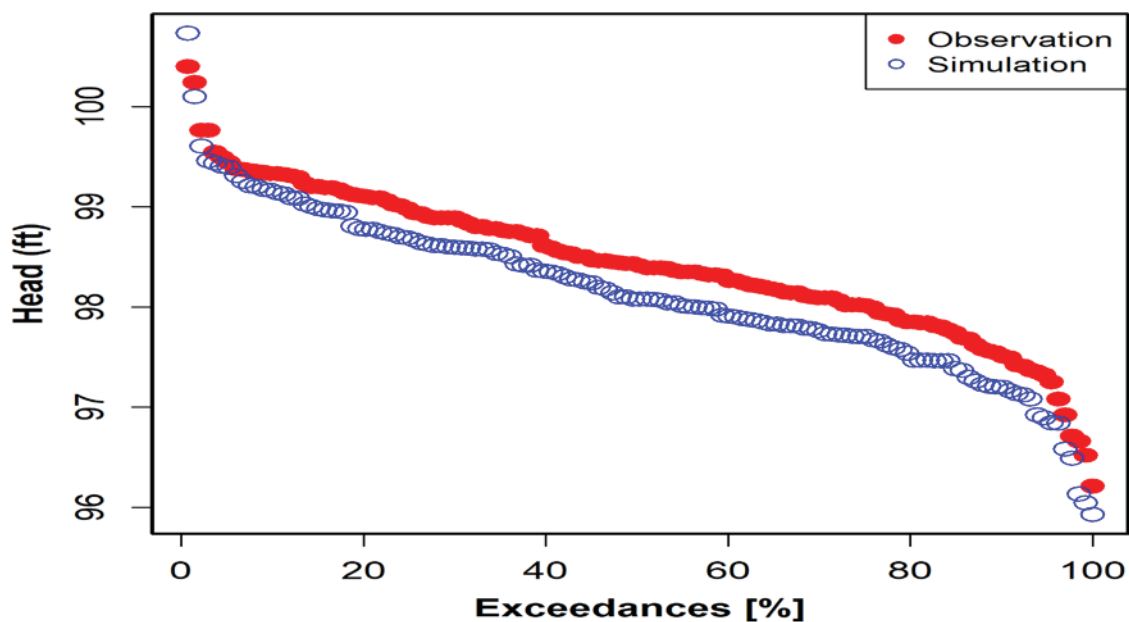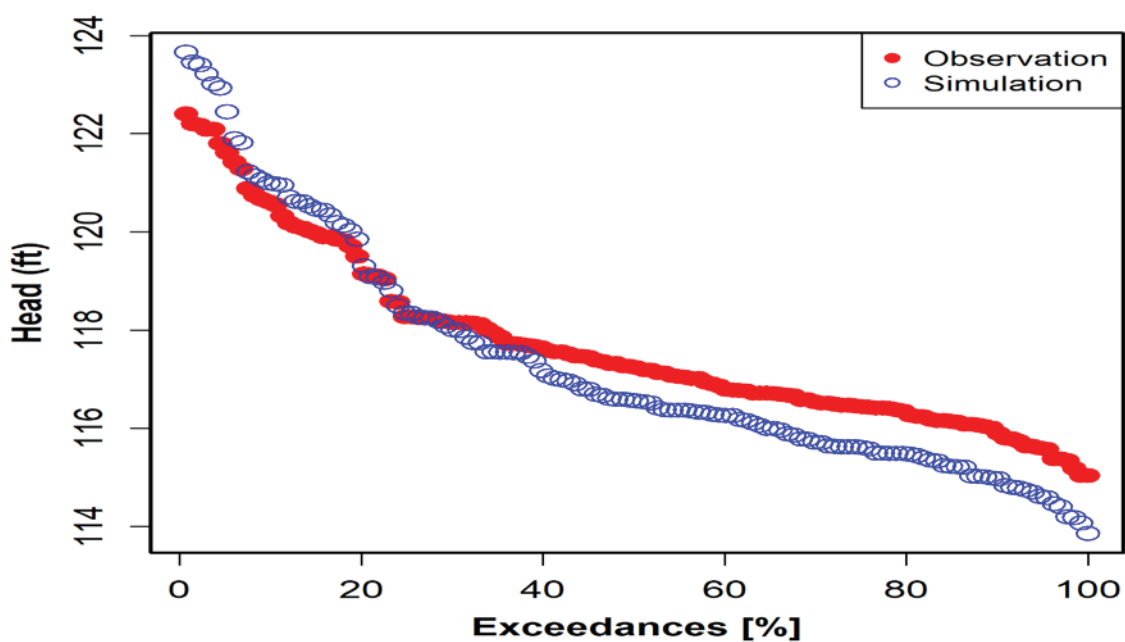
Figure 137. Simulated versus observed head duration (Ft NAV88) for the SA at monitor wells TB3_GW2 Tibet-Butler Preserve and Romp CL-3 (USGS5274545081342503) within the CFWI area of the ECFTX model.
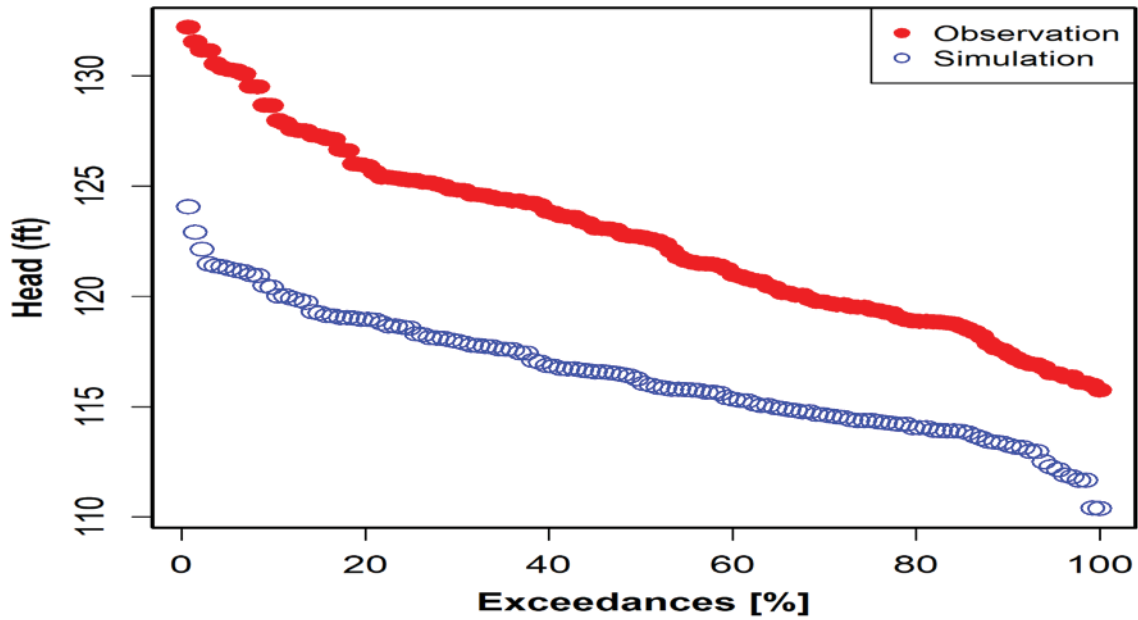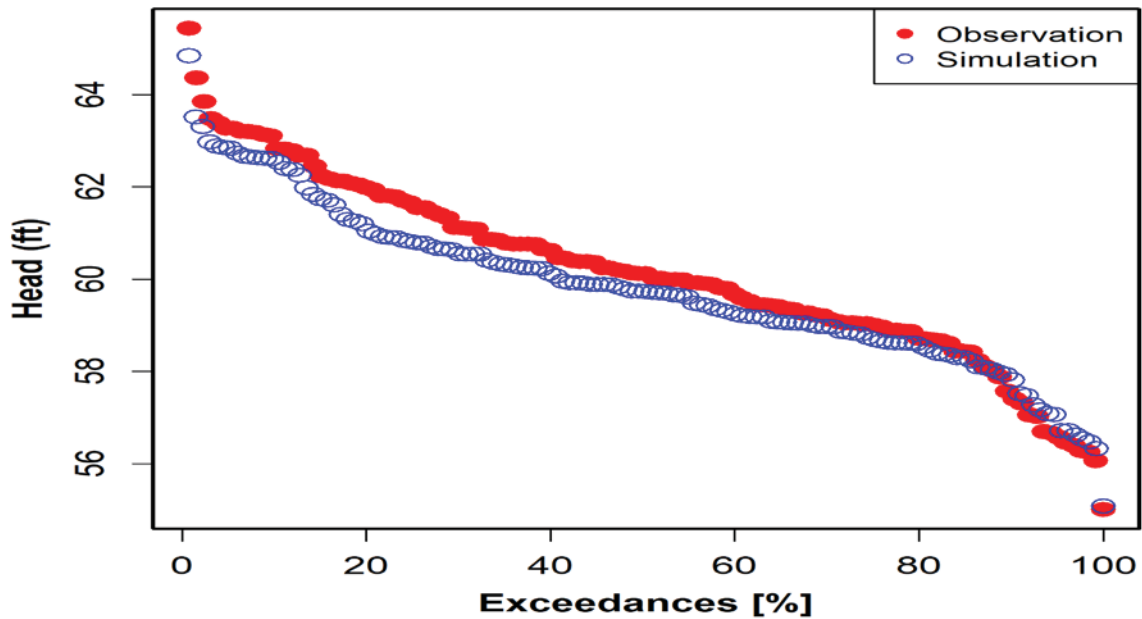
Figure 138. Simulated versus observed head duration (Ft NAV88) for the SA at monitor well Plymouth Tower (STRWMD51005097) and the UFA monitor well OSF-14 within the CFWI area of the ECFTX model.
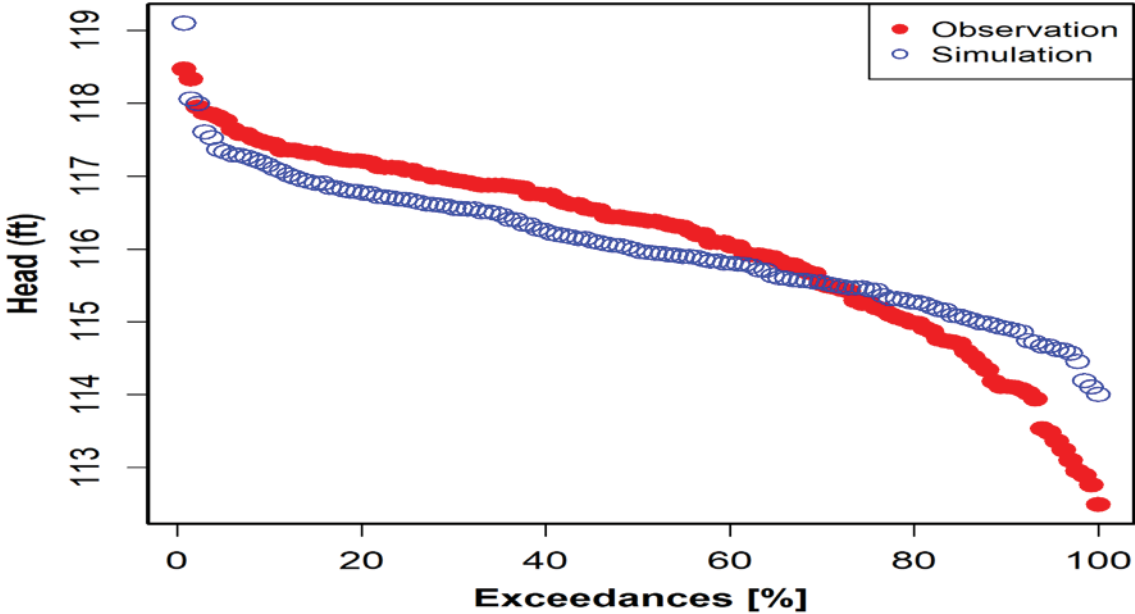
Figure 139. Simulated versus observed head duration (Ft NAV88) for the UFA at monitor wells
Romp 88 (USGS281837081544101) and L-0877 Hilochee (SJRWMD19564474) within the CFWI
area of the ECFTX model.
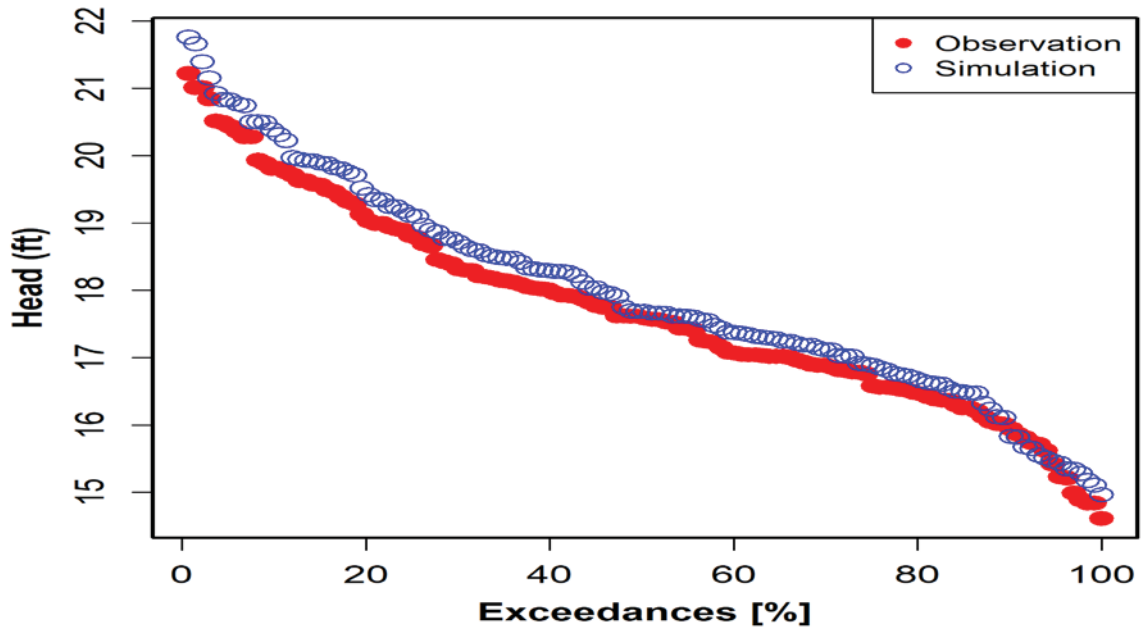
Figure 140. Simulated versus observed head duration (Ft NAV88) for the UFA at monitor wells S-1224 Geneva Fire Station (SJRWMD01850098) and OR-47 (USGS283253081283401) within the CFWI area of the ECFTX model.
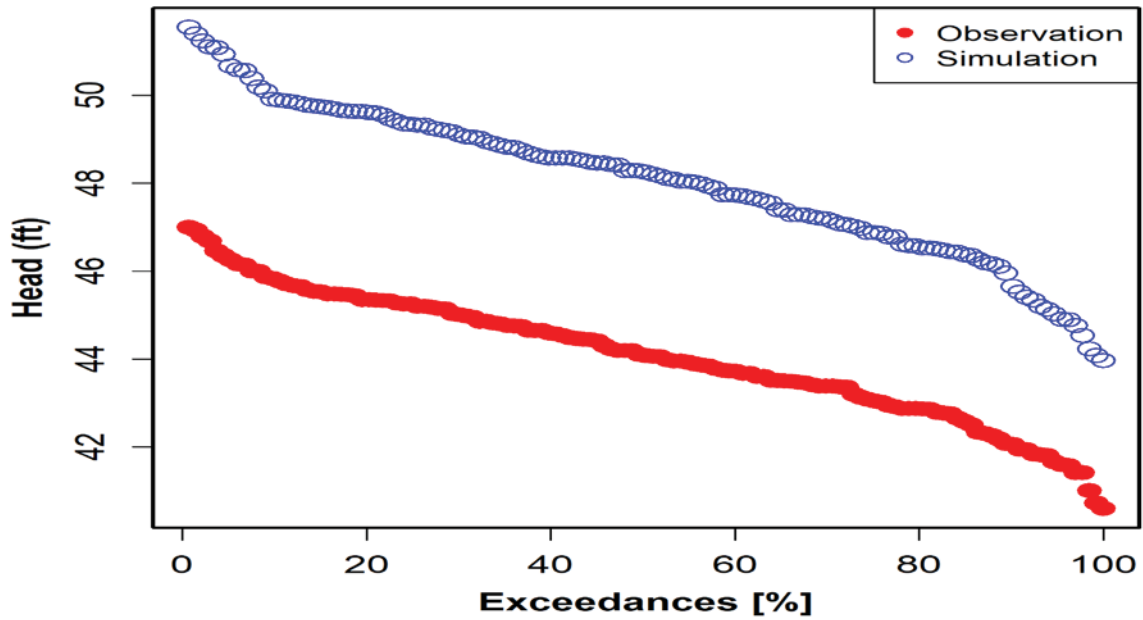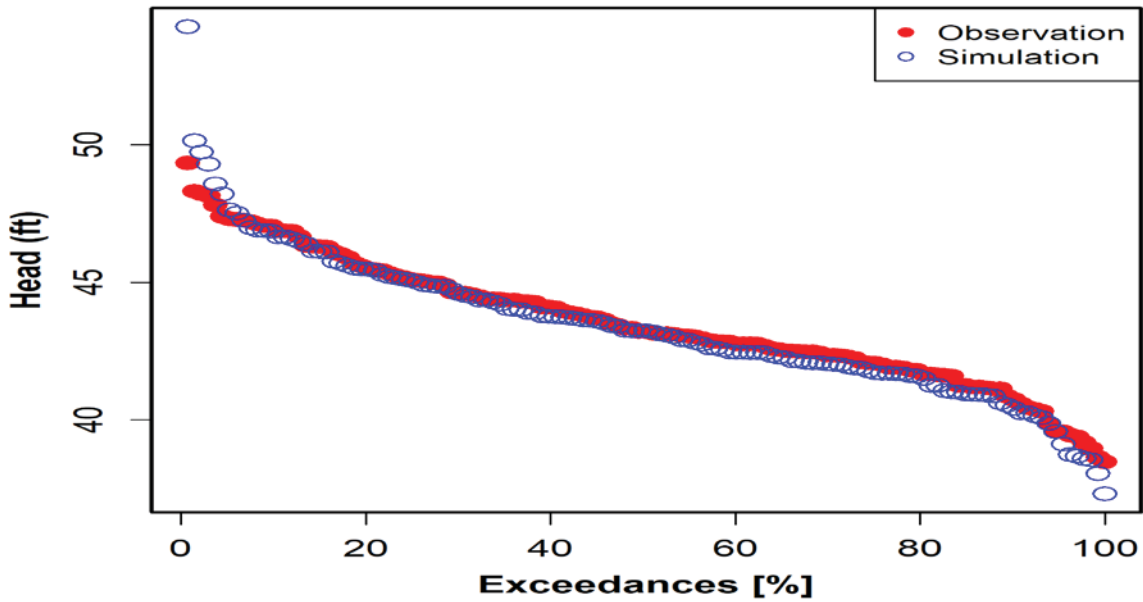
Figure 141. Simulated versus observed head duration (Ft NAV88) for the UFA at monitor well OSF-52 and LFA monitor well S-1329 (SJRWMD09991670) within the CFWI area of the ECFTX model.
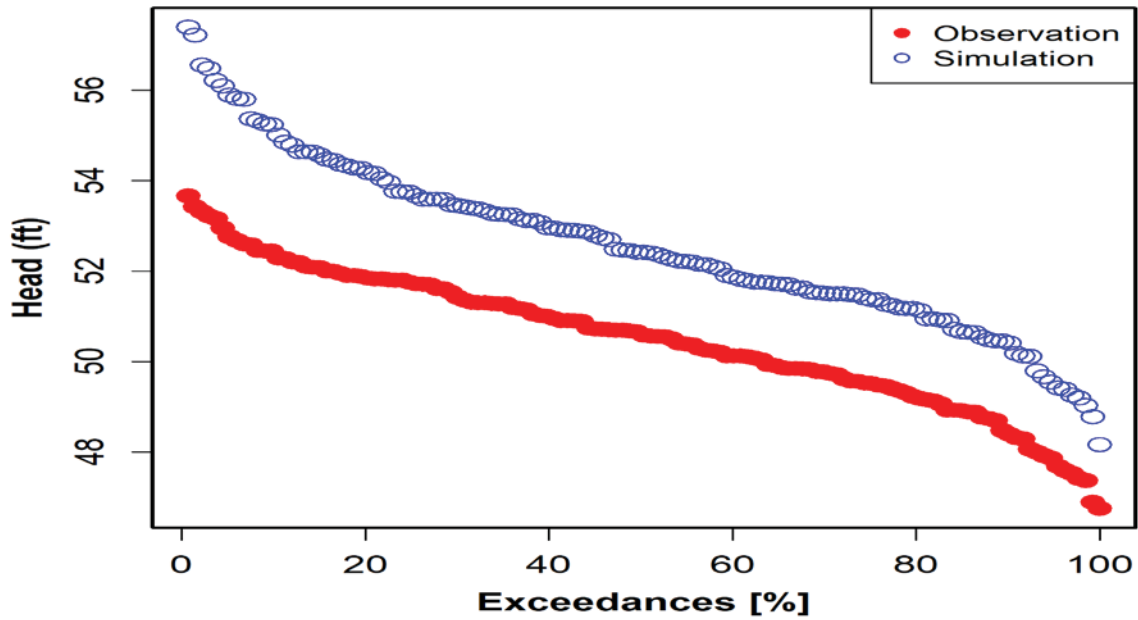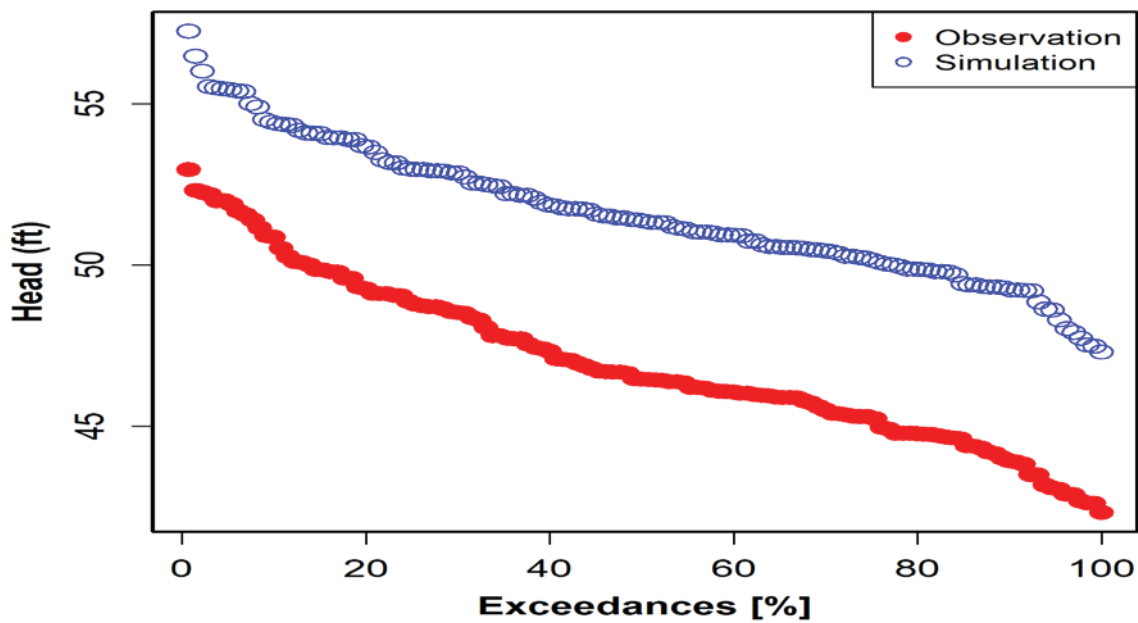
Figure 142. Simulated versus observed head duration (Ft NAV88) for the LFA at monitor wells OSF-97 and ORD794 Plymouth Tower (SJRWMD51004173) within the CFWI area of the ECFTX model.
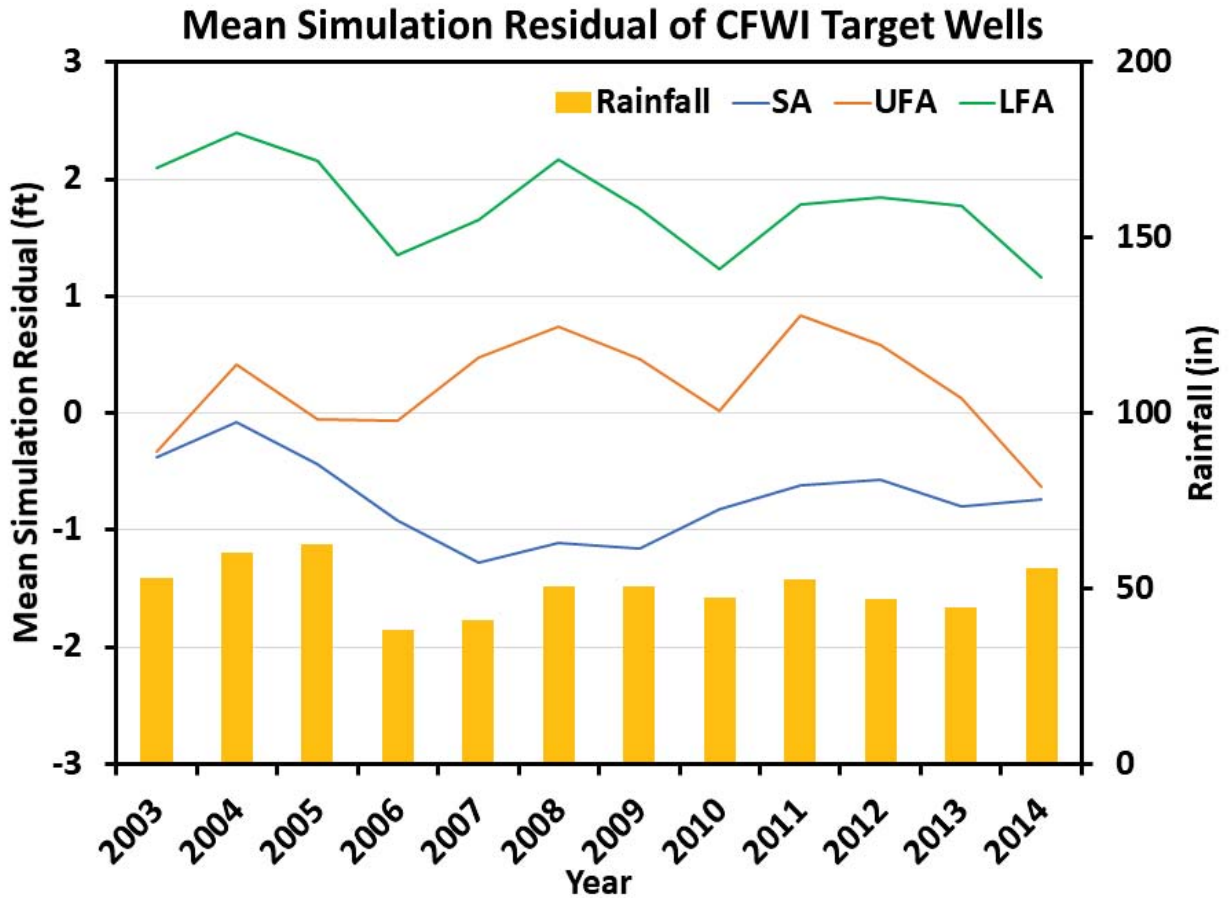
Figure 143. Simulated versus observed mean error by aquifer by year in the CFWI area from 2003 through 2014. Annual rainfall average within the domain is shown in the bar graph.
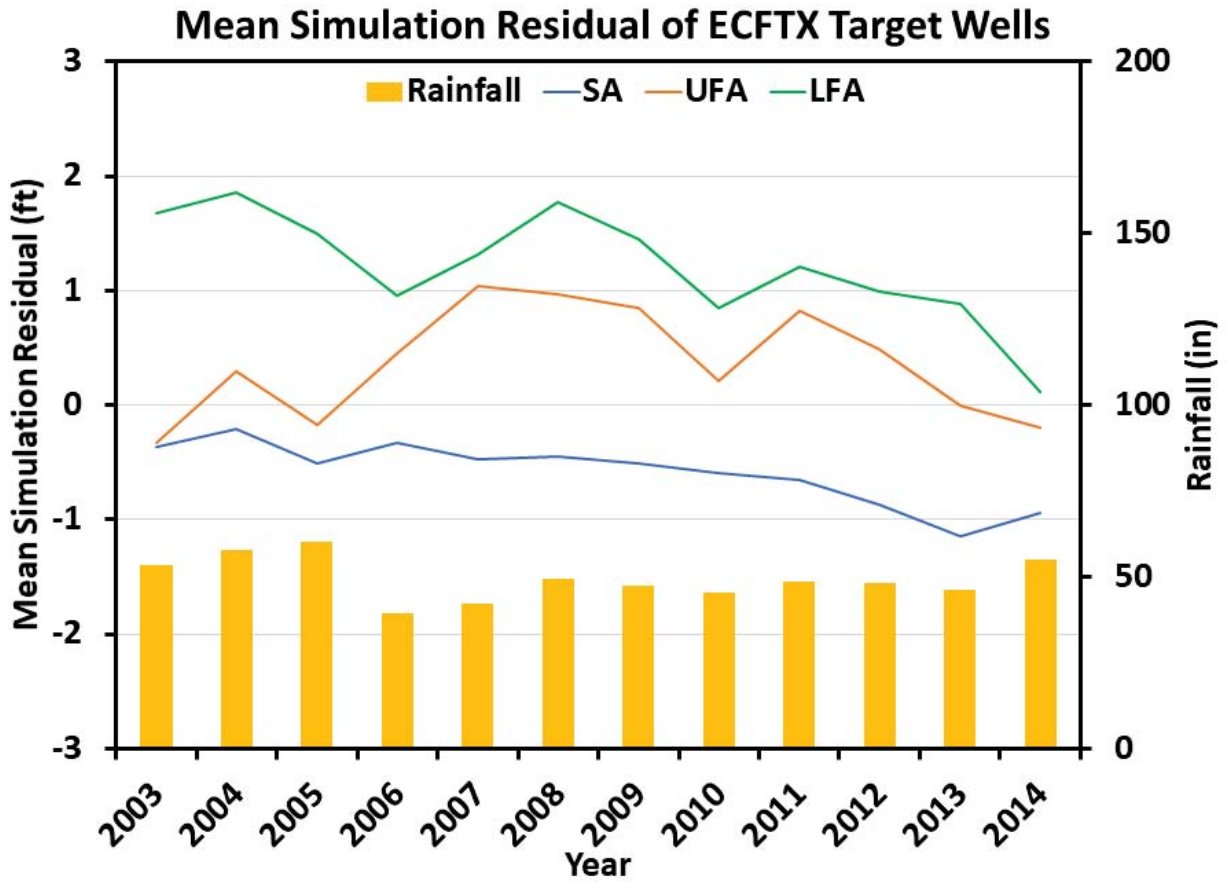
Figure 144. Simulated versus observed mean error by aquifer by year in the ECFTX domain from 2003 through 2014. Annual rainfall averaged within the domain is shown in the bar graph.
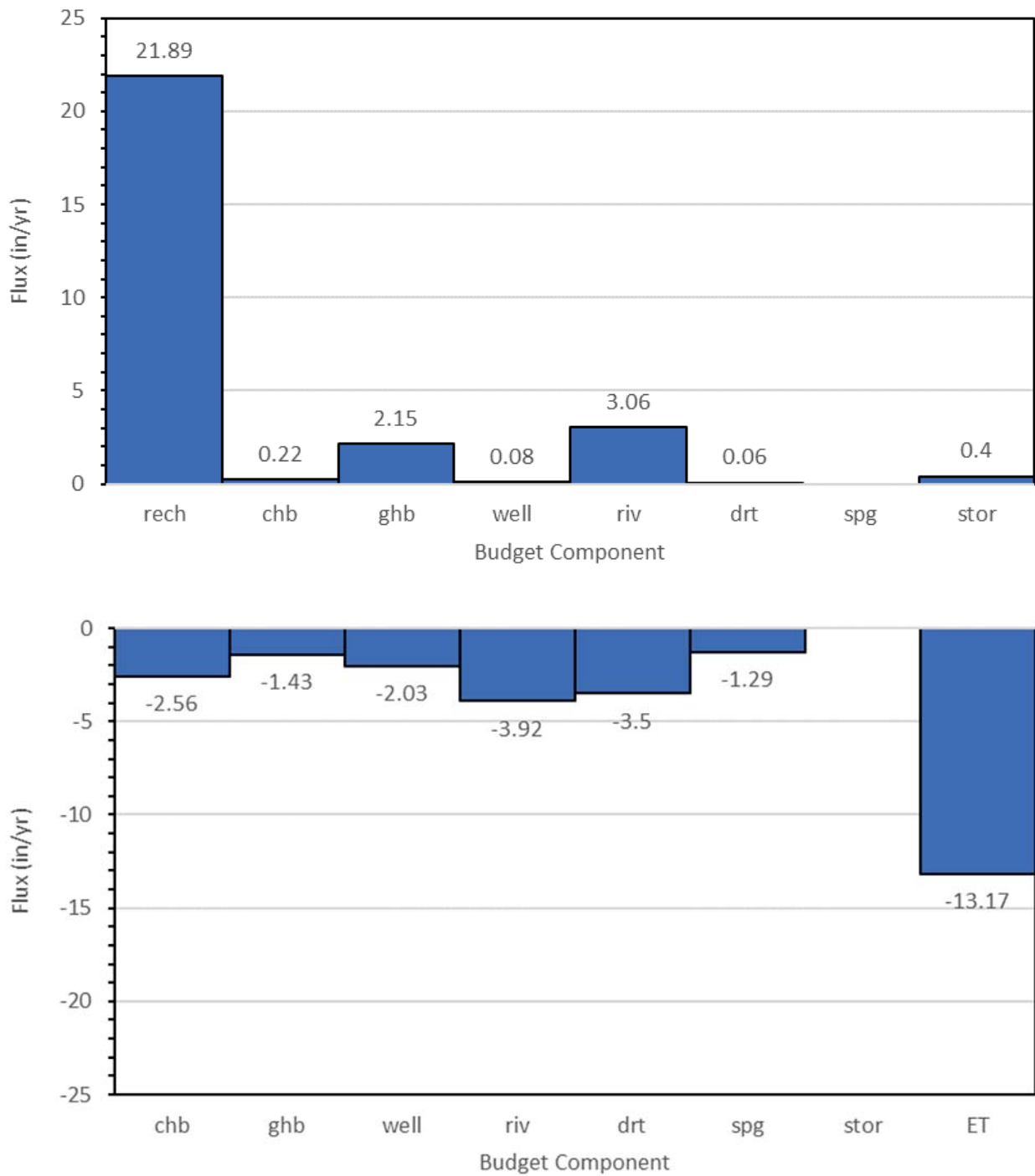
Figure 145. Inflow and outflow fluxes for major budget components during the calibration period (2004-2012) in the ECFTX model.
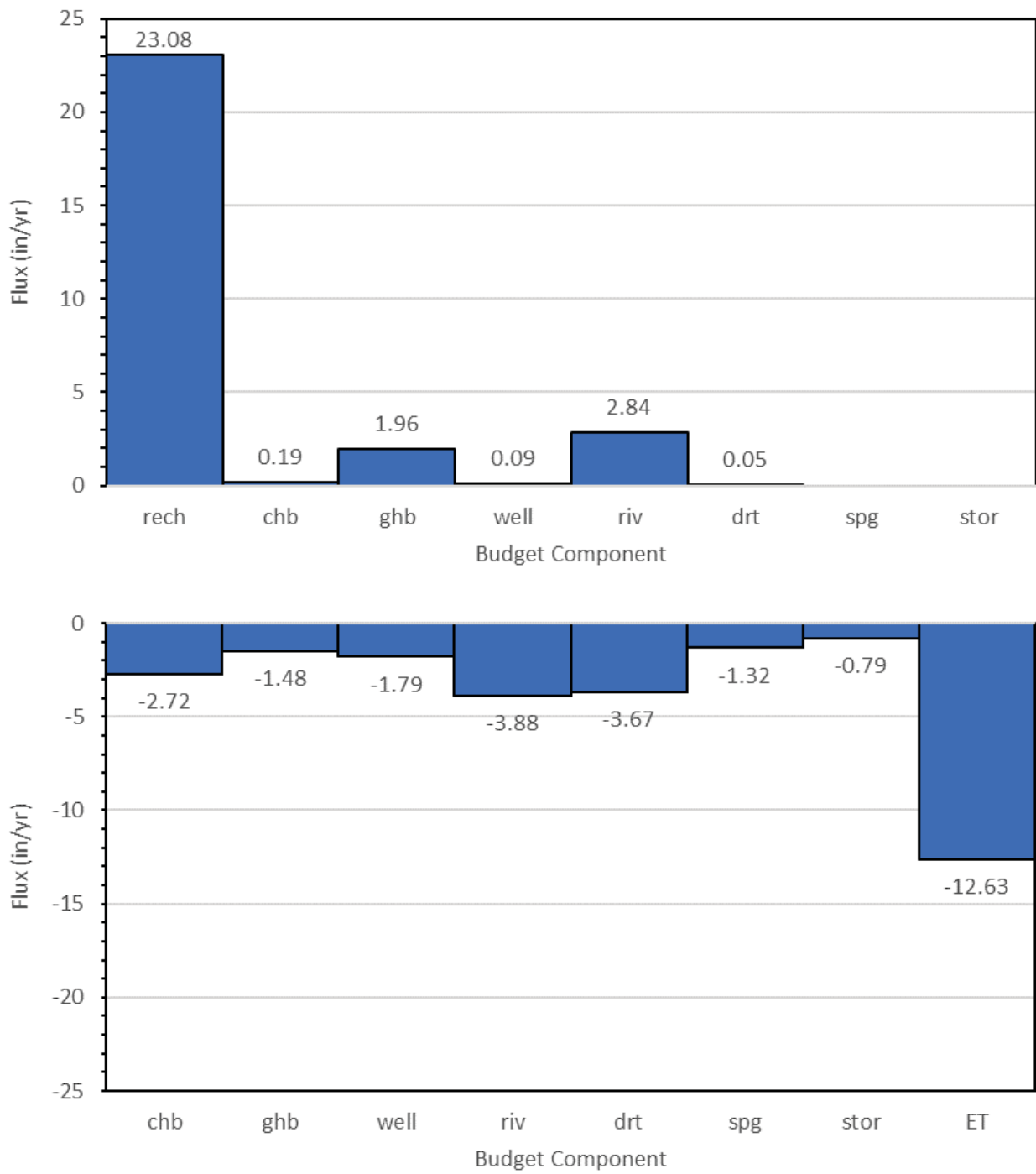
Figure 146. Inflow and outflow fluxes for major budget components during the verification period (2013-2014) in the ECFTX model.
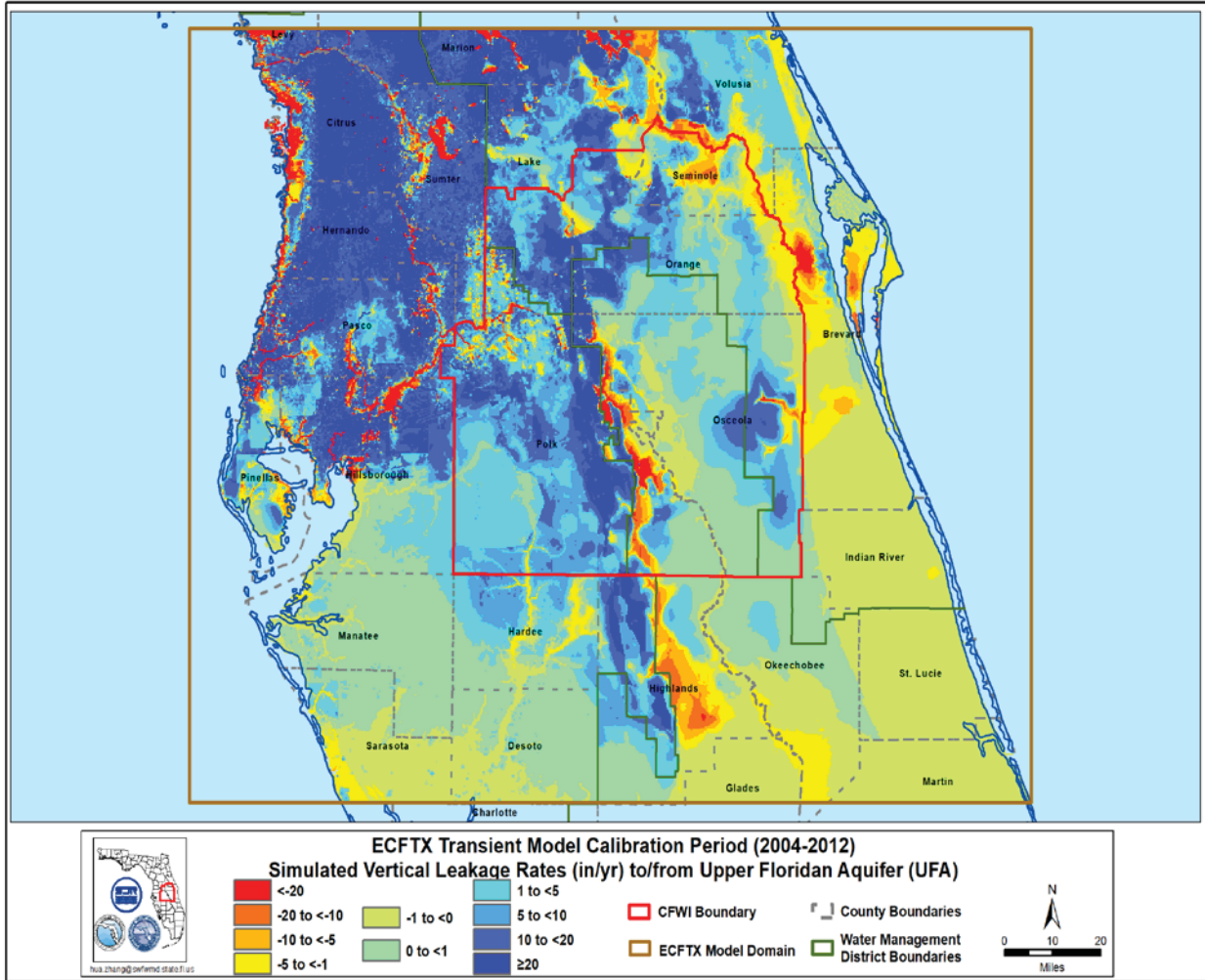
Figure 147. Average vertical leakage into or from the UFA during the calibration period (2004-2012). Negative values are upward leakage.

Figure 148. Basins and stream gaging stations used for structure flow calibration.
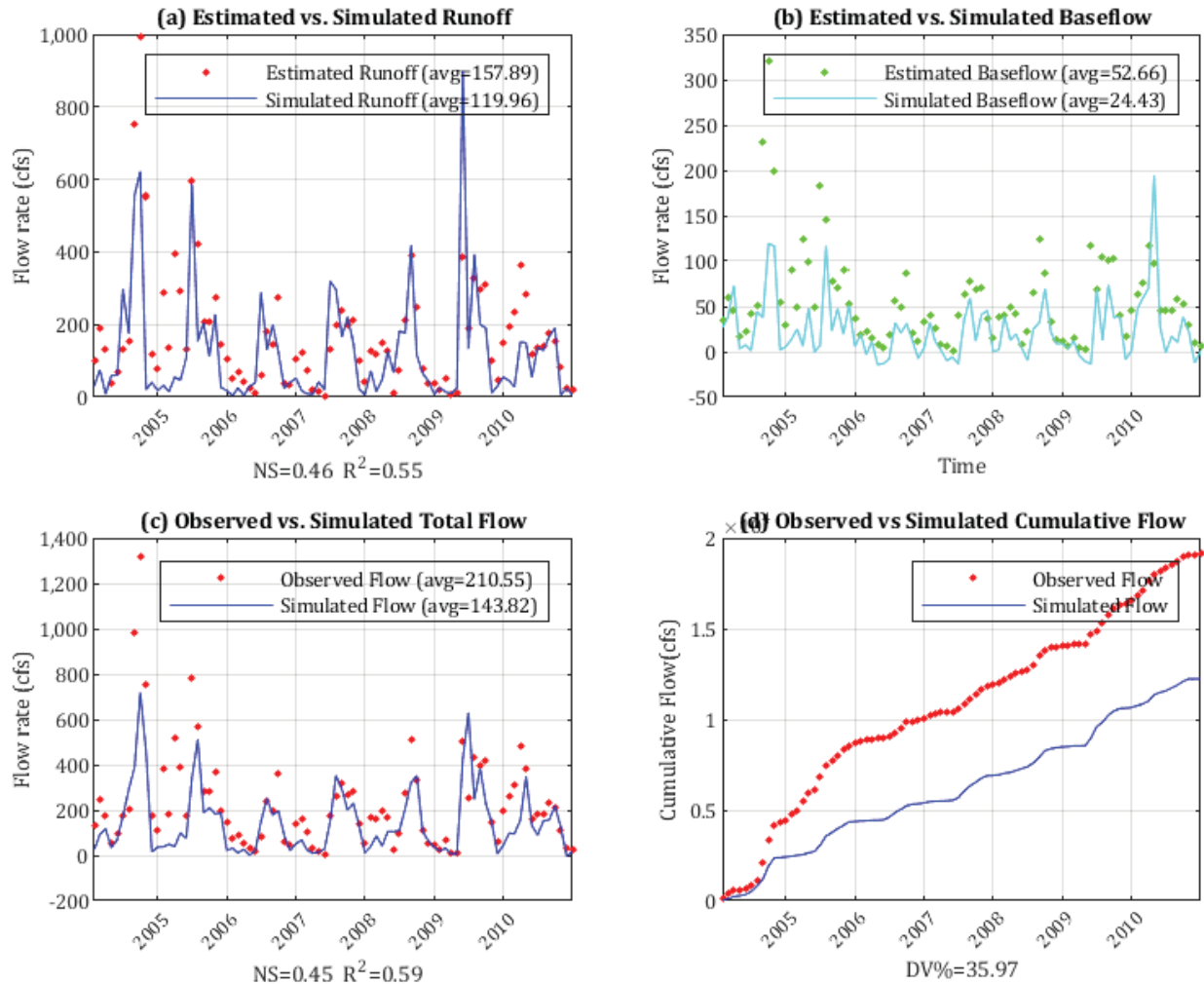
Figure 149. Comparison of (a) estimated vs. simulated runoff (b) estimated vs. simulated baseflow (c) observed vs. simulated total structure flow (d) observed vs. simulated total cumulative flow for Shingle Creek Watershed

CHAPTER 6 – SENSITIVITY ANALYSIS

Sensitivity analysis is a part of the model calibration process used to evaluate model input parameters to determine how they impact model outputs such as heads and flows. Sensitivity analysis is a quantitative evaluation of the impact of variability or uncertainty in model inputs on the degree of calibration of a model and on its results or conclusions. The analysis is essential in understanding how the simulated system conforms with the conceptual model, and the results can be used to determine which model input parameters are more significant in adjusting the simulated heads and flows and how they relate to the observed values (Reilly and Harbaugh, 2004).

6.1 Parameters and Methodology

Both automated and manual techniques can be implemented during a sensitivity analysis. Due to the transient nature of the model, a manual approach to sensitivity analysis was used to determine which model input parameters were most sensitive within the East Central Floridan Transient Extended Model domain (ECFTX). In this approach, one parameter is changed at a time so the effect of its variations on the model could be individually assessed. Parameter ranges were varied within acceptable ranges based upon a predetermined data range for each parameter calculated from known values.

The sensitivity analysis was used to determine which parameters are most sensitive to:

- simulated heads at the groundwater monitoring wells

- simulated flows at the Magnitude one and two springs

- simulated structure flows -at gaged watershed outlets

Table 29 shows the model input parameters used in the sensitivity analysis and the different multipliers that were applied to the calibration parameters. The tested parameters include vertical hydraulic conductivity (Kv) in Model layers 1 through 11; horizontal hydraulic conductivity (Kh) in Model layers 1 through 11; specific storage (Ss) in Model layers 1 through 11; specific yield (Sy) in Model layers 1 through 3; conductance values for drains, rivers, and General Head Boundary (GHB) cells; gross recharge (applied groundwater recharge); maximum saturated zone Evapotranspiration rates (ET); and the ET extinction depth. For each parameter, several model runs were completed using the various multipliers identified in Table 29. The maximum saturated zone ET and gross recharge are MODFLOW inputs derived from a pre-processor and therefore should not be confused with MODFLOW simulated ET or net recharge (gross recharge minus MODFLOW simulated ET).Specific yield values did not use multipliers; instead, the values shown in Table 29 were used as fixed values for each layer analyzed in the sensitivity runs. Additional model runs replacing time-varying heads in the GHB cells with a constant-head boundary in addition to a no-flow boundary (GHB conductance equal to 0) in Model layers 1 through 11 were also simulated. A total of 192 model runs were conducted to complete the sensitivity analysis. The simulation period for the sensitivity analysis is from January 1, 2004 to December 31, 2012, which is the same as the calibration period for the ECFTX Model and is used to compare spring and structure flows. Both the calibration and verification (January 1, 2013 to December 31, 2014) period were used to evaluate the model's sensitivity to simulated heads due to several Lower Floridan Aquifer monitor wells with observation data that are relatively new and not available during the calibration period.

Table 29. Parameters and multipliers of sensitivity analysis for the ECFTX Model.

Parameters	Multipliers			
Vertical Hydraulic Conductivity Model layers 1 – 11	0.1	0.2	5	10
Horizontal Hydraulic Conductivity Model layers 1 – 11	0.1	0.2	5	10
Specific Storage Model layers 1 – 11	0.01	0.1	10	100
Specific Yield Model layers 1 – 3*	0.05	0.15	0.2	0.25
Drain Conductance (DRN Package)	0.01	0.1	10	100
Drain Conductance (DRT Package)	0.01	0.1	10	100
River Conductance	0.01	0.1	10	100
General Head Boundary Conductance	0.01	0.1	10	100
Maximum Saturated Zone Evapotranspiration (ET)	0.8	0.9	1.1	1.2
Gross Recharge	0.8	0.9	1.1	1.2
ET Extinction Depth	0.5	0.75	1.5	2.0

*Specific yield was set to the fixed values shown in Figure 29.

6.2 Sensitivity Results

Sensitivity results are grouped by monitor well water levels, spring flows and structure discharges. The primary parameters that show the greatest sensitivity are presented initially with a discussion on changes to the entire model for each parameter change following. Monitor well water level results are further subdivided by primary aquifers which includes the Surficial Aquifer (SA), the Upper Floridan Aquifer (UFA) and the Lower Floridan Aquifer (LFA). Results are presented into four major sensitivity categories including:

1. Not sensitive -- changes to mean absolute error (MAE) are less than 0.1 feet and the total number of wells exhibiting this exceeds 50 percent.

2. Slightly sensitive -- changes in the MAE of between 0.1 and 0.5 feet at over 50 percent of the wells.

3. Moderately sensitive -- at least 50 percent of the wells showing change in the MAE between 0.5 and 1.0 feet.

4. Sensitive -- over 50 percent of the wells show changes of at least 1.0 feet in the MAE compared to the calibration value.

Determination of the degree of sensitivity assigned to changes in spring flows are based on the mean absolute error (MAE) of the springs, including an examination of the most sensitive parameter for the overall model domain as well as for each individual spring. Sensitivity of spring flows are examined by looking at 17 Magnitude 1 and 2 springs that were presented in the calibration section. The level of sensitivity is determined by comparing the difference between the calibrated MAE and the MAE of each sensitivity run. Four categories for springs sensitivity based on these differences are:

1. Less than 1% are insensitive.

2. Between 1% and 5% are minimally sensitive.

3. Between 5% and 10% are moderately sensitive.

4. Greater than 10% are sensitive.

Individual springs that are sensitive to a given parameter are provided in the discussion. Determination of the degree of sensitivity assigned to changes in structure flows are based on total flow at the gauges, including an examination of the most sensitive parameter for the overall domain as well as for each individual basin. Sensitivity of structure flows is examined by looking at the 40 basins that were presented in the calibration section. The level of sensitivity for the basins is determined by looking at the deviation of volume (DV), the Nash-Sutcliffe (NS) coefficient, and the coefficient of determination (R^2). The most sensitive parameters were identified by looking at the difference between the DV for the calibration run and each sensitivity run. The level of sensitivity based on the DV follows the same criteria that was used for the spring flows. Additional sensitive parameters were identified using the difference between the NS coefficient for the calibration run and the individual sensitivity runs. Four categories for structure flow sensitivity based on NS coefficient differences are:

1. Less than 0.05 in the NS coefficient are considered insensitive

2. Between 0.05 and 0.1 are minimally sensitive

3. Between 0.1 and 0.25 are moderately sensitive

4. Greater than 0.25 are sensitive.

The coefficient of determination, R^2, was initially used to identify additional sensitive parameters; however, upon further examination of the results, R^2 did not have significant variation between the 192-sensitivity model runs. This was expected, because none of the parameters were time dependent, which ultimately does not impact the R^2 value. Therefore, it was not used as a screening tool for identifying sensitive parameters.

6.2.1 Primary Sensitive Parameters to Monitor Well Water Levels

The top five most sensitive parameters over the model domain that affect monitor well water levels are presented in Table 30. The table shows the difference from the calibrated model for the MAE at each individual well. A negative value indicates the parameter causes a worsening of the calibration while a positive value indicates improvement to the calibration. It is grouped into two categories, the first being which parameter causes the greatest number of wells to change over 1 foot in either direction and with the highest change in the model MAE, while the second set is which parameter causes the greatest number of wells to change over 0.1 feet in either direction regardless of the change in the MAE. The overall model results suggest changing aquifer properties in the intermediate confining unit (ICU) and the primary production zones (Model layers 3 and 5) of the UFA causes the greatest magnitude of change (Figure 150). Parameters that cause changes to the majority of the monitor well water levels, but to a lesser degree, occurs in changes to variations in maximum evapotranspiration, gross recharge and riverbed conductance. Some variations of the most sensitive parameters exist between the aquifers. For example, the

SA is more sensitive to extreme changes in the hydraulic conductivity of Model layer 1 as well as gross recharge while the LFA is sensitive to variations in horizontal hydraulic conductivities (Kh) of the ICU or to the Kh of Model layer 5 (the Avon Park Permeable Zone (APPZ)).

Table 30. Most Sensitive Parameters Influencing Monitor Well Water Levels.

Top Five Parameters with Greatest Percentage of Wells in Sensitive Category								
		Difference from Calibrated Mae (ft)						
Parameter	Multiplier	< -1.0	-0.5 to -1.0	-0.1 - -0.5	+/- 0.1	0.1 – 0.5	0.5- 1.0	> 1.0
Kh Layer 5	X 10	40%	5%	10%	25%	7%	4%	9%
Kh Layer 3	X 10	38%	6%	8%	27%	6%	4%	11%
Kv Layer 2	X 10	34%	7%	11%	28%	8%	3%	8%
Kv layer 2	X 0.1	32%	5%	9%	30%	8%	5%	11%
Kv Layer 2	X 5	29%	7%	11%	32%	8%	4%	8%
Top Five Parameters with Greatest Number of Wells in the Slightly Sensitive Category								
		Difference from Calibrated MAE (ft)						
Parameter	Multiplier	< -1.0	-0.5 to -1.0	-0.1 - -0.5	+/- 0.1	0.1 – 0.5	0.5- 1.0	1.0
Gross Recharge	X 0.8	20%	12%	16%	13%	17%	13%	8%
Gross Recharge	X 1.2	12%	17%	21%	15%	15%	9%	11%
ET Depth	X 0.5	3%	13%	29%	21%	21%	10%	3%
Gross Recharge	X 0.9	6%	11%	24%	24%	26%	7%	2%
DRT Conductance	X 0.01	16%	10%	22%	24%	17%	7%	4%

NOTES:
Kh = horizontal hydraulic conductivity
Kv = vertical hydraulic conductivity
ET = Evapotranspiration
DRT = Drain Return Package

6.2.2 Primary Sensitive Parameters to Spring Flows

Figure 151 shows the overall results of the 192-sensitivity model runs based on the number of Magnitude 1 and 2 springs meeting the calibration criteria of mean error within +/- 10%. Overall, it does not appear that the spring flows are very sensitive to the majority of the parameters tested. The most sensitive parameters are shown in Figure 151 with red representing the drain conductance, pink representing the aquifer properties in the ICU, and purple, black and green representing aquifer properties in the UFA, specifically Model layers 3, 4, and 5, respectively.

The most sensitive variations of the top 5 most sensitive parameters over the model domain that impact spring flows are presented in Table 31. The table presents the percentage of spring flows whose difference from calibrated MAE fall within a specified category. A negative value indicates the parameter causes a worsening of the MAE, while a positive value indicates an improvement to the MAE. A difference of 10% or greater in over 50% of the Magnitude 1 and 2 springs indicates the springs are sensitive to the given parameter. A difference between 5% to 10% in at least 50%

of the springs is considered moderately sensitive, a difference between 1% to 5% in at least 50% of the springs is considered minimally sensitive, and differences less than 1% in greater than 50% of the springs is considered an insensitive parameter. The overall results of the sensitivity analysis, as shown in Table 31 show that changes to the drain cell conductance as well as changes to the aquifer properties of the ICU and UFA caused the greatest magnitude of change. This sensitivity is expected because the springs are simulated using the MODFLOW Drain package and the springs are discharge points for the UFA.

Table 31. Most Sensitive Parameters Influencing Spring Flows.

| Parameter | Multiplier | Difference from Calibrated Mean Absolute Error (MAE) % | | | | | | |
		< -10%	-5% to -10%	-5% to -1%	+/- 1%	1% to 5%	5% to 10%	> 10%
Drain	100	82%	6%	6%	0%	0%	6%	0%
Drain	10	76%	12%	6%	0%	0%	6%	0%
Drain	0.1	100%	0%	0%	0%	0%	0%	0%
Drain	0.01	100%	0%	0%	0%	0%	0%	0%
Kv of Layer 2	0.2	53%	6%	12%	23%	6%	0%	0%
Kv of Layer 2	0.1	59%	12%	0%	17%	12%	0%	0%
Kh of Layer 3	10	65%	23%	0%	12%	0%	0%	0%
Kh of Layer 3	5	65%	17%	6%	6%	6%	0%	0%
Kh of Layer 4	10	53%	0%	17%	18%	12%	0%	0%
Kh of Layer 4	5	53%	0%	6%	41%	0%	0%	0%
Kh of Layer 5	10	71%	12%	6%	12%	0%	0%	0%
Kh of Layer 5	5	53%	18%	24%	0%	6%	0%	0%

6.2.3 Primary Sensitive Parameters to Structure Flows

Figure 152 shows the overall results of the 192-sensitivity model runs based on the number of structure flows meeting the calibration criteria of a deviation of volume within +/- 15%. Overall, it does not appear the structure flows are very sensitive to the majority of the parameters tested. Figure 153 shows the number of structure flows meeting the calibration criteria for NS coefficient greater than 0.5 for each of the 192 sensitivity runs. Overall, NS calibration does not appear to be very sensitive to the variations or parameters that were tested. Additionally, unlike the sensitivity to the DV criteria, there are very few sensitivity runs that resulted in an increase in the number of calibrated structure flows. The most sensitive parameters are shown in Figure 152 and 153 with red representing the gross recharge, light blue representing the maximum ET rate, pink representing the extinction depth, purple representing the DRT Conductance, and black and green representing the sensitive aquifer properties in the SA and ICU, respectively.

The most sensitive variations and parameters over the model domain impacting structure flows are presented in Table 32. The table presents the percentage of structure flows whose difference from calibrated DV or calibrated NS fall within a specified category. A negative value indicates the parameter causes a worsening of the DV or NS, while a positive value indicates an improvement to the DV or NS. For the deviation of volume, a difference of 10% or greater in over 50% of the structure flows indicates the basins are sensitive to the given parameter. A difference between 5% to 10% in at least 50% of the basins is considered moderately sensitive, a difference between 1% to 5% in at least 50% of the basins is considered minimally sensitive, and differences

less than 1% in greater than 50% of the basins is considered an insensitive parameter. For the NS coefficient, a difference of 0.25 or greater in over 50% of the structure flows indicates the basins are sensitive to the given parameter. A difference between 0.1 and 0.25 in at least 50% of the basins is considered moderately sensitive, a difference between 0.05 to 0.01 in at least 50% of the basins is considered minimally sensitive, and differences less than 0.05 in greater than 50% of the basins is considered an insensitive parameter. The overall results of the sensitivity analysis, as shown in Table 32 show changes to gross recharge, ET, and extinction depth are the most sensitive parameters for the DV calibration criteria, while DRT conductance and aquifer parameters in the SA and ICU are also sensitive. Although these same parameters are moderately to minimally sensitive for the calibration based on the NS coefficient, none of the variations of the parameters that were tested had at least 50% of the basins meeting the criteria for a sensitive parameter, therefore further analysis and discussion of sensitivity based on the NS coefficient is not included.

Table 32. Most Sensitive Parameters Influencing Structure Flows.

Parameter	Multi plier	Difference from Calibrated Deviation of Volume %						
		< -10%	-5% to -10%	-5% to -1%	+/- 1%	1% to 5%	5% to 10%	> 10%
Gross Recharge	x 1.2	78%	5%	0%	0%	0%	5%	13%
Gross Recharge	x 1.1	45%	33%	5%	0%	5%	8%	5%
Gross Recharge	x 0.9	5%	8%	5%	0%	5%	15%	63%
Gross Recharge	x 0.8	13%	5%	0%	0%	0%	5%	78%
Max ET	x 1.2	8%	5%	5%	0%	3%	18%	63%
Max ET	x 0.8	53%	28%	3%	0%	5%	5%	8%
Extinction Depth	x 2.0	15%	3%	0%	0%	0%	0%	83%
Extinction Depth	x 1.5	5%	10%	3%	0%	0%	15%	68%
Extinction Depth	x 0.5	80%	3%	0%	0%	0%	8%	10%
DRT Conductance	x 0.1	3%	3%	10%	0%	13%	10%	63%
DRT Conductance	x 0.01	3%	5%	8%	0%	8%	8%	70%
Kh in Layer 1	x 10	60%	8%	13%	5%	0%	3%	13%
Kv in Layer 2	x 10	28%	5%	8%	13%	10%	5%	33%

Parameter	Multiplier	Difference from Calibrated NS						
		< -0.25	-0.10 to -0.25	-0.10 to -0.05	+/- .05	.05 to .10	0.10 to 0.25	> 0.25
Gross Recharge	x 1.2	23%	18%	13%	28%	3%	3%	15%
Gross Recharge	x 1.1	8%	18%	18%	38%	3%	5%	13%
Extinction Depth	x 0.5	13%	25%	28%	15%	5%	8%	8%
DRT Conductance	x 100	10%	15%	15%	43%	0%	13%	5%
Kh in Layer 1	x 10	23%	15%	25%	18%	5%	8%	8%
Kh in Layer 1	x 5	15%	18%	15%	35%	3%	10%	5%

6.2.4 Results by parameter groupings

A total of 192 different sensitivity simulations were analyzed, which can be roughly grouped into three broad categories. These include variations of the aquifer and confining unit parameters, stress-related variables, and surface water-groundwater controlling factors. Embedded in these broad categories are 49 distinct groupings of like variables. For example, one of these like groupings would include multiplying the calibrated value of the SA by a factor of 10, 5, 0.2, 0.1 at each cell with the original calibration result to provide a reference point.

Changes to aquifer properties include global changes in the Kh and Kv by factors of 10, 5, 0.2 and 0.1 individually for layers 1 through 11. Changes in specific yield (Sy) were globally set to values of 0.25, 0.2, 0.15 and 0.5 for layers 1 through 3 where the aquifers can change from confined to unconfined conditions. The aquifer specific storage (Ss) was varied by factors of 100, 10, 0.1 and 0.01 for each individual layer.

Surficial Aquifer

The Kh of the SA is slightly sensitive to variations away from the calibrated values. Changes in the global MAE of the model decreased by 0.74 ft, 0.48 ft., 0.21 ft., and 0.48 ft from the calibrated model for multiplication factors of 10, 5, 0.2 and 0.1, respectively. The percentage of total wells showing slight sensitivity ranged between 54 to 70 percent, with 14 to 25 percent falling in the sensitive category depending upon the simulation. In general, the model is slightly sensitive to the variations in the Kh for the SA and the UFA. The LFA shows moderate sensitivity to increased values of Kh. The overall model is unaffected by changes in the Kv of layer 1. Figure 154 shows the sensitivity of monitor well water levels to changes in the Kh of the three aquifers for both the CFWI and the model domain. The center point represents the calibrated value with the values on each side showing the increasing or decreasing multiplication factors. Similar plots are included for every major parameter change and its effects on the monitor well heads, spring flows and structure discharges in Appendix M.

Variations in the magnitude of both Sy and Ss for the SA showed no appreciable changes for any simulation in the MAE of the simulated heads. The model is insensitive to these parameters by individual aquifer. Additional analysis was done to check the transient sensitivity of the model to Sy. For this analysis the residual difference between the sensitivity runs and the calibration run for each stress period and each well were analyzed. The model shows limited sensitivity within SA wells when Sy is set to 0.05 but is insensitive to the other variations of Sy. When the Sy of Layer 1 is set to 0.06, 25% of the wells have a residual difference of greater than 1 foot for at least 50% of the time and 45% of the wells have a residual difference of greater than 0.5 foot for at least 50% of the time,

The spring flows for the Magnitude 1 and 2 springs are only minimally sensitive to variations in the magnitude of Kh and Kv of the SA. Bugg Spring and Apopka Spring are the only two which show sensitivity to the different variations in Kh, while Sulphur Spring and Chassahowitzka Spring show sensitivity to the different variations in Kv. Variations to Sy and Ss for the SA showed no appreciable changes for any simulation in the ME of the simulated spring flows.

The structure flows are sensitive to the Kh of the SA when multiplied by a factor of 10. This variation results in 73% of the structure flows having a deviation in the DV% of greater than 10%. Overall performance of the structures is worse than the calibrated model. All other variations of Kh are moderately sensitive, with the factors of 0.2 and 0.1 resulting in slightly more structure meeting the calibration criteria for DV%. Variations of Kh are the most sensitive parameter for the following basins: 10, 12, 16, 17, 20, 25, 27, 28, 35, 36, 41, 49, and 67. A map of the basins are shown in Figure 148. Basins are also identified by name and basin id in structure flow tables found in Appendix N. Structure flows are minimally sensitive to all variations of Kv, Ss, and Sy.

Intermediate Confining Unit

Variations of the Kh of the ICU are insensitive but do show some slight degradation of the global MAE by 0.34 and 0.16 feet at the higher multipliers. Unlike Kh, Kv of the ICU may be the most sensitive parameter in the model.

Kv of the ICU increases the global MAE by 2.28 ft, 1.57 ft., 1.50 ft., and 2.84 ft from the calibrated model when multiplication factors of 10, 5, 0.2 and 0.1 are applied, respectively. The increase in the MAE of 2.84 feet when the Kv is multiplied by 0.1 is the worse observed in any of the simulations. The percentage of total wells showing slight sensitivity ranges between 67 to 72 percent with 37 to 43 percent falling in the sensitive category, depending upon the simulation. For every variation, over 50 percent of the wells in both the UFA and LFA fall in the sensitive category. In general, the model is slightly sensitive to variations in the Kv of the ICU for the SA. The UFA and LFA are sensitive to any variation of Kv. Variations in the magnitude of both the Sy and Ss for the ICU showed no appreciable changes for any simulation in the MAE of the simulated heads. The model is insensitive to these parameters either for the overall model or by individual aquifer. Additional analysis was done to check the transient sensitivity of the model to Sy. For this analysis the residual difference between the sensitivity runs and the calibration run for each stress period and each well were analyzed. The results of this analysis show that the model's transient response is also insensitive to variations of Sy in Layer 2.

Simulated spring flows are sensitive to variations of the Kv of the ICU. When this parameter is multiplied by a factor of 5 or 10, the model appears to be moderately sensitive, with many springs having a deviation from the calibrated MAE greater than 5%. When this parameter is multiplied by a factor of 0.2 or 0.1, the model appears to be sensitive, with many springs having a deviation

from the calibrated MAE greater than 10%. Additionally, Gum Spring and Apopka Spring were most sensitive to Kv of the ICU. Kh in the ICU is not a sensitive parameter for spring flows; however, Sulphur Spring, Weeki Wachee Spring, Chassahowitzka Spring, Homosassa Spring, Gum Spring, and Bugg Spring all show sensitivity to variations of the parameter. Variations to the Sy and Ss for the ICU showed no appreciable changes for any simulation in the ME of the simulated spring flows.

Variations in the magnitude of Kh for the ICU are minimally sensitive for the structure flows. However, variations in the magnitude of Kv for the ICU are sensitive when the parameter is multiplied by 10, and moderately sensitive for all the other variations. Although Kv is a sensitive parameter, there is only a minimal difference (reduced by 1 basin) in the number of structures meeting the DV % calibration criteria. Variations of Kh and Kv of the ICU are the most sensitive parameter for the following basins: 9, 24, 27, 46, 47, 58, 62, and 71. Variations of Ss and Sy for the ICU are not a sensitive parameter for structure flows.

Upper Floridan Aquifer

Increasing the Kh of Model layer 3 by factors of 10 and 5 increases the MAE of the model by 1.54 and 0.57 feet, respectively. Sensitivity by aquifer varies from none to slightly sensitive for the SA, sensitive for the UFA, and moderately sensitive for the LFA. Decreasing the hydraulic conductivity of Model layer 3 shows little change in the MAE. At these lower values, both the UFA and LFA are moderately sensitive while the SA is insensitive.

The model's response to changes in the Kh of Model layer 4 is like Model layer 3 although more muted. The MAE increases by 1.72 ft. and 0.75 feet when it is increased by factors of 10 and 5. A reduction of the Kh of Model layer 4 shows little change from the calibrated values. In general, the SA is insensitive to the changes. The UFA and LFA are moderately sensitive when Model layer 4 values are increased by a factor of 10 and only slightly sensitive to the other changes.

Kh of the APPZ (Model layer 5), is another extremely sensitive model parameter. Increasing the Kh by a factor of 10 results in the MAE increasing by 2.77 feet compared to the calibration. This change is the second greatest deviation from the calibration of any simulation except for when Kv of the ICU was multiplied by 0.1. In addition, 75 percent of all wells show some sensitivity with 49 percent falling in the sensitive category which is the most of any simulation.

All three aquifers showed some sensitivity to the variable, with the SA being the least affected. Both the UFA and the LFA have nearly 70 percent of the wells within the sensitive category, with changes greater than 1 foot and over 95 percent of the wells being slightly to moderately sensitive. Although not as extreme, multiplying the Kh of the APPZ by 5 results in an increase in the MAE of 1.41 feet. For this case, 70 percent of the wells are slightly sensitive with 36 percent falling in the sensitive category. All three aquifers showed some sensitivity to the variable with the SA being slightly sensitive and both the UFA and LFA as sensitive. Decreasing the parameter by 0.2 and 0.1 provides similar results in that the SA is relatively insensitive to those changes, the UFA is moderately sensitive and the LFA is sensitive to reductions in the Kh of the APPZ.

Changes to the Kv for Model layers 3, 4 and 5 showed no appreciable changes for any simulation in the MAE of the simulated heads. The model is insensitive to this parameter for these layers either for the overall model or by individual aquifer.

Variations in the magnitude of the Sy in Model layer 3 and the Ss for Model layers 3 and 4 showed no appreciable changes for any simulation in the MAE of the simulated heads. The model is insensitive to these parameters either for the overall model or by individual aquifer. Additional analysis was done to check the transient sensitivity of the model to Sy. For this analysis the residual difference between the sensitivity runs and the calibration run for each stress period and each well were analyzed. The results of this analysis show that the model's transient response is also insensitive to variations of Sy in Layer 3. Some slight sensitivity was detected in the LFA when the Ss for Model layer 5 was increased by a factor of 100. Other changes to the Ss in Model layer 5 had little effect.

Sulphur Spring, Bugg Spring, Volusia Blue Spring, and Alexander Spring were all most sensitive to the aquifer properties of the UFA, namely the Kh. Simulated spring flows are sensitive to variations of Kv of the UFA. When this parameter is multiplied by a factor of 5 or 10, the model appears to be sensitive, with many springs having a deviation from the calibrated MAE greater than 10%. However, when this parameter is multiplied by a factor of 0.2 or 0.1, the model appears to be minimally sensitive, with most springs having a deviation from the calibrated MAE less than 5%. Kh of the UFA is not a sensitive parameter for the spring flows. Variations to Sy and Ss for the UFA showed no appreciable changes for any simulation in the ME of the simulated spring flows.

Overall, variations in the magnitude of aquifer properties for the UFA are minimally sensitive for the structure flows. However, on an individual basin basis, the following basins are sensitive to Kv in Layer 4: 5, 14, 33, 40, 43, and 70. Additionally, basin 11 is sensitive to Kh in Layer 5.

Middle Confining Unit

Changes to the aquifer parameters in the Middle Confining Unit (MCU) does not significantly change the overall MAE of the model, nor does it affect the SA. Changes to the Kh of Model layer 6 shows some slight sensitivity to the UFA and LFA when it is multiplied by 10 but otherwise it is insensitive. Changes to the Kv of Model layer 6 does not impact the UFA but does cause the LFA to become slightly sensitive for every case. Variations in the magnitude of both Kh and Kv for Model layer 7 has little effect.

Changes to the Kh of Model layer 8 indicates variations of this parameter are insensitive to the model overall. However, modifications to the Kv of Model layer 8 impacts the LFA. When it is increased, the LFA indicates moderately sensitive tendencies while it reverts to the slightly sensitive category when it is reduced.

Variations in the magnitude of the Ss for Model layers 7 and 8 showed no appreciable changes for any simulation in the MAE of the simulated heads. The model is insensitive to these parameters by aquifer. Some slight sensitivity was detected in the LFA when the Ss for layer 6 was increased by a factor of 100. Other changes to the Ss in Model layer 6 had little effect. Variations to Kh, Kv, and Ss for the MCU showed no appreciable changes for any simulation in the ME of the simulated spring flows, and the DV of the structure flows.

Lower Floridan Aquifer

Changes to aquifer parameters in the LFA does not significantly change the overall MAE of the model nor does it affect the SA or the UFA. Increasing the Kh of the upper production zone of the LFA (Model layer 9) by a factor of 10 suggests it is sensitive with over 50 percent of the LFA wells

showing changes of greater than 1 foot. When it is multiplied by a factor of 5, the LFA is considered moderately sensitive. Reducing the Kh or any changes to the Kv of Model layer 9 indicates the LFA is insensitive. Similarly, changes to the Kh of Model layer 10 shows little change while varying the Kv suggests the LFA is slightly sensitive in all cases. The LFA is moderately sensitive when the Kh of Model layer 11 increased and slightly sensitive when it is decreased. The LFA is insensitive to changes to Kv.

Changes to the Ss of Model layers 9 through 11 results in similar findings. When the storage is increased by two orders of magnitude for any layer, the LFA becomes slightly sensitive to those changes. However, it is insensitive to changes of one order of magnitude or less.

Variations to the Kh, Kv, and Ss for the LFA showed no appreciable changes for any simulation in the mean error of the simulated spring flows, and the DV of the structure flows.

6.2.5 Stresses and related variables

Changes to model stresses evaluated include increasing or decreasing the maximum saturated zone ET and gross recharge rates by factors of 1.2, 1.1, 0.9 and 0.8 across the model domain. Adjustments to the extinction depth are multiplication factors of 2.0, 1.5, 0.75 and 0.5.

Maximum Saturated Zone Evapotranspiration (ET)

Variations in maximum groundwater ET rates did not show widespread changes across the model domain. ET -tested here is the maximum saturated zone ET that can occur at the water table, which can be several to tens of feet below land surface along the ridge areas and near surface in the flatland regions. Multiplying the maximum saturated zone ET by 0.9 or 1.1 results in no significant change for any aquifer. When the parameter is multiplied by 1.2 or 0.8, all three aquifers show slight sensitivity to the parameter with over 60 percent of the wells reflecting noticeable changes although none of the wells indicate high sensitivity to the parameter.

Variations in the magnitude of the maximum groundwater ET shows only a minimal sensitivity to the error within the spring flows. None of the individual magnitude 1 and 2 springs showed a sensitive difference in error for the variations of this parameter.

Unlike simulated heads and spring flows, the structure flows are very sensitive to variations in the maximum ET rate. When a factor of 1.2 is applied to the maximum ET rate, 70% of the structures have a difference in DV % from the calibrated DV greater than 10%. The number of basins that are calibrated based on the DV calibration criteria increases from 10 to 16. When a factor of 1.1 is applied to the maximum ET rate, the structure flows are only moderately sensitive. The number of basins that are calibrated based on the DV calibration criteria increases slightly from 10 to 11. When a factor of 0.9 is applied to the maximum ET rate, the structure flows are only moderately sensitive, however, unlike the previous variations, the number of basins that are calibrated based on the DV calibration criteria decreases slightly from 10 to 9. When a factor of 0.8 is applied to the maximum ET rate, 60% of the structures have a difference in DV % from the calibrated DV greater than 10%. The number of basins that are calibrated based on the DV calibration criteria decreases from 10 to 6. The following basins are most sensitive to variations in maximum ET rate: 20, 28, 29, 50, 55, 80 and 81.

Evapotranspiration Extinction Depth

Changes to the ET extinction depths show slightly more sensitivity than the maximum saturated zone ET rates. Increasing the extinction depths result in the SA being somewhat insensitive while the UFA and LFA show slightly sensitive tendencies. Increasing the depth did not show any noticeable change to the overall MAE of the model. The MAE does not change by decreasing the extinction depth with all three aquifers showing slight sensitivity to the reductions. Over 60 percent of the wells respond as slightly sensitive when the extinction depth is reduced by a quarter and near 80 percent of the wells are slightly sensitive when it is reduced by one half. However, less than 6 percent of the wells respond with changes of greater than 1 foot in the worst case.

Variations in the magnitude of the ET extinction depth shows only a minimal sensitivity to the error within the spring flows. Only one of the 17 springs, Gum Spring, showed a sensitive difference in error for the variations of this parameter.

ET extinction depth is one of the most sensitive parameters with regards to structure flow calibration. When a factor of 2.0 is applied to the gross recharge, 98% of the structures have a difference in DV % from the calibrated DV greater than 10%. The number of basins that are calibrated based on the DV calibration criteria increases from 10 to 17. When a factor of 1.5 is applied to the ET extinction depth, 73% of the structures have a difference in DV % from the calibrated DV greater than 10%. The number of basins that are calibrated based on the DV calibration criteria increases from 10 to 15. When a factor of 0.75 is applied to the ET extinction depth, structure flow is moderately sensitive, however, unlike the previous variations, the number of basins that are calibrated based on the DV calibration criteria decreases from 10 to 8. When a factor of 0.5 is applied to the ET extinction depth, 90% of the structures have a difference in DV % from the calibrated DV greater than 10%. The number of basins that are calibrated based on the DV calibration criteria decreases from 10 to 2. The following basins are most sensitive to variations in ET extinction depth: 21, 31, 34, 38, 50, 55, 80, and 81.

Gross Recharge

Unlike changes to some of the hydraulic conductivities that can result in extreme changes at individual wells, variation in gross recharge is a significantly sensitive model parameter regarding the sheer number of wells it can affect. For instance, all three aquifers show slight sensitivity when the gross recharge is multiplied by 0.9 or 1.1 but all three aquifers move into the moderately sensitive category when it is multiplied by 1.2 or 0.8. Although the changes at the individual well level are widespread, the values are not large in that the global MAE does not noticeably change for any of the simulations except when it is reduced by 0.8, and even then, it only is reduced by approximately 0.27 feet. Regarding percentage of wells affected, 85 percent of the wells have some sensitivity when multiplied by 1.2, 74 percent of the wells have some sensitivity at 1.1, 76 percent of the wells have some sensitivity at 0.9, and 87 percent of the wells at a multiplier of 0.8 which is the highest percentage of wells showing signs of sensitivity of any of the 192 sensitivity simulations.

Variations in the magnitude of the gross groundwater recharge shows only a minimal sensitivity to the error within the spring flows. Gum Spring, Bugg Spring, Apopka Spring, Crystal Spring, and Chassahowitzka Spring show a sensitive difference in error for some of the variations of this parameter.

Gross recharge is one of the most sensitive parameters with regards to structure flow calibration. When a factor of 1.2 is applied to the recharge, 90% of the structures have a difference in DV % from the calibrated DV greater than 10%. The number of basins that are calibrated based on the DV calibration criteria decreases from 10 to 4. When a factor of 1.1 is applied to the recharge, 50% of the structures have a difference in DV % from the calibrated DV greater than 10%. The number of basins that are calibrated based on the DV calibration criteria decreases from 10 to 7. When a factor of 0.9 is applied to the recharge, 68% of the structures have a difference in DV % from the calibrated DV greater than 10%, however, unlike the other variations, the number of basins that are calibrated based on the DV calibration criteria increases from 10 to 17. When a factor of 0.8 is applied to the recharge, 90% of the structures have a difference in DV % from the calibrated DV greater than 10%. The number of basins that are calibrated based on the DV calibration criteria increases from 10 to 15. The following basins are most sensitive to variations in recharge: 3, 5, 12, 14, 17, 24, 29, 31, 33, 40, 43, 46, 62, 70, and 75.

6.2.6 Surface-groundwater Interaction

Changes to boundary conditions that affect surface-groundwater interactions evaluated includes adjustments to the river, general head, drain, drain return packages and includes changes to the conductance terms by factors 100, 10, 0.1 and 0.01. In addition, in layers where the constant head cells or the general head cells are in contact with the ocean, or in the deeper layers the 10,000 mg/l TDS, these terms were also simulated with a zero-conductance term to simulate a no-flow boundary at the saltwater interface.

General Head Boundaries

Changes to the general head boundaries produce varying results depending upon the simulations. The number of general head cells in the SA and ICU is limited which results in the variable being insensitive to any changes for those layers. A similar condition exists when the general heads are adjusted in the UFA (Model layers 3 through 5). In this case, no noticeable change occurs to any aquifer for any simulation except when the GHB is set to zero. When the GHB is set to zero for Model layers 3 through 5, the SA and the UFA remain insensitive, the LFA becomes slightly sensitive and the overall MAE only changes by 0.26 feet.

When the MCU and the LFA general heads are modified, a slightly different result occurs. For all instances, the SA and UFA remain insensitive to parameter variations and the LFA is slightly sensitive when the GHB is multiplied by values of 0.1 or greater. When the GHB cells in the LFA are multiplied by 10 and 100, there is a slight improvement in the MAE of the LFA wells; however, the higher GHB conductance values result in large fluxes along the coastal boundaries, which does not occur in the natural system. When the GHB is multiplied by 0.01 or zero, the LFA moves into the sensitive category although the MAE does not change noticeably. Sensitivity continues to increase when all layers are adjusted simultaneously. Like the previous results, multiplication factors of 0.1 or greater results in minimal change to the MAE, with the SA and UFA being insensitive and the LFA being only slightly sensitive.

When all GHB values are multiplied by 0.01, the global MAE changes from 3.24 feet in the calibration to 3.77 feet in the sensitivity run, with the SA remaining insensitive, the UFA becoming slightly sensitive and the LFA entering the moderately sensitive category. When the GHBs are effectively turned off for the entire model, the global MAE changes from 3.24 feet in the calibration to 4.21 feet in the sensitivity run. The SA continues to be insensitive, primarily because the constant heads in the upper layer are still active as constant head boundaries, but the UFA shows

some slight sensitivity. The LFA produces the largest change with 97 percent of the wells showing slight sensitivity and over 60 percent of the LFA wells in the sensitive category. This is the largest change to the LFA wells excluding variations in the Kh of the ICU and extremely high values for the APPZ.

Most of the variations in the magnitude of the GHB conductance showed no appreciable changes for any simulation in the MAE of the simulated spring flows. The model is predominantly insensitive to these parameters either for the overall model or for individual springs. The exceptions are when all layers are multiplied by a factor of either 0.1,0.01, or 0, or when the LFA GHB conductance is multiplied by 0.01 or 0. For these variations of the GHB conductance, the model is minimally sensitive, with Rainbow Spring and Gum Spring showing the most sensitivity to this parameter.

Variations in magnitude of GHB conductance is only minimally sensitive to structure flow calibration. There is no change in the number of structure flows meeting the DV calibration criteria when compared to the calibrated model.

Drain, River and Drain Return Conductance Terms

Varying the drain conductance term generally produces similar results regardless of the multiplication factor. The SA is insensitive to variations in the parameter while the UFA and LFA are slightly sensitive to these changes. A slightly worse situation exists for variations of the drain return (DRT) conductance term. In this case, all three aquifers are only slightly sensitive regardless of the change. The variations in the MODFLOW River package also result in both the SA and LFA being insensitive to the parameter with the UFA being slightly sensitive for all multipliers except for 0.01. In that case, all three aquifers show some slight sensitivity.

For some of the sensitivity runs there may be several wells that show an improvement in the statistics for that site, but it may not be widespread for every monitor well in the model to show improvement and the overall net change may be negative. For instance, Figure 155 shows the location of monitor wells showing a net improvement in the calibration of greater than 1.0 feet when the drain conductance was modified.

ME of the spring flows are only minimally sensitive to variation of riverbed conductance from a global model perspective. Sulphur Spring, Crystal Spring, Weeki Wachee Spring, Chassahowitzka Spring, and Gum Spring show a sensitive difference in error for some of the variations in the riverbed conductance. Drain conductance is the single most sensitive parameter for the spring flows. This is to be expected, since springs were simulated using the MODFLOW drain package. When drain conductance was multiplied by a factor of 0.1 and 0.01, all 17 Magnitude 1 and 2 springs showed a sensitive difference in ME. When drain conductance was multiplied by a factor of 10 and 100, a significant majority of the springs, 13 out of 17 and 14 out of 17, respectively, showed a sensitive difference in ME. ME of spring flows are only minimally sensitive to variation of drain return flow conductance from a global model perspective. None of the springs are sensitive to a reduction of the DRT conductance. Variations increasing the conductance term show Crystal Spring, Chassahowitzka Spring, Homosassa Spring, and Gum Spring are sensitive.

Structure flows are minimally sensitive to variations in the magnitude of the riverbed and drain conductance. However, basins 7 and 71 are most sensitive to the riverbed conductance. This occurs mainly in situations where the stream flow is dominated by the baseflow/spring flow. For

example, basin 7 (Wekiva basin) has several springs that contributes to stream flow and therefore is very sensitivity to drain conductance. When DRT conductance is multiplied by a factor of 10 or 100, the structure flows are only minimally sensitive. When DRT conductance is multiplied by a factor of 0.1 or 0.01, the difference in DV from the calibrated model is sensitive for 65% and 73% of the structures, respectively. Structure flow calibration based on the DV criteria also improves for these runs. Variations in DRT conductance is the most sensitive parameter for the following basins: 7, 10, 11, 16, 21, 25, 34, 35, 36, 38, 41, 48, 49, and 58.

Constant Head

The constant head cells are primarily located in the SA. Changing the constant head cells to no-flow along the northern and southern boundaries has little effect on the model MAE either overall or by aquifer. However, adjusting the constant head cells to no flow along the eastern and western boundaries or across the entire model domain causes the global mean absolute error to get worse by approximately 1.4 feet for each of these two cases. Although the change in the mean absolute error is high relative to many of the other runs, it appears to be confined to a lessor number of wells being negatively affected a greater magnitude. Evaluation of these results suggest the SA is insensitive, the UFA is slightly sensitive and the LFA is moderately sensitive. The final run for this parameter was setting the general head cells to constant heads for all layers. This did not change the MAE, nor does it impact the SA or UFA. The LFA is only slightly sensitive in this case.

The majority of the changes to the constant heads showed no appreciable changes for any simulation in the MAE of the simulated heads. The model is predominantly insensitive to these parameters either for the overall model or by individual springs. The one exception is when all layers are set to constant heads. The model is only minimally sensitive to this simulation; however, out of all the sensitivity parameters, Chassahowitzka Spring was most sensitive to setting all layers to constant head.

The majority of the variations in constant heads is only minimally sensitive to structure flow calibration, except for when GHB is converted to constant head in all layers, which is insensitive. The number of calibrated basins is slightly reduced for variations in constant head.

6.2.7 Summary/Conclusion

Overall, based on the results of the sensitivity analysis, the model is most sensitive to changes in the hydraulic conductivity of the ICU and UFA including both producing zones, the drain conductance term, and the recharge rates. The results from the global model sensitivity changes indicate changing any parameter model wide does not result in an improvement in the overall model calibration and modifying the most sensitive of parameters generally results is a net degradation of the calibration statistics. This would tend to suggest the model appears to be reasonably calibrated. While there may be instances when a sensitivity run might appear superior to the calibration run for one or more parameters at the local scale, the calibration run was superior when considering the mean absolute error, the deviation of volume, Nash-Sutcliffe coefficients and the R^2 across the model domain.

6.3 Model Limitations

Overall, the transient groundwater-flow model reasonably simulates regional hydrologic conditions across the project area. Simulated potentiometric surfaces are in good visual agreement with regional UFA potentiometric-surface maps prepared by the USGS. The shapes of the simulated and observed potentiometric-surface contours are similar, indicating model-simulated, groundwater-flow patterns are in good agreement with observed conditions. Residual statistics and maps presented in Chapter 5 also demonstrate the good agreement between observed and simulated water levels.

The model also adequately simulates spring discharges and river baseflow. There was a -3.5 percent error between total simulated and estimated/observed springflow during the transient calibration period. That error was two percent for the two-year verification period from 2013-2014. Simulated baseflow was within the range of estimated baseflow at 15 out of 18 gaging stations that were not significantly affected by highly managed basins. These results provide verification that the modeling results are reasonable.

Even though the model adequately represents the groundwater-flow patterns and fluxes within the model domain, there are some areas outside the CFWI area where model residual head errors are significant, particularly in steep hydraulic gradient areas centered near the East Pasco High and southern Lake Wales Ridge. Localized head changes in the proximity of some major wellfields in the Tampa Bay region were also difficult to simulate given the regional nature of the application. Furthermore, although the model generally reproduces the temporal water-level trends at most of the monitoring wells, there are significant differences between observed and simulated temporal water-level response at specific wells. These differences are not unexpected, given the use of aquifer parameter zones during calibration and the limitations of the available hydrogeologic data. In these instances, the various qualitative and quantitative calibration criteria were balanced to achieve the best overall calibration. Despite these differences, the calibrated model reasonably simulates the regional and three-dimensional hydrogeologic features of the project area.

Potential users of the ECFTX model should note because of recognized data limitations, model simulation is more appropriate at the sub-regional and regional scales rather than at the very local or site-specific scales for simulation of hydrologic conditions. Grid cell sizes are a uniform 1,250 feet. Any simulation results at a scale of a few hundred feet would be problematic unless a finer grid discretization is utilized.

The conceptual model used to construct the model for the project area is a simplified representation of the true groundwater-flow system. The Floridan aquifer system is composed mainly of carbonate rocks some of which have undergone significant karstification and some of which have undergone fracture development, all of which can be characterized as an extremely complex, heterogeneous aquifer system. Even though, there may be numerous zones of differential pathways associated with secondary porosity features, it is believed the secondary porosity features are so ubiquitous that an equivalent porous medium model is appropriate for the model domain. This viewpoint is supported by Hickey (1984; 1989) who showed that the hydraulic and mass transport response characteristics of a fractured dolostone within the UFA could be effectively modeled using the equivalent porous medium assumption. In general, spatially and volumetrically averaged hydraulic properties of the carbonate rocks can be determined in a sub-regional to regional scale via aquifer performance tests. These

properties are included in the model cells to reflect spatially and volumetrically averaged properties. The fact that the model can simulate heads and fluxes in a reasonable manner under a variety of conditions provides confidence that the equivalent porous medium assumption is applicable. Kuniansky (2016) also found in a study of Wakulla Springs that equivalent porous medium assumption is valid in karst terrains when examining heads and flows for annual, monthly, or seasonal average hydrologic conditions.

Various model parameters and boundary conditions were determined based on land-use distribution, configuration of waterways and other surface-water bodies, and climatic conditions during the calibration period of the model. If any of these factors were to significantly change, parameters such as recharge, ET, and river conductance may need to be modified.

6.4 Recommendations for Future Data Collection

The Data, Monitoring, and Investigative Team (DMIT), in coordination with the HAT have identified and prioritized areas within the CFWI that would benefit from additional data collection for model calibration. The selection process is described by the DMIT in the *CFWI Regional Monitoring Program: Summary Report*. The summary report can be found on the CFWI website (www.cfwiwater.com). As part of the DMIT's continuing efforts to assist the HAT, an annual 5-year Work Plan is submitted to the CFWI Steering Committee for approval outlining a review of site prioritization, updated well construction costs, updated monitoring and testing sites, and a record of work completed in preceding fiscal years. These annual reports can also be found on the CFWI website.

The DMIT focus of future data collection includes infilling portions of the CFWI area between existing data collection and monitoring sites. Data collection and future monitoring will be undertaken to further understand the spatial extent and hydraulic properties of the ICU, MCUs I and II, and portions of the LFA. Also, there is a need for additional information about both the degree of interaction between wetlands/lakes and the underlying UFA and the spatial distribution of semi-confined and well-confined conditions in the UFA.

6.5 Future Model Refinements

A review and discussion about boundary conditions and the recharge methodology used in the model should be undertaken to assess their strengths and limitations for future model refinements. Results from the sensitivity analysis indicate the model is sensitive to the uncertainty of some parameters. The most sensitive parameters in this model are the Kv of the ICU, Kh of the UFA and the areal recharge. Priority should continue to be assigned for data collection related to these parameters in order to minimize the predictive model uncertainty.

For future major calibration updates regarding the model, it is recommended a parameter estimation technique, such as PEST, be used as a final step after initial manual calibration of the model. In addition, an uncertainty analysis should be untaken regarding key head and flux targets.

The ECFTX Model underwent a major peer-review upgrade to support the development of the 2020 CFWI Regional Water Supply Plan. The updates to the model to support the CFWI 2025 RWSP are envisioned to include:

- Updated model layering and aquifer parameters associated with new wells principally installed as part of the DMIT Workplan.

- Updated water use information from 2015 onward.

- Updated water level information from 2015 onward for wells, lakes, and wetlands and spring flows.

- Re-calibration of the existing model with these data updates.

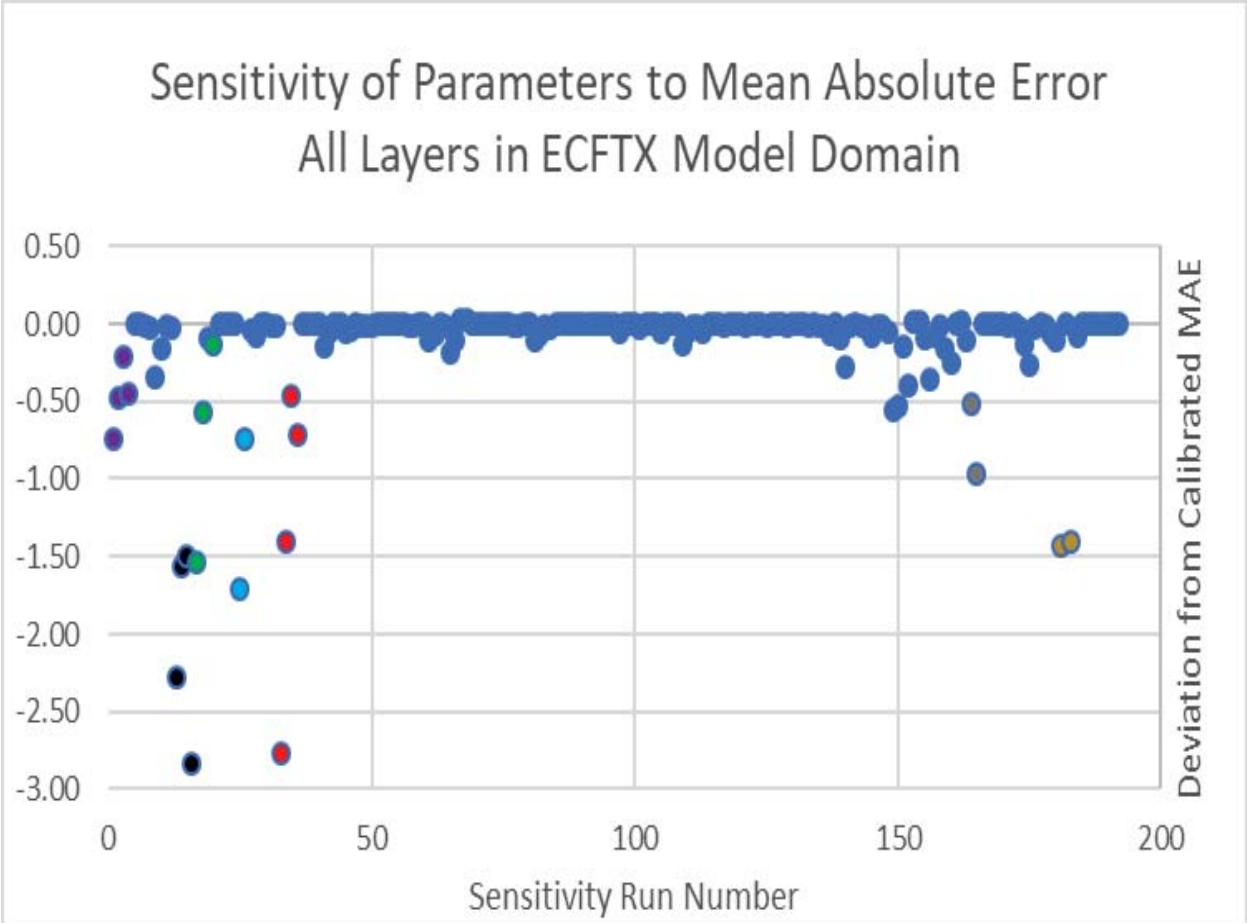- Model documentation.

CHAPTER 6 - FIGURES

Figure 150. Change in mean absolute error for each sensitivity run. Purple is layer 1, green is layer 3, light blue is layer 4 and red is layer 5 horizonal hydraulic conductivity; dark blue is layer 2 vertical hydraulic conductivity; gray is general head boundaries
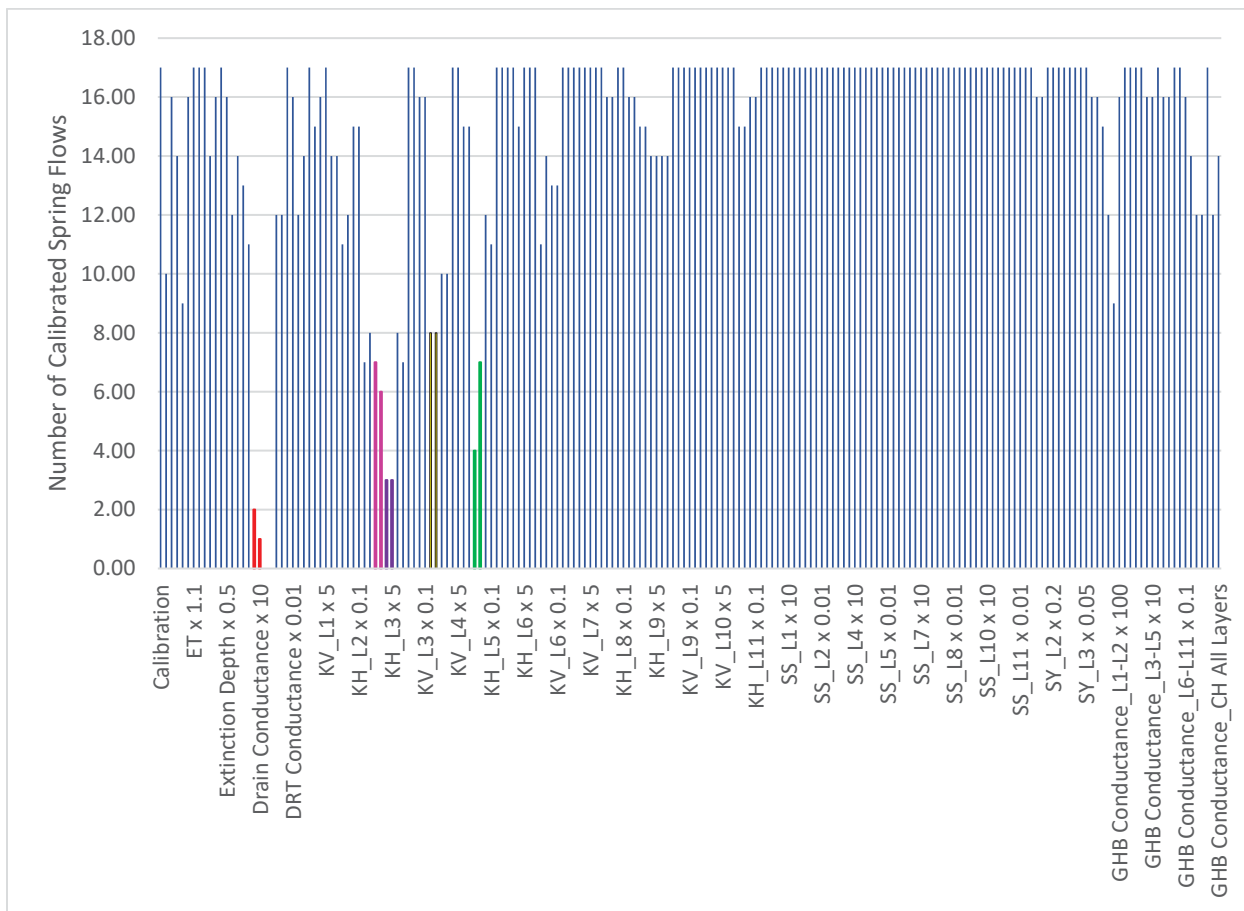
Figure 151. Number of Magnitude 1 and 2 springs meeting the calibration criteria of error within +/- 10%. Bars in red are the number of calibrated springs with variations to drain conductance, bars in pink are the number of calibrated springs with variations to aquifer properties in ICU, bars in purple, black, and green are the number of calibrated springs with variations to aquifer properties in UFA.
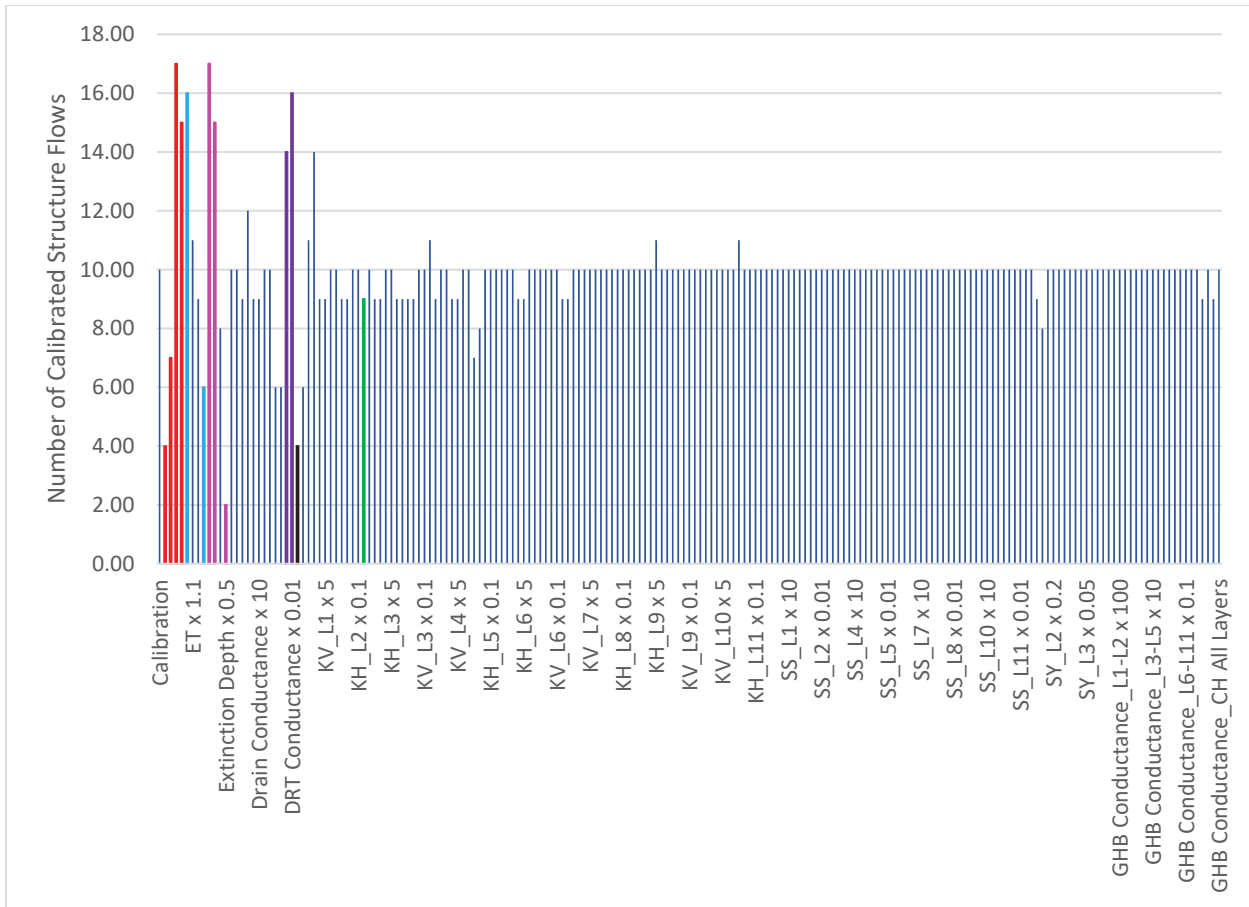
Figure 152. Number of structure flows meeting the calibration criteria of a deviation of volume within +/- 15%.
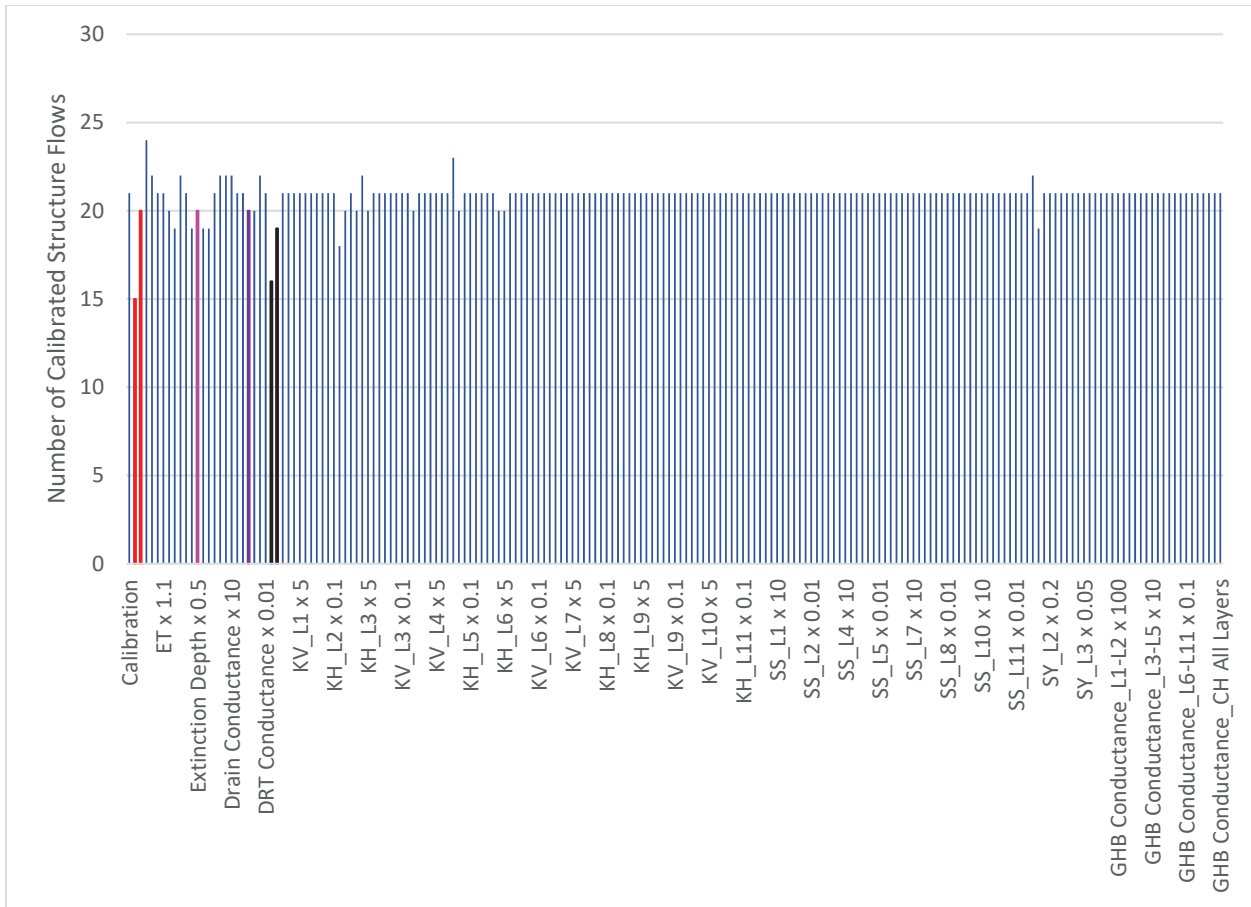
Figure 153. Number of structure flows meeting the calibration criteria of a NS Coefficient greater than 0.5.
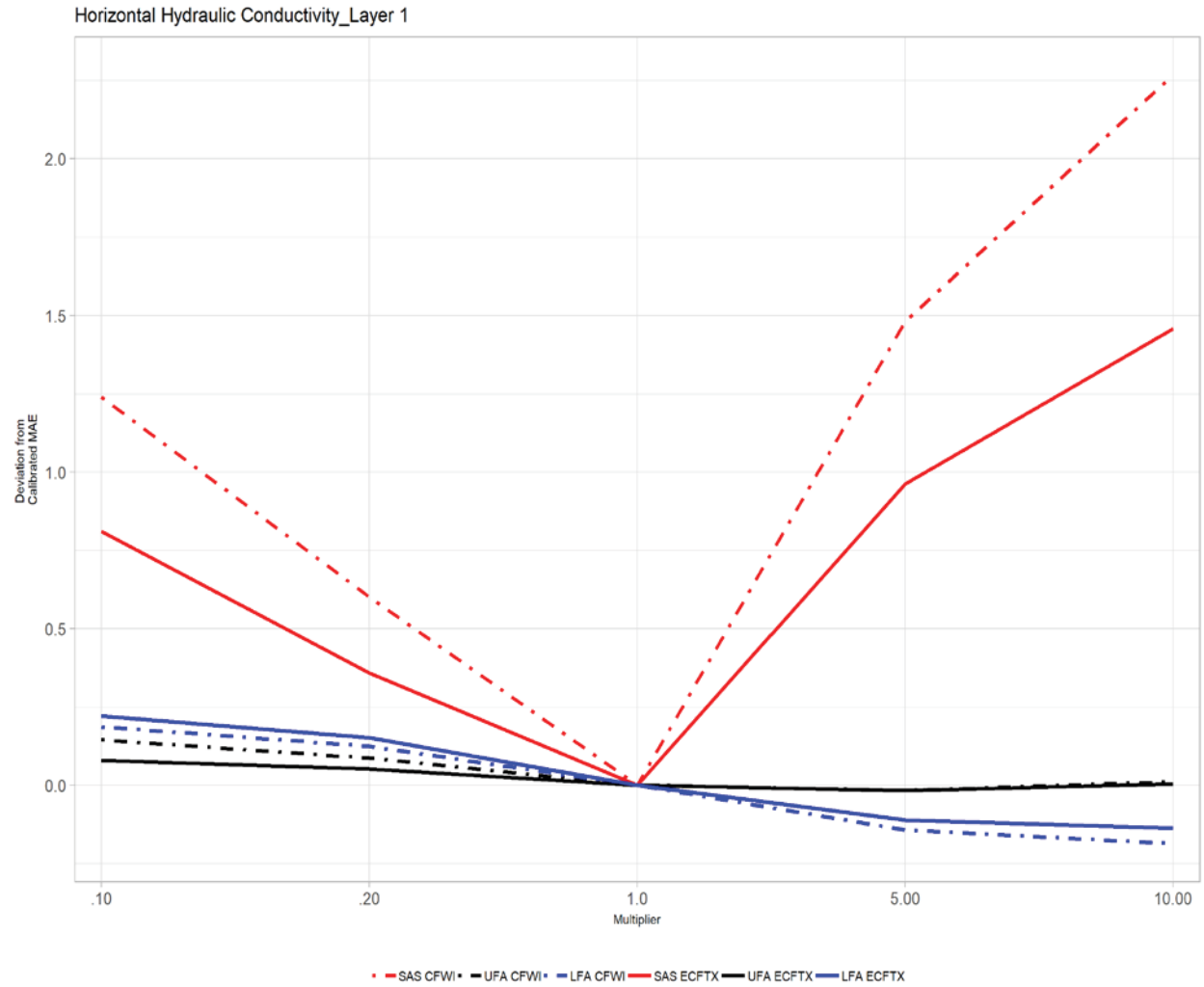
Figure 154. Sensitivity of simulated heads to changes in Kh of the SA in groundwater monitoring wells. Wells are grouped by aquifer and by domain. Sensitivity is shown as a deviation from the calibrated MAE.

Figure 155. Monitor Wells showing improvement of over 1 foot in the MAE resulting from changes to the drain conductance terms.

REFERENCES

Andersen, P., B. Jacobs, and L. Konikow, 2007, Peer Review Report – East Central Florida Transient Model, South Florida Water Management District.

Bandara, U. 2018, Development and Verification of a Numerical Model to Simulate Evapotranspiration and Recharge for Regional Scale Groundwater Models. Florida Water Resource Conference. April 2018. Daytona Beach, FL.
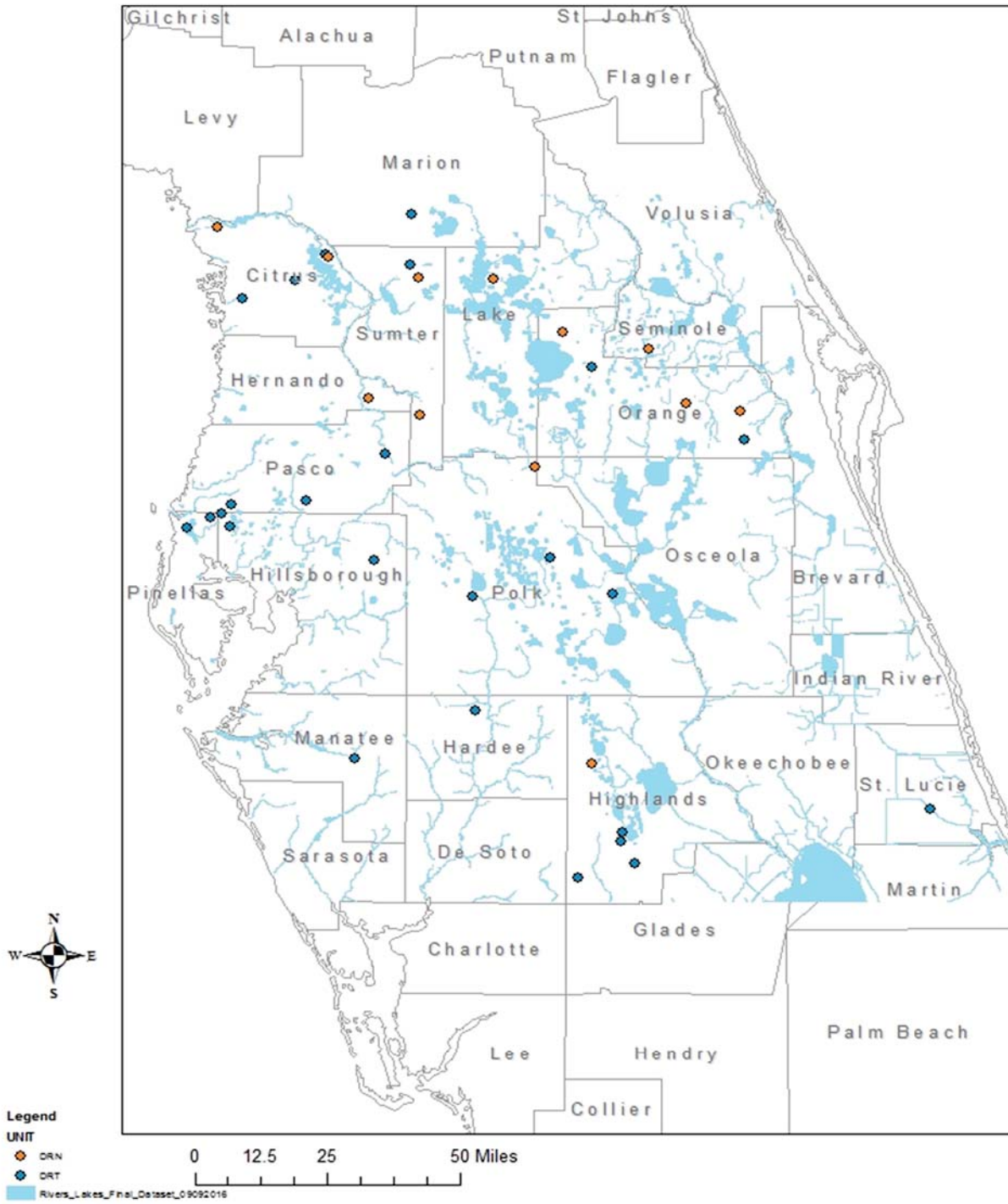
Banta, E.R., 2000, MODFLOW-2000, the U.S. Geological Survey Modular Ground-Water Model Documentation of Packages for Simulating Evapotranspiration with a Segmented Function (ETS1) and Drains with Return Flow (DRT1): U.S. Geological Survey Open-File Report 00-466, 127 p.

Basso, R., 2010, Hydrologic Conditions of the Green Swamp and an Evaluation of Potential Groundwater Withdrawal Impacts to MFL Wetlands, Southwest Florida Water Management District Technical Memorandum, 11 p.

Basso, R., 2011, Hydrogeologic Provinces within West-Central Florida, Southwest Florida Water Management District Technical Report, 48 p.

Basso, R. and Hood, J., 2005, Assessment of Minimum Levels for the Intermediate Aquifer System in the Southwest Florida Water Management District, Southwest Florida Water Management District Technical Report, 60 p.

Bellino, J., Kuniansky, E., O'Reilly, A., and Dixon, J., 2018, Hydrogeologic Setting, Conceptual Groundwater Flow System, and Hydrologic Conditions 1995-2010 in Florida and Parts of Georgia, Alabama, and South Carolina, U.S. Geologic Survey, Scientific Investigations Report 2018-5030, 103 p.

Boniol, D., M. Williams, and D. Munch, 1993. Mapping Recharge to the Floridan Aquifer Using a Geographic Information System. Technical Publication SJ93-5, St. Johns River Water Management District, Palatka, FL.

Brooks, H. K. 1981, Geologic Map of Florida, Florida Cooperative Extension Service, IFAS, University of Florida, Gainesville, Florida.

Bush, P. and Johnston, R., 1988, Ground-water hydraulics, regional flow, and ground-water development of the Floridan aquifer system in Florida and in parts of Georgia, South Carolina, and Alabama, Professional Paper 1403-C., 80 p.

CFWI. 2014a. *Central Florida Water Initiative Regional Water Supply Plan Planning Document*, Final Draft. Central Florida Water Initiative. http://www.cfwiwater.com.

CFWI. 2014b. *Central Florida Water Initiative Regional Water Supply Plan Appendices*. Appendix C-I, Evaluation of Water Quality Degradation Potential in the CFWI Planning Area. Central Florida Water Initiative. http://www.cfwiwater.com.

Flannery, M., Chen, X., Dixon, L., Estevez, E., Leverone, J., 2011, *The Determination of Minimum Flows for the Lower Myakka River.* Brooksville, FL.

Flannery, M., Chen, X., Heyl, M., Munson, A., Dachsteiner, M. 2008, *The Determination of Minimum Flows For the Lower Alafia River Estuary* Brooksville, FL.

Geovariances, 2011, Modeling of the Hydrostratigraphic units of Florida – Peer Review of SJRWMD ISATIS Project , 16 p.

Goudenhoofdt, E. and L. Delobbe. 2009. Evaluation of Radar-Gauge Merging Methods for Quantitative Precipitation Estimates. Hydrol. Earth Syst. Sci. 13:195-203.

Harbaugh, A.W., 2005, MODFLOW-2005, The U.S. Geological Survey Modular Ground-Water model—The Ground-Water Flow Process: U.S. Geological Survey Chapter 6 of Book 6, Conceptualization and Implementation of Stress Packages.

Harbaugh, A.W., 2005, MODFLOW-2005 The U.S. Geological Survey Modular Ground-Water Model – The Ground-Water Flow Process, USGS, Techniques and Methods, Book 6, Chapter 16, Modeling Techniques, Section A, Ground Water, 196 p.

Helsel, D.R. and R.M. Hirsch. 1992. Statistical Methods in Water Resources. Studies in Environmental Science Volume 49. Elsevier, Amsterdam, The Netherlands. 522 pp.

Hickey, J.J., 1982. Hydrogeology and Results of Injection Tests at Waste-Injection Test Sites in Pinellas County, Florida. U.S. Geological Survey Water-Supply Paper 2183.

Hickey, J.J., 1984. Field Testing the Hypothesis of Darcian Flow Through a Carbonate Aquifer, Ground Water, Vol. 22, No. 5, pp.544-547.

Hickey, J.J., and Wilson, W.E., 1982, Results of deep-well injection testing at Mulberry, Florida: U.S. Geological Survey Water-Resources Investigations Report 81-75, 15 p.

Hoblit, B.B., C. Castello, L. Liu, and D. Curtis, 2003, *Creating a seamless map of gage-adjusted radar rainfall estimates for the state of Florida:* Proceedings of the EWRI World Water and Environmental Congress, Philadelphia, PA.

Hoblit, Brian C. and David C. Curtis, 2000, "Next Generation Rainfall Data", Proceeding from the ASCE Watershed and Operations Management 2000 Conference, Ft. Collins, CO.

Hood, J., Kelly, M., Basso, R., Morales, J., 2010, *Proposed Minimum Flows and Levels for the Upper and Middle Withlacoochee River.* Brooksville, FL.

Huebner, S.R., Pathak, C. and Hoblit, B.C., 2003. Development and Use of a NEXRAD Database for Water Management in South Florida. ASCE EWRI World Water and Environmental Resources Congress Proceedings. ASCE, Reston, Virginia.

Jensen, M.E., R.D. Burman, and R.G. Allen (ed). 1990. Evapotranspiration and Irrigation Water Requirements. American Society of Civil Engineers, Eng Pract. Manual No. 70. 332 p.

Kuniansky, E.L., 2016, Simulating groundwater flow in karst aquifers with distributed parameter models—Comparison of porous-equivalent media and hybrid flow approaches: U.S. Geological Survey Scientific Investigations Report 2016–5116, 14 p., available online at https://dx.doi.org/10.3133/sir20165116.

McDonald, M.G., and Harbaugh, A.W., 1988, A modular three-dimensional finite-difference ground-water flow model: U.S. Geological Survey Techniques of Water-Resources Investigations, book 6, chap. A1, 586 p.

McGurk, B., and P.F. Presley. 2002. Simulation of the effects of groundwater withdrawals on the Floridan aquifer system in east-central Florida: Model expansion and revision. Technical Publication SJ2002-3. Palatka, Fla.: St. Johns River Water Management District.

Merritt, M.L., and L.F. Konikow, 2000, Documentation of a computer program to simulate lake-aquifer interaction using the MODFLOW ground-water model and the MOC3D solute-transport model: U.S. Geological Survey Water Resources-Investigations Report 00-4167, 146 p.

Metz, P.A., 2016, Discharge, water temperature, and water quality of Warm Mineral Springs, Sarasota County, Florida: A retrospective analysis: U.S. Geological Survey Open-File Report 2016–1166, 31 p.

Müllner, D. 2013. Fastcluster: Fast Hierarchical, Agglomerative Clustering Routines for R and Python. Journal of Statistical Software 53(9):1-18.

Niswonger, R.G., Panday, Sorab, and Ibaraki, Motomu, 2011, *MODFLOW-NWT, A Newton formulation for MODFLOW-2005*: U.S. Geological Survey Techniques and Methods 6-A37, 44 p. Available online at http://pubs.er.usgs.gov/publication/tm6A37.

Reilly, T.E. and A.W. Harbaugh. 2004. Guidelines for Evaluating Ground-Water Flow Models U.S. Geological Survey Scientific Investigations Paper 2004-5038, 30.

Restrepo, J.I., and J.B. Giddings. 1994. Physical Based Methods to Estimate ET and Recharge Rates Using GIS. Effects of Human-Induced Changes on Hydrologic Systems, American Water Resources Association, Bethesda, MD.

Rumbaugh, J., 2019., Revised Calibration of the District Wide Regulation Models Version 3 and Version 4 for the Southwest Florida Water Management District, Chapter 3, DWRM 3 Development, p 16.

SEGS Ad Hoc Committee, 1986, Hydrogeological units of Florida: Florida Geological Survey Special Publication 28, 8 p.

Sepulveda, N. 2002. Simulation of Ground-Water Flow in the Intermediate and Floridan Aquifer Systems in Peninsular Florida. U.S. Geological Survey WRI Report 02-4009, U.S. Geological Survey, Tallahassee, Florida. 130 pp.

Sepulveda, N., C.R. Tiedeman, A.M. O'Reilly, J.B. Davis, and P. Burger, 2012. Groundwater Flow and Water Budget in the Surficial and Floridan Aquifer Systems in East-central Florida: U.S. Geological Survey Scientific Investigations Report 2012–5161, 214 p.

SFWMD, 2013. *Volume III, Water Use Permitting Manual,* South Florida Water Management District, West Palm Beach, FL.

Shah, N., M. Nachabe, and M. Ross. 2007. Extinction depth and evapotranspiration from ground water under land covers: Ground Water 45(3):329-338.

Skinner, C.L., 2006. Developing a Relationship between NEXRAD Generated Rainfall Values and Rain Gauge Measurements in South Florida. Thesis Completed to Fulfill Requirements of Master of Science Degree, Florida Atlantic University, Boca Raton, Florida.

Smajstrla, A.G. 1990. Technical Manual. Agricultural Field Scale Irrigation Requirements Simulation (AFSIRS) model, Version 5.5. Agricultural Engineering Department, University of Florida, Gainesville, FL.

Smajstrla, A.G. 1990. User's Guide. Agricultural Field Scale Irrigation Requirements Simulation (AFSIRS) model, Version 5.5. Agricultural Engineering Department, University of Florida, Gainesville, FL.

Smith, B. and S. Rodriguez. 2017. Spatial Analysis of High-Resolution Radar Rainfall and Citizen-Reported Flash Flood Data in Ultra-Urban New York City. Water 9(736). 17 pp.

The South Florida Water Management District. https://www.sfwmd.gov/our-work/kissimmee-river Accessed September 9, 2019.

Southwest Florida Water Management District, 1996, Northern Tampa Bay Water Resource Assessment Project, Surface-Water/Ground-Water Interrelationships.

Southwest Florida Water Management District, 1999, Aquifer Characteristics within the Southwest Florida Water Management District, 111 p.

Southwest Florida Water Management District, 2006, *Lower Hillsborough River Low Flow Study Results And Minimum Flow Recommendation.* Brooksville, FL.

Southwest Florida Water Management District, 2010, *Proposed Minimum Flows and Levels for the Lower Peace River and Shell Creek.* Brooksville, FL.

Spechler and Kroening (2007), Hydrology of Polk County, Florida, U. S. Geological Survey Scientific Investigations Report 2010-5097.

The St. Johns River Water Management District. https://www.sjrwmd.com/waterways/st-johns-river/ Accessed September 9, 2019.

Steiner, M., J.A. Smith, S.J. Burges, C.V. Alonso, and R.W. Darden. 1999. Effect of bias adjustment and rain gauge data quality control on radar rainfall estimation. Water Resources. Res. 35(8):2,487-2,503.

Stewart, J. 1980. Areas of Natural Recharge to the Floridan Aquifer in Florida, U. S. Geological Survey Map Series 98.

Stokes, J., 2005. Recharge Areas of the Floridan Aquifer in the St. Johns River Water Management District, SJRWMD, Palatka, FL.

Sumner, D.M., 1996, Evapotranspiration from Successional Vegetation in a Deforested Area of the Lake Wales Ridge, Florida.

Sumner, D.M., 2017, Evapotranspiration (ET) at Blue Cypress marsh site, daily data, Indian River County, Florida, June 1, 1995 – October 20, 2014: U. S. Geological Survey data release.

Sumner, D.M., Hinkle, C.R. and Becker, K.E., 2017, Evapotranspiration (ET) at University of Central Florida urban site, daily data, Orange County, Florida, January 29, 2009 - September 27, 2012: U.S. Geological Survey data release.

Sutherland. 2000. Methods for Estimating Effective Impervious Cover. Article 32 in The Practice of Watershed Protection, Center for Watershed Protection, Ellicott City, MD.

Swancar, Amy, 2017, Evapotranspiration data at Starkey pasture site, Pasco County, Florida, January 2010 - April 2016: U.S. Geological Survey data release.

Tibbals, C.H., 1990. Hydrology of the Floridan Aquifer System in East-central Florida, U.S. Geological Survey Professional Paper 1403-E, 98p.

United States Department of Agriculture, TR-55, United States Department of Agriculture, Natural Resource Conservation Service, Conservation Engineering Division, Technical Release 55, June 1986.

White, W.A.,1970, The Geomorphology of the Florida Peninsula. Geological Bull. 51. Bureau of Geology, Florida Department of Natural Resources, Tallahassee. 164 p.

Williams, L.J., A.D. Dausman, and J.C. Bellino. 2011. Relation of aquifer confinement and long-term groundwater-level decline in the Floridan aquifer system: Proceedings of the 2011 Georgia Water Resources Conference, April 11-13, 2011, Athens, Georgia.

Williams, L. and Kuniansky, E., 2016, Revised hydrogeologic framework of the Floridan aquifer system in Florida and parts of Georgia, Alabama, and South Carolina (ver. 1.1, March 2016): U.S. Geological Survey Professional Paper 1807, 140 p.

Winsburg, M.D. 2003. *Florida Weather.* Second Edition. University Press of Florida, Gainesville, FL.

Wunderlin, R.P., 2010, Central Highlands of Florida, U.S.A., North America Regional Centre of Endemism: CPD Site NA29 website: http://botany.si.edu/projects/cpd/na/na29.htm.

Yobbi, D., 1996. Analysis and Simulation of Ground-Water Flow in Lake Wales Ridge and Adjacent Areas of Central Florida: U.S. Geological Survey Water-Resources Investigations Report 94-4254, 82 p.

Zahina-Ramos, J., D. MacIntyre, J. Bays, S. Denton, A. Janicki, and C. Uranowski, 2013, *Development of Environmental Measures for Assessing Effects of Water Level Changes on Lakes and Wetlands in the Central Florida Water Initiative Area, Final Report*, (http://cfwiwater.com/pdfs/CFWI_Environmental_Measures_finalreport.pdf.

LIST OF APPENDICES

Appendix A. Hydraulic conductivity of each layer in the ECFTX model.

Appendix B. Vertical hydraulic conductivity of layers 2,6, 8, and 10 in the ECFTX model.

Appendix C. Specific storage of each layer in the ECFTX model.

Appendix D. Additional information on River package development in the ECFTX model.

Appendix E. Additional information on River package development for lakes in the ECFTX model.

Appendix F. Additional information on agricultural return flow and landscape irrigation return flow in the ECFTX model.

Appendix G. Simulated versus observed water level hydrographs for all target wells in the ECFTX model.

Appendix H. Simulated versus observed flow hydrographs for all measured springs in the ECFTX model.

Appendix I. Simulated versus observed May and September potentiometric surface maps in the ECFTX model.

Appendix J. Flooded cell extent by stress period in the ECFTX model.

Appendix K. Dry cell extent by stress period in the ECFTX model.

Appendix L. Simulated versus observed head duration hydrographs for all target wells in the ECFTX model.

Appendix M Mean Inflow and outflow components of the ECFTX model from 2003-2014.

Appendix N. Major parameter changes and their effects on the monitor well heads, spring flows and structure discharges.

Appendix O. Structure flow tables and basin information.

All appendices located at:

ftp://ftp.cfwi.cfwiwater.com/pub/HAT/ECFTX_Report